GEOLOGICAL SURVEY OF CANADA
COMMISSION GÉOLOGIQUE DU CANADA

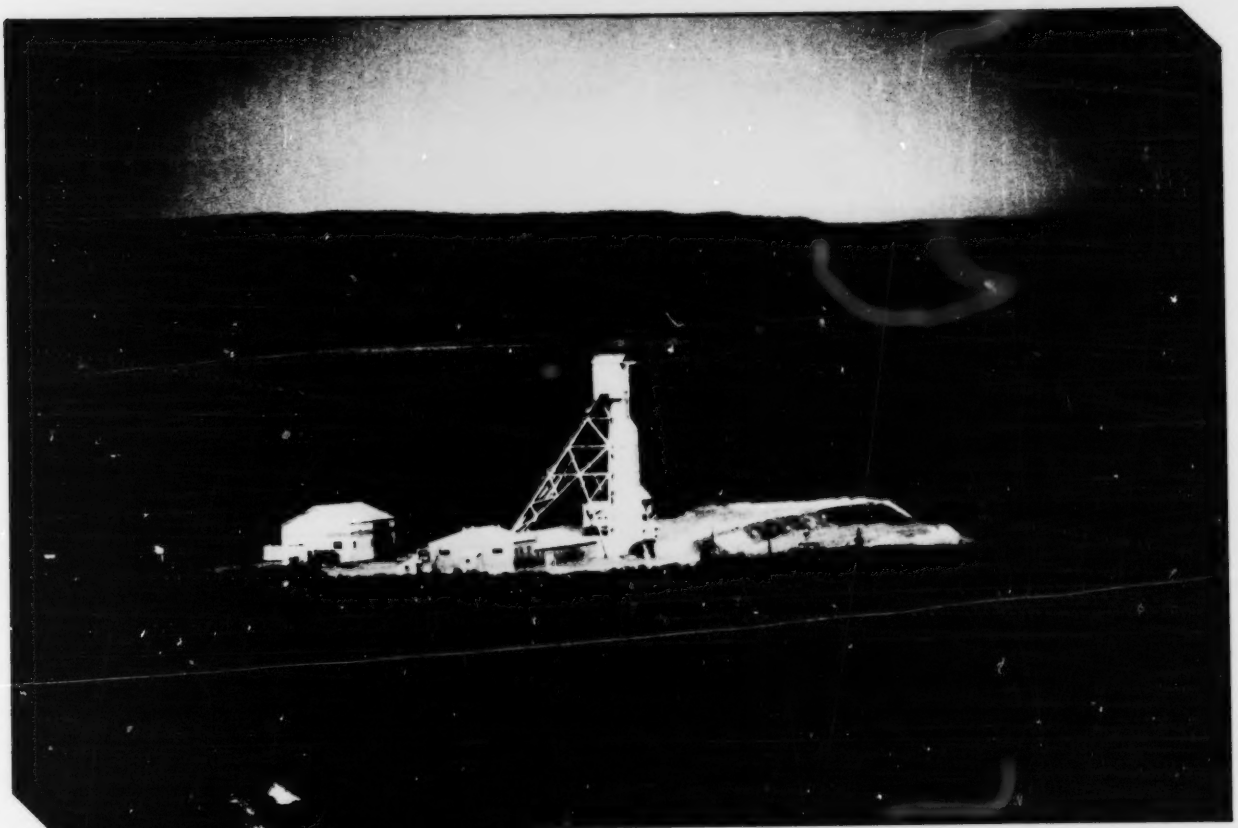

PAPER 86-24

BUCHANS GEOLOGY, NEWFOUNDLAND

edited by
R.V. KIRKHAM

Canada

88-00842/

DEPARTMENT OF MINES AND ENERGY
GOVERNMENT OF NEWFOUNDLAND AND LABRADOR

Contribution to
CANADA-NEWFOUNDLAND CO-OPERATIVE MINERAL PROGRAM 1982-1984
and to
CANADA-NEWFOUNDLAND MINERAL DEVELOPMENT AGREEMENT 1984-1989

Field and laboratory studies for most of the reports were supported by the Canada-Newfoundland co-operative mineral program, and costs of publication of the volume were carried by the Canada-Newfoundland Mineral Development Agreement, a subsidiary agreement under the Economic and Regional Development Agreement.

Contribution au
PROGRAMME COLLABORATIF CANADA-TERRE-NEUVE RELATIF AUX MINÉRAUX 1982-1984
et à
L'ENTENTE CANADA-TERRE-NEUVE SUR L'EXPLOITATION MINÉRALE 1984-1989

Le concours du Programme collaboratif Canada-Terre-Neuve relatif aux minéraux a permis la réalisation des études sur le terrain et en laboratoire qui sont à la base de la plupart des rapports, et l'Entente Canada-Terre-Neuve sur l'exploitation minérale, une entente auxiliaire relevant de l'Entente de développement économique et régional, a assumé les frais associés à la publication du volume.

Energy, Mines and Resources Canada
Énergie, Mines et Ressources Canada

GEOLOGICAL SURVEY OF CANADA
PAPER 86-24

BUCHANS GEOLOGY, NEWFOUNDLAND

edited by
R.V. KIRKHAM

1987

©Minister of Supply and Services Canada 1987

Available in Canada through

authorized bookstore agents and other bookstores

or by mail from

Canadian Government Publishing Centre
Supply and Services Canada
Ottawa, Canada K1A 0S9

and from

Geological Survey of Canada offices:

601 Booth Street
Ottawa, Canada K1A 0E8

3303-33rd Street N.W.,
Calgary, Alberta T2L 2A7

A deposit copy of this publication is also available
for reference in public libraries across Canada

Cat. No. M44-86/24E Canada: $30.00
ISBN 0-660-12632-X Other countries: $36.00

Price subject to change without notice

Cover Photographs

View to the west of MacLean headframe. Low terrain in foreground is underlain by the Buchans Group and high terrain in background is underlain by the Topsails igneous terrane. Photograph by W.P. Binney.

Polylithic breccia-conglomerate with abundant rigid lithic clasts (nonmetallic, various shades of grey) and relatively uncompacted sulphide clasts with both regular and scalloped surfaces (mainly sphalerite and galena with minor chalcopyrite and pyrite), MacLean Extension Orebody. Specimen is about 11 cm wide. Sample: R.V. Kirkham (KQ-83-15A).

Preface

The papers in this volume are chiefly a product of the Canada-Newfoundland co-operative mineral program 1982-84, and involved industry, the Newfoundland Department of Mines and Energy, Memorial University of Newfoundland, and the Geological Survey of Canada.

Although the papers deal with such diverse topics as geochemistry, isotopic geology, mineral deposits, paleontology, petrology, and sedimentology, the majority are concerned with geophysics, stratigraphy, and structural geology. These studies have resulted in a fundamental re-interpretation of the stratigraphy and structure of the Buchans mine.

The mine closed in 1984, because its reserves were exhausted after 57 years of production. Although the total quantity of ore mined was modest, the average grade was remarkably high, and the amount of contained zinc, lead, copper, silver, and gold made the deposits very productive. The studies recorded here add important documentation concerning one of Canada's major mines and, by advancing the general knowledge of volcanogenic massive sulphide deposits, will assist exploration for this type of deposit in Newfoundland and elsewhere.

R.A. Price
A/Assistant Deputy Minister
Geological Survey of Canada

Préface

Les articles de cette publication sont en grande partie la résultante du Programme coopératif sur les minéraux Canada - Terre-Neuve 1982-84 et la participation de l'industrie, du ministère des Mines et de l'Énergie de Terre-Neuve, de l'Université Memorial de Terre-Neuve et de la Commission géologique du Canada.

Même si ces articles abordent différents domaines telles que la géochimie, la géologie isotopique, les gîtes minéraux, la paléontologie, la pétrologie et la sédimentologie, il reste que la majorité des sujets traités relève de la géophysique, de la stratigraphie et de la géologie structurale. Ces études sont le résultat d'une réinterprétation en profondeur de la stratigraphie et de la structure de la mine Buchans.

La mine cessa ses activités en 1984 à cause de l'épuisement de ses réserves survenant après cinquante-sept ans de production. Même si la quantité de minerais extrait fut relativement faible, la teneur moyenne fut remarquablement élevée et le pourcentage de zinc, de plomb, de cuivre, d'argent et d'or a fait en sorte que les gisements furent très productifs. Cet ouvrage est une importante contribution, d'une part, parce qu'il fait connaître une des principales mines canadiennes et d'autre part, par les renseignements généraux qu'il apporte sur les gisements de sulfures volcanogéniques massifs; il rendra un service conséquent dans l'exploration de ces types de gisements à Terre-Neuve et partout ailleurs.

Le sous-ministre adjoint
intérimaire de la
Commission géologique du Canada
R.A. Price

Contents

Page	
1	**Introduction** *R.V. Kirkham*
23	Tectonic setting of the Buchans Group *R.V. Kirkham* (Report 1)
35	Stratigraphy and structure of the Buchans Group *J.C. Thurlow* and *E.A. Swanson* (Report 2)
47	Aspects of the structural geology of the Buchans area *K.R. McClay* (Report 3)
59	Middle Ordovician conodonts from the Buchans Group *G.S. Nowlan* and *J.G. Thurlow* (Report 4)
63	Interpretation of an aeromagnetic gradiometer survey in the Buchans area *L.J. Kornik, J.G. Thurlow* and *J.B. Whalen* (Report 5)
69	The relationship of the Topsails igneous terrane to the Buchans Group *J.B. Whalen* and *K.L. Currie* (Report 6)
75	Geology and origin of orebodies in the Lucky strike area *J.L. Jambor* (Report 7)
107	A sedimentological investigation of MacLean channel transported sulphide ores *W.P. Binney* (Report 8)
149	Geology and genesis of granitoid clasts in the MacLean Extension transported orebody *P.W. Stewart* (Report 9)
177	Evaluation of a resurgent caldera and aspects of ore deposition and deformation at Buchans *R.V. Kirkham* and *J.G. Thurlow* (Report 10)
195	Geology and geochemistry of the Skidder Basalt *J.W. Pickett* (Report 11)
219	Geology and mineralogy of the Tulks deposit *J.L. Jambor* and *D.M. Barbour* (Report 12)
227	Detailed lead isotope study of Buchans and related ores *G.L. Cumming* and *D. Krstic* (Report 13)
235	Deep multifrequency and transient electromagnetic surveys near Buchans *A.K. Sinha* and *L.E. Stephens* (Report 14)
251	Mise-à-la-masse experiments in the MacLean Extension Orebody *C.J. Mwenifumbo* (Report 15)
263	Natural gamma ray logging in volcanic rocks: the Mudhole and Clementine base metal prospects *C.J. Mwenifumbo* and *P.G. Killeen* (Report 16)
273	Preliminary results of detailed structural analysis at Buchans *T.J. Calon* and *F.K. Green* (Report 17)
In pocket	Aeromagnetic vertical gradient map, Buchans, Newfoundland, 12A/15. Geological Survey of Canada, Geophysical Series, Map C40 097G.

INTRODUCTION

R.V. Kirkham

The Buchans mine, with reserves exhausted, was closed in 1984 after 57 years of production. During its life it produced, from several orebodies, a total of 16 196 876 tonnes of ore with an average grade of 14.51% Zn, 7.56% Pb, 1.33% Cu, 126 grams Ag/tonne and 1.37 grams Au/tonne (J.G. Thurlow, personnal communication, 1985) making it one of the world's richest and most productive volcanogenic, massive sulphide districts. The amount of ore produced was not remarkable but the high average grade and amount of contained metals made it a very productive mine. It was the most important base and precious metal producer in Newfoundland.

A number of projects were carried out at Buchans under the Canada-Newfoundland co-operative mineral program 1982-84. The projects were designed to improve the geological understanding of the Buchans deposits, to aid in exploration and possibly help reduce impending serious unemployment in the area, if more ore could be located. The projects were also designed to take advantage of the last underground access to the MacLean Extension Orebody where more detailed geological and geophysical studies were possible. An improved knowledge of Buchans deposits hopefully will help in the search for more ore not only at Buchans but also in other parts of Newfoundland and elsewhere.

This volume attempts to bring under one cover most of the main findings of the work carried out under the 1982-1984 co-operative mineral program, but some work was not part of this program. The paper by Thurlow and Swanson (Report 2) was part of continuing company studies and these authors kindly agreed to prepare this essential update on stratigraphy and structure of the Buchans area for this volume. The work by Whalen and Currie in the Topsails igneous terrane (Report 6) was not directed specifically towards Buchans but since it covered an adjacent area these authors agreed to discuss how the geology of the Topsails igneous terrane relates to that of the Buchans Group. G.L. Cumming and D. Krstic of the University of Alberta (Report 13) were involved in a detailed Pb-isotope study of deposits in the Buchans area and agreed to incorporate their findings into this volume, even though their work was not part of the Canada-Newfoundland co-operative mineral program. Since the end of the 1982-84 co-operative mineral program, structural geology studies have continued at Buchans under the successor Canada-Newfoundland Mineral Development Agreement. Preliminary results of this work are presented in the paper by T.J. Calon and F.K. Green (Report 17). Although most of the work for the volume was done during the 1982-1984 period, some report preparation continued to 1986.

INTRODUCTION

R.V. Kirkham

Ses réserves épuisées, la mine Buchans a fermé en 1984 après avoir été exploitée pendant 57 ans. Elle a produit au total 16 196 876 tonnes de minerai ayant une teneur moyenne de 14,51 % en Zn, de 7,56 % en Pb, de 1,33 % en Cu, de 126 g d'Ag par tonne et de 1,37 g d'Au par tonne (J.G. Thurlow, communication personnelle, 1985); ce district de sulfures massifs d'origine volcanique a donc été l'un des plus productifs et des plus riches du monde. Étant donné la teneur moyenne élevée et la quantité de métal contenu, cette mine a été très productive, même si la quantité de minerai produite n'a pas été remarquable; a été le plus important producteur de métaux communs et de métaux précieux de Terre-Neuve.

Un certain nombre de projets ont été effectués à Buchans, dans le cadre du programme coopératif Canada – Terre-Neuve sur les minéraux de 1982-1984. Ces projets visaient à améliorer notre connaissance de la géologie des gisements de Buchans, à faciliter l'exploration et peut-être même à contribuer à réduire le problème du chômage dans la région en découvrant d'autres minerais. Ces projets devaient également permettre de profiter du dernier accès souterrain au gisement de la prolongation de MacLean, où il était possible de poursuivre des études géologiques et géophysiques détaillées. Une meilleure connaissance des gisements de Buchans facilitera la recherche d'autres minerais non seulement à Buchans, mais aussi ailleurs à Terre-Neuve.

Le présent volume a pour objet de rassembler la plupart des principaux résultats qui découlent des travaux effectués aux termes du programme de 1982-1984; cependant, certains travaux ne faisaient pas partie de ce programme. Le rapport 2 par Thurlow et Swanson, préparé dans le cadre d'une étude permanente entreprise par la société, présente une mise à jour de la stratigraphie et la structure de la région de Buchans. Les travaux effectués par Whalen et Currie dans le terrane igné de Topsails (rapport 6) ne portaient pas spécifiquement sur les gisements de Buchans mais, étant donnée qu'ils couvraient une partie de la région contiguë, les auteurs ont accepté de présenter une discussion des liens qui existent entre la géologie du terrane igné de Topsails et la géologie du groupe de Buchans. G.L. Cumming et D. Krstic de l'Université de l'Alberta (rapport 13) ont participé à une étude détaillé des isotopes de plomb dans les gisements de la région de Buchans, et ils ont bien voulu présenter leurs conclusions dans ce volume, bien que leurs travaux ne fassent pas partie du programme coopératif Canada – Terre-Neuve sur les minéraux. Depuis que le programme coopératif sur les minéraux de 1982-1984 a pris fin, l'étude de la géologie structurale de Buchans s'est poursuivie dans le cadre de l'Entente Canada – Terre-Neuve sur l'exploitation minérale. Le rapport 17, par T.J. Calon et F.K. Green décrit les résultats provisoires de ces travaux. Bien que la plupart des travaux aient été effectués de 1982 à 1984, la préparation de certains rapports s'est poursuivie jusqu'en 1986.

La publication de ce volume suit de très près la parution du volume sur les masses minéralisées de Buchans (Swanson *et al.*, 1981), publié pour marquer le 50e anniversaire de l'Association géologique du Canada. Le présent volume complète celui de l'Association et porte sur les aspects de la géologie de Buchans qui

This volume follows closely on the heels of the Geological Association of Canada Special Paper marking the 50th anniversary of mining of the Buchans orebodies (Swanson *et al.*, 1981). This present volume supplements the 50th anniversary volume and concentrates on those aspects of Buchans geology that were deemed to be most closely related to immediate exploration concerns. Certain problems relevant to exploration that were either identified in the 50th anniversary volume or were unanswered at that time were selected for study during the 1982-1984 period. In general, theoretical and genetic studies without direct application to exploration were not emphasized. Nevertheless, company- and government-sponsored work since 1982 has demonstrated that major revisions to the geology as presented in the 50th anniversary volume are necessary and that much of the theoretical modeling presented in that volume was premature and based on geological assumptions now known to be incorrect. Many of the major geological changes are based on fundamental reinterpretations of the stucture and stratigraphy at Buchans. Much of this work was carried out by J.G. Thurlow, formerly with Abitibi-Price Inc., and his colleagues with additional, lesser contributions by government-sponsored workers. Many basic structural and stratigraphic problems remain to be solved and work at Buchans in continuing. Reinterpretation of Buchans geology has already led to the identification of new exploration targets.

Besides increasing the understanding of the general structural and stratigraphic relations at Buchans, other advances have also been made. The geology of the main Lucky Strike area has been documented more fully and reinterpreted by J.L. Jambor. J.W. Pickett was able to demonstrate that the Skidder Basalt, containing the Skidder Cu-Zn Prospect, has ophiolite affinities and, therefore, should not be included in the Buchans Group. Both conodont and U-Pb zircon dates support a Middle Ordovician age for the Buchans Group, which is more compatible with the ages of other subaqueous mixed basalt-rhyolite volcanic sequences in central Newfoundland. The younger, Late Ordovician – Early Silurian age, accepted previously for the Buchans Group, is clearly incorrect. Dating of the Topsails granites as Early Silurian by Whalen and Currie indicates that the Buchans Group was complexly faulted and overthrust by the Hungry Mountain Complex before or during the Early Silurian. The Buchans area, therefore, had a protracted Ordovician history that included ophiolite formation and emplacement, extensive subaqueous basalt-rhyolite volcanism and associated ore deposition, and complex thrust faulting, followed by the emplacement during the Early Silurian of large amounts of mafic and felsic igneous material in the Topsails igneous terrane immediately to the west and north of the area.

One of the most spectacular features of Buchans geology is the well-preserved, breccia-conglomerate

semblent le plus étroitement liés à l'exploration. Certains problèmes ayant trait à l'exploration qui avaient été posés dans le volume du 50e anniversaire ou qui n'étaient pas résolus à l'époque, ont été étudiés au cours de la période allant de 1982 à 1984. En général, les études théoriques et génétiques qui ne s'appliquent pas directement à l'exploration n'ont pas été soulignées. Néanmoins, les travaux parrainés par les sociétés et par le gouvernement et entrepris depuis 1982 ont révélé qu'il serait nécessaire de réviser l'interprétation de la géologie présentée dans le volume du 50e anniversaire et qu'un grand nombre des modèles théoriques qui s'y trouvent sont faux, puisqu'ils se fondent sur des suppositions géologiques qui se sont révélées incorrectes. Une grande partie des principaux changements apportés à la géologie se fondent sur une réinterprétation fondamentale de la structure et de la stratigraphie de Buchans. Bon nombre de ces travaux ont été effectués par J.G. Thurlow, anciennement de l'Abitibi-Price Inc., et collègues, avec l'aide de travailleurs parrainés par le gouvernement. Il reste à résoudre de nombreux problèmes fondamentaux ayant trait à la géologie structural et à la stratigraphie de la région; les travaux se poursuivent à Buchans. La réinterprétation de la géologie de la région de Buchans a déjà permis de trouver d'autres zones d'intérêt.

Outre les données qui permettent d'améliorer nos connaissances des liens structuraux et stratigraphiques généraux à Buchans, d'autres données ont également été recueillies. J.L. Jambor a documenté en détail et réinterprété la géologie de la zone principale de Lucky Strike. J.W. Pickett a montré que le basalte de Skidder, qui contient l'indice de cuivre et de zinc Skidder, possède des affinités ophiolitiques et ne devrait donc pas être inclus dans le groupe de Buchans. La datation de conodontes et la datation isotopique (U-Pb) du zircon indiquent que le groupe de Buchans date de l'Ordovicien moyen, ce qui correspond mieux aux âges d'autres séquences volcaniques basaltiques-rhyolitiques mixtes subaquatiques dans la partie centrale de Terre-Neuve. Le groupe de Buchans ne daterait donc pas de l'Ordovicien récent-Silurien ancien, âge plus récent qui avait déjà été proposé. Whalen et Currie ont trouvé que les granites de Topsails datent du Silurien ancien, ce qui indique que le groupe de Buchans a été faillé à plusieurs reprises et chevauché par le complexe de Hungry Mountain avant ou durant le Silurien ancien. L'histoire de la zone de Buchans au cours de l'Ordovicien est donc longue et comprend la formation et la mise en place d'ophiolites, un volcanisme basaltique-rhyolitique subaquatique répandu et l'accumulation connexe de minerais, ainsi que la formation de failles chevauchantes composées, suivie par la mise en place au cours du Silurien ancien d'énormes quantités de matériaux ignés felsiques et mafiques dans le terrane igné de Topsails, immédiatement à l'ouest et au nord de la région.

Les minerais clastiques bien conservés à brèches conglomératiques forment un des éléments les plus spectaculaires de la géologie de la région de Buchans. Les recherches effectuées par Binney et d'autres confirment les interprétations antérieures de la géologie, soit que ces minerais ont été déposés par des coulées de débris subaquatiques. Ces travaux montrent également qu'il est possible de cartographier diverses composantes des coulées de débris, ce qui peut faciliter l'exploration et la planification des mines. Les minerais riches à matrice de sulfures et de barytine au centre des coulées de débris sont entourés d'unités grossières à brèches conglomératiques qui contiennent d'abondants clastes sulfurés et lithiques; ces deux unités sont entourées de dépôts relativement massifs et amor-

fragmental ores. Work by Binney and others has confirmed previous interpretations that these were deposited by subaqueous debris flows. This work has demonstrated also that various components of the debris flows can be mapped and can aid in exploration and mine planning. High-grade, sulphide- and barite-matrix ores in the centres of the debris flows are flanked by coarse breccia-conglomerate units with abundant sulphide and lithic clasts and both of these units are surrounded by relatively massive, structureless deposits of arenaceous conglomerate and sandstone with minor amounts of clastic sulphides. In many areas the breccia-conglomerate deposits were demonstrated to have steep, abrupt snouts, indicating high angles of repose and matrix strength.

Many of the debris flows associated with ore contain granitoid clasts. These granitoid clasts had always been an enigma in Buchans geology, since they were the only clast type for which the source was unknown. Stewart, using petrology, petrochemistry and radiometric dating, has demonstrated that these clasts were probably derived from a subvolcanic intrusion(s) related to Buchans Group rhyolites. The association with fragmental ores suggests strongly that phreatomagmatic eruptions were responsible for both the granitoid clasts and triggering the sulphide-rich debris flows.

The airborne gradiometer survey is the first government-sponsored survey of this kind carried out in Newfoundland. It is particularly useful for identifying magnetic differences and gradients between rock units and for tracing lithologic units through covered areas. In the Buchans area, magnetic features are outlined best in the Topsails granitoid and Hungry Mountain crystalline terranes but not so well, unfortunately, in the Buchans Group volcanic rocks (see map in pocket). Nevertheless, some structural and stratigraphic trends are evident in the volcanic rocks and the maps are useful for general lithological distributions, particularly diabase intrusions, and for outlining fault traces.

Most Buchans ores, because of their elongate shapes, gentle plunges, high zinc and barite contents, low pyrite contents and fragmental natures, have not been particularly amenable to electromagnetic exploration techniques. Nevertheless, the geophysical experiments indicate that certain electromagnetic methods, such as mise-à-la-masse, especially used in conjunction with geology, could be useful in exploration. High-energy, deep-penetrating, multifrequency electromagnetic techniques could also have application for certain Buchans ore types in selected areas. Gamma ray logging could also prove useful in correlating lithologic units between drillholes and identification of alteration zones.

Although the studies reported in this volume should help clarify some aspects of Buchans geology, many problems remain unsolved. The most pressing problems, especially for exploration, are basic stratigraphic

phes de conglomérat arénacé et de grès qui contiennent de faibles quantités de sulfures clastiques. À de nombreux endroits, les dépôts de brèches conglomératiques ont des fronts abrupts et raides qui indiquent que l'angle de repos était raide et que la matrice est très résistante.

Bon nombre des coulées de débris associées au minerai contiennent des clastes granitoïdes. Ces clastes granitoïdes avaient toujours représenté une énigme puisque leur source était inconnue. Stewart s'est fondé sur la pétrologie, la pétrochimie et la datation isotopique pour montrer que ces clastes dérivent vraisemblablement d'intrusions hypabyssales liées aux rhyolites du groupe de Buchans. L'association des clastes granitoïdes et des minerais clastiques porte à croire que ces clastes auraient été formés par des éruptions phréatomagmatiques, qui auraient également déclenché les coulées de débris riches en sulfures.

Le levé au gradiomètre aéroporté est le premier levé de ce genre entrepris par le gouvernement à Terre-Neuve. Il permet de déterminer les variations et les gradients magnétiques des diverses unités lithologiques et de tracer ces unités lorsqu'elles sont enfouies. Dans la région de Buchans, les caractéristiques magnétiques s'expriment le mieux dans le terrane granitoïde de Topsails et le terrane cristallin de Hungry Mountain; ces caractéristiques sont malheureusement moins bien exprimées dans les roches volcaniques du groupe de Buchans (voir la carte en pochette). Néanmoins, les roches volcaniques font voir certaines tendances structurales et stratigraphiques et les cartes sont donc utiles pour déterminer la répartition lithologique générale, notamment des intrusions de diabase, et pour tracer les lignes de failles.

La plupart des minerais de Buchans ont une forme allongée; ils sont riches en zinc et en barytine et pauvres en pyrite, ils ont une nature clastique et ils plongent doucement; on ne peut donc pas les déceler à l'aide de méthodes électromagnétiques. Les expériences géophysiques ont néanmoins révélé que certaines méthodes électromagnétiques telles que la méthode de la mise à la masse, utilisées en conjonction avec l'étude de la géologie, pourraient servir à des fins de prospection. Des méthodes électromagnétiques multifréquences à forte énergie, qui pénètrent en profondeur, pourraient également servir pour certains types de minerais dans des régions particulières. La diagraphie par rayons gamma pourrait également se révéler utile pour la corrélation des unités lithologiques entre les forages et la détermination des zones d'altération.

Les études décrites dans ce volume permettront d'éclaircir certains aspects de la géologie de Buchans; cependant, il reste bon nombre de problèmes à résoudre. Les problèmes les plus pressants, notamment en ce qui a trait à l'exploration, portent sur les liens stratigraphiques et structuraux fondamentaux aux environs de la mine. Les travaux se poursuivent dans ces domaines. D'autres questions à résoudre concernent l'épaisse séquence arkosique (anciennement appelée "Footwall Arkose" mais faisant maintenant partie de la formation de Sandy Lake) et ses liens stratigraphiques avec les laves en coussins et les roches volcaniques felsiques. Des unités arkosiques massives, presque entièrement dépourvues de traits distinctifs, dont les contacts sont difficiles à voir dans une région de failles composées, présentent certains problèmes stratigraphiques et sédimentologiques particuliers. L'origine de l'arkose et ses liens avec d'autres unités sont mal connus (p. ex., voir Thurlow et Swanson, 1987). Cas (1979) a décrit des dépôts à écou-

and structural relationships in the mine area. Work on these problems is continuing.

The thick arkosic sequence (formerly called "Footwall Arkose" but now part of Sandy Lake Formation) and its stratigraphic relationships with pillow lavas and felsic volcanic rocks are also problematic. The relationship of the arkose with other units and its origin are not well understood (e.g. see Thurlow and Swanson, 1987). Massive, relatively featureless arkosic units with poorly exposed contacts in an area of complex faults present some special stratigraphic and sedimentological problems. Cas (1979) described possible similar,massive, thick arenaceous mass-flow deposits in the Early Devonian Merrions Tuff in eastern Australia, which interestingly are interlayered with lavas and felsic and intermediate pyroclastic rocks. He interprets these arenites to be products of cold emplacement in a deep basin of large volumes of angular, sand-sized quartz and feldspar. If Bouma cycles are present they tend to be severely top- and middle-truncated. The thick arkosic units at Buchans may have similarities to those in the Merrions Tuff described by Cas.

Contact relationships of the Buchans Group with all other units are not well documented. The stratigraphic top and bottom of the Buchans Group are unknown. The contact with ophiolitic Skidder Basalt has not been observed. To the northwest of Buchans, rocks of the Hungry Mountain Complex in the Topsails igneous terrane have been thrust over the Buchans Group but the nature and amount of movement on this fault have not been established. The new radiometric date on rhyolite in the Roberts Arm Group to the northeast (Dunning *et al.*, 1986) supports the long-held view that the two groups are correlative but the nature and distribution of lithofacies within the two groups are still poorly documented. Complex faulting within the two groups and poor outcrop in many areas compound stratigraphic problems. Work on the general geology of the Buchans-Roberts Arm belt is continuing.

With current re-evaluation of the structural and stratigraphic setting of the Buchans ores, considerable uncertainty exists concerning the volcanic settings of the ores. What is the importance of the dominantly bimodal suite? Was the area under extension with many, major block faults and were central volcanic complexes present? Were calderas present and, if so, what was their nature, distribution and degree of control on ore formation? Before such questions can be answered satisfactorily, the basic stratigraphy and structural relationships of the Buchans area must be established and more surface and subsurface information is required.

Detailed studies of Buchans ores indicate the intriguing possibility that they have been sheared during both sedimentary transport and later tectonic deformation. The ramifications for interpretation of ore textures at Buchans are obvious but work necessary to elaborate

lement massique, épais, massifs et probablement similaires au taf de Merrions du Dévonian ancien dans l'est de le Australie; ce qui attire l'attention, c'est ces dépôs sont intercalés avec les laves et les roches pyroclastiques felsiques à intermédiaires. Cas donne comme origine de ces comites d'être le résultat d'une sédimentation à température froide dans un bassin profond d'une énorme quantité de sable à grains anguleur de quartz et feldspeth. Si les cydes de Bourma sont présents ils ont tendance d'être sévèrement trouqués au sommet à au centre. Les unités d'arkose épaisses de Buchans pouvent avoir une similitude avec ce tuf de Merrions d'écrit par Cas.

Les contacts entre le groupe de Buchans et toutes les autres unités sont mal documentés. On n'a pas trouvé le sommet et la base stratigraphiques du groupe de Buchans, ni le contact avec le basalte ophiolitique de Skidder. Au nord-ouest de Buchans, les roches du complexe de Hungry Mountain dans le terrane igné de Topsails ont été poussées sur le groupe de Buchans, mais on ne connaît pas la nature de la faille ni l'ampleur du mouvement qui s'y est produit. La nouvelle datation isotopique de la rhyolite du groupe de Robert Arm au nord-est (Dunning *et al.*, 1986) appuie une hypothèse de longue date selon laquelle il existe une corrélation entre les deux groupes; cependant, la nature et la répartition des lithofaciès à l'intérieur des deux groupes demeurent mal documentées. La formation de failles composées à l'intérieur des deux groupes et l'absence de bons affleurements à de nombreux endroits aggravent les problèmes stratigraphiques. L'étude de la géologie générale de la zone de Buchans-Robert Arm se poursuit.

La réévaluation actuelle du milieu structural et stratigraphique des minerais de Buchans donne lieu à de nombreuses questions sur les milieux volcaniques des minerais. Quelle est l'importance de l'ensemble bimodal? La région a-t-elle subi une extension et y a-t-il eu formation de nombreux gros blocs faillés; y existait-il des complexes volcaniques centraux? Y trouvait-on des calderas et dans l'affirmative, quelle sorte? Quelle était leur répartition et comment ont-elles contrôlé la formation du minerai? Avant de pouvoir répondre à ces questions il faudrait établir les liens structuraux et stratigraphiques fondamentaux de la région de Buchans et obtenir de plus amples données sur la surface et la subsurface.

L'étude détaillée des minerais de Buchans révèle que ces minerais ont peut-être été cisaillés au cours du transport sédimentaire et de la déformation tectonique subséquente. L'importance de l'interprétation de la structure des minerais de Buchans est évidente, mais on n'a pas encore entrepris les travaux qui permettront de reconstituer l'évolution de ces structures, et ces travaux pourraient s'avérer difficiles puisqu'on ne connaît pas les structures d'origine des minerais en place et que les affleurements de minerais déformés tectoniquement dans les zones de Lucky Strike et d'Oriental sont peut nombreux. Néanmoins, en regard de bon nombre d'autres gisements de sulfures massifs d'origine volcanique, les minerais de Buchans sont bien conservés. S'il s'avère impossible de reconstituer l'histoire de la déformation et de la transformation de la structure des minerais de Buchans, il nous sera extrêmement difficile de comprendre pleinement la transformation des structures dans les gisements plus déformés et métamorphisés.

Cumming et Krstic ont découvert des différences subtiles mais néanmoins mesurables dans les rapports d'isotopes de plomb des minerais de Buchans, ainsi que des différences marquées entre les gisements de Buchans et d'autres gisements de la région. Outre

on the development of ore textures has not been done and may be difficult without knowledge of original textures of in situ ores and adequate exposures of tectonically deformed ores in the Lucky Strike and Oriental areas. Nevertheless, relative to many other volcanogenic massive sulphide deposits, the Buchans ores are well preserved. If the deformational history and transformation of ore textures at Buchans cannot be established, it is then doubtful that the transformation of ore textures in more highly deformed and metamorphosed deposits can be understood fully.

Cumming and Krstic have identified that subtle but measurable differences in Pb-isotope ratios exist in Buchans ores and that marked differences exist between the Buchans deposits and other deposits in the region. Besides the important implications that this has for Pb-isotope studies and ore genesis, the distinct measurable differences between deposits in this part of central Newfoundland also indicates that Pb isotopes offer a potential means of tracing glacially transported sulphides. A number of sulphide-bearing glacial erractics have been found in the Buchans area but the locations of some do not seem to fit established glacial transport directions. Glacial transport directions in this part of Newfoundland are complex and Pb isotopes might help trace ore sulphides back to their sources.

Acknowledgments

Without the complete co-operation of Abitibi-Price Inc. and ASARCO Inc. and their representatives, J.G. Thurlow and E.A. Swanson, this work and volume on Buchans would not have been possible. E.A. Swanson's extensive experience and knowledge of the geology of the area were irreplacable assets. Without any reservations, J.G. Thurlow contributed his help and extensive knowledge to all projects. Only with his persistent work in trying to trace orebodies, and their faulted offsets and to identify new exploration targets was he able to recognize the importance of high-angle reverse and thrust faults in the area. D.M. Barbour, who has much experience in the area, also contributed much information and help with many of the projects. The projects were planned in the fall of 1981 largely through group discussions by J.G. Thurlow, E.A. Swanson, D.M. Barbour, P.L. Dean, B.F. Kean, J.L. Jambor, J.M. Franklin, R.S. Hildebrand, P.E. Killeen, W.H. Poole and R.V. Kirkham. D.F. Strong of Memorial University, with his long experience in the study of mineral deposits in Newfoundland, supervised Stewart's and Pickett's M.Sc. theses which were done under Canada-Newfoundland co-operative mineral program 1982-84.

R.D. Lancaster of the Geological Survey of Canada did a commendable job in co-ordinating and helping

l'importance que ces différences peuvent avoir en ce qui a trait à l'étude des isotopes de plomb et de l'origine des minerais, les différences mesurables qui existent d'un dépôt à un autre dans cette zone de la partie centrale de Terre-Neuve révèlent que l'utilisation des isotopes de plomb pourrai être un moyen de retracer les sulfures transportés par la glace. Un certain nombre de blocs erratiques sulfurés ont été découverts dans la région de Buchans, mais leurs emplacements actuels ne semblent pas concorder avec les directions de transport glaciaire déjà établies. Les directions de transport glaciaire sont complexes dans cette partie de Terre-Neuve et l'étude des isotopes de plomb pourrait aider à retrouver la source des minerais sulfurés.

Remerciements

Cette publication et le volume sur Buchans n'auraient jamais été achevés sans la pleine collaboration des sociétés Abitibi-Price Inc. et ASARCO Inc. et de leurs représentants, J.G. Thurlow et E.A. Swanson. La vaste expérience de E.A. Swanson et ses connaissances détaillées de la géologie de la région ont été irremplaçables. J.G. Thurlow a collaboré à tous les projets et y a apporté ses vastes connaissances. Les travaux qu'il a effectués en vue de détecter les masses minéralisées et leurs rejets et d'identifier de nouvelles zones d'intérêt lui ont permis de reconnaître l'importance des failles chevauchantes et des failles inverses à fort pendage dans la région. D.M. Barbour, qui possède une vaste expérience de la région, a également donné de l'information et de l'aide pour un grand nombre de projets. Les projets ont été planifiés durant l'automne 1981, au cours de discussions auxquelles ont participé J.G. Thurlow, E.A. Swanson, D.M. Barbour, P.L. Dean, B.F. Kean, J.L. Jambor, J.M. Franklin, R.S. Hildebrand, P.E. Killeen, W.H. Poole et R.V. Kirkham. D.F. Strong de l'Université Memorial possède une vaste expérience de l'étude des gisements minéraux à Terre-Neuve; il a supervisé les thèses de maîtrise de Stewart et Pickett, qui ont été entreprises aux termes du programme coopératif Canada – Terre-Neuve sur les minéraux de 1982-1984.

R.D. Lancaster de la Commission géologique du Canada a coordonné le dessin d'un grand nombre des diagrammes publiés dans ce volume et y a également participé. K. Nguyen, J.J. Carrière et W.G. Young ont également participé à la cartographie et à d'autres aspects de la préparation du rapport. R.W. Sullivan, W.D. Loveridge et O. van Breemen de la Section de la géochronologie ont fourni à P.W. Stewart des dates établies par datation à l'U-Pb du zircon. G. Lemieux de la Section de la photographie a fourni de nombreuses photos d'échantillons. T. Scaga et le personnel du Centre de traitement de texte se sont chargés du transfert sur ordinateur et du traitement définitif des manuscrits. J.G. Thurlow, est non seulement co-auteur de quatre textes de ce volume mais a aussi contribué à la révision de plusieurs autres et fourni plusieurs idées originales. W.P. Binney, G.R. Dunning, M.B. Lambert, D.F. Strong, H.S. Swinden, J.L. Jambor, W.D. Sinclair, R.I. Thorpe, H.K. Poulsen, W.H. Poole et J.M. Duke ont également participé à la vérification d'un ou de plusieurs manuscrits, tandis que W.H. Poole a participé à plusieurs des aspects administratifs des projets et à la production définitive du volume.

with the drafting of many diagrams for this volume. K. Nguyen, J.J. Carrière and W.G. Young also helped with cartography and with other aspects of preparation of the report. R.W. Sullivan, W.D. Loveridge and O. van Breemen of the Geochronology Section provided the U-Pb zircon dates for P.W. Stewart. G. Lemieux and R.J. Kelly of the Photography Section also provided many photographs of samples. T. Scaga and staff of the Word Processing Centre were responsible for the computer transfer and final processing of manuscripts. J.G. Thurlow not only co-authored four papers for the volume but reviewed many of the others offering much constructive advice. W.P. Binney, J.M. Duke, G.R. Dunning, J.L. Jambor, M.B. Lambert, W.H. Poole, H.K. Poulsen, W.D. Sinclair, D.F. Strong, H.S. Swinden and R.I. Thorpe provided valuable assistance with the editing of one or more manuscripts and W.H. Poole helped with many of the administrative aspects of the projects and with the final production of this volume.

REFERENCES

Cas, R.
1979: Mass-flow arenites from a Paleozoic interarc basin, New South Wales, Australia: mode and environment of emplacement; Journal of Sedimentary Petrology, v. 49, p. 29-44.

Dunning, G.R., Krogh, T.E., Kean, B.F., O'Brien, S., and Swinden, H.S.
1986: U/Pb zircon ages of volcanic groups from the central mobile belt, Newfoundland (abstract); in Geological Association of Canada – Mineralogical Association of Canada – Canadian Geophysical Union, Joint Annual Meeting, Program with Abstracts, v. 11, p. 66.

Swanson, E.A., Strong, D.F. and Thurlow, J.G., (ed.)
1981: The Buchans Orebodies: Fifty Years of Geology and Mining; Geological Association of Canada, Special Paper 22, 350 p.

Thurlow, J.G. and Swanson, E.A.
1987: Stratigraphy and structure of the Buchans Group; in Buchans Geology, Newfoundland, ed. R.V. Kirkham; Geological Survey of Canada, Paper 86-24, Report 2.

BIBLIOGRAPHIE

Cas, R.
1979: Mass-flow arenites from Paleozoic interarc basin, New South Wales, Australia: mode and environment of emplacement; Journal of Sedimentary Petrology, v. 48; p. 29-44.

Dunning, G.R., T.E. Krogh, B.F. Kean, S. O'Brien et H.S. Swinden
1986: U/Pb zircon ages of volcanic groups from the central mobile belt, Newfoundland (résumé); dans: Geological Association of Canada – Mineralogical Association of Canada – Canadian Geophysical Union, Joint Annual Meeting, Program with Abstracts, vol. 11, p. 66.

Swanson, E.A., D.F. Strong et J.G. Thurlow (rédacteurs)
1981: The Buchans Orebodies : Fifty Years of Geology and Mining; Association géologique du Canada, rapport spécial nº 22, 350 pages.

Thurlow, J.G. et E.A. Swanson
1987: Stratigraphy and structure of the Buchans Group; dans: Buchans Geology, Newfoundland, R.V. Kirkham (rédacteur); Commission géologique du Canada, étude 86-24, rapport 2.

PLATES

Plate 1. Some project leaders at the base of the Lucky Strike glory hole. From left to right: L. Boone (assistant), J.W. Pickett, W.P. Binney, J. Carroll (foreground-assistant), J.G. Thurlow, J.L. Jambor and P.W. Stewart. Timbers in background are from caved stopes[1].

Plate 2. Typical variolitic pillow lava of the Skidder Basalt. Photograph by J.W. Pickett.

[1]Field photographs are by R.V. Kirkham and most hand specimens were photographed by G. Lemieux unless otherwise mentioned. Captions were prepared by R.V. Kirkham and many were reviewed by J.G. Thurlow and W.P. Binney.

Plate 3. Characteristic bedded interflow jasper and pyrite with minor chalcopyrite and sphalerite in the Skidder Basalt. Specimen is 9.5 cm long. Drillhole SK-37A-40 feet, collected by J.W. Pickett.

Plate 4. Semi-massive pyrite and lesser chalcopyrite with irregular jasper clasts. Skidder prospect. Specimen is 5 cm long. Drillhole SK-37A-46 feet, collected by J.W. Pickett.

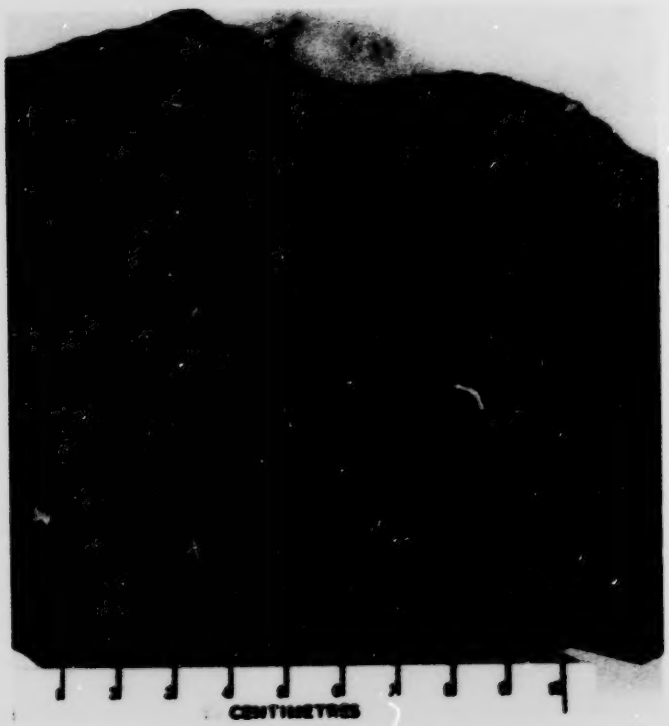

Plate 5. Feeder Granodiorite with typical white plagioclase, pink K-feldspar, 6 mm-diameter clear quartz and dark biotite (altered to chlorite) phenocrysts, Wiley's River area. Photograph by J.G. Thurlow.

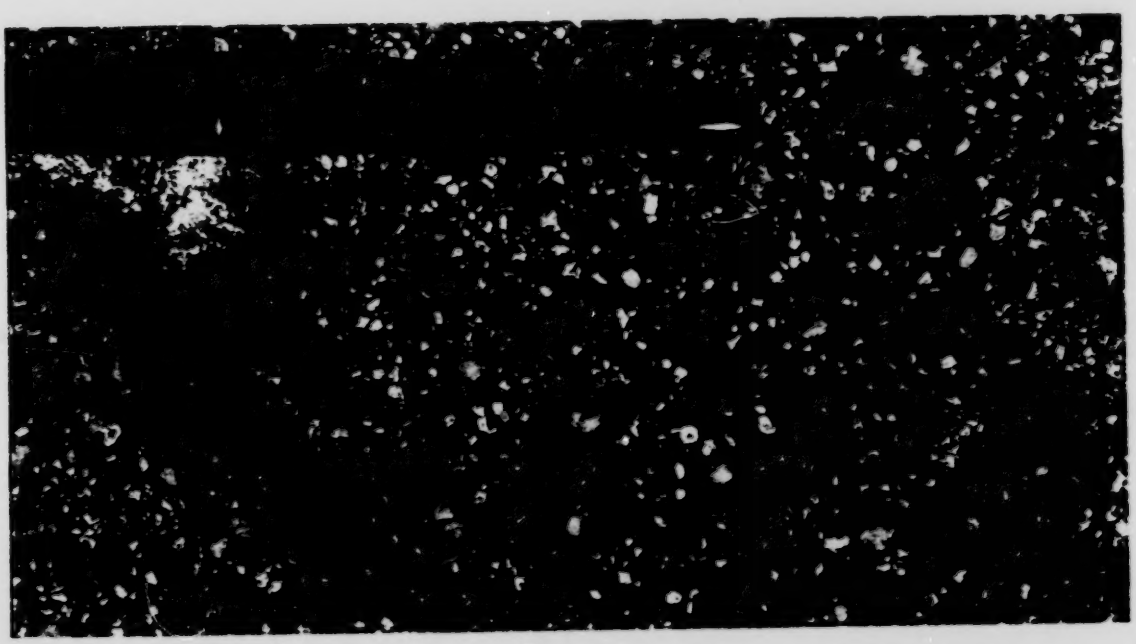

Plate 6. Lundberg Hill Formation rhyolite with abundant zoned plagioclase and 5 to 8 mm-diameter quartz phenocrysts set in an aphanitic matrix. Photograph by J.G. Thurlow.

Plate 7. Mafic volcanic breccia with elongate quartz-filled amygdules, Ski Hill Formation, type locality at Ski Hill. Central fragment is 10 cm across. Photograph by J.G. Thurlow.

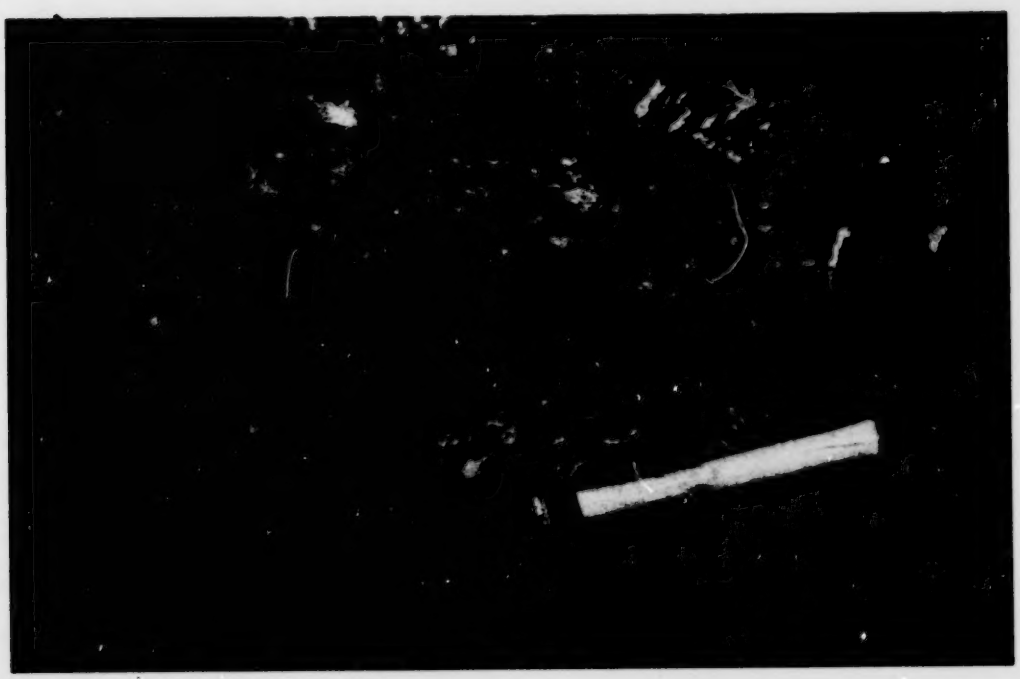

Plate 8. Pillow with radiating, quartz-filled amygdules in basaltic flow near the top of the Ski Hill Formation, about 3000 west, 20 level, MacLean Extension area.

Plate 9. Riedel shear in Ski Hill Formation at Ski Hill. Photograph by K.R. McClay.

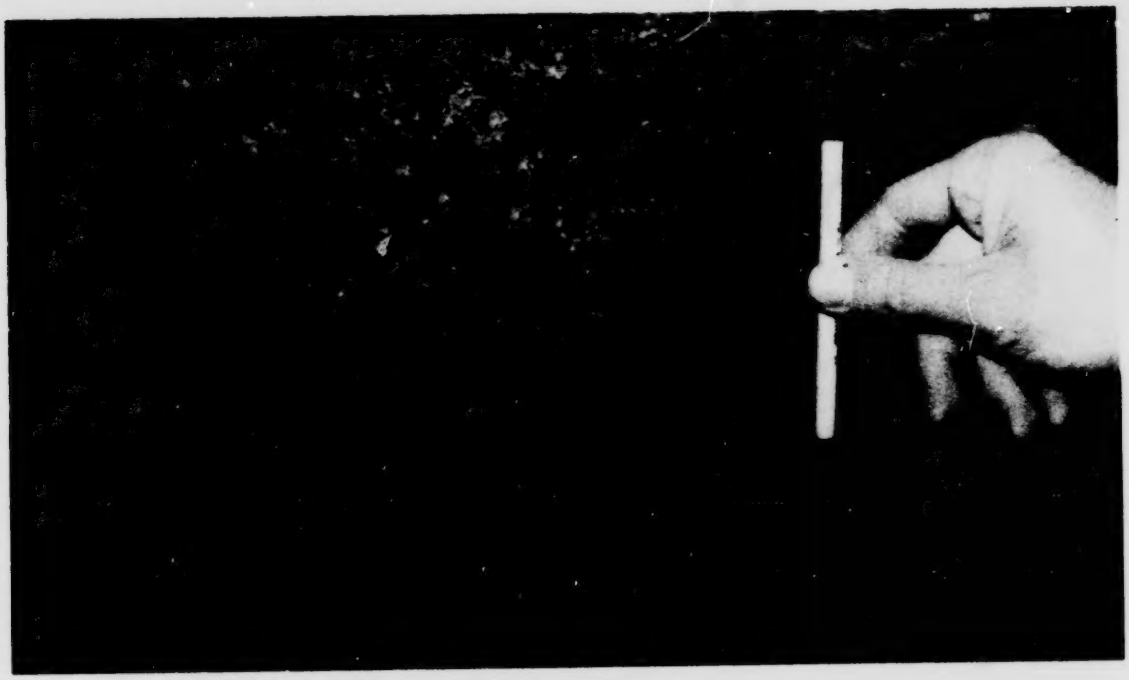

Plate 10. Rhyolitic, quartz-feldspar crystal tuff with dark, elongate pumice fragments in Buchans River Formation, 21 level, above MacLean Extension Orebody.

Plate 11. Sandy Lake Formation pillow breccia with fragments displaying radial and concentric fractures and concentric calcite-filled amygdules. Photograph by J.G. Thurlow.

Plate 12. Matrix-supported conglomeratic arkose in Sandy Lake Formation near powerhouse on Buchans River east of Buchans. Most arkose in this area does not contain conspicuous pebbles.

Plate 13 (above). Typical, irregular pyrite-quartz veins ("stockwork") in altered volcanic rocks, upper north side of Lucky Strike glory hole.

Plate 14. Fragmental sphalerite (grey) - chalcopyrite (yellow) ore central part of Lucky Strike glory hole. Sample: J.L. Jambor.

Plate 15. Typical siltstone breccia of Buchans River Formation with well-bedded and massive siltstone and granitoid clasts, about 3000 west, 20 level, MacLean Extension area, stratigraphically above the pillow lava of Ski Hill Formation illustrated in Plate 8 and below the MacLean Extension Orebody.

Plate 16. Two sulphide- and barite-rich polylithic breccia-conglomerate debris flow units separated by well-bedded siltstone and overlain by felsic crystal tuff, lower ore unit, 20-6-1 sublevel, MacLean Extension Orebody. Differential compaction of siltstone and tuff can be noted around siltstone clast with altered rims at the top of the lower breccia-conglomerate unit and sphalerite-rich clasts at the top of the upper unit. Scale is 10 cm long. Photograph by W.P. Binney.

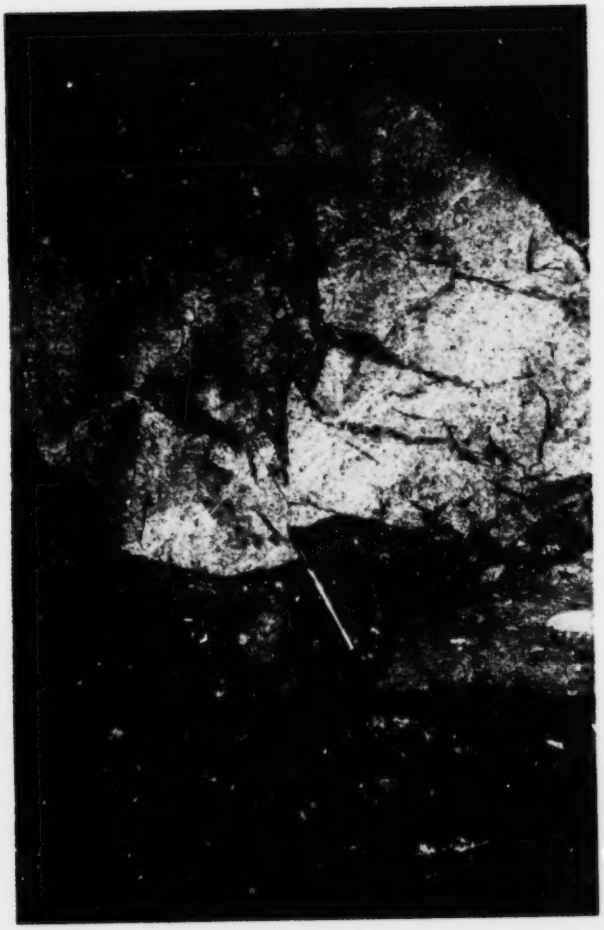

Plate 17. Large granitoid clast (dated sample) in lower ore unit, 20 level, MacLean Extension Orebody. Note the truncated veins and associated alteration zones that cut diagonally across the clast and the sharp contact of the lower ore unit with underlying felsic crystal tuff. Photograph by P.W. Stewart.

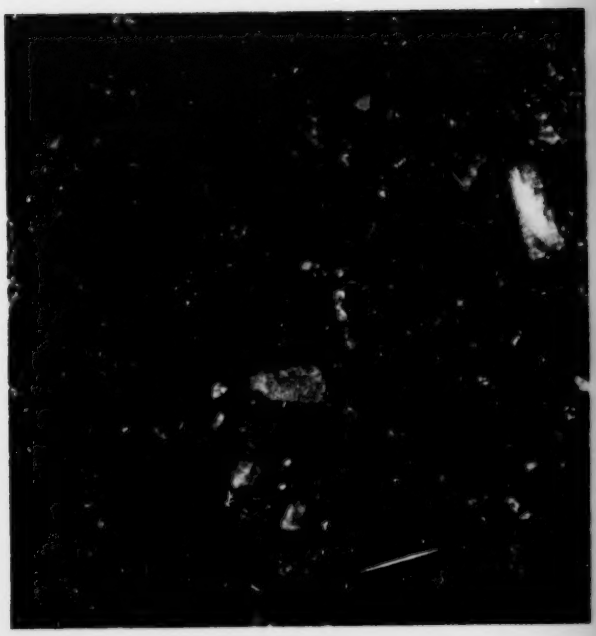

Plate 18 (above). Extremely large sphalerite (minor galena) clast in coarse polylithic breccia-boulder conglomerate bed near snout of a debris flow, 20-5 sublevel, lower ore unit, MacLean Extension Orebody. Other clast types include granitoid, dense and amygdaloidal basalt and siltstone. Photograph by P.W. Stewart.

Plate 19 (top right). Sulphide- and barite-rich debris-flow ore, 20-1 sublevel, MacLean Orebody. Sphalerite (medium grey, metallic), galena (light grey gains), chalcopyrite and pyrite (yellow, metallic), barite (white), rhyolite (pale nonmetallic clasts), and siltstone and mafic volcanic clasts (variable green and grey nonmetallic clasts) set in a fine grained, baritic sulphide-lithic detrital matrix.

Plate 20 (bottom right). Arenaceous conglomerate with interbedded tuffaceous sandstone and siltstone near polylithic breccia-conglomerate beds, Buchans River Formation, 20 level, MacLean Extension area. Note small fault cutting tuffaceous siltstone beds.

Plate 21 (top right). Typical sulphide-poor arenaceous conglomerate with abundant granitoid clasts (white, red and pink; medium grained), siltstone (medium green-grey) and a variety of altered volcanic lithologies (pale grey, green clasts), 20-5 drive, MacLean Extension area. Specimen is cut by late calcite veinlets (white), one at the top of the specimen showing a small fault offset of a granitoid clast. Sample: W.P. Binney (KQB-82-52).

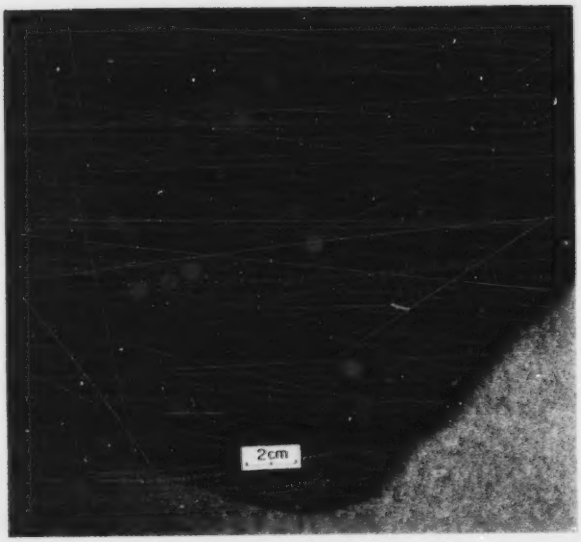

Plate 22 (below). Typical deformed, anastomosing discontinous wispy-layered sulphide matrix ore with a few more rigid siltstone and volcanic clasts, 20-1 sublevel, MacLean Orebody. Sulphides show evidence of high but variable strain. Layering is probably a result of a combination of shear deformation with grain comminution during sedimentary transport and compaction of only semi-consolidated sulphide clasts. The galena (light grey) in sphalerite (medium grey) and barite (dark grey, nonmetallic) occur interstitially in small gash or 'pull-apart' structures indicating textural equilibrium. The yellowish material is pyrite and chalcopyrite grains and clasts. Sample: R.V. Kirkham (KQ-74-35).

Plate 23 (left). Polylithic breccia-conglomerate showing prominent inverse grading from the base of a debris flow bed, 20-6 drive, lower ore unit, MacLean Extension Orebody. Sample is upright. Medium grey metallic clasts are sphalerite (minor galena), yellow metallic clasts are pyrite and chalcopyrite, medium green-grey clasts are siltstone, and darker green-grey clasts are volcanic rocks. Sample: W.P. Binney (KQB-82-76).

Plate 24 (above). Sulphide-rich, polylithic breccia-conglomerate with ragged pyrite-chalcopyrite (yellow), sphalerite (metallic medium grey), barite (white to pale grey), altered siltstone (pale and medium green-grey), basalt (dark grey) clasts, 17 level, MacLean Orebody. Sample: W.P. Binney (KQB-82-190).

Plate 25 (right). Sphalerite (medium grey), chalcopyrite (yellow), pyrite (pale brassy yellow), galena (minor, light grey), lithic (dark and medium grey) clasts in a baritic sulphide matrix, 20 level MacLean Extension Orebody. Clasts are elongated along the bedding. Sample: W.P. Binney (KQB-82-42).

Plate 26. Typical baritic sulphide ore with sphalerite (medium grey), galena (light grey), chalcopyrite (yellow), pyrite (pale brassy yellow), siltstone (pale and medium green-grey) and volcanic (medium and dark green-grey) clasts, Two Level Orebody, northeast corner of Lucky Strike glory hole. Most galena and chalcopyrite occur in gash or 'pull-apart' tension structures indicating textural equilibrium with more competent (harder) sphalerite and pyrite hosts. In the centre of the large elongate sphalerite (chalcopyrite) clast in the middle of the specimen are thin highly deformed but probably relic galena (light)-barite (dark grey) beds. Even though still doubtful, this is one of the best canidates for relic bedding in a sulphide clast. Sample: R.V. Kirkham (KQ-83-19A).

Plate 27. Fragmental barite matrix ore with abundant, elongate brownish sphalerite (minor galena), white barite clasts and bronze-coloured pyritic clasts. 20-8 stope, above 20 level, upper ore unit, MacLean Extension Orebody.

Plate 28. Low-grade, baritic fragmental ore, 20-4 drive, lower ore unit, MacLean Extension Orebody. White clasts are fragments of large barite crystals, medium grey metallic mineral is sphalerite, light grey is galena (minor), yellow is chalcopyrite, and lithic clasts include granitoid, siltstone and volcanic lithologies. Sample W.P. Binney (KQB-82-104).

Plate 29a. Polylithic breccia-conglomerate ore, MacLean Extension Orebody. Medium grey metallic clasts with irregular contacts are sphalerite (galena); yellow metallic clasts are chalcopyrite and pyrite; bedded medium green-grey clasts are siltstone; medium green-grey clast with pale rim in centre of specimen is siltstone with an altered rim; pale clast at top-centre is altered rhyolite, and pale granular clast at top-right is granitoid. Specimen is cut by late calcite veinlets. Sample: R.V. Kirkham (KQ-84-32A).

Plate 29b. Detail of crudely layered sphalerite-rich clast with prominent scalloped margin. Light grey interstitial material is galena. The scalloped margin is probably the result of loading during compaction of a semi-consolidated sulphide clast.

Plate 30a. Typical arenaceous conglomerate, near the polylithic boulder-breccia beds, MacLean Extension area. Green-grey lithic clasts are a variety of volcanic and siltstone lithologies and white, granular clast in lower right with unusual irregular embayed surface is granitoid. Sample: R.V. Kirkham (KQ-84-32B).

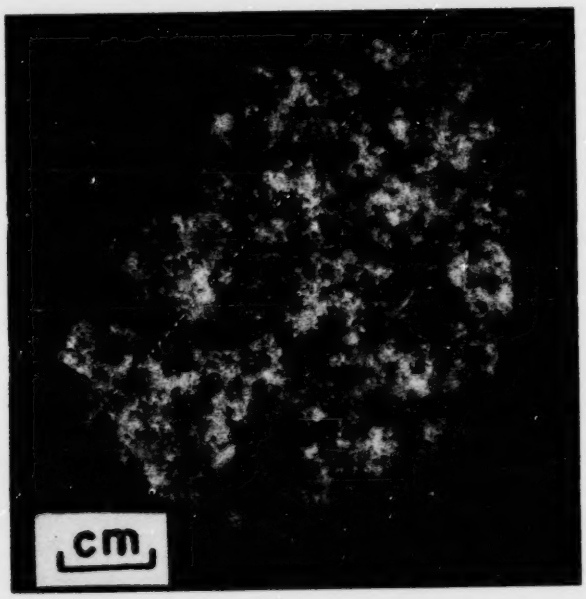

Plate 30b. Detail of porphyritic (quartz) granitoid clast showing irregular embayed surface. Origin of the surface is uncertain but normal sedimentary abrasion was an unlikely cause. Based on discussions with M.B. Lambert, "sand-blasting" and fragment impacts in a diatreme were plausible contributing factors.

Tectonic setting of the Buchans Group

Project 700059

R.V. Kirkham[1]

Kirkham, R.V., Tectonic setting of the Buchans Group; in Buchans Geology, Newfoundland, ed. R.V. Kirkham; Geological Survey of Canada, Paper 86-24, p. 23-34, Report 1, 1987.

Abstract

Until recently the Buchans-Roberts Arm volcanic belt, containing the Buchans and other volcanogenic sulphide deposits, was interpreted to be part of a Late Ordovician-Early Silurian volcanic arc. This paper summarizes new geochronological and geological data and uses them as a framework to reinterpret the tectonic setting of the Buchans deposits.

The Buchans Group consists of a late Arenig – early Llanvirn (Middle Ordovician) subaqueous, mainly bimodal suite of basalt and rhyolite. These volcanic rocks and succeeding Llandeilo and Caradocian (Middle to Upper Ordovician) black shale and chert probably formed during a period of widespread extension in central Newfoundland, while ophiolites were being obducted onto the continental shelf of North America in western Newfoundland. Easterly dipping subduction under the Topsail igneous terrane, and probably other volcanic belts in central Newfoundland, was terminated at this time. In Late Ordovician or earliest Silurian time remnants of ophiolites and arcs to the east of Buchans were underthrust to the west beneath the newly amalgamated Topsails igneous terrane and North American continent. This period of convergence was followed by extension and voluminous intrusive and extrusive bimodal igneous activity in the Topsails igneous terrane during the Early Silurian, including the emplacement of peralkaline granites and rhyolites.

The Buchans deposits, although possibly in an area that was previously a volcanic arc, formed in a subaqueous, volcanic environment during a period of foundering rather than during constructive calc-alkaline arc volcanism. This setting is analogous to that of the Kuroko district in Japan and other polymetallic, massive sulphide districts. Extensional subaqueous settings rather than constructive island arcs should be sought for rhyolite-associated, massive sulphide deposits.

Résumé

Jusqu'à très récemment, la zone volcanique de Buchans-Roberts Arm, qui contient les gisements de Buchans et d'autres gisements de sulfures d'origine volcanique, était considérée comme faisant partie d'un arc insulaire datant de l'Ordovicien récent-Silurien ancien. Ce rapport résume les nouvelles données géologiques et géochronologiques et présente une nouvelle interprétation du milieu tectonique des gisements de Buchans.

Le groupe de Buchans se compose d'un ensemble subaquatique, de nature surtout bimodale, de basalte et de rhyolite qui daterait de l'Arénigien récent ou du Llanvirnien ancien (Ordovicien ancien à moyen). Ces roches volcaniques et le schiste noir et le chert llanvirniens et caradociens (Ordovicien moyen à récent) qui les ont suivi se sont probablement accumulés au cours d'une période d'extension répandue dans la partie centrale de Terre-Neuve, pendant que des ophiolites étaient obductées sur le plateau continental nord-américain dans l'ouest de Terre-Neuve. Une zone de subduction à inclinaison est qui se trouvait sous le terrane igné de Topsails et probablement sous d'autres zones volcaniques dans la partie centrale de Terre-Neuve, aurait cessé son activité à cette époque. Au cours de l'Ordovicien récent ou au tout début du Silurien, des restes d'ophiolites et d'arcs volcaniques à l'est de Buchans ont subi un sous-charriage vers l'ouest-nord-ouest sous le terrane igné de Topsails nouvellement formé et le continent nord-américian.

[1]Geological Survey of Canada, 601 Booth St., Ottawa, K1A 0E8

Cette période de convergence a été suivie, au début du Silurien, par la mise en place de vastes quantités de matériaux ignés extrusifs et intrusifs, y compris des rhyolites et des granites peralcalins, dans le terrane igné de Topsails.

Les gisements de Buchans, qui pourraient se situer dans un ancien arc insulaire, se sont formés dans un milieu volcanique basaltique-rhyolitique bimodal, subaquatique, au cours d'une période de destruction, plutôt que d'accrétion d'arcs insulaires associés au volcanisme calco-alcalin. Ce milieu est analogue à celui du district de Kuroko au Japon et à ceux d'autres zones de sulfures massifs polymétalliques. Les sufures massifs associés aux rhyolites se retrouveraient donc dans des milieux d'extension subaquatique plutôt que dans des arcs volcaniques en accrétion.

INTRODUCTION

As geological studies progressed at Buchans during the 1982-84 period and new radiometric and fossil dates were acquired, existing tectonic models had to be modified in order to explain many aspects of the geology. This paper offers an interim tectonic model to account for geological features at Buchans. Such models tend to be ephemeral and can be expected to be superseded by more satisfactory ones as more geological, geochronological, geochemical, geophysical and paleomagnetic data are acquired.

Previous models supported the concept that Buchans deposits formed in a Late Ordovician-Early Silurian[1] island-arc environment post-dating Caradocian and Ashgillian (Late Ordovician) black shale and greywacke sequences that overlie older island-arc sequences of the Central Volcanic Belt of Newfoundland (e.g. Dean, 1978; Kean *et al.*, 1981; Strong, 1982; Dean and Meyer, 1983; Swinden and Thorpe, 1984). Conodont (Nowlan and Thurlow, 1984, 1987) and radiometric ages (Stewart, 1986; Whalen and Currie, 1986; Whalen *et al.*, in press; Dunning *et al.*, 1986, in press) indicate that the Buchans Group is Middle Ordovician and not Ordovician-Silurian as previously supposed. These ages are only slightly different from those of the 'older arc sequences' (Dunning *et al.*, 1986, in press), indicating that none of the presumed island-arc sequences with massive sulphide deposits is as young as Silurian.

In general, an island-arc setting has been assigned to submarine volcanic sequences that contain rhyolite-associated, polymetallic, massive sulphide deposits in central Newfoundland. Such designations can be questioned since available evidence does not support constructive arc volcanic settings as sites of formation of polymetallic, massive sulphide deposits (e.g. Sillitoe, 1982; Ohmoto and Skinner, 1983). The occurrence of the Miocene Kuroko deposits in the Green Tuff region of Japan has perhaps had too great an influence in the assignment of rhyolite-associated, volcanogenic, massive sulphide deposits to island-arc settings. Recent evidence indicates that the Japanese arc system was being dismembered and foundering at the time of formation of Kuroko deposits and not undergoing constructive arc volcanism (eg. Ohmoto, 1983; Guber and Merrill, 1983; Lallemand and Jolivet, 1986; Kimura and Tamaki, 1986). The Hokuroku district was probably about 3500 m below sea level at the time of ore formation (Guber and Merrill, 1983) and was not, at that time, in a constructive island-arc setting. No convincing modern example exists of volcanogenic massive sulphide deposits forming during constructive, calc-alkaline, island-arc volcanism. Under these circumstances, other evidence, such as lithochemical information, should be sought for identification of the tectonic settings and the nature of the volcanic environments at the time of ore formation. In areas, such as central Newfoundland, the tectonic settings of submarine volcanic sequences is undoubtedly more complex than a series of simple island arcs as is commonly postulated.

REGIONAL SETTING OF THE BUCHANS GROUP

The Buchans Group lies on the western edge of the mixed volcanic-sedimentary terrane of central Newfoundland (Fig. 1). Whalen and Currie (1987) include it in the Topsails igneous terrane, based on general similarities to the Glover Formation to the west and intrusions in the Topsail igneous terrane which conceivably could have been the source of granitoid clasts in the Buchans Group. The thrust fault between the Hungry Mountain Complex and Buchans Group, a major zone of dislocation (Thurlow, 1981a; Thurlow and Swanson, 1987; Calon and Green, 1987), is also a logical boundary between the dominantly granitic, crystalline terrane of the Topsails to the west and the dominantly volcanic and sedimentary terranes of central Newfoundland to the east. Nevertheless, contact relations of the Buchans Group with all surrounding sequences are poorly known and several possibilities exist. For this paper the eastern boundary of the Topsails igneous terrane is tentatively considered to be the Hungry Mountain Thrust.

To the south, the Buchans Group is either in fault contact with, or sits conformably on, the Skidder Basalt. Previously the Skidder Basalt was considered to be part of the Buchans Group (e.g. Thurlow and Swanson, 1981). However, studies by Pickett and Barbour (1984) and Pickett (1987) indicate that the Skidder Basalt has ophiolitic affinities and, therefore,

[1]The boundaries between Ordovician and Silurian epochs are after Barnes et al. (1981) and the time chart developed for Canadian DNAG volumes. The boundary between the Early and Middle Ordovician is in the upper part of the Arenig; the boundary between the Middle and Late Ordovician is in the upper part of the Caradocian, and the boundary between the Early and Late Silurian is at the boundary between the Llandovery and Wenlock. These boundaries differ from those presented by Palmer (1983).

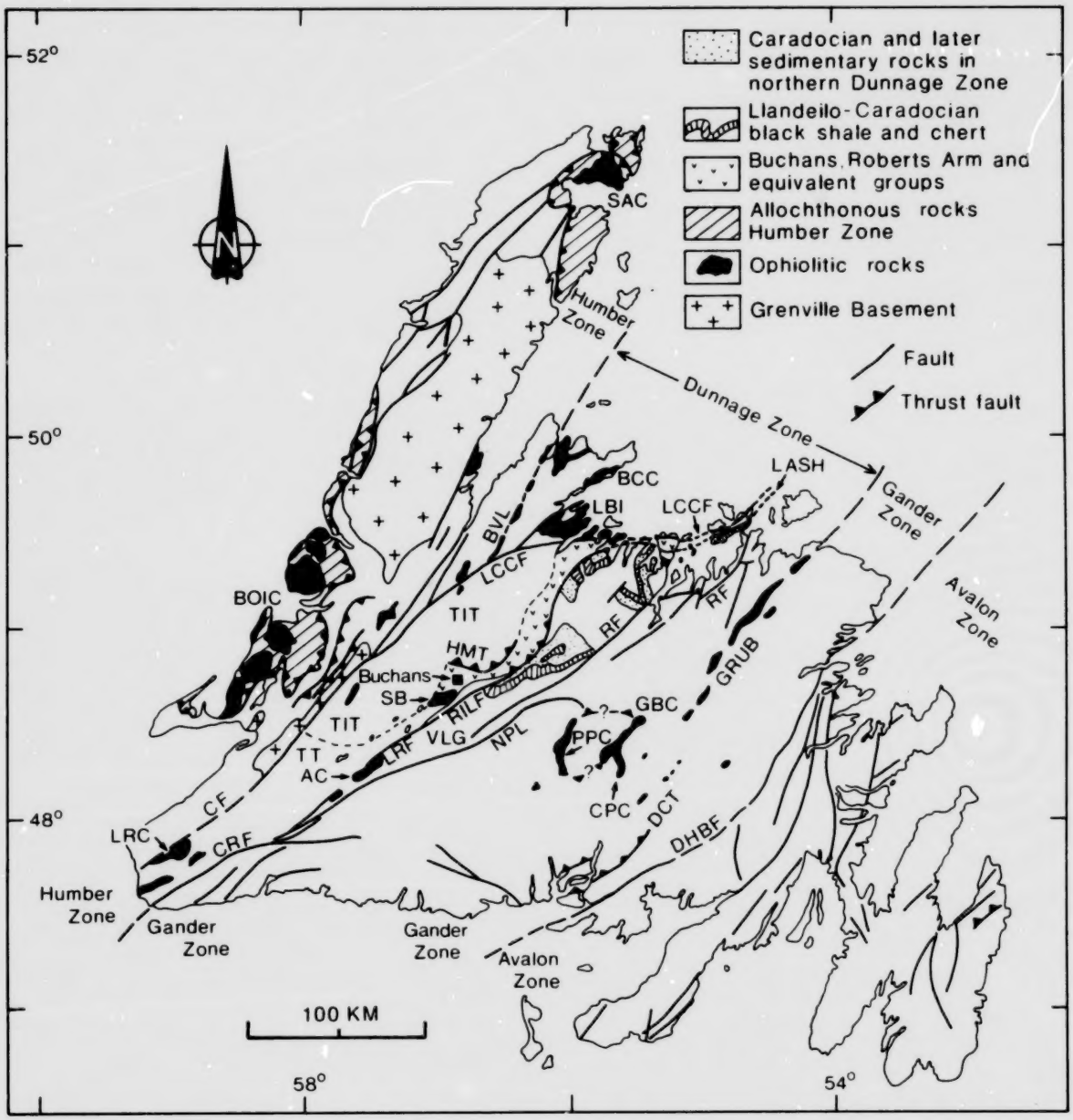

Figure 1. Map of Newfoundland showing selected geological and tectonic features. Data were adapted from Williams (1978, 1982), Kean *et al.* (1981), Hibbard (1983), Colman-Sadd and Swinden (1984), Dunning and Krogh (1985) and Arnott *et al.* (1985).

AC = Annieopsquotch Complex,
BCC = Betts Cove Complex,
BOIC = Bay of Islands Complex,
BVL = Bay Verte Lineament,
CF = Cabot Fault,
CRF = Cape Ray Fault,
CPC = Coy Pond Complex,
DCT = Day Cove Thrust,
DHBF = Dover-Hermitage Bay Fault,
GRUB = Gander River Ultramafic Belt,
GBC = Great Bend Complex,
HMT = Hungry Mountain Thrust,
LASH = Lukes Arm- Sops Head Fault,
LCCF = Lobster Cove-Chanceport Fault,
LRC = Long Range Complex,
LRF = Lloyds River Fault,
NPL = Noel Paul's Line,
PPC = Pipestone Pond Complex,
RF = Reach Fault,
RILF = Red Indian Lake Fault,
SAC = St. Anthony Complex,
SB = Skidder Basalt,
TIT = Topsails igneous terrane,
TT = Tonalite terrane and
VLG = Victoria Lake Group.

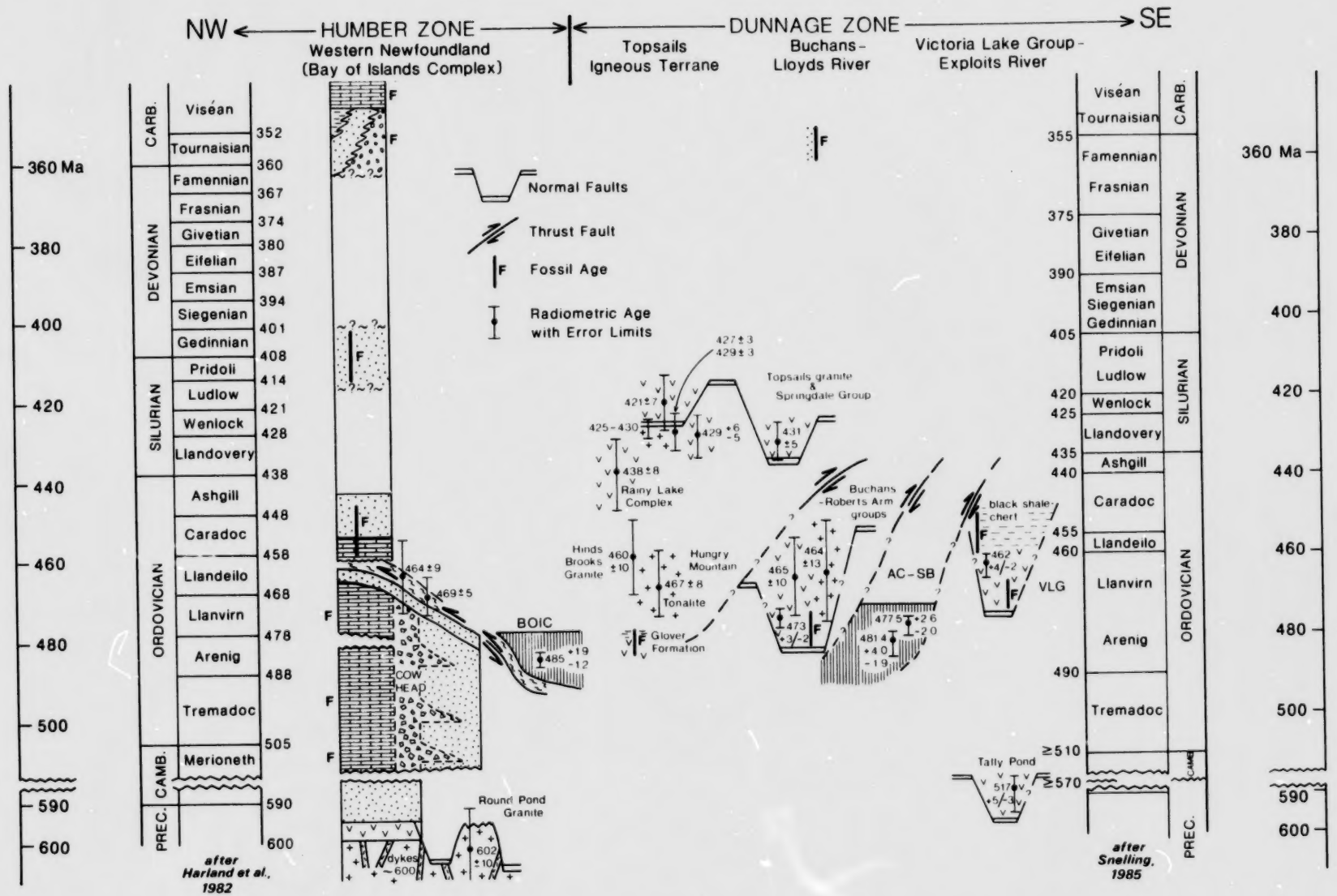

Figure 2. Schematic cross-section from western to central Newfoundland through the Buchans area illustrating stratigraphic, geochronological and tectonic information. Time scales are after Harland *et al.* (1982) and Snelling (1985). See Figure 1 for abbreviations.

should not be included in the Buchans Group. Nevertheless, the contact between the two groups has not been observed.

To the east of Buchans, the Buchans Group structurally overlies the Lower to Middle Ordovician Victoria Lake Group in the south and Middle to Upper Ordovician black shale and greywacke in the north, along a presumed high-angle reverse fault (Kean *et al.*, 1981; Thurlow, 1984; Kean and Evans, 1986). This fault brings the Buchans Group in contact with progressively younger rocks to the north (Kean *et al.*, 1981). Farther to the southwest, the Skidder Basalt is possibly in contact with the Victoria Lake Group along the same presumed high-angle reverse fault suggesting that the fault is probably a major regional structure (Fig. 1).

GEOCHRONOLOGY OF EVENTS

Until recently the geochronology of events in central Newfoundland were not well known. However, with continued mapping and more precise conodont and U-Pb zircon dates some rock units and events have been dated more accurately. Geochronologic work is continuing and will undoubtedly lead to a much refined understanding of the geological history of the area. Figure 2 illustrates some of the more important geological events in a schematic cross-section from the obducted ophiolites in the Bay of Islands Complex in the west, across the Topsails igneous terrane, through the Buchans area and Exploits valley, to the Victoria Lake Group in the east. Two absolute time scales are given for reference, although correlation of absolute time and fossil zones for the Ordovician are poorly known.

In the west, along the leading edge of the North American continent, a stable carbonate platform developed from Lower Cambrian to Llandeilo on an Atlantic-type, passive continental margin (Fig. 2; Stevens, 1970; Williams, 1971; Casey and Kidd, 1981; James and Stevens, 1982; Casey and Dewey, 1984). Slope deposits including Cow Head breccia and Middle Arm Point Formation formed to the east of the carbonate platform (e.g. Casey and Dewey, 1984; James and Stevens, 1986).

Dunning and Krogh (1985) have dated a sample of trondhjemite from the Bay of Islands Complex at 485.7 + 1.9/ -1.2 Ma by the U-Pb zircon method. This date is interpreted to be the age of formation of the Bay of Islands Complex. ^{40}Ar-^{39}Ar dates on amphibolites from the metamorphic aureole under the ophiolite at North Arm Mountain average 469 ± 5 Ma (recalculated using new constants) reported by Dallmeyer and Williams (1975) and Dallmeyer (1983, personal communication in Dunning and Krogh, 1985) and 464 ± 9 Ma for the metamorphic aureole at North Arm Mountain and Table Mountain (after Archibald and Farrar, 1976; recalculated by Dunning and Krogh, 1985) are taken to indicate the time of emplacement of the Bay of Islands Complex. Therefore, about 17 to 22 Ma lapsed between the formation of the Bay of Islands Complex and its emplacement onto the leading edge of North America.

In the southern part of the Humber Zone on the Port au Port Peninsula the allochthonous rocks of the Humber Arm Supergroup are overlain unconformably by marine Middle Ordovician rocks of the Long Point Group (Fig. 2; Rogers, 1965; Bergstrom *et al.*, 1974; Schillereff and Williams, 1979). These rocks stratigraphically date the emplacement of the allochthons in western Newfoundland as Middle Ordovician.

Recently acquired dates indicate that an extensive belt of tonalite, granodiorite and granite was emplaced during the Middle Ordovician to the west of the Buchans-Roberts Arm belt. In the Topsails igneous terrane, sedimentary rocks interlayered with volcanic rocks of the Glover Formation have yielded sparse conodont fauna indicating a mid to late Arenig age (Nowlan and Thurlow, 1987). Whalen and Currie (1987) and Whalen *et al.* (in press) report U-Pb zircon dates of 467 ± 8 Ma for tonalite in the Hungry Mountain Complex and 460 ± 10 Ma for the possibly closely related but slightly younger massive Hinds Brook granite. Dallmeyer and Hibbard (1984) reported a very similar pattern of U-Pb zircon emplacement dates for Burlington Granodiorite (about 460 to 465 Ma) and Dumamagon Granite (about 440-460 Ma) in the Baie Verte Peninsula area to the northeast of the Topsails igneous terrane. Dunning and Chorlton (1985) and Dunning (personal communication, 1986) reported that a K-Ar hornblende age of 455 ± 14 Ma on foliated tonalite along the Burgeo road in the Tonalite terrane to the south of the Topsails igneous terrane (Fig. 1) has also been confirmed by U-Pb zircon dates to be the approximate probable age of emplacement of similar foliated tonalitic rocks in that area.

The Early Silurian was marked by extensive felsic and mafic igneous activity in the Topsails igneous terrane and adjacent areas, mainly to the west of the Buchans-Roberts Arm belt. Whalen (1986) and Whalen *et al.* (in press) report a U-Pb zircon age of 438 ± 8 Ma for the Rainy Lake complex in the southwestern part of the Topsails igneous terrane, making it the oldest dated member of the Topsails igneous suite. They have also obtained U-Pb zircon dates of 429 ± Ma on Topsails peralkaline amphibole granite, 427 ± 3 Ma on high-level quartz-K-feldspar porphyry and 429 ± 4 Ma on Springdale Group rhyolite. These dates are essentially identical with the U-Pb zircon dates on subaerial rhyolites of 429 ± 6/-5 Ma in the Springdale Group to the north (Chandler *et al.*, in preparation) and 431 ± 5 Ma near the Annieopsquotch Complex to southeast (Chandler and Dunning, 1983). These dates indicate that Early Silurian felsic igneous activity extended well to the northeast and southwest of Buchans. Bell and Blenkinsop (1981) reported a compatible Rb-Sr isochron date of 421 ± 7 Ma for Topsails peralkaline granite.

Thurlow (1981a) demonstrated that Topsails granites cut the Hungry Mountain Thrust, thereby bracketting the period of thrusting between about 465 to 475 Ma, the age of the Buchans Group, and 425 to 430 Ma, the age of emplacement of Topsails granites, that is, at some time between the Middle Ordovician and middle Silurian.

In the Lloyds and Exploits River areas of central Newfoundland trondhjemite bodies of the Annieopsquotch Complex to the southwest of Buchans have been dated as $481.4 + 4.0/-1.9$ and $477.5 + 2.6/-2.0$ Ma (Dunning and Krogh, 1985). Conodonts from near the top of the Victoria

Lake Group indicate an age of late Llanvirn to early Llandeilo (Kean and Jayasinghe, 1982). Preliminary U-Pb zircon dates for Victoria Lake Group and Tally Pond rhyolites are $462 + 4/-2$ and $517 + 5/-3$ Ma, respectively (Dunning *et al.*, 1986 and oral communication, 1986). The considerably older date for the Tally Pond rhyolite indicates that it should probably be separated from the Victoria Lake Group. Conodonts from limestone clasts in the Buchans Group indicate an age of latest Arenig-early Llanvirn (Nowlan and Thurlow, 1984, 1987), slightly older than those in the Victoria Lake Group. These clasts are interpreted to be coeval with the Buchans Group. U-Pb zircon dates for the Buchans Group rhyolite are 465 ± 10 Ma (Stewart, 1987) and $473 + 3/-2$ Ma, Dunning *et al.* (in press). A granitoid clast in a sulphide-bearing debris flow at Buchans yielded an imprecise date of 464 ± 40 Ma by the U-Pb zircon method (Stewart, 1987), supporting the concept that the granitoid clasts in the debris flows were derived from a subvolcanic intrusion(s) related to Buchans Group rhyolites. These U-Pb zircon dates are compatible with the conodont fossil ages for the Buchans Group. A rhyolite sample from the Roberts Arm Group to the northeast yielded a U-Pb zircon age of 473 ± 2 Ma supporting the long term correlation of the Buchans and Roberts Arm groups (Dunning *et al.*, in press). This age suggests that an earlier reported Rb-Sr date of 464 ± 13 Ma on a subvolcanic granitic intrusion is reasonable but does not support the 447 ± 7 Ma date on Roberts Arm felsite (Bostock *et al.*, 1979).

Black shale, chert and greywacke in the Exploits valley to the northeast of Buchans contain graptolites indicating a Llandeilo-Caradocian age (e.g. Dean, 1978; Bergstrom *et al.*, 1974; Dean and Meyer, 1983; Arnott *et al.*, 1985). This age supports the concept that pelagic and turbiditic sedimentation followed submarine volcanism in this part of Newfoundland. This period of sedimentation pre-dated final closure of the marine basin and uplift of Ordovician volcanic and sedimentary terranes of central Newfoundland prior to subaerial deposition of Lower Silurian redbeds and volcanic rocks. Closure of this marine basin could have been accomplished by compressive movements on the Hungry Mountain Thrust, the presumed high-angle reverse fault between the Buchans and Victoria Lake groups and related faults (Fig. 1). Upper Ordovician marine rocks to the east of the Topsails igneous terrane indicate that this part of the Iapetus Ocean remained open after closure of the marine basin to the west along the Baie Verte-Brompton Line.

Subaerial and some marine Silurian and Carboniferous clastic sedimentary and volcanic rocks, including redbeds, occur in several small sedimentary basins from western to eastern Newfoundland (e.g. Williams, 1978; Hibbard, 1983). In most places these clastic sediments were deposited unconformably on older sequences. Currie *et al.* (1986) pointed out, that since widespread Upper Ordovician to Lower Silurian (430 ± 15 Ma) intrusive and extrusive rocks cut and overlie numerous terrane boundaries, then the terranes of central Newfoundland were probably largely amalgamated by Early Silurian time. Spores from fluviatile rocks near Red Indian Lake southwest of Buchans indicate an Early Carboniferous age (Barss, 1974). Paleomagnetic studies of Carboniferous rocks by Irving and Strong (1984a, b) indicate that no large (greater than 100 to 200 km) transcurrent displacements occurred in central Newfoundland after the Carboniferous.

TENTATIVE TECTONIC MODEL FOR THE BUCHANS AREA

This paper attempts to integrate available geochronological and geological data into a coherent tectonic model. The general model of Casey and Dewey (1984) and Casey *et al.* (1985) for the obduction of ophiolites in western Newfoundland is extended to the east into the Buchans area. Such an extension is based on the precarious assumption that, since the Middle Ordovician, no major strike-slip displacements have occurred between the Bay of Islands Complex in the west and Buchans area in the east. Irving and Strong (1984a, b) indicate that no major lateral displacements have occurred since the Carboniferous but these data do not negate the possibility that such displacements occurred between the Middle Ordovician and Carboniferous. Strike-slip faults with modest displacements (10 to perhaps as much as 100 km?) and possibly even larger displacements (greater than 100 km) should not affect the model greatly, provided that the Topsails igneous terrane and at least some of the volcanic belts of central Newfoundland were part of the arc(s) above the easterly dipping subduction zone(s) responsible for obduction of ophiolites in western Newfoundland.

Rifting in western Newfoundland, perhaps about 600 Ma, as indicated by a U-Pb zircon date of 602 ± 10 Ma on the Round Pond granite near Deer Lake (Williams *et al.*, 1985) and an ^{40}Ar-^{39}Ar age of about 600 Ma on rift-related mafic dykes and lavas in the Long Range of the Humber Zone (Stukas and Reynolds, 1974; Strong, 1974), initiated the opening of this part of the Iapetus Ocean during the Late Proterozoic. Along the eastern continental margin of North America a carbonate platform developed from Early Cambrian to Llandeilo in western Newfoundland along a stable Atlantic-type margin (e.g. Stevens, 1970; Williams, 1971; Casey and Dewey, 1984; James and Stevens, 1986). Slope deposits, including Cow Head breccia and interlayered greywacke, formed in deeper water to the east of the platform. How wide this ocean basin was is unknown but it was probably large considering the amount oceanic crust that was probably consumed by Ordovician subduction and the time since initial rift-opening of the basin (Casey and Dewey, 1984; Casey *et al.*, 1985).

Critical to the model for obduction of ophiolites in western Newfoundland is that during much of the Early and Middle Ordovician an easterly dipping subduction zone, probably overlain by an island arc, existed somewhere to the east of North America (Casey and Dewey, 1984; Fig. 3). A segment of oceanic crust, the Bay of Islands Complex, was trapped in the arc-trench gap to the west of the arc (e.g. Malpas and Stevens, 1977; Casey and Dewey, 1984). This model implies that during the Early and Middle Ordovician a volcanic arc(s) existed in central Newfoundland perhaps in the Topsail igneous terrane and in other volcanic belts of central Newfoundland. The Middle Ordovician tonalites and

related granitoid rocks are evidence that the Topsails igneous terrane and areas to the northeast and southwest could have been part of the foundation of such an arc. In the Middle Ordovician, about the time of formation of the Buchans Group, the leading edge of North America encountered this easterly dipping subduction zone and the trapped oceanic crust in the forearc region was obducted onto the continental shelf of North America. By Llandeilo time obduction was complete, presumably terminating the subduction and associated arc volcanism (in part in the Topsails igneous terrane?) as the arc was amalgamated with North America (Fig. 3). Other workers, such as Searle and Stevens (1984), postulate an arc above an easterly dipping subduction zone to the east of North America but view ophiolite emplacement as a product of back-thrusting to the west of oceanic crust of the down-going slab over the continental shelf deposits of North America.

The Buchans Group, consisting dominantly of a bimodal suite of basalt and rhyolite (Thurlow, 1981b; Thurlow and Swanson, 1987), is postulated to have formed during a period of extension after calc-alkaline constructive arc volcanism had ceased. The entire Buchans Group was deposited in a subaqueous environment indicating that at the time of formation of the orebodies the area was below sea level (J.G. Thurlow, personal communication, 1982). If the Kuroko deposits in Japan can be used as an example, an arc in the Buchans area might have been extensively dismembered and rifted during this interval of bimodal volcanism. The dominantly bimodal character and subaqueous environment deposition of the Buchans Group, rather than any major documented block faults of this age, are the lines of evidence to support extension at this time in the Buchans area. Analogies with areas of Cenozoic bimodal volcanism suggest that this is not an unreasonable assumption and that bimodal, rift-related volcanism can closely follow subduction-related arc volcanism (e.g. Lipman, 1980). At the time of formation of the Buchans Group, the underlying oceanic slab could have broken away, falling vertically putting the area under tension and thus permitting the rise of large volumes of mafic magma into the lower crust (e.g. Fig. 3, Llanvirn). Some of this mafic magma rose to surface and was extruded as basalt but it also could have caused extensive melting of the lower crust to produce the Buchans Group rhyolites. Caradocian black shale, chert and greywacke in the Exploits River valley to the northeast of Buchans could be evidence of continued widespread extension into the Upper Ordovician in north-central Newfoundland.

The Buchans Group, with its abundant rhyolite, probably did not directly overlie the Skidder Basalt oceanic crust. The large volume of rhyolite at Buchans suggests a more sialic foundation. Therefore, as no felsic rocks underlying the Buchans Group are known, the nature and extent of the foundation are unknown. The easterly to southeasterly directed thrusts in the Buchans area suggest that the Buchans Group possibly formed to the west of its present position.

The foundered Middle to Late Ordovician marine basin(s) in central Newfoundland might have been an intra-arc to back-arc basin(s) that attained absyssal depths. However, so little evidence exists that it also might have been a much larger basin with extensive oceanic crust and a degree of complexity comparable to parts of the southwest Pacific. The widespread distribution of Llandeilo-Caradocian pelagic black shale and chert, nevertheless, suggests that at this time significant parts of what is now north-central Newfoundland was starved of coarse clastic sediments and was not in close proximity to sediment source areas.

The foundering of volcanic terranes in central Newfoundland was followed closely by a period of compression resulting in thrusting of the Hungry Mountain Complex over the Buchans Group and possibly Buchans Group in turn over the Victoria Lake Group probably during the Late Ordovician. These easterly directed thrusts could reflect the transport of the newly amalgamated North America–Topsails igneous terrane over oceanic and arc terranes, the last relics of the Iapetus Ocean to the east. Possibly the earliest stages of this overthrusting could have been accompanied by westerly-directed subduction under a Topsails igneous terrane arc but extensive subduction-related igneous rocks of this age have not been recognized. However, in the Springdale Group to the north, Coyle and Strong (1986b) have recognized a mixed assemblage of calc-alkaline rocks with discrete silica gaps ranging from basalt to high-silica rhyolite but including andesite and other rocks which might have been products of subduction. Whalen (1986) suggested recently that the oldest dated member of the Topsails igneous suite, the Rainy Lake complex (438 ± 8 Ma), could also have arc affinities. During this period of convergence, the Topsails igneous terrane probably underwent major uplift with significant erosion of the Middle Ordovician volcanic arc carapace (Fig. 3). This erosion and closure of the marine basin to the east in the Late Ordovician were probably responsible for the large amounts of coarse clastic basin fill that occurs in the northern Dunnage Zone of central Newfoundland (e.g. Dean, 1978; Bergstrom *et al.*, 1974; Arnott *et al.*, 1985).

Recently, several authors have suggested that the Dunnage Zone, at least in part, is allochthonous and has been thrust to the east over the Gander Zone (e.g. Currie *et al.*, 1980; Karlstrom *et al.*, 1982; Wonderley and Neuman, 1984; Colman-Sadd and Swinden, 1984; Elliott and Williams, 1986). The emplacement of the thrust sheets is not well documented but Colman-Sadd and Swinden (1984) suggested that final emplacement probably post-dated the middle Silurian, the age of the youngest parts of the underlying Botwood Group. If this is the case then this deformation might have been related to the final closure of Iapetus bringing North America and the Dunnage Zone in contact with the Gander and Avalon zones to the east (Fig. 1). As depicted in Figure 3 (Llandovery-Wenlock), some of the allochthonous ophiolite fragments in central Newfoundland, such as the Pipestone and Coy Pond complexes, could have been derived from one or more sutures to the west.

At the time of emplacement of Topsails intrusive rocks and Springdale volcanic rocks to the north in the Early Silurian (about 425-430 Ma), the Topsails igneous terrane

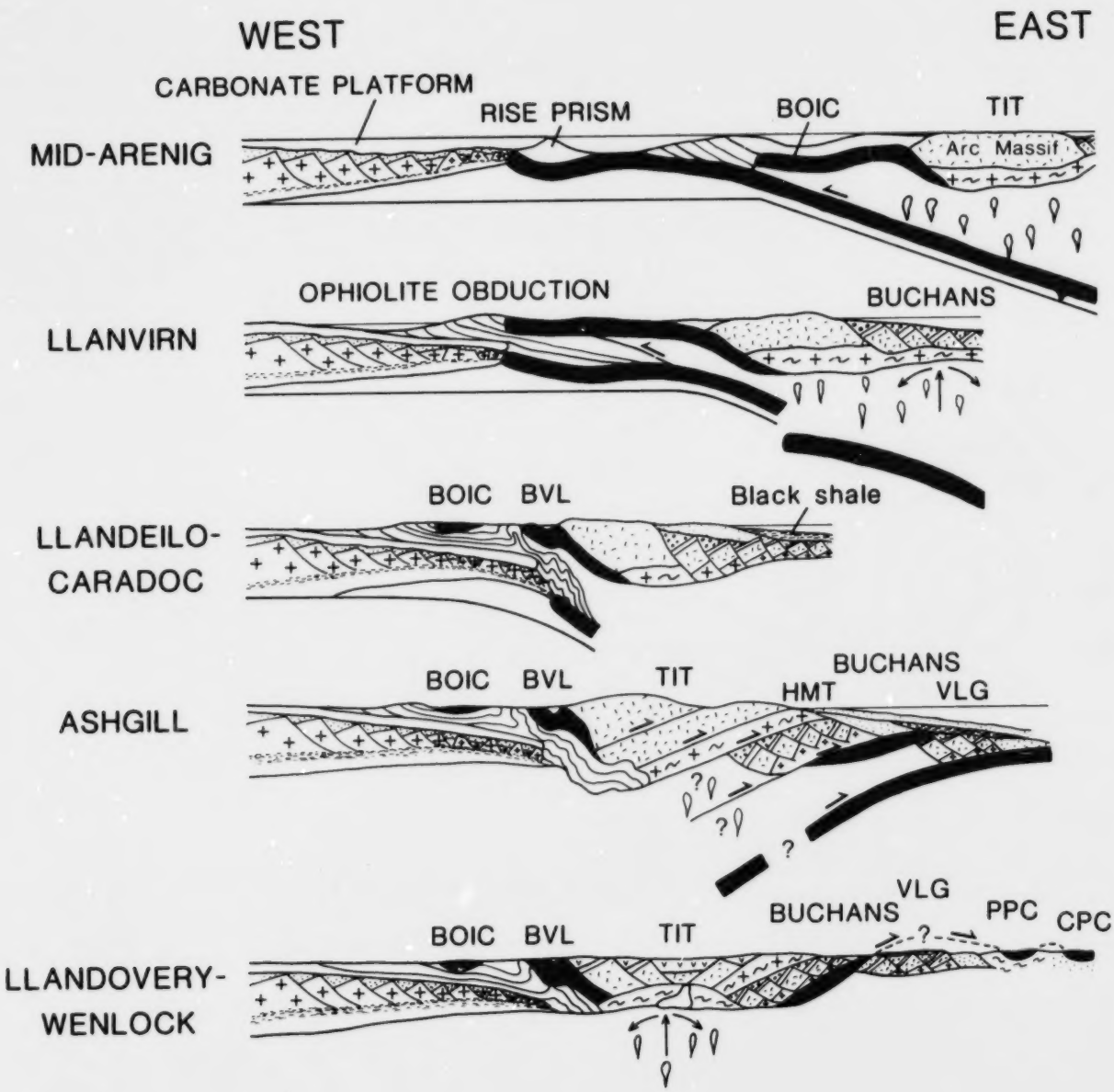

Figure 3. Schematic plate tectonic reconstructions for the Buchans area from Lower Ordovician to Lower Silurian. The western parts of the diagrams are largely after Casey and Dewey (1984) and Casey *et al.* (1985). See Figure 1 for abbreviations.

was characterized by extensive A-type magmas and bimodal igneous activity (Whalen and Currie, 1983; Coyle *et al.*, 1985; Coyle and Strong, 1986a). The A-type magmas indicate extensive reworking of continental crust which is consistent with the view that the Topsails igneous terrane was ensialic and the site of repeated magmatic activity during the Ordovician and Early Silurian. Judging by more modern counterparts, such as the Basin and Range Province in the western United States, the Topsails bimodal igneous activity suggests that the area, once again, was under extension during the Early Silurian (Fig. 3).

Compression in the Early to Middle Ordovician in the Humber Zone in western Newfoundland followed by extension in the Topsails igneous terrane and Buchans area to the

east in the Dunnage Zone in the Middle and early Late Ordovician, then compression in the Late Ordovician and Early Silurian and finally extension again in the late Early Silurian indicate rapidly alternating compressional and extensional tectonic events over relatively short distances. Such patterns indicate that generalization of tectonic regimes over large areas and long periods of time in the Appalachians should be made with caution.

ACKNOWLEDGMENTS

W.H. Poole, J.G. Thurlow and H.S. Swinden reviewed the paper and made several useful comments.

REFERENCES

Archibald, D.A. and Farrar, E.
1976: K-Ar ages of amphibolites from the Bay of Islands ophiolite and the Little Port Complex, western Newfoundland, and their geological implications; Canadian Journal of Earth Sciences, v. 13, p. 520-529.

Arnott, R.J., McKerrow, W.S., and Cocks, L.R.M.
1985: The tectonics and depositional history of the Ordovician and Silurian rocks of Notre Dame Bay, Newfoundland; Canadian Journal of Earth Sciences, v. 22, p. 607-618.

Barnes, C.R., Norford, B.S. and Skevington, D.
1981: The Ordovician System in Canada-Correlation chart and explanatory text; International Union of Geological Sciences, Publication No. 8, 27 p.

Barss, M.S.
1974: Palynological zonation of the Carboniferous and Permian rocks of the Atlantic Provinces; in Report of Activities, Part B, November 1973 to March 1974; Geological Survey of Canada, Paper 74-1, Part B, p. 135-136.

Bell, K. and Blenkinsop, J.
1981: A geochronologic study of the Buchans area, Newfoundland; in The Buchans Orebodies: Fifty Years of Geology and Mining, ed. E.A. Swanson, D.F. Strong and J.G. Thurlow; Geological Association of Canada, Special Paper 22, p. 91-111.

Bergstrom, S.M., Riva, J. and Kay, M.
1974: Significance of conodonts, graptolites, and shelly faunas from the Ordovician of western and north-central newfoundland; Canadian Journal of Earth Sciences, v. 11, p. 1625-1660.

Bostock, H.H., Currie, K.L., and Wanless, R.K.
1979: The age of the Roberts Arm Group, north-central Newfoundland; Canadian Journal of Earth Sciences, v. 16, p. 599-606.

Calon, T. and Green, K.
1987: Preliminary results of detailed structural analysis at Buchans; in Buchans Geology, Newfoundland, ed. R.V. Kirkham; Geological Survey of Canada, Paper 86-24, Report 17.

Calon, T. and Green, K.
1987: Preliminary results of detailed structural analysis at Buchans; in Buchans Geology, Newfoundland, ed. R.V. Kirkham; Geological Survey of Canada, Paper 86-24, Report 17.

Casey, J.F. and Dewey, J.F.
1984: Initiation of subduction zones along transform and accreting plate boundaries, triple-junction evolution, and forearc spreading centres – implications for ophiolitic geology and obduction; in Ophiolites and Oceanic Lithosphere, ed. I. Gass, S.J. Lippard and A.W. Shelton; Blackwell, London, p. 269-290.

Casey, J.F. and Kidd, W.S.F.
1981: A parallochthonous group of sedimentary rocks unconformably overlying the Bay of Islands ophiolite complex, North Arm Mountain, Newfoundland; Canadian Journal of Earth Sciences, v. 18, p. 1035-1050.

Casey, J.F., Elthon, D.L., Siroky, F.X., Karson, J.A., and Sullivan, J.
1985: Geochemical and geological evidence bearing on the origin of the Bay of Islands and Coastal Complex ophiolites of western Newfoundland; Tectonophysics, v. 116, p. 1-40.

Chandler, F.W. and Dunning, G.R.
1983: Fourfold significance of an early Silurian U-Pb zircon age from rhyolite in redbeds, southwest Newfoundland; in Current Research, Part B, Geological Survey of Canada, Paper 83-1B, p. 419-421.

Chandler, F.W., Sullivan, R.W., and Currie, K.L.
– The age of the Springdale Group, western Newfoundland and correlative rocks – evidence for a Llandovery overlap assemblage in the Canadian Appalachians. (in preparation)

Colman-Sadd, S.P. and Swinden, H.S.
1984: A tectonic window in central Newfoundland? Geological evidence that the Appalachian Dunnage Zone may be allochthonous; Canadian Journal of Earth Sciences, v. 21, p. 1349-1367.

Coyle, M. and Strong, D.F.
1986a: Geology of the southern and northern margins of the Springdale caldera, Newfoundland; in Current Research, Part A, Geological Survey of Canada, Paper 86-1A, p. 499-506.
1986b: Nested calderas in the Silurian of west central, Newfoundland (abstract); in Geological Association of Canada, Mineralogical Association of Canada, Canadian Geophysical Union, Joint Annual Meeting, Program with Abstracts, v. 11, p. 59-60.

Coyle, M., Strong, D.F., Gibbons, D., and Lambert, E.
1985: Geology of the Springdale Group, central Newfoundland; in Current Research, Part A, Geological Survey of Canada, Paper 85-1A, p. 157-163.

Currie, K.L., Chandler, F.W. and Whalen, J.B.
1986: A Silurian event in Atlantic Canada and its implications for Appalachian tectonics (abstract); Geological Association of Canada, Mineralogical Association of Canada, Canadian Geophysical Union, Joint Annual Meeting, Program with Abstracts, v. 11, p. 61.

Currie, K.L., Pickerill, R.K., and Pajari, G.E.
1980: An early Paleozoic plate tectonic model of Newfoundland; Earth and Planetary Science Letters, v. 48, p. 8-14.

Dallmeyer, R.D. and Hibbard, J.
1984: Geochronology of the Baie Verte Peninsula, Newfoundland: implications for the tectonc evolution of the Humber and Dunnage zones of the Appalachian Orogen; Journal of Geology, v. 92, p. 489-512.

Dallmeyer, R.D. and Williams, H.
1975: $^{40}Ar/^{39}Ar$ ages for the Bay of Islands metamorphic aureole: their bearing on the timing of Ordovician ophiolite obduction; Canadian Journal of Earth Sciences, v. 12, p. 1685-1690.

Dean, P.L.
1978: The volcanic stratigraphy and metallogeny of Notre Dame Bay, Newfoundland; Memorial University of Newfoundland, Geology Report 7, 204 p.

Dean, P.L. and Meyer, J.R.
1983: Lithochemistry of Middle Ordovician chert and shale: Newfoundland Department of Mines and Energy, Mineral Development Division, Open File 1317, 24 p.

Dunning, G.R. and Chorlton, L.B.
1985: The Annieopsquotch ophiolite belt of southwest Newfoundland: geology and tectonic significance: Geological Society of America, Bulletin, v. 96, p. 1466-1476.

Dunning, G.R. and Krogh, T.E.
1985: Geochronology of ophiolites of the Newfoundland Appalachians; Canadian Journal of Earth Sciences, v. 22, p. 1659-1670.

Dunning, G.R., Krogh, T.E., Kean, B.F., O'Brien, S., and Swinden, H.S.
1986: U/Pb zircon ages of volcanic groups from the central mobile belt, Newfoundland (abstract); in Geological Association of Canada – Mineralogical Association of Canada – Canadian Geophysical Union, Joint Annual Meeting, Program with Abstracts, v. 11, p. 66.

Dunning, G.R., Kean, B.F., Thurlow, J.G. and Swinden, H.S.
– Geochronology of the Buchans, Roberts Arm and Victoria Lake groups and Mansfield Cove Complex; Canadian Journal of Earth Sciences. (in press)

Elliott, C.G. and Williams, P.F.
1986: The tectonics and depositional history of the Ordovician and Silurian rocks of Notre Dame Bay, Newfoundland: discussion; Canadian Journal of Earth Sciences, v. 23, p. 586-588.

Guber, A.L. and Merrill III, S.
1983: Paleobathymetric significance of the foraminifera from the Hokuroku district; in The Kuroko and Related Volcanogenic Massive Sulfide Deposits, ed. H. Ohmoto and B.J. Skinner; Economic Geology, Monograph 5, p. 55-70.

Harland, W.B., Cox, A.V., Llewellyn, P.G., Pickton, G.A.G., Smith, A.G., and Walters, R.
1982: A geologic time scale; Cambridge University Press, 109 p.

Hibbard, J.
1983: Geology of Newfoundland (Preliminary version); Newfoundland Department of Mines and Energy, Mineral Development Division, Map 83-106.

Irving, E. and Strong, D.F.
1984a: Palaeomagnetism of the Early Carboniferous Deer Lake Group, western Newfoundland: no evidence for mid-Carboniferous displacement of "Acadia"; Earth and Planetary Science Letters, v. 69, p. 379-390.
1984b: Evidence against large-scale Carboniferous strike-slip faulting in the Appalachian-Caledonian orogen; Nature, v. 310, p. 762-764.

James, N.P. and Stevens, R.K.
1982: Anatomy and evolution of a Lower Paleozoic continental margin; International Association of Sedimentologists, Guidebook, No. 2B, 75 p.
1986: Stratigraphy and correlation of the Cambro-Ordovician Cow Head Group, western Newfoundland; Geological Survey of Canada, Bulletin 366, 143 p.

Karlstrom, K.E., van der Pluum, B.A., and Williams, P.F.
1982: Structural interpretation of the eastern Notre Dame Bay area, Newfoundland: regional post-Middle Silurian thrusting and asymmetrical folding; Canadian Journal of Earth Sciences, v. 19, p. 2325-2341.

Kean, B.F. and Evans, D.T.W.
1986: Metallogeny of the Tulks Hill volcanics Victoria Lake Group, central Newfoundland; in Current Research; Newfoundland Department of Mines and Energy, Mineral Development Division, Report 86-1, p. 51-57.

Kean, B.F. and Jayasinghe, N.R.
1982: Geology of the Badger map area (12A/16) Newfoundland; Newfoundland Department of Mines and Energy, Mineral Development Division, Report 81-2, 37 p.

Kean, B.F., Dean, P.L., and Strong, D.F.
1981: Regional geology of the Central Volcanic Belt of Newfoundland; in The Buchans Orebodies: Fifty Years of Geology and Mining, ed. E.A. Swanson, D.F. Strong and J.G. Thurlow; Geological Association of Canada, Special Paper 22, p. 65-78.

Kimura, G. and Tamaki, K.
1986: Collision, rotation, and back-arc spreading in the region of the Okhotsk and Japan seas; Tectonics, v. 5, no. 3, p. 389-401.

Lallemand, S. and Jolivet, L.
1986: Japan Sea: a pull-apart basin?; Earth and Planetary Science Letters, v. 76, p. 375-389.

Lipman, P.W.
1980: Cenozoic volcanism in the western United States: Implications for continental tectonics; in Studies in Geophysics; National Academy of Sciences, Washington, p. 161-174.

Malpas, J. and Stevens, R.K.
1977: The origin and emplacement of the ophiolite suite with examples from western Newfoundland; Geotectonics, v. 11, no. 6, p. 453-466.

Nowlan, G.S., and Thurlow, J.G.
1984: Middle Ordovician conodonts from the Buchans Group, central Newfoundland, and their significance for regional stratigraphy of the Central Volcanic Belt; Canadian Journal of Earth Sciences, v. 21, p. 284-296.
1987: Middle Ordovician conodonts from the Buchans Group; in Buchans Geology, Newfoundland, ed. R.V. Kirkham; Geological Survey of Canada, Paper 86-24, Report 4.

Ohmoto, H.
1983: Geologic setting of the Kuroko deposits, Japan: Part I. Geologic history of the Green Tuff region; in The Kuroko and Related Volcanogenic Massive Sulfide Deposits, ed. H. Ohmoto and B.J. Skinner; Economic Geology, Monograph 5, p. 9-24.

Ohmoto, H. and Skinner, B.J. (ed.)
1983: The Kuroko and Related Volcanogenic Massive Sulfide Deposits; Economic Geology, Monograph 5, 604 p.

Palmer, A.R.
1983: The Decade of North American Geology 1983 geologic time scale; Geology, v. 11, p. 503-504.

Pickett, J.W.
1987: Geology and geochemistry of the Skidder Basalt; in Buchans Geology, Newfoundland, ed. R.V. Kirkham; Geological Survey of Canada, Paper 86-24, Report 11.

Pickett, J.W. and Barbour, D.M.
1984: Geology of the Skidder prospect, Buchans, Newfoundland; in Current Research, Part A, Geological Survey of Canada, Paper 84-1A, p. 581-586.

Rodgers, J.
1965: Long Point and Clam Bank formations, western Newfoundland; Geological Association of Canada, Proceedings, v. 16, p. 83-94.

Searle, M.P. and Stevens, R.K.
1984: Obduction processes in ancient, modern and future ophiolites; in Ophiolites and Oceanic Lithosphere, ed. I. Gass, S.J. Lippard and A.W. Shelton; Blackwell, London, p. 303-319.

Schillereff, S. and Williams, H.
1979: Geology of the Stephenville map area, Newfoundland; in Current Research, Part A, Geological Survey of Canada, Paper 79-1A, p. 327-332.

Sillitoe, R.H.
1982: Extensional habits of rhyolite-hosted massive sulfide deposits; Geology, v. 10, p. 403-407.

Snelling, N.J.
1985: An interim time-scale; in The Chronology of the Geological Record, ed. N.J. Snelling; British Geological Survey, Memoir No. 10, p. 261-265.

Stevens, R.K.
1970: Cambro-Ordovician flysch sedimentation and tectonics in west Newfoundland and their possible bearing on a proto-Atlantic Ocean; in Flysch Sedimentology in North America, ed. J. Lajoie; Geological Association of Canada, Special Paper 7, p. 165-177.

Stewart, P.W.
1987: Geology and genesis of granitoid clasts in the MacLean Extension transported orebody; in Buchans Geology, Newfoundland, ed. R.V. Kirkham; Geological Survey of Canada, Paper 86-24, Report 10.

Strong, D.F.
1974: Plateau lavas and diabase dikes of northwestern Newfoundland; Geological Magazine, v. 111, p. 501-514.
1982: Tectonic and metallogenic evolution of the Canadian Appalachians; in Prospecting in Areas of Glaciated Terrain-1982, ed. P.H. Davenport; The Canadian Institute of Mining and Metallurgy, Symposium Volume, p. 1-36.

Stukas, V. and Reynolds, P.H.
1974: $^{40}Ar/^{39}Ar$ dating of the Long Range dikes, Newfoundland; Earth and Planetary Science Letters, v. 22, p. 256-266.

Swinden, H.S. and Thorpe, R.I.
1984: Variations in style of volcanism and massive sulphide deposition in Early to Middle Ordovician island-arc sequences of the Newfoundland Central Mobile Belt; Economic Geology, v. 79, p. 1596-1619.

Thurlow, J.G.
1981a: The Buchans Group: Its stratigraphic and structural setting; in The Buchans Orebodies: Fifty Years of Geology and Mining, ed. E.A. Swanson, D.F. Strong and J.G. Thurlow; Geological Association of Canada, Special Paper 22, p. 79-90.
1981b: Geology, ore deposits and applied rock geochemistry of the Buchans Group, Newfoundland; Unpublished Ph.D. thesis, Memorial University of Newfoundland, 305 p.
1984: A geological field guide to the Buchans area; in Mineral Deposits of Newfoundland – A 1984 Perspective, compiled by H.S. Swinden; Newfoundland and Labrador Department of Mines and Energy, Report 84-3, p. 141-146.

Thurlow, J.G. and Swanson, E.A.
1981: Geology and ore deposits of the Buchans area, central Newfoundland, in The Buchans Orebodies: Fifty Years of Geology and Mining, ed. E.A. Swanson, D.F. Strong and J.G. Thurlow; Geological Association of Canada, Special Paper 22, p. 113-142.
1987: Stratigraphy and structure of the Buchans Group; in Buchans Geology, Newfoundland, ed. R.V. Kirkham; Geological Survey of Canada, Paper 86-24, Report 2.

Whalen, J.B.
1986: Geochemistry of the mafic and volcanic components of the Topsails igneous suite, western Newfoundland; in Current Research, Part B, Geological Survey of Canada, Paper 86-1B, p. 121-130.

Whalen, J.B. and Currie, K.L.
1983: The Topsails igneous terrane of western Newfoundland; in Current Research, Part A, Geological Survey of Canada, Paper 83-1A, p. 15-23.
1987: The relationship of the Topsails igneous terrane to the Buchans Group; in Buchans Geology, Newfoundland, ed. R.V. Kirkham; Geological Survey of Canada, Paper 86-24, Report 6.

Whalen, J.B., Currie, K.L., and van Breeman, O.
– Episodic Ordovician-Silurian plutonism in the Topsails igneous terrane, western Newfoundland; Royal Society of Edinburgh, Earth Sciences Division, Transactions. (in press)

Williams, H.
1971: Mafic-ultramafic complexes in western Newfoundland and the evidence for their transportation: A review and interim report; Geological Association of Canada, Proceedings, A Newfoundland Decade, v. 24, p. 9-25.
1978: Tectonic lithofacies map of the Appalachian orogen; Memorial University of Newfoundland, Map 1.
1982: Geology of the Canadian Appalachians; in Perspectives in Regional Geological Synthesis (Planning for the Geology of North America), ed. A.R. Palmer; Decade of Northern American Geology, Special Publication 1, p. 57-66.

Williams, H., Gillespie, R.T., and van Breemen, O.
1985: A late Precambrian rift-related igneous suite in western Newfoundland; Canadian Journal of Earth Sciences, v. 22, p. 1727-1735.

Wonderley, P.F. and Neuman, R.B.
1984: The Indian Bay Formation: fossiliferous Early Ordovician volcanogenic rocks in the northern Gander Terrane, Newfoundland, and their regional significance; Canadian Journal of Earth Sciences, v. 21, p. 525-532.

- 2 -

Stratigraphy and structure of the Buchans Group

J.G. Thurlow[1], and E.A. Swanson[2]

Thurlow, J.G. and Swanson, E.A., Stratigraphy and structure of the Buchans Group; in Buchans Geology, Newfoundland, ed. R.V. Kirkham; Geological Survey of Canada, Paper 86-24, p. 35-46, Report 2, 1987.

Abstract

A significant revision of Buchans Group stratigraphy and structure is presented in this paper. The new model suggests a considerably simplified stratigraphic column with a corresponding increase in structural complexity from those presented previously. A formal lithostratigraphic subdivision of the Buchans Group into four formations is proposed. The Buchans orebodies form members within the newly designated Buchans River Formation.

The revised stratigraphy combined with correlations of thrust faults has permitted identification of duplex structures, antiformal stacks and other features common in thrust belts. Facies distributions suggest that some thrusts propagated along early, high-angle, normal faults which were active at the time of deposition and were important in determining the positions of paleochannels that contain the transported ores.

The recognition that all of the major orebodies are bounded by thrusts and that structural footwall rocks are the stratigraphic hangingwall, has led to important new exploration ideas and strategies.

Résumé

Cette étude présente une révision détaillée de la stratigraphie et de la structure du groupe de Buchans. Selon la nouvelle interprétation, l'échelle stratigraphique serait beaucoup plus simple et la géologie structurale beaucoup plus complexe que ce qui avait été présenté auparavant. Les auteurs proposent une subdivision officielle en quatre formations de la lithostratigraphie du groupe de Buchans. Les masses minéralisées de Buchans formeraient des termes à l'intérieur de la nouvelle formation de Buchans River.

La révision de la stratigraphie et la mise en corrélation des failles chevauchantes ont permis de reconnaître la présence de duplex, de piliers antiformes et d'autres détails trouvés couramment dans les zones de charriage. La répartition des faciès porte à croire que certaines nappes de charriage ont longé d'anciennes failles normales à fort pendage qui étaient actives au moment de la mise en place et qui ont contribué à déterminer la position des paléochenaux contenant les minerais déplacés.

L'identification, que toutes les masses minéralisées soient limitées par des failles de poussé et cette structure rocheuse située au-dessous constitue la stratigraphie de la structure du dessus, fait en sorte que ces structures rocheuses sont un guide pour d'importantes idées de nouvelles stratégies et de nouvelles exploitations.

[1]BP Canada-Selco Division, P.O. Box 789, Corner Brook, Newfoundland A2H 6G7 (formerly with Abitibi-Price Inc.)
[2]38 Ennis Avenue, St. John's, Newfoundland A1A 1Y8 (formerly with ASARCO Inc.)

INTRODUCTION

Despite ascribing an epigenetic origin to the orebodies, the earliest geologists at Buchans recognized the stratigraphic control on the distribution of ores (Newhouse, 1931; George, 1937). The association of mineralization with key sequences of lithologies was the prime guide to deep diamond drilling which formed an important part of exploration at Buchans (Swanson, 1981). Though largely empirical, this approach proved highly successful. The importance of stratigraphy was emphasized with the recognition of the synvolcanic origin of the ores and subsequently further applied with recognition of their sedimentological transported nature. A complex stratigraphic model involving four volcanic cycles evolved (Thurlow et al., 1975) though this, and earlier models, lacked the basic understanding of the regional and local structure. The recognition of first the Hungry Mountain Thrust, and then the Skil Hill – Buchans River Thrust, in the mid 1970s, began a decade-long reappraisal of all aspects of the geology. The result of this work is an improved understanding of the nature and extent of the thrust faults and their role in disrupting the stratigraphic succession which in turn permits the formal stratigraphic subdivision proposed in this paper.

The model presented suggests a considerably simplified stratigraphy with a corresponding increase in structural complexity than that presented previously (e.g. Thurlow and Swanson, 1981). Division of the Buchans Group into lower and upper subgroups is abandoned and the various stratigraphic "sequences" have been consolidated into four formations. A number of venerable stratigraphic names are abandoned because they contravene allowable nomenclature in the North American Stratigraphic Code. Included among these are the "Intermediate Footwall", "Footwall Basalt" and "Footwall Arkose" (the latter two are now considered to lie stratigraphically in the hangingwall of the orebodies!). Introduction of new names is unfortunate but, since they conform to the Stratigraphic Code and are based upon specific relationships preserved in diamond-drill core, hopefully they will be of more lasting significance.

The Buchans Group has been subjected to several episodes of faulting including a period of significant thrust movement. Lithological contacts are typically the locus of strain and indeed most major lithological contacts, as preserved in diamond-drill core, are now sheared and/or intruded by late diabase sills. As a consequence, reconstructed prethrust stratigraphy is based upon rare contacts which are unsheared and indisputably conformable. The location of these contacts, and other information primarily of interest to future workers, is given in an appendix.

STRATIGRAPHY OF THE BUCHANS GROUP

Introduction

The stratigraphy of the Buchans Group is summarized in Table 1 and shown schematically in Figure 1. The Buchans Group can be envisaged as a thrust belt composed of a series of sheets separated by significant thrust faults (Fig. 2). The Buchans orebodies occur as part of the newly designated Buchans River Formation within two such thrust sheets; and Lucky Strike sheet which hosts the Lucky Strike, Rothermere and MacLean orebodies and the structurally higher Oriental sheet, which hosts the Oriental Orebodies. The stratigraphic

Table 1. Stratigraphy of the Buchans Group

Formation	Maximum Thickness in Oriental Block	Maximum Thickness	Lithologies	Former Stratigraphic Names
Sandy Lake Formation	200m	2000m?	Basaltic pillow lava, pillow breccia intertonguing with coarse grained, redeposited clastic rocks of felsic volcanic derivation (arkosic conglomerate, arkose, wacke, siltstone). Local abundant tuff, breccia, polylithic pyroclastic breccia and tuffaceous sedimentary rocks.	Sandy Lake Basalt, Upper Arkose, Lake Seven Basalt, Footwall Arkose, Footwall Basalt, part of Prominent Quartz sequence.
Buchans River Formation	200m	400m?	Felsic tuff, rhyolite, rhyolite breccia, pyritic silstone, wacke, polylithic breccia-conglomerate, granite boulder conglomerate, high-grade in situ and transported sulphide orebodies.	Lucky Strike Ore Horizon sequence, Oriental Ore Horizon sequence, parts of Intermediate Footwall.
Ski Hill Formation	1000m?	1000m?	Basaltic to andesitic pyroclastic rocks, breccia, pillow lava, massive flows. Minor felsic tuff.	Ski Hill sequence, parts of Intermediate Footwall, Oriental Intermediate.
Lundberg Hill Formation	200m minimum	1000m?	Felsic pyroclastic rocks, coarse pyroclastic breccia, rhyolite, tuffaceous wacke, siltstone, lesser basalt, minor chert and magnetic iron-formation.	Part of Prominent Quartz sequence, Wiley's Prominent Quartz sequence, Little Sandy sequence (?).

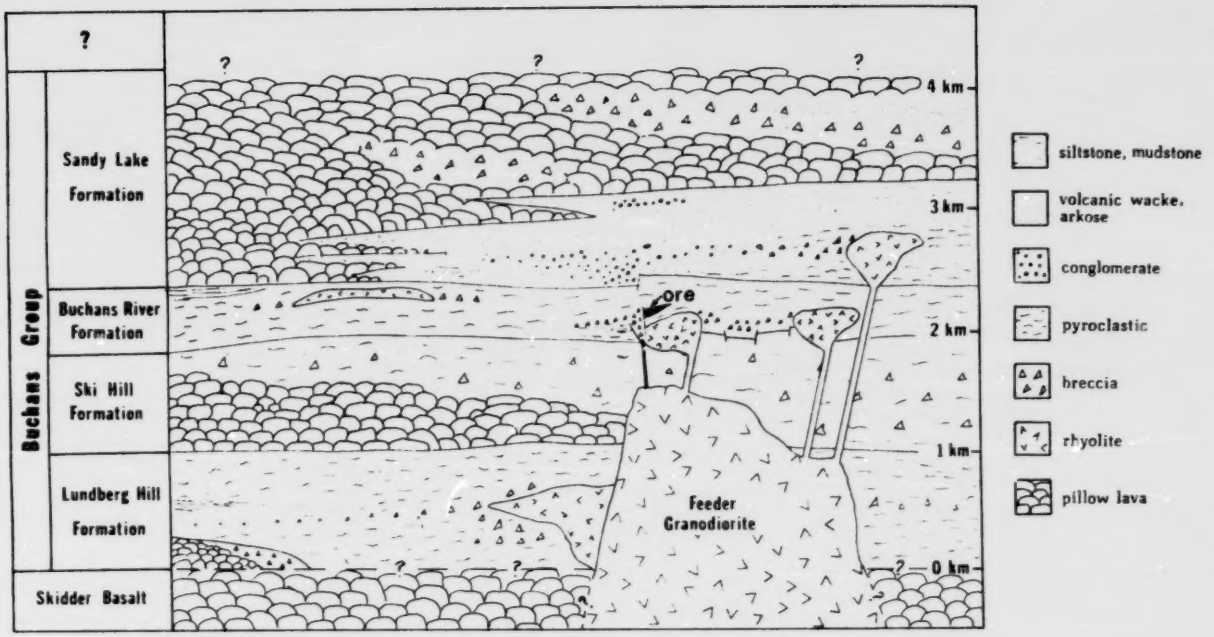

Figure 1. Schematic reconstructed stratigraphy of the Buchans Group. The orebodies form members within the Buchans River Formation.

sequence of the Buchans Group is best preserved within the Oriental sheet, and hence, this block was chosen for definition of the stratigraphy. This same succession is repeated in the Lucky Strike sheet though less completely and with greater disruption by faults. Other unnamed thrust sheets, both structurally higher and lower, are much more poorly understood than the two economically important blocks. All of the major thrust sheets are cut by relatively lesser thrusts with displacements of a few hundred metres or less.

The regional structural and stratigraphic setting of the Buchans Group has been discussed in detail by Thurlow (1981a) and will be reviewed only briefly here. The Buchans Group lies structurally above both the Victoria Lake Group (Kean, 1977) and the ophiolitic Skidder Basalt (Pickett and Barbour, 1984; Pickett, 1987). Neither contact is exposed and structural-stratigraphic relationships can only be inferred and are thus controversial. Pickett (*op cit*) suggested that the Buchans Group lies with fault-modified conformable contact upon the Skidder Basalt. Nowlan and Thurlow (1984) suggested that the Buchans Group is thrust upon the Victoria Lake Group. The Feeder Granodiorite is considered to be a subvolcanic plutonic facies of the Buchans Group (Thurlow, 1981a; Stewart, 1987) and is herein considered part of the Buchans Group. However, the authors feel that formal designation of this unit must await further petrographic study and clarification of field relationships. The upper contact of the Buchans Group is both an intrusive contact against granites of the Silurian Topsails Granite, or a fault contact against structurally overlying deformed plutonic rocks of the Hungry Mountain Complex (Thurlow, 1981a; Whalen and Currie, 1983, 1987). Carboniferous red sandstone and conglomerate unconformably overlie the Buchans Group in the Red Indian Lake basin.

The recognition of additional thrust faults within the Buchans Group has resulted in a lowering of the thickness estimate of the Buchans Group from 5 km-9 km (Thurlow and Swanson, 1981) to 3 km-6 km. The proposed stratigraphic subdivision is based upon observed relationships only from the most studied part of the Buchans Group. With further study, scope exists for additional formations to be added either at the base or top of the stratigraphic pile.

Lundberg Hill Formation

The Lundberg Hill Formation (mainly the former "Prominent Quartz Sequence") is the lowest recognized mappable unit within the Buchans Group. The stratigraphic base of this formation in the Oriental block is not seen both because drill holes stop short of the base and elsewhere because the unit bottoms on the major Ski Hill thrust fault (Fig. 1). The formation occupies a known surface and subsurface area of more than 200 square kilometres and may reach a maximum thickness of approximately 1 km. Within the Oriental block, the dominant lithologies are rhyolitic pyroclastic rocks which are characterized by prominent 5 mm–10 mm quartz phenocrysts and smaller zoned plagioclase crystals. In other thrust blocks, these felsic pyroclastic rocks are interbedded

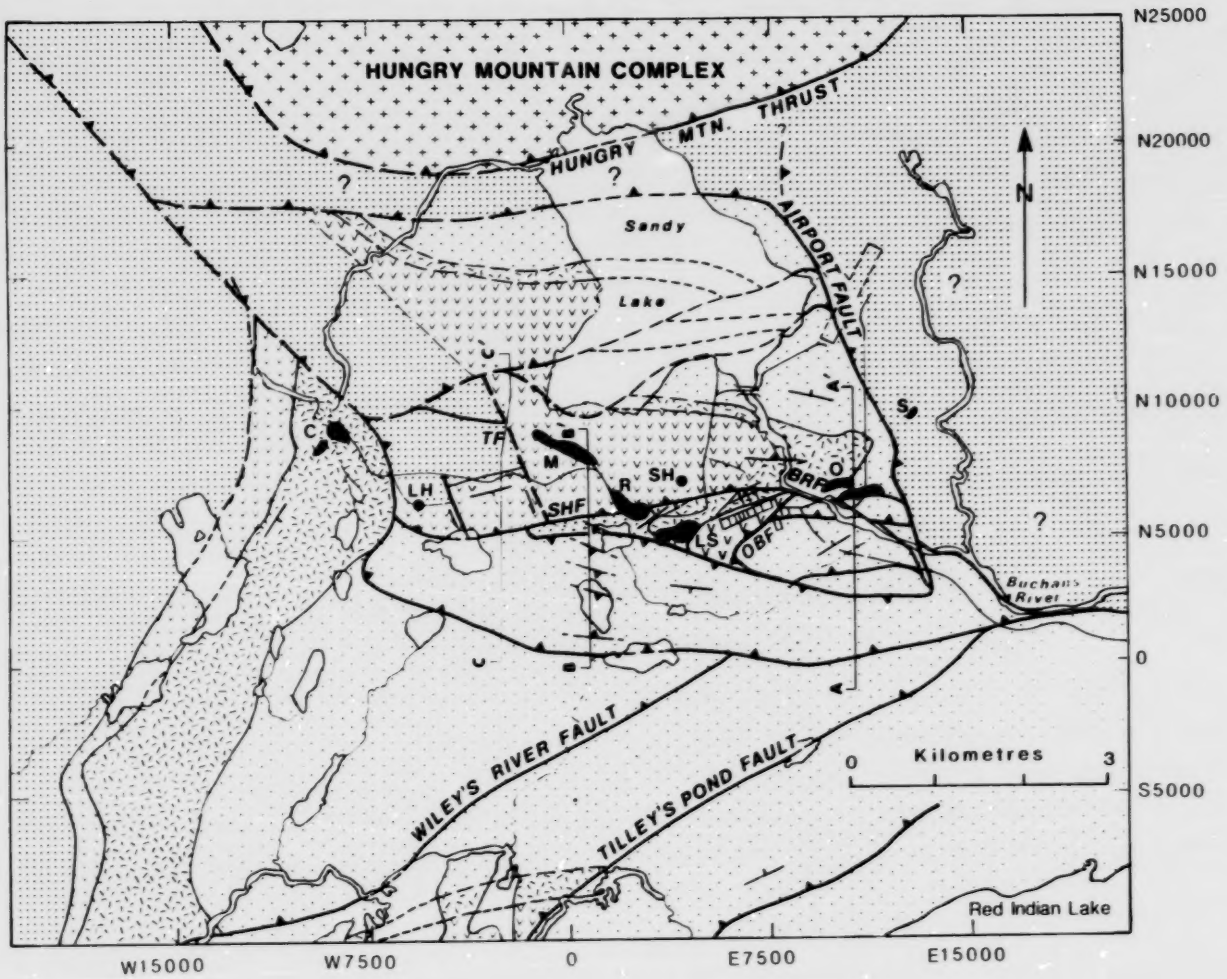

Sandy Lake Formation

Buchans River Formation

Ski Hill Formation

Lundberg Hill Formation

Geological contacts
(defined, approximate).....

Thrust fault.....

Bedding.....

Mine co-ordinates N5000

Figure 2. Simplified structural-stratigraphic map of the Buchans area. Section lines A-A', B-B', C-C' refer to Figures 4, 5, 6, respectively. BRF is Buchans River Fault, LH is Lundberg Hill, OBF is Old Buchans Fault, SH is Ski Hill, SKF is Ski Hill Fault, and TF is tear fault.
Major faults only are shown. Extreme outlines of orebodies are projected to surface. Deposits are: C = Clementine; LS = Lucky Strike; M = MacLean; O = Oriental; R = Rothermere, and S = Sandfill.

with subaqueous, dominantly epiclastic, pyroclastic flows which grade upward from a base of polylithic breccia through pumiceous pyroclastic rock into tuffaceous wacke, siltstone and cherty mudstone. Rhyolite bodies containing either large or small quartz phenocrysts, bedded tuffaceous sedimentary rocks with multicoloured mudstone-chert and basaltic pillow lava units locally form important units within the formation.

Ski Hill Formation

The Ski Hill Formation consists of a thick pile of black to dark green breccia, pyroclastic rocks and pillow lava of basaltic to andesitic composition. It conformably overlies pyroclastic and tuffaceous sedimentary rocks of the Lundberg Hill Formation in a number of diamond-drill holes north of Lake Seven and reaches a maximum thickness of approximately 1 km. Most flows and fragments in breccias are amygdular and porphyritic with plagioclase and augite phenocrysts. Amygules filled with combinations of calcite, chlorite, prehnite and pumpellyite are typical throughout the Buchans Group but the Ski Hill Formation also contains abundant zones with distinctive elongate quartz-filled amygdules. Hematite is not abundant, except near the stratigraphic top of the unit.

In areas removed from epigenetic stockwork sulphides and alteration, the contact between pillow breccia of the Ski Hill Formation and overlying felsic pyroclastic rocks of the Buchans River Formation is gradational over several metres both in diamond-drill core and numerous underground exposures in the vicinity of the MacLean and MacLean Extension orebodies.

In the vicinity of the Lucky Strike and Oriental in situ orebodies, a zone of significant hydrothermal alteration obscures the contact between the Ski Hill and Buchans River formations. This zone, previously called the "Intermediate Footwall", is a complex, poorly understood stratigraphic package which has been altered extensively and modified significantly by faults. In general, altered rocks of recognizable mafic composition underlie altered, quartz-poor felsic lithologies. The former are assigned to the Ski Hill Formation and the latter to the Buchans River Formation.

Buchans River Formation

The Buchans River Formation (formerly "Lucky Strike and Oriental Ore Horizon sequences") hosts all of the major volcanogenic sulphide orebodies of the Buchans Group. Its surface and subsurface distribution is well known in the immediate vicinity of the orebodies and its complex internal stratigraphy has been mapped in detail, in selected areas. In the vicinity of the orebodies, the maximum thickness is in the range of 200 to 400 m. The stratigraphy in the vicinity of Maclean Extension Orebody is summarized in Figure 3. In general, the formation consists of lowermost quartz-poor pumiceous pyroclastic rocks, rhyolite and pyritic siltstone, overlain by quartz-rich rhyolite and crystal-vitric tuff and the transported ore breccias. These are in turn overlain by a thick sequence of felsic tuff with local quartz and feldspar phyric rhyolite. In the vicinity of Lucky Strike and Oriental orebodies, all units below the ore have been silicified, chloritized and sericitized extensively.

In the Oriental block the distribution and thickness of the formation is controlled by a linear, northeast-trending paleotrough which was active during deposition. Early coalescing rhyolite breccia domes are overlain by breccia, debris flows and pyroclastic units which fill the trough.

Sandy Lake Formation

The felsic tuff of Buchans River Formation in the Oriental block is overlain conformably by both hematitic basaltic pillow lava-pillow breccia and by arkosic volcaniclastic conglomerate which form the base of the lithologically complex Sandy Lake Formation. These disparate lithologies intertongue and are interbedded locally, though, in general, basalt is more common at the base of the Formation in the Sandy Lake area and arkosic conglomerate is predominant at the base in the Oriental-Sandfill area. The arkosic conglomerate is matrix supported and mainly contains rounded rhyolite cobbles with 5 to 10 mm quartz phenocrysts identical to those in the Lundberg Hill Formation. It occupies and levels the remnants of the paleotopographic trough which controlled deposition of the underlying Buchans River Formation. Some interbedding near the contact between the two formations is present as one lens of arkose occurs within tuffs of the Buchans River Formation. This lens of arkose, and that of the overlying Sandy Lake Formation evidently were derived from a different source than the volcanic units of the underlying Buchans River Formation. Similarly, the basalt and arkose of the Sandy Lake Formation appear to have filled the basin episodically from different sources (directions?). Although they intertongue and have limited interbedding, little mixing of the two lithologies has occurred, i.e., basaltic detritus in arkose is absent, except for rare rounded cobbles of basalt and arkosic detritus does not form interpillow material.

In the Lucky Strike fault slice, a lithologically more diverse sequence forms the base of the Sandy Lake Formation. These include felsic pyroclastic rocks (some with prominent quartz phenocrysts), polylithic breccia-conglomerate, arkose, wacke, siltstone and graded pumiceous pyroclastic flows. These are conformably overlain by a significant basaltic member (the Lake Seven Basalt of Thurlow and Swanson, 1981).

STRUCTURE OF THE BUCHANS AREA

Introduction

Advances have been made in decipering the complex structure of the Buchans area but the reader will readily appreciate that this paper represents only an interim report. It is anticipated that a much more sophistocated understanding will emerge from detailed studies now being sponsored by the Geological Survey of Canada. The dominant structural event affecting the Buchans area is an episode of pre-Topsails

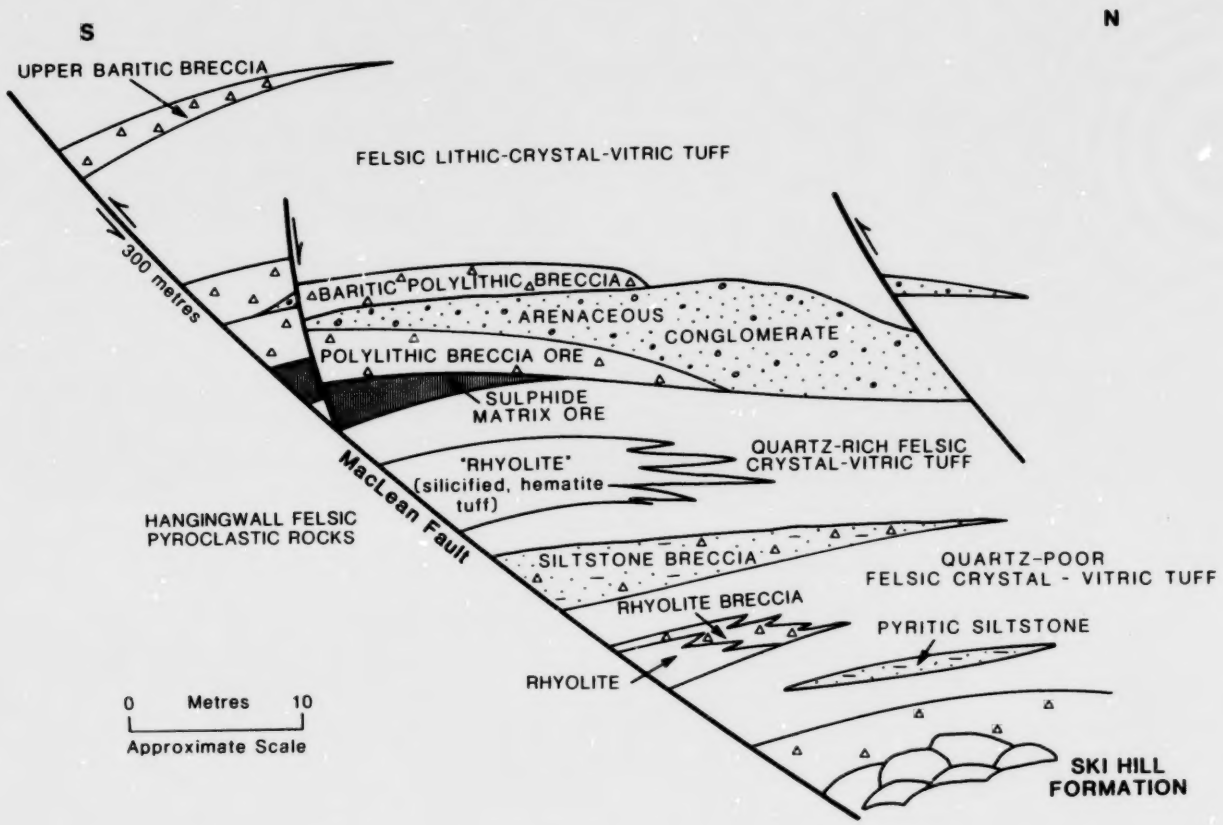

Figure 3. Schematic stratigraphy of the Buchans River Formation in the vicinity of MacLean Extension Orebody.

Granite thrust faulting which disrupts the orebodies and units of the Buchans Group.

Nature of the fault zones

Individual faults are generally narrow zones of brittle shear. The width of fault zones varies directly with displacement on the fault and ranges from a few centimetres in faults with displacements of 30 m or less to several metres wide in faults with displacements of a kilometre or more. Fault gouge is lithified typically by secondary quartz-epidote though many faults have been reactivated and contain seams of unlithified clayey gouge which was generally not recovered in older drill core. Many fault planes have been intruded by diabase sills which emanate from gabbroic bodies associated with the Topsails Granite. In some drill cores, fault blocks are "sealed" by diabase and show no evidence of shearing.

Distribution and characteristics of thrust faults

A map (Fig. 2) and unbalanced cross-sections (Figs. 4, 5, 6) illustrate the major structural elements. A closed elliptical structure, defined by faults, is present in the immediate vicinity of the Town of Buchans and is of key importance in understanding the local structure (Fig. 2). Inside this structure, northeast striking and northwest facing basaltic and arkosic rocks structurally underlie the Oriental and Lucky Strike orebodies. These rocks, traditionally termed the "Footwall Arkose" and "Footwall Basalt" are herein considered to form part of the Sandy Lake Formation and thus to lie stratigraphically above the ores. The Old Buchans Fault (Fig. 2) is a significant thrust bringing rocks of the older Ski Hill and Buchans River formations over those of the younger Sandy Lake Formation. The Old Buchans Fault joins the Ski Hill and Buchans River faults. These faults in turn bring older rocks, including Oriental Orebodies, structurally over the younger Sandy Lake rocks and repeat the Lucky Strike stratigraphy at Oriental. Between the Old Buchans and Ski Hill faults occur a series of lesser thrusts with displacements of 300 m or less. Detailed correlation of these economically significant faults was an important aspect of underground exploration in the MacLean and MacLean Extension areas. A small-scale duplex structure is developed below MacLean Orebody (Fig. 5) between the floor and roof thrusts, Buchans River and MacLean faults, respectively (terminology used is after Dahlstrom, 1970; Boyer and Elliott, 1982; Butler, 1982).

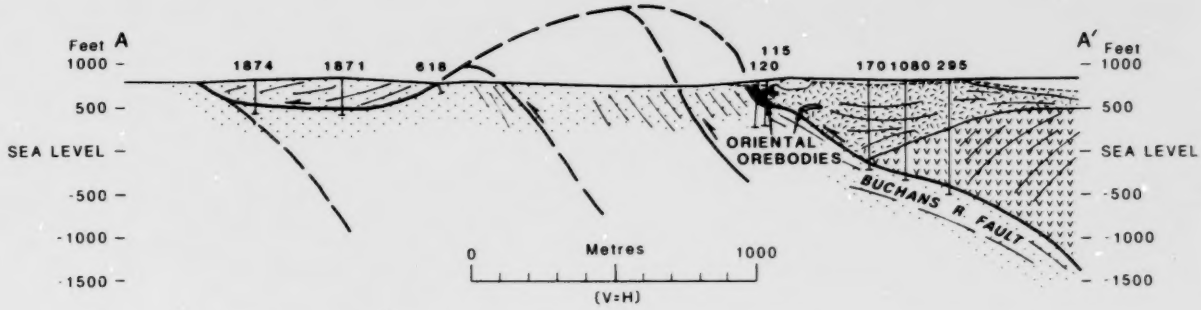

Figure 4. North-south vertical section looking west along mine co-ordinate E11,000. See Figure 2 for location of section line. Many minor faults which emanate from the Buchans River Fault and disrupt the Oriental Orebodies are not shown.

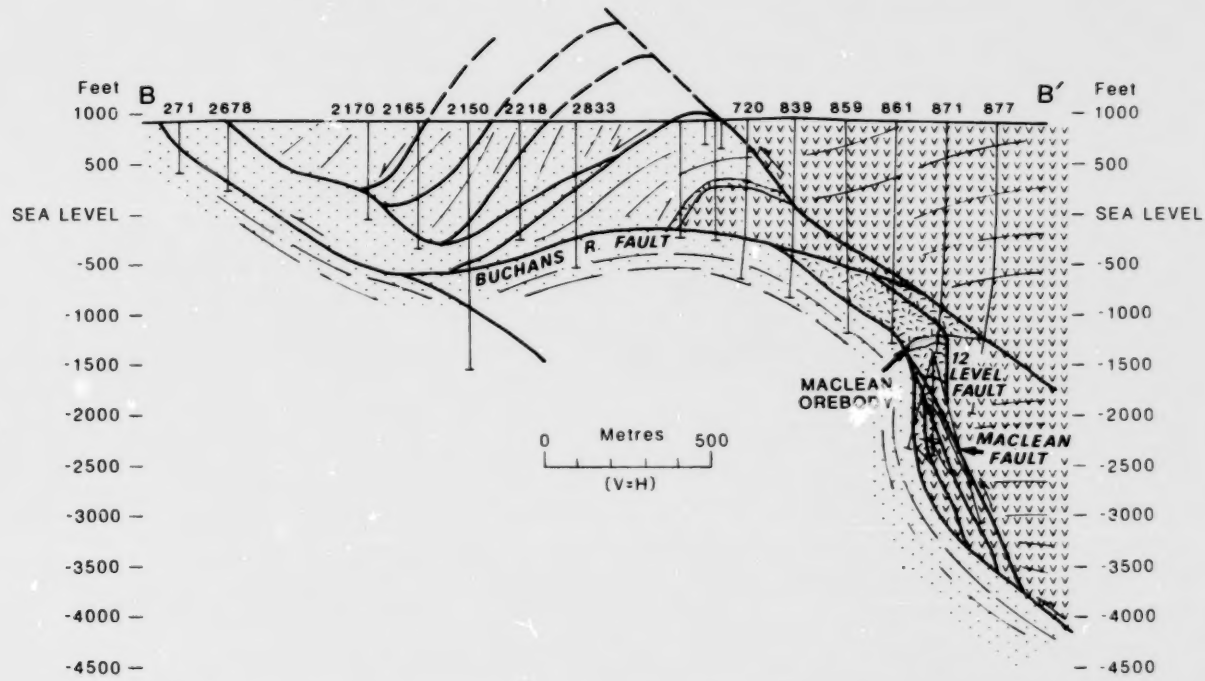

Figure 5. North-south vertical section looking west along mine co-ordinate E1000. See Figure 2 for location of section. Late diabase dykes and sills are omitted.

Above the MacLean Fault, asymetric folds developed with bedding locally overturned and facing the north-dipping fault. The hinge of one such folded ore bed can be traced through detailed drilling for 300 m with east-west trend and sub-horizontal plunge, suggesting thrust movement directly up-dip from the north. A foreland-dipping duplex was developed and is exposed at surface within steeply south-dipping strata south and west of Lucky Strike. Only the major faults in this this structure are shown in Figure 5 and detailed correlation along strike has not yet been attempted (Fig. 2). An antiformal stack (see Boyer and Elliott, 1982, Fig. 12) involving the Ski Hill, Buchans River and Sandy Lake formations is formed at the base of this duplex (Fig. 5). This structure can be traced in the surface and subsurface over a length of 5 km and is important in determining the present disposition of Lucky Strike and Rothermere orebodies.

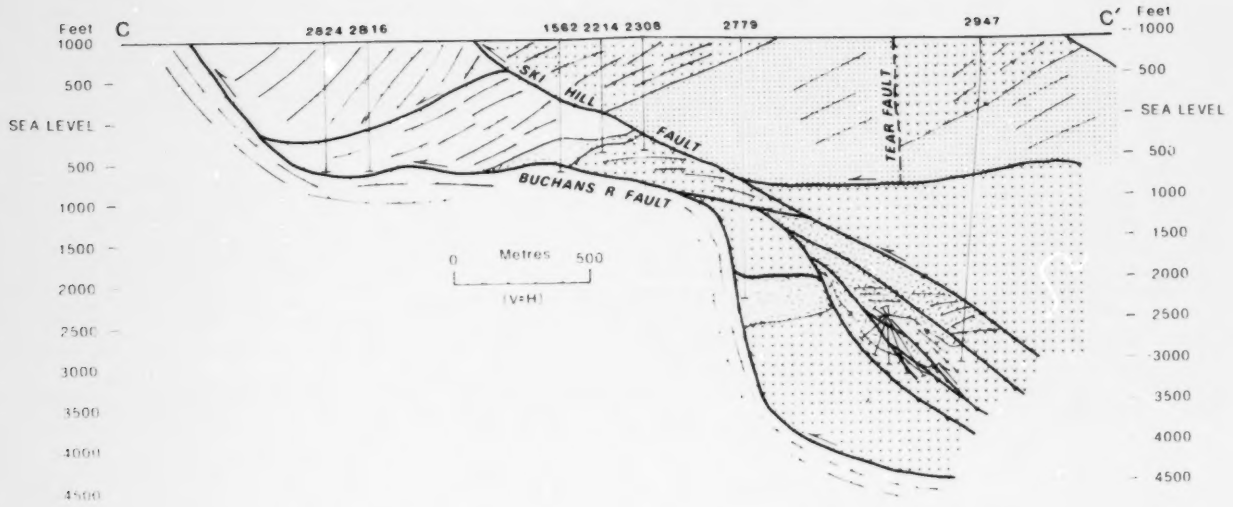

Figure 6. North-south vertical section looking west along mine co-ordinate W2500. See Figure 2 for location of section. Strike of the tear fault is subparallel to the section line (Fig. 2).

The Ski Hill Fault is a significant thrust which causes structural repetition of the Oriental Orebodies and their host lithologies on top of the sequence containing the Lucky Strike Orebodies. The displacement on the fault can be estimated by measuring the offset on the Ski Hill-Buchans River formations contact in the blocks above and below the fault. Assuming north to south displacement, movement on the fault was approximately 1 km. The Ski Hill Fault forms an anomalously straight planar surface (Fig. 5, 6) which, had it rode "piggyback" on the Buchans River Fault, should have been folded in a manner similar to the Buchans River Fault. The fact that it is not folded suggests that it developed later and is therefore out of sequence (K. Green, personal communication, 1985). Rocks below the fault young westward along the fault whereas rocks above the fault young eastward along the fault again suggesting that the fault is of later generation.

An anticlinal axis is present at surface north of, and parallel to, the Ski Hill-Buchans River fault system. This fold was evidently generated during thrusting since the stratigraphy becomes homoclinal north-dipping in the subsurface beneath the Ski Hill Fault.

A secondary transverse tear fault (see Dahlstrom, 1970, Fig. 45) has its downward termination on a thrust fault, west of MacLean Orebody (Fig. 2 and 6). Movement on this fault can be measured accurately due to its effect on the contact between the Lundberg Hill and Ski Hill formations (Fig. 7). The block west of the tear fault has moved an additional 450 m on the Ski Hill Fault relative to the block to the east. The attitude of the tear fault suggests thrust movements from the north northwest.

Mafic to felsic volcanic rocks presumed to belong to the Lundberg Hill Formation are thrust upon the Sandy Lake Formation along the northwest-striking Airport Fault (Fig. 2). The fault geometry suggests the presence of a larger scale duplex structure developed between the Airport and Buchans River faults.

Polydeformed plutonic rocks of the Hungry Mountain Complex were emplaced upon the Buchans Group along the Hungry Mountain Thrust (Fig. 2). This major fault can be traced at least 60 km along strike and probably records thrust movement in the order of tens of kilometres. The fault zone has a variable north-dipping attitude but is everywhere subparallel to stratigraphy in the underlying Buchan Group. It is marked by mylonite within the Hungry Mountain Complex and by the development of a penetrative foliation and an inverted metamorphic aureole within the Buchans Group. Mineral lineations and axes of small recumbent folds suggest a general movement direction from north to south. Dykes from the Early Silurian Topsails Granite (Whalen and Currie, 1987) cut the mylonite and thus date the thrust event as pre-Topsails Granite.

Early fault structures

The great number and magnitude of thrust faults obscure earlier structural history but some observations and inferences can be made. The transported ore breccias of MacLean Orebody overlie approximately 100 m of pyritic siltstone (Fig. 5). The ore and siltstone have a narrow linear fault-bounded distribution strongly suggestive of a paleotopographic channel. Drilling in search of ore above the 12 Level Fault and below the MacLean Fault (Fig. 5) has

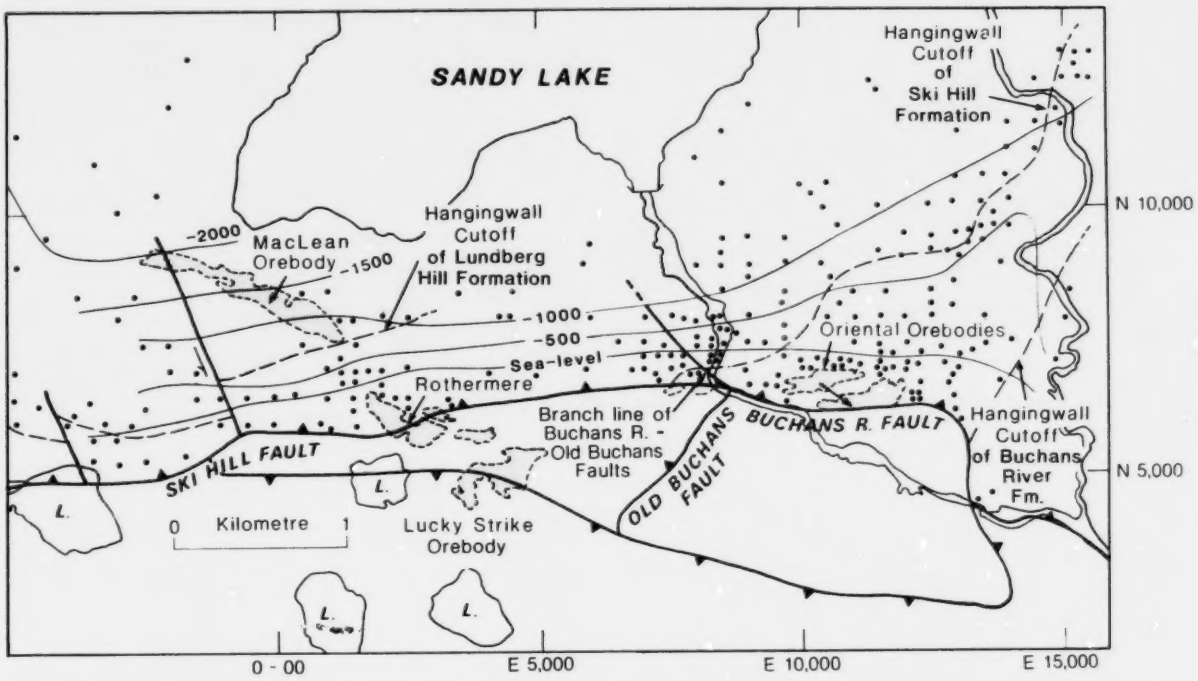

Figure 7. Map showing structural contours on the Ski Hill-Buchans River fault system. Mine co-ordinates and contour values related to sea level are in feet. Lines of intersection of the fault plane with the stratigraphic top of formations lying above the fault are shown as hangwall cutoff lines. Note the displacement of the hangingwall cutoff of the Lundberg Hill Formation along the tear faults. The branch line formed by the intersection of the Old Buchans and Buchans River faults is also shown. Dots are only those vertical diamond-drill holes collared north of the Ski Hill-Buchans River fault and give an indication of degree of control of the data. The surface expression of the Buchans River-Ski Hill fault ranges from 700 feet above sea level in the east to 1000 feet above sea level in the west of the map area.

revealed only minor ore breccia and footwall siltstone. This implies that the structures (graben?) which channelled these transported ores were relatively abrupt and deep and that the later thrust faults propagated preferentially along earlier fault planes that bounded the depression.

North of Oriental a broader subsurface basin trends northeast through the Sandfill area and is marked by a linear arrangement of rhyolite domes and flanking breccia and pyroclastic rocks. These lithologies lie above the Buchans River fault which forms a northeast trending hangingwall ramp which truncates these units (Fig. 7). In this area as well, a connection between depositional trends and late thrust faults suggests an influence of early structures on the distribution of lithologies.

The Lucky Strike and Oriental areas are characterized by strong sericitic, chloritic and silicic alteration which must have been localized by a fracture network which existed at the time of ore deposition. These areas are characterized now by abundant faults. It is suggested that these zones, weakened by early structural breaks and alteration, formed the locus for thrust and other fault movements. Thus, the empirical association of structural complexity and ore is viewed, in part, as a genetic link and not a result of more detailed geological study or coincidence.

Late faults

The late structural history of the Buchans Group has only been the subject of casual observation. Small-scale, high-angle, listric normal faults with displacements of less than 10 m bottom in thrust faults at the MacLean Extension area (Fig. 3). These fault surfaces are annealed and interpreted to be earlier than later movements on pre-existing thrust faults which are now manifested by unconsolidated clayey to sandy fault gouge.

Kornik et al. (1987) and McClay (1987) give evidence for additional late transverse and thrust fault movements. We anticipate that, with further study, the complex history of faulting within the Buchans Group will become much better understood and that the region will become an important

area for establishing the structural style of much of central Newfoundland.

EXPLORATION SIGNIFICANCE

Standard exploration practice in volcanogenic massive sulphide terranes is to explore the sulphide-bearing horizon both down dip and along strike. This approach was taken at Buchans since the earliest days of the mine, and for a period, was substantially successful. However, exploration reached a point in the mid 1970s where the full extent of the known ore horizon at both Oriental and Lucky Strike had been largely tested by diamond drilling.

The ongoing improvements in the understanding of structure and stratigraphy revealed that all of the major orebodies are bounded, in part, by thrust faults. Since thrusts bring older rocks on younger rocks, a new exploration opportunity was identified and tested by attempting to drill through stratigraphic hangingwall rocks below MacLean and MacLean Extension orebodies. This approach met with technical success and other settings of this nature remain to be tested.

On a larger scale, the recognition that the former "Footwall Basalt" and "Footwall Arkose" belong to the post-ore Sandy Lake Formation opens substantial new areas for exploration. These lithologies comprise most of the Buchans Group between the town of Buchans and Red Indian Lake. Because they were considered to be footwall rocks, they were relatively unexplored and have been the subject of very little diamond drilling. The new stratigraphic succession implies that the ore-bearing Buchans River Formation lies undiscovered below these rocks. A significant exploration challenge for the next few years will first be the identification of the ore-bearing host rocks and then the finding of ore within them. This work will come about only through an improved understanding of the internal stratigraphy of the Sandy Lake Formation and a better understanding of both local and regional structural patterns.

ACKNOWLEDGMENTS

We acknowledge useful discussions with D.M. Barbour, W.P. Binney, H. Helmstaed, J.L. Jambor, R.V. Kirkham, K.R. McClay and J.A. McGregor. Special thanks are due T.J. Calon who supplied a series of key references which gave meaning to structures which had puzzled us for some time. R.V. Kirkham kindly arranged for drafting of diagrams by the Geological Survey of Canada. We are grateful to BP Canada-Selco Division, Abitibi-Price Inc. and ASARCO Inc. for permission to publish.

REFERENCES

Boyer, S.E., and Elliott, D.
1982: Thrust systems; American Association of Petroleum Geologists, Bulletin, v. 66, p. 1196-1230.

Butler, R.W.H.
1982: The terminology of structures in thrust belts; Journal of Structural Geology, v. 4, p. 239-245.

Dahlstrom, C.D.A.
1970: Structural geology in the eastern margin of the Canadian Rocky Mountains; Canadian Association of Petroleum Geologists, Bulletin, v. 18, p. 332-406.

George, P.W.
1937: Geology of lead-zinc-copper deposits at Buchans, Newfoundland: American Institute of Mining and Metallurgical Engineers, Technical Publication 816-1, 22 p.

Kean, B.F.
1977: Geology of the Victoria Lake map area (12A/6), Newfoundland; Newfoundland Department of Mines and Energy, Report 77-4, 11 p.

Kornik, L.J., Whalen, J.B., and Thurlow, J.G.
1987: Interpretation of aeromagnetic gradiometer survey in the Buchans area; in Buchans Geology, Newfoundland, ed. R.V. Kirkham; Geological Survey of Canada, Paper 86-24, Report 5.

McClay, K.R.
1987: Aspects of the structural geology of the Buchans area; in Buchans Geology, Newfoundland, ed. R.V. Kirkham; Geological Survey of Canada Paper 86-24, Report 3.

Newhouse, W.H.
1931: Geology and ore deposits of Buchans, Newfoundland: Economic Geology, v. 26, p. 399-414.

Nowlan, G.S., and Thurlow, J.G.
1984: Middle Ordovician conodonts from the Buchans Group, central Newfoundland, and their significance for regional stratigraphy of the Central Volcanic Belt; Canadian Journal of Earth Sciences, v. 21, p. 284-296.
1987: Middle Ordovician condonts from the Buchans Group; in Buchans Geology, Newfoundland, ed. R.V. Kirkham; Geological Survey of Canada, Paper 86-24, Report 4.

Pickett, J.W.
1987: Geology and geochemistry of the Skidder Basalt; in Buchans Geology, Newfoundland, ed. R.V. Kirkham; Geological Survey of Canada, Paper 86-24, Report 11.

Pickett, J.W. and Barbour, D.M.
1984: Geology of the Skidder prospect, Buchans, Newfoundland; in Current Research, Part A, Geological Survey of Canada, Paper 84-1A, p. 581-586.

Relly, B.H.
1960: The geology of the Buchans mine; Unpulished Ph.D. thesis, McGill University, 281 p.

Stewart, P.W.
1987: Geology and genesis of granitoid clasts in the MacLean Extension transported orebody; in Buchans Geology, Newfoundland, ed. R.V. Kirkham; Geological Survey of Canada, Paper 86-24, Report 9.

Swanson, E.A.
1981: Development of genetic concepts and exploration practice at Buchans; in The Buchans Orebodies: Fifty Years of Geology and Mining, ed. E.A. Swanson, D.F. Strong and J.G. Thurlow; Geological Association of Canada, Special Paper 22, p. 311-324.

Thurlow, J.G.
1981a: The Buchans Group: Its stratigraphic and structural setting; in The Buchans Orebodies: Fifty Years of Geology and Mining, ed. E.A. Swanson, D.F. Strong and J.G. Thurlow; Geological Association of Canada, Special Paper 22, p. 79-90.
1981b: Geology, ore deposits and applied rock geochemistry of the Buchans Group, Newfoundland; Unpublished Ph.D. thesis, Memorial University of Newfoundland, 305 p.

Thurlow, J.G., and Swanson, E.A.
1981: Geology and ore deposits of the Buchans area, central Newfoundland; in The Buchans Orebodies: Fifty Years of Geology and Mining, ed. E.A. Swanson, D.F. Strong, and J.G. Thurlow; Geological Association of Canada, Special Paper 22, p. 113-142.

Thurlow, J.G., Swanson, E.A. and Strong, D.F.
1975: Geology and lithogeochemistry of the Buchans polymetallic sulphide deposits, Newfoundland; Economic Geology, v. 70, p. 130-144.

Whalen, J.B. and Currie, K.L.
1983: The Topsails terrane of western Newfoundland; in Current Research, Part A, Geological Survey of Canada, Paper 83-1A, p. 15-23.
1987: The relationship of the Topsails igneous terrane to the Buchans Group; in Buchans Geology, Newfoundland, ed. R.V. Kirkham; Geological Survey of Canada, Paper 86-24, Report 6.

APPENDIX 1

This appendix contains data necessary for the formal designation of new lithostratigraphic units including the locations in diamond-drill core of important lithological contacts. Contacts are typically the locus for later shear and thus unsheared, well-preserved contacts are of prime importance in erecting the stratigraphy. Also given are comments relating the rationale of some stratigraphic decisions and other information of use to future workers.

The stratigraphic succession is defined in the panel of rocks overlying the Ski Hill Fault (the Oriental block) and assignment of formational names to rocks outside this fault block is done mainly on the basis of lithological and stratigraphic similarities. As the structure of the area becomes better understood, stratigraphic revisions outside the Oriental block will undoubtedly become necessary.

Derivation of Formational Names

1) Lundberg Hill Formation: Naming of this unit is complicated by the fact that no permanent geographic feature marks the limited area of sub-outcrop of the formation in the Oriental thrust slice. Lundberg Hill, though underlain immediately by rocks of the Ski Hill Formation, is the site of key diamond-drill holes (e.g. holes 2925 and 2927) which intersect a major formation of felsic pyroclastic rocks conformably below Ski Hill lithologies. The hill is termed "Hill B" on some older maps.

2) Ski Hill Formation: The Formation is named after a prominent topographic knob 600 m north of Lucky Strike Orebodies. The outrop comprises mafic pyroclastic breccia typical of the Ski Hill Formation.

3) Buchans River Formation: The Buchans River cuts through and exposes a variety of felsic pyroclastics rocks, including breccia, immediately north of Old Buchans. These lithologies form part of the suite of rocks which hosts the Oriental Orebodies and they are herein collectively termed the Buchans River Formation.

4) Sandy Lake Formation: The Lake 2 km north of the town of Buchans (Fig. 1) is called Sandy Lake by local residents despite being called "Buchans Lake" on government topographic maps. The major sequence of basaltic and arkosic rocks occurring east of the Lake are named after this feature.

Location of Important Lithological Contacts

1) Lundberg Hill-Ski Hill Contact: diamond-drill hole 2927 at 106 feet (32.3 m): mine co-ordinates of hole are N7000, W5000. Similar contact relations can be seen in holes 2105, 2841 and 2925.

2) Ski Hill-Buchans River Contact: diamond-drill hole 2775 at 1045 feet (318.6 m): Mine co-ordinates of hole are N8644, E12,908. Similar contact relations can be seen in hole 2853 and in outcrop at Stacey's Point. In the Lucky Strike fault slice the conformable contact was mapped at many localities underground below MacLean Extension Orebody and is cored in many diamond-drill holes in this area.

3) Buchans River-Sandy Lake Contact: Felsic volcanic rocks of the Buchans River Formation are overlain locally by basaltic rocks and elsewhere by arkose and conglomerate. Conformable contacts with arkosic rocks are preserved in diamond-drill holes 1640 at 880 feet (268.3 m) co-ordinates N9662, E13456, 1683, 1872, 1720 at 1130 feet (344.5 m) and 2902, all holes were collared immediately northeast of Oriental Orebodies. Conformable contacts of basalt on Buchans River Formation are preserved in holes 2853 (co-ordinates N11, 508, E8500) and 1582. At least one lens of arkosic rock is considered to be part of the Buchans River Formation

near its upper contact in holes 1606, 1683 and 1568 (approximate co-ordinates N10,000, E14,000).

Comments on the Sandy Lake Formation

At the present time, to separate the disparate lithologies of basalt and arkose of this unit into separate formations is not possible. Within the Oriental thrust slice neither basalt nor arkose seems to be as voluminous as in other areas of the Buchans Group and the stratigraphic relationships between basalt and arkose are ambiguous. Both lithologies may directly overlie the Buchans River Formation. Basalt lies conformably on arkose (e.g. hole 1582 at N10,090, E11,456) and elsewhere arkose lies conformably on basalt (e.g. hole 1934 at N12,547, E14,604).

Outside of the Oriental block, large areas of basalt and arkose form separate mappable units which are assumed to be stratigraphically correlative with basalt and arkose of the Sandy Lake Formation. These separate units could each be accorded formational status but the stratigraphic relationships between them and those with other established formations are not known. Basalt and arkose must be amalgamated into one formation until the stratigraphic and structural relationships are established more clearly.

Another problem arises in attempting to establish the contact between the Sandy Lake and Buchans River formations in the Lucky Strike fault block. In this area arkosic rocks form an integral part of a sequence of rhyolitic breccia, pumiceous polylithic breccia, crystal-vitric tuff and related wacke and siltstone. These rocks are characterized by 2 mm–4 mm quartz grains, distinctly coarser than the 0.5 mm–2 mm quartz of the underlying Buchans River Formation. These rocks are conformably overlain by basaltic pillow lava (e.g. hole 799 at N5351, E893). The abrupt first stratigraphic appearance of these units containing larger quartz grains is interpreted as the contact between the Buchans River and Sandy Lake formations.

Carbonate clasts, some of which are fossiliferous (Nowlan and Thurlow, 1984, 1987), occur in breccias with the larger quartz grains in the Lucky Strike slice (e.g. holes 2932, 629, 799), in arkose of the Sandy Lake Formation north of Oriental (e.g. hole 1670), in the Wiley's Lake area (e.g. holes 2933, 2764) and in breccias in a felsic volcanic sequence immediately south of Lucky Strike (e.g. holes 1874, 609). The revised stratigraphy proposed in this paper implies that all of these carbonate clast occurrences are from the same general stratigraphic level near the base of the Sandy Lake Formation. Also, in the same general stratigraphic position, are a number of occurrences of sulphide clasts (Thurlow, 1981b, p. 97). These apparently correlate with an occurrence of a sulphide boulder in the arkose above Oriental Orebodies reported by Relly (1960, p. 82 and 97).

- 3 -

Aspects of the structural geology of the Buchans area

K.R. McClay[1]

McClay, K.R., Aspects of the structural geology of the Buchans area; in Buchans Geology, Newfoundland, ed. R.V. Kirkham; Geological Survey of Canada, Paper 86-24, p. 47-57, Report 3, 1987.

Abstract

The polymetallic massive sulphide-barite orebodies of the Buchans area occur in an imbricated sequence of Ordovician felsic and mafic volcanic rocks - the Buchans Group. The dominant structure in the mine area is a series of duplex structures 'pushed up' into an antiformal stack. Deformation is brittle with the development of brittle shear zones, joints and only local development of ductile deformation fabrics adjacent to major thrust faults. Dynamic and kinematic analysis of minor structures reveal two possible tectonic transport directions in the thrust sequence - one to the southeast and a hither to unrecognized southwestern movement pattern. This pattern of repetition of stratigraphy along major thrust faults with complex movement patterns has important implications for future exploration.

Résumé

Les masses minéralisées polymétalliques massives à sulfures et à barytine de la région de Buchans se trouvent dans une séquence imbriquée de roches volcaniques felsiques et mafiques ordoviciennes, le groupe de Buchans. Aux environs de la mine, la structure dominante est une série de duplex qui ont été poussés vers le haut pour former un amas antiforme. La déformation est de nature cassante et on y trouve des zones formées par cisaillement cassant et des joints; par endroits, le long des principales failles chevauchantes, les roches ont acquis une pétrofabrique sous l'effet d'une déformation ductile. L'analyse dynamique et cinématique des structures secondaires révèle la présence de deux directions possibles de transport tectonique dans la séquence de nappes de charriage, l'une vers le sud-est et l'autre, auparavant inconnue, vers le sud-ouest. Cette répétition de la stratigraphie le long des principales failles chevauchantes aux mouvements complexes aurait d'importantes répercussions sur l'exploration à l'avenir.

INTRODUCTION

The polymetallic, Kuroko-like baritic sulphide ores of the Buchans area occur in Ordovician felsic volcanic rocks of the Buchans Group in central Newfoundland. Detailed descriptions of the regional geology and of these spectacular sulphide deposits are found in Swanson *et al.* (1981), Thurlow (1984) and this volume. Recent structural and stratigraphic reinterpretations of the Buchans area by J.G. Thurlow has changed drastically the understanding of Buchans Group geology (Thurlow 1984 and personal communication).

Thurlow (1984) has identified major repetitions of stratigraphy along south to southeast verging thrust faults. This recent interpretation (Thurlow, 1984; Thurlow and Swanson, 1987) has allowed the subdivision of the Buchans Group into four formations (Fig. 1) which are repeated by a series of listric duplex thrust faults (Fig. 1, 2). The lowest stratigraphic unit, the Lundberg Hill Formation comprises primarily of felsic fragmental rocks (formerly called "Prominent Quartz Sequence") (Thurlow and Swanson, 1987). Ski Hill Formation comprises basaltic to andesitic pillow lava, breccia and pyroclastic rocks and overlies the Lundberg Hill Formation. Above the Ski Hill Formation is the Buchans River Formation containing the ore horizon, felsic volcanic breccia and siltstone. Overlying the ore-bearing sequence is the Sandy Lake Formation comprising arkose, mudstone, siltstone, conglomerate and stratigraphically equivalent felsic pyroclastic rocks intertongueing with hematitic pillow lava and breccia. Thurlow (1984 and personal communication) has identified

[1]Department of Geology, University of London Royal Holloway and Bedford New College, Egham, Surrey TW20 OEX UK.

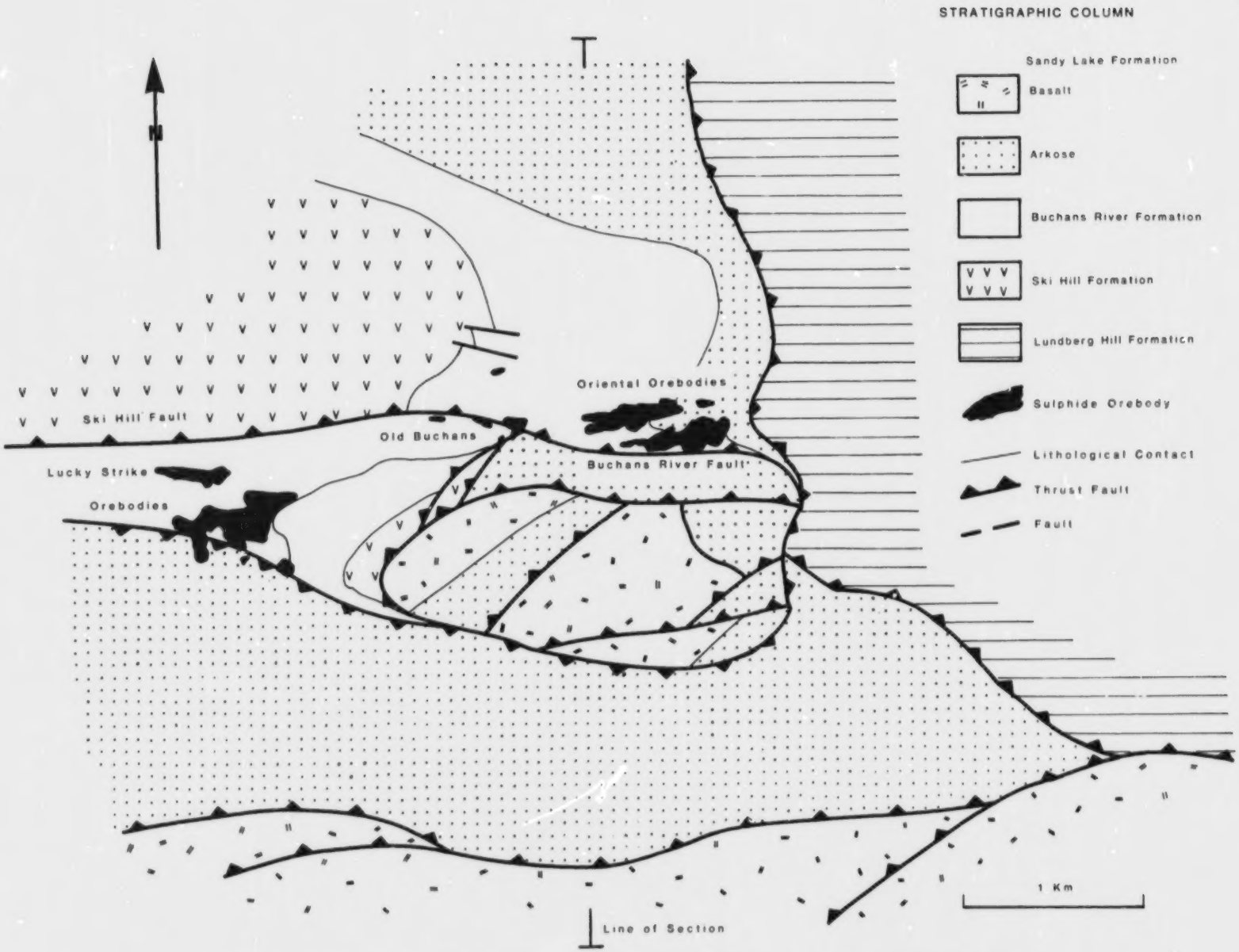

Figure 1. An interpretation of the geology of the Buchans area (adapted from Thurlow and Swanson, 1987).

this stratigraphic sequence wholly or partly repeated in thrust fault-bounded panels in the Buchans area. The reinterpreted geology in the immediate vicinity of the town of Buchans is shown in Figure 1 and a schematic cross-section illustrating the thrust relationships is shown in Figure 2.

In the Buchans area the grade of metamorphism is very low prehnite-pumpellyite facies (Thurlow, 1981). The massive volcanic rocks are strongly jointed and pervasive foliations are developed only locally adjacent to major thrust faults.

This paper presents a review of the structure of the Buchans area and a geometric dynamic and kinematic analysis of structures in the sulphide deposits and their host rocks. It is based on limited field observations and relies heavily upon the important revisions of stratigraphy carried out by J.G. Thurlow (1984) and Thurlow and Swanson (1987).

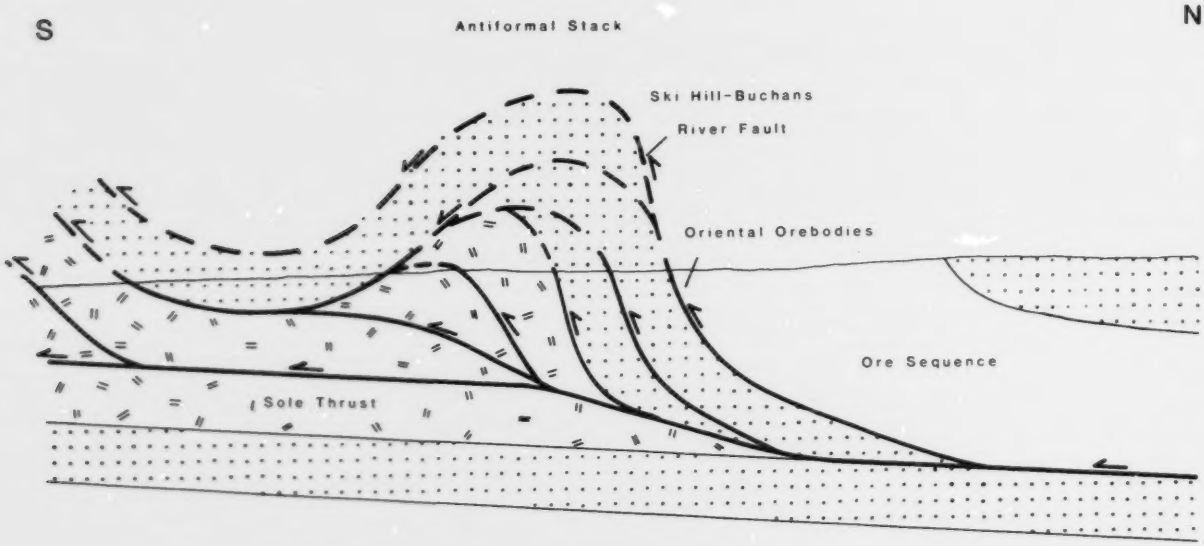

Figure 2. Schematic cross-section through the central Buchans area. The units are the same as in Figure 1.

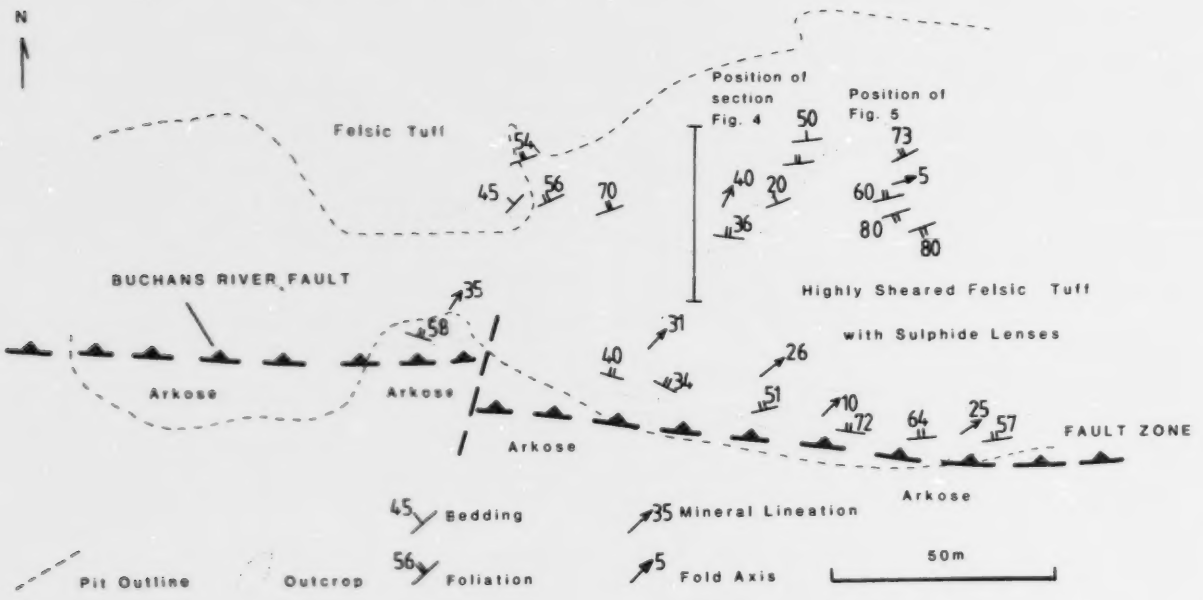

Figure 3. Sketch map of structural features in the Oriental West pit.

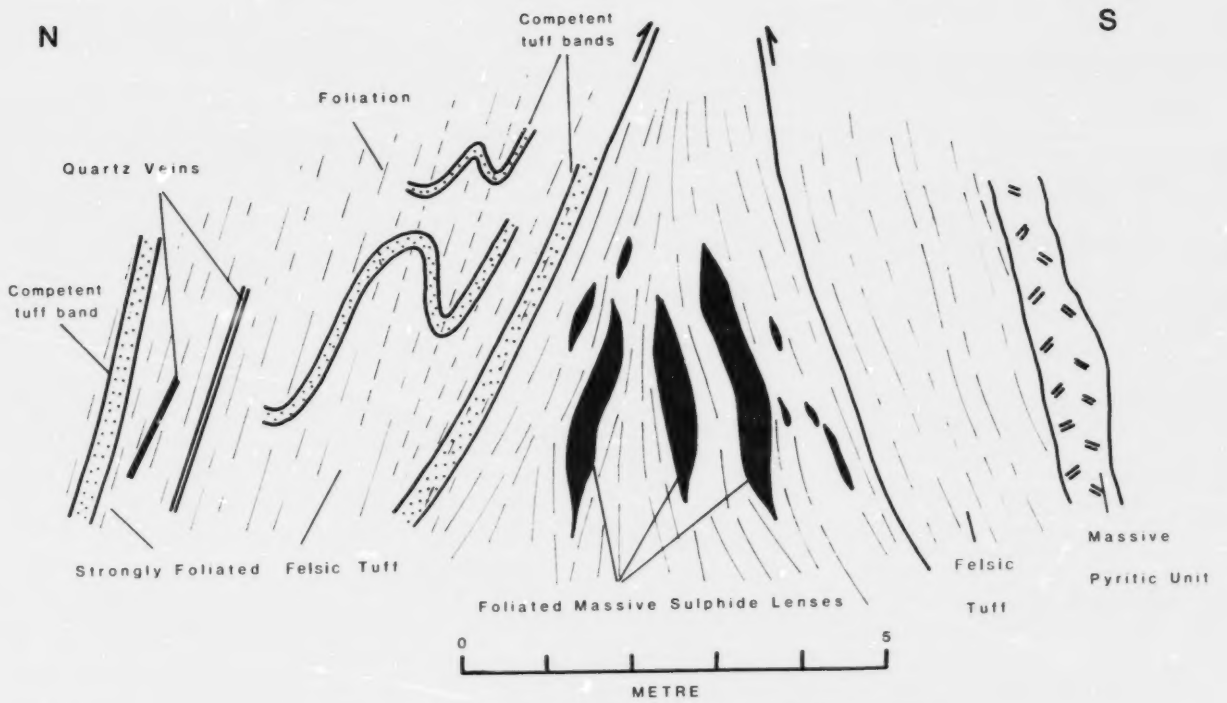

Figure 4. Section through sheared sulphide lenses-Oriental West pit.

Figure 5. Folded felsic tuffs with axial planar foliation Oriental West pit. View to east.

Figure 6. Sheared barite-sulphide lens truncated against a discrete northerly dipping shear fault-Oriental East pit. Viewed to West.

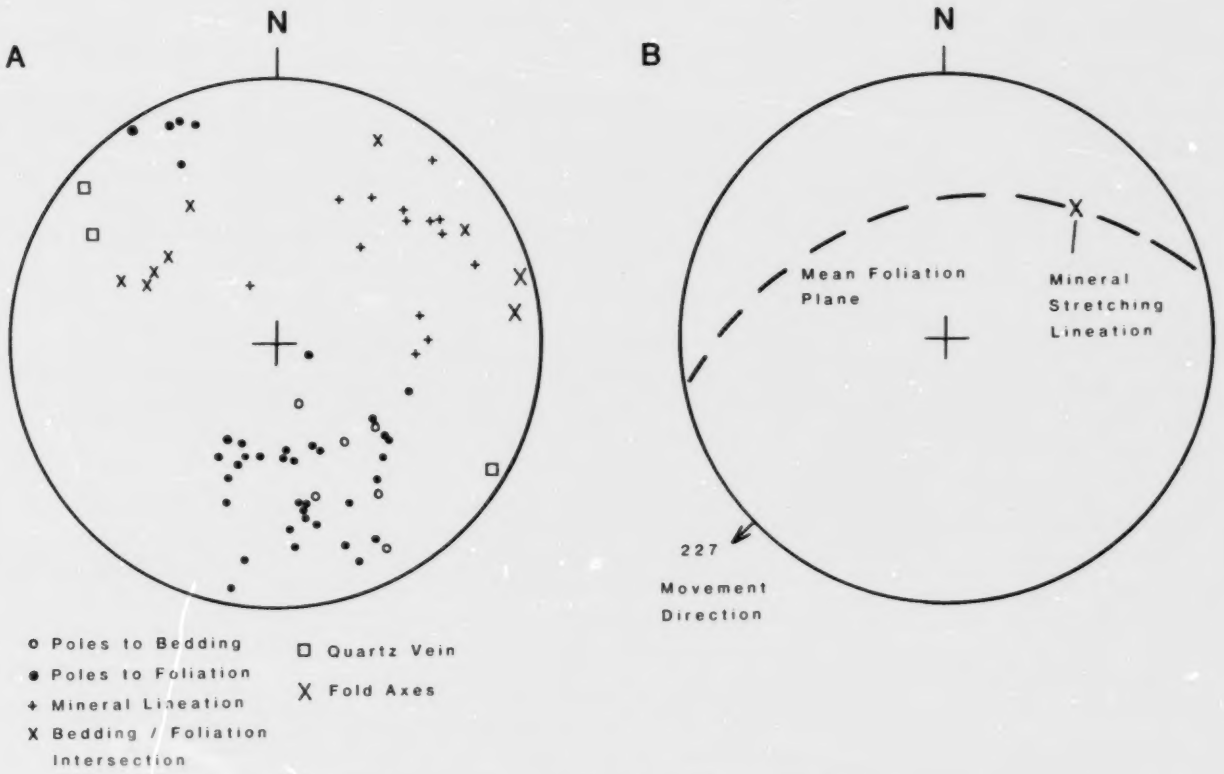

Figure 7. Structural data from the Oriental West pit.

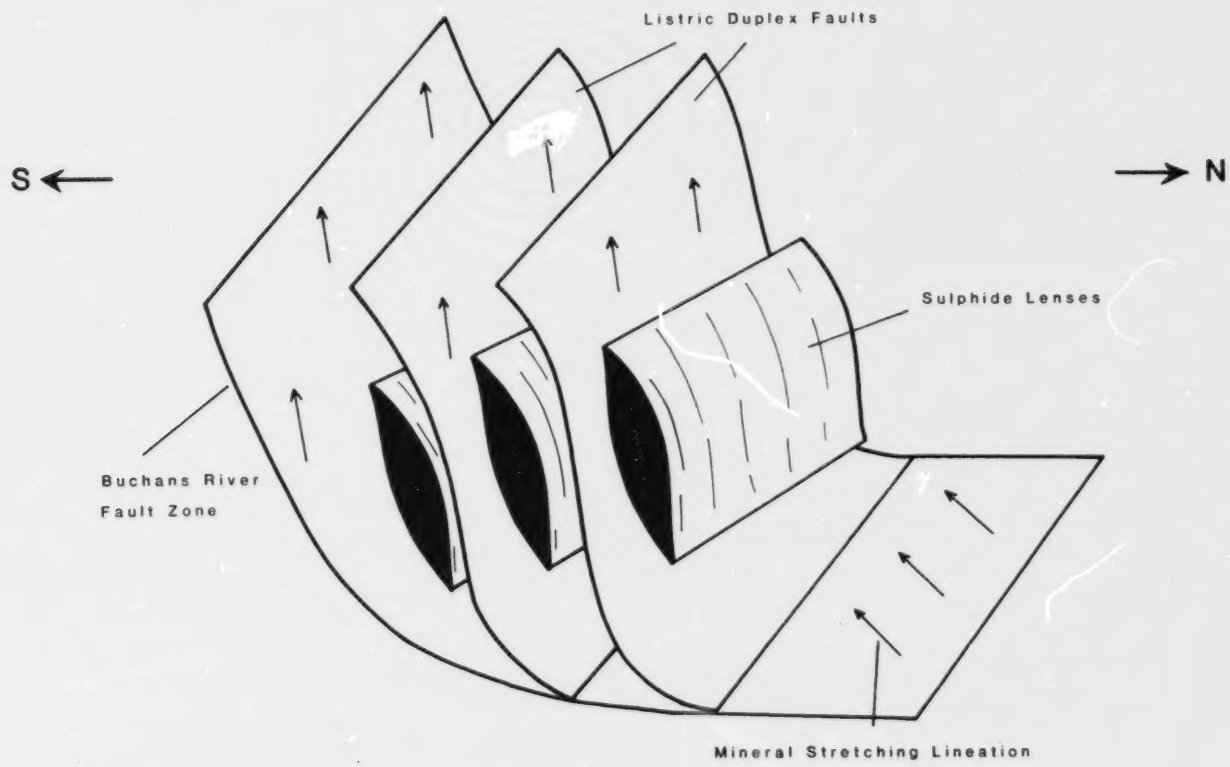

Figure 8 Schematic cross-section through the Oriental Orebodies showing individual sulphide lenses plunging to the northwest.

LOCAL STRUCTURE

The structure is dominated by a series of thrust faults which form a complex culmination pattern typical of an antiformal stack (Boyer and Elliott, 1982). The extensive repetition of units occurs along listric thrust faults. Three orientations of thrust faults are found: E-W, NE-SW, and NW-SE.

An interpreted cross-section through part of the Buchans area is shown in Figure 2. The Oriental Orebodies occur in

Figure 9. Slickensides on fault plane in felsic tuff 20 Level Maclean Extension Orebody.

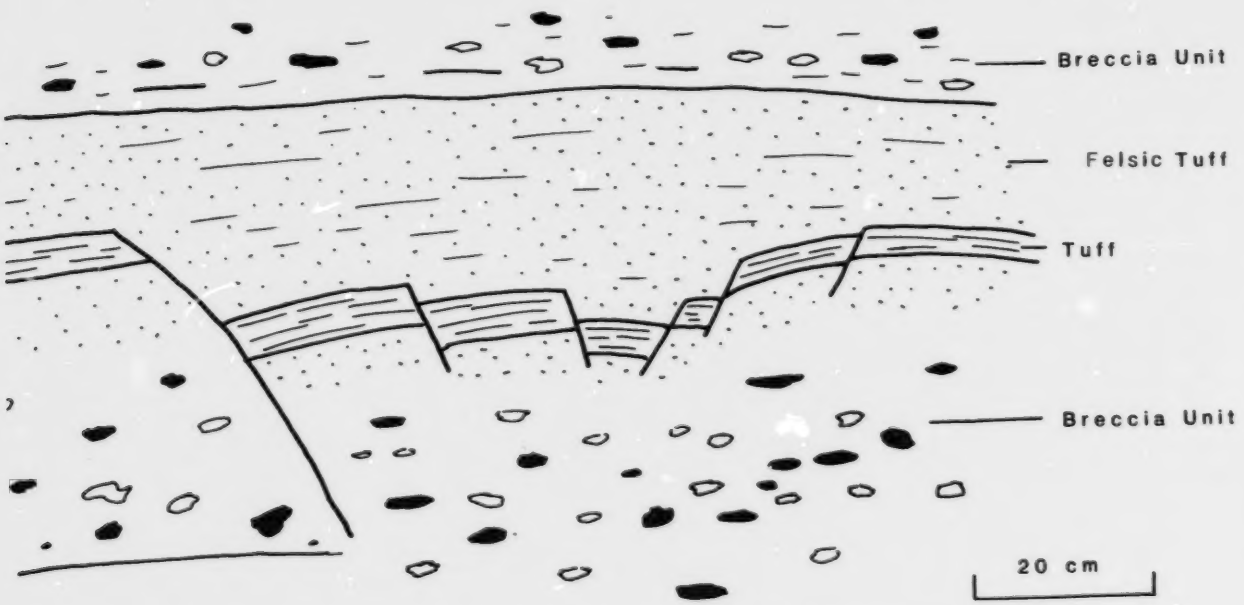

Figure 10. Syndepositional extension faults in interbedded felsic tuff and fragmental units. Note undeformed overlying breccia layer, 20 level, Maclean Extension Orebody.

Buchans River Formation in the hangingwall of the Ski Hill – Buchans River Fault (Fig. 2). The Ski Hill – Buchans River Fault is underlain by Sandy Lake Formation arkose repeated along listric thrust faults-forming a duplex (Boyer and Elliott, 1982). This duplex is presumed to be 'pushed up' over a footwall ramp in the basal or sole thrust thus forming an antiformal stack (Fig. 2) which gives rise to the distinctive outcrop pattern of Figure 1. The 'sole' thrust and footwall ramp have yet to be identified.

Such interpretations of the geometry of the Buchans structures need to be further developed and tested extensively. Recognition of this structural style, however, is extremely important in that it opens new ground for exploration for blind orebodies.

Minor structures and kinematic analysis

Some detailed mapping and structural analysis was carried out on surface and underground at Buchans and the results are summarized below.

Oriental Orebodies

Remnants of the Oriental Orebodies (Fig. 1) are found in abandoned pits. Mapping of the West pit (Fig. 3) shows that the sulphide orebodies consisted of a series of highly sheared lenses in the immediate hangingwall of the Buchans River Fault (Fig. 3). Massive fractured arkose is found in the footwall of the fault whereas the hangingwall comprises strongly foliated Buchans River Formation felsic tuffs with sulphide and barite lenses. The foliation in these rocks is strongly

Figure 11. Shear joints in massive pillow breccia of the Ski-Hill Formation, Ski Hill.
a) Structural data showing shear joints and shear zones.
b) Stress analysis of dextral shear zones.
c) Stress analysis of sinistral shear zones.
d) Synopsis of stress analysis of shear zones and joints.

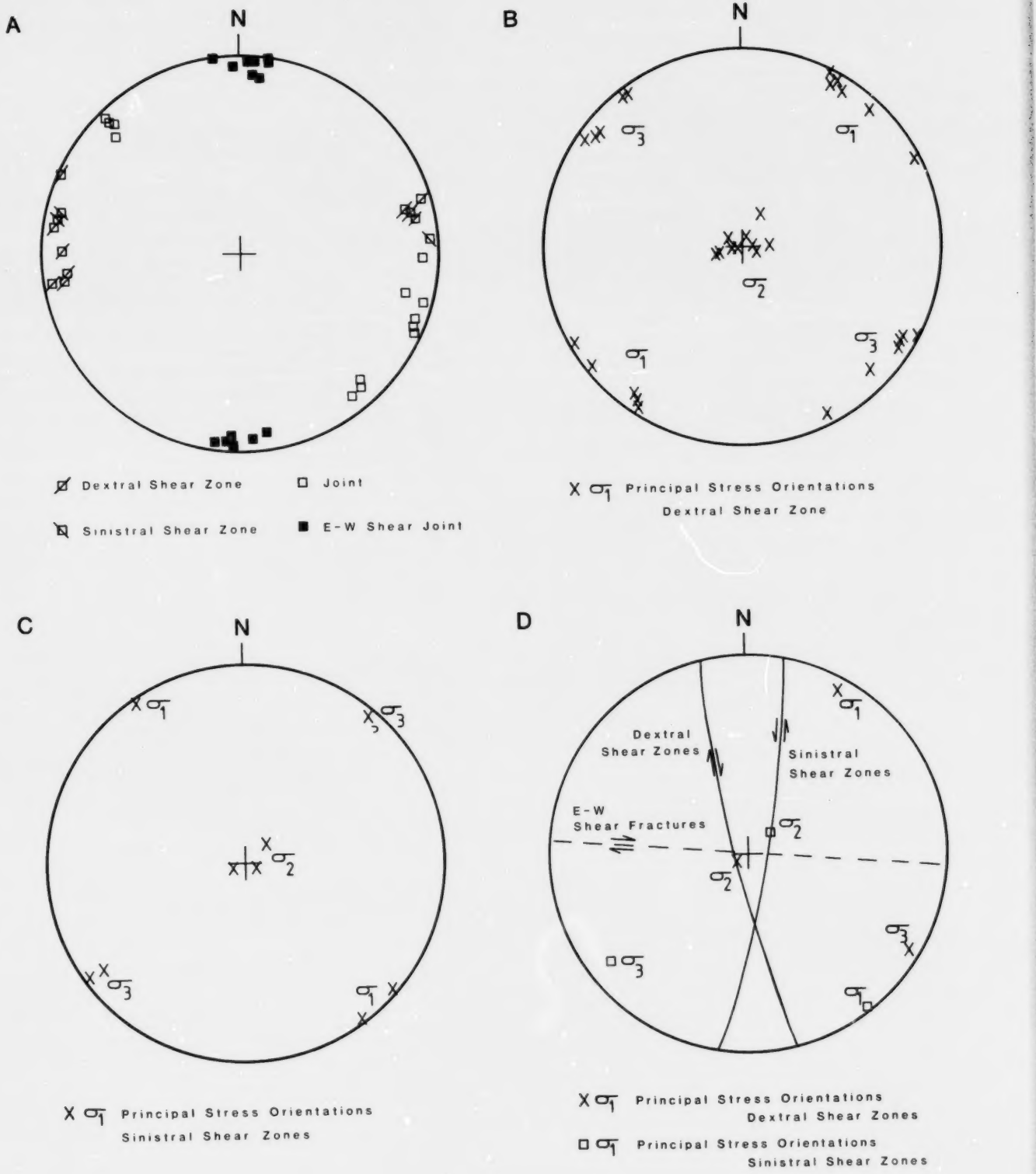

Figure 12. Structural data from the Ski Hill area.

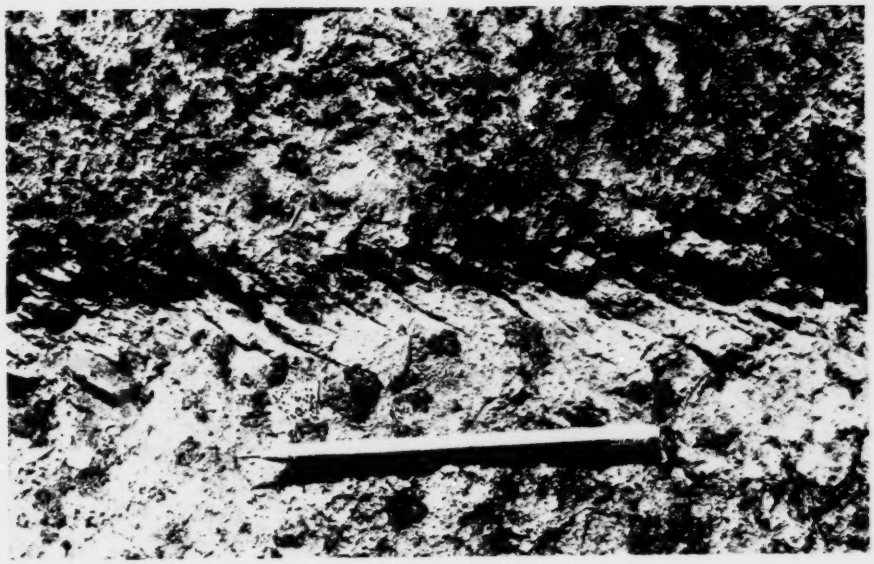

Figure 13. Dextral shear zone in massive pillow breccia of the Ski-Hill Formation, Ski Hill. Note the development of well-formed Riedel shear fractures.

Figure 14. East-west shear fracture with the development of Riedel fractures showing dextral motion. Ski Hill massive pillow breccia.

developed and dips at moderate to shallow angles (Fig. 3). A northeasterly plunging mineral stretching lineation is developed in the foliation plane (Fig. 3).

The sulphide-barite lenses are strongly foliated and are found in listric shear zones within folded and sheared felsic tuffs (Fig. 4). The folded tuff units (Fig. 5) have a strong penetrative axial planar foliation sub-parallel to the shear zones (Fig. 4 and 5). In places the folded barite-sulphide lenses are truncated against discrete shear planes (Fig. 6). Structural data collected from the Oriental pits show a mean foliation plane dipping 40-50° to 348° with a marked mineral stretching lineation indicating up dip movement on shear planes towards 227° (Fig. 7). Figure 8 is a synoptic diagram of the structure of the Oriental Orebodies as they occur in the highly sheared hangingwall of the Buchans River Fault. Movement on this fault plane was in part towards 227°.

Maclean Extension Orebody

Limited underground observations in felsic volcanic rocks that host the MacLean Extension transported fragmental ores (Binney *et al.*, 1983; Binney, 1987) indicate two directions of thrust faults – one set of thrust faults which dip 40-50° northeast with apparent movement directions towards the southwest and a second set of thrust faults dipping northwest with apparent movement directions to the southeast. The relative ages of these fault systems has yet to be determined. In this part of the sequence penetrative foliations are not developed but individual discrete fault planes commonly have very well-developed slickensides (Fig. 9).

Syndepositional extensional fractures are found within the ore zone stratigraphy (Fig. 10) indicating extension during deposition of the sulphides and their host rocks.

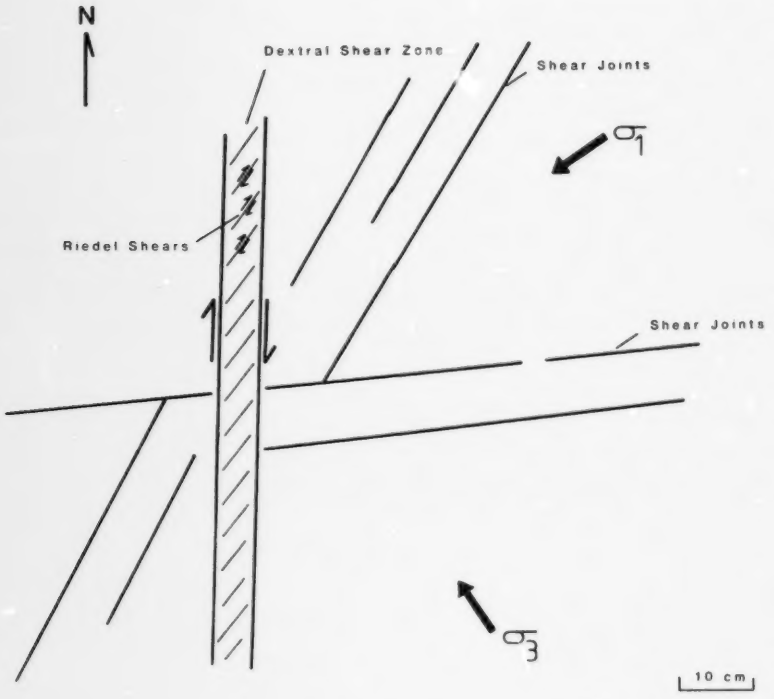

Figure 15. Synopsis of shear zones and joint geometry on Ski Hill.

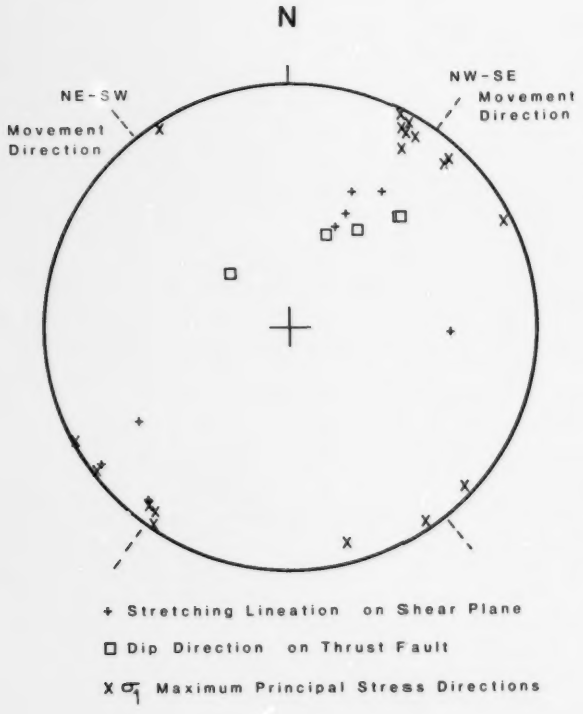

Figure 16. Synopsis of kinematic and dynamic analyses in the Buchans area showing possible movement directions on thrust faults.

Ski Hill Area

The massive pillow lava, breccia and pyroclastic rocks of the Ski Hill Formation occur in the hangingwall of the Ski Hill Fault (Fig. 1) and structurally overlie the Lucky Strike Orebodies (Fig. 1). These rocks are not foliated but contain penetrative and consistent fracture systems. Near conjugate shear joints (Fig. 11) are well developed as are small (up to 20 cm wide but 4-10 m long) shear zones. These approximately north-south shear zones (Fig. 12) show characteristic development of Riedel fractures (Fig. 13) and both dextral and sinistral displacements. Cutting these shear joints and shear zones is a penetrative set of large east-west oriented shear joints (Fig. 14). Riedel fractures associated with these large penetrative joints indicates some dextral movement (Fig. 14). In addition minor mafic dykes are found in this east-west joint system, indicating a component of dilation during this later deformation.

Dynamic analysis of the shear zones and shear fractures in the Ski Hill area indicates two movement patterns – (a) a dominant movement to the southwest as indicated by north-east-southwest oriented maximum principal stress directions σ_1 (Fig. 12b) and (b) a less well-defined movement to the southeast defined by northwest-southeast oriented σ_1 directions (Fig. 12c).

The northeast-southwest σ_1 direction is associated with prominent, well-developed dextral shear zones (Fig. 15) whereas the northwest-southeast σ_1 orientation is associated with less well-developed sinistral shear zones (Fig. 12d).

DISCUSSION AND CONCLUSIONS

Deformation in the Buchans Group (Fig. 1) is dominated by brittle processes with only the local development of ductile deformation fabrics adjacent to major thrust faults. Kinematic and dynamic analysis of deformation fabrics and fractures reveals two possible tectonic transport directions during thrust faulting and imbrication of the Buchans Group stratigraphy (Figs. 1, 2). The suggested probable deformation sequence is: (a) northwest → southeast directed thrust faults with the development of sinistral shear zones and shear joints; foliation development in major fault zones; (b) Late northeast → southwest directed movement on thrust faults (some may have been pre-existent) with the development of a local mineral stretching lineation, dextral shear zones and conjugate shear fractures (Fig. 15), and (c) Late E-W dextral shear jointing-in part dilational (accompanied by dyke emplacement).

This deformation sequence gave rise to the complex arrangement of duplex thrust faults in the Buchans area (Figs. 1 and 2). The probable movement history on these faults is seen to have been complex with more than one period of non-orthogonal movement on individual fault planes. Movement directions are summarized in Figure 16. Further research is needed to relate the mesoscopic movement patterns as discussed in this paper with the regional fault patterns (see Thurlow and Swanson, 1987). This paper has demonstrated that detailed kinematic and dynamic analysis of minor brittle failure structures can provide valuable insights into fault movement histories. Thurlow (1984) has previously suggested that the dominant direction of thrusting was to the southeast whereas this paper has demonstrated that in addition to a southeast transport direction there is also a component of movement towards the southwest. Recognition of these fault patterns and the application of modern concepts of thrust tectonics (Boyer and Elliott, 1982) will lead to a greater understanding of Buchans area geology and the identification of new exploration targets.

ACKNOWLEDGMENTS

Fieldwork at Buchans was supported by the Geological Survey of Canada. Special thanks go to Geoff Thurlow for introducing the author to Buchans geology and providing many informative discussions. Rod Kirkham and Tyson Birkett also provided assistance and stimulating discussions. Tom Easter ably assisted with the photographic reproductions.

REFERENCES

Binney, W.P.
1987: A sedimentological investigation of MacLean channel transported sulphide ores; in Buchans Geology, Newfoundland, ed. R.V. Kirkham; Geological Survey of Canada, Paper 86-24, Report 8.

Swanson, E.A., Strong, D.F. and Thurlow, J.G. (eds.)
1981: The Buchans Orebodies: Fifty Years of Geology and Mining. The Geological Association of Canada, Special Paper 22, 350 p.

Thurlow, J.G. and Swanson, E.A.
1987: Stratigraphy and structure of the Buchans Group; in Buchans Geology, Newfoundland, ed. R.V. Kirkham; Geological Survey of Canada, Paper 86-24, Report 2.

- 4 -

The significance of Middle Ordovician conodonts from the Buchans Group

Godfrey S. Nowlan[1] and J. Geoffrey Thurlow[2]

Nowlan, Godfrey S. and Thurlow, J. Geoffrey, The significance of Middle Ordovician conodonts from the Buchans Group; in Buchans Geology, Newfoundland, ed. R.V. Kirkham; Geological Survey of Canada, Paper 86-24, p. 59-62, Report 4, 1987.

Abstract

The authors previously have reported Middle Ordovician (Whiterockian) conodonts from carbonate clasts in the Buchans Group and have suggested that these conodonts indicate the age of at least part of the unit. No new conodont data from the Buchans Group are presented herein, but their significance is reviewed in the light of new information presented in this volume and elsewhere. In terms of the revised stratigraphy presented in this volume, all the clasts are from approximately the same stratigraphic level near the base of the Sandy Lake Formation. Radiometric dates reported in this volume are more in accord with the age indicated by conodonts than were previous results. New lead isotope evidence presented elsewhere suggest different source materials for the Buchans and Victoria Lake groups and thus the two units may not be lateral facies equivalents as previously suggested by the authors. In fact the slight difference in age suggested by conodonts from the two groups may thus be significant. Conodonts and other fossils from the Glover Formation in the Grand Lake area suggest that the unit is considerably older than the Buchans Group. Conodont colour alteration indices suggest that the Sandy Lake Formation may once have been buried to depth 5700-9000 m, although the overall thermal regime resulting from plutonism has not been taken into account.

Résumé

Les auteurs avaient déjà signalé la présence de conodontes de l'Ordovicien moyen (Whiterockien) dans des clastes carbonatés du groupe de Buchans; ils ont suggéré que ces conodontes représentent l'âge d'au moins une partie de l'unité. Cette étude ne fournit aucune nouvelle donnée sur les conodontes du groupe de Buchans, mais elle examine l'importance de ces restes en regard des nouvelles informations données dans ce volume et ailleurs. Pour ce qui est de la stratigraphie révisée présentée dans ce volume, tous les clastes proviennent plus ou moins du même niveau stratigraphique près de la base de la formation de Sandy Lake. Les dates isotopiques données dans ce volume concordent mieux avec l'âge indiqué par les conodontes que ne l'avaient fait les résultats antérieurs. D'après les nouvelles données sur les isotopes de plomb présentées ailleurs, les matériaux qui ont donné le groupe de Buchans et ne seraient pas les mêmes que ceux qui ont produit le groupe de Victoria Lake; ainsi, contrairement à une hypothèse proposée par divers chercheurs, il se peut que ces deux unités ne représentent pas des faciès latéraux équivalents. En réalité, la légère différence d'âge donnée par les conodontes tirés des deux groupes pourrait donc se révéler très importante. Les conodontes et d'autres fossiles provenant de la formation de Glover aux alentours de Grand Lake laissent supposer que l'unité est beaucoup plus ancienne que le groupe de Buchans. Ces indices laissent supposer que la formation de Sandy Lake aurait jadis été enfouie à une profondeur d'entre 5 700 et 9 000 mètres, bien qu'on n'ait pas tenu compte du régime thermique global résultant du plutonisme.

[1]Geological Survey of Canada, 601 Booth St., Ottawa, K1A 0E8
[2]BP Canada-Selco Division, P.O. Box 789, Corner Brook, Newfoundland A2H 6G7 (formerly with Abitibi-Price Inc.)

INTRODUCTION

The recovery of Middle Ordovician conodonts from the Buchans Group was reported by Nowlan and Thurlow (1984) and the reader is referred to that publication for a detailed account of the occurrence and conclusions. This contribution is intended to provide only a brief summary of the significance of the conodonts in the context of the advances in knowledge of Buchans Group geology presented in this volume. No new conodont data are available, except for a sparse fauna from the Glover Formation (see below).

STRATIGRAPHIC POSITION OF SAMPLES

Nowlan and Thurlow (1984) reported Middle Ordovician conodonts from carbonate clasts within breccia units of the Buchans Group. The conodont-bearing clasts came from diamond-drill core in two distinct areas: a northern region just west of the town of Buchans (Hole 2932) and the Wiley's River area about 4-5 km south of Buchans (Holes 2764, 2933 and 3311, see Nowlan and Thurlow, 1984, Fig. 1). The northern occurrences were considered to be from the uppermost part of the "Lucky Strike ore horizon sequence", about 100 m above the ore horizon itself, and the southern occurrences were thought to form part of the "prominent quartz sequence" at a lower stratigraphic level. Nowlan and Thurlow (1984) acknowledged that correlation between the two areas was uncertain because of the complexity of thrust faulting in the area. Recent reinterpretation of the stratigraphy and fault patterns in the Buchans area has led to the production of new, simplified stratigraphic nomenclature and to the recognition of a much more intricate pattern of faults (Thurlow and Swanson, 1987). Their work suggests that all the carbonate clasts are from approximately the same stratigraphic level near the base of the Sandy Lake Formation that overlies the ore-bearing Buchans River Formation.

AGE, PALEOGEOGRAPHY AND CORRELATION

One of the main conclusions of Nowlan and Thurlow (1984, p. 290, 291) is that the carbonate clasts hosting the conodonts are of local Buchans Group origin, probably derived from carbonates formed around active volcanic islands. They supported this conclusion by pointing to the difficulty of deriving clasts from elsewhere into the demonstrably shallow water and active volcanic setting of the Buchans Group. Potential sources such as the Table Head Group, deposited on the western margin of the Iapetus Ocean were discounted because of the improbability of clasts travelling downslope, across the sea bottom and upward to the shallow volcanic setting. Another line of evidence supporting this conclusion is that all the other clasts in the breccia can be shown to be of local origin. Nowlan and Thurlow (1984) were therefore of the opinion that the age indicated by the condonts is indeed the age of the Buchans Group.

The conodont assemblage in the Buchans Group is characterized by specimens of "*Cordylodus horridus*" Barnes and Poplawski and *Histiodella holodentata* Ethington and Clark. These and other species recovered indicate a Whiterockian (latest Arenig-early Llanvirn age). This is a slightly older assemblage than that indicated by conodonts from the Victoria Lake Group (Kean and Jayasinghe, 1980) which suggest an age near the Llanvirn-Llandeilo boundary. The similarity in age of the two groups led Nowlan and Thurlow (1984) to suggest that they might be lateral facies equivalents. New Pb isotope evidence presented by Swinden and Thorpe (1984) suggest substantially different source areas for Pb in the Buchans sulphide deposits as compared to volcanogenic deposits in the Victoria Lake Group and therefore that the two groups may not be facies equivalents. In light of this new information the slight age difference indicated by conodonts may be of greater significance than previously considered. However, on the basis of the fossil evidence we cannot agree that the Buchans Group is younger than the Victoria Lake Group as suggested by Swinden and Thorpe (1984, p. 1597, 1613). The fact that conodonts from the uppermost Victoria Lake Group are younger than conodonts from the upper part of the Buchans Group supports the southerly to southeasterly overthrust pattern suggested for the region, with older Buchans Group rocks thrust over younger Victoria Lake Group rocks. This tectonic style is in part similar to that proposed for parts of Notre Dame Bay (e.g. Karlstrom *et al.*, 1982) and is in agreement with suggestions that the Dunnage Zone is allochthonous (Colman Sadd and Swinden, 1985). The conodont data from the Buchans Group lend support to the regional structural-stratigraphic models of Nelson and Kidd (1979), Kusky and Kidd (1985) and others who propose a pre-Caradoc age for the Buchans and Roberts Arm groups.

Conodonts have also been recovered from a locality within the Glover Formation 75 km west-southwest of Buchans (GSC loc. 97971, 98687). The Glover Formation has been suggested as a possible correlative of the Buchans Group because of lithological similarity (Whalen and Currie, 1983). The conodont fauna is sparse and poorly preserved but includes representatives of *Periodon flabellum* (Lindström), *Protopanderodus rectus* (Lindström) and *Scolopodus* sp. aff. *S. gracilis* Ethington and Clark (Nowlan, 1982). This meagre assemblage suggests a mid to late Arenig (Early Ordovician) age.

The locality from which the conodonts were obtained is 2.3 km northeast of a previously known graptolite locality in strata of the Glover Formation (GSC 87420) reported by Dean (1976, p. 236) and by Williams and St. Julien (1978, p. 227, Fig. 44.2). The graptolites identified by R.B. Rickards and D. Skevington indicate a mid-Arenig (Didymograptus protobifidus Zone) age. On the available evidence, the Glover Formation is considerably older than the Buchans Group.

RADIOMETRIC DATES

Several attempts have now been made to date the Buchans Group radiometrically. Bell and Blenkinsop (1981) obtained a Rb-Sr whole rock isochron of 447 ± 18 Ma, suggesting an age younger than that indicated by the conodonts. Stewart (1987) report dates from zircons in rhyolite (465 ± 10 Ma)

and granitoid clasts (464 ± 40 Ma). Granite of the Topsails igneous terrane, which intrudes the Buchans Group and transects the thrust faults has also been the subject of radiometric investigation. Bell and Blenkinsop (1981) report Rb/Sr ages of 387 ± 16 and 421 ± 7 and more recently, zircons have yielded U-Pb dates in the range of 425-430 Ma (Whalen and Currie, 1987). These Early Silurian dates suggests an upper limit on the age of the Buchans Group and the timing of thrusting.

THERMAL MATURATION

Apart from the age of the Buchans Group the conodonts may also indicate the depth of tectonic burial of the Sandy Lake Formation at Buchans. As reported by Nowlan and Thurlow (1984) the conodonts recovered have a colour alteration index (CAI) of 4 indicating that the strata have been heated to temperatures of 190°-300°C (see Epstein *et al.*, 1977). Assuming an average thermal gradient of about 1°C per 30 m, this may suggest that the Sandy Lake Formation was once buried to a depth of 5700-9000 m. The contribution to the overall thermal regime made by the intrusion of the Topsails Granite is uncertain and not taken into account in this estimate. The conodonts from the Victoria Lake Group reported by Kean and Jayasinghe (1980) were noted by Stouge (the author of the original unpublished report) to have a CAI of 5 (Kean, personal communication, 1984). This higher level of thermal alteration might be expected in the more deeply buried, lower structural slices, although it must be emphasized that other factors such as local intrusive and volcanic activity may have played a role in the thermal history of the region.

REFERENCES

Bell, K. and Blenkinsop, J.
1981: A geochronological study of the Buchans area, Newfoundland; in The Buchans Orebodies: Fifty Years of Geology and Mining, ed. E.A. Swanson, D.F. Strong and J.G. Thurlow; Geological Association of Canada, Special Paper 22, p. 91-111.

Colman Sadd, S.P. and Swinden, H.S.
1985: A tectonic window in central Newfoundland? Geological evidence that the Appalachian Dunnage Zone may be allochthonous; Canadian Journal of Earth Sciences, v. 21, p. 1349-1367.

Dean, P.L.
1977: A report on the geology and metallogeny of the Notre Dame Bay area; Mineral Development Division, Department of Mines and Energy, Government of Newfoundland and Labrador, Report 77-10, 17 p.

Dean, W.T.
1976: Some aspects of Ordovician correlation and trilobite distribution in the Canadian Appalachians; in The Ordovician System: Proceedings of a Paleontological Association Symposium, Birmingham, September 1974, ed. M.G. Bassett; University of Wales Press and National Museum of Wales, Cardiff, p. 227-250.

Epstein, A.G., Epstein, J.B., and Harris, L.D.
1977: Conodont color alteration – an index to organic metamorphism; United States Geological Survey, Professional Paper 995, 27 p.

Karlstrom, K.E., van der Pluijm, B.A., and Williams, P.F.
1982: Structural interpretation of the eastern Notre Dame Bay area, Newfoundland: regional post-Middle Silurian thrusting and asymmetrical folding; Canadian Journal of Earth Sciences, v. 19, p. 2325-2341.

Kean, B.F. and Jayasinghe, N.R.
1980: Badger map area (12A/16), Newfoundland; Mineral Development Division, Department of Mines and Energy, Government of Newfoundland and Labrador, Report 80-1, p. 37-43.

Kusky, T.M. and Kidd, W.S.F.
1985: Middle Ordovician conodonts from the Buchans Group, central Newfoundland, and their significance for regional stratigraphy of the Central Volcanic Belt: Discussion; Canadian Journal of Earth Sciences, v. 22, p. 484, 485.

Nelson, K.D.
1981: Melange development in the Boones Point Complex, north-central Newfoundland; Canadian Journal of Earth Sciences, v. 18, p. 433-442.

Nelson, K.D. and Kidd, W.S.F.
1979: The age of the Roberts Arm Group, north-central Newfoundland: Discussion; Canadian Journal of Earth Sciences, v. 16, p. 2068-2070.

Nowlan, G.S.
1982: Report on a single sample collected for conodont analysis by E. Erdmer (I.S.P.G., Ottawa) from 3 km northeast of the northeast corner of Corner Pond, south of Glover Island, west central Newfoundland; Ottawa Paleontology Section, Geological Survey of Canada, Report 05-GSN-1982 (unpublished).

Nowlan, G.S. and Thurlow, J.G.
1984: Middle Ordovician conodonts from the Buchans Group, central Newfoundland, and their significance for regional stratigraphy of the Central Volcanic Belt; Canadian Journal of Earth Sciences, v. 21, p. 284-296.

Stewart, P.W.
1987: Geology and genesis of granitoid clasts in the MacLean Extension transported orebody; in Buchans Geology, Newfoundland ed. R.V. Kirkham; Geological Survey of Canada, Paper 86-24, Report 9.

Swinden, H.S. and Thorpe, R.
1984: Variations in style of volcanism and massive sulphide deposition in Early to Middle Ordovician island arc sequence of the Newfoundland Central Mobile Belt; Economic Geology, v. 79, p. 1596-1619.

Thurlow, J.G. and Swanson, E.A.
1987: Stratigraphy and structure of the Buchans Group; in Buchans Geology, Newfoundland, ed. R.V. Kirkham; Geological Survey of Canada, Paper 86-24, Report 2.

Whalen, J.B. and Currie, K.L.
1983: The Topsails igneous terrane of western Newfoundland; in Current Research, Part A, Geological Survey of Canada, Paper 83-1A, p. 15-23.

Whalen, J.B. and Currie, K.L.
1987: Relationship of the Topsails Igneous Terrane to the Buchans Group; in Buchans Geology, Newfoundland, ed. R.V. Kirkham; Geological Survey of Canada, Paper 86-24, Report 6.

Williams, H. and St.-Julien, P.
1978: The Baie Verte – Brompton line in Newfoundland and regional correlations in the Canadian Appalachians; in Current Research Part A, Geological Survey of Canada, Paper 78-1A, p. 225-229.

- 5 -

Interpretation of an aeromagnetic gradiometer survey in the Buchans area

L.J. Kornik[1], J.B. Whalen[1], and J.G. Thurlow[2]

Kornik, L.J., Whalen, J.B., and Thurlow, J.G., Interpretation of an aeromagnetic gradiometer survey in the Buchans area; in Buchans Geology, Newfoundland, ed. R.V. Kirkham; Geological Survey of Canada, Paper 86-24, p. 63-67, Report 5, 1987.

Abstract

The Buchans and Badger map areas of central Newfoundland were surveyed in August, 1983 with the Geological Survey of Canada's aeromagnetic gradiometer system. The vertical gradient and total field maps are extremely useful in outlining the shape, interrelationships and structural effects of the Topsails intrusions. In light of the poor outcrop and complex structure in this part of Newfoundland these maps give structural information otherwise not obtainable. Ubiquitous northeast-trending structural magnetic anomalies appear to reflect the position and shape of the individual intrusive centres in the Topsails igneous terrane and also appear to outline, along with northwest trends, the composition and fabric of remnants of the older Hungry Mountain Complex. The aeromagnetic data indicate the presence of northwest-trending faults within the Buchans Group which truncate and displace magnetic units. These magnetic units represent structurally controlled dykes, sills and laccoliths of possibly early Topsails mafic igneous activity. Information on the stress regime prevailing at the time of intrusion, as deduced from the magnetic data, should be pertinent to an understanding of faults in the Buchans Group.

Résumé

En août 1983, un levé a été effectué à l'aide du gradiomètre aéromagnétique de la Commission géologique du Canada dans les régions cartographiques de Buchans et de Badger, dans la partie centrale de Terre-Neuve. Les cartes produites du gradient vertical et du champ total sont très utiles pour délimiter la forme, les liens et les effets structuraux sur les roches encaissantes des intrusions de Topsails. Ces cartes fournissent des détails structuraux qui autrement n'auraient pas été obtenus, étant donné le nombre très restreint d'affleurements dans cette partie de la province. Les anomalies magnétiques structurales ubiquistes à orientation nord-est semblent traduire la position et la forme des divers centres intrusifs dans le terrane igné de Topsails et délimiter, conjointement avec les orientations nord-ouest, la composition et la texture des restes du complexe plus ancien de Hungry Mountain. En outre, les données aéromagnétiques révèlent la présence, à l'intérieur du groupe de Buchans, de failles à orientation nord-ouest qui traversent et ont déplacé des unités magnétiques. Ces unités magnétiques représentent des filons, des filons-couches et des laccolites qui étaient soumis à un contrôle structural et qui pourraient avoir été formés par une des premières phases d'activité du magma igné mafique de Topsails. Les données magnétiques fournissent des renseignements sur le régime de contraintes qui dominait au moment de l'intrusion; ces informations aideront à mieux connaître les failles dans le groupe de Buchans.

[1]Geological Survey of Canada, 601 Booth St., Ottawa K1A 0E8
[2]BP Canada-Selco Division, P.O. Box 789, Corner Brook, Newfoundland, A2H 6G7 (formerly with Abitibi-Price Inc.).

INTRODUCTION

The Buchans and Badger map areas of western Newfoundland were surveyed with the Geological Survey of Canada's aeromagnetic gradiometer system in August, 1983. This survey was carried out under the Canada-Newfoundland co-operative mineral program.

The extensive drift cover in the survey area makes geological mapping difficult. Based on existing maps (Kean, 1979; Kean & Jayasinghe, 1982; Whalen and Currie, 1983a, b), the area can be subdivided into three main zones: (a) the Topsails igneous terrane in the north and west, (b) a central zone consisting of the Buchans and Victoria Lake groups and Carboniferous clastic sedimentary rocks and (c) the Crippleback Lake intrusive complex in the southeast corner.

The total field and vertical gradient maps of the Buchans and Badger map areas were compiled from east-west survey lines flown at an altitude of 150 metres with a spacing of 300 metres. The maps were coloured with the Applicon colour plotter and published at the scale of 1:50,000. The vertical gradient map of the Buchans map area is included with this volume. Other types of enhanced and derived aeromagnetic maps were produced to aid in the interpretation but are not included in this paper.

AEROMAGNETIC LITHOLOGIC CORRELATIONS

Comparison of available geological data with the new aeromagnetic data indicates that the Topsoils igneous terrane is characterized by magnetic anomalies which reveal both contact relationships of the granitoid Topsails intrusions with the adjacent Buchans Group and structures within the Topsails intrusions related to their final emplacement. A lack of correspondence exists between mapped lithological units and magnetic anomalies within areas underlain by the Buchans Group. Magnetic anomalies within the Buchans Group appear to be correlatable with mafic dykes and sills which probably represent early mafic Topsails intrusions. The areas mapped as Victoria Lake Group and Carboniferous sedimentary rocks lack magnetic anomalies or have extremely weak or diffuse magnetic anomalies. The Crippleback Lake intrusive complex is characterized by magnetic anomalies similar to those within the Topsails igneous terrane.

The southern margin of the Topsails igneous terrane is characterized by arcuate contacts outlined by strong magnetic anomalies or clusters of strong anomalies. These anomalies correlate with areas of mafic rocks of the older Hungry Mountain Complex, which appear to be disrupted and intruded by Topsails granitoid intrusions. Drill logs at Buchans indicate a mixed assemblage of mafic and felsic rocks in the Topsails intrusions in the Buchans area. This mixed assemblage has also been documented by Whalen *et al.* (1984) in the area to the west of Buchans. The Topsails igneous terrane contains ovoid high-level intrusions separated by screens and roof pendants of older igneous rocks. Four plutons or intrusive centres exist in the surveyed area (Fig. 1) as well as portions of others centred to the north of the study area. In the Badger map area, the Skull Hill syenite (Area 1 in Fig. 1) and an area of Hungry Mountain Complex roof rocks (Area 2 in Fig. 1) constitute two intrusive centres. In the Buchans map sheet a complex intrusive centre occurs in the northeast corner (Area 3 in Fig. 1) and another ovoid centre (Area 4 in Fig. 1) occurs directly north of the town of Buchans.

Each individual intrusive centre contains different and distinct patterns of magnetic screen and cover rocks and non-magnetic felsic intrusive rocks. The pattern of magnetic anomalies produced by screens or cover rocks appears to arise from magnetic rocks fractured and then pulled apart and separated by intervening non-magnetic intrusive material. This seems to be a consistent and pervasive feature as this texture occurs even in the least magnetic portions of the intrusive centres. Units immediately above or adjacent to the ovoid intrusions usually have strong magnetic anomalies associated with them which are presumed to be areas underlain by the Hungry Mountain Complex.

As mentioned above, the Buchans Group apparently does not contain obvious magnetic anomalies correlatable to volcanic or sedimentary lithologic units. The linear magnetic anomalies within the Buchans Group are interpreted to reflect diabase or mafic dykes intruded during an early stage of the Early Silurian Topsails igneous activity (Whalen & Currie, 1987). Less distinct anomalies are interpreted to be sills intruded along subhorizontal thrust faults. These magnetic anomalies are very disrupted, a pattern interpreted to be a result of extensive later faulting. Mafic lavas in the Buchans Group do not appear to have a positive magnetic expression, probably due to the alteration of magnetite to hematite in these volcanic rocks.

AEROMAGNETIC STRUCTURAL INTERPRETATION

Patterns present in the aeromagnetic data in the Topsail igneous terrane differ from those present over plutons in Nova Scotia north of Halifax and from various igneous regimes in the Canadian Shield. The aeromagnetic data suggest a unique and complex igneous style compared to that revealed by other vertical gradiometer surveys. The aeromagnetic maps over the Buchans Group also indicte a complicated and complex structural environment. Aeromagnetic anomalies suggest that structures change with depth and a "veneering" of structures is present in many localities. This complexity is due to the complicated thrust faults present in these localities (e.g. Thurlow and Swanson, 1987; McClay, 1987).

Contacts of the intrusive Topsails igneous terrane are clearly delineated on the aeromagnetic maps. These maps reveal a consistent northeast fabric which appears to be related to the trend of units in the Hungry Mountain Complex and to mafic dykes in the Buchans Group. A set of northwest-trending faults cuts all units in the map area. Arcuate trends or truncations attributed to thrust faults occur in the Buchans

Group immediately adjacent to the boundary zones of Hungry Mountain Complex rocks at the southern contacts of the intrusive granitic bodies in the Buchans area.

The entire area of Buchans and Victoria Lake group rocks is interpreted to contain southeast-trending strips 5 to 8 kilometres wide bounded by major northwest faults or fault zones. These strips also contain smaller faults parallel to the larger ones. Major faults appear to originate from emplacement centres of the larger intrusive lobes of Topsails granite (Fig. 1). These faults are very conspicuous in areas where the linear magnetic anomalies in the adjacent Buchans Group are truncated and displaced.

The patterns of magnetic anomalies present in the Topsails igneous terrane suggest structural features such as those produced by Ramberg (1981) in centrifuge models of thin-skinned diapirs. Initially, as indicated by these models expansion of thin, brittle cover produces a typical "pull-apart" texture in the magnetic patterns. Further expansion in the centrifuge models produces parallel folds or imbricate "shingles" of brittle cover material around the periphery of the diapir. Such linear structures parallel to diapir boundaries appear to be present in several places along the boundaries of the Topsails intrusions. Greater expansion of the thin-skinned cover over the diapirs creates expansion faults or tear shears in the brittle boundary structures. Probable tear or expansion faults are indicated by the magnetic patterns in many places along the boundaries of the Topsails intrusions. We interpret the magnetic anomaly patterns as exhibiting all of the features related to thin-skinned diapirism as illustrated by Ramberg (1981). The model suggested for the Topsails intrusions is a mature high-level diapir centred to the north off the map area. This diapir reached its vertical buoyancy level in the crust, became very viscous and spread laterally into the surrounding rocks where it crystallized. Magnetic rocks of the Hungry Mountain Complex appear to be the brittle, thin-skinned roof of the diapir throughout most of the survey area. In the map area the erosion level has just penetrated the roof over much of the lateral lobes of the diapir.

The simple concentric and pull-apart structures indicated in centrifuge models appear to be modified in Topsails intrusions by later lateral movement of magma towards the contacts. Uplift and displacement of adjacent Buchans Group rocks by such movement is evidenced by thrust faults and uplift parallel to the intrusive contacts. As well, this lateral flow may have produced tensional and tear faults filled with granitic material in the boundary areas and large east-northeast tensional fractures in the mobile roof plates perpendicular to the flow direction. This set of large parallel expansion shears are obvious in the aeromagnetic maps in the Topsails igneous terrane north of the town of Buchans. We

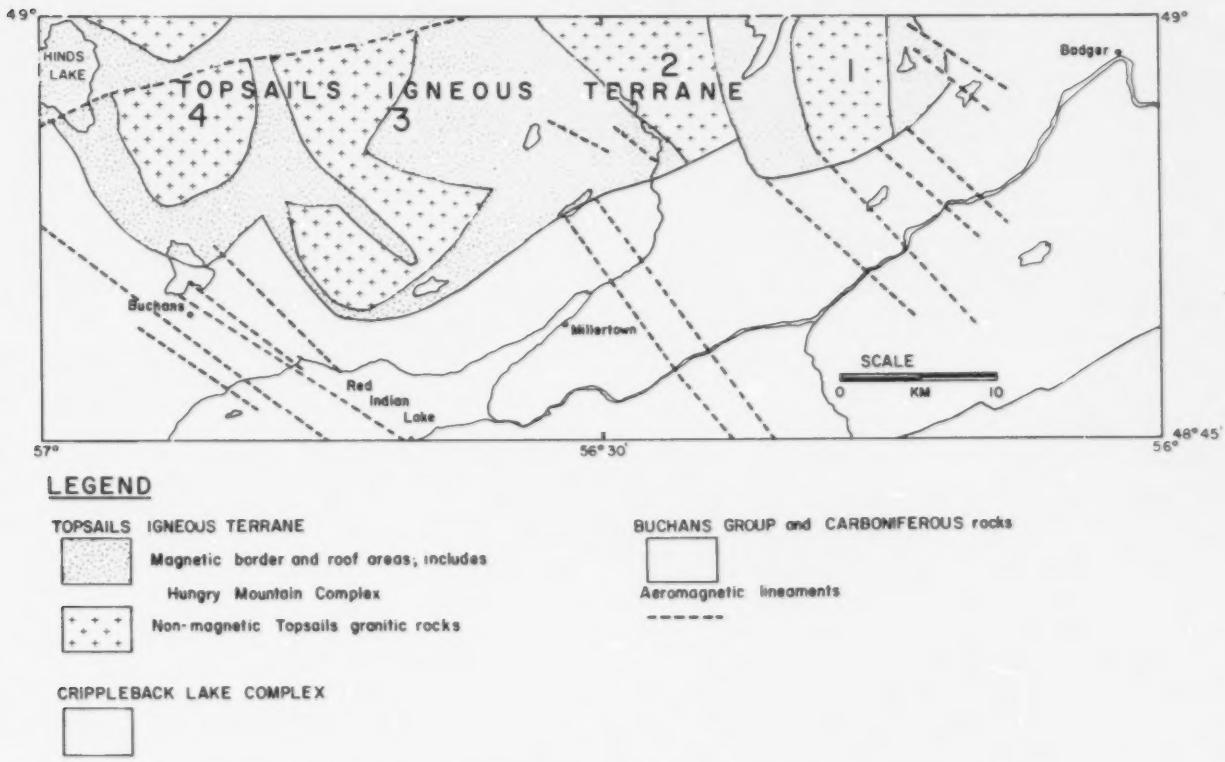

Figure 1. Generalized geology of the Buchans area as interpreted from aeromagnetic data.

believe that flow perpendicular to the linear imbricate shingles at the boundaries of the intrusions rotated these shingles into the flow direction and away from the contacts. Such rotation of contact blocks appears to be outlined clearly by a clockwise fanning of magnetic anomalies along the western contact zone of the Topsails igneous terrane north of the town of Buchans. Magnetic patterns also indicate another type of movement of magma beneath the cover-rocks within the Topsails intrusions. These areas of flow are portrayed clearly by magnetic patterns resembling "sea-pack ice flow". Features such as abutting of adjacent anomalies and interdigitization of anomalies suggests that flow of viscous magma has selectively rotated, submerged and overidden blocks, thus changing the "pull-apart" structures into compressional structures.

A close examination of magnetic patterns in the Skull Hill intrusion (Area 1 in Fig. 1), suggests that the northeastern edge is segmented by numerous parallel northwest trending faults with each slice progressively uplifted towards the southwest. Along the south side of the Skull Hill intrusion a lateral southeastly directed displacement of the adjoining Buchans Group is indicated in two major fault bounded blocks with smaller inter-block adjustments along parallel northwest-trending faults. A major northwest-trending zone of displacement, approximately two kilometres wide, occurs along the southwestern edge of the Skull Hill intrusion and appears to be traceable across the Buchans and the Victoria Lake groups. The magnetic anomaly patterns over the intrusion suggest that roof rocks suffered east-west displacements as well as southwest-northeast extension. This pattern could be the result of fracturing of roof rocks over a vertically rising intrusion and displacement of rocks to the south due to lateral movement in a southwest direction. Complicated interference patterns appear to have been produced by interaction between the southward lateral movement away from the Skull Hill centre and southeasterly directed lateral movement away from the adjacent intrusive centre to the west. Magnetic anomaly patterns suggest southwesterly directed thrust slices along the southwest corner of the Skull Hill intrusion. These thrusts are involved with the southeasterly directed faults in the Buchans Groups away from the intrusive centre to the west (Area 3 in Fig. 1).

The magnetic features of Area 2 in Figure 1, the area of Hungry Mountain roof rocks, suggests disruption and extension in both southwest and southeast directions. Individual blocks appear chaotic in orientation due to what appears to be selective rotation of adjacent blocks. Its southwestern boundary is characterized by a sharp northwest-trending alignment of magnetic anomaly truncations against the larger intrusive lobe to the west in which prominent flow textures are present (Area 3 in Fig. 1).

The intrusive centre (Area 3 in Fig. 1), which occupies the northeastern quarter of the Buchans map sheet, is larger and more complicated than the others. Several areas of weaker amplitude magnetic anomalies, interpreted to be more homogeneous amphibole granite, occur in this lobe bounded by more magnetic screens and rafts of roof rocks. Magma flow into a postulated bulge of granitic material under the Buchans Group in the vicinity of Millertown appears to have caused magnetic roof rocks at the western edge of Area 2 to be dragged into the adjacent Area 3 resulting in compressional "sea-pack ice flow" features. This flow ends at the middle of the southeastern contact with the Buchans Group in a hinge point from which the magnetic anomalies radiate outward in a fan. This pattern suggests progressive southeast extension east from the hinge point toward the northeastern contact of Area 3. This region also has well-developed southwest compression structures. At this hinge point magnetic anomalies can be moved and fitted back together by 1 kilometre of movement on the southern limb and 2 kilometres of movement on the northern limb. This movement is marked by a "trail" of small weak and separate magnetic anomalies which are interpreted to represent a "detrital trail" of stretched and boundinaged or shattered brittle roof rocks. This detrital trail is interpreted to be due to extension of brittle material in a viscous medium. Drill cores from short holes in this area indicates the assimilation of amphibolitic material in granite with some flow layering. Similar evidence for longer detrital trails presumably also caused by brittle extension, is present along this contact west of the hinge point. Five kilometres or more of movement, due to flow, appears to be possible from the magnetic data. These areas have a consistent topographic expression outlined by many parallel watercourses at right angles to the inferred extension direction. Immediately northwest of this area of flow-patterned magnetic anomalies is a screen of rafts of Hungry Mountain rocks about five kilometres wide which trends in a north-northeast direction to the north edge of the map. Different apparent senses of movement and rotation of these rafts occur in various parts of this screen. Northwest of this screen along the western edge of Area 3 is an area of magnetic anomalies with lower amplitudes and a more uniform texture which is underlain by more homogeneous coarse grained amphibole granite. Magnetic patterns in these areas suggest typical pull-apart structures with both southeast and southwest extensions between the magnetic anomalies. The original arcuate southwest boundary of this lobe, appears to have been modified by southeasterly flow of magma along this contact. This late southeasterly flow, which originated from an area along the eastern edge of Area 4, produced compressional textures in the magnetic anomalies at the junction of Areas 3 and 4. This late flow is interpreted to have also produced and modified the fault structures in the adjacent Buchans Group rocks. The southwest extensional features in Areas 3 and 4 appear to be manifested as thrust faults in the Buchans Group. As mentioned earlier a screen of Hungry Mountain rocks characterized by flow-patterned magnetic anomalies occurs between Areas 3 and 4. The northwestern contact of Area 4, another region of radiating magnetic anomalies contains less obvious flow patterns. The fan structure diverges in a clockwise direction, presumably produced by Topsails intrusive material dragging and rotating the originally parallel imbricate shingles away from the contact and perpendicular to the flow direction.

SUMMARY AND CONCLUSIONS

The aeromagnetic data in the Buchans and Badger map areas are extremely useful in delineating the shape, interrelationships and structural effects on host rocks of Topsails intrusions. Patterns and fabric of magnetic anomalies in the Topsails igneous terrane indicate that the granitic intrusions spread from central cores which intruded and displaced the Hungry Mountain Complex and adjacent Buchans Group rocks. Areas of roof pendants or screens between these intrusive centres display a typical "pull-apart" structure which also exists in a subdued manner in all parts of the Topsails igneous terrane. Lateral subhorizontal movement of these stocks resulted in relative displacement of strips of adjacent Buchans Group rocks along northwest-trending faults and fault zones. Interaction between arcuate lobe boundaries also resulted in complex relationships of intersecting thrust planes in adjacent Buchans rocks. The magnetic data significantly augment geological mapping by helping outline the intrusive structures developed during the emplacement of high-level granitic bodies into brittle older igneous and volcanic-sedimentary rocks. The intrusive mechanism may resemble those described for post-orogenic granites elsewhere (Ehlers & Bergman, 1984; Holder, 1979) or generated in models (Ramberg, 1970) in which funnel-shaped ring intrusions are formed, and the intruding granite lifts zones or slices of shattered host rocks. In the Buchans Group, magnetic anomalies particularly highlight possibly earlier Silurian Topsails mafic igneous activity. These structurally controlled dykes, sills and laccoliths reflect the tensional environment prevailing at the time of emplacement and probably record information pertinent to an understanding of faulting and thrusting in the Buchans Group rocks and orebodies. The area is extremely complicated structurally and much further information on this area should be forthcoming from further study of the aeromagnetic data and a more rigorous correlation with new geological data.

REFERENCES

Ehlers, C. and Bergman, L.
1984: Structure and mechanism of intrusion of two post-orogenic granite massifs, southwestern Finland; in Precambrian Tectonics Illustrated, ed. A. Kroner and R. Greiling; Stuttgart, Germany, p. 173-190.

Geological Survey of Canada
1985: Aeromagnetic Vertical Gradient Map, Buchans, Newfoundland; 12 A/15, Geological Survey of Canada, Geophysical Series, Map C40 097G.

Geological Survey of Canada
1985: Aeromagnetic Vertical Gradient Map, Badger, Newfoundland; 12 A/16, Geological Survey of Canada, Geophysical Series, Map C40 096G.

Geological Survey of Canada
1985: Aeromagnetic Total Field Map, Buchans, Newfoundland; 12 A/15, Geological Survey of Canada, Geophysical Series, Map C20 356G.

Geological Survey of Canadda
1985: Aeromagnetic Total Field Map, Badger, Newfoundland; 12 A/16, Geological Survey of Canada, Geophysical Series, Map C20 355G.

Holder, M.T.
1979: An emplacement mechanism for post-orogenic granites and its implication for their geochemical features; in Origin of Granite Batholiths, Geochemical Evidence, ed. M.P. Atherton and J. Tarney; Shiva Publications Limited, Cheshire, United Kingdom, p. 116-128.

Kean, B.F.
1979: Buchans, Newfoundland; Newfoundland Department of Mines and Energy, Mineral Development Division, Map 79-125.

Kean, B.F. and Jarasinghe, N.R.
1982: Geology of the Badger Map Area (12A16), Newfoundland; Newfoundland Department of Mines and Energy, Mineral Development Division, Report 81-2.

McClay, K.R.
1987: Aspects of the structural geology of the Buchans area; in Buchans Geology, Newfoundland, ed. R.V. Kirkham; Geological Survey of Canada, Paper 86-24, Report 3.

Ramberg, H.
1970: Model studies in relation to intrusion of plutonic bodies; in Mechanism of Igneous Intrusion, ed. G. Newall and N. Rast; Geological Journal, Special Issue, Gallery Press, Liverpool, p. 261-272.
1981: Gravity, deformation and the Earth's crust, second edition; Academic Press, London.

Thurlow, J.G. and Swanson, E.A.
1987: Stratigraphy and structure of the Buchans Group; in Buchans Geology, Newfoundland, ed. R.V. Kirkham; Geological Survey of Canada, Paper 86-24, Report 2.

Whalen, J.B. and Currie, K.L.
1983(a): The Topsails igneous terrane of western Newfoundland, in Current Research, Geological Survey of Canada, Paper 83-1A, p. 15-23.

Whalen, J.B. and Currie, K.L.
1983(b): The Topsails igneous terrane, western Newfoundland, 1:100,000 map and marginal notes., Geological Survey of Canada, Open File 923.

Whalen, J.B. and Currie, K.L.
1987: The relationship of the Topsails igneous terrane to the Buchans Group; in Buchans Geology, Newfoundland, ed. R.V. Kirkham; Geological Survey of Canada, Paper 86-24, Report 6.

The relationship of the Topsails igneous terrane to the Buchans Group

J.B. Whalen[1] and K.L. Currie[1]

Whalen, J.B. and Currie, K.L., The relationship of the Topsails igneous terrane to the Buchans Group; in Buchans Geology, Newfoundland, ed. R.V. Kirkham; Geological Survey of Canada, Paper 86-24, p. 69-73, Report 6, 1987.

Abstract

The granitic Topsails igneous terrane separates the volcanic sequences of central Newfoundland from the continental and mioclinal terrane of western Newfoundland. Indirect evidence suggests the Topsails igneous terrane to be floored by Precambrian continental crust. In Middle Ordovician time this isolated continental fragment was surrounded by volcano-sedimentary complexes, including the Buchans Group. During Middle to Late Ordovician time parts of the surrounding oceanic crust were emplaced on the Topsails igenous terrane. The plutonic history came to an end with very extensive peralkaline granite emplacement in the Early Silurian. The Buchans Group may have formed a volcanic arc on the edge of the Topsails igneous terrane, or it may have formed as a result of extensional tectonics breaking up the margin of the terrane.

Résumé

Le terrane igné granitique de Topsails sépare les séquences volcaniques de la partie centrale de Terre-Neuve du terrane continental et mioclinal de l'ouest de Terre-Neuve. Des indices indirectes portent à croire que le terrane igné de Topsails repose sur une croûte continentale précambrienne. Au cours de l'Ordovicien moyen, ce fragment continental isolé était entouré de complexes volcano-sédimentaires, y compris le groupe de Buchans. Au cours de l'Ordovicien moyen et de l'Ordovicien récent, certaines parties de la croûte océanique environnante ont été déplacées par dessus le terrane igné de Topsails. La fin de l'histoire plutonique a été marquée par la mise en place, sur de grandes étendues, de granite peralcalin au début du Silurien. Le groupe de Buchans peut avoir formé un arc insulaire en bordure du terrane igné de Topsails, ou s'être formé suivant la fragmentation de la marge du terrane au cours d'un stade de distension.

INTRODUCTION

The mainly granitic Topsails igneous terrane separates the oceanic volcanic sequences of central Newfoundland from the autochthonous continental and mioclinal terrane of western Newfoundland (Fig. 1). The Topsails terrane has been mapped recently and described in detail (Whalen and Currie, 1982, 1983a,b, 1984). A simplified version of our geological map appears as Figure 2. In this paper we present some implications of our work for the interpretation of the geology of the Buchans area.

Major tectonic breaks separate the Topsails igneous terrane from juxtaposed terranes (Fig. 1). The Baie Verte-Brompton line (Williams and St. Julien, 1978) and the drift-filled valley of Birchy Lake, thought to contain the Lobster Cove Fault (Dean and Strong, 1977) separate terranes containing Topsails-type peralkaline granite from the Fleur de Lys terrane to the northwest. To the west of the Topsails igneous terrane a steeply dipping fault exposed in Connors Brook and thought to extend the length of Grand Lake (Hyde

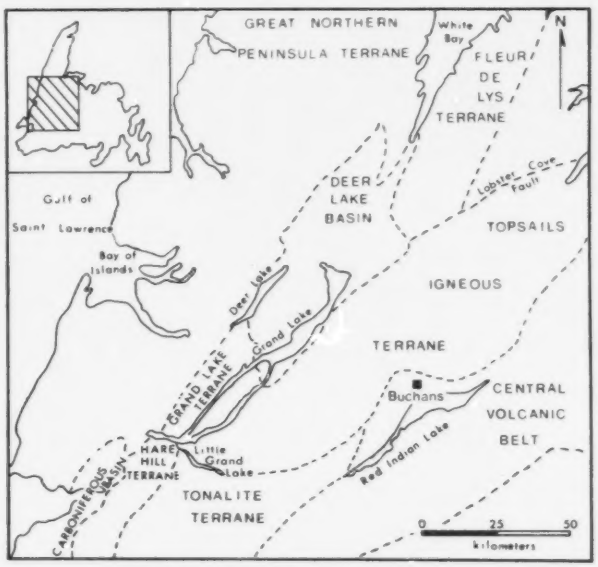

Figure 1. Location of the Topsails igneous terrane and other geological terranes of western Newfoundland.

[1]Geological Survey of Canada, 601 Booth Street, Ottawa, K1A 0E8

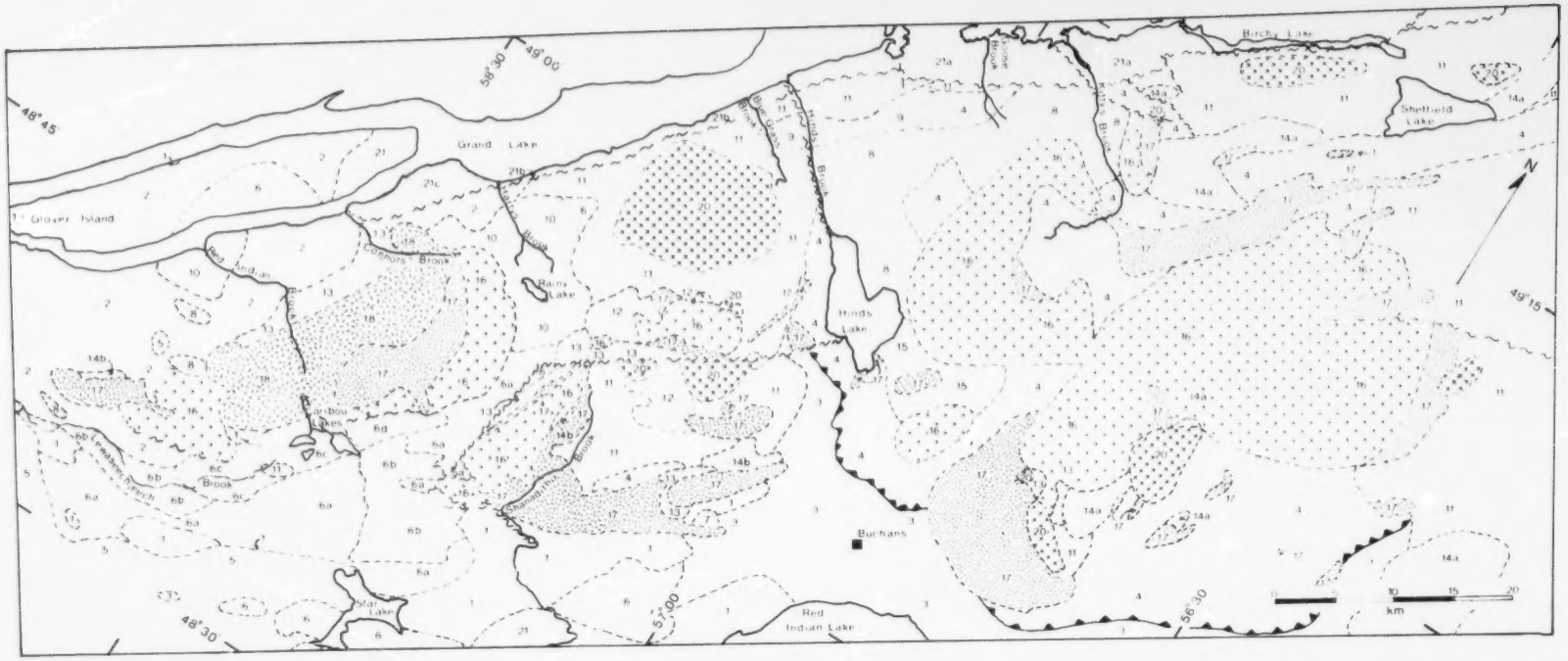

Period	Unit	Description	Symbol
Carboniferous	Howley Beds	Grey sandstone, minor conglomerate and siltstone	21c
	Little Pond Brook Formation	Grey to green muscovitic sandstone, quartz pebble conglomerate	21b
	North Brook and Rocky Brook fms.	Pink to orange conglomerate and sandstone, granite wash	21a
		unconformity	
		Quartz feldspar porphyry, rhyolite, minor basalt, composite dykes	20
		relations uncertain	
		diabase and porphyry dykes	19
		intrusive contact	
		Massive white biotite-amphibole, two-feldspar granite	18
		gradational to intrusive contact	
		fine- to medium-grained amphibole ± pyroxene, pink biotite (-muscovite) granite and aplite	9
		relations uncertain	
		pink biotite-amphibole potash feldspar porphyritic, two-feldspar granite	8
		relations uncertain	
	Feeder Granodiorite	pink to red, biotite-amphibole, two feldspar granite	7
		relations uncertain	
		massive to moderately foliated granodiorites with many small mafic to ultramafic fragments. Relations between sub-units uncertain 6a-biotite granite to granodiorite, minor amphibole granodiorite 6c-amphibole-biotite quartz-eye porphyritic	6

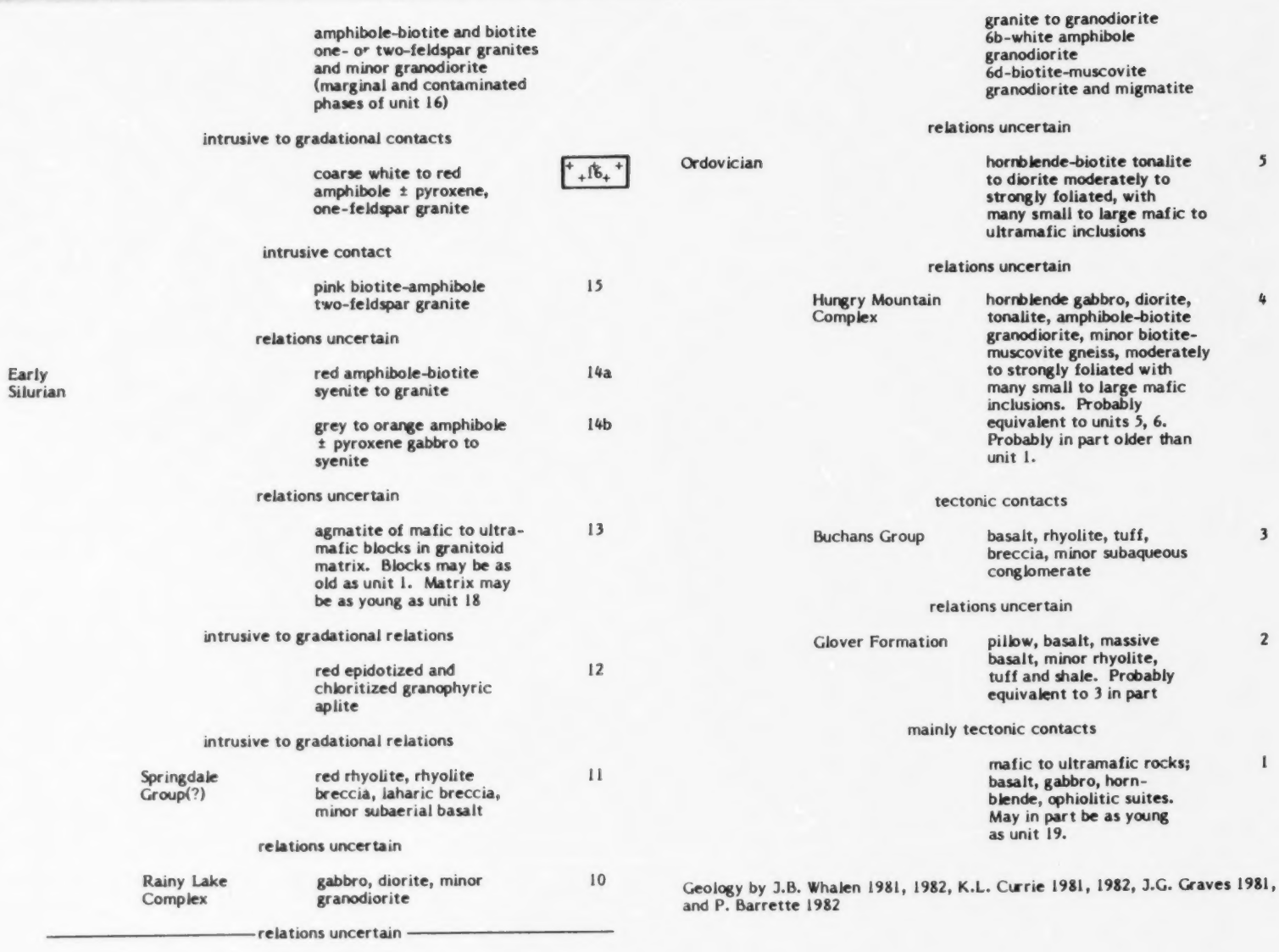
amphibole-biotite and biotite one- or two-feldspar granites and minor granodiorite (marginal and contaminated phases of unit 16)
intrusive to gradational contacts
coarse white to red amphibole ± pyroxene, one-feldspar granite
16
intrusive contact
pink biotite-amphibole two-feldspar granite
15
relations uncertain
Early Silurian
red amphibole-biotite syenite to granite
14a
grey to orange amphibole ± pyroxene gabbro to syenite
14b
relations uncertain
agmatite of mafic to ultramafic blocks in granitoid matrix. Blocks may be as old as unit 1. Matrix may be as young as unit 18
13
intrusive to gradational relations
red epidotized and chloritized granophyric aplite
12
intrusive to gradational relations
Springdale Group(?)
red rhyolite, rhyolite breccia, laharic breccia, minor subaerial basalt
11
relations uncertain
Rainy Lake Complex
gabbro, diorite, minor granodiorite
10
relations uncertain
granite to granodiorite
6b-white amphibole granodiorite
6d-biotite-muscovite granodiorite and migmatite
relations uncertain
Ordovician
hornblende-biotite tonalite to diorite moderately to strongly foliated, with many small to large mafic to ultramafic inclusions
5
relations uncertain
Hungry Mountain Complex
hornblende gabbro, diorite, tonalite, amphibole-biotite granodiorite, minor biotite-muscovite gneiss, moderately to strongly foliated with many small to large mafic inclusions. Probably equivalent to units 5, 6. Probably in part older than unit 1.
4
tectonic contacts
Buchans Group
basalt, rhyolite, tuff, breccia, minor subaqueous conglomerate
3
relations uncertain
Glover Formation
pillow, basalt, massive basalt, minor rhyolite, tuff and shale. Probably equivalent to 3 in part
2
mainly tectonic contacts
mafic to ultramafic rocks; basalt, gabbro, hornblende, ophiolitic suites. May in part be as young as unit 19.
1
Geology by J.B. Whalen 1981, 1982, K.L. Currie 1981, 1982, J.G. Graves 1981, and P. Barrette 1982

Figure 2. Simplified geological map of the Topsails igneous terrane.

and Ware, 1981), separates the Topsails igneous terrane from the deformed Deer Lake Carboniferous basin. To the south observations of brittly deformed and altered peralkaline granite (unit 16) suggest the Topsails igneous terrane has been thrust at a low angle over older foliated granodiorite. These observations, and the discovery of probable deformed and metamorphosed equivalents of the peralkaline granite in the Hare Hill region to the southwest (Whalen and Currie, 1984), suggest that major deformation to the south and west of the Topsails igneous terrane post-dated the emplacement of the peralkaline granite.

In the Buchans region Thurlow (1981) showed that the Hungry Mountain complex (unit 4) of the Topsails igneous terrane was thrust over the Buchans Group (unit 3), but that dykes and sills of Topsails-type granites (unit 17) cut the Hungry Mountain complex, the Buchans Group and the mylonitized thrust contact between them. The post-granite deformation noted south and west of the Topsails igneous terrane appears to be absent from the Buchans area. Rb-Sr and zircon ages (Whalen et al., in press) document that the Topsails-type igneous rocks (units 11-20) all formed in a brief period of Early Silurian time between about 425 and 430 Ma. The formation and deformation of the Buchans rocks and their ores must therefore be pre-Early Silurian. Conodonts (Nowlan and Thurlow, 1984), and imprecise Rb/Sr (Bell and Blenkinsop, 1981) and U/Pb zircon (Stewart, 1986) radiometric dates suggest a Middle Ordovician age of formation for the Buchans Group.

The difference in composition between the potassic, salic magmatic rocks of the Topsails igneous terrane and the generally more mafic compositions predominant in surrounding areas indicates a fundamental difference in the nature of the crust beneath these juxtaposed areas. The huge volumes of silicic and potassic magmas generated in the Topsails igneous terrane in Early Silurian time require a pre-existing, salic lower crustal source. The Humber Zone to the west (Fig. 1) displays Grenvillian potassic gneisses and megacrystic granites, whereas the Central Volcanic Belt to the east has been interpreted to be remnants of volcanic arcs underlain by mafic crust (Strong, 1977). The Topsails igneous terrane may be underlain by Humber-like Precambrian basement extending north from Little Grand Lake to the Burlington Peninsula (Strong et al., 1985). If so, it must represent a continental fragment or sliver separated from the Humber Zone by the Baie Verte-Brompton line (Williams and St. Julien, 1978). Similarly a major break must exist between the Topsails igneous terrane and the oceanic or island arc sequences of the Central Volcanic Belt. We outline below reasons for supposing the Buchans Group to be part of the Topsails igneous terrane rather than the Central Volcanic Belt.

The Hungry Mountain complex of the northern Topsails igneous terrane (unit 4) includes deformed ultramafic, gabbroic, tonalitic and granodioritic rocks of diverse ages associated in intricate relationships and heterogeneous on both large and small scale. Bell and Blenkinsop (1981) obtained poorly defined Rb/Sr isochrons of 400 ± 60 and 660 ± 70 Ma from the Hungry Mountain complex. A foliated tonalite sample representing one of the younger phases of the complex yielded U-Pb zircon upper and lower intercept ages of 2090 ± 75 and 467 ± 8 Ma (Whalen *et al.*, in press). Lithologically similar deformed tonalitic (unit 5) and granodioritic (unit 6) rocks occur on the southern margin of the Topsails igneous terrane. Just south of the Topsails igneous terrane in the Puddle Pond area, Dunning (written communication, 1983) found tonalites (of unit 5) to have cores of old zircon (approximately 1300 Ma), and the data plotted on a mixing line with a Late Ordovician lower intercept, interpreted to be the age of crystallization. Based on field work (Dunning, 1981; Dunning *et al.*, 1982) and zircon dating in western Newfoundland (Dunning and Krogh, 1983), the ophiolitic fragments (unit 1) in units 4, 5 and 6 may be Lower Ordovician in age (479-495 Ma). The lithological and chronological similarities between the Hungry Mountain complex (unit 4) and units 5 and 6 suggest that they may be roughly equivalent post-ophiolite intrusive units. However, relations within the Hungry Mountain complex are poorly understood and older material may be present. By contrast, a diorite from the compositionally similar Rainy Lake complex (unit 10) gave an unexpectedly young Late Ordovician to Early Silurian (438 ± 8 Ma) zircon age (Whalen *et al.*, in press). The Rainy Lake complex (unit 10), the tonalite terrane (unit 5) and the mafic parts of the Hungry Mountain complex (unit 4) compositionally and lithologically resemble island-arc intrusive suites described by Whalen (1985). They may represent "mantle" or M-type intrusive suites (White, 1979; Pitcher, 1983) which have chemical and isotopic compositions like island arc volcanic rocks, and probably derived by partial melting of subducted oceanic crust or mantle beneath island arcs.

Granitic rocks younger than the M-type granites but older than the Silurian Topsails anorogenic or A-type granites cut the middle to late Arenig (G.S. Nowlan, personal communication, 1982) Glover Formation. Lithologically and structurally correlative intrusive rocks occur to the east and in the Hinds Brook granite which has given a late Middle Ordovician (460 ± 10 Ma) zircon age (Whalen *et al.*, in press). One of the similar granite clasts in the Buchans orebodies (Stewart, 1986) yielded an almost identical, but very imprecise, zircon age of 464 ± 40 Ma suggesting a possible source for the clasts.

We found no close correlatives of the Buchans Group in the Topsails igneous terrane. However, the Middle to Late Arenig Glover Formation consists mainly of basaltic rocks with subordinate felsic fragmental and flow units, and minor sedimentary rocks (Knapp *et al.*, 1979). Since fossils recovered from carbonate clasts within breccia units of the Buchans Group suggest a Late Arenig to Early Llanvirn age (Nowlan and Thurlow, 1984), both lithologic and stratigraphic evidence indicate the Glover Formation is similar to, but slightly older than, the Buchans Group. The Glover Formation clearly forms part of the Topsails igneous terrane. The Buchans Group arguably contains clasts derived from the Topsails igneous terrane. Accumulating evidence therefore points to formation of the Buchans Group in a Middle Ordovician volcanic environment fringing the continental fragment of the Topsails igneous terrane. At present we do

not know the exact nature of this environment. If it was a volcanic arc built on the edge of the continent, the Hungry Mountain complex and equivalents could represent deeper levels of the Buchans Group igneous activity. On the other hand, the essentially bimodal character of the Buchans volcanism, and the peralkaline nature of much of the Topsails igneous activity may indicate a long period of tensional tectonics with subsidence and basin formation on the margin of the Topsails igneous terrane.

REFERENCES

Bell, K. and Blenkinsop, J.
1981: A geochronologic study of the Buchans area, Newfoundland; in The Buchans Orebodies: Fifty Years of Geology and Mining, ed. E.A. Swanson, D.F. Strong and J.G. Thurlow; Geological Association of Canada, Special Paper 22, p. 91-111.

Dean, P.L. and Strong, D.F.
1977: Folded thrust faults in Notre Dame Bay, central Newfoundland; American Journal of Science, v. 77, p. 97-108.

Dunning, G.R.
1981: The Annieopsquotch ophiolite complex, southwestern Newfoundland, and its regional relationships; in Current Research, Part B, Geological Survey of Canada, Paper 81-1B, p. 11-15.

Dunning, G.R., Carter, P.J., and Best, M.A.
1982: Geology of Star Lake (west half), southwest Newfoundland; in Current Research, Part B, Geological Survey of Canada, Paper 82-1B, p. 21-26.

Dunning, G.R. and Krogh, T.
1983: Tightly clustered, precise, U/Pb (zircon) ages of ophiolites from the Newfoundland Appalachians (abstract); Geological Society of America, Northeastern Section, Abstracts with Program, v. 15, no. 3, p. 136.

Hyde, R.S. and Ware, M.J.
1981: Notes on the geology of parts of the Deer Lake (12 H/3) and Rainy Lake (12 A/14) map-areas; Newfoundland Department of Mines and Energy, Mineral Development Division, Map 81-17.

Knapp, D., Kennedy, D., and Martineau, Y.
1979: Stratigraphy, structure and regional correlation of rocks at Grand Lake, western Newfoundland; in Current Research, Part A, Geological Survey of Canada, Paper 79-1A, p. 317-325.

Neale, E.R.W. and Nash, W.O.
1963: Sandy Lake (east half), Newfoundland; Geological Survey of Canada, Paper 62-28.

Nowlan, G.S. and Thurlow, J.G.
1984: Middle Ordovician conodonts from the Buchans Group, central Newfoundland and their significance for regional stratigraphy of the Central Volcanic Belt; Canadian Journal of Earth Sciences, v. 21, p. 284-296.

Pitcher, W.S.
1983: Granite and tectonic environment; in Mountain Building Processes, ed. K. Hsu; Academic Press, London, p. 19-40.

Stewart, P.W.
1984: Geochemistry of granitoid clasts from MacLean Extension orebody, Buchans, Newfoundland, and implications on their possible source; in Current Research, Part A, Geological Survey of Canada, Paper 84-1A, p. 467-472.
1986: Geology and genesis of granitoid clasts in transported sulphide ores; in Buchans Geology, Newfoundland, ed. R.V. Kirkham; Geological Survey of Canada, Paper 86-24, Report 9.

Strong, D.F.
1977: Volcanic regimes of the Newfoundland Appalachians; in Volcanic Regimes in Canada, ed. W.R.A. Baragar, L.C. Coleman, and J.M. Hall; Geological Association of Canada, Special Paper 16, p. 61-90.

Thurlow, J.G.
1981: The Buchans Group: its stratigraphic and structural setting; in The Buchans Orebodies: Fifty Years of Geology and Mining, ed. E.A. Swanson, D.F. Strong and J.G. Thurlow; Geological Association of Canada, Special Paper 22, p. 79-90.

Whalen, J.B.
1985: Geochemistry of an island arc plutonic suite: the Uasilau-Yau Yau intrusive complex, New Britain, P.N.G.; Journal of Petrology, v. 26, p. 603-632.

Whalen, J.B. and Currie, K.L.
1982: Volcanic and plutonic rocks in the Rainy Lake area, Newfoundland; in Current Research, Part A, Geological Survey of Canada, Paper 82-1A, p. 17-22.
1983a: The Topsails igneous terrane of western Newfoundland; in Current Research, Part A, Geological Survey of Canada, Paper 83-1A, p. 15-23.
1983b: Geology of the Topsails igneous terrane, western Newfoundland; Geological Survey of Canada, Open File 923.
1984: Peralkaline granite near Hare Hill south of Grand Lake, Newfoundland; in Current Research, Part A, Geological Survey of Canada, Paper 84-1A, p. 181-184.

Whalen, J.B., Currie, K.L. and Van Breemen, O.
– Episodic Ordovician-Silurian plutonism in the Topsails igneous terrane, western Newfoundland; Transactions of the Royal Society of Edinburgh. (in press)

White, A.J.R.
1979: Sources of granite magmas (abstract); Geological Society of America Abstracts with Programs 11, p. 539.

Williams, H. and St. Julien, P.
1978: The Baie Verte-Brompton line in Newfoundland and regional correlations in the Canadian Appalachians; in Current Research, Part A, Geological Survey of Canada, Paper 78-1A, p. 225.

- 7 -

Geology and origin of the orebodies in the Lucky Strike area

J.L. Jambor[1]

Jambor, J.L., Geology and origin of the orebodies in the Lucky Strike area; in Buchans Geology, Newfoundland, ed. R.V. Kirkham; Geological Survey of Canada, Paper 86-24, p. 75-106, Report 7, 1987.

Abstract

Rocks exposed in the Lucky Strike area consist mainly of volcanic breccia and tuff of the Ski Hill Formation overlain by felsic tuff of the Buchans River Formation. Conformably overlying the Buchans River Formation is prominent quartz tuff which comprises part of the Sandy Lake Formation. The stratigraphic relations of Thurlow and Swanson (1987) dictate that all of the above are in a fault block thrust over young arkosic and basaltic rocks that also are part of the Sandy Lake Formation. Preserved within the fault block are indications of the sequence of events that led to the evolution of the economically important orebodies at Lucky Strike.

Initially, the uppermost part of the Ski Hill Formation was penetrated by an extensive stockwork zone that underlies much of the northern part of the area. The stockwork zone is most intense in proximity to the Lucky Strike shaft, and this site is concluded to have been an area of hydrothermal venting. The quartzose, blanket-like Engine House Orebody to the southeast of Lucky Strike merges with the upper part of the stockwork zone and is thought to be an early, synsedimentary body. Near the inferred vent area, sulphide-rich tuff was deposited locally and a subsequent debris flow formed the barite-rich North Orebody at the base of the Buchans River Formation. Following a period of quiescence marked by widespread siltstone deposition, renewed volcanism disturbed the sulphide pile that had accumulated in the vent area, and roughly contemporaneous deposition of the Two Level and Main orebodies ensued. The Two Level Orebody is a ribbon-like, baritic debris flow deposit that was concentrated in a northwest-trending channel, whereas the Main Orebody is a blanket-like Pb-Zn-rich sulphide breccia that was deposited in a basin adjacent to the Two Level channel. Felsic tuff deposited on these orebodies locally contains additional thin layers of transported sulphides; thus, several episodes of sulphide dispersion took place, but all are focused near the Ski Hill – Buchans River contact.

The upper part of the Two Level Orebody was displaced 130 m southeastward along a shallow-dipping, pre-diabase fault. Significant deformation of the Main Orebody is evident from vertical folding of its southeastern part. As well, a tuff layer through the middle of the ore zone was tilted vertically and the upper part was locally overturned, probably as a result of deformation related to late-stage diabase intrusion. Textures of the sulphides indicate that no significant metamorphism of the orebodies has occurred.

Résumé

Les roches affleurant dans la région de Lucky Strike se composent surtout de brèches et de tufs volcaniques de la formation de Ski Hill, et du tuf felsique de la formation susjacente de Buchans River. Un tuf quartzique qui fait partie de la formation de Sandy Lake repose en concordance sur la formation de Buchans River. Les liens stratigraphiques établis par Thurlow et Swanson (1986) révèlent que toutes ces roches font partie d'un bloc faillé chevauché sur des roches arkosiques et basaltiques récentes qui font également partie de la formation de Sandy Lake. Des détails conservés à l'intérieur du bloc faillé révèlent la série d'événements qui a mené l'évolution des corps minéralisés économiquement importants à Lucky Strike.

À l'origine, la partie supérieure de la formation de Ski Hill a été coupée par une vaste zone de stockwerks qui repose sous une grande partie de la zone nord de la région. La zone de stockwerks est plus marquée à proximité du puits Lucky Strike, et cet endroit aurait été marqué par la présence de cheminées

[1]CANMET, 555 Booth Street, Ottawa, Canada K1A 0G1

hydrothermales. Le gisement stratiforme quartzeux de Engine House se situe au sud-est de Lucky Strike et se joint à la partie supérieure de la zone de stockwerks; ce gisement serait une ancienne masse synsédimentaire. Un tuf riche en sulfures s'est accumulé par endroits près des cheminées hydrothermales, et une coulée de débris plus récente a formé le gisement North riche en barytine à la base de la formation de Buchans River. Après une période de repos marquée par l'accumulation répandue d'aleurolite, une nouvelle phase volcanique a perturbé l'amas de sulfures qui s'était accumulé près des cheminées; le gisement de Main et le gisement de Two Level se sont accumulés plus ou moins en même temps. Le gisement de Two Level est un dépôt de coulées de débris riche en barytine, en forme de ruban, qui s'est formé dans un chenal à orientation nord-ouest, tandis que le gisement de Main est un brèche stratiforme sulfurée riche en plomb et en zinc qui s'est accumulée dans un bassin contigu au chenal de Two Level. Du tuf felsique accumulé sur ces gisements contient par endroits d'autres couches minces de sulfures transportés; il y a donc eu plusieurs phases de dispersion des sulfures et toutes ces phases ont été concentrées près du contact de Ski Hill – Buchans River.

La partie supérieure du gisement de Two Level a été déplacée vers le sud-est sur une distance de 130 mètres, le long d'une faille à faible pendage qui s'est formée avant l'intrusion de la diabase. Le gisement de Main a été fortement déformé, et la partie sud-est du gisement a été plissée verticalement. En outre, une couche de tuf qui traverse le centre de la zone minéralisée a été plissée verticalement et la partie supérieure de cette couche a été déversée localement, vraisemblablement à la suite d'une déformation associée à l'intrusion tardive de la diabase. La texture des sulfures révèle que les gisements n'ont pas été fortement métamorphisés.

INTRODUCTION

Within the three genetically related ore types recognized to occur at Buchans, viz., stockwork, in situ, and mechanically transported ores (Thurlow and Swanson, 1981), the Main Orebody at Lucky Strike was considered to be representative of the in situ ore type, beneath which was an extensive stockwork source zone. The nature and distribution of this stockwork zone have been described by Thurlow and Swanson (1981) and Kowalik *et al.* (1981).

In conjunction with other Buchans-area geological studies undertaken as part of the Canada–Newfoundland cooperative mineral program 1982-84, it was proposed that a detailed mineralogical study be done to document the nature of the Lucky Strike stockwork sulphides and their associated hydrothermal alteration. Characterization of the alteration assemblage was considered to be desirable in that the results would provide useful comparisons with alteration zones noted in other parts of the Buchans area. Recent publication of a compendium of Buchans geology (Swanson *et al.*, 1981) had laid the groundwork for the proposed alteration study, and it was expected that the work would be relatively routine. Although only a few years have passed since the appearance of the compendium, the interval has seen enormous changes in the concepts of Buchans geology (this volume). Similarly, the geological framework in the Lucky Strike area is now recognized as being much more complex than was thought previously; folding and faulting have played major roles in determining the shape and disposition of the orebodies. The recognition of these complexities changed the objective from the initially proposed study of an established package of hydrothermally altered rocks, to one in which fundamental questions arose: what is the stratigraphic sequence in the Lucky Strike area, and which of the quartz- and sulphide-rich rocks, some of which are spatially above the orebodies, represent stockwork mineralization? Perhaps one of the most useful contributions of this study is the current general acceptance that the Lucky Strike geology is much more complex structurally than was known previously, and that the structural aspects merit the attention of specialists in this field. Recent work under the sponsorship of the Canada–Newfoundland Mineral Development Agreement include such structural investigations by T.J. Calon and F.K. Green of Memorial University of Newfoundland.

METHOD OF STUDY

Except for the Lucky Strike shaft, the underground workings in the vicinity of the Lucky Strike glory hole are inaccessible. Most of this study is based on examinations of drill cores and logs. An excellent program of core storage was maintained throughout the exploration and mining history of Buchans; although the core record is generally superb, it is poorest for the early drilling of the Lucky Strike deposit and no core remains for several holes drilled in this area.

The geological record for the Lucky Strike area consists mainly of a series of plans for the surface (elevation approximately 930 feet or 290 m), 880 (feet) level, and 840, 800, 760, 720, 640, 540, and 350 levels. These plans, of which the surface one is reproduced here as Figure 1, were prepared in 1937 and for the most part have been unmodified since then. Also available was a series of cross-sections that showed the outlines of the orebodies, but no geology. In some areas these cross-sections were extremely useful in defining orebody contacts and the configuration of a tuffaceous waste zone in the Main Orebody, but in other cases the diagrams were misleading in that they defined mineable ore rather than the geological orebody, the two not always being coincident.

For examination of the Lucky Strike glory hole, the only data available were a drillhole location map and a topographic map, both at 1 inch to 100 feet (1 cm to 12 m). The

Table 1. Stratigraphy of the Buchans Group (Thurlow and Swanson, 1987)

Formation	Former Stratigraphic Names
Sandy Lake Formation	Sandy Lake basalt, Upper Arkose, Lake Seven Basalt, Footwall Arkose, Footwall Basalt.
Buchans River Formation	Lucky Strike Ore Horizon sequence, Oriental Ore Horizon sequence, parts of Intermediate Footwall.
Ski Hill Formation	Ski Hill sequence, parts of Intermediate Footwall, Oriental Intermediate.
Lundberg Hill Formation	Prominent Quartz sequence, Wiley's Prominent Quartz sequence, Little Sandy sequence (?)

latter was prepared in 1975 and showed contour intervals at 10 feet (3.05 m). It was not intended that the glory hole be geologically mapped in the present study, though this was what eventually evolved. The grid used for the mapping was constructed on chain and compass traverses from only a few reference points at the eastern and northeastern periphery of the pit; within the pit nearly all the lines were laid out using the Jacob's staff principle and marker pegs at 25-foot (7.5 m) intervals.

GENERAL GEOLOGY

The general geology of the Lucky Strike area is shown in Figures 1 and 2, and the partial stratigraphic column for the Buchans area is given in Table 1. Formation names and the stratigraphic sequence are those of Thurlow and Swanson (1987), who also give descriptions of the various rock types which make up the formations.

The oldest stratigraphic unit, the Lundberg Hill Formation (Table 1), is not present in the map area. For correlative purposes, however, it should be noted that unit 8 of Figure 2 has been considered in the past (e.g. Swanson *et al.*, 1981) to be part of the former Prominent Quartz sequence. Unit 8 is now thought to be different from other "prominent quartz" rocks and has been assigned to the Sandy Lake Formation rather than to the Lundberg Hill Formation.

The eastern part of the map area (Fig. 2) is represented by rocks of the Ski Hill Formation. Unit 1 consists largely of grey felsic tuff and breccia with numerous narrow sections of interbedded siltstone that is finely but inconspicuously well bedded. Much of the tuff and breccia are characterized by abundant black, typically sharply angular volcanic fragments pseudomorphed by chlorite. The rocks locally contain small amounts of base metal sulphides, but for the most part are only weakly pyritiferous and could be considered as barren relative to the more sulphide-rich assemblages that occur in the vicinity of the glory hole. Unit 1 is considered to be part of the siltstone and breccia assemblage that occurs beneath the Main Orebody, and only a few metres beneath the floor of the western end of the glory hole.

Unit 2 in the Ski Hill Formation (Fig. 2) is a stockwork zone whose eastern boundary varies from sharp to gradational with unit 1. The pronounced northeasterly trend of the stockwork zone is arbitrary and arises only because the stockwork boundary in drillhole 282 at the northeastern corner of Figure 2 has been projected vertically to surface. No outcrop occurs in the area. In the northeastern part of the glory hole area the stockwork zone is overlain by a varied assemblage of tuff and volcanic breccia (unit 3, Fig. 2). The assemblage is locally highly pyritiferous and contains sulphide clasts as well as pebbles and cobbles of stockwork-altered felsite. The assemblage is overlain by the North Orebody, which is highly baritic and is of the mechanically transported ore type.

Unit 4 (Fig. 2) consists mainly of black, massive to amygdaloidal flows, amygdaloidal tuff breccia, and local felsic tuff. The flows are sulphide-barren, but parts are hematitic and veined abundantly by epidote. The predominant amygdule mineral is calcite. Unit 4 has good continuity along its southwestern dip, but at surface along strike the unit is faulted at its northwestern end. At surface the flows mark the approximate boundary between the Ski Hill and Buchans River formations, and indicate also that minor basaltic magmatism intervened between stockwork formation and the subsequent deposition of the major orebodies at Lucky Strike. The flows are separated from the underlying stockwork zone by a thin layer of greenish cherty tuff and chert containing minor interlayers of well-bedded sandstone and grit. Identical cherty rocks, more clearly in the Buchans River Formation, occur 500 m to the northwest in association with one of the major baritic orebodies of the mechanically transported type.

Unit 5 (Fig. 2) consists mainly of siltstone and breccia-conglomerate; the latter is locally ore-bearing, and some contains granitoid clasts. According to Thurlow and Swanson (1987), the lowermost part of the Buchans River Formation in general consists of "quartz-poor pumiceous pyroclastic rocks, rhyolite and pyritic siltstone, overlain by quartz-rich rhyolite and crystal-vitric tuff and the transported ore breccias. These are in turn overlain by a thick sequence of felsic tuff with local quartz and feldspar-phyric rhyolite". The latter sequence of felsic tuff with local rhyolite forms most of the northern part of the map area (Fig. 2, unit 6). The felsic tuff is similar at the northern and southeastern perimeter of the glory hole, but along its western side the rocks are hematitic, and farther west the rocks are pink rather than green. The upper part of the felsic tuff unit is sulphide-barren, but the lower part contains several layers rich in transported sulphides. In the northern part of the map area the base of the felsic tuff is intercalated locally with breccia-conglomerate, wacke, and siltstone that host the largest of the transported barite-rich ore lenses in the northeastern part of the glory hole area (Fig. 2). The breccia-conglomerate is restricted to the northern part of the map area (Fig. 2) and trends northwesterly. The unit is typically thin, but about a 10-m thickness overlies siltstone in the northeast. Siltstone in this assemblage is typically barren except for extremely sparse detrital pyrite and traces of

sphalerite (Thurlow and Swanson, 1981). The siltstone occurs at the top of the Ski Hill Formation and in the lowermost part of the Buchans River Formation. The younging direction appears to be toward the north and east.

Overlying the Buchans River Formation in the southern and southwestern part of the Lucky Strike area is the southwesterly dipping Sandy Lake Formation. At its base is arkose (unit 7, Fig. 2), previously designated as the Upper Arkose

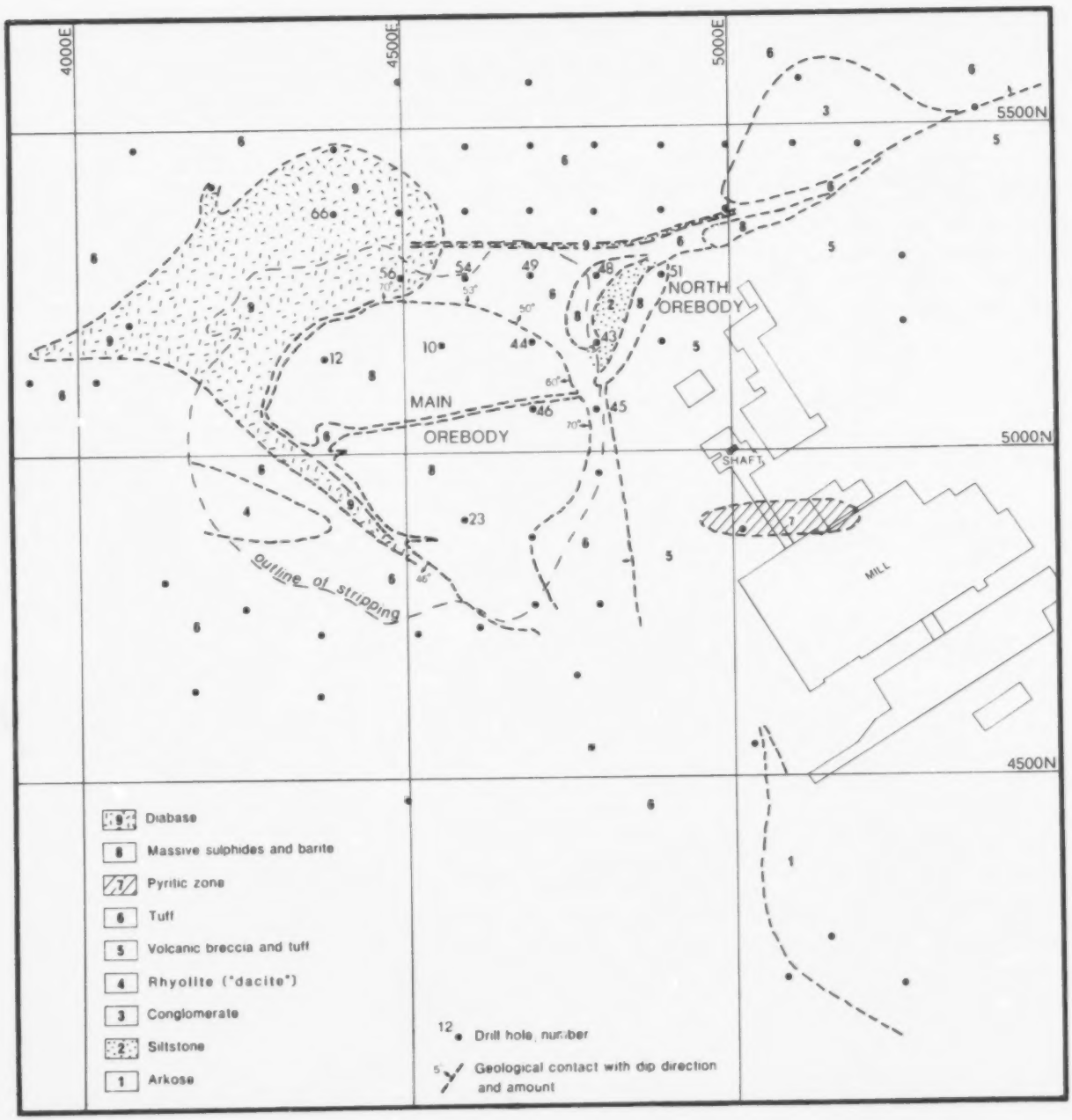

Figure 1. Company surface plan showing the geology and original configuration of the orebodies at Lucky Strike, with minor revision of the legend. Grid co-ordinates are in feet.

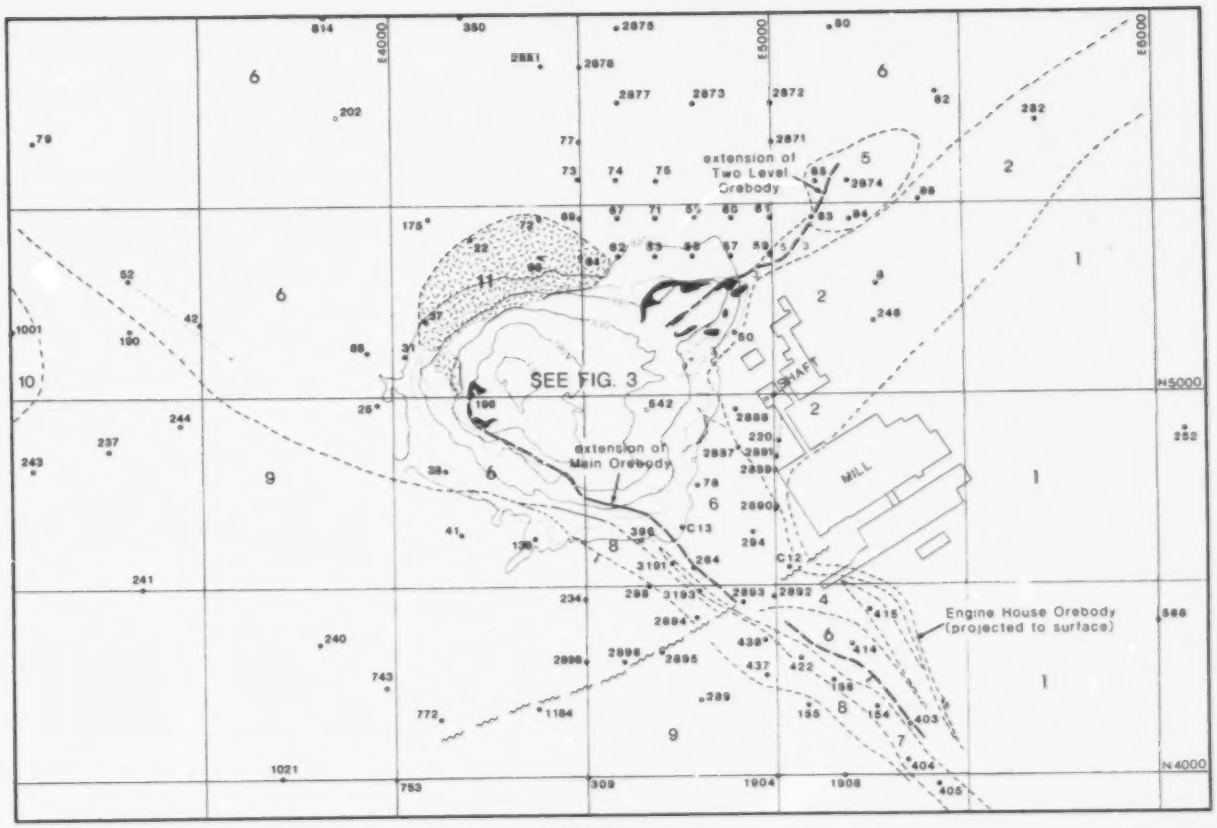

LEGEND

- 11 Diabase
- SANDY LAKE FORMATION
- 10 Basalt (Lake 7 basalt)
- 9 Prominent quartz tuff
- 8 Mudstone, siltstone
- 7 Arkose
- BUCHANS RIVER FORMATION
- 6 Mainly felsic crystal tuff
- 5 Breccia-conglomerate, siltstone
- 4 Black massive to amygdaloidal flows
- SKI HILL FORMATION
- 3 Mainly pyritic tuff and breccia
- 2 Stockwork zone
- 1 Volcanic breccia, lapilli tuff, minor siltstone
- 74 Drillhole, number
- 202 Important underground drillhole
- Orebody remnants
- —730— Contour of Glory hole, interval in feet

Figure 2. Geology map of the Lucky Strike area. Grid co-ordinates and contour elevations of the glory hole are in feet. Geology of the glory hole is shown in Figure 3.

(J.G. Thurlow, written communication, 1986; see Table 1). Catherall (1960) noted that the upper contact of the arkose is conformable with the mudstone-siltstone of unit 8 (Fig. 2), and his observation is supported by drill-core intersections (e.g. hole #437)[1] showing the mudstone conformably interbedded with finer grained variants of the arkose.

The arkose pinches out to the northwest and was not observed in the glory hole. Most of the area to the west of the arkose consists of massive "prominent quartz" tuff that has been intersected in numerous drillholes and is exposed in several outcrops at the edge of the glory hole. The tuff typically contains abundant white quartz phenocrysts averaging 4-6 mm. This unit is conformable with the underlying Buchans River felsic tuffs, and in a few areas the two are difficult to distinguish near the contact. Similarly, at the western edge of the glory hole the prominent quartz tuff is gradational downward to dark green massive tuff with less

[1]Contact reference specimens are stored at the Geological Survey of Canada.

5000E
4500E
4100E
5300N
5000N
4700N
cover
cover
extension of
Main Orebody
6Ab
6Aa
6Ba
6Bb
6Bc
9
9a
8
7
2
1

LEGEND: LUCKY STRIKE GLORY HOLE

9 diabase; 9a: diabase with included and intermixed tuff; 9b: dyke; 9c: sill.

SANDY LAKE FORMATION

8 prominent quartz tuff

7 siltstone and carbonaceous mudstone

BUCHANS RIVER FORMATION

6A/B 6A: mainly layered crystal-vitric tuff; 6Aa: mainly pinkish; 6Ab: mainly greenish; 6Ac: white, altered and schistose; 6Ad: with abundant barite lenses; 6Ae: with barite and sulphide fragments.
6B: siliceous, pyritiferous felsic tuff and breccia with minor black schistose interlayers; 6Ba: intensely pyritiferous and siliceous, locally semi-massive pyrite and quartz (some veins); 6Bb: moderately siliceous and pyritiferous; 6Bc: chloritic felsic tuff with lithic fragments and negligible sulphides (similar to 6Ab).

5 massive sulphides and barite; 5a: Main Orebody, massive sulphides; 5b: Main Orebody, mainly barite; 5c: Two Level Orebody, mainly barite with lithic and sulphide clasts

4 clastic sedimentary rocks; 4a: siltstone gradational with 4b sandstone or wacke; 4c: siltstone breccia-conglomerate

3 North Orebody, mainly barite with lithic barite and sulphide clasts.

SKI HILL FORMATION

2 pyritiferous tuff and volcanic breccia beneath the North Orebody; 2a: mainly massive, coarsegrained pyrite; 2b: siliceous and highly pyritiferous with sulphide-rich clasts; 2c: black, chloritic, pyritiferous tuff and breccia; 2d: tuff and breccia with sparse pyrite and sphalerite and negligible silicification

1 stockwork zone with discrete quartz-sulphide veinlets.

Geological contact: defined, assumed

Inferred fault with dip

Bedding: tops known, tops unknown, foliation

Lineation direction and plunge; minor folds, plung.

Surface drillhole, number; significant underground drillhole

Limit of outcrop

Figure 3. Geological map of the Lucky Strike glory hole.

abundant quartz eyes that average only 2-3 mm in diameter. Much of the prominent quartz tuff basal contact is, however, marked by the appearance of well-laminated, black, carbonaceous mudstone and dark, massive cohesive siltstone containing sparse pebbles, some of which are jasperoidal. Outcrops in the glory hole show mudstone underlying siltstone, but in drill core (e.g. hole #298) the mudstone has been noted to occur in unsheared contact with prominent quartz tuff.

At the western extremity of the map area (Fig. 2), basaltic lava with pillow breccia and tuff layers was intersected in one drillhole (1001) in which the tuff is transitional to the underlying prominent quartz tuff. These barren basaltic rocks, formerly known as the Lake Seven Basalt (Table 1), are now included in the Sandy Lake Formation (Thurlow and Swanson, 1987).

In summary, the Sandy Lake Formation in the Lucky Strike area is considered here to consist of the following units in upward stratigraphic succession: arkose (the former Upper Arkose), mudstone-siltstone, prominent quartz tuff (part of the former Prominent Quartz sequence) and basalt (the former Lake Seven Basalt). These rocks overlie the Buchans River Formation. The conformable contact reported by Thurlow and Swanson (1981) for Ski Hill rocks overlying prominent quartz tuffs refers to prominent quartz rocks now assigned to the Lundberg Hill Formation.

The two remaining units in the Sandy Lake Formation correspond to the former Footwall Arkose and former Footwall Basalt (Table 1). These two units are not exposed at bedrock surface at Lucky Strike, but occur at depth. Arkose equivalent to the former Footwall Arkose (J.G. Thurlow, written communication, 1986) was intersected near the bottom of inclined drillhole 282 in the northeastern part of the map area (Fig. 2). The contact is marked by abundant core losses and schistosity that are indicative of a fault contact. The stratigraphic relationships (Table 1) dictate that at this site the older Ski Hill Formation has been thrust over the arkosic unit.

The remaining unit, the former Footwall Basalt, underlies part of the Lucky Strike area. As these basaltic rocks are overlain by the older Ski Hill and Buchans River formations, the stratigraphic relations (Table 1) dictate that the whole of the map area is a block that has been thrust over the Sandy Lake Formation. This topic is discussed in a later section.

Thin diabase dykes and sheets occur sporadically in the map area, and a large diabase intrusion makes up the northwestern wall of the Lucky Strike glory hole (unit 11, Fig. 2). These intrusions are the youngest major rock type in the area. The dykes and sheets, including parts of the main diabase mass, commonly have chilled margins or unsheared contacts.

At the northeastern end of the glory hole a steeply dipping diabase dyke, 2 to 4 m thick and striking easterly, cuts the Two Level baritic orebody (Fig. 3). The dyke is traceable to 175 m below surface, but nowhere are contacts with the main diabase evident. Likewise, two diabase sheets, each 1 to 3 m

thick and separated by a similar thickness of felsic tuff (Unit 6Aa in Fig. 3), are exposed in the southwestern wall of the glory hole but disappear in rubble before reaching the main intrusion. Contacts of the main intrusion are well exposed locally, particularly at the western end of the glory hole; in this area the basal contact of the diabase is sharp and unsheared, but above it the contacts are highly irregular and much intermingling occurs with layers of tuff. The northerly striking fault with westerly dip (Fig. 3) follows one such tuff layer. Only a minor rubble zone in bedrock marks the probable southwesterly extension of the fault into felsic tuff. Displacement seems to have been insignificant and the fault is probably a minor shear zone of no importance. Steeply dipping, east-trending slickensided surfaces also occur in the diabase in this area, but are also thought to be of no significance in marking major fault displacements.

The geology near the glory hole (Fig. 3) is discussed in conjunction with the descriptions of the orebodies that occurred in this area. The sizes, grades, and general character of these orebodies are given in Table 2.

TWO LEVEL AND NORTH OREBODIES

The orebody remnants exposed in the northeastern corner of the glory hole are parts of two major lenses that are barite-rich and consist of sulphides and lithic fragments in a matrix of fragmental barite. Baritic transported ores of this type make up part of the Rothermere, MacLean, and MacLean Extension orebodies, and have been recognized to be subaqueous debris flows (Binney *et al.*, 1983). Examples from the glory hole are shown in Figure 4.

Barite lenses in the northeastern part of the glory hole have two distinct stratigraphic positions, one above siltstone and the other below (Fig. 3). The above-siltstone baritic lens dips northwest and has subsurface continuity for a considerable distance in this direction. The lens is referred to here as the Two Level Orebody, a name originally applied to a westerly trending subsurface baritic orebody whose eastern limit was approximatelky at E4000 N5700 (Fig. 2).

Company geological plans show the Two Level Orebody near the pit as having a distinctly lensoid shape, but this

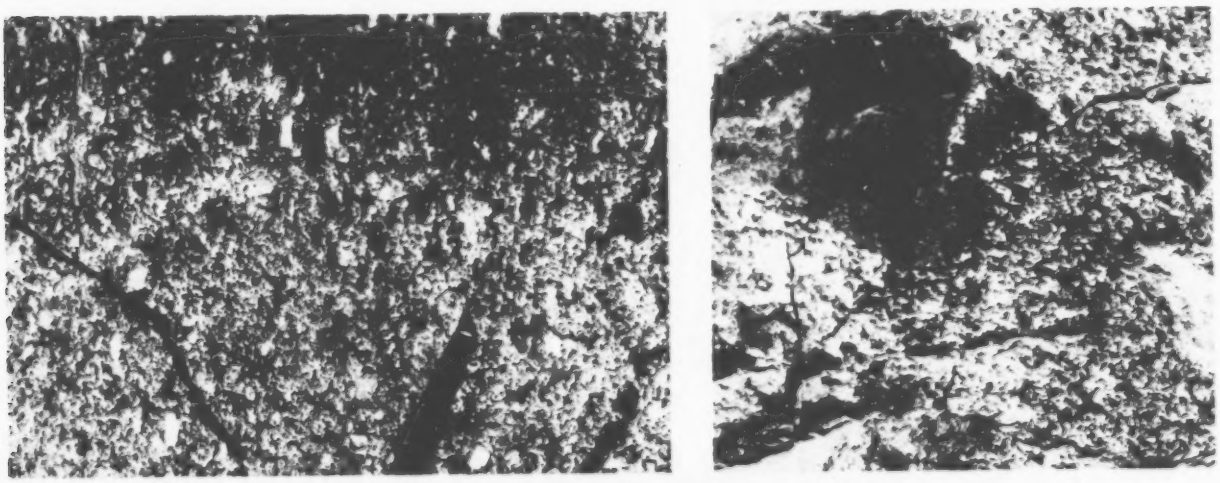

Figure 4. Typical texture of transported ore in the Two Level Orebody exposed in the glory hole. The barite matrix contains white barite fragments and black massive sulphide clasts rich in galena and sphalerite. Right photograph shows a larger sphalerite-galena clast.

Table 2. Grades and tonnages milled from orebodies in the Lucky Strike area[1]

Orebody	Type	Tonnes	Zn %	Pb %	Cu %	Ag (g/t)	Au (g/t)
Main Orebody	brecciated, massive "black ore"	5,050,459	18.42	8.61	1.63	112.5	1.68
North orebodies[2]	baritic debris flows	546,100	8.20	4.54	0.46	122.7	1.68
Two level[3]	baritic debris flows	298,724	8.02	4.56	0.50	124.8	1.61
Engine House[4]	quartzose, possible stockwork	140,909	4.75	1.59	1.54	25.0	0.58

1. Adapted from Thurlow and Swanson (1981).
2. Includes the displaced eastern part of the Two Level Orebody in the terminology of this paper.
3. Undisplaced, northwestern part only.
4. Approximate tonnage and grade mined from estimated total reserves of 454,545 tonnes (after Catherall, 1960).

probably reflects the custom of outlining ore rather than geological boundaries. Drillhole intersections indicate that the orebody is very broad relative to its thickness, and the orebody extends beyond both the northern and eastern boundaries of the glory hole northeastern quadrant of Figure 3. Some of the baritic intersections in this northeastern area are less than a metre thick, but good continuity is evident in east-west cross-sections to N5465, though not beyond it. Figure 5 shows an east-west cross-section at N5365.

In the glory hole the siltstone base of the Two Level Orebody is conformable and cohesive. A few metres to the south and west, however, the siltstone is highly fractured and pencil-shaped cleavage fragments only a few centimetres thick are characteristic. Immediately east of drillhole 48 (Fig. 3) the siltstone is folded to an almost vertical dip adjacent to a minor northeasterly fault accompanied by irregular offshoots from the adjoining diabase dyke.

Despite the northwesterly dip and trend of the orebody, its upper contact in the most westerly exposure in the glory hole has a southward dip. The hangingwall surface of the barite is slightly rough, with coarse flutes and weakly developed steps that indicate a southward relative movement of the hangingwall tuff. Southeast of drillhole 44 the hangingwall tuff seems to reverse its dip, thus suggesting that a minor synformal structure was present in this area. In addition, at the westernmost exposure of the Two Level outcrop, both the top and the bottom contacts of the barite dip southward (Fig. 3). This feature indicates transgression of the siltstone bedding, and suggests that there was some ore deposition in a southward-facing minor branch of the northwesterly trending main paleochannel.

Overlying the Two Level Orebody north of the glory hole are predominantly greenish crystal-vitric felsic tuffs shown in Figure 3 as Unit 6Ab. In drill cores these tuffs are interbedded locally with the Two Level Orebody and its associated clastic rocks; as well, similar transported sulphides appear higher in the tuff sequence (Fig. 5), but for the most part appreciable thicknesses of the tuff are sulphide-barren. In the northern part of the glory hole, however, the Two Level Orebody is overlain by a northeasterly trending assemblage of mixed tuff and volcanic breccia, large parts of which are characterized by being highly pyritiferous and highly siliceous (Unit 6B in Fig. 3). Drill-core preservation in this area is poor and thus little is known of the configuration of the sulphide-rich, siliceous assemblage north of the outcrop area; the limited data available indicate that the assemblage does not continue, at least with its outcrop traits, beyond the northern or northwestern edge of the glory hole. At the glory hole, however, drillholes through the siliceous assemblage intersected the Two Level Orebody and siltstone footwall, thus indicating that the broader geological relationships in this area are not much different from those evident in outcrop.

The rocks making up the siliceous-pyritiferous assemblage (Unit 6Ba) are diverse. Immediately west of the expo-

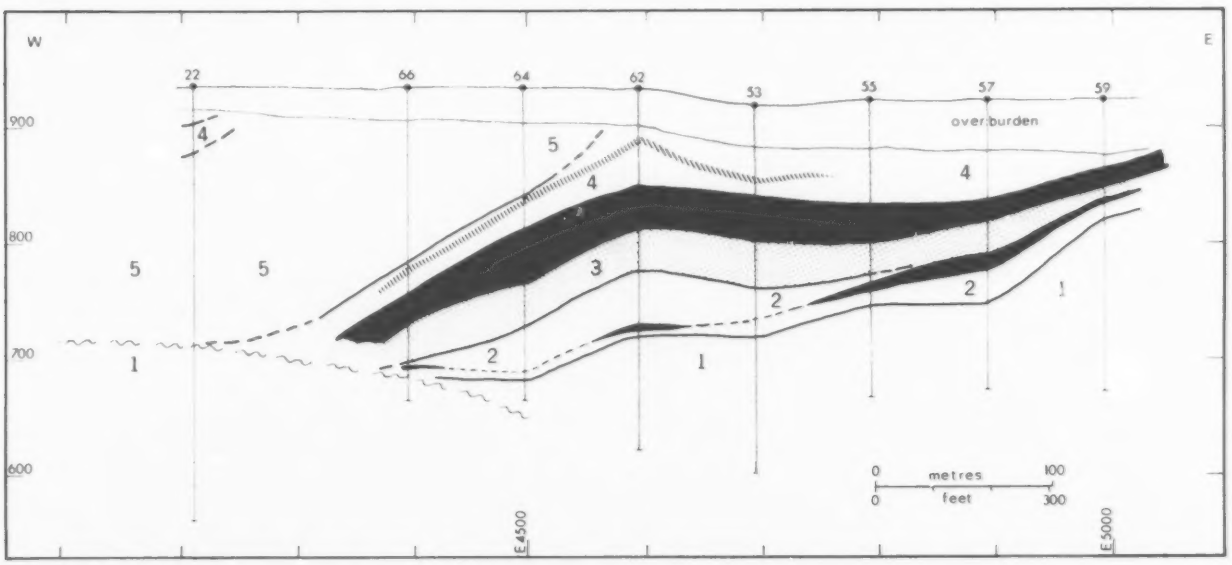

Figure 5. East-west cross-section at co-ordinate N5365 (see Fig. 2 for location). Slash pattern represents a low-grade Zn-Pb zone in felsic tuff and breccia (4) overlying a thick baritic lens (solid black) considered to be an extension of the Two Level Orebody. Stippled unit 3 is mainly siltstone; it is underlain by the North Orebody (solid black) associated with tuff and felsic breccia (2) above the stockwork zone (1). The baritic lenses evidently terminate against a fault near the base of the main diabase intrusion (5). Elevations and co-ordinates are in feet; see Figures 2 and 3 for drillhole locations.

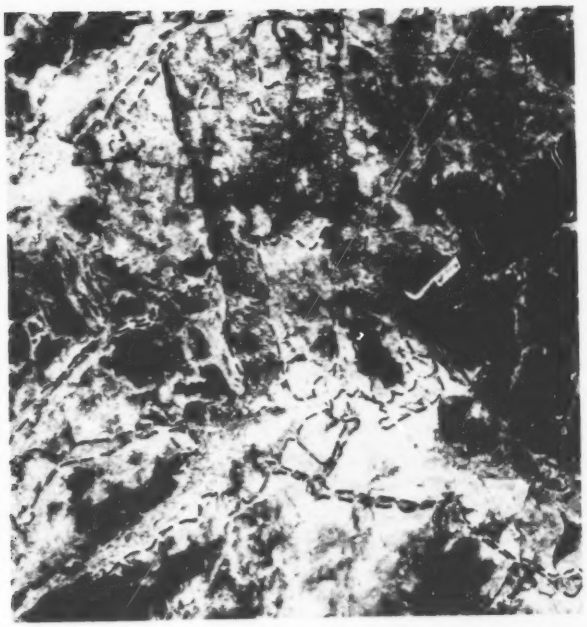

Figure 6. Highly siliceous zone containing irregular pyrite veinlets in an outcrop (unit 6Ba in Figure 3) above the Two Level Orebody near drillhole 54 (Fig. 3).

sure of the Two Level Orebody is a large outcrop that, at the top of the glory hole, is pervasively siliceous and megascopically appears as massive quartz with well-defined, irregular, steeply dipping veins of pyrite accompanied by small amounts of chalcopyrite and trace amounts of sphalerite and galena (Fig. 6). Deeper in the pit, however, the veins disappear, the rocks are gradationally less siliceous, and planar structure roughly matching the trend of the underlying tuffs is evident. Immediately west and north of drillhole 54 (Fig. 3) similar siliceous rocks are present, but farther west the pervasive silicification is laterally discontinuous and the rocks are recognizable as siliceous, variably pyritiferous tuffs that are well foliated and locally contain black, chlorite-rich schistose tuff layers. Parts of this area also have pebbles to metres-wide blocks of coarse-grained massive pyrite; these blocks appear to be pyrite rubble, but exposures are not good enough to determine whether the rubble represents transported debris or has some other origin.

The contact between units 6Ba and 6Bb in Figure 3 is an arbitrary separation of the highly siliceous-pyritiferous rocks (6Ba) from the underlying tuffs that are more chloritic, less siliceous, and contain less disseminated pyrite. These underlying tuffs contain numerous lithic and pyritic pebbles, and one exposure shows a 3-m wide boulder of massive pyrite. No quartz-sulphide veinlets characteristic of stockwork-type mineralization were observed in these lower rocks.

The contact between the hangingwall of the Two Level Orebody and the siliceous-pyritiferous assemblage is separated by barren tuff (6Bc in Fig. 3) whose upper contact is not exposed. When this study first began, it was assumed that unit 6Ba represented a stockwork zone whose appearance above the transported baritic orebody was a consequence of thrust faulting. Two questions therefore arise: (a) is the assemblage thrust-faulted, and (b) is the assemblage a stockwork zone?

Although a specific fault has not been observed, a faulted, stockwork origin for these rocks is supported by: (1) the highly siliceous character of the rocks; (2) the local presence of sulphide veins as shown in Figure 6; (3) the presence of siliceous, pyritic masses similar to those underlying the North Orebody, and which are interpreted here to have temporally preceded deposition of the Two Level Orebody; (4) the lateral extension of the siliceous rocks to the western side of the glory hole, where they overlie the Main Orebody (Fig. 3), whereas similar siliceous rocks typically underlie the Orebody; (5) the contact between the top of the Two Level Orebody and the highly siliceous assemblage, although not exposed, is obviously abrupt.

If the siliceous assemblage is not a stockwork zone, then there is no need to assume the presence of a thrust fault. The following support an alternative viewpoint that the rocks are a highly altered assemblage deposited on the Two Level Orebody rather than thrust over it: (1) the veins shown in Figure 6 are exceptional and nearly all the assemblage is a pervasive-type alteration devoid of anastomosing veinlets; (2) the siliceous assemblage at the top of the glory hole is gradational downward to much less altered rock and the assemblage is unlike the stockwork zone that underlies much of Lucky Strike; (3) the less altered assemblage contains boulders and pebbles of massive pyrite, thus showing that consolidation and transportation of sulphides preceded the formation of the highly siliceous assemblage, and therefore would have preceded the assumed stockwork formation; (4) the apparently restricted occurrence of the siliceous assemblage and its presence above both the Two Level and Main orebodies would require that the top, as well as the bottom, of the assemblage be fault bounded.

Neither thrust faulting nor in situ alteration satisfactorily explains all of the features observed in the siliceous assemblage. In choosing between the alternatives, however, the writer would opt for in situ alteration.

Two Level Fault

The Two Level Orebody dips northwesterly and is continuous down-dip to near drillhole 66 (E4400, Fig. 3), at which point the orebody is on the 720 level, approximately 70 m below surface. Subsurface plans show that the orebody terminates abruptly just below the 720 level, but reappears farther northwest (Fig. 7) at approximately E4000 N5700. The latter segment is the portion to which the name Two Level Orebody was originally applied by the company. Figure 8 shows the effects of restoration by assuming a horizontal displacement of approximately 130 m along N50°W. Little doubt exists that the lens exposed in the glory hole and the originally defined Two Level Orebody are the same unit.

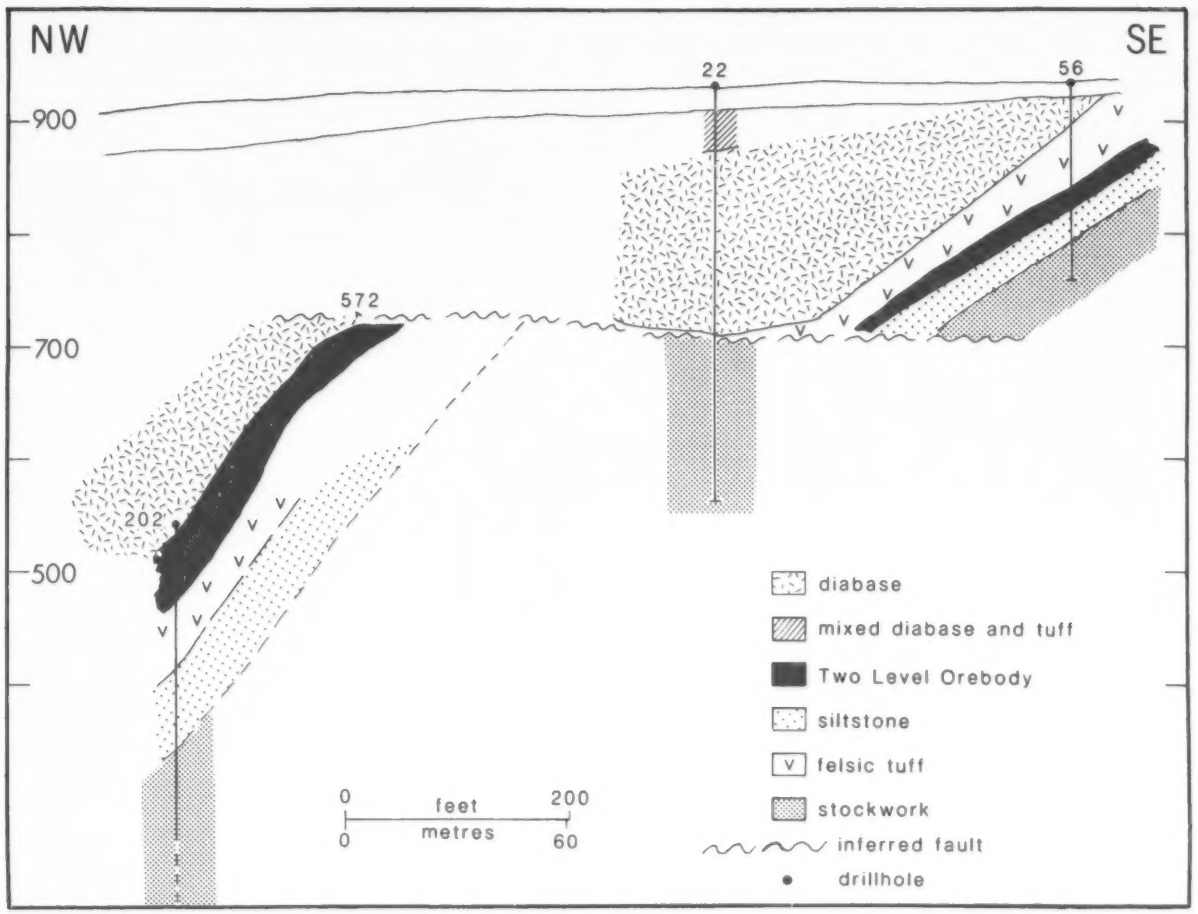

Figure 7. Northwest-southeast cross-section of the Two Level Orebody showing the displacement along an inferred flat-lying fault (see Figure 2 for drillhole locations).

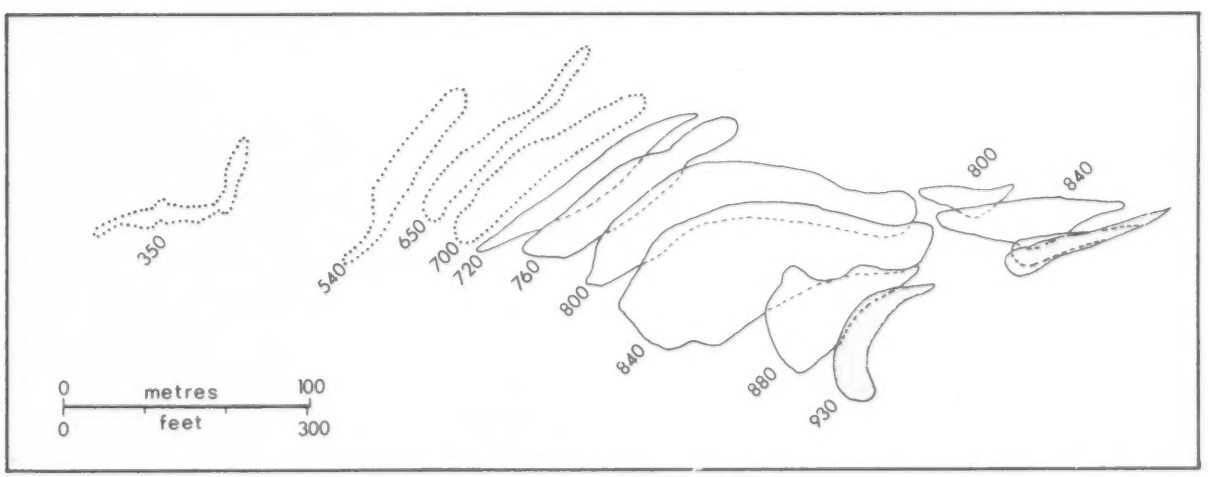

Figure 8. Company plans of the Two Level Orebody at different elevations (in feet above mean sea level). Dotted lines show the orebody in its present position (350 to 700 levels), and solid outlines are the orebody above the 700 level, restored after displacement of approximately 130 m along N 50°W. Shaded pattern is the original surface outline in the glory hole at an elevation of about 930 feet (Fig. 1).

The character and attitude of the plane along which the orebody was offset are not known; presumably the displacement was related either to a low-angle fault, or to dilation offset which attended diabase intrusion. As exemplified in Figure 7, the diabase footwall contact followed the general dip of the country rock, but in the vicinity of the offset the diabase footwall had a flat to slight southeasterly dip (Fig. 9). As well, however, the trace of the Two Level hangingwall-footwall contact has been distorted below and to the east of the diabase mass (Fig. 9). The contact distortion and orebody offset, if related, cannot be accounted for readily by diabase intrusion. A relatively flat-lying fault with a component of easterly dip is inferred, with the upper part of the Two Level Orebody having been translated southeastward.

North Orebody

Beneath the siltstone and tuff assemblage that forms the footwall of the Two Level Orebody in the glory hole is a second baritic transported orebody which is referred to here as the North Orebody (unit 3a, Fig. 3). This orebody evidently extended to surface as a single large lens (Fig. 1). Much of the seemingly large area of outcrop in the glory hole (Fig. 3) merely represents thin footwall remnants of the orebody along the dip-slope of the pit.

The North Orebody and Two Level Orebody are similar in that both are transported ores consisting mainly of fragmental barite with abundant sulphide and lithic clasts. Locally the upper contact of the North Orebody abuts on the overlying

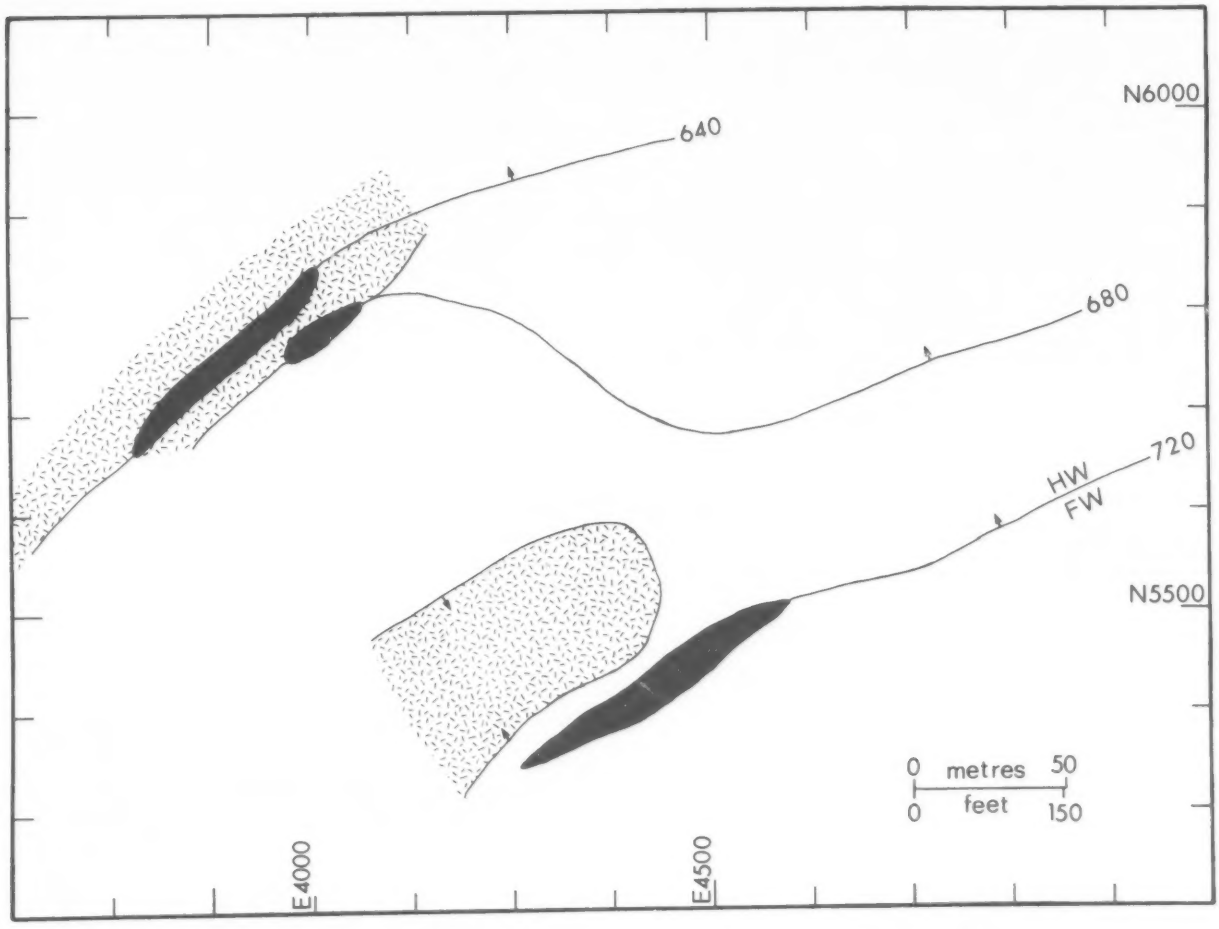

Figure 9. Company plans for the 720, 680, and 640 levels showing the Two Level Orebody (solid black) and adjacent overlying diabase intrusion (pattern). Northeasterly-trending lines are the contact between felsic tuffs and the Two Level footwall rocks; displacement of this contact may have occurred by southeasterly movement as indicated in Figure 7.

siltstone along a thin foliated chloritic contact rather than a large shear zone. Parts of the base of the orebody are much enriched in sphalerite, galena, and chalcopyrite. The basal contact is irregular in detail, the barite and sulphides evidently having filled minor depressions, a metre or so in depth, in the underlying highly pyritiferous tuff and tuff breccia. The dip-slope remnants of the orebody are considered to reflect primary indentations in the footwall rocks, a concept that is supported by lateral changes in the lithology of the basal rocks over distances of only a few metres.

The Two Level Orebody dips northwesterly and is traceable for considerable distances both to the northwest and to the east of the glory hole. The North Orebody has a similar trend, but is thinner and more discontinuous. The abrupt western contact in the glory hole near drillhole 44 (Fig. 3) reflects a western plunge of the orebody beneath tuff identical to that which overlies the southward-dipping top of the Two Level Orebody. The westerly plunge of the North Orebody is traceable through drillhole 44 and for about 15 m farther west, gradually thinning in this direction. Thus the orebody in this area is beneath the floor of the glory hole; at surface, this area was originally overlain by the Main Orebody which extended southeasterly to within 5 m of drillhole 45 (Figs. 1 and 3).

The three small barite outcrops near drillhole 45 (Fig. 3) consist of fragmental, transported-type ore. The most easterly of the outcrops is mound-like, with intensely silicified tuff following the contours of the rounded surface (Fig. 10). These three baritic outcrops, one of which is merely a down-dip exposure at a lower elevation, are thought to form a westerly dipping mass that is an extension of the North Orebody.

In summary, the North Orebody is concluded to be a sheet-like deposit of transported baritic ore that was formed prior to the deposition of the Two Level Orebody and its associated siltstone base. A contrary viewpoint is that the North Orebody and the Two Level Orebody are stratigraphically equivalent and have been separated along an unexposed fault (J.G. Thurlow, written communication, 1986). To achieve such equivalence, however, the assumed fault must cut between the orebodies in the glory hole, and more specifically, must be along the hangingwall of the North Orebody. A major shear zone is not present at this site, but in view of the apparent difficulty in recognizing major shears it is perhaps more significant that a fault at this position would not account for the substantially different lithological assemblages that underlie each orebody.

MAIN OREBODY

The Lucky Strike Main Orebody contained about 5 million tonnes of fine grained high-grade ore that averaged more than 26 per cent Zn + Pb (Table 2). The principal ore minerals – sphalerite and galena – were accompanied by appreciable amounts of chalcopyrite and lesser quantities of tetrahedrite; these four minerals apparently accounted for all but a tiny fraction of the zinc, lead, copper, and silver in the deposit. Unlike its predominance in most massive sulphide deposits, pyrite evidently was much less abundant than sphalerite and was only slightly more abundant than galena (Thurlow and Swanson, 1981). Barite was the chief gangue mineral, but orebody remnants show that calcite is also a major constituent and occurs pervasively with the barite. The fine grained,

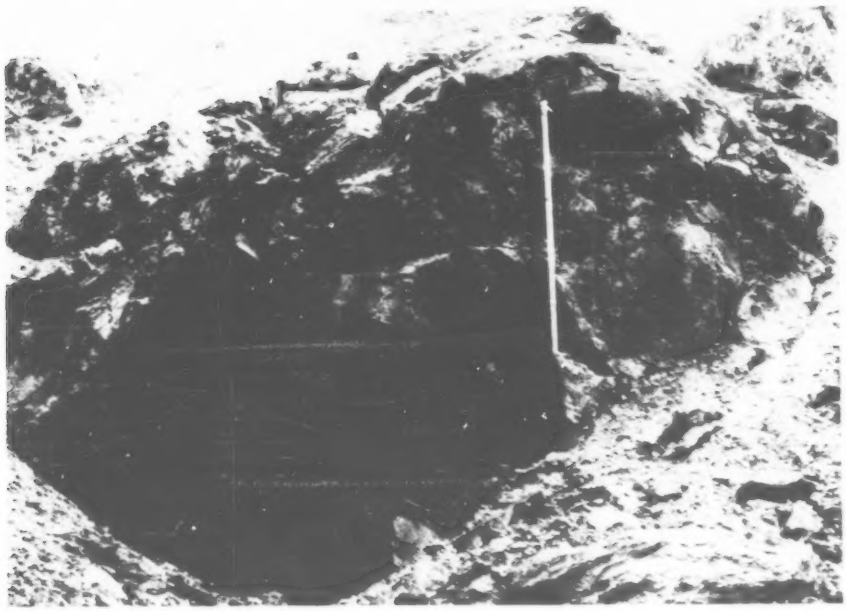

Figure 10. Outcrop of North Orebody fragmental barite near drillhole 45 showing the curved nature of both the barite and the overlying siliceous tuff. The lower and upper contacts of the barite dip toward the viewer. The staff is 1.56 m (5 ft.) long.

intergrown character of the sulphides is apparent in several of the photomicrographs published by Strong (1981), and also is evident from the extremely fine grind that was used to process the ore (Buchans Staff, 1955).

The thickest, highest grade mass of the Main Orebody had an inverted hemispherical shape as shown by George (1937), Thurlow and Swanson (1981), Kowalik *et al.* (1981), and others. This shape, however, depicts only a small part of the orebody, the overall structure of which was sheet-like rather than an isolated bulbous mass.

Remnants of the Main Orebody are exposed in the floor of the glory hole, and along its southern and western walls. Part of the oxidized surface ore of the Main Orebody, although no longer available, was stockpiled for several decades and was sampled for this study. None of the massive sulphide intersections from surface drillholes above the glory hole has been preserved, but Main Orebody intersections in several underground holes beyond the limits of the glory hole are available. In addition, one vertical underground drillhole (No. 28) that was collared on the 840 level (about 30 m below surface) approximately 20 m west of drillhole 10 (Fig. 3) intersected about 11 m of the main massive sulphide zone. This intersection is especially important as it is the only core record preserved of the orebody that originally occupied the higher parts of the glory hole. The core from this drillhole confirms other observations that much of the Main Orebody consisted of sulphide breccia. The fragmental nature of the ore accounts for the observation by most writers that the orebody lacked the well-defined lamination typical of at least parts of most massive sulphide deposits.

Despite the brecciated character of the massive sulphides, the orebody was not a uniform mass of heterolithic breccia, and rather substantial lateral and vertical variations in mineralogy were present. For example, a crude metal zoning was noted by George (1937), who reported that more than 90 per cent of the ore in the Main Orebody was classed as a lead-zinc ore, and the remainder as copper-zinc ore. For lead-zinc ore George cited assays of Cu 1.2, Pb 9.9, Zn 20.8%, and $BaSO_4$ 30.0%; copper-zinc ore was reported as Cu 6.1, Pb 1.6, and Zn 13.2%. He also noted (1937, p. 504) that "In general the footwall sections contain more sphalerite, chalcopyrite and pyrite and less barite, galena and gold-silver minerals than the parts closer to the hanging wall". This concentration of copper-rich ore along the base of the orebody (though not restricted to it) is readily explained if the brecciation is an in situ feature. Indeed, a peculiar trait of the brecciated ore, where well defined, is that the fragments at a specific site are overwhelmingly similar rather than diverse, exactly as one would expect from in situ brecciation (Fig. 11). Contrary features are that the breccia ore is known to have been widespread, and thus the deformation leading to in situ brecciation should have been fairly penetrative; nevertheless, evidently unbrecciated, or at least dissimilar ore, occurs within a metre of breccia. Other contrary features are (1) the relatively large size of unbroken fragments, and their clearly random position, amidst finer breccia; (2) the presence of small breccia fragments included in larger ones, without indications of local deformation, and (3) the presence of colloform sulphide overgrowths on breccia fragments. The last two indicate that brecciation occurred prior to the cessation of sulphide crystallization. It is concluded, therefore, that the brecciated textures are a syndepositional rather than post-ore feature, and they reflect the movement of fragmental sulphides over some unknown distance. The presence of crude zoning of metals as noted by George (1937) is not at variance with this conclusion, especially since sulphide accumulation evidently did not occur as a single, unbroken continuum, as is noted farther below.

The blanket-like shape and mineralogical variations of the Main Orebody on a broader scale are evident in the western and southern parts of the deposit. Exposures in the glory hole in these areas show that the ore is highly baritic and is of ore grade only locally. The thick section of ore at the western side of the glory hole thins rapidly to the southwest, and becomes reddish from hematite staining. The staining accentuates the fragmental character of the barite, which is similar to that in the Two Level and North orebodies but lacks their high proportion of lithic and sulphide clasts. At the southern extremity of the floor of the glory hole (Fig. 3) the barite is less than a metre thick, and it continues to thin eastward to the edge of the glory hole, at which point barite, sulphides and sheared tuff interlayers have a combined thickness of only a few centimetres. Southeastward continuity of the mineralized zone is evident from several drillhole intersections (Fig. 2) in which the maximum true thickness of the barite-sulphide zone is of the order of 2 to 3 m but is typically much less. Most of the barite-sulphide intersections are present as two layers separated by 1 to 3 m of felsic tuff. This separation is thought to be significant because a similar tuff layer traversed the main part of the orebody in the glory hole and was referred to by the company as the "waste band" (Fig. 1).

The southeastern extension of the Main Orebody has continuity almost to the edge of the map area (Fig. 2) and to a vertical depth of at least 100 m. The orebody did not extend north or east of the glory hole, but to the west a gradual thinning and change to highly baritic, low-grade ore is evident. In the subsurface area to the west with co-ordinates E3400 to E3800, and N4500 to N4900 (Fig. 2), high-grade lead-zinc ore is present at the same stratigraphic position and was named the New Year Orebody. This ore zone, which has a northwesterly strike and southwesterly dip, and which extends to at least 150 m below surface, is clearly a continuation of the Main Orebody and was distinguished solely by ore grade. An interesting feature noted by Relly (1960) is that this area contained boulders of ore, 2.2 to 2.5 m in diameter, surrounded by soft clay-like altered tuff. These boulders were mined and evidently contained metal grades similar to those in the adjacent main part of the ore zone.

In summary, the Main Orebody sulphides are concluded to have been transported rather than deposited in situ, and much or most of the Pb-Zn-Cu black ore was an accumulation of sulphide breccia. A contrary viewpoint is that some or much of the ore was a "sulphide mylonite". Polished sections

of samples from the Main Orebody show, however, that the sulphides vary from crudely layered to chaotic. Sphalerite, galena, and chalcopyrite intergrowths occur in irregular patches, delicate replacement textures are widespread, and minute randomly distributed blebs of chalcopyrite and galena disseminated in a sphalerite host form a typical texture. Pyrite is fine grained and commonly shows growth zoning in crystals, or colloform textures. These features simply are not compatible with mylonitic or any other type of strong deformation or metamorphism.

The detailed study by Eldridge *et al.* (1983) of mineral textures in Japanese Kuroko ores also included a few examples of Buchans sulphides. These examples are from the West Oriental deposit and from the Lucky Strike pit (R.V. Kirkham, written communication, 1987). Eldridge *et al.*

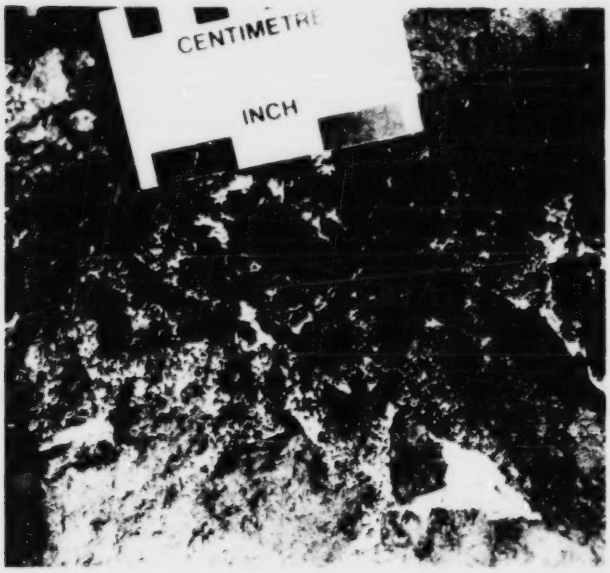

Figure 11a. Massive sulphide breccia ore from near the bottom of the Lucky Strike Main Orebody in the central part of the glory hole. Weathering has enhanced the contrast between the dark sulphides and the white, barite-rich matrix.

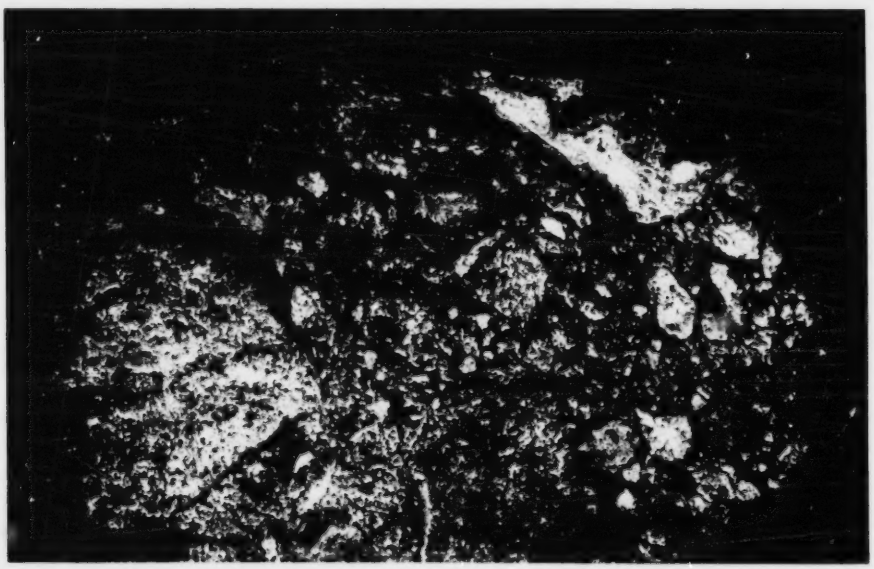

Figure 11b. Same piece, slabbed and polished. Large and small fragments at bottom left consist mainly of pyrite and abundant chalcopyrite, and largest fragment at top right consists predominantly of chalcopyrite and sphalerite (GSC Photo 204266).

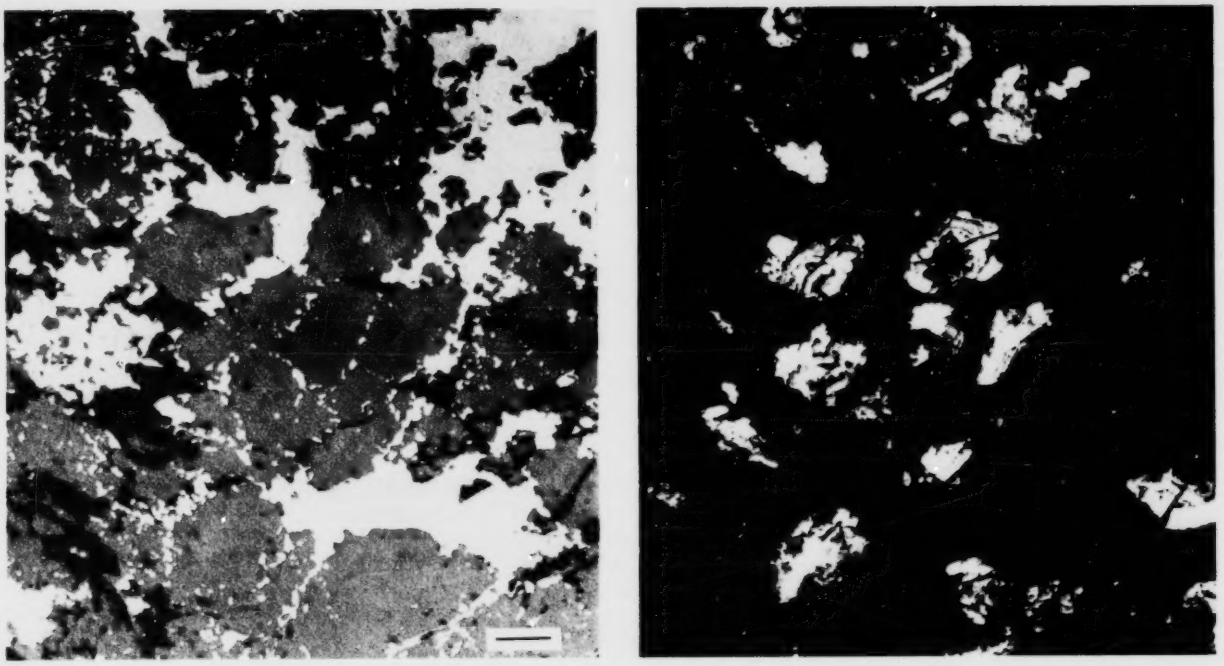

Figure 12. Typical texture of Main Orebody sulphides as seen in reflected light (left photo). Galena (white) is present as blebs and large, irregular patches amidst a mass of sphalerite (main grey). Equivalent photo in transmitted light (right) shows chromatic growth zones preserved in sphalerite, most of which is rendered opaque. Bar scale represents 0.1 mm. Sample is from the subsurface, western part of the Main Orebody; drillhole 167 at 5 feet (approximate co-ordinates N5200 E3700, 720 level).

noted that one of the most significant textures demonstrating the virtually pristine character of the Kuroko and Buchans ores is the preservation of primary depositional features such as growth banding in sphalerite. A few polished thin sections of samples randomly selected from the Main Orebody showed that this feature is present in all of the samples (Fig. 12, 13). Rather than being mylonitic, the Main Orebody sulphides are an outstanding example of an undeformed Kuroko-type black ore.

Waste band

The blanket-like form of the Main Orebody is evident from extensions beyond the western and southern limits of the glory hole. The high-grade orebody that existed in the glory hole is considered here to be a thicker part of the blanket whose shape was modified by folding and faulting.

The mineralogical and textural diversity of the Main Orebody has been referred to above, and considerable heterogeneity in the ore zone has been implied. Drillhole data for the glory hole area are sparse, but the presence of lithic fragments in the ore is noted in a few places in the core logs. As well, as many as four felsic tuff layers, each more than a metre thick, occurred at least locally in the ore. Some of this tuff was intercalated with sulphides and formed low-grade ore. Unfortunately, except for the thickest layer nothing is known about the attitude or continuity of the layers.

Figure 1 shows that the orebody at surface was traversed completely by a "waste band" that, near surface, was steeply dipping and 2 to 4 m thick. The waste layer was intersected in a few drillholes but no core is preserved; the rock was logged variously as sheared quartz porphyry, quartz porphyry breccia, and schist, thus suggesting that the rock was equivalent to schistose felsic tuff or tuff breccia. The tuff layer thinned at depth and is not shown on company plans and cross-sections deeper than the 800 level (about 40 m below surface). As is indicated by a few drill intersections, however, the dip of the layer was probably relatively low at depth and the layer, whether continuous or discontinuous, was traceable to the 720 level in the area west of the glory hole.

Figure 14 shows that the east-northeast strike of the waste layer at surface changed to southwest at depth, and that along the western side of the orebody the layer dipped more steeply than along the eastern side. The 800 level plan shows only two attitude measurements (Fig. 14), but these indicate that the layer dip flattened at depth. Figure 15 shows the configuration of the waste layer in north-south cross-section.

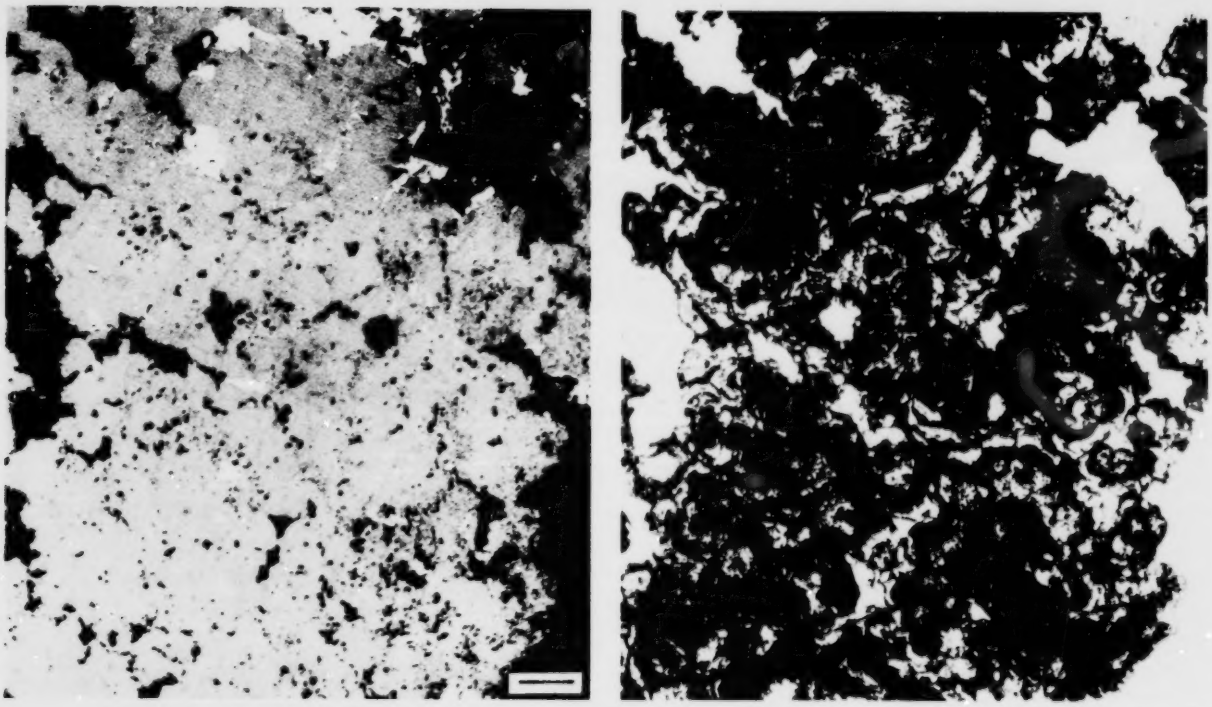

Figure 13. Reflected-light photo (left) showing numerous blebs of chalcopyrite in a sphalerite mass (main grey). The same area in transmitted light (right) shows the well-developed zoning of the sphalerite. Bar scale represents 0.2 mm. Sample is from drillhole 28 at 1 foot, from the 840 level near the centre of the mined-out Main Orebody.

At surface the waste layer was almost at right angles to the strike of the adjacent country rocks, whereas at depth the strike approached or equalled that of the host rocks. The waste layer, considering its area, thickness, and enclosure in massive sulphides, can be assumed to have had a relatively shallow to moderate dip that subsequently was steepened and locally overturned (Fig. 15). The steepest dips and most pronounced overturn occur in the upper part of the northwestern sector of the orebody. Possibly the folding was related to intrusion of the main diabase mass that borders the northwestern part of the orebody, but a relationship to southward thrusting along the Ski Hill Fault is an alternative possibility. Figure 16 is an east-west cross-section which shows that the western contact of the orebody adjacent to the diabase was vertical.

Orebody contacts

The entire northern part of the Main Orebody dipped steeply southward along a contact similar to that shown in the Figure 15 cross-section. From surface to the 680 level, inclusive, the Main Orebody did not extend beyond approximately N5250 (at deeper levels the orebody is not well defined in this area). In contrast to the southward dip of this Main Orebody contact, the adjacent rocks in the glory hole dip northward (Fig. 3), thus suggesting that the northern contact of the orebody must have been a fault. This fault follows the northern and eastern contact of the orebody (Fig. 3) and coincides with a narrow rim of sheared tuff bordering the orebody as shown on company plans.

The contacts of the orebody in the southern and eastern parts of the glory hole area are more complicated. As mentioned previously, the strike of the waste layer at surface was almost at a right angle to that of the country rock adjoining on the east. Beneath the Main Orebody significant deformation and shearing is evident in the southern part of the glory hole near drillhole 40 (Fig. 3). The basal contact of the barite at this site is schistose chlorite tuff, less than a metre thick, containing an S-shaped boudin indicating relative movement of the hangingwall was about N55°E. The hangingwall tuffs and barite dip moderately to the southwest. Tuffs beneath the fault have steep to vertical dips (Fig. 17), and footwall exposures closest to the fault also show a slight drag compatible with northeasterly thrusting. The fault plane did not precisely follow the bottom of the orebody, as is evident from unfaulted contacts along the steeply dipping orebody remnants that form an arcuate pattern in the southeastern part of the glory hole (Fig. 3). That the fault is present several metres below the

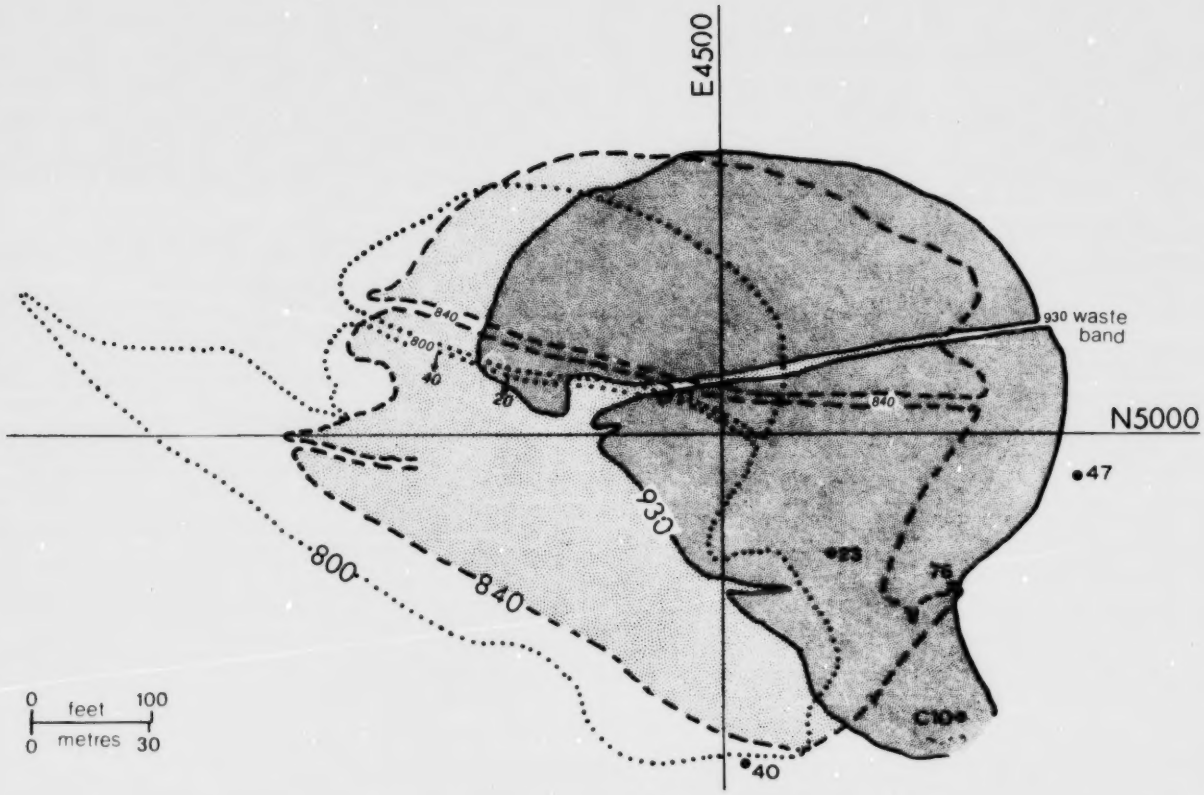

Figure 14. Company plans for the surface (930), 840, and 800 levels showing the outlines of the Main Orebody and the configuration of the "waste band" of felsic tuff. Numbered drillholes (solid dots) are referred to in the text.

orebody contact is suggested by the occurrence of schistose, folded tuffs (unit 6Ac, Fig. 3) which extend northward to the proximity of the fault along the northeastern periphery of the glory hole. Probably the northern and southern faults are the same structure, and this fault underlies the whole of the Main Orebody.

Folding of the southeastern part of the Main Orebody contact is evident from the arcuate orebody remnants that extend from near drillhole 40 to drillhole 76, where a topographically higher knoll of waste rock indicates that the orebody contact changed strike abruptly and trended westerly toward drillhole 23 (Fig. 3). The arcuate orebody remnants are topographically lower than those exposed in the pit wall near drillhole 40, and the two cannot be connected except by tight folding. This folding has west to northwest trends and thus seems to be related to north-south compression. In addition, however, minor refolding is evident in the crenulated tuffs of unit 6Ac (Fig. 3), and in an exposure near drillhole 76. At the latter site, strongly hematitic felsic tuff with remnants of ore is folded tightly and dips vertically to form an outcrop face about 3 m high. At the top of the vertically dipping tuff has been refolded and has only a moderate dip to the west. The contact of the mineable part of the orebody in this area apparently had a similar shape, the configuration of which suggests that the steep folding of the orebody contact was followed by minor movement to the east or southeast, possibly as a local response to intrusion of the main diabase mass.

Central part of the glory hole

Outcrops in the central part of the glory hole consist of three principal rock types: (1) massive sulphides and barite, (2) well-foliated to schistose felsic tuff, predominantly of a crystal-vitric type, and (3) highly siliceous, sulphide-rich breccia. The massive sulphides occur at substantially different elevations in the pit, the differences presumably reflecting the general westward slope of the orebody and the irregularities of the footwall contact (Fig. 19). In the deepest, western part of the glory hole (see contours in Fig. 2), the basal contact of the orebody occurs against a schistose layer that is thought to be the continuation of the thrust fault exposed near drillhole 40.

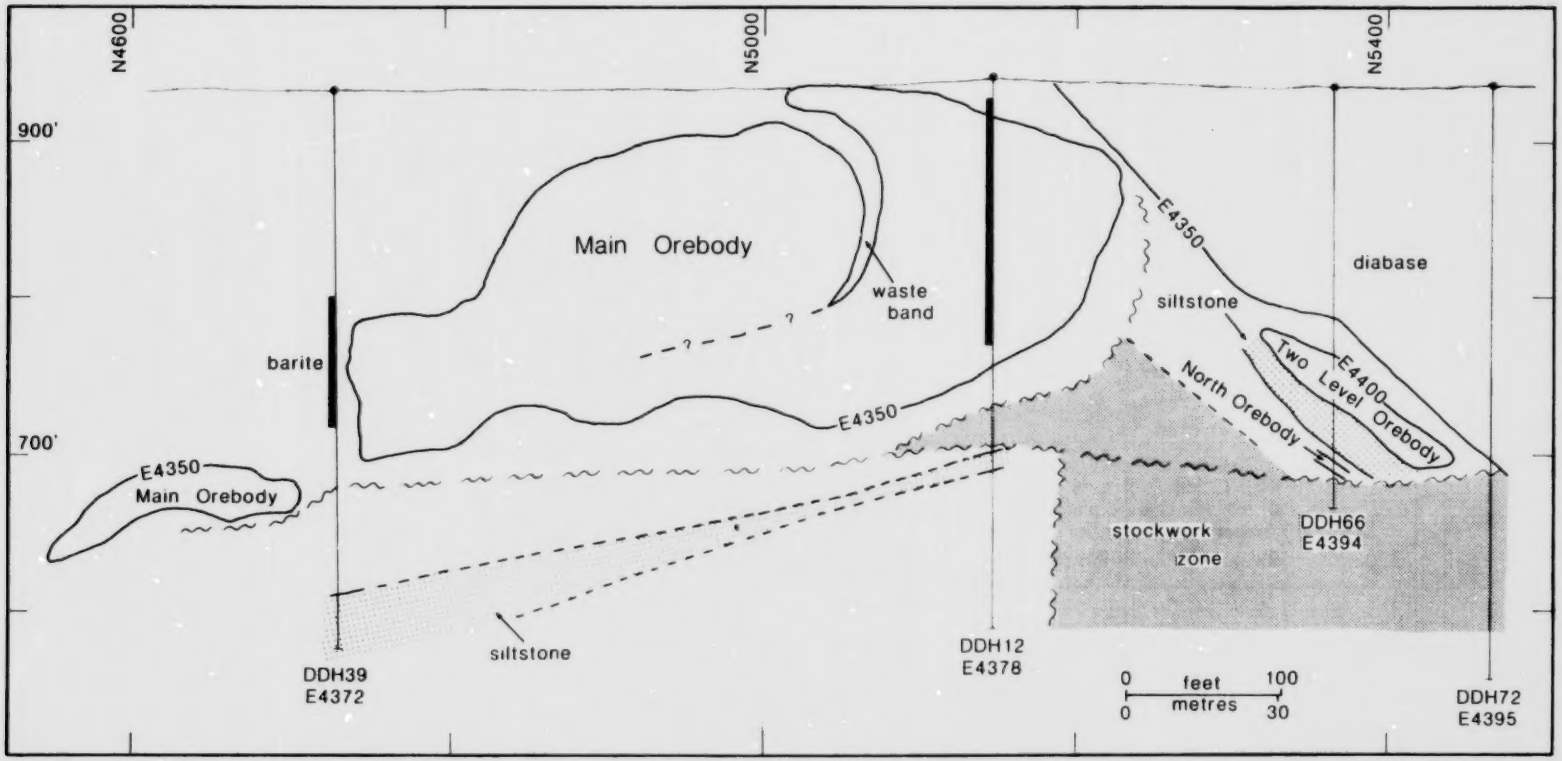

Figure 15. North-south cross-section approximately along E4350 showing the position of the "waste band" and the outline of the Main Orebody and Two Level orebodies according to company data (see Fig. 2 and 3 for drillhole locations). Stippled pattern shows the distribution of siltstone; the south and lower contacts of the stockwork zone are inferred to be faults.

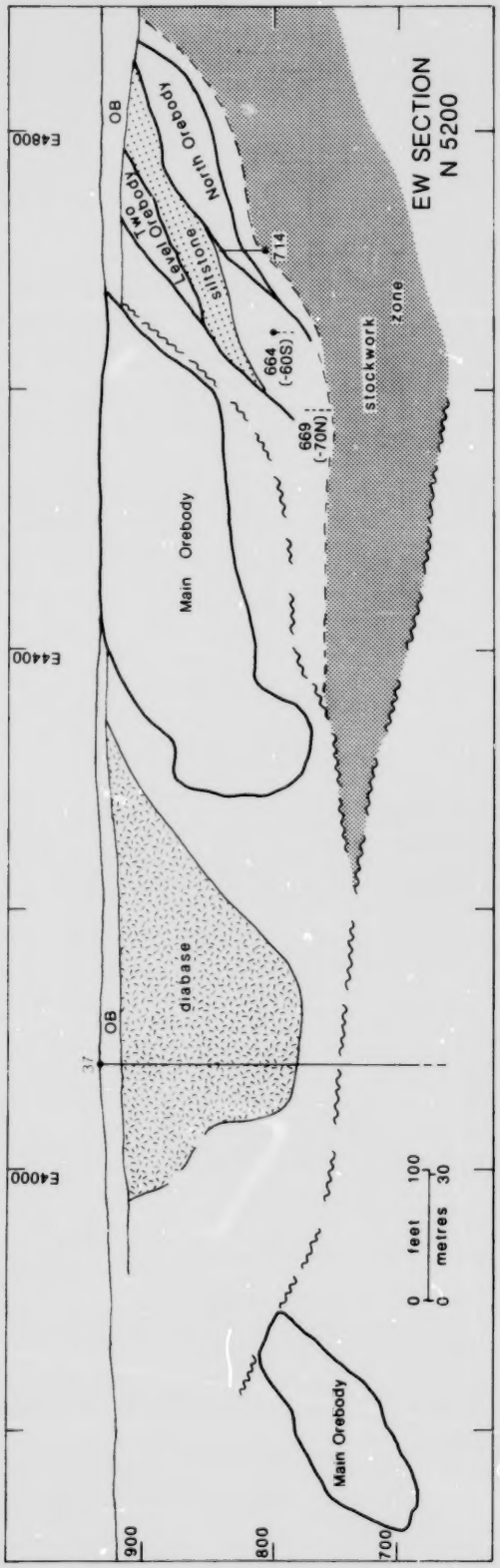

Figure 16. East-west cross-section along N5200 through the Main Orebody (company data), and the interpreted configuration of the Two Level and North orebodies (see Fig. 2 and 3 for drillhole locations). Siltstone (stippled) underlies the Two Level Orebody, and a thin layer of volcanic rocks relatively low in sulphides intervenes between the North Orebody and underlying stockwork zone. Faults are inferred. The lithology in the lower part of drillhole 37 is uncertain.

The schistose felsic tuff in the centre of the glory hole is similar to that which occurs along the eastern wall of the pit. In both areas the tuff is green but takes on a somewhat silvery sheen from weathering, and in both areas thin barite lenses or layers occur locally (unit 6Ad). The outcrop in the glory hole near E4400 contains pods of barite up to 1 m long and 0.3 m wide, and these have undulose, variable attitudes. The outcrop at N4865 and E4500 consists predominantly of barite-sulphide lenses that plunge 40°W, roughly similar to the thrust direction of the fault near drillhole 40.

The schistose felsic tuff occurs beneath a large part of the Main Orebody, but the thickness of the tuff is generally only 5 to 10 m. The exact relationship between massive sulphides and the highly siliceous sulphide-rich breccia in the glory hole is less clear. The orebody remnants vary from seemingly homogeneous high-grade massive sulphides, to sulphide breccias, to sulphide-rich rubble that contains highly pyritic fragments, blocks of ore-grade sulphides with barite, and siltstone fragments up to 18 × 25 cm. The siltstone is similar to that which forms the footwall of the Two Level Orebody. The siliceous, sulphide-rich breccia varies from tuffaceous to massive, and in outcrop typically has a coarse, knobby, rusty surface derived from siliceous pebbles and cobbles. Similar rock makes up a large part of the west-trending knoll near drillhole 76 (Fig. 3).

Northeastern side of glory hole

The final part of the glory hole to be described is the area near drillholes 47, 46, and 45 (Fig. 3). Near drillhole 47 schistose felsic tuff which has negligible disseminated sulphides is succeeded northward by black to dark green, northerly striking chloritic tuff that is highly pyritic. The contact between the two rock types seems to be along a poorly exposed fault marked only by a chloritic surface rather than a well-defined gouge zone. The northerly striking pyritiferous tuff has a variable but generally high sulphide content that seems to be related to the tuff bedding or layering rather than being vein-controlled. Some areas have enough pyrite to form semi-massive sulphides, and some contain sufficient base metals to form low-grade ore. Most of the sulphides are disseminated, but discrete pebbles and fragments also occur.

The area adjacent to drillhole 45 (Fig. 3) was mentioned previously with reference to the North Orebody. The two most easterly barite outcrops are dip-slope remnants of the same body; between these and the northwestern barite outcrop is massive, coarse grained pyrite overlain by the same highly siliceous tuff that overlies the barite. The massive pyrite extends downslope, where it was overlain by the Main Orebody, a remnant of which occurs about 20 m south of drillhole 46 (Fig. 3). This remnant of high-grade Zn-Pb ore is at a slightly lower elevation than the massive pyrite, and presumably occurred in a local irregularity in the footwall of the Main Orebody.

Outcrops adjacent to drillhole 45 contain less pyrite, are slightly more tuffaceous, and contain numerous siliceous and massive pyrite pebbles. Some of the pyrite is evidently present as huge boulders; one of these, 2 to 3 m across, shows

Figure 17. View to the east, from near drillhole 40 in the south part of the glory hole, showing a barite-rich part of the Main Orebody overlain by hematitic felsic tuff, both of which dip moderately southwest (Fig. 3). Beneath the barite are steeply dipping tuffs, parts of which are pale grey (middle of photograph). The steeply dipping tuffs follow an arcuate trend toward the middle left of the photo (i.e., from drillhole 40 toward drillhole 76 in Fig. 3).

siliceous tuff draped over its top in the same kind of relationship noted for the nearly massive barite (Fig. 10). Minor, fine grained, schistose tuffaceous layers in this area have small folds with axes trending about 75° and plunging about 35°W.

The massive pyritic rocks described above closely resemble some parts of the pyritiferous assemblage that occurs along the northern wall of the glory hole, west of the Two Level Orebody. Connecting the two areas stratigraphically would suggest that these were unconformably deposited above the Two Level Orebody and its underlying siltstone. Unfortunately, the geology of the intervening area is obscure because of the former presence of the Main Orebody, and because of poor drill-core preservation. Indications are, however, that siliceous, pyritiferous rocks formed a narrow belt around the northern and eastern periphery of the Main Orebody. J.G. Thurlow (written communication, 1986) has suggested that the siliceous assemblage was thrust to its current position.

Many of the rocks that have been described for the glory hole are sulphide-rich, or highly siliceous, or both. The stratigraphic position and mode of origin of some of these rocks is controversial, but in some areas, such as that immediately beneath the North Orebody, the weight of evidence suggests that the sulphides originated by syndepositional accumulation rather than by stockwork epigenesis. The presence of stockwork-altered cobbles amidst these sulphide-rich, pyritic volcanic rocks indicates their post-stockwork age.

Southeast of the glory hole a small, low-grade, copper-rich zone referred to as the Engine House Orebody (Fig. 2) formed a separate underground mine reported to consist of stockwork mineralization (Thurlow and Swanson, 1981). In view of the conclusion reached about the nature of the mineralization in the glory hole area, the Engine House Orebody was of special interest for revealing the characteristics of stockwork sulphides in the area.

ENGINE HOUSE OREBODY

The Engine House workings have been dammed and flooded, and thus nearly all of the information about the orebody comes from drillhole logs and cores, and from the thesis by Catherall (1960). According to Catherall, during 1944-1951 about 140,000 tonnes of ore were mined from total reserves of about 400,000 tonnes grading 1.54% Cu, 4.75% Zn, and 1.59% Pb. The copper content thus was similar to that of Main Orebody, but other metals were substantially lower (Table 2). The orebody was centered in an area about 100 m below surface and near drillholes 437, 436, and 422 (Fig. 2). Access was from the Lucky Strike underground workings.

Although the shape of the Engine House deposit is irregular, in the mined area the form is distinctly blanket-like and the ore came from a thicker-than-average part of the blanket (Fig. 19). Drill cores show that the ore consists of white quartz containing chalcopyrite, pyrite, sphalerite, galena, and small amounts of tetrahedrite. The sulphides occur predominantly as disseminated grains, wisps, and trains of grains in a relatively uniform sulphide-quartz assemblage, distinct from clear-cut veins. Catherall (1960) reported the presence of white quartz as irregular blebs, lenses, and stringers, but the exact nature of these is not clear and he does not specifically

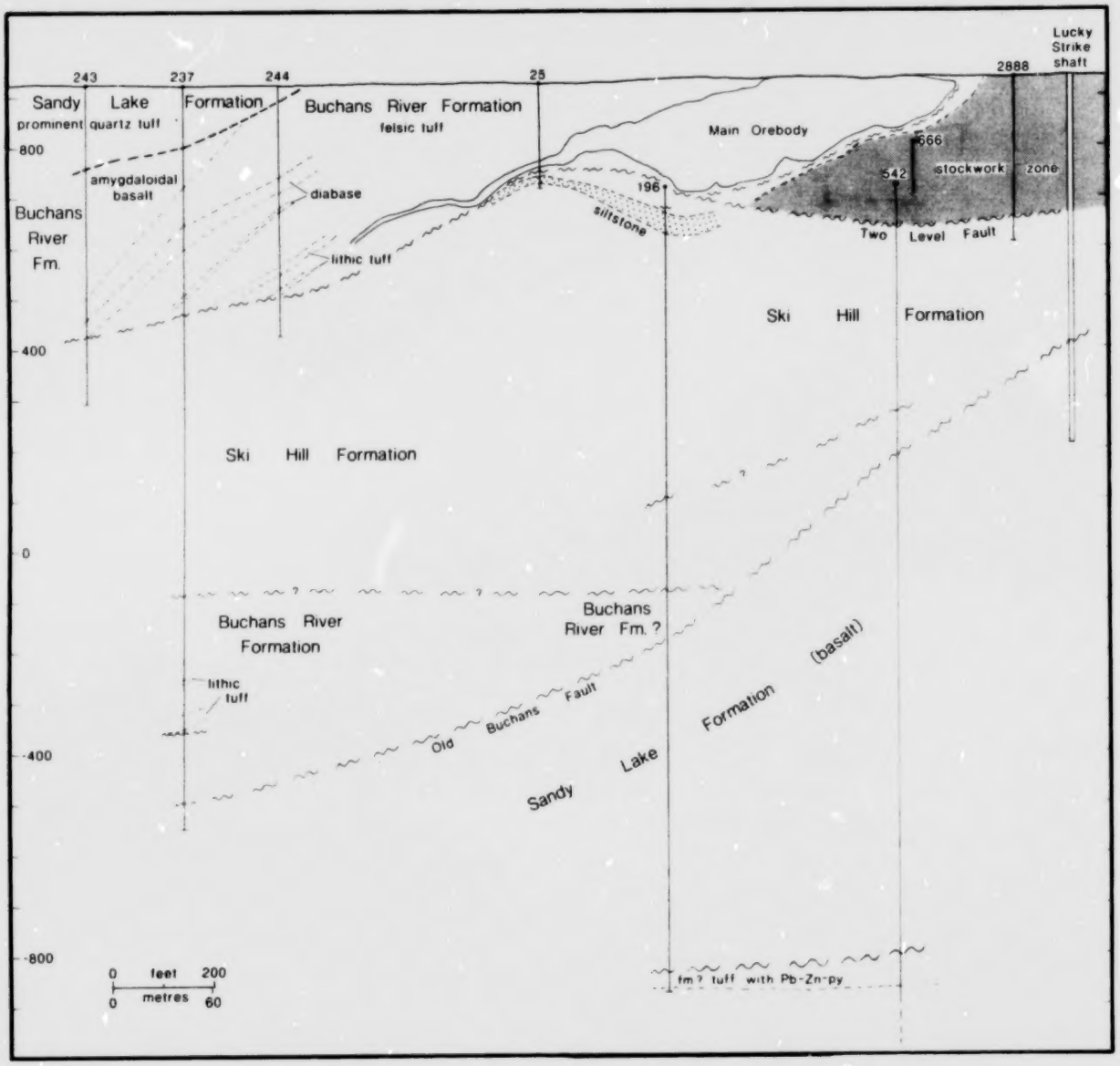

Figure 18. East-west cross-section at N5000, with Main Orebody outline from company data (see Fig. 3 for drillhole locations). The stockwork zone is in the Ski Hill Formation and is terminated by an inferred fault. Stippled pattern represents siltstone which is interpreted to be equivalent to the unit that underlies the Two Level Orebody. Contact of Sandy Lake Formation in the Lucky Strike shaft is from Kowalik *et al.* (1981).

refer to the presence of quartz-sulphide veinlets. Catherall did conclude, however, that silicification and pyrite crystallization were followed by strong fracturing and the introduction of quartz and the ore sulphides. J.G. Thurlow (written communication, 1986) reported that, from his personal underground observations, the orebody was characterized by a network of quartz-sulphide veins cutting a strongly silicified host.

The orebody contacts vary from sharp, without apparent faults, to the local presence of a completely gradational footwall. In the latter, anomalous silica is absent and discontinuous seams or disseminated grains of chalcopyrite conform with tuff layers rather than cross-cutting them. In several areas many centimetres of barren tuff are interspersed with the sulphide-bearing tuff so that the boundary is completely arbitrary. Where the contact is sharp, the orebody is

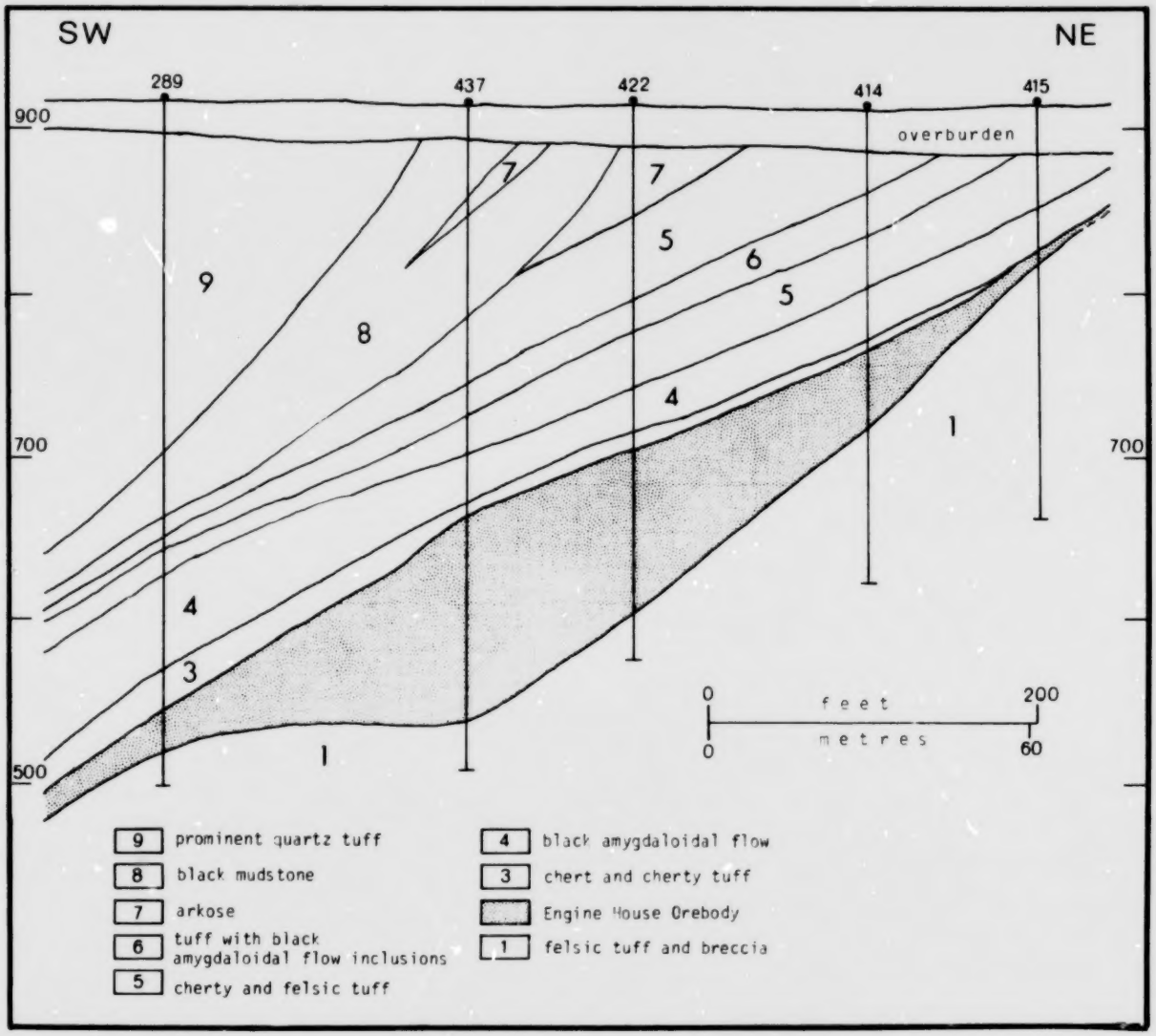

Figure 19. Northeast-southwest cross-section of the Engine House Orebody in the southeastern part of the map area (Fig. 2).

typically bounded by pale green to buff, barren chert or cherty tuff. Catherall (1960) noted that chert up to 1 m thick occurred in sharp contact along part of the base of the orebody; a similar buff, waxy-lustre, barren unit occurs extensively along the top of the orebody.

Despite the presence of almost massive quartz or pervasive silicification in the main part of the orebody, a few short (10 to 20 m) underground holes drilled in the ore zone show rare occurrences of clear-cut quartz-sulphide veins in silicified tuff. The veinlets occur within the orebody and do not affect the statements made about the sharp or gradational nature of the orebody contacts. The underground holes also show that massive barite up to 1 m thick, and baritic massive sulphides (greater than 30% Pb + Zn) up to 1.5 m thick, occur in the ore zone but lack lateral continuity. Catherall (1960) observed that barite and associated lead and zinc increased near the centre of the orebody; the barite apparently occurred as a matrix rather than as a vein mineral, and in places massive barite was present. From a detailed examination of assay data, Catherall also concluded that the highest average grades of copper occurred along a zone, 3 to 9 m thick, that followed and abutted on the hangingwall contact of the deposit.

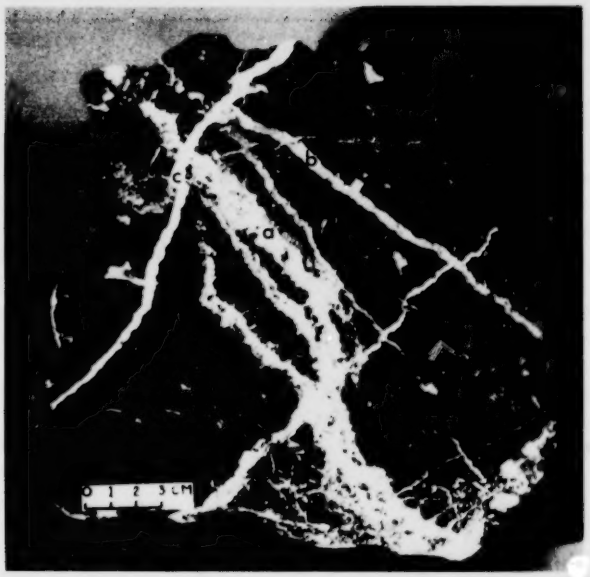

Figure 20. Stockwork veinlets in altered volcanic float from the Lucky Strike glory hole. Relatively wide quartz-pyrite veinlets (a) are cut by narrower veinlets of quartz-sphalerite-galena-chalcopyrite (b), in turn cut by pink calcite (c). (GSC Photo 204266E).

Extensions of the Engine House zone

Down-dip the Engine House Orebody diminishes to less than 1 m in thickness, but parts nevertheless are interpreted here to be traceable for at least 100 m in a down-dip, southwesterly direction. In the extreme southeastern area a similar waning occurs southeasterly along strike. The up-dip projection to surface through drillhole 415 (Fig. 19) is more uncertain in that sulphides are erratic, are of low grade (2% combined base metals), and anomalous silicification is absent. Underground, the northwestern strike extension of the orebody loses continuity in the vicinity of a minor northeasterly-striking fault (Fig. 2). The fault dips to the northwest at about 65°, and is shown on company mine plans of the 640 and 540 levels as a faulted and crushed zoned, the sense of movement of which is uncertain. At surface the fault seems to mark the termination of amygdaloidal basalt (Fig. 2), but with no significant offset of the arkosic unit or the extension of the Main Orebody.

Near-surface sulphides intersected in drillhole 2890 and others to the north (Fig. 2) probably represent the continuation of the Engine House Orebody. In cores from these holes the proportion of barite is higher than occurs in the mined area, but otherwise the mineralized zone is similar. The host Ski Hill Formation in this northern area consists predominantly of pale grey breccias with intercalated buff to grey siltstone. Unreplaced fragments of the assemblage occur within the mineralized zone, and many of these remnants contain sharply defined quartz-sulphide veinlets. Coincident with the widening of the mineralized zone the amount of massive milky quartz declines, and anastomosing quartz-sulphide veinlets characteristic of a stockwork are abundant.

The presence of typical stockwork veinlets at some sites at Lucky Strike raises several questions concerning the nature and origin of the Engine House Orebody. First, the sheet-like form of the orebody is most unusual for a stockwork zone. To account for the orebody shape it has been suggested that the body might be fault-bounded. This suggestion, however, is at variance with the sharp to gradational, unfaulted contacts reported above (the faulted versus unfaulted alternatives can be judged by examining cores such as those from underground drillholes 725 and 727). Secondly, the association of the orebody and concordant cherty sediments is unlikely to be merely coincidental. Thirdly, network veinlets typical of stockwork are not obvious in Engine House cores despite the highly siliceous character of the ore, and despite the fact that such veinlets are readily recognizable at other sites. The fourth and final point centres on the textures of some of the minerals. Reconnaissance microscopic observations indicate that the Engine House pyrite is similar to that in stockwork veinlets in that the grains are well crystallized and lack well-developed growth zones. Much of the pyrite has been affected by brittle deformation as is indicated by fractured grains with matching walls. Nevertheless, sphalerite zoning is well preserved in some grains. Quartz is typically minutely dusty, and in some sections the grains form anhedral masses. In other sections the dusty particles clearly outline growth zones in chalcedony. None of these textures is genetically definitive, but also present along and beneath the base of the orebody are abundant detrital pyrite grains and rare ore clasts which indicate that the Engine House area must have been exposed at the time of ore formation. Consequently, the unorthodox (and strongly criticized) conclusion is that the Engine House Orebody originated largely as a siliceous chemical precipitate. To the north, the siliceous zone is thought to be a relatively thin capping that overlies and merges with well-defined epigenetic stockwork veins in the vicinity of the Lucky Strike shaft. This merger suggests that the shaft area was the probable discharge site for the siliceous precipitates.

Stockwork zone

The breccia, tuff, and intercalated siltstone assemblage that makes up the bulk of the Ski Hill Formation east of the Engine House Orebody is sulphide-barren in that only traces of disseminated matrix pyrite, and rare moderately pyritic breccia fragments are present. The pyritic fragments are distinctive in that the pyrite is characteristically extremely fine grained. Similar rocks occur adjacent to the mill and extend beneath the floor of the glory hole. To the north and northeast, however, the arenaceous components are minor or missing and the rocks are largely a mixed assemblage of medium to dark green tuff and volcanic breccia. Much of the breccia is fine grained, has diverse fragments, and appears to be a greener and finer grained version of the breccias that occur in the siltstone-breccia assemblage.

A zone of intense stockwork replacement underlies the eastern part of the glory hole and extends to the vicinity of the

the Lucky Strike shaft. Within this zone, siliceous replacement and quartz veins with associated sulphides, barite, and calcite typically make up 50% to 80% of the rock. Pyrite is abundant and commonly forms semi-massive sulphides in a siliceous matrix. Most of the pyrite is fine grained; where crystals are megascopically evident, relatively few exceed 1 mm along an edge. Sphalerite and lesser amounts of galena occur both in quartz veins and as disseminated grains in the more pervasively altered rock; in places core lengths of several metres contain 8 to 10% combined Zn + Pb. Chalcopyrite content is variable, but several assay intervals of 1 to 2 m were noted in which Cu values exceed 5%. These high base metal values are not anomalous relative to the near-surface stockwork to the east of the glory hole; for example, drillhole 220 near the mill (Fig. 2) averaged 9.85% combined Zn + Pb over a continuous interval of 13.4 m.

Judging from the virtual absence of stopes outlined on company cross-sections available to the writer, only a minute amount of the Lucky Strike stockwork zone was mined. Despite the impressive assay data cited above, metal values are erratic and average grades are substantially lower when mineable volumes are considered. The only large stope in this ore type evidently was elongate in a north-south direction and extended from about 15 m north of drillhole 45, southward almost to drillhole 47 (Fig. 3). The floor of the stope was approximately the 760 level, and the roof was 3 to 4 m above it.

An excellent description of the general aspects of the stockwork mineralogy is given by Kowalik *et al.* (1981). A decrease in the intensity of the stockwork zone toward the northeast is marked principally by a decline in pervasive sulphides and quartz, and by the commensurate increase in the proportion of host rock; thus the number of sharply defined quartz-sulphide veinlets increases, but the total volume of sulphides and quartz decreases. Calcite also increases at the expense of barite. Additional waning of stockwork intensity continues with increasing depth and to the northeast beyond the map area; the decline in intensity is evident from the progression to narrower and fewer veinlets in which pyrite-quartz supplants the mixed base metal sulphide assemblage.

The northwestern boundary of the stockwork zone at surface simply reflects the presence of overlying felsic tuffs of the Buchans River Formation (Fig. 2). The tuffs average about 70 m in thickness along the northern part of the map-area (Fig. 2), and thickness increases northward and westward. Thus the stockwork zone in these areas has not been penetrated to great depths, but the limited drill data suggest that the zone decreases in intensity both toward the north and with increasing depth to the northwest. Probably weak stockwork continues northward to the easterly striking Ski Hill thrust (Thurlow and Swanson, 1987).

Host rocks for the stockwork zone in the northern area are a mixed assemblage of tuffs, flows, and volcanic breccia that are typically massive rather than well layered. Aphanitic grey to tan felsite or felsite breccia is abundant locally and provides some of the best examples of intense stockwork replacement. No large concentration of felsite that could be deemed a genetically related body for the stockwork zone has been observed within the map area.

The configuration of the stockwork zone beneath the glory hole, and the relationship to the Main Orebody, is shown in Figures 15, 16 and 18. The Main Orebody was not in direct contact with the stockwork zone; in most areas the orebody was underlain by several metres of green, well-foliated felsic tuff containing negligible sulphides. The stockwork zone lies beneath the green tuff, and extends northwesterly beyond drillhole 175 (Fig. 2), penetrating to unknown depths in this area. In contrast, the contact between intense stockwork veining and barren rock beneath the eastern part of the glory hole is extremely abrupt (Fig. 18), and is accompanied by poor core recovery. The abrupt change occurs at various elevations, but most are approximately between the 600 and 640 levels. The sharp demarcation is attributed to the presence of a flat-lying, inferred fault.

FAULTS

Thurlow and Swanson (1987) have described the numerous thrust faults that occur in the Buchans area. The presence of two major thrust faults in the Lucky Strike block is based entirely on the stratigraphic and structural relationships defined by Thurlow and Swanson.

Buchans River Fault

The southward dipping Buchans River Fault is a major thrust that strikes slightly north of west and cuts through the Lucky Strike area (Fig. 7 of Thurlow and Swanson, 1987). The approximate co-ordinates of the fault at surface in Figure 2 are N4000 E6000 to N5000 E4000, and the fault therefore would cut through the Lucky Strike orebody and its enveloping rocks.

No evidence of a major, southward dipping fault along the above co-ordinates was found in the present study. Continuity of the Main Orebody in the southern and western parts of the map area is evident not only from the presence of massive sulphides and barite, but also because the ore zone is closely associated with a distinctive grey lithic tuff that contains variable amounts of quartz and feldspar crystals, and has scattered irregular to round felsic inclusions typically a few millimetres to a centimetre in diameter. The most characteristic trait of the tuff is its poor induration, and even large-diameter cores are readily broken by hand. The tuff, which is typically only a few metres thick, chiefly overlies the Main Orebody but locally straddles or underlies it where the ore zone is thin. At elevations roughly corresponding to the 540 level, the tuff extends from the extreme southeastern part of the map area (drillholes 1904 and 1908, Fig. 2) to about N5000 E3400.

Old Buchans Fault

The Old Buchans Fault to the east of Lucky Strike has thrust the Ski Hill and Buchans River formations over the younger

Sandy Lake Formation (Thurlow and Swanson, 1987). The stratigraphic relations therefore dictate that the Old Buchans Fault is present at depth in the northeastern corner of the Lucky Strike area, in inclined drillhole 282 (Fig. 2), where stockwork-altered Ski Hill rocks overlie arkose of the Sandy Lake Formation at a vertical depth of about 235 m. Although the arkose is not known to occur elsewhere at Lucky Strike, equivalently young rocks of the Sandy Lake Formation are represented in the map area by the unit known formerly as the Footwall Basalt (Table 1). These basaltic rocks in the Lucky Strike area are overlain by the stratigraphically older Ski Hill Formation (Thurlow and Swanson, 1987), and thus their contact can be used to define the thrust plane of the Old Buchans Fault. The general configuration of the contact is evident in Figure 17 of Thurlow and Swanson (1981).

Only a few drillholes in the Lucky Strike block have penetrated the Sandy Lake basaltic unit, and even in these holes it is difficult to distinguish Ski Hill from Sandy Lake rocks. Relly's (1960) illustration showing the "Structural Contour on Main Footwall Horizon", which presumably was based on company data, clearly includes rocks belonging in the Ski Hill Formation and thus does not depict the contact. The cross-sections shown by Kowalik *et al.* (1981) are thought to include altered Ski Hill rocks (e.g. drillhole 2891) and possibly parts of the Buchans River Formation (e.g. drillhole 1904), but these sections otherwise seem to be a much better representation of the possible Sandy Lake basaltic contact. Near the central part of the glory hole (drillhole 542, Fig. 18) the possible contact is about 220 m below surface, or roughly at the same elevation as the Ski Hill–arkose fault contact in the extreme northeastern part of the map area. In the northwestern part of the area, however, the contact is at a much lower elevation, and is about 480 m below surface in drillhole 202 (Fig. 2; see also the Figure 2 cross-section in Kowalik *et al.*, 1981).

The position of the Ski Hill–Sandy Lake contact is uncertain in the western part of the map area. The possible position of the contact is shown in Figure 18, but a much more thorough on-site study is necessary to establish the lithological correlations from drillhole to drillhole. For example, the previously mentioned poorly indurated lithic tuff that is associated with the Main Orebody can be traced from the southwestern area (drillhole 1021, Fig. 2) northward through holes 240, 241, 244 and 237. Dips of the tuff are moderate, and in all holes except 237, the tuff is at elevations appropriate for continuity from the glory hole area; in drillhole 237, however, the tuff is about 280 m deeper than expected from the projection from the adjacent drillhole (Fig. 18). This anomaly, also evident in another hole to the east, suggests that the Ski Hill Formation in this area may have been thrust over the Buchans River Formation. A more detailed study extending to the west of the map area is needed to resolve the structural and lithological relationships.

Other faults and folds

Company plans of the Lucky Strike deposit show only three minor folds and a total of about a dozen faults, all of which are on the 800, 540, and 350 levels. Two of the folds have axial planes striking northeast, and the other strikes northwest. Many of the faults are accompanied by the notation W.H.N., indicating that they were mapped by W.H. Newhouse during the period 1927-1929 (Swanson, 1981). One of the faults on the 540 level is noted specifically as stopping against an east-trending diabase dyke that is the continuation of the intrusion exposed along the northern lip of the glory hole. Other faults cut the dyke, thus indicating at least two ages for the faults. Strikes and dip directions of the faults are not in any definable pattern. The only fault shown as having an offset is thought to continue to surface and appears in the southeastern corner of Figure 2. On the 540 level this fault is shown as having a displacement of a few metres, but beds offset at opposite ends of the fault give contradictory movement directions; a few metres of northeasterly movement of the southeastern block is the more probable alternative, and this offset could be accommodated readily in the configuration shown in Figure 2.

All rocks in the glory hole area have local slickenside surfaces and local areas of schistosity, but no major offsets were defined by direct observation. The presence and importance of the two significant faults in the glory hole area are largely inferred, and problems exist in deciphering the continuity of the faults because of a lack of observational data. One of the faults, which is exposed at the southern end of the pit near drillhole 40 (Fig. 3), has been described already. The fault occurs at the base of the orebody and apparently continues northward along this contact to at least the 720 level, as is discussed below. At surface in the southeastern corner of the glory hole, between drillholes C14 and 76, the arcuate orebody remnants do not have a faulted base. The rocks here are highly folded, and the fault is thought to be present in strongly schistose, altered tuff a few metres below the orebody contact. The schistose tuff extends northward and evidently is continuous with the arcuate fault along the northern half of the glory hole (Fig. 3). There is ample evidence that the rocks at the Main Orebody contact, or a few metres below it, are highly contorted in the glory hole area, thus suggesting that the fault extended beneath the main part of the orebody and dipped northwestward to the 720 level.

On the 720 level the Two Level Orebody has been offset by the assumed continuation of the above fault (Fig. 7, 8). Figure 23 shows the assumed pre-fault position of the Two Level Orebody, and the direction of movement used to achieve the restoration.

The second major fault in the glory hole area forms the northern boundary of the Main Orebody. This fault is thought to be steeply dipping, but possibly merged with the fault that offset the Two Level Orebody. In the northern part of the glory hole the waste band and the north contact of the Main Orebody dipped steeply south, suggesting that both were steeply folded; in addition, however, the Main Orebody contact shows an abrupt discontinuity against the assemblage containing the Two Level Orebody (Fig. 25), thus indicating that the two were separated by a west-trending fault roughly along N5250.

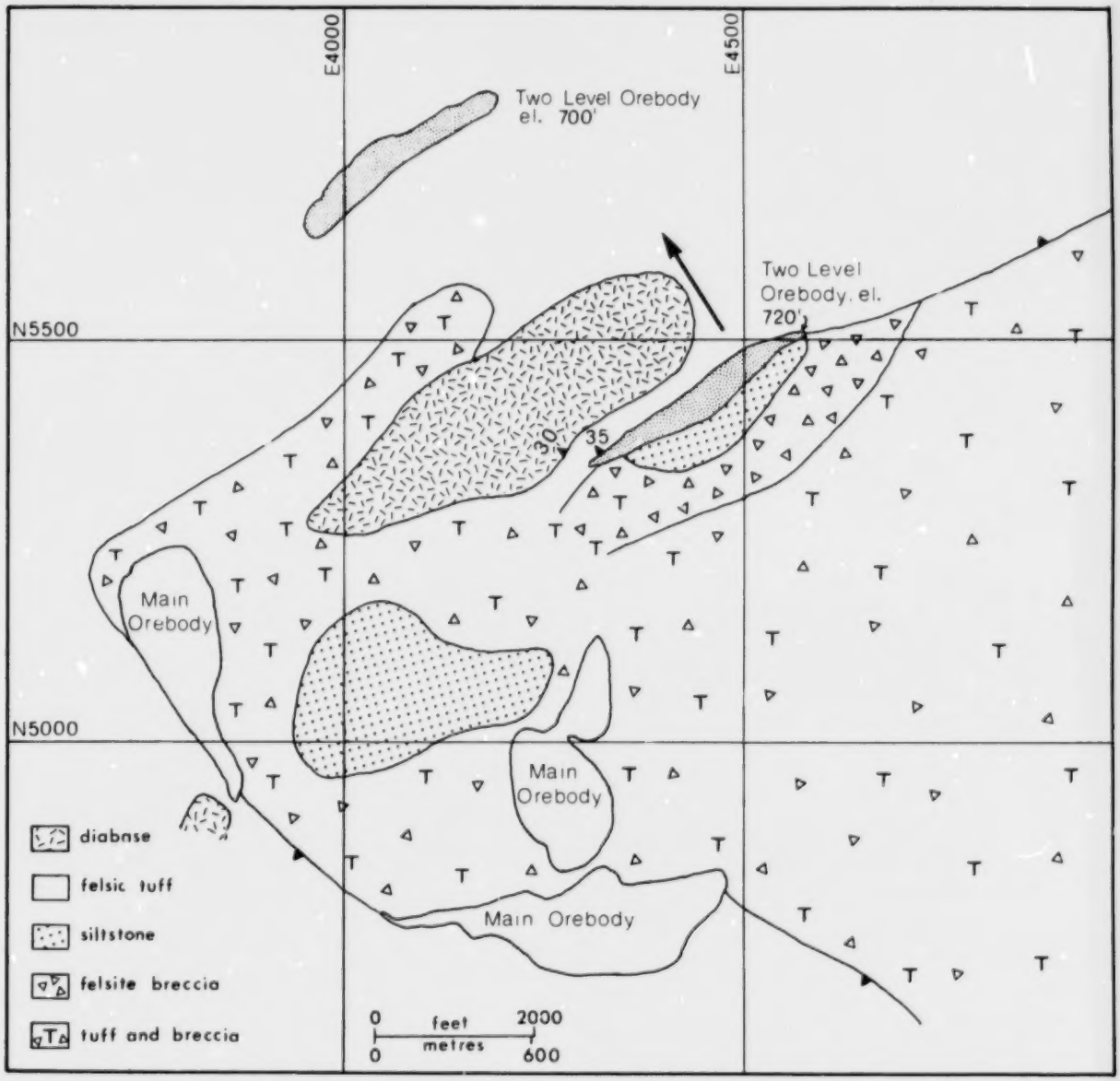

Figure 21. Company plan of the geology of the 720 level approximately 210 feet below surface, with the Two Level Orebody at elevation 700 feet added. Arrow indicates the displacement direction used for the restoration shown in Figure 23.

A pre-diabase age for the northern contact fault is suggested from the fact that parts of the western near-surface contact (and inferred fault) mimic each local irregularity in the diabase outline. The diabase and Main Orebody are close to each other at surface, but their separation increases gradually with depth. The dip of the folded northern contact of the Main Orebody and waste band diminish similarly, thus suggesting that the steep to overturned contact of the upper part of the orebody, as contrasted with the relatively shallow dip of its lower part, reflects deformation related to diabase intrusion.

Although the fault along the northern part of the Main Orebody has been concluded to be pre-diabase, it was assumed initially that displacement of the Two Level Orebody was post-diabase. It may be significant that company plans do not show that the base of the diabase on the 720 level as a fault

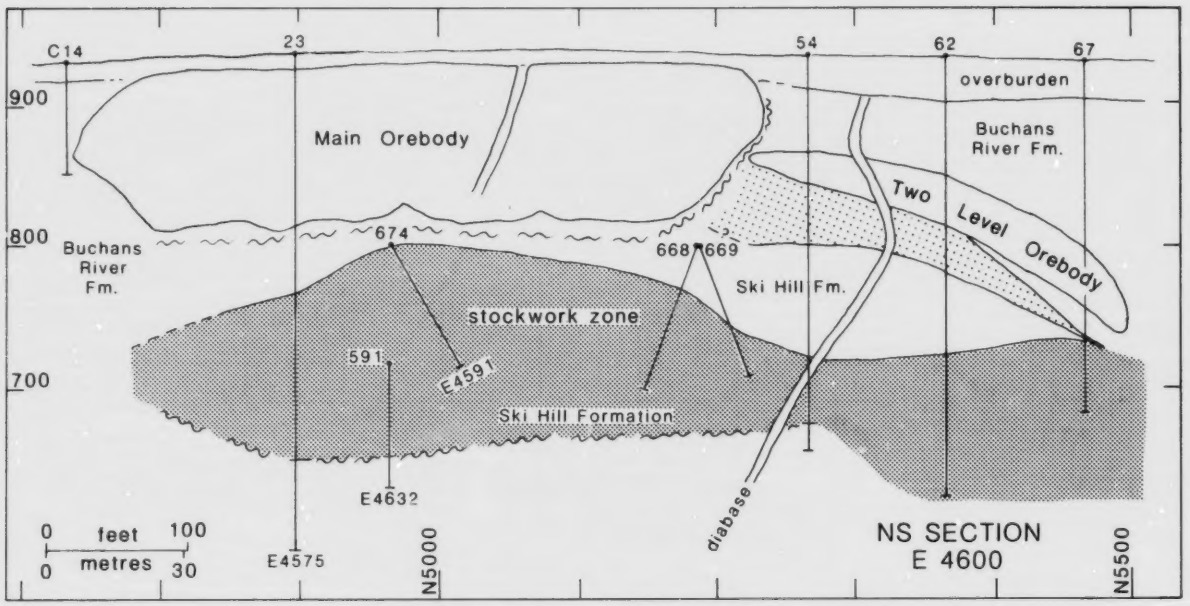

Figure 22. North-south cross-section at E4600 showing the configuration of the Main Orebody (company data); waste band added from information on company plans.

contact. Diabase footwall contacts in a 720 level drift through the intrusion show that the northwestern dip of the intrusion is interrupted for a short distance by an abrupt change to a gentle southeastern dip. As this abrupt change coincides with the offset plane of the Two Level Orebody (Fig. 8), possibly the intrusion was deflected by the pre-existing fault. Supporting this possibility is the continuity of the diabase dyke that occurs on the northern lip of the glory hole, and which is reasonably assumed to be an offshoot of the main diabase mass. The dyke is almost vertical and is continuous from surface to the 540 level, which indicates that intrusion must have occurred after offset of the Two Level Orebody.

MINERALOGICAL NOTES

Before proceeding with a discussion of the genesis of the Lucky Strike deposits, a few notes on miscellaneous mineralogical observations are recorded. One mineral not noted previously to occur at Buchans is laumontite, but this zeolite is widespread in small amounts and has been observed at many sites and in various lithologies throughout the Buchans River Formation, in the Ski Hill Formation, and in diabase. A random check confirmed that laumontite also is present in the former Upper Buchans Subgroup of Thurlow (1981), thus indicating that the mineral is regional in extent. The typical occurrence is as pink veinlets along easily separable hairline fractures; rare veinlets up to 2 cm wide have been observed. The widespread presence of laumontite imposes constraints on maximum temperatures of the regional metamorphism (Liou, 1971, 1979).

George (1937) reported that oxidation of the top of the Main Orebody was extensive, and that some parts contained a gossan almost 2 m thick. Apparently this material was stripped and stockpiled; although none remains now, at the time this study was begun a small amount of the oxidized ore was stockpiled at the edge of the glory hole near the Lucky Strike shaft. Sporadic colorful blooms were present, and a suite of these was collected. Green coatings reflect the presence of brochantite $Cu_4(SO_4)(OH)_6$, antlerite $Cu_3(SO_4)(OH)_4$, and ktenasite $(Cu,Zn)_5(SO_4)(OH)_6 \cdot 6H_2O$; the last is known from only two other localities (Raade *et al.*, 1977). Sky-blue coatings invariably are serpierite $Ca(Cu,Zn)_4(SO_4)_2(OH)_6 \cdot 3H_2O$, and all yellow to yellow-brown pulverulent coatings were found to be beaverite $Pb(Cu,Fe)_3(SO_4)_2(OH)_6$, or solid-solution members of similar composition in the jarosite group. Other minerals identified in the assemblage are smithsonite, anglesite, hemimorphite, gypsum, chalcanthite, rozenite, and gunningite. The last three are evanescent water-soluble sulphates.

EVOLUTION OF THE OREBODIES

The stratigraphic relations of Thurlow and Swanson (1987) indicate that the lithological assemblages in the Lucky Strike block have been thrust over basaltic rocks that form part of the Sandy Lake Formation. The thrust plane lies at considerable depths, however, and within the thrust block the distribution and intensity of stockwork alteration suggest that a substantial part of the mineralization record has been preserved.

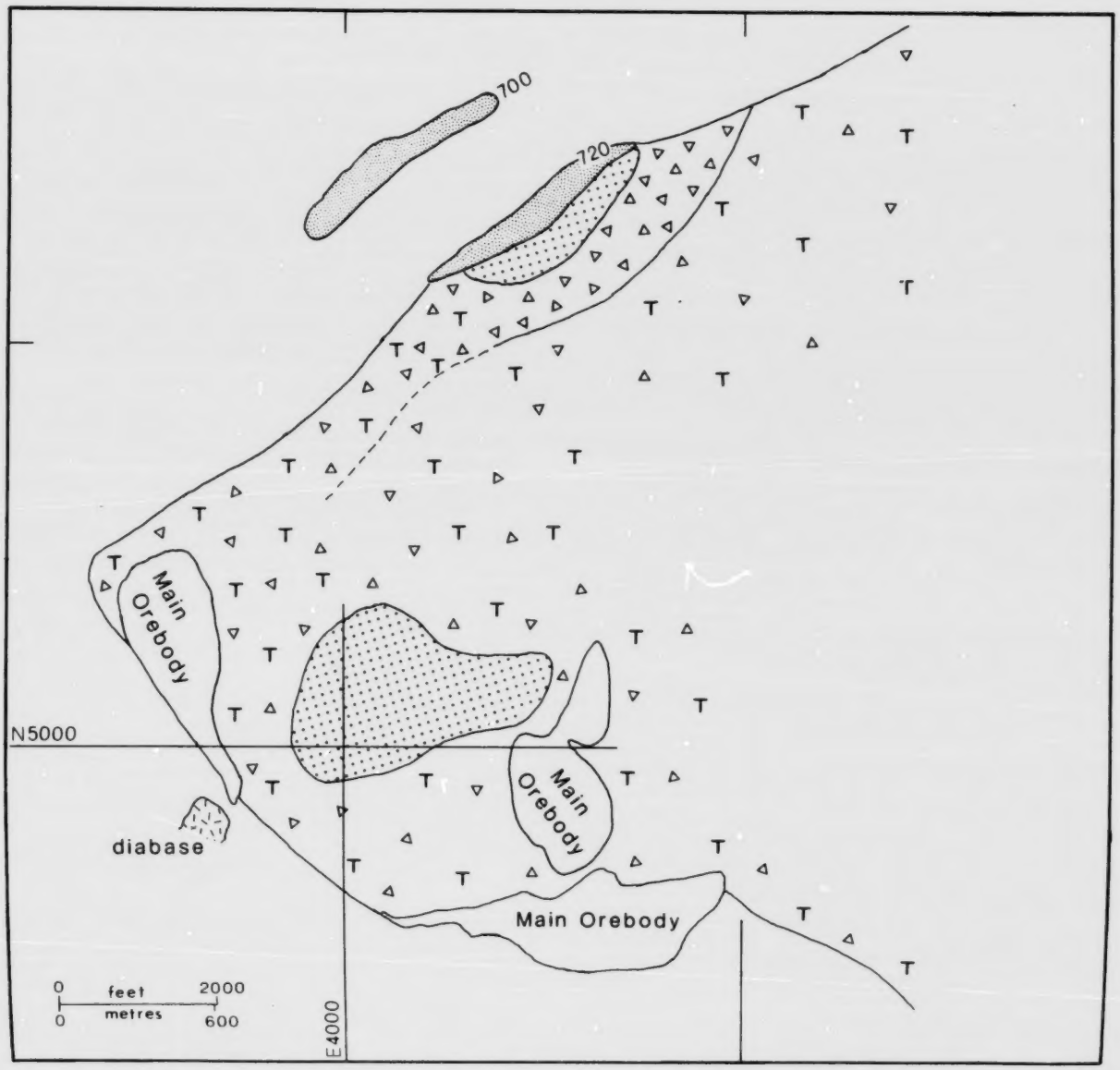

Figure 23. Geology of the 720 level restored by northwesterly translation along the inferred flat-lying fault (see Fig. 21 for legend).

The initiation of significant sulphide deposition seems to have begun during the accumulation of the upper part of the Ski Hill Formation, and is represented mainly by the widespread but sparse presence of pyritiferous lithic fragments in which the pyrite is extremely fine grained. Subsequently, the uppermost part of the Ski Hill Formation was penetrated by a stockwork in which the network of quartz-sulphide veinlets is well defined. The stockwork zone is much less extensive than the Ski Hill assemblage in the Lucky Strike area (Fig. 2), and stockwork intensity is greatest near the eastern part of the Lucky Strike glory hole.

Within the stockwork zone abundant veins containing quartz, pyrite, sphalerite, galena, chalcopyrite, barite and calcite are evident in remnants of host rocks. Also present, however, are substantial amounts of sulphide-bearing, almost massive quartz. Along the western contact which represents

the top of the stockwork zone (Fig. 2), are rare indications that some of the sulphides are clasts, and some of the barite in the siliceous zone is fragmental. These features are indicative of transportation, but the assemblage nevertheless is completely gradational with the well-resolved, underlying epigenetic stockwork zone. In this early stage of mineralization, therefore, it is thought that some of the silica-rich hydrothermal fluids associated with stockwork formation were discharged onto the paleosurface and subsequently were precipitated as siliceous ore. The Engine House Orebody in the southeastern part of the area, although shown as an extension of the stockwork zone (Fig. 2), is distant from the main stockwork centre and is the thicker part of a more extensive, blanket-like siliceous body. The shape of the orebody is interpreted here to be primary rather than fault-derived, and the orebody is thought to be a syndepositional feature rather than a stockwork zone.

The area in the northeastern part of the glory hole provides the most complete stratigraphic record of the events that preceded massive sulphide deposition. In this area, deposition of the upper part of the Ski Hill Formation was followed by additional accumulation of a new assemblage of layered tuffs and volcanic breccia that is typically chloritic and devoid of siltstone. These rocks, shown as unit 2 in Figure 3, vary from sulphide-rich to barren, but the group as a whole contains substantial amounts of various sulphides, of which pyrite is by far predominant. Despite their high sulphide content, these rocks do not contain discrete veinlet-type stockwork mineralization; the sulphide minerals are mainly disseminated, though some larger aggregates are recognizable as clasts.

The origin of these sulphide-bearing rocks is thought to be similar to that described for Kuroko deposits (Kuroda, 1983). Following stockwork development, there was sea-floor venting of hydrothermal fluids and an attendant build-up of sulphides near the requisite vents, sited as described below. Continued volcanic activity is represented by the host tuffs and volcanic breccia of unit 2, and their contained sulphides represent incorporated clastic fragments, grains, and probably minute particles that subsequently recrystallized. The stratigraphic upper part of unit 2 shows that with time a substantial increase in the volume of sulphides was deposited. Although none of the massive, transported orebodies had yet been deposited, the hydrothermal system was probably fully mature, and consolidation of the accumulated ore pile had proceeded to the point where pyrite aggregates, fragmental barite, and galena-sphalerite were transported as clasts to the upper part of the Ski Hill Formation. Crystallization of coarse grained pyrite was such that coherent pyritite masses were transported as large blocks that presumably were broken and move downslope from the accumulated sulphide pile. This stage culminated with the gravity-flow transportation (Binney, 1987) and deposition of the baritic, fragmental ore constituting the relatively small North Orebody. The transportation of sulphides was relatively minor in volume at this stage, and the distribution was restricted to a fan or mound near the Lucky Strike shaft. The fan extended outward for 100 to 200 m, thinning to the north and west. The interval of quiescence that followed the formation of the North Orebody is marked by the deposition of a laterally extensive unit of siltstone, part of which directly underlies the Two Level Orebody. Accumulation of the main ore pile that provided the source of the large transported type orebodies may have occurred during this quiescent interval.

Renewed volcanism and vigorous clastic deposition followed the formation, and at least partial induration, of the siltstone. Locally the top of the siltstone was broken into intraformational breccia, some of which was incorporated into the lower part of the fragmental, transported baritic ore of the Two Level Orebody. Other areas show that minor parts of the siltstone are intercalated with breccia-conglomerate containing low-grade ore clasts, and with crystal-vitric felsic tuff. Thus, the deposition of breccia-conglomerate, the transportations and deposition of the Two Level Orebody, and the onset of felsic tuff accumulation began at roughly the same time. The breccia-conglomerate, some of which contains granitoid clasts (Stewart, 1987), does not occur beneath the Main Orebody, but felsic tuff and siltstone do. Barite- and sulphide-rich breccia with fist-size siltstone fragments is present locally at the base of the Main Orebody, thereby suggesting that the siltstone was still exposed, or re-exposed, at the time of formation of the transported ores. Therefore, the Two Level and Main Orebodies must have been deposited at similar times.

The Two Level Orebody is mainly baritic with minor sulphides, whereas a large part of the Main Orebody consisted chiefly of sulphides. Although this distinction is a generalization, it serves to demonstrate the lithological dissimilarity of the two orebodies. Both orebodies are blanket- to ribbon-like, but their thickest parts indicate that deposition of the Two Level Orebody must have been focused in an extremely elongate northwest-trending channel (the MacLean channel), whereas the shape of Main Orebody indicates that its deposition was centred in a more equant depression to the southwest of the North Orebody.

Despite the different mineralogical compositions of the Two Level and Main orebodies, both are visualized as having been drawn from the same source. The Two Level Orebody is interpreted to be a debris flow, or flows, containing much material from the barite-rich portion of a highly evolved ore pile (Eldridge *et al.*, 1983). The Main Orebody is less diverse with respect to lithic inclusions and corresponds closely with slumped Kuroko-type "black ore". The dominating feature in the Main Orebody is the widespread presence of breccia textures that were formed from partly consolidated sulphides (Fig. 11). The same texture has been observed in Kuroko deposits and has been referred to as intraformational breccia (Yui and Ishitoya, 1983). The prevalance of this type of breccia in the Main Orebody intuitively suggests that transportation of the ore was over a short distance. Nevertheless, the breccia texture has been retained in sulphides that span an observed horizontal distance of approximately 400 m; the retention of the texture over this type of distance alone indicates that the sulphide source need not have been immediately adjacent to the existing orebody.

Deposition of the Two Level and Main orebodies was followed by continued accumulation of felsic tuff. In the early stages the tuff was accompanied by intermittent additions of clastic sulphides, some of which are concentrated into thin, low-grade layers (Fig. 5). Additionally, if the highly siliceous, pyritiferous unit above the Two Level and Main orebodies in the glory hole (unit 6Ba, Fig. 3) is in place rather than thrust-faulted, then the downward, as well as lateral, gradations to siliceous tuff suggests that the quartzose rock was formed by hydrothermal alteration of tuff. To achieve this alteration it is assumed that the preceding disturbance and bulk movement of orebody sulphides either permitted or initiated the renewed venting of hydrothermal fluids. At this stage, however, the hydrothermal system was waning, and conditions may have been similar to those pertaining to Kuroko deposits wherein late-stage deposition of siliceous exhalites occurs above the massive sulphide ores. In Kuroko deposits these exhalites form by slow mixing of hydrothermal fluids with cold seawater within unconsolidated sediments (Ohmoto *et al.*, 1983; Kalogeropoulos and Scott, 1983).

Irrespective of faults, the distribution of stockwork impregnation at Lucky Strike shows that the hydrothermal system from which the orebodies evolved was concentrated in the upper part of the Ski Hill Formation throughout the northern half of the area. Additionally, however, the distribution of sulphides deposited after stockwork development shows a focal pattern leading toward the east side of the glory hole. The most significant evidence supporting the presence of a hydrothermal centre in this area is the outward decrease in the intensity of the stockwork zone. Much of the main plumbing system evidently lay above the present erosional surface.

ACKNOWLEDGMENTS

The co-operation and assistance of J.G. Thurlow and D.M. Barbour, formerly with Abitibi-Price Inc. (now BP Canada – Selco Division), and E.A. Swanson, formerly with ASARCO Inc., were essential in the undertaking of this study. Particular acknowledgment is due to R.V. Kirkham and J.G. Thurlow for their continued interest and valuable discussions during the progress of the work, and for incisive critical reviews of the manuscript. Since the inception of this study alternative opinions have been expressed vigorously for almost all aspects of the geology of Lucky Strike, and it is perhaps too generous simply to label the conclusions reached here as highly unorthodox. As is evident from the contrary viewpoints specifically expressed in only a few representative places in the text, prior review does not signify acquiescence or agreement; the conclusions expressed here are the sole responsibility of the author.

REFERENCES

Binney, W.P.
1987: A sedimentological investigation of MacLean channel transported sulphide ores; in Buchans Geology, Newfoundland; ed. R.V. Kirkham; Geological Survey of Canada, Paper 86-24, Report 8.

Binney, W.P., Thurlow, J.G. and Swanson, E.A.
1983: The MacLean Extension Orebody, Buchans, Newfoundland; in Current Research, Part A, Geological Survey of Canada, Paper 83-1A, p. 313-319.

Catherall, D.J.
1960: Engine House Orebody, Buchans, Newfoundland; B.Sc. Thesis, Royal School of Mines, London, England, 89 p.

Eldridge, C.S., Barton, P.B., Jr. and Ohmoto, H.
1983: Mineral textures and their bearing on formation of the Kuroko orebodies; in The Kuroko and Related Volcanogenic Massive Sulfide Deposits, ed. H. Ohmoto and B.J. Skinner; Economic Geology, Monograph 5, p. 241-281.

George, P.W.
1937: Geology of lead-zinc-copper deposits at Buchans, Newfoundland; Transactions of the American Institute of Mining and Metallurgical Engineers, v. 126, p. 488-511.

Kalogeropoulos, S.I. and Scott, S.D.
1983: Mineralogy and geochemistry of tuffaceous exhalites (Tetsusekiei) of the Fukazawa mine, Hokuroko District, Japan; in The Kuroko and Related Volcanogenic Massive Sulfide Deposits, ed. H. Ohmoto and B.J. Skinner; Economic Geology, Monograph 5, p. 412-432.

Kowalik, J., Rye, R.O. and Sawkins, F.J.
1981: Stable-isotope study of the Buchans, Newfoundland, polymetallic sulphide deposits; in The Buchans Orebodies: Fifty Years of Geology and Mining, ed. E.A. Swanson, D.F. Strong and J.G. Thurlow; Geological Association of Canada, Special Paper 22, p. 229-254.

Kuroda, H.
1983: Geological characteristics and formation environments of the Furutobe and Matsuki Kuroko deposits, Akita Prefecture, northeast Japan; in The Kuroko and Related Volcanogenic Massive Sulfide Deposits, ed. H. Ohmoto and B.J. Skinner; Economic Geology, Monograph 5, p. 149-166.

Liou, J.G.
1971: P-T stabilities of laumontite, wairakite, lawsonite and related minerals in the system $CaAl_2Si_2O_8$-SiO_2-K_2O; Journal of Petrology, v. 12, p. 370-411.

Liou, J.G.
1979: Zeolite facies metamorphism of basaltic rocks from the East Taiwan Ophiolite; American Mineralogist, v. 64, p. 1-14.

Ohmoto, H., Mizukami, M., Drummond, S.E., Eldridge, C.S., Pisutha-Arnond, V. and Lenagh, T.C.
1983: Chemical processes of Kuroko formation; in The Kuroko and Related Volcanogenic Massive Sulfide Deposits, ed. H. Ohmoto and B.J. Skinner; Economic Geology, Monograph 5, p. 570-604.

Raade, G., Elliott, C.J. and Fejer, E.E.
1977: New data on ktenasite; Mineralogical Magazine, v. 41, p. 65-70.

Relly, B.H.
1960: The Geology of the Buchans Mine; unpublished Ph.D. Thesis, McGill University, Montreal, Quebec, 281 p.

Staff (Buchans Mining Company, Limited)
1955: Buchans operation, Newfoundland; Canadian Mining and Metallurgical Bulletin, v. 55, p. 349-353.

Stewart, P.W.
1987: Geology and genesis of granitoid clasts in the MacLean Extension transported orebody; in Buchans Geology, Newfoundland, ed. R.V. Kirkham; Geological Survey of Canada, Paper 86-24, Report 9.

Strong, D.F.
1981: Notes on ore mineralogy of the Buchans district; in The Buchans Orebodies: Fifty Years of Geology and Mining, ed. E.A. Swanson, D.F. Strong and J.G. Thurlow; Geological Association of Canada, Special Paper 22, p. 143-160.

Swanson, E.A.
1981: Development of genetic concepts and exploration practice at Buchans; in The Buchans Orebodies: Fifty Years of Geology and Mining, ed. E.A. Swanson, D.F. Strong, and J.G. Thurlow; Geological Association of Canada, Special Paper 22, p. 311-324.

Swanson, E.A., Strong, D.F. and Thurlow, J.G. (editors)
1981: The Buchans Orebodies: Fifty Years of Geology and Mining; Geological Association of Canada, Special Paper 22, 350 p.

Thurlow, J.G.
1981: The Buchans Group: its stratigraphic and structural setting; in The Buchans Orebodies: Fifty Years of Geology and Mining, ed. E.A. Swanson, D.F. Strong, and J.G. Thurlow; Geological Association of Canada, Special Paper 22, p. 79-89.

Thurlow, J.G. and Swanson, E.A.
1981: Geology and ore deposits of the Buchans area, central Newfoundland; in The Buchans Orebodies: Fifty Years of Geology and Mining, ed. E.A. Swanson, D.F. Strong and J.G. Thurlow; Geological Association of Canada, Special Paper 22, p. 113-142.

Thurlow, J.G. and Swanson, E.A.
1987: Stratigraphy and structure of the Buchans Group; in Buchans Geology, Newfoundland, ed. R.V. Kirkham; Geological Survey of Canada, Paper 86-24, Report 2.

Yui, S. and Ishitoya, K.
1983. Some textures of the ores from the Ezuri Kuroko deposits, Akita Prefecture, Japan; in The Kuroko and Related Volcanogenic Massive Sulfide Deposits, ed. H. Ohmoto and B.J. Skinner; Economic Geology, Monograph 5, p. 224-230.

- 8 -

A sedimentological investigation of Maclean channel transported sulphide ores

Contract 08GR.23233-2-0500

W.P. Binney[1]

Binney, W.P., A sedimentological investigation of MacLean channel transported sulphide ores; in Buchans Geology, Newfoundland, ed. R.V. Kirkham; Geological Survey of Canada, Paper 86-24, p. 107-147, Report 8, 1987.

Abstract

Transported massive sulphide ores of the Buchans camp account for over 50 per cent of the ore produced. Detailed distribution and sedimentary transport of ores in the MacLean channel has been studied using underground mapping, clast counts, drill core data, metal contents (Cu, Pb and Zn) and microscopic study of the sulphide and lithic detritus. Debris flows are recognized as the primary means of transport for sulphide and lithic detritus in the MacLean channel. Other ore-bearing sedimentary deposits result from slumping of massive ore and high-density turbidity current transport.

The degree of lithification of the sulphide and barite sediments in the hydrothermal source area is reflected in the types of deposit in the MacLean channel. Poorly lithified sulphides and barite plastically deform during transport to produce sulphide and barite matrix ore where the hydrothermally-derived sediment forms a matrix for volcanic and sedimentary clasts. Polylithic breccia-conglomerate and arenaceous conglomerate contain discrete clasts of sulphides and barite in a matrix of fine grained lithic detritus; the product of brittle failure of lithified sulphides and barite in the hydrothermal source area.

Transport direction of ore in a few places in the MacLean channel has been determined by mapping of debris flow margins, clast orientations and analysis of facies assemblages. These studies indicate that most ore-bearing sediment was transported from the east to the west with a lesser volume from the west or southwest in the western MacLean channel.

The deposition of transported ore was determined by the internal shear strength of the debris and the slope over which the debris was moving. A decrease in slope was the main reason for deposition of transported ore in the MacLean channel.

Résumé

Les sulfures massifs déplacés du gisement de Buchans sont à l'origine de plus de 50 % du minerai produit. La répartition et le transport sédimentaire des minerais dans le chenal MacLean ont été étudiés en détail en utilisant diverses méthodes telles que la cartographie du souterrain, le comptage des clastes, l'étude des carottes de sondage, l'évaluation de la teneur en métaux (Cu, Pb et Zn) et l'étude microscopique des débris sulfurés et lithiques. Les coulées de débris auraient été le principal mécanisme de transport des débris lithiques et sulfurés dans le chenal MacLean. D'autres dépôts sédimentaires métallifères ont été produits par le glissement de minerais massifs et par des courants de turbidité très denses.

Le type de gisement trouvé dans le chenal MacLean est fonction du degré de lithification subi dans la zone source des solutions hydrothermales par les sédiments à sulfures et à barytine. Les sulfures et la barytine mal lithifiés subissent une déformation plastique au cours du transport et produisent un minerai à matrice à sulfures et à barytine, tandis que les clastes volcaniques et sédimentaires ont pour matrice des sédiments d'origine hydrothermale. La brèche-conglomérat polygénique et le conglomérat arénacé contiennent des clastes distincts de sulfures et de barytine dans une fine matrice de débris lithiques; ces conglomérats ont été produit par l'effondrement cassant de sulfures et de barytine lithifiés dans la zone source des solutions hydrothermales.

[1]Falconbridge Limited, P.O. Box 1140, Timmins, Ontario P4N 7H9

La direction de transport du minerai a été déterminée à certains endroits dans le chenal MacLean en cartographiant les marges des coulées de débris, en déterminant l'orientation des clastes et en analysant les associations de faciès. Ces études indiquent que la plupart des sédiments métallifères ont été transportés de l'est vers l'ouest, bien que dans la partie ouest du chenal, une plus petite quantité de ces sédiments ait été transportée de l'ouest ou du sud-ouest.

L'accumulation du minerai transporté était fonction de la résistance au cisaillement interne et de la pente sur laquelle les débris étaient transportés. Le minerai transporté s'est déposé dans le chenal MacLean principalement parce que l'angle du talus y était plus faible.

INTRODUCTION

A detailed stratigraphic and sedimentological description of the transported massive sulphide ores of the MacLean and MacLean Extension orebodies is presented. The type and size of clasts and mineralogical content of the matrix in addition to the interrelationships of clasts and matrix and the recognition of distinctive facies assemblages are considered in determining the provenance and distribution of the transported ore. Particular attention has been given to features of the 'high grade' mineralized beds for which exploration guides are suggested.

Research leading to this report included seven months of fieldwork at Buchans and additional laboratory study from July, 1982 to January, 1984.

Fieldwork consisted of mapping the character and distribution of the ore-bearing units in the MacLean Extension and locally the MacLean orebodies. Counts of the size, position and lithology of clasts were carried out at 42 locations with data on more than 4,000 individual clasts recorded. Clast measurements were corrected for density differences between sulphide and lithic fragments and size distributions plotted. Clasts percentages by area were also calculated. The studies were concentrated in the MacLean Extension orebody, undergoing development and in the initial stages of mining, in 1982 and 1983. Few ore exposures remain in the MacLean orebody where mining ceased in early 1982 and most of the older workings were inaccessible at the time of study. Diamond-drill core from both orebodies was relogged and the general stratigraphy of the ore sequence was examined both underground and in drill core.

Samples of the clasts and matrix of the ore-bearing units were collected for microscopic examination of the occurrence, intergrowths and habit of the sulphide, sulphate and carbonate minerals. Identification of the size and type of lithic detritus was aided by thin sections. Studies of the transported massive sulphide ores in thin and polished section are difficult due to macroscopic and microscopic heterogeneity of ore beds.

ACKNOWLEDGMENTS

The author wishes to thank the geological staff of Abitibi-Price Mineral Resources and ASARCO Inc., especially chief geologists Geoff Thurlow and Eric Swanson (now retired), respectively, for their helpful comments and discussions. The underground investigation of the ores in the MacLean channel would not have been possible without the co-operation received from Ed Kelly (MacLean superintendent) and the mining department of ASARCO Incorporated.

Dr. R.V. Kirkham provided advice, support and guidance throughout this project. His critical reading and comments on the manuscript are also appreciated. Helpful discussions with Dr. D.F. Sangster, Dr. J. Jambor and Dr. W.H. Poole during visits to Buchans provided many new ideas for consideration. Dr. Marcos Zentilli, Dalhousie University, provided both encouragement and technical support throughout the study.

In addition to the professional assistance received from the above-mentioned people, I would also like to thank Mrs. Dora Barnes who provided my wife and I not just with lodging but constant assistance, encouragement and a sense of the history and people of Buchans. Alma and Don White with their companionship and enthusiasm made life in Buchans during 1982 and 1983 a pleasurable experience.

The completion of this research project would not have been possible without the assistance of my wife, Lynn, who aided with underground photography, read manuscript drafts and showed a great measure of tolerance for my long hours spent in the final preparation of this paper.

STRATIGRAPHY IN THE MACLEAN CHANNEL

The sedimentological study of the transported ore and surrounding rocks was confined to the Buchans River Formation (Thurlow and Swanson, 1987) in the MacLean channel exposed in the MacLean and MacLean Extension workings. In the western MacLean Extension area (drive 20-4, Fig. 1) and in part of the MacLean workings (supply raise, Fig. 1) the contact of the Buchans River Formation and underlying pillow breccias of the Ski Hill Formation (Thurlow and Swanson, 1987) is exposed.

The MacLean channel in the study area is bounded to the south by the MacLean Fault and to the northeast by the 12 Level Fault. The confluence of the two high-angle reverse faults to the east determines the eastern limit of the MacLean channel in the MacLean workings (Fig. 2). Other fault-bounded portions of the channel contain the Rothermere, Two Level and North orebodies which occur east of the study area (Thurlow and Swanson, 1987).

Simplified stratigraphic sections constructed from underground mapping and new drill logs are presented in Figure 2. The sections illustrate lithological variation in the

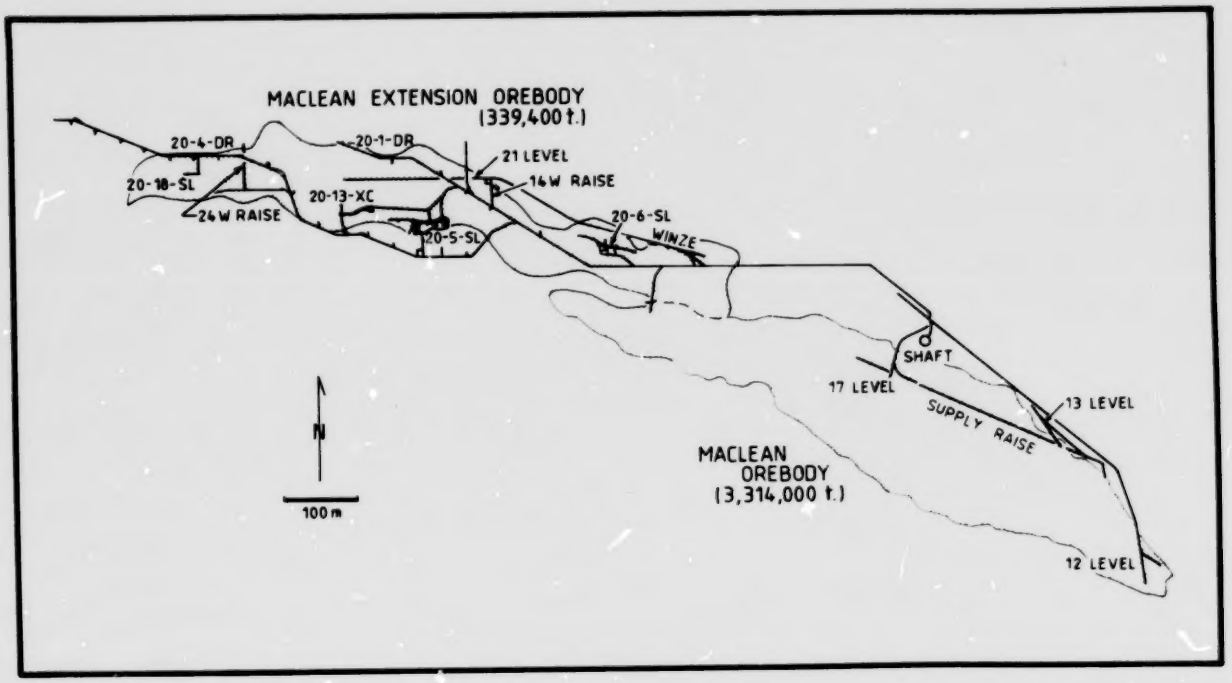

Figure 1. Plan projection of some workings accessible in 1982 and 1983 in the MacLean and MacLean Extension areas that were examined in this study (from ASARCO plans).

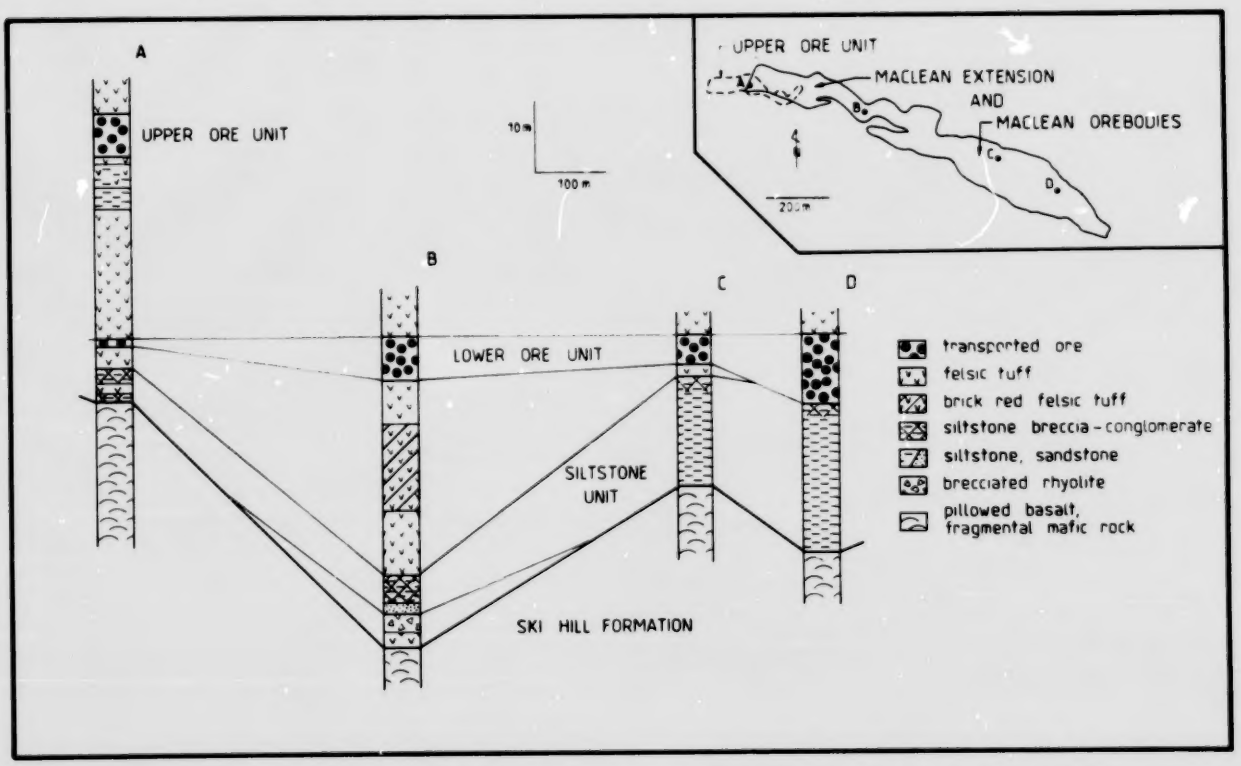

Figure 2. Simplified stratigraphic sections of the ore sequence in the MacLean channel. Map insert shows a plan projection of the ore units with the position of the stratigraphic sections noted.

ore sequence along the MacLean channel in the MacLean-MacLean Extension area. Due to the limited stratigraphic extent of the underground workings and diamond-drill holes, only the basal stratigraphy of the ore sequence is known in detail.

Throughout the exposed length of the MacLean channel the ore sequence overlies hematized basaltic pillow lava, broken pillow breccia and fragmental mafic rock of the Ski Hill Formation.

Locally, at the base of the ore sequence (section B, Fig. 2), green felsic tuff is overlain by breccia with 10 to 30 cm subangular blocks of quartz-veined, reddish-brown rhyolite in a fine grained green siliceous matrix.

Overlying the rhyolite breccia, or the Ski Hill Formation, is the siltstone unit of the ore sequence (Fig. 3). This unit, the most laterally extensive of all members of the ore sequence, occurs under the Lucky Strike and Rothermere orebodies in addition to extending throughout the MacLean workings. In the eastern part of the exposed channel (sections C and D, Fig. 2) the siltstone unit includes light to medium grey, massive to finely laminated, pyritic siltstone and fine grained sandstone with some 5 to 10 cm-thick interbeds of medium to coarse grained sandstone. Microscopically, the siltstone comprises fine grained sand- and silt- sized, angular to subangular quartz and altered feldspar grains dispersed in a silt- to clay-sized matrix of indeterminate mineralogy. Detrital pyrite forms up to 20 per cent of the rock with individual grains less than two-thirds the size of the corresponding silicate detritus. In grab samples from the MacLean waste dump, siltstone blocks contain a variety of sedimentary structures indicative of turbulent sediment transport. These features include graded beds, partial Bouma sequences (Walker, 1979) with massive, fine grained sandstone beds, planar laminae and cross-bedding, and loading structures resulting from deposition of medium to fine grained sand on unconsolidated silt (Fig. 4). The loading features vary from small cuspate structures to complete disruption of the bedding.

Figure 3. Siltstone breccia-conglomerate overlying fragmental mafic rocks of the Ski Hill Formation; 20-4 drive, MacLean Extension area.

Figure 4. Siltstone underlying the MacLean Orebody. Darker areas are medium- to fine-grained sandstone and lighter areas are siltstone. Specimen shows load structures on tops of beds, plane lamination, grading and ripple drift cross-lamination typical of turbidity current deposits. (GSC 204076-A)

In eastern exposures of the MacLean channel on the 13 and 17 levels (Fig. 1), the upper part of the siltstone unit comprises clasts of siltstone, rhyolite, other volcanic rock fragments and rare granitoid fragments in a silt-to clay-sized matrix, identical to that of the siltstone. Pyrite occurs throughout this breccia-conglomerate with a few corroded grains of sphalerite up to 250 mm in length. Altered siltstone clasts are present in this breccia-conglomerate. This alteration occurs as a slight bleaching and a lack of pyrite in the clast margin. Locally, the siltstone unit at the eastern end of the MacLean channel is capped by a thin bed of medium- to coarse-grained sandstone containing quartz, altered feldspar, volcanic rock fragments, graphic quartz-feldspar intergrowths and biotite.

The character of the siltstone unit changes to the west in the MacLean channel (sections A and B, Fig. 2) where the unit includes sandstone, siltstone breccia-conglomerate and interbedded lithic felsic tuff. In the breccia-conglomerate, blocks of siltstone in excess of 1 m in length coexist with smaller fragments of siltstone, altered siltstone, rhyolite, jasper, basalt and sphalerite-pyrite in a matrix of quartz, altered feldspar and altered vitric tuff. These breccia-conglomerate beds are interpreted as debris flow deposits. Although a great variety of clast types have been recognized, unaltered siltstone fragments comprise greater than 80 per cent of the clasts. To the west the proportion of altered to unaltered siltstone clasts decreases. At section B (Fig. 2) 13 per cent of siltstone clasts have at least some alteration rimming. This proportion decreases to 3 per cent at section A (Fig. 2) and 150 m west of section A less than 1 per cent of the clasts contain any alteration. At each location 100 siltstone clasts were recorded and the proportion calculated based on the area of each clast. Within the siltstone unit lithic felsic tuff interbeds are proportionately more abundant to the west.

In summary, the siltstone unit in the eastern part of the MacLean channel is massive with only minor sandstone and breccia-conglomerate beds at the top of the section. To the west the unit thins and includes a greater proportion of sandy, tuffaceous and siltstone breccia-conglomerate beds than in situ siltstone beds.

The siltstone unit is overlain directly by the lower ore unit in the eastern part of the MacLean channel (section D, Fig. 2). Due to a lack of access in the old MacLean workings this contact was observed only in drill core where a gradational contact exists between the siltstone breccia-conglomerate or sandy top of the siltstone unit and the basal transported ore bed of the lower ore unit. In all accessible areas studied (sections A, B, C, Fig. 2) in both the MacLean and MacLean Extension workings a thin to thick section of green felsic tuff overlies the siltstone unit and forms the substrate for the lower ore unit.

Macroscopically the green felsic tuff is identical in all exposures but microscopic examination indicates local differences. Most green felsic tuff contains 1 to 2 mm embayed quartz and altered plagioclase crystals in a microcrystalline to cryptocrystalline matrix. Distinctive broken zoned feldspar crystals (Fig. 5) and variations in the accessory mineral content were noted locally.

Figure 5. Broken zoned plagiolase crystal in green felsic tuff underlying the lower ore unit; drillhole 3214, 1100W, MacLean Extension area.

Section B (Fig. 2) represents an area (150 by 100 m) in the MacLean Extension workings where brick red felsic tuff occurs within the lower green felsic tuff unit. The brick-red matrix containing feldspar and quartz crystals, has lead to this rock being referred to informally as 'rhyolite' in mine terminology. It is easily distinguished from the brown-red, quartz-veined and brecciated rhyolite that forms the base of the ore sequence in section B (Fig. 2). Microscopically the brick-red felsic tuff comprises 20 to 40 per cent, 2 to 2.5 mm angular to subrounded plagioclase (oligoclase) crystals and lesser numbers of embayed quartz crystals in a microcrystalline matrix of quartz and feldspar. The feldspar phenocrysts are only slightly altered but the accessory ferromagnesian minerals are extensively altered to chlorite. No hematite veining was observed in the thin section studied.

Both the upper and lower contacts between brick-red felsic tuff and green felsic tuff are poorly defined due to hematite veining and associated reddish alteration of the green tuff. Locally, blocks of brick-red tuff are found in the basal 1 m of the overlying green tuff.

The lower ore unit, which overlies the lower tuff unit, is described in detail in the section on sedimentary geology of the ore-bearing units. This unit forms the main ore deposits in the MacLean channel including all of the MacLean Orebody and most reserves in the MacLean Extension Orebody. The orebodies represent complex sedimentary filling of channels in the volcanic and sedimentary substrate with varying proportions of sulphides, barite, volcanic, siltstone and granitoid detritus. The transported sulphide and barite minerals occur in large clasts or as fine grained clastic matrix to lithic detritus.

Overlying the lower ore unit is a thick unit of felsic tuff with 1 to 2 mm embayed quartz and highly altered feldspar crystals in a fine grained altered matrix which includes sericite and calcite. Lithic fragments are common and include

barite and sulphide clasts in addition to the more abundant sedimentary and volcanic clasts.

A bed of grey-green siltstone and interbedded felsic crystal tuff forms a distinct marker in the upper tuff sequence (Fig. 6). The siltstone is similar to that found locally at the top of the lower ore unit and includes angular to subangular quartz grains and a lesser number of highly altered feldspar grains dispersed in a silt-to clay-sized matrix. The average grain size of the quartz and feldspar is approximately 0.5 mm. Sulphides form less than 1 per cent of the rock and include 0.2 mm pyrite grains and sparse corroded grains of sphalerite.

Overlying the siltstone, 5 to 10 cm-diameter fragments of felsic tuff are enclosed by a silty to tuffaceous matrix, the 'squeezed siltstone unit'. Microscopically the fine grained immature matrix of the siltstone is indistinguishable from the highly altered aphanitic matrix of the tuff. Prominent quartz and feldspar crystals in the tuff are distinct from smaller broken quartz grains dispersed in the siltstone. The content of interstitial silt-sized material decreases up section where blocks of felsic tuff are enclosed by a light green felsic tuff matrix. The tuff unit, or a thin bed of yellowish-green felsic crystal tuff, overlies the silty beds and forms a substrate for the upper ore unit.

Figure 6. Siltstone with thin interbeds of dacitic tuff (darker discontinuous beds) between the lower and upper ore units; 20-4 drive, MacLean Extension workings.

The upper ore unit is limited to the MacLean Extension area and is not as widespread as the lower ore unit (Fig. 2). Important features of the upper ore unit include its high barite content, low sulphide content and great lateral extent of individual beds relative to their thickness. A more detailed description of the upper ore unit is provided in the section on underground geology.

Overlying the upper ore unit are altered yellow-green felsic tuff and hematized felsic pyroclastic rocks, the youngest rocks of the ore sequence exposed in underground workings in the MacLean channel.

Small felsite and numerous diabase dykes, many with chilled margins, cut the ore sequence in the MacLean channel. Large diabase dykes have been emplaced along faults and occur at offsets of the ore beds.

SEDIMENTARY GEOLOGY OF ORE-BEARING UNITS OF THE MACLEAN CHANNEL

This section on the sedimentary geology of the ore units in the MacLean channel considers lithologies in the ore units, configuration of the basin of deposition, detailed underground and diamond-drill core observations and results of clast counts and other detailed studies.

Lithological units

Lithological descriptions of the rocks in the ore units of the ore sequence were presented by Swanson and Brown (1962), Thurlow et al. (1975), Thurlow and Swanson (1981), Walker and Barbour (1981), Calhoun and Hutchinson (1981) and Binney et al. (1983). In these studies the varying occurrence of sulphide minerals both as a matrix to lithic detritus and as discrete clasts within the sedimentary rocks have been described.

A continuum in rock lithologies exists from a sulphide or barite matrix with layers of fine grained lithic detritus or scattered larger lithic clasts, through sulphide and barite blocks and lithic clasts in a lithic matrix, to arenaceous conglomerate with minor pebble-sized detritus including rare sulphide and barite clasts. Three lithological units described by Binney et al. (1983) for the MacLean Extension Orebody are: sulphide matrix ore, polylithic breccia-conglomerate and arenaceous conglomerate. Added to these units in the current report is barite matrix ore, a significant rock type in the eastern part of the MacLean Orebody. These lithologies, with various descriptive modifiers, account for most units in the MacLean and MacLean Extension orebodies.

Sulphide and barite matrix ore

These two lithologies, sulphide and barite matrix ore, are the end members of a series of sedimentary rocks in the MacLean

channel. A fundamental property of "matrix ores" is the fine grained mixture of sphalerite, galena, chalcopyrite, pyrite, barite and lesser amounts of lithic detritus as a matrix for larger lithic and less abundant sulphide clasts.

Sulphide matrix ore was noted on 12, 13 and 17 levels in the MacLean workings and on 20 level in the MacLean Extension workings (Fig. 1). Barite matrix ore is an important part of the lower ore unit on 12 level in the MacLean workings and forms the economic portion of the upper ore unit in the MacLean Extension Orebody (Fig. 2). The limited exposures of ore in the MacLean workings include most ore types when compared with the more extensive drill-core record from the orebody.

Discontinuous layers of chalcopyrite-pyrite, sphalerite-galena and barite occur in sulphide matrix ore. Fine grained lithic detritus in the matrix of the ore includes single quartz grains, aggregates of altered plagioclase, and graphic intergrowths of quartz and altered feldspar. A continuous gradation exists from high-grade sulphides with lithic clast-rich layers (Fig.7) to rock with a lithic-sulphide matrix.

Coarse grained (clasts greater than 1 cm long) lithic detritus comprises 5 to 20 per cent of the sulphide matrix ore. Although clasts in excess of 1 metre were observed, most clasts are less than 20 cm in their apparent maximum dimension. Coarse grained lithic detritus is angular to subangular, with some subround clasts noted in the MacLean Extension sulphide matrix ore. Clasts types include siltstone, rhyolite, basalt and in some sections barite, massive sulphide fragments (usually chalcopyrite-pyrite-rich) and stockwork sulphides (pyrite-chalcopyrite veinlets in altered, silicified volcanic rocks). No granitoid or other crystalline rock fragments were observed, although fine grained crystalline detritus is found in the matrix.

Barite matrix ore occurs in the eastern part of the MacLean channel near the stratigraphic top of the lower ore unit. Barite predominates as the major mineral in the matrix, although sphalerite, galena, calcite and minor fine grained lithic detritus were observed. Coarse grained detritus within the barite-rich matrix includes altered intermediate volcanic rocks, altered siltstone, white rhyolite, sphalerite-galena, chalcopyrite-pyrite and both light- and dark-coloured barite clasts. The clasts vary from small broken angular fragments to elongate siltstone blocks up to 50 cm in length. The proportion of coarse grained detritus ranges from about 0 to 50 per cent of the rock mass.

Three distinct cycles of deposition of barite matrix ore occur on 12 level. At the base of each cycle the matrix is rich in sphalerite and galena and coarse grained lithic detritus is abundant. Toward the top of each cycle a gradual change to a massive very fine grained barite matrix occurs and the size and number of lithic clasts decrease. The uppermost part of some cycles is a section of massive white barite containing only scattered lithic clasts less than 5 cm in length. These cycles of barite matrix ore must be of limited extent since they were not observed on 13 level or in drill core from the area.

Barite matrix ore in the upper ore unit of the MacLean Extension Orebody includes barite crystal clasts in addition to siltstone, rhyolite, basalt, massive sulphide and stockwork clasts dispersed in a matrix of barite, sphalerite and galena. Two beds of barite matrix ore are separated, and overlain by, sandy to conglomeratic sedimentary rocks (Binney *et al.*, 1983).

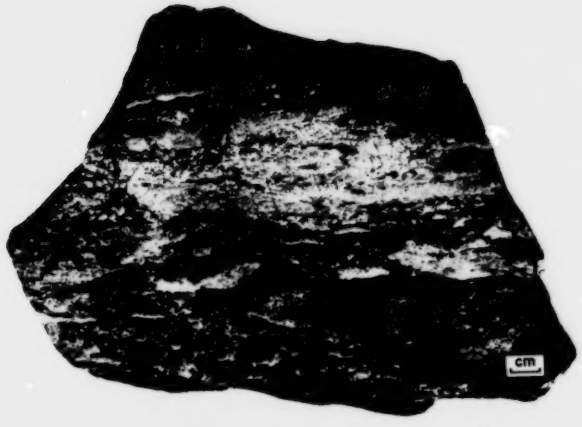

Figure 7. Sulphide matrix ore with small lithic fragments (dark grey to black) and irregular sphalerite-galena or pyrite-chalcopyrite clasts without lithic detritus (light grey); 17 level, MacLean Orebody. (KQB-82-186, GSC 204076-D)

Polylithic breccia-conglomerate

Polylithic breccia-conglomerate comprises the broad central part of the lithological continuum from sulphide or barite matrix ore to arenaceous conglomerate. It occurs throughout the lower ore unit in the MacLean channel.

On 12 level of the MacLean Orebody, this lithology forms a bed of undetermined thickness overlying siltstone breccia-conglomerate and underlying sulphide matrix ore. Angular to subangular clasts comprise greater than 70 per cent of the rock. The dominant clast types are siltstone, rhyolite and altered felsic rocks, but basalt, and a few clasts of sphalerite-galena also are present. Most clasts are 5 to 20 cm in apparent maximum dimension, but clasts up to 50 cm have been observed. This polylithic breccia-conglomerate is atypical in comparison with those of the MacLean Extension Orebody due to the small amount of matrix and the angular, breccia appearance of much of the unit.

Numerous polylithic breccia-conglomerate beds occur in the MacLean Extension Orebody where they constitute a significant percentage of the ore grade material. The sulphides occur as blocks of sphalerite-galena or pyrite-chal-

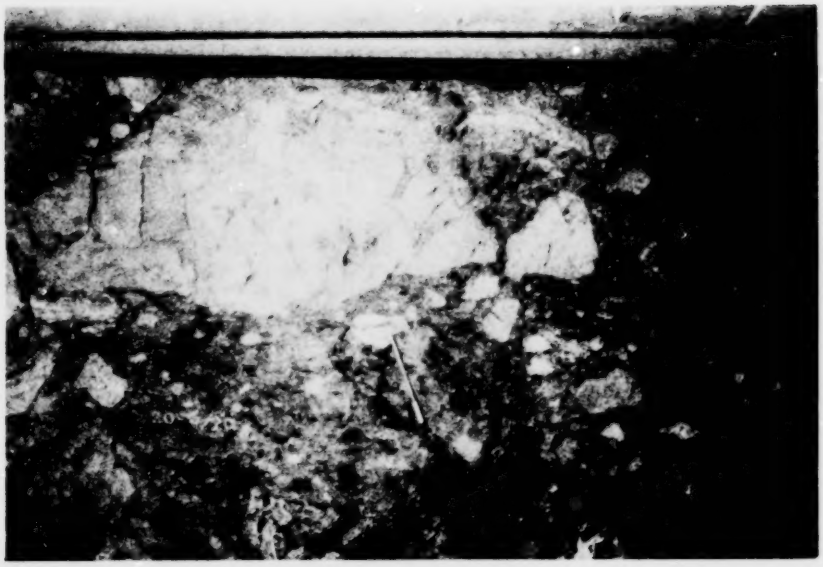

Figure 8. Polylithic breccia-conglomerate with coarse sulphide and lithic clasts supported in a sand-sized matrix. Large block above pencil is sphalerite-galena. Pencil is 15 cm long. 20-6-SL MacLean Extension workings.

copyrite- sphalerite-galena in a lithic pyritic matrix. Typical polylithic breccia-conglomerate in the MacLean Extension Orebody contains 20 to 40 per cent angular to subrounded clasts greater than 1 cm long in a matrix of fine grained, sand-sized clastic detritus (Fig. 8). The detritus forming the matrix includes quartz, altered feldspar, pyrite, sphalerite, galena, barite and small lithic grains. Coarse fragment lithologies include: rhyolite, siltstone, altered felsic volcanics, basalt, silicified basalt cut by sulphide veins, granitoid, sphalerite-galena, chalcopyrite-pyrite (+ sphalerite and/or galena) and single crystal clasts and crystalline aggregates of barite. Dominant clast lithologies were used in mapping certain polylithic breccia- conglomerates in the MacLean Extension area. Granitic and baritic were applied as modifiers where granitoid and barite clasts, respectively, form anomalously high percentages of the coarse fragments. In most locations beds cannot be separated on clast lithology because of high local variability and gross similarities in bed appearance.

Granitoid clasts are more rounded than coexisting sulphide and volcanic detritus. Some granitoid clasts are cut by barite veinlets and microbreccia zones which terminate at clast margins (Fig. 9). Such veins support the concept that granitoid clasts were derived from an igneous-hydrothermal feeder system.

Sorting in the polylithic breccia-conglomerate beds is poor, with blocks of greater than 4 m apparent maximum dimension intermixed with large numbers of smaller clasts in a matrix of fine grained, sand-sized detritus. Lithic clasts of 30 to 60 cm apparent maximum dimension are common in the polylithic breccia-conglomerate, but, the majority of clasts are less than 15 cm apparent maximum dimension. The large clasts are not found at the base of the bed but are supported by the matrix of finer grained detritus.

Two important features of polylithic breccia-conglomerate were observed in specific lithological positions. A sulphide clast-bearing conglomerate with few lithic clasts but containing sphalerite-galena, chalcopyrite-pyrite and chalcopyrite- pyrite-sphalerite-galena fragments in a lithic-pyritic matrix occurs adjacent to sulphide matrix ore in 20-13-XC (Fig. 1). The second feature, which occurs with, or in close proximity to, the sulphide clast-bearing conglomerate, is plastically deformed sulphide fragments (Fig. 23). First described by Thurlow and Swanson (1981), the plastically deformed sulphide fragments are best seen where sulphide clasts are draped over, and have irregular contacts with, adjacent lithic detritus. The plastic deformation results from the transport and deposition of only partially indurated sulphide fragments and indicates an extremely gentle transport process. Both of the features occur at the termination of viscous debris flow deposits.

Arenaceous conglomerate

With a decrease in the size and number of clasts and a consequent increase in the proportion of the lithic, pyritic clastic matrix, polylithic breccia-conglomerate grades into arenaceous conglomerate. This lithological unit was not observed in the MacLean workings.

Aranaceous conglomerate is widely distributed throughout the MacLean Extension Orebody. In the sections studied the matrix comprises medium grained, sand- to granule-sized, angular, quartz, altered feldspar and small lithic clasts (Fig. 10). Pyrite, the main sulphide mineral, occurs as discrete clastic grains and as thin beds of subhedral grains in lithic detritus. Irregular blebs of sphalerite-galena also occur in the matrix but are less abundant than pyrite.

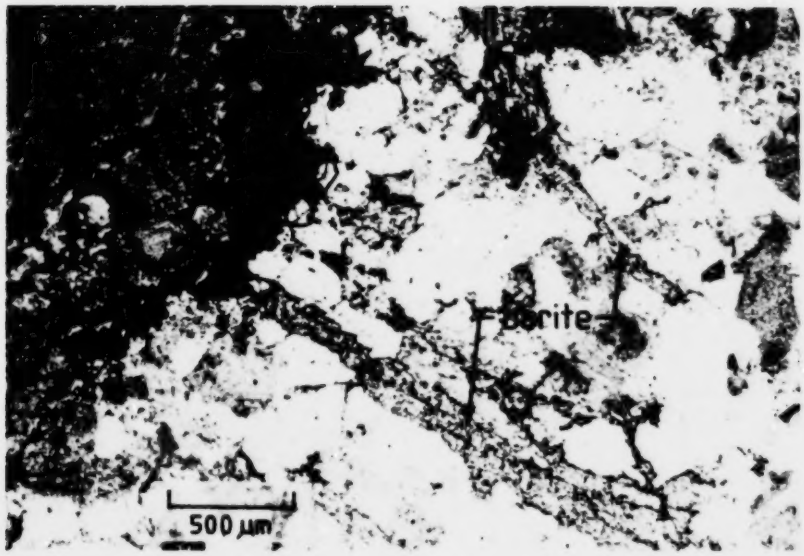

Figure 9. Barite veinlets cutting a granitoid clast and terminated at the boundaries of the clast in polylithic breccia-conglomerate. Matrix to the clast includes sulphides (black) and altered clastic detritus (grey). Transmitted light, 20-6-SL, MacLean Extension workings (KQB-82-75).

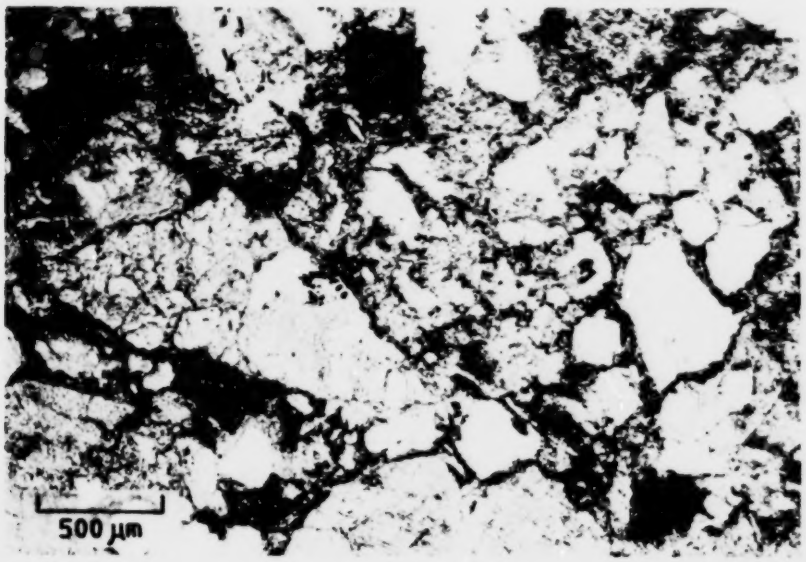

Figure 10. Photomicrograph of poorly sorted, angular quartz, feldspar and small lithic fragments forming the matrix of the arenaceous conglomerate. Discrete sulphide grains (black) are subhedral pyrite. 20-4 drive, MacLean Extension workings (KQB-82-108A).

Lithic fragments are subangular to subround and form less than 10 per cent of the rock. Local normal grading of clasts was observed. The lithic fragments are pebble- to cobble-sized with most less than 10 cm in apparent maximum dimension. Clast types include rhyolite, granite, siltstone, basalt, jasper, sulphides and barite.

A related lithological unit of the arenaceous conglomerate is the fine grained sandstone to siltstone which caps the lower ore unit in many locations in the MacLean Extension area. In the sandstone, quartz and altered feldspar grains of fine to coarse grained sand size are dispersed in a silt to clay size matrix. Grading of the mineral grains occurs in some 2 to 5 cm-thick beds.

Fine grained sandstone beds are also found in the upper ore unit of the MacLean Extension Orebody. Fine grained sandstone interbedded with felsic tuff, overlies the first and underlies the second ore cycle in sharp contact. The sandstone contains graded beds of barite crystals up to 1 cm long, but no coarse grained lithic detritus.

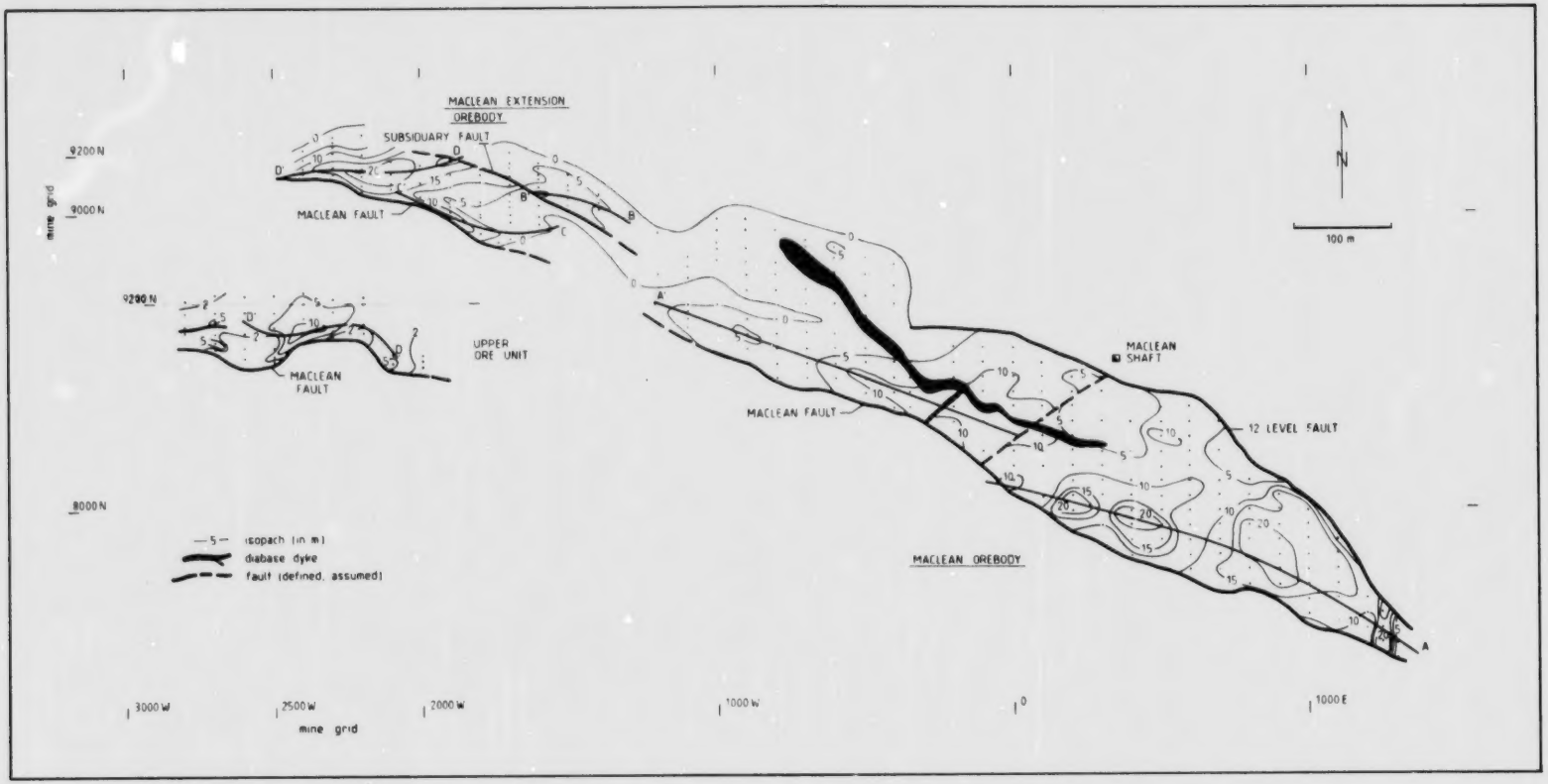

Figure 11. Isopach map of the lower and upper ore units in the MacLean and MacLean Extension areas. Isopach contours are in metres, and the mine grid is in feet. Dots represent data points used in contouring. For clarity the upper ore unit is offset due south of its actual position. The upper ore unit is unfolded with 9200N as a fixed reference line. A-A′ to D-D′ are the positions of longitudinal sections presented in Figures 12 to 15.

Thickness variations of ore units

Isopach maps for the upper and lower ore units of the ore sequence in the MacLean and MacLean Extension orebodies are presented in Figure 11. The stratigraphic thickness of the lower ore unit in the MacLean Orebody was obtained by measurement of stope height as plotted on 1:720 mine sections spaced 100 feet (30.5 m) apart. Thicknesses were corrected for the dip of the beds and the results confirmed by comparison with data from level plans which show the complete geology of the ore sequence. For the area including the MacLean Extension Orebody, thicknesses of the lower and upper ore units were obtained by direct measurement from drill sections plotted at a scale of 1:360. For the lower ore unit in the MacLean Extension Orebody open folding about west-trending axes was ignored and data plotted where measured on the mine grid. All isopach data were plotted on a plan projection of the lower ore unit. The upper ore unit had to be restored to its original attitude due to significant overturning in the vicinity of the main MacLean Fault. The 9200N mine co-ordinate was used as a fixed reference for restoration.

The mine co-ordinate system was used to locate features on isopach and other maps in this study. The co-ordinates, expressed in feet north, east and west of the grid origin, have not been converted to metres in this report. To do so would cause confusion.

Thickness errors on the isopach map are thought not to exceed ± 1 m for the drill sections and ± 2 m for the stope sections. The isopach maps were constructed using 262 control points for the lower ore unit and 34 for the upper ore unit. Any errors in unit thickness would not affect significantly the contours which are at 5 m intervals.

Ore unit thickness on the isopach map includes sulphide matrix ore, barite matrix ore, polylithic breccia-conglomerate and arenaceous conglomerate. This thickness does not represent mineable ore, especially in the MacLean Extension area where extensive beds of low-grade arenaceous conglomerate are present. (Fig. 15).

The lower ore unit is truncated to the south in both the MacLean and MacLean Extension orebodies by the main, northwest-trending, north-dipping MacLean reverse fault (Fig. 11) (Thurlow and Swanson, 1986). The northern margin of the MacLean Orebody is also a fault (12 level Fault, Fig. 11).

At the fault-bounded eastern end of the MacLean Orebody a north-trending accumulation of transported ore in excess of 20 m thick (Fig. 11) results from the juxtaposition of several individual beds of sulphide matrix and barite matrix ore. A series of disconnected deeper basins form a crude west-trending trough from 1300E to 0+00 (section A′-A, Figs. 11 and 12). In this trough, the lower ore unit exceeds 20 m thick at several locations. In contrast, to the north of the trough, the lower ore unit does not exceed 10 m thick over a large area. About 0+00 a northeast- trending lineament offsets the contours. To the west of this offset, the thickest section of the lower ore unit is centrally located between the bounding faults. The maximum total thickness of the lower ore unit decreases to 10 to 15 m.

The MacLean channel bifurcates to the west. The thicker southern channel pinches out at about 1100W but was noted again in the MacLean Extension Orebody at 1600W. To the north the lower ore unit is laterally extensive, but thin (Fig. 11). The two channels coalesce about 2000W in the MacLean Extension Orebody. Here, in excess of 20 m of sediment fill forms the lower ore unit in a west-trending channel.

Although the MacLean Extension Orebody is smaller than the MacLean Orebody, the channel fill is recognized to be more complex, with a greater proportion of lithic detritus in the deposit.

The upper ore unit of the ore sequence occurs only in the MacLean Extension area. It is bounded to the south by the main MacLean Fault that defines the limit of the lower ore unit. In Figure 11 the fault is curved sharply due to the restoration of the bedding in the unit to a horizontal plane. Immediately east of 2500W the beds of the upper ore unit thicken rapidly and form a mound-like accumulation of sediment. Away from this mound the beds are thin but laterally extensive. No well-defined channel exists for the upper ore unit.

In summary, within the confines of the main MacLean and 12 level faults, the MacLean channel includes thick accumulations of detritus in the east (0+00 to 1300E) and the west (2000W to 2500W) with an area between of thin sedimentary fill. Due to a lack of diamond-drill holes, the extent of the channel beyond the faults is unknown.

Ore unit stratigraphy

Longitudinal sections showing detailed stratigraphy of ore units in the main elongate depressions of the MacLean channel are presented in Figures 12, 13, 14 and 15. The section for the MacLean Orebody (Fig. 12) is an uncorrected plot of the geology as determined from mine and drill records. In the MacLean Extension area, west-trending folds of the ore units affect the vertical position of the sections. To allow for this, shematic sections are used with geological information from drillholes and sections adjusted vertically to conform to the assumed regional dip. Assumed regional dips are obtained by using minimum slope angles consistent with sediment transport processes for coarse bouldery detritus.

Within the main MacLean channel (section A-A′, Fig. 12) a simple stratigraphic assemblage is present. Altered and fresh felsic tuff and siltstone of the ore sequence underlie the lower ore unit and overlie fragmental mafic rocks of the Ski Hill Formation. Polylithic breccia-conglomerates containing sedimentary, volcanic, granitoid and minor sulphide and barite clasts form the basal beds of the lower ore unit. These breccia-conglomerate beds are separated by thin felsic tuff interbeds, most too thin to be shown on the section. Overlying the breccia-conglomerate beds is massive sulphide matrix ore. The sulphide matrix ore in the MacLean Orebody forms one extensive bed within the main depression as shown on the section. A small bed of sulphide matrix ore occurs at the east end of the area and possibly several other discrete sulphide matrix ore beds occur off the line of section.

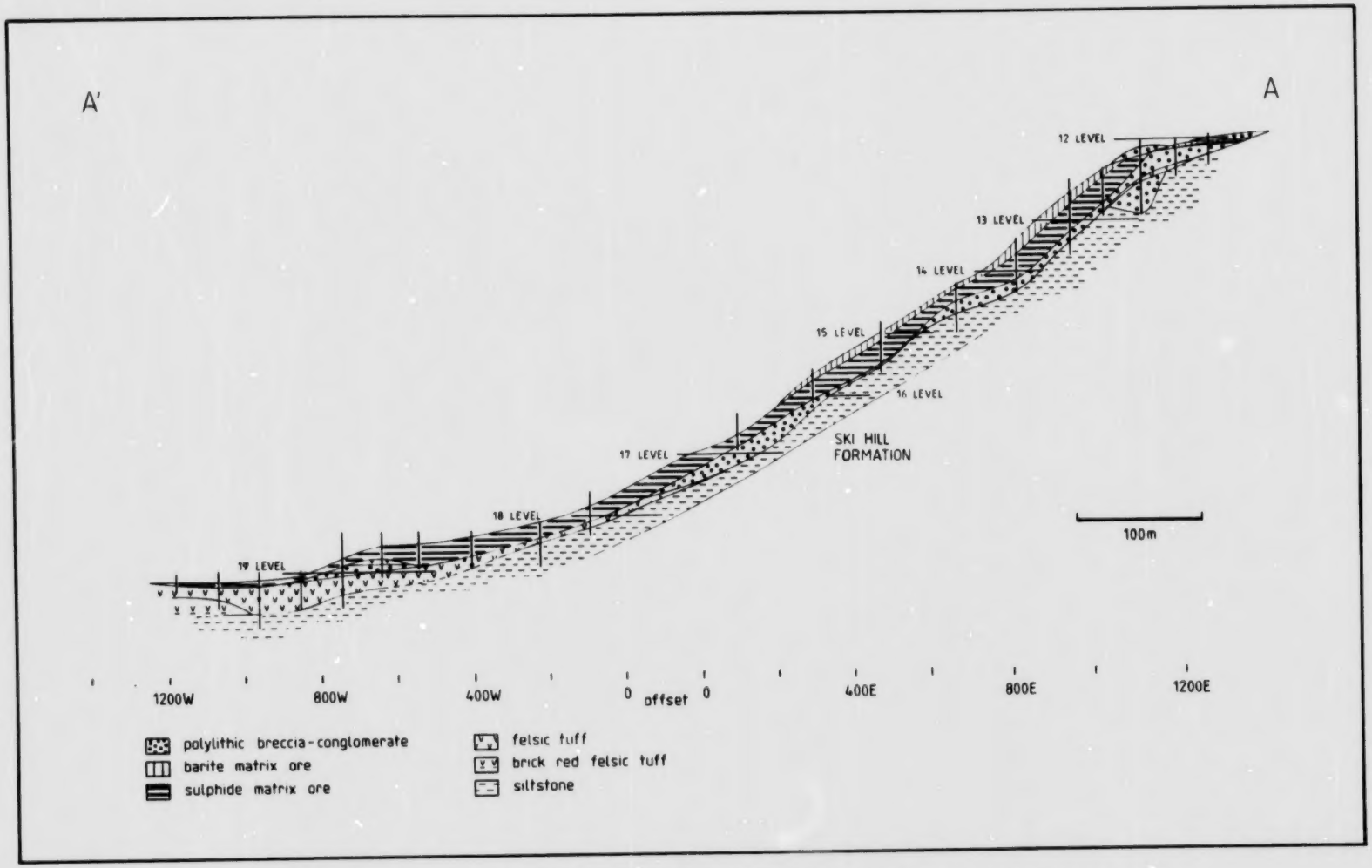

Figure 12. Longitudinal section of the MacLean Orebody along A-A′ (Fig. 11) showing ore beds and underlying rocks of the ore sequence. Vertical and horizontal bars represent data sites from level plans and E-W mine sections. Easting and westing refer to the mine grid (in feet).

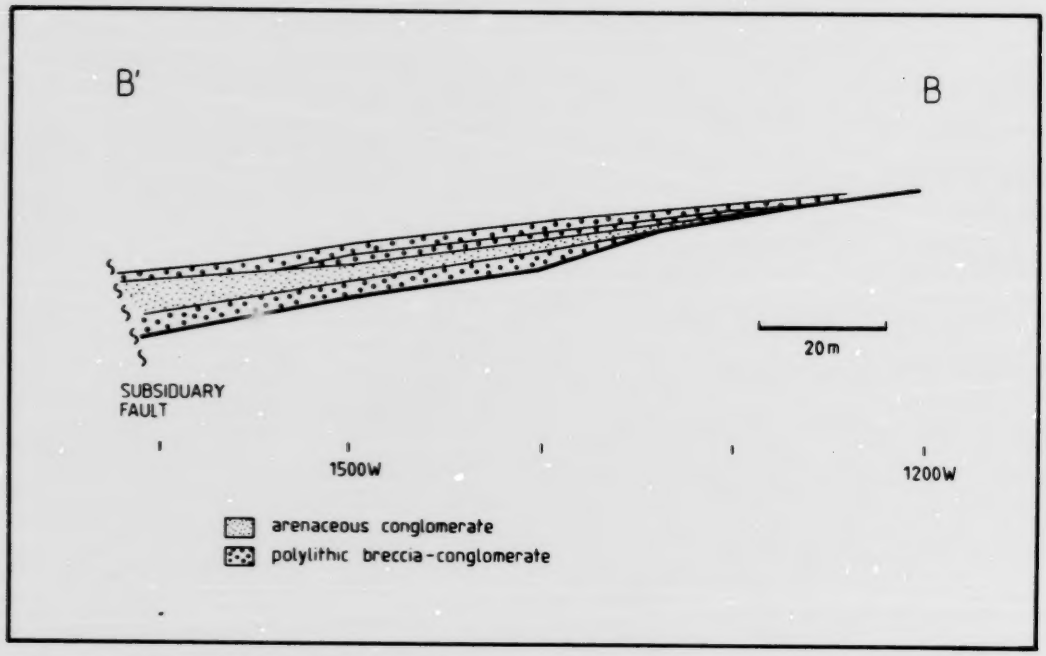

Figure 13. Schematic longitudinal section B-B', northeast part of the MacLean Extension Orebody (Fig. 11). Westing locations refer to the mine grid (in feet).

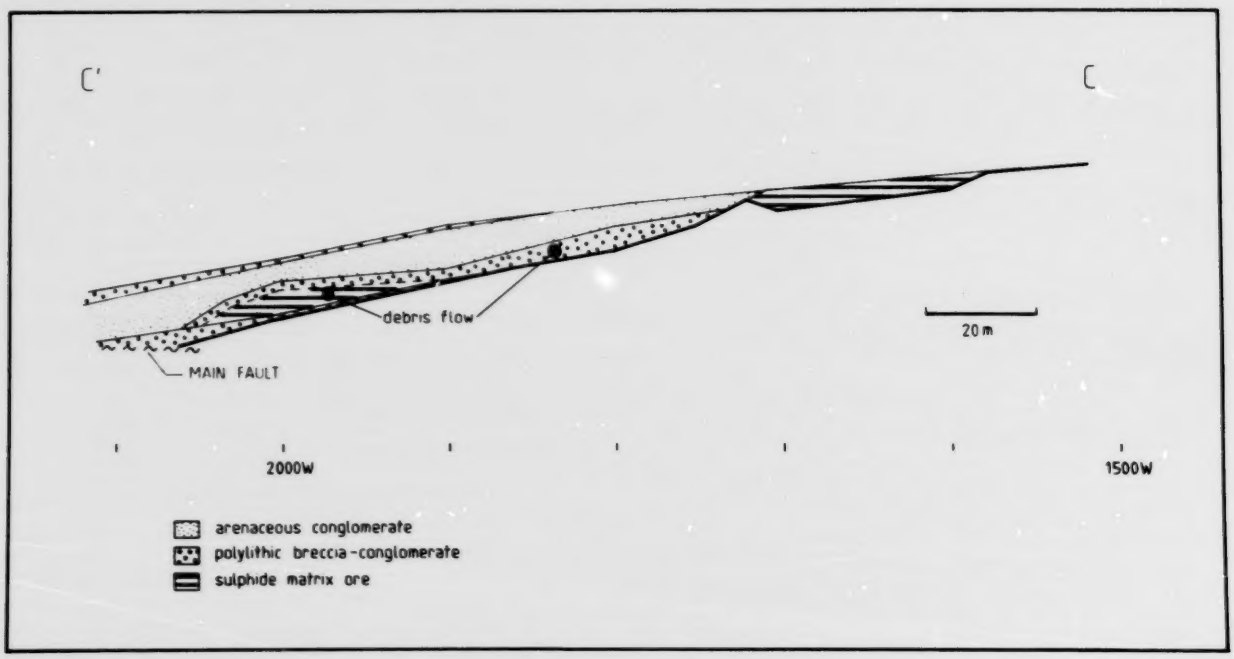

Figure 14. Schematic longitudinal section C-C' southeast part of the MacLean Extension Orebody (Fig. 11). Westing locations refer to the mine grid (in feet). The debris flow noted on C-C' is described in greater detail in Figure 20 and accompanying text.

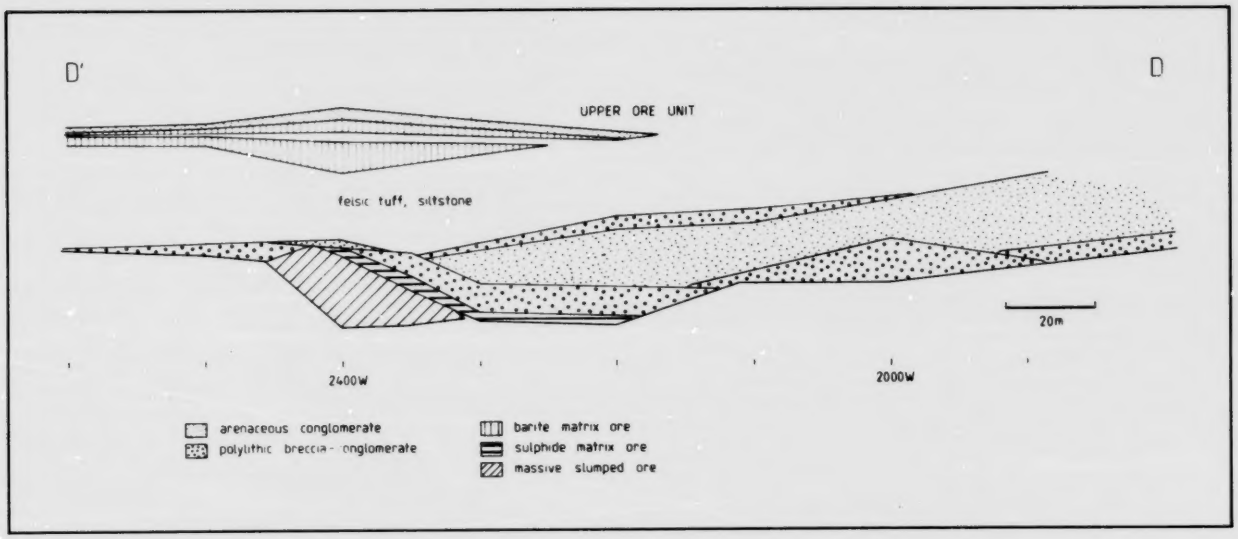

Figure 15. Schematic longitudinal section D-D′ MacLean Extension Orebody based on diamond-drill sections 100 feet apart from 1800W to 2600W (Fig. 11). Westing locations refer to the mine grid (in feet).

At the western end of section A-A′ the sulphide matrix ore forms the top of the lower ore unit. To the east, it is overlain by barite-rich beds containing a variety of lithic clasts. A detailed description of the unique cyclic deposition of barite matrix ore with graded clasts at the extreme east end of the exposed MacLean channel is found in the section on vertical variations in clast size and type.

The longitudinal section of the MacLean channel shown in section A′-A can be simplified to polylithic breccia-conglomerate at the base of the lower ore unit, overlain by sulphide matrix ore which in turn is overlain by barite matrix ore.

The schematic longitudinal sections of the bifurcated MacLean channel in the MacLean Extension Orebody are markedly different than in the MacLean Orebody. To the west of the MacLean Orebody polylithic breccia-conglomerate is a major ore type with clasts of sphalerite-galena, pyrite-chalcopyrite and barite (±sphalerite-galena) in a lithic matrix. Polylithic breccia-conglomerate beds occur near the base and at the top of the lower ore unit. The sulphide matrix ore occurs at the base of the stratigraphic section and a thick bed of low-grade arenaceous conglomerate overlies the basal sulphide beds.

In the north channel (section B-B′, Fig. 13) polylithic breccia-conglomerate and an interbed of arenaceous conglomerate extend from the subsiduary fault in the west to pinch out against the substrate of felsic tuff in the east. The beds are thin but laterally extensive. The uppermost polylithic breccia-conglomerate bed in this area contains abundant barite clasts and, similar to the MacLean Orebody, barite is concentrated near the top of the ore unit.

A limited, but economically important, sulphide matrix ore bed occurs at the eastern end of the south channel of the MacLean Extension Orebody (section C-C′, Fig. 14). To the west, polylithic breccia-conglomerate beds are separated by a thick bed of arenaceous conglomerate. The blunt, high-angle contacts outlined on this section define the limits of a debris flow with lateral and terminal boulder dams and a high-grade sulphide-rich flow centre. Detailed descriptions of this flow are presented in this paper. The basal polylithic breccia-conglomerate extends into the area of section D-D′, (Fig. 15). It forms distinct mound at 2000W (Fig. 15).

The section along the main channel in the western part of the MacLean Extension area (section D-D′, Fig. 15) contains a number of lithologically distinct beds. Unique to this area is a thick lens of massive slumped pyrite-chalcopyrite-sphalerite-galena-barite ore with no lithic clasts or streaky laminar layering (Fig. 16). However, some specimens contain relict disturbed beds of pyrite- chalcopyrite and barite. This ore lens is thought to be a slump deposit from in situ massive sulphides. The sulphide lens overlies unaltered felsic tuff, siltstone breccia-conglomerate and fragmental mafic rocks of the Ski Hill Formation. It apparently was derived from the south or southwest, off the line of the longitudinal section.

Overlying the massive slumped ore is sulphide matrix ore which includes lithic detritus and a sheared sulphide matrix. This sulphide matrix ore is overlain by polylithic breccia-conglomerate with sulphide and barite fragments in a clastic matrix (Fig. 15). This sequence of beds appears to have a source in the western end of the channel in the vicinity of the massive slumped ore. The source was spatially, but not temporally, separate from the source of the polylithic breccia-

Figure 16. Massive pyrite-chalcopyrite (light grey) interbedded with and cut by sphalerite-galena (dark grey). A small barite vein (white) cuts the sulphides, 2400W raise, MacLean Extension Orebody.

conglomerate and arenaceous conglomerate which were derived from the east.

In the western end of the MacLean channel a second or upper ore unit is exposed. Two barite-rich detrital and overlying sandstone cycles form this upper ore unit which thickens in close proximity to the underlying massive slumped ore. Within the upper ore unit the second cycle of deposition is laterally more extensive than the lower cycle. Both cycles extend further west than the pinch-out of the lower ore unit.

The general sequence of sediment-fill in the western part of the channel is initial deposits of sulphide matrix ore and polylithic breccia-conglomerate overlain by arenaceous conglomerate. The lower ore unit is capped by more polylithic breccia-conglomerate with abundant granitoid and barite clasts. Tuff and siltstone buried the lower ore unit, followed by the two episodes of barite matrix ore deposition of the upper ore unit.

Underground geology

All available exposures of ore-bearing units of the MacLean channel were mapped underground at a scale of 1:60 and plotted at a scale of 1:120. To outline in detail each of the drives and sublevels that were mapped is beyond the scope of this report. Only two areas will be dealt with, portraying important sedimentary features in the MacLean channel.

Sublevel 20-6-1 of the MacLean Extension workings is described to illustrate complex depositional features of the lower ore unit. Detailed sections of sublevel walls are presented in Figure 17 with a plan view of the workings showing stope outlines as of November, 1983.

Stratigraphy of the ore sequence at this location is presented in section B of Figure 2. Greater than 20 m of brick-red felsic tuff is overlain by approximately 10 m of green felsic tuff which underlies the lower ore unit. Blocks of the brick-red tuff are noted in the basal metre of the overlying green tuff. This portion of the ore sequence is exposed in the raise between 20 level and the 20-6-1 sublevel.

The contact of the lower ore unit and the felsic tuff is complicated locally by faults, but generally trends west and dips from 5 to 35 degrees to the north. In the cross-section of the ore unit (X-X', Fig. 17), dips flatten to the north giving the distinct impression of a series of offlapping beds deposited at the base of a steep slope. Within the lower ore unit in sublevel 20-6-1, six beds or groups of beds have been separated based on their lithological characteristics and contact relations. Beds are labelled *A* to *F* on Figure 17 for ease of identification. The designations have no regional significance and apply only to the beds in this area.

Within *A* three separate beds have been distinguished. A description of grain size variations in these three beds is presented in Figure 26. *A1*, the basal polylithic breccia-conglomerate, overlies green felsic tuff. Large lithic and sulphide blocks from 1 m to greater than 4.5 m apparent maximum dimension are a distinctive feature of this bed. Lithic clast types include basalt, altered silicified basalt, rhyolite, altered felsic volcanics and granitoid rocks. Ore clasts include pyrite-chalcopyrite-sphalerite-galena, sphalerite-galena, barite-sphalerite-galena and massive barite. The matrix of this coarse blocky bed includes centimetre-sized fragments of granitoids, massive rhyolite, felsic tuff, basalt and barite with sand- sized single crystal fragments of quartz and altered feldspar. Chlorite and matrix sulphides are interstitial to the lithic detritus.

Overlying *A1* in a small area is bed *A2*. It is distinguished from *A1* by its smaller clasts (most less than 15 cm apparent maximum dimension) and the greater proportion of barite in the matrix. A large proportion of the clasts in this bed are either sulphides or barite. The fine grained matrix includes quartz and altered feldspar grains, intergranular calcite, discrete grains of euhedral pyrite and anhedral irregular blebs of sphalerite-galena.

A3 is the uppermost bed of polylithic breccia-conglomerate in group *A*. Plastically deformed sulphide fragments are present in addition to lithic clasts to 30 cm apparent maximum dimension. The matrix is a mixture of angular and subangular quartz and altered feldspar grains, small lithic clasts, euhedral pyrite and anhedral sphalerite-galena blebs.

Marginal to *A* beds, and gradational with them, is arenaceous conglomerate (*Am*). The matrix forms over 90 per cent of the rock and includes granitic detritus in addition to the matrix constituents mentioned for the polylithic breccia-conglomerates. Interstitial chlorite was noted but no barite

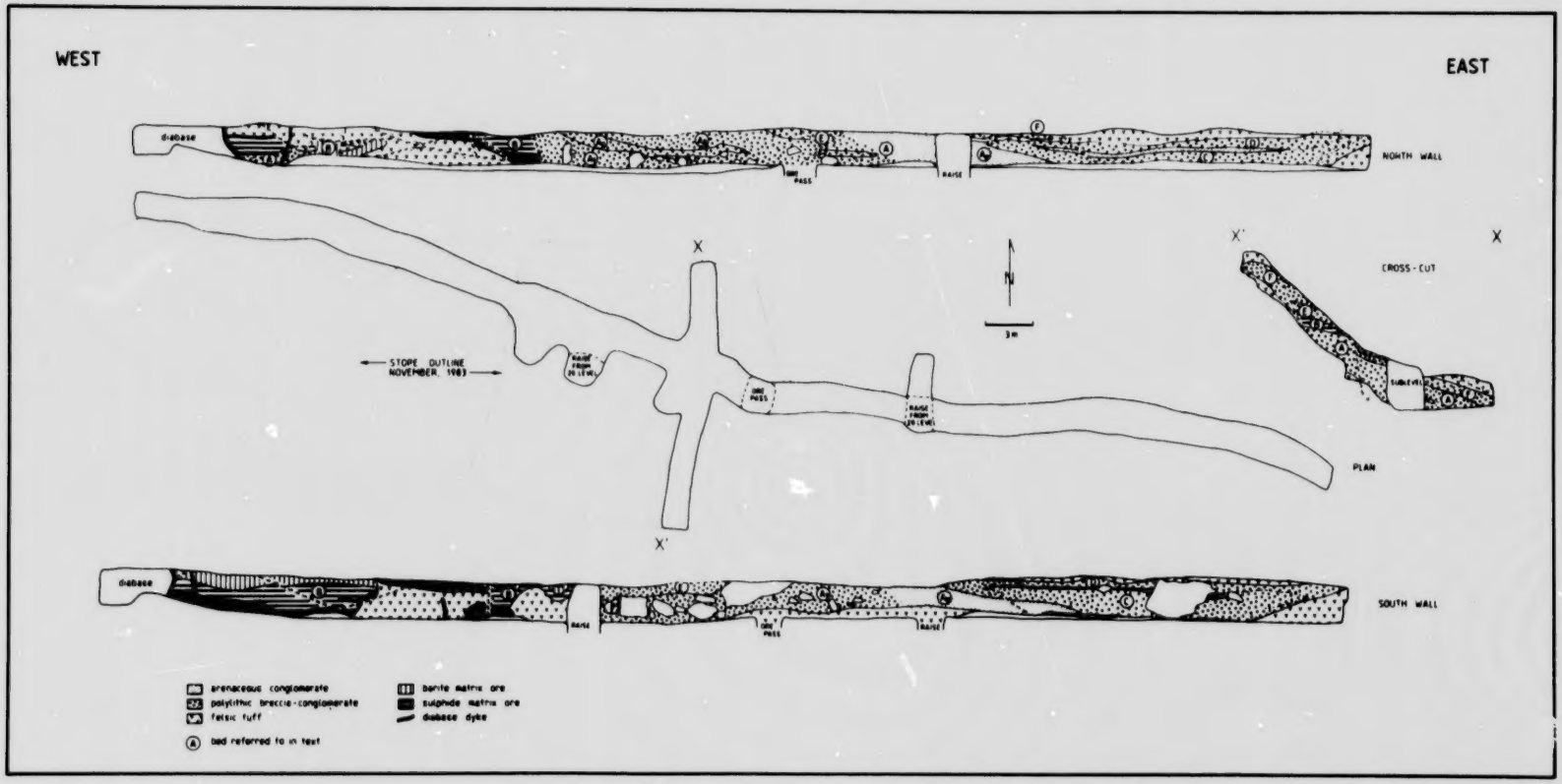

Figure 17. Plan and wall sections of sublevel 20-6, MacLean Extension workings. Letters are bed designations referred to in the text. Large boulders (blank) are shown to scale.

was observed in the matrix of the arenaceous conglomerate. Clast types include granitoid, siltstone, rhyolite and sulphides, all less than 15 cm in apparent maximum dimension.

The beds of group *A* occur in the central portion of the sublevel and pinch out against underlying green felsic tuff to the east and south. Faults complicate contact relations to the west.

The relative ages of beds overlying group *A* have not been established due to the lack of superposition of beds. For the purpose of this description, sulphide matrix ore is assumed to preceed polylithic breccia-conglomerate.

Bed *B*, comprising sulphide matrix and barite matrix ore, overlies *A* in the cross-cut of the sublevel and to the west sits directly on a green felsic tuff substrate. The bed contains a large number of volcanic, granitoid, siltstone and sulphide clasts in a matrix of sulphides, barite and calcite with much admixed lithic detritus. Bed *B* is a transitional lithology with sulphides as both clasts and in the matrix of the rock.

Bed *C*, a polylithic breccia-conglomerate unit, is exposed in the eastern part of the sublevel and occupies a channel underlain in the west by arenaceous conglomerate of the *A* group beds (*Am*) and in the east by felsic tuff. The polylithic breccia-conglomerate is the basal bed of the lower ore unit within this north-trending channel. Coarse detritus occurs in this bed with many clasts ranging from 20 to 50 cm apparent maximum length. The largest block noted is 4.4 m long where exposed by the sublevel (Fig. 17). The mixture of clast types and matrix for bed *C* is typical of polylithic breccia-conglomerate described previously. Bed *C* is overlain by 20 to 50 cm of sandstone and arenaceous conglomerate. The sandy beds are medium grey-green to grey-pink in colour and massive to finely laminated. Individual laminae do not extend more than 5 to 10 m laterally across the channel. The content of tuffaceous detritus (crystals, glass shards) in the sandstone increases towards the top of the bed. The sandy beds abut, but do not cover, the large boulder in the centre of the channel.

The last unit in the eastern part of the sublevel is another polylithic breccia-conglomerate bed labelled *D*. This thin bed contains crowded lithic and sulphide clasts to 50 cm length in a matrix of fine grained lithic detritus, barite, pyrite, quartz and altered feldspar. Small granitoid clasts are abundant in the matrix. Bed *D* abuts and only partially covers the large lithic fragment (Fig. 17).

Granitic polylithic breccia-conglomerate of bed *E* overlies both beds *B* and *A* in the central part of the sublevel. Bed *E* contains granitoid and other lithic clasts in a matrix of small volcanic and granitoid fragments, quartz, altered feldspar chlorite, pyrite and sphalerite-galena.

Lithic felsic tuff overlies bed *E* in the eastern part of the sublevel. In marginal areas, on the north wall of the sublevel, felsic tuff and intercalated sandstone separates beds *D* and *F*.

Bed *F*, a baritic polylithic breccia-conglomerate, overlies the extremities of beds *A*, *E* and the felsic tuff. The bed includes barite and sulphide clasts to 50 cm apparent length and lithic clasts to 80 cm apparent length. The matrix includes subangular to subround quartz, altered feldspar, barite and small lithic fragments. A blunt marginal termination of bed *F* with the adjoining tuff (Fig. 17) indicates some internal strength when it was deposited. Overlain by an undetermined thickness of green felsic tuff, *F* is the uppermost bed of the lower ore unit in sublevel 20-6-1.

The distribution of beds *A* through *F* illustrates the complexity of bed deposition of the lower ore unit in this part of the MacLean channel. The local nature of individual beds demonstrates that detailed sedimentological and stratigraphic investigation using only drill core data could be quite misleading. Simple correlation of beds between drill holes is complicated by their similar lithologies. Studies of sublevel 20-6-1 demonstrate that several channels could be involved in ore deposition. The matrix strength of polylithic breccia-conglomerate beds is indicated by their high-angle marginal contacts and coarse matrix supported sediment load. Size variation of boulders and orientation of the eastern channel in the sublevel suggest the source of sediment in the lower ore unit in sublevel 20-6-1 was to the south, towards the western end of the main MacLean Orebody (Fig. 11, 33 at 1000W).

Sublevel 20-18 exposed the complete ore-bearing section of the upper ore unit in the MacLean Extension Orebody. In contrast to the complexity of the lower ore unit, beds of the upper ore unit in sublevel 20-18 include two cycles which are continuous over a sizeable area (Fig. 15).

Detailed sections along the walls of the sublevel are presented in Figure 18. To illustrate the stratigraphic continuity of the sequence a drill section from 100 m to the east is presented for comparison.

The upper ore unit in sublevel 20-18 overlies massive yellow-green felsic tuff along an irregular contact. The barite-rich base of the first cycle of ore deposition comprises single broken barite crystals to 1 cm in length and clasts of siltstone, rhyolite, altered felsic volcanics, basalt and sulphides in a matrix of barite, sphalerite, galena, calcite and lesser quartz and altered feldspar. About 5 to 10 per cent of the matrix is sphalerite and galena which occur as irregular mineral aggregates between the barite crystals. Sorting is poor, with lithic fragments to 50 cm apparent length dispersed in the matrix.

Above this 0.6 to 1.0 m thick basal bed is sandstone and interbedded felsic tuff. The sandstone beds comprise medium- to coarse-grained-sized quartz and altered feldspar in an altered silt- to clay-sized matrix. Barite crystal clasts are normally graded in some sandy beds. The principal sulphide in the sandstone is pyrite, occurring as discrete euhedral to subhedral grains with lithic detritus. In a few places, fine grained sphalerite and galena are present in the sandstone. The interbedded felsic tuffs have an altered aphanitic matrix containing 0.5 to 1 mm altered feldspar and embayed quartz crystals. These tuff beds are more abundant near the top of the section and locally form a separate unit.

The base of the second cycle is a 0.4- to 0.8 m-thick bed of barite matrix ore. Sphalerite and galena comprise 10 per cent of the matrix with some calcite. Fine grained lithic

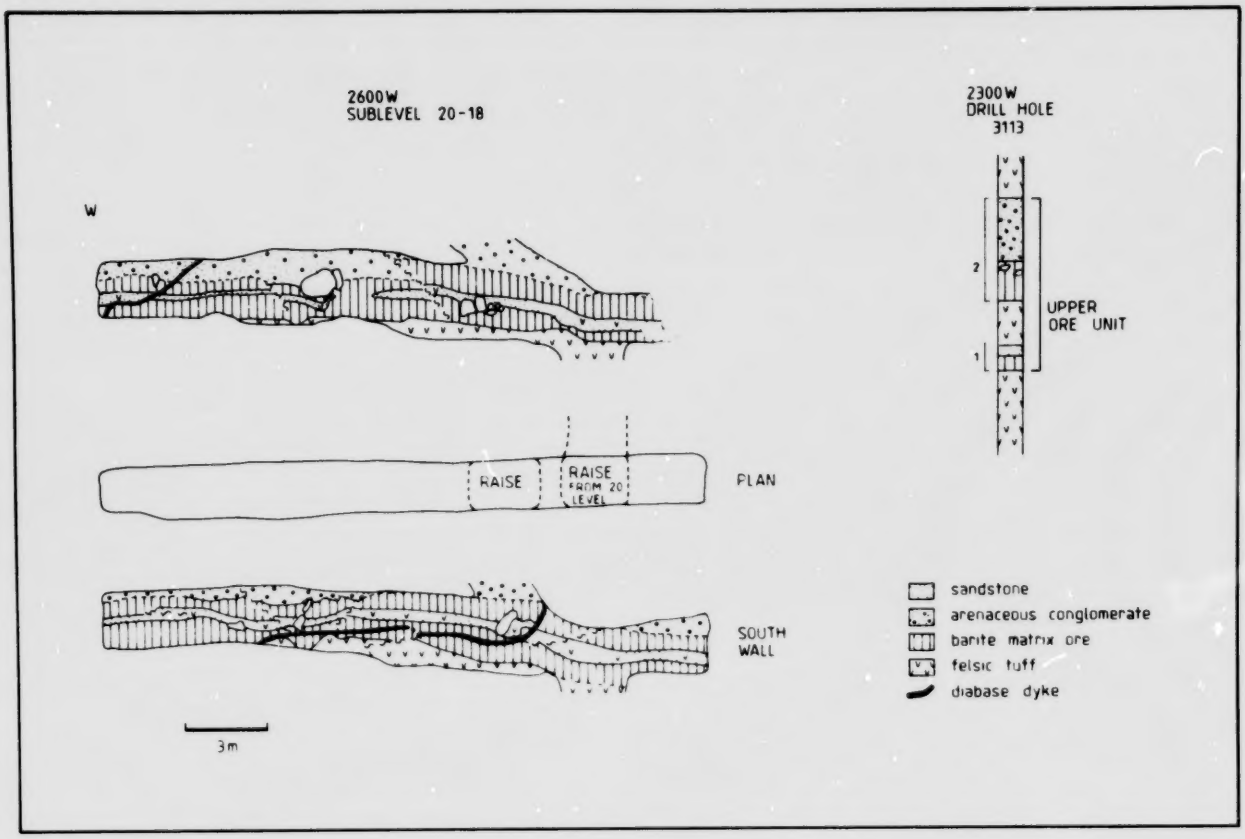

Figure 18. The upper ore unit of the MacLean channel in sublevel 20-18 and drillhole 3113 area. Large boulders (blank) are shown to scale. Westing locations refer to the mine grid (in feet).

detritus occurs throughout the unit being more abundant towards the top of the bed. A gradational contact exists with the overlying arenaceous conglomerate. This ore bed contains boulders of sphalerite-galena to 80 cm length. The largest boulders penetrate the underlying sandstone and felsic tuff, which were only partly lithified at the time of deposition of these heavy clasts (Fig. 19).

Above the second barite-rich bed in sublevel 20-18 is an undetermined thickness of arenaceous conglomerate with 10 to 20 cm clasts of siltstone, rhyolite and basalt dispersed in a sandy matrix.

In hole 3113 the upper ore unit is underlain by felsic tuff. The first depositional cycle comprises sulphide-rich barite matrix ore containing clasts of rhyolite and siltstone to 5 cm intersected diameter at the top of the bed. This basal bed is overlain by fine grained barite and quartz sandstone with interbedded tuff which grades upward into a section of massive felsic tuff (Fig. 18). A barite matrix ore bed containing altered felsic volcanic and siltstone clasts greater than 10 cm intersected diameter is the lowest unit in the second ore cycle. Arenaceous conglomerate with clasts of siltstone and rhyolite overlies the barite matrix ore. The arenaceous conglomerate contains fewer clasts higher in the section and is overlain by lithic and crystal felsic tuff (Fig. 17).

Between sublevel 20-18 and drillhole 3113 the stratigraphy is unchanged except for the thickness variations of beds. Unlike the lower ore unit which comprises a complex assemblage of laterally restricted beds, the two cyclical ore beds are more uniform and extensive.

Characteristic features of debris flows

Although previous authors (including Thurlow, 1977; Thurlow and Swanson, 1981; Walker and Barbour, 1981, and Calhoun and Hutchinson, 1981) recognized the importance of subaqueous sediment gravity flow or debris flow for the transport of massive sulphide ores at Buchans, the distinctive features of the flow margins were not described by these authors.

Middleton and Hampton (1976) reviewed the mechanics of flow, methods of deposition and textures and structures of debris flows. Debris flow is considered to be the non-

Figure 19. Large block of sphalerite and galena of the second barite matrix ore unit has penetrated the underlying sandy-tuff and lower ore bed. The steel plate is 12.6 cm on a side. Upper ore unit, sublevel 20-18, MacLean Extension Orebody.

turbulent downslope movement of mixtures of granular solids, clay minerals, water and, at Buchans, sulphides, in response to the pull of gravity. When the driving stress of gravity decreases below the strength of the debris, the flow 'freezes' in position. On freezing, the fabric and textures of the flow during transport are preserved.

An important feature, diagnostic of debris flows, is a blunt, steep-sided profile resulting from the matrix strength of the debris. Marginal bouldery deposits are formed at the snout and sides of the flow, in some cases creating levees which contain the flow above the level of the substrate. Sharp and Nobles (1953, p. 551-552), in observing a film of a subaerial debris flow gave a graphic description of the flow front.

> *A bouldery embankment formed at the front of the more viscous surges and the boulders therein rolled, twisted and shifted about but for the most part did not appear to be rolled under. Instead they were pushed along by the finer more fluid debris impounded behind the bouldery dam and swept along by the mud leaking through it.*

Other features of debris flow deposits such as random fabric, variable clast size and variable matrix (Nardin *et al.*, 1979) are all present in the ore beds of the MacLean channel.

The lateral and snout deposits of a debris flow in the south channel area in the MacLean Extension workings will be described. The extent of the flow and its position within the south channel are shown in Figure 20. Mine openings include a drive at location B (20-5-SL) into the lateral deposits of the flow and a cross-cut at location A (20-13-XC) which traverses the flow near its snout (Fig. 20).

At location B the core and lateral deposits of the debris flow sit directly on green felsic tuff. The main body of the debris flow includes sheared, but recognizable, blocks of sphalerite-galena in sulphide matrix ore (Fig. 21). Sulphide clasts greater than 1 cm length predominate in the coarse grained central portion of the flow but siltstone, rhyolite and other lithic clasts are also present (Fig. 20). Granitoid clasts are rare in this area. The matrix includes sulphides, fine grained lithic detritus and minor barite.

The contact of the main body of the debris flow and its coarse bouldery marginal deposits are at a high angle to the felsic tuff substrate. At location B the lateral deposits of the flow include large, plastically deformed blocks of sphalerite-galena mixed with subround granitoid blocks which are in excess of 30 cm apparent length (Fig. 21). Siltstone, rhyolite and other lithic clasts also border the flow but are less abundant. The matrix to the coarse blocky detritus comprises fine grained lithic detritus and discrete granular sulphides, principally pyrite. The flow margin at location B is less than 2 m in width, although it appears more extensive on the wall section as the drive follows the trend of the flow.

Away from the main body of the debris flow the lateral deposits include a greater proportion of lithic detritus. The overall amount of coarse detritus decreases with a proportionate increase in sand-sized matrix. The lateral flow deposits grading into arenaceous conglomerate are shown schematically in Figure 20.

Near the snout of the debris flow, in the cross-cut at location A, the flow overlies polylithic breccia-conglomerate of an earlier flow. The breccia- conglomerate has an immature, sand-sized matrix with abundant crystalline detritus and few sulphide grains. The main body of the debris flow at location A (Fig. 22) contains small clasts of sphalerite-galena, barite-sphalerite, siltstone and rhyolite dispersed in a matrix of barite, sphalerite, galena, quartz, altered feldspar and small lithic fragments. The contact of the debris flow and its marginal deposits are at a high angle to the underlying polylithic breccia-conglomerate substrate.

At location A, the marginal debris flow deposits close to the snout of the flow are more extensive than the lateral deposits described at location B. Bounding the flow is a sulphide-rich breccia-conglomerate with plastically de-

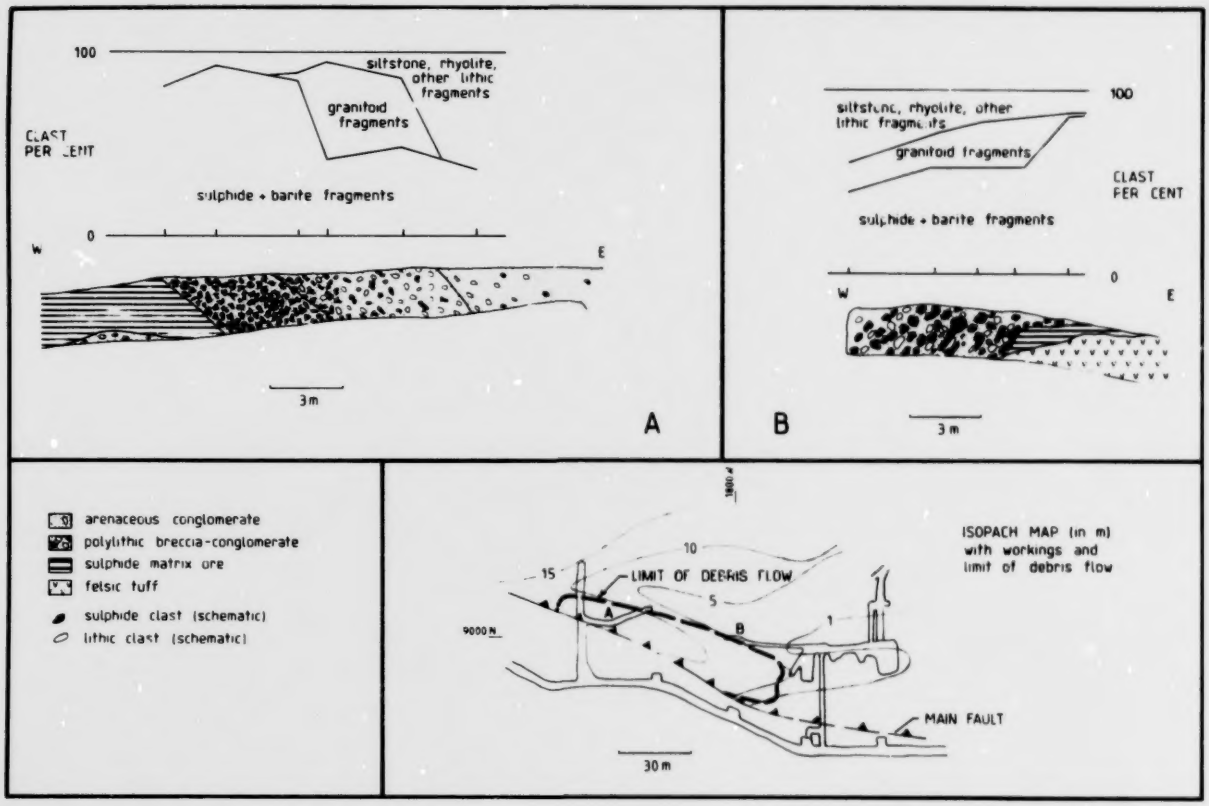

Figure 20. Anatomy of a debris flow. Plan shows the workings exposing the debris flow and isopach contours which outline the depositional channel. Two wall sections with corresponding clast proportion plots illustrate the marginal deposits of the flow.

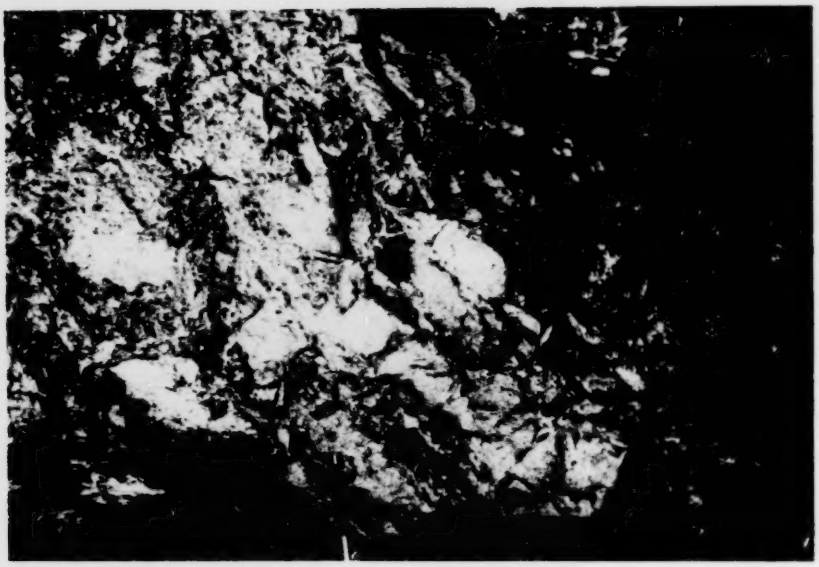

Figure 21. Debris flow comprising elongate sphalerite-galena blocks partly sheared and in a matrix of lithic and sulphide detritus. The flow is bounded on the right by large granitoid and sulphide clasts. Note the high angle contact between the flow detritus and the underlying felsic tuff. The pencil is 14.5 cm long. Lower ore unit, 20-5-SL, MacLean Extension Orebody (location B, Fig. 20).

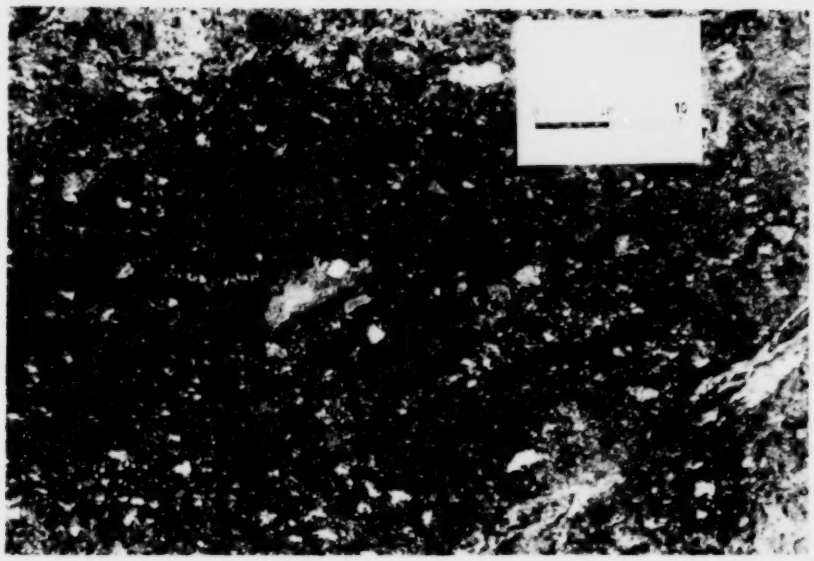

Figure 22. Main body of the debris flow illustrated in Figure 20, location A. The flow comprises a matrix of sulphides, barite and fine grained lithic detritus containing small, discrete lithic, sulphide and barite clasts. Lower ore unit, 20-13-XC, MacLean Extension Orebody.

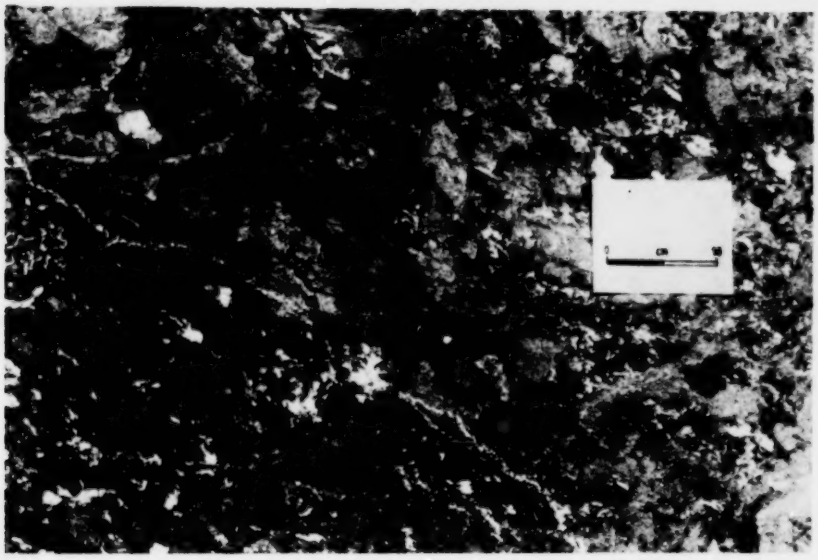

Figure 23. Contact of the sulphide matrix ore (lower left) in main body of the debris flow and associated marginal sulphide-rich breccia-conglomerate (upper right) at location A, Figure 20. In the sulphide-rich breccia-conglomerate plastically deformed sulphide fragments occur in a matrix of fine grained lithic detritus and pyrite. Lower ore unit, 20-13-XC, MacLean Extension Orebody.

formed blocks of sphalerite-galena and pyrite-chalcopyrite to 75 cm apparent length in a matrix of quartz, altered feldspar, discrete pyrite grains, chlorite and small lithic fragments. Figure 23 illustrates both the contact of the sulphide-rich breccia-conglomerate with the core of the flow, and the irregular margins of the plastically deformed sulphide fragments against adjacent clastic detritus. This sulphide-rich breccia-conglomerate grades laterally into polylithic breccia-conglomerate containing abundant granitoid and sulphide clasts. Not only in this flow, but throughout the MacLean Extension area, marginal debris flow deposits are the principal location for concentrations of large, subround granitoid clasts up to 50 cm apparent length (Fig. 24). The irregular but subrounded margins of granitoid clasts in Figure 24 may support the hypothesis that granitoid fragments were derived by explosive brecciation of the underlying volcanic feeder (stock) and ejection from the volcanic vent (Stewart, 1987). The plot of clast proportions (Fig. 20), shows the concentration of granitoid fragments is laterally restricted near the snout of the flow at location A. The sulphides occurring in the

matrix of the polylithic breccia-conglomerates are principally 30- to 55 mm-sized grains of pyrite. The remainder of the matrix comprises a mixture of angular quartz and feldspar, granitoid and volcanic fragments.

Further from the main body of the debris flow the range of clast types increases, the sulphide clasts have more discrete boundaries and the overall percentage of clastic matrix increases. Sulphides occur as pebble- to boulder-sized clasts, euhedral grains of pyrite, or in a few places, as irregular blebs of sphalerite- galena, in the lithic matrix. Large granitoid clasts are not abundant.

The outer sandy lithologies beyond the bouldery debris flow margin have a broad lateral extent but at their extremities they have angular contacts against the substrate. The extreme margin of the flow system is not observed at location A but the outer lithology observed is arenaceous conglomerate with only 10 to 15 per cent clasts greater than 1 cm length. The clasts are dispersed in a lithic, pyritic matrix with abundant angular grains.

Figure 24: Large, irregular granitoid blocks bordering the sulphide-rich breccia- conglomerate in the boulder dam of the debris flow (location A, Fig. 20). Lower ore unit, 20-13-XC, MacLean Extension workings.

These debris flow deposits containing massive sulphide clasts can be compared to subaerial sandy flows described by Sharp and Nobles (1953) and Johnson (1970, p. 433-445) and subaqueous flows discussed by Middleton and Hampton (1976). The debris flow itself is a mixture of sulphides, barite and fine grained lithic detritus. Laminar shear during flow probably disaggregated poorly indurated sulphide clasts. Competent lithic fragments were unaffected. The presence of partly lithified sulphide fragments transported as discrete clasts but deformed by loading after deposition confirms the non-turbulent, laminar or plastic nature of debris flows suggested by Fisher (1971), Middleton and Hampton (1976) and others. The debris flow was confined within a marginal boulder dam which includes coarse sulphide and granitoid fragments cast out of the flow. The damming helped retain and elevate the flow above the substrate. Near the snout of the debris flow the boulder dam is internally sorted with dense, plastically deformed sulphide fragments between the main flow body and the outer debris dam of competent sulphide blocks, granitoid and other coarse lithic detritus.

Polylithic breccia-conglomerate and arenaceous conglomerate outside the boulder dam may be deposits of finer grained, less dense material which breached or leaked through the coarse boulder dam or may be entirely separate overbank deposits. Hampton (1972) developed a model for the initiation of turbidity currents by debris flows. The process could account for the crudely graded beds which overlie, or are adjacent to, some debris flow deposits in the MacLean Extension area. The extent of the arenaceous conglomerate beyond the debris flow margin is a function of the method of transport which could include singly, or in combination, grain flow, fluidized flow or turbidity.

High-angle contacts between debris flow deposits and underlying substrate, and recognition that such deposits represent the exact configuration of the flow, permits the determination of the finite yield strength of the flow detritus.

Economically the recognition of debris flow margins is important as they represent grade boundaries between ore and low-grade, subeconomic arenaceous conglomerate. The orientation of the marginal deposits indicates the direction of sediment transport and the size of the bouldery detritus in the flow is a function of the slope of the substrate at the time of deposition (Binney, 1984).

CLAST COUNT STUDIES

Detailed count studies are used to quantify the variation in clast size and type, within and between lithologically distinct beds. Important in the genesis of the lower and upper ore units is the source and transport direction of the sulphide detritus. Previous authors, including Walker and Barbour (1981) and Calhoun and Hutchinson (1981), have inferred the direction of sediment transport by reference to the lateral heterogeneity of clast proportions in individual beds. Their work is re-examined using the more detailed clast counts of the present study.

Methods and manipulation of data

The size, lithology and stratigraphic position were recorded for in excess of 4000 clasts located at 40 sites. Sections were chosen to include the maximum stratigraphic extent of the lower ore unit and were cleaned with water and scrubbed to facilitate examination of the clasts. At each section, a grid was marked on the wall 0.5 m wide by the maximum exposed height of the lower ore unit (as low as 0.5 m but typically 1 to 2 m). The grid was oriented with respect to visible bedding planes and had vertical divisions every 10 cm. Within the grid, for every clast over 1 cm in apparent length, the observed length and width, clast type and its height in centimetres above the base of the grid were recorded. Bedding planes cutting the grid were noted so delineation of clast size and type within individual thin beds was possible. A 1 cm lower cutoff in clast size was a practical decision based on the difficulty of seeing small clasts in dim underground light.

The length measurements of sulphide and barite clasts were corrected for density differences between sphalerite-, galena-, pyrite- and barite-rich clasts and the coexisting lithic detritus. Corrected clast lengths, denoted by open circles in all plots of clast length versus height in bed (Fig. 25, 26, 27), are also used in the cumulative per cent versus phi diagrams (Fig. 30, 31).

The correction of clast lengths is based on a model for the settling of coarse grains (greater than 1 to 2 mm). The settling velocity (w) of a granular solid (density, ρs) in a fluid (density, ρf) is:

$$W = \left(\frac{4}{3} \cdot \frac{(\rho s - \rho f)\cdot g \cdot D}{C_D \cdot \rho f}\right)^{1/2}$$

where C_D is the drag coefficient, g is the acceleration due to gravity and D the grain diameter.

To correct the clast lengths for density differences:

$$W \propto \left(\frac{\rho s - \rho f}{\rho f}\right)^{1/2}$$

An assumption is made that the clasts are settling in water ($\rho = 1.0\ g\cdot cm^{-3}$). This gives a minimum correction factor for sulphide and barite clasts relative to lithic detritus ($pSL = 2.7\ g\cdot cm^{-3}$). The correction equation is:

$$\text{Length}_{corr} = \text{Length}_{meas.} \left(\frac{\rho s - \rho f}{psL - pf}\right)^{1/2} =$$

$$\text{Length}_{meas.} \left(\frac{(\rho s - 1)\ g\cdot cm^{-3}}{1.7\ g\cdot cm^{-3}}\right)^{1/2}$$

The assumed clast density for different types of sulphide and barite clasts is calculated based on mineralogical examination to determine "average" clast compositions. As an example, for sphalerite-galena clasts the assumed density is $4.7\ g\cdot cm^{-3}$. The correction factor for these clasts is:

$$\left(\frac{(4.7-1)\ g\cdot cm^{-3}}{(2.7-1)\ g\cdot cm^{-3}}\right)^{1/2} = 1.48.$$

Correction factors vary from 1.09 for pyritic stockwork fragments to 1.48 for sphalerite-galena fragments. The factors are minimums as conservative values are chosen for the density of the sulphide and barite clasts.

The position of the clasts is plotted versus the corrected clast length for all sections using the method of Walker (1975).

For each measured section, the percentage, by area, of each type of clast was determined. This percentage by area reflected the true relationship between clasts, as some types, particularly granitoid and sulphide clasts, were few in

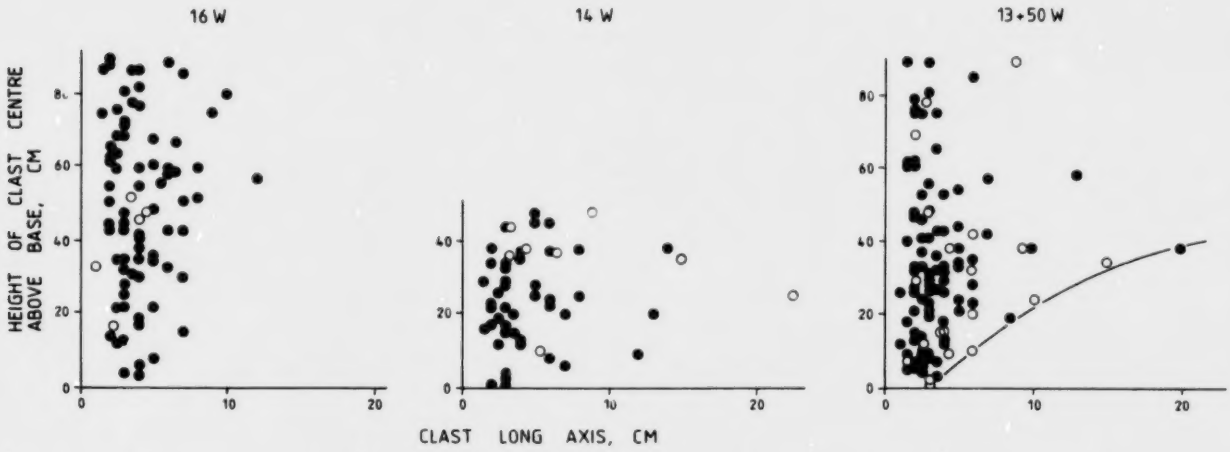

Figure 25. Vertical and lateral variation in clast size for a granitoid-rich polylithic breccia-conglomerate bed in the lower ore unit. Locations refer to westings on the mine grid. Curved line on the 13 + 50W section is the limit of the largest clast size over the inversely graded basal 40 cm of the section. Solid circles are lithic clasts, open circles are corrected clast lengths for sulphide and barite clasts.

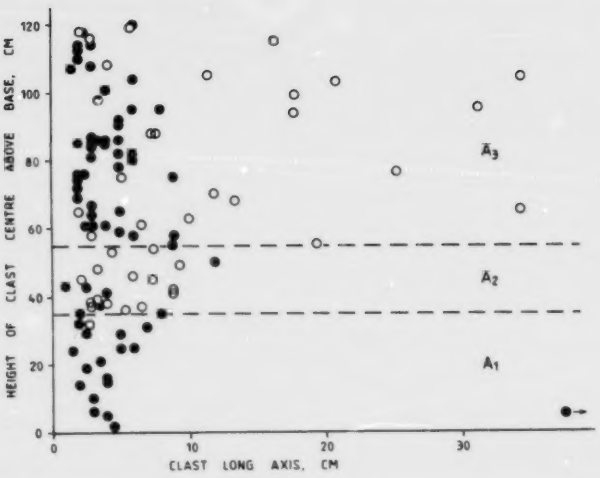

Figure 26. Vertical variation in clast size, lower ore unit, sublevel 20-6-1. Bed designations (A1, A2, A3) refer to detailed descriptions of this sublevel as shown in Figure 17. Solid circles are lithic clasts, open circles are corrected clast lengths for sulphide and barite clasts.

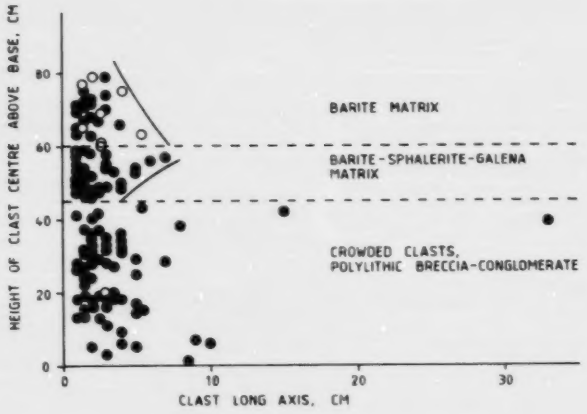

Figure 27. Vertical clast-size variation in one depositional cycle of the lower ore unit, 12 level, MacLean Orebody. Curved lines show the limit of maximum clast size in inversely and normally graded parts of the cycle. Solid circles are lithic clasts, open circles are corrected clast lengths for sulphide and barite clasts.

number in a selected area but significant due to their large size with respect to other lithic detritus.

The data from the present study may not be comparable directly with that presented by Calhoun and Hutchinson (1981). Their clast counts are not stated as weighted by area or just presented as raw data in the form of the total number of clasts.

Figure 28. A portion of the third depositional cycle, 12 level, MacLean Orebody. The base of the cycle, below the pencil, comprises coarse, unsorted lithic clasts with little matrix. The remainder of the cycle comprises smaller lithic clasts dispersed in a barite-sulphide matrix. Clast size increases up to the top of the pencil and then shows a progressive decrease up the cycle. Siltstone clasts at the base of the section have altered rims. Steel plate is 12.6 cm along a side.

Vertical variation in clast size and type

Vertical variation in clast size and type was examined for beds of the lower ore unit in the MaacLean Extension Orebody. A granitoid-rich polylithic breccia-conglomerate bed exposed at several locations permitted determination of the lateral variation within a single stratigraphic unit.

Most of the beds of the lower ore unit have a random internal fabric and no vertical grading of clasts. These features occur in sulphide and barite matrix ore, polylithic breccia-conglomerate and most sections of arenaceous conglomerate. Barite matrix ore in the lower ore unit of the MacLean Orebody is one of the few documented examples of normal grading in ore beds. Figures 27 and 28 show one cycle of deposition of this barite matrix ore.

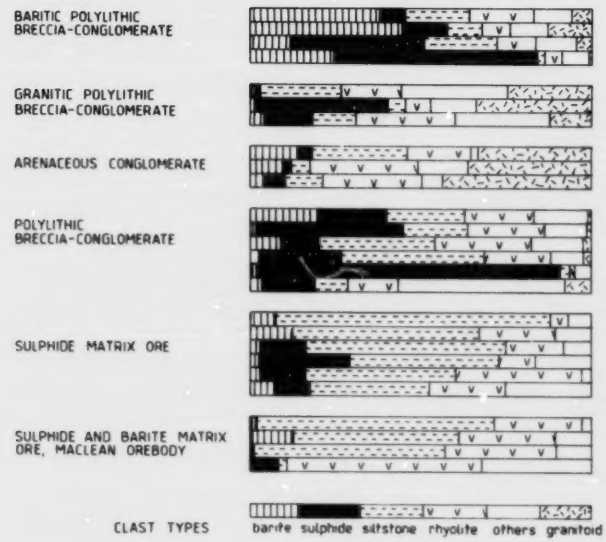

Figure 29. Proportions of clast types (by area) for selected beds of the lower ore unit. Sections are from workings in the MacLean Extension Orebody except where noted. Beds are presented in stratigraphic order; within each group, lower sections are from eastern exposures, overlying sections are from progressively further west.

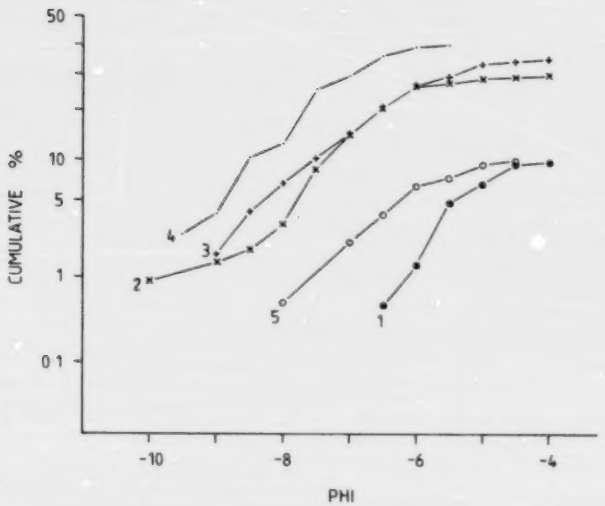

Figure 30. Cumulative per cent versus phi size for five measured sections across the margin of a debris flow in the MacLean Extension area (location A, Fig. 20). Truncated size distributions are presented as only detritus coarser than $-3\emptyset$ were measured. Sections are: 1 from debris flow, 2 to 4 from bouldery margin of flow, 5 from arenaceous conglomerate bounding flow.

Figure 25 presents complete sections through a bed of granitoid-rich polylithic breccia-conglomerate from three locations. The diagram is based upon the length and position measurements of 251 clasts. All sections are located in south-trending drifts so comparisons of clast length should not be biased by different section orientations. Several features of the sections are noted. The absolute number of sulphide and barite clasts (open circles) decreases from east to west. The total number of large clasts (greater than 10 cm apparent length) also decreases to the west. In the section at 13 + 50W the basal 40 cm of the bed is inversely graded. No grading occurs in the other two sections.

A bed of baritic polylithic breccia-conglomerate, overlying the granitoid-rich polylithic breccia-conglomerate, is unsorted and has a decrease in the number of sulphide and barite clasts to the west. No consistent trend was observed in the maximum size of clasts in the baritic bed.

A vertical section through three beds of the lower ore unit in sublevel 20-6-1 is shown in Figure 26. Lithic, sulphide and barite detritus are unsorted within each bed. The lower bed, of which only the top is exposed by the grid section, contains coarse- to fine-grained lithic detritus with one clast to 52 cm apparent length. This clast is not atypical for this lower bed; the lack of similar sized clasts in the section is a reflection of the limited width of the grid (0.5 m). At 35 cm height, the proportion of lithic to sulphide and barite clasts changes dramatically and the overall average size of the detritus increases slightly from the underlying bed. Above 55 cm height is polylithic breccia-conglomerate containing plastically deformed sulphide fragments. This bed is coarser grained than the underlying beds; about one-quarter of the measured clasts are greater than 10 cm in length. All of the large clasts are sulphides. The stratigraphy of the lower ore unit in sublevel 20-6-1 is complex and more beds were exposed in the back of the drive. Individual beds measured were not laterally extensive and further mining outlined their pinch-out within 30 m of the measured section. Figure 26 illustrates the variability in both the size and type of clasts in different beds deposited at the same location.

Graded beds occur in the barite matrix ore of the lower ore unit on 12 level of the MacLean workings (Fig. 28). The base of a sedimentary cycle is formed by an unsorted bed with fine- to coarse-grained, elongate siltstone and rhyolite clasts (crowded clast section, Fig. 27). Overlying this division with a distinct break in clast size is barite-sphalerite-galena matrix and barite matrix ore with both density grading in the matrix and clast-size grading. The proportion of siltstone to rhyolite clasts, the two principal types, remains constant throughout the cycle. The basal 15 cm of the matrix ore unit is inversely size graded (Fig. 27); the maximum clast length of 7 cm occurs just above the pencil tip in Figure 28. Above this inversely graded base the maximum clast length decreases to 3 cm at the top of the observed section. Clasts at the top of the matrix ore section were not measured, however the clast size drops rapidly below the 1 cm limit for measurement. Associated with this clast size gradation, the proportion of barite to sulphides also increases from the base to the top of the matrix

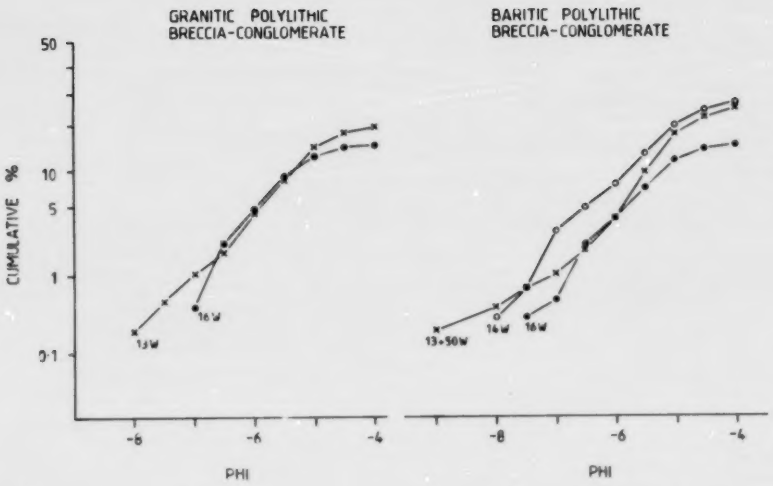

Figure 31. Lateral variations in cumulative per cent versus phi size distributions for two polylithic breccia-conglomerate beds. Baritic polylithic breccia-conglomerate overlies granitoid clast-rich polylithic breccia-conglomerate and forms the uppermost bed of the lower ore unit in this part of the MacLean channel. Locations refer to west co-ordinates on the mine grid (in feet).

ore unit. In the upper part of the cycle, larger barite clasts occur in a matrix of massive barite.

Size grading in the arenaceous conglomerate beds in the MacLean Extension workings is common but not laterally extensive. This grading is portrayed by fine pebble-sized lithic detritus or by sand- to silt-sized quartz grains. None of this grading was quantified by clast counts, although it was easily recognized during mapping and thin section studies.

Clast percentages

Percentages of clast types by area were calculated for all measured sections. In Figure 29 data for lower ore unit beds are plotted in stratigraphic order with sulphide matrix ore at the base, overlain by polylithic breccia-conglomerate, arenaceous conglomerate and finally the polylithic breccia-conglomerate beds that cap the lower ore unit in the MacLean Extension Orebody. Within individual beds each section is from an exposure of the bed west of the underlying section.

Several trends are shown by the data in Figure 29. Towards the top of the lower ore unit a greater proportion of sulphide and barite clasts coexist with the lithic detritus. The proportion of barite to sulphide clasts also increases. As polylithic breccia-conglomerate and arenaceous conglomerate contain few sulphide grains in the matrix, the proportion of sulphides as clasts rather than matrix increases up the stratigraphic section. Within the lithic component of the coarse clastic detritus, granitoid clasts occur only in polylithic breccia-conglomerate and arenaceous conglomerate. Granitoid clasts were not observed in sulphide or barite matrix ore, although small aggregates of quartz and feldspar crystals were noted in thin sections of these lithologies.

Calhoun and Hutchinson (1981) used the ratio of the number of assumed proximally derived clasts to the number of assumed distally plus proximally derived clasts to infer a direction for the debris flow transport of sulphide ore. Making several assumptions about the source and geology of the ore deposits, the authors defined siltstone as a distal clast type and rhyolite, sulphides and barite as proximal clast types. Based on only four sections, they found the ratio decreased down the proposed flow direction (to the west). In other words, the proportion of siltstone clasts increased with respect to rhyolite, sulphide and barite clasts. An unfounded assumption of the erosive ability of debris flows was used to account for the observed results.

In comparing the data of Calhoun and Hutchinson (1981) with the results obtained in this study, only one bed shows a similar systematic change in the clast proportions. In the sulphide matrix ore exposed on 20 level, from east to west the proportion of siltstone clasts increases (Fig. 29). This trend, and those presented by Calhoun and Hutchinson could result from infiltration by a debris flow of a mound of loose siltstone blocks partially obstructing the channel. The siltstone fragments might have been incorporated into a debris flow but, because of the laminar nature of flow, mixing would be slow and most of the siltstone clasts would remain in the snout of the flow. This model to explain the lateral clast variations is highly speculative and the results of the clast counts by Calhoun and Hutchinson could result from spurious sampling of a heterogeneous bed.

In the polylithic breccia-conglomerate and arenaceous conglomerate beds no systematic changes in clast proportions occur vertically, laterally or longitudinally. The methods of Calhoun and Hutchinson appear to be of questionable use in determining the flow direction of the sulphide-bearing debris flows. More positive results are obtained from direct observation of the contacts and sedimentary features of the ore-bearing beds combined with comparisons with modern debris flows.

Clast size distributions within beds

The distribution of clast sizes for individual beds is examined by means of cumulative per cent versus phi (Ø) diagrams. Corrected clast lengths are expressed in phi units, $\emptyset = -\log_2 \frac{d}{d_o}$ where d is the grain diameter (in this case the long diameter d_l) and d_o is the standard grain diameter (1 mm).

The range of sizes examined is $-3\emptyset$ to $-11\emptyset$ as only clasts greater than 1 cm length were measured. To allow for this sampling bias the data are cumulated to the percentage of the unit that contains clasts greater than 1 cm length. For example, if 70 per cent of the unit is matrix then the coarse fraction is cumulated to a total of 30 per cent as the other part of the size distribution was not measured. A source of error inherent in constructing size distributions from wall sections is the measurement of only the apparent maximum dimension of the clasts. In this study all sections compared have similar orientations removing a potential source of error due to anistotropic sediment fabrics.

All size distributions demonstrate the poor sorting and large size of clasts in most beds. Sorting on a diagram of this type is shown by the slope of the line. A theoretical bed of all one grain size would be shown as a vertical line and a bed with an infinite variety of grain sizes would plot as a horizontal line.

Figure 30 illustrates variations in the size distribution of the sediments within and on the margin of the debris flow at 20-13-XC (location A, Fig. 20) 20 level. The size distributions are labelled from the sulphide matrix interior of the flow (1) to the arenaceous conglomerate outside the flow (5). Within the main body of the debris flow (1) the sediment is better sorted than in the other sections. Maximum clast sizes do not exceed $-7\emptyset$ and the total cumulated percentage of clasts greater than $-4\emptyset$ in size is 10 per cent. The dam of coarse bouldery sulphide and lithic detritus flanking the sulphide matrix main body of the flow (2, 3, 4, Fig. 30) is very poorly sorted and contains a greater proportion of coarse detritus with cumulated percentages in the range of 30 to 40 per cent. With greater distance from the interior of the flow the detritus of a given coarse phi size is more abundant. This may reflect the progressive casting out of coarse detritus to the margin of the flow. The results could also be influenced by clast lithologies. Coarse grantitoid and lithic detritus in the boulder dam increase away from the main body of the flow with a corresponding decrease in the percentage of smaller, more dense, sulphide fragments. Although the sulphide clasts are corrected for the density difference, the correction factors are conservative and the diagram may not reflect true hydraulically equivalent clasts. Arenaceous conglomerate flanking the debris flow contains fewer coarse grained clasts than the debris fan but is also poorly sorted. The coarse bouldery debris flow marginal deposits occur at the front and side of the flow.

Data are presented in Figure 31 for the size distribution of clasts in two separate beds. The granitoid clast-rich polylithic breccia-conglomerate and baritic polylithic breccia-conglomerate are the uppermost beds of the lower ore unit over an area exceeding 6000 m^2 of the MacLean Extension Orebody. Both beds are poorly sorted with maximum clast sizes in the baritic polylithic breccia-conglomerate approximately one phi unit less (or clasts twice the size) the clasts in the granitoid clast-rich polylithic breccia-conglomerate. Blatt et al. (1972, p. 161) suggest debris flows on moving downslope show a progressive, though ineffective elimination of coarser materials. This elimination of coarse detritus is not clearly shown by these beds, perhaps due to the limited lateral extent exposed in the underground workings. The length of the largest clast does decrease to the west in both beds. This is not a clear and regular relationship for all phi sizes, as shown by the size distribution for the baritic polylithic breccia-conglomerate at 14W. This section may be closer to the margin of the bed where coarse detritus would accumulate. The lateral heterogeneity within the bed and its marginal deposits may mask any progressive downslope changes, negating the usefulness of size distributions in determining flow directions.

TRANSPORT DIRECTION STUDIES

Several methods were considered for their effectiveness in determining transport directions for the sulphide-bearing debris flows in the MacLean channel. These can be divided into methods providing direct evidence of flow orientation and methods where flow orientations are inferred from calculation or theory.

The most direct evidence of flow orientation is provided by documenting individual debris flow margins. This was possible in parts of the MacLean Extension Orebody and a detailed description of one flow margin was presented in a previous section. The margins of debris flows are recognized by high-angle contacts between debris in the flow and substrate of sedimentary or volcanic rocks and distinctive boulder dam deposits. Within the limited underground exposures complete margins enclosing debris flows cannot be traced. Delineation of entire flow margins would give an absolute direction of flow. However, incomplete exposure requires this flow direction to be inferred. Known debris flow marginal deposits and channels containing discrete flows for the MacLean channel are shown in Figure 32.

On 12 level further direct evidence of a transport direction by preferred clast orientations was noted in the MacLean Orebody. Four distinct episodes of ore deposition occur at this location; the upper three contain elongate siltstone and rhyolite clasts in a matrix of barite, sphalerite, galena and sand-sized lithic detritus. Figure 33 is a plan of the stope wall showing these cycles.

Size distribution and a photograph of a cycle are presented in Figures 27 and 28. Elongate siltstone and rhyolite clasts are aligned parallel with bedding and perhaps more important, have a preferred orientation on bedding surfaces.

Underground, configuration of the walls in the 12 level stope allowed measurement of the long axis trend of 25 clasts (long axis: short axis greater than 3:2) in the second depositional cycle (location 2, Fig. 33). Several oriented specimens

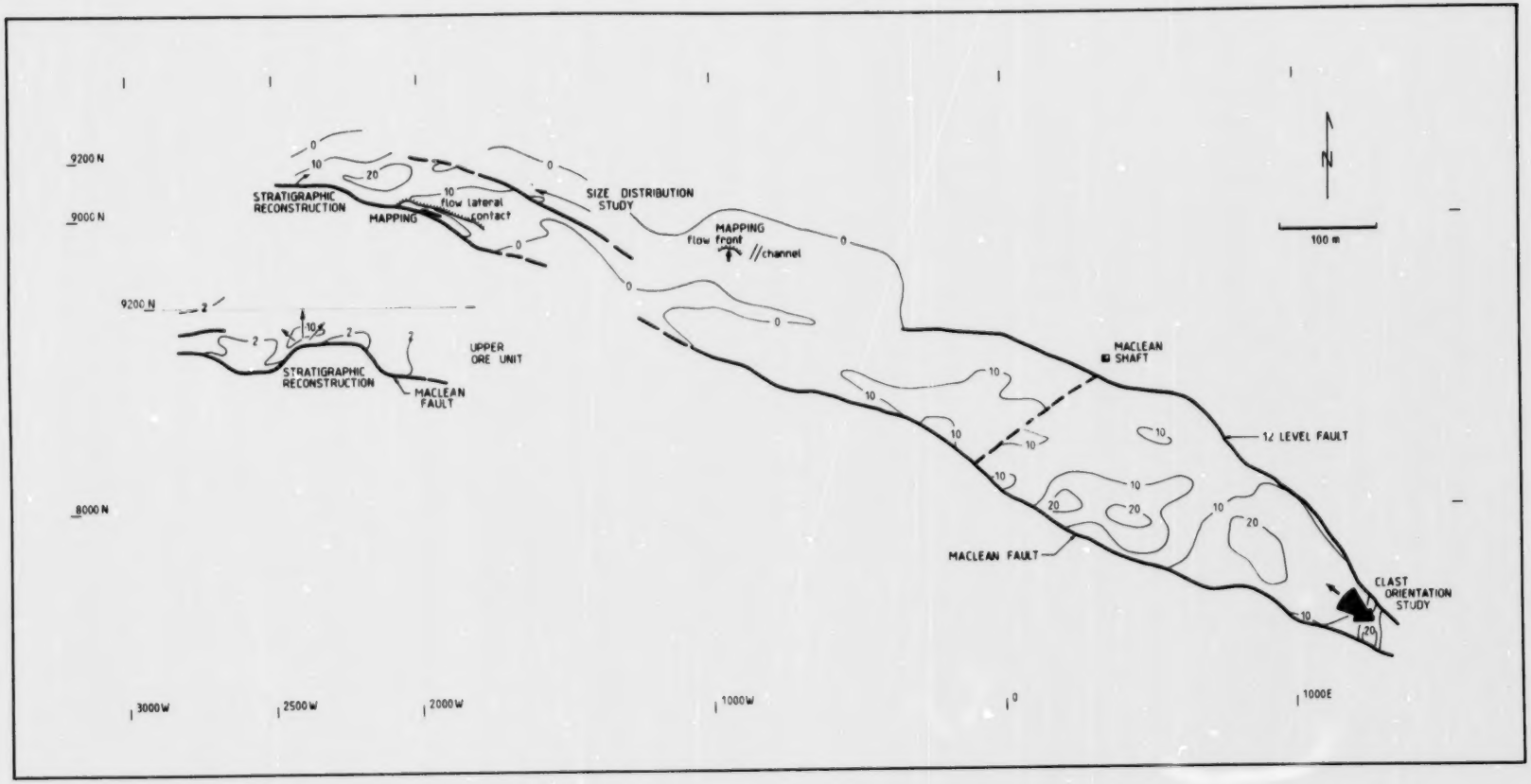

Figure 32. Summary of the transport directions. Method of determination is noted adjacent to the implied transport direction. Double arrows are based on physical features and single arrows are based on facies associations or theoretical considerations. Limited isopach data are presented to convey the shape of the depositional basin. Upper ore unit is offset for clarity.

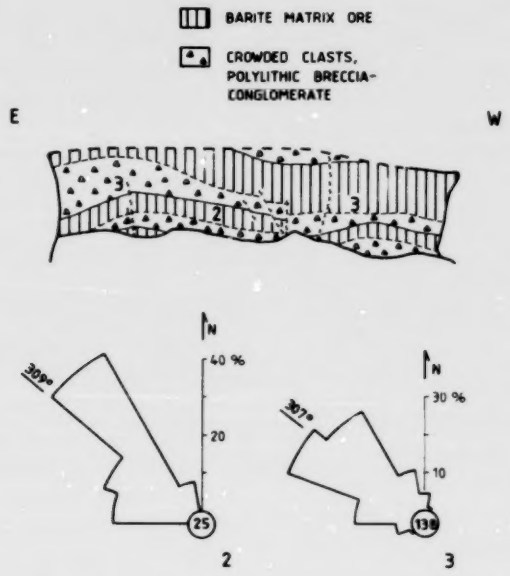

Figure 33. Section along the stope south wall, 12 level, MacLean Orebody, showing cyclic deposition of crowded-clast polylithic breccia-conglomerate and barite matrix ore in the lower ore unit. Rose diagrams illustrate the preferred orientation of elongate clasts in cycles 2 and 3. The number of clast orientations measured in each cycle is shown in the centre of the circle.

were collected from the third cycle for slabbing along bedding planes and measurement of clast orientations (locations 3, Fig. 33).

Results of the orientation study are presented in Figure 33. Within the 95 per cent confidence level and sampling orientation errors of ±2°, all samples show a preferred orientation of clasts to 308°. Only half of each rose diagram is shown. Because of lack of imbrication of clasts, data could also be plotted in the southeast quadrant of the diagram; however regional disposition of lithological units in the MacLean channel indicates flow to the southeast was unlikely.

Cook's (1979) study of gravity flow in Paleozoic continental slope deposits exposed in Nevada determined that clasts whose long dimensions are parallel to bedding also have their long dimension parallel to the paloeflow direction. This result is in accord with model studies of debris flow by Lindsay (1968) who determined that clasts in a flow develop a preferred fabric when the clasts are horizontal and oriented parallel to the flow. Clast orientation data from 12 level, therefore, indicates paleoflow to 308° or along the long axis of the MacLean channel (Fig. 32).

Indirect evidence bearing on the transport direction is based on the property of debris flows to eject coarse material and leave it as boulder lag deposits along the course of the flow. Boulder beds with little included matrix are recognized in the eastern part of the MacLean channel. Changes in size distribution for a polylithic breccia-conglomerate bed in the MacLean Extension Orebody are shown in Figure 25. The coarsest fraction of the bed decreases in size to the west but this relationship is not regular for all clasts sizes due to lateral variations in clast size and the heterogeneous nature of the rock type.

Calhoun and Hutchinson (1981) studied clast proportions in the MacLean ore beds to determine a flow direction. They suggested that erosion of underlying siltstone in the ore sequence by debris flows would cause an increase in the percentage of these clasts downslope. The relationship was developed on examination of four sections from widely separated parts of the MacLean Orebody. The present detailed clast studies have failed to support Calhoun and Hutchinson's methods and results.

Detailed stratigraphic sections of the basin's long axis have been constructed (Figs. 12, 13, 14, 15). These diagrams, based on drill data and underground observations, indicate that most of the sediment fill in the lower ore unit of the MacLean channel was transported to the west. The lithological progression away from the source area and up section of sulphide matrix ore – polylithic breccia-conglomerate – arenaceous conglomerate has been recognized . Exception to the westward transport of sediment include the massive slumped ore, sulphide matrix ore and polylithic breccia-conglomerate in the western end of the MacLean channel (section D'-D, Fig. 15, 32). Isopach maps and the stratigraphic succession in this area indicate sediment transport was from the south or southwest in the western part of the known MacLean channel. Thickness changes indicate a similar source for the upper ore unit (Fig. 32). The results are important, since they suggest another, as yet undiscovered, sulphide source to the south or southwest.

ALTERED LITHIC CLASTS

Altered clasts in the transported ore of the MacLean channel vary from large blocks (in excess of 2 m) of bleached, altered, sulphide-bearing and silicified pillow basalt to small clasts of siltstone with thin, light green alteration rims. Thurlow and Swanson (1981) suggest alteration occurred before transport and was the result of fracturing, permeation and alteration by hydrothermal fluids of autochthonous sedimentary and volcanic rocks. Subsequent violent explosion and/or earthquake broke the rock along small fractures and generated clasts with concentric alteration rims. Fragments that broke across alteration zones yielded clasts having only partial alteration rims (Thurlow and Swanson, 1981).

Siltstone is the most common altered clast type in the MacLean channel. The pale rims of siltstone clasts are depleted in pyrite; the light green colour results from alteration of clay minerals (e.g. Fig. 28).

Stratigraphically, the lowest altered silt clasts observed occur in the siltstone breccia-conglomerate of the ore sequence in the western part of the MacLean channel (sections A, B, Fig. 2). Although greater than 80 per cent of all clasts are siltstone in this unit, only 5 to 15 per cent of them have

alteration rims. This observation suggests that the siltstone clasts in this breccia-conglomerate were not derived from an area of intense hydrothermal activity.

Within the lower ore unit, 25 to 35 per cent of the siltstone clasts have at least partial alteration rims. In some beds up to 80 per cent of the siltstone clasts are altered. Either the clasts in the lower ore unit were derived from a different source area than the clasts in the underlying siltstone breccia-conglomerate, or, the hydrothermal system was more active and encompassed a greater proportion of the source area of the siltstone clasts.

DISTRIBUTION AND TEXTURES OF SULPHIDES AND BARITE

A detailed study of the ore minerals and their intergrowths was beyond the scope of this investigation, however, several features of sedimentological interest were noted in polished and thin sections.

Both sulphides and barite are important ore components at Buchans. Sphalerite, galena, pyrite and chalcopyrite are the principal sulphides and barite, with or without sulphides, is important in the MacLean orebodies.

As discussed previously under rock lithologies, a division occurs between those rocks with sulphides and barite as discrete clasts and rocks where lithic clasts occur in a matrix of sulphides and/or barite. The principal lithological divisions are:

1) Matrix ores:
   a) sulphide-dominant matrix with sphalerite, galena, pyrite, chalcopyrite, minor lithic detritus and barite.
   b) barite-dominant matrix ore with barite, sphalerite, galena, minor calcite and lithic detritus.

2) Breccia-conglomerate
   a) polylithic breccia-conglomerate
   b) sulphide clast-bearing breccia-conglomerate
   c) siltstone breccia-conglomerate

3) Arenaceous conglomerate

In sulphide matrix ore (1a) the dominant feature is wispy, discontinuous layered pyrite and chalcopyrite in relatively massive sphalerite and galena (Fig. 7) The layering comprises either small subhedral pyrite grains or pyrite partly replaced and enclosed by chalcopyrite (Fig. 34). Another type of layering is barite and minor sphalerite, interlayered with massive sulphides (Fig. 35). The layers are typically 0.5 to 1.0 mm thick, although some pyrite-chalcopyrite layers to 1 cm thick have been noted.

Barite matrix ore (1b) differs from sulphide matrix ore (1a) as it contains discrete blocks of sphalerite-galena or pyrite-chalcopyrite in addition to a low content of matrix sulphides.

In breccia-conglomerate (2a, 2b, 2c) and arenaceous conglomerate (3) sulphides occur as clasts in a matrix of sand-sized lithic detritus and pyrite. Although minor amounts of sphalerite and galena occur with the matrix pyrite (Fig. 36), the economic component of the rock is primarily as sulphide clasts. This is in contrast to the sulphide matrix ore with important economic concentrations of sulphides in the matrix. Barite occurs in polylithic breccia-conglomerate and arenaceous conglomerate either as large clasts of barite intergrown with sphalerite and galena, or as discrete single crystal clasts up to several centimetres in length. At a few localities, the latter clasts are rimmed by chlorite, perhaps formed by late reaction of trapped interstitial fluids within the enclosing sediments.

Remnants of lithified sulphide material included in the ore-bearing beds provide information on ore genesis. These sulphide remnants, which occur in the sulphide matrix ore and as sulphide clasts, include colloform pyrite, pyrite overgrowths on sphalerite and granular sphalerite.

Colloform pyrite (Fig. 37) forms a discontinuous 1 to 2 mm thick layer within a sulphide clast. Several broken fragments of a colloform pyrite layer also occur in the same clast.

Pyrite encrustations on sphalerite are fractured and partially replaced by chalcopyrite (Fig. 38). Some pyrite encrustations in this rock specimen of sulphide matrix ore are broken suggesting abrasion during transport of the ore.

In contrast to these two atypical pyrite structures, granular sphalerite occurs in many samples of both clasts and sulphide matrix ore. In polished sections inclusion free, rounded sphalerite grains are rimmed by galena or occur in a matrix of finely intergrown sphalerite-galena. Elongate to equant, transparent sphalerite grains are enclosed by galena, pyrite and barite in some thin sections (Figs. 39 and 40). These textures observed in lithified sulphide fragments are similar to those in stratabound Kuroko-type ores deposited at the sediment-water interface (Lambert and Sato, 1974).

Examples of "pyritic stockwork", which could have been derived from hydrothermal 'feeder' system, occur as clasts in all types of transported ore. Within these clasts, "crushed" pyrite texture is abundant (Fig. 41). Pyrite is fractured and partially replaced by later sulphides, principally chalcopyrite. This texture is found within veins of stockwork fragments and as discrete smaller fragments in the polylithic breccia-conglomerate and arenaceous conglomerate.

Large sulphide clasts in the polylithic breccia-conglomerate are, in some cases, partly rimmed by sphalerite and galena. Individual clasts with coarse grained sulphide intergrowths in their interior may contain 5- to 10 mm-wide margins of similar, but finely intergrown sulphides. Sulphide redistribution in plastically deformed sulphide fragments in polylithic breccia-conglomerate (2a) and sulphide conglomerate (2b) indicate mobilization of sulphides after the clasts formed. The predominant clast type is sphalerite-galena-pyrite. The less abundant pyrite-and chalcopyrite-rich clasts tend to be less deformed. Plastically deformed sulphide clasts have extremely contorted boundaries resulting from loading of lithic clasts and matrix. This plastic behaviour is demonstrated by sulphide clast boundaries protruding be-

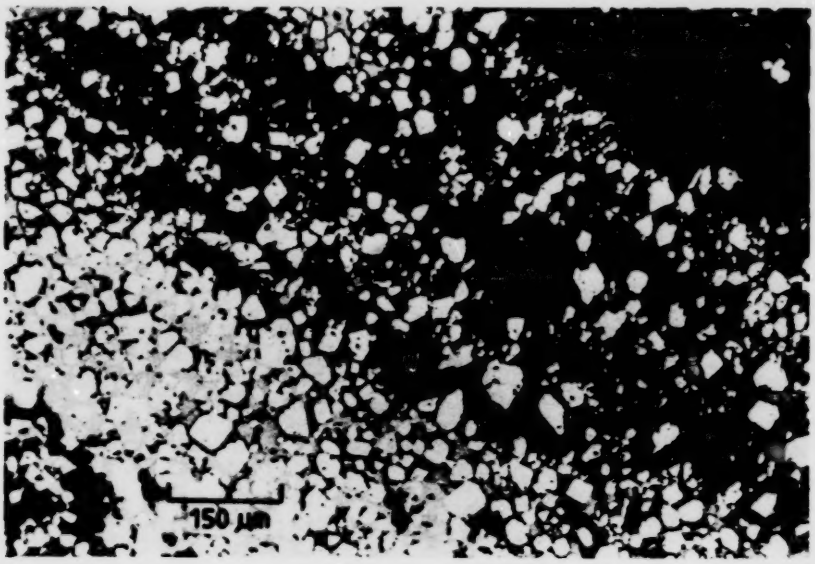

Figure 34. Layers of pyrite grains (white), in places with chalcopyrite (light grey), in a "matrix" of sphalerite (dark grey) and barite (black), Lower ore unit, MacLean Extension Orebody. Reflected light (KQB-82-35).

tween fragments of adjacent lithic detritus (e.g. Fig. 42). These plastically deformed clasts are typical of debris flows overlying sulphide matrix ore. In sulphide matrix ore, poorly lithified clasts were destroyed by the laminar shear of debris flow. Plastically deformed sulphide fragments were adequately lithified to fracture in the source area and be transported as clasts. Truncated barite-calcite veinlets in sulphide clasts predate the transport of the sulphides. The lithification was not complete and after deposition and loading by other detritus some flow of sulphides occurred within the clasts.

In summary, the sulphide clasts and lithic fragments containing sulphides in the transported ore can be identified as being derived from stratabound and stockwork feeder systems of typical volcanogenic, massive sulphide deposits. The state of lithification in the sulphidic sediments in the source area is indicated by the mode of occurrence of sulphides in the transported ore. Sulphide matrix ores were poorly lithified and transport destroyed the original clast boundaries, although a variety of original habits are still observed in the sulphide grains. Plastically deformed sulphide clasts were indurated well enough to survive transport but not loading during deposition. Sulphide clasts in most polylithic breccia-conglomerate were affected principally by brittle failure in the source area and show little, but some, evidence of sulphide redistribution during or immediately after transport.

METAL CONTENTS

The relationship of Cu, Pb, Zn and barite to stratigraphic position was determined for several beds in the MacLean channel. For each bed Cu, Pb and Zn values for each drill intersection were computed from split drill-core assays. The use of drillhole data gives an unbiased sampling of the bed as data is not obtained from a pre-chosen metal-rich area. Cu, Pb

Figure 35. Layers and small masses of barite (light) intercalated with sulphides (black). Remnant of a thin sphalerite bed occurs as a slightly lighter area within the opaque sulphides. Lower ore unit, 17 level, MacLean Orebody. Transmitted light (KQB-82-187).

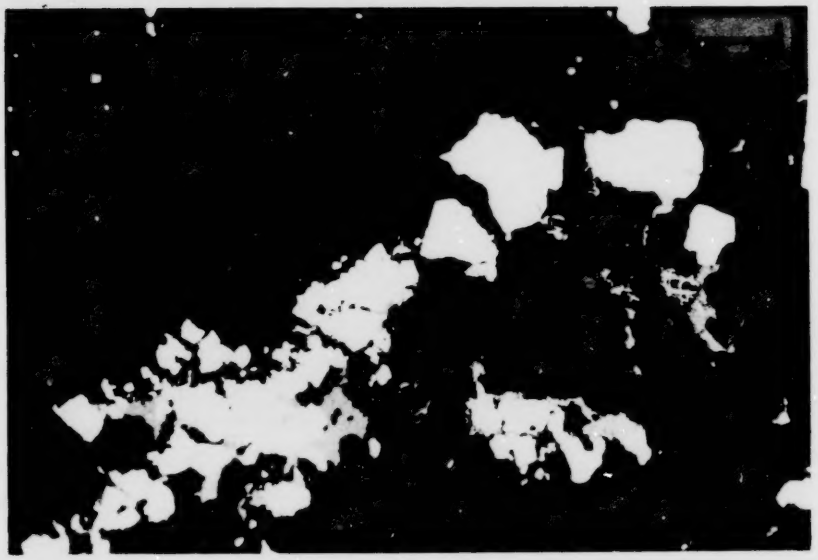

Figure 36. Anhedral grains of pyrite (white) and small masses of sphalerite (grey) and chalcopyrite (rough, grey) in the lithic matrix of a polylithic breccia-conglomerate. Lower ore unit, MacLean Extension Orebody. Reflected light (KQB-82-135).

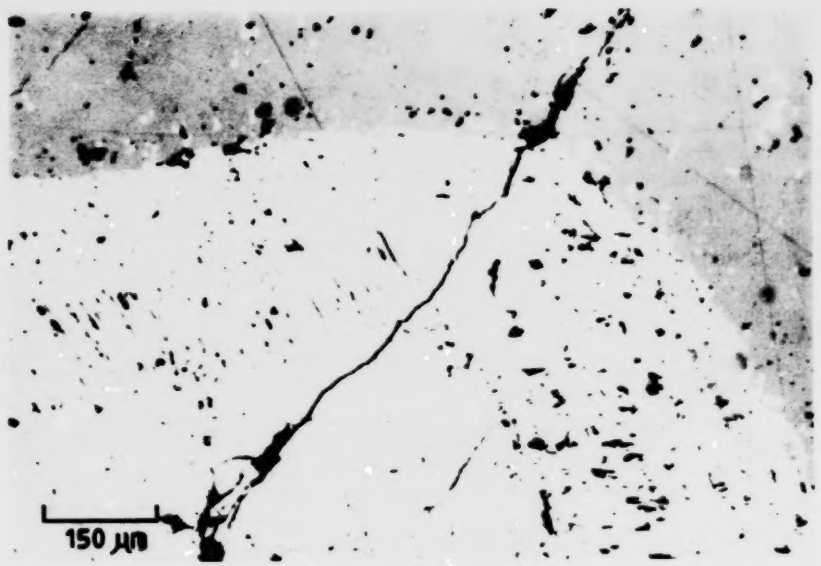

Figure 37. Detailed view of the margin of a colloform pyrite layer. Small intergrown layers of chalcopyrite occur with the pyrite. The layer occurs within a sulphide clast in a polylithic breccia-conglomerate. Lower ore unit, MacLean Extension Orebody. Reflected light (KQB-82-99).

and Zn were chosen for this investigation, as they are well above the detection limits of assay methods used at Buchans. Values for the barite content of beds were estimated from examination of drill core and underground exposures.

For each bed the total metal content (Cu + Pb + Zn), the estimated barite content and the range of values for the Cu/(Pb + Zn) ratio are presented in Figure 43. The beds are plotted in a generalized schematic stratigraphic succession.

The massive slumped ore at the west end of the MacLean channel in the MacLean Extension Orebody is plotted at the base of the figure. This bed is thought to be a slumped portion of an in situ orebody and is not directly comparable with other transported ore observed in the MacLean channel which contains admixed lithic detritus. At the base of the section, above the slumped ore, is polylithic breccia-conglomerate from the MacLean Orebody. This bed contains minor barite and less than 10 per cent combined

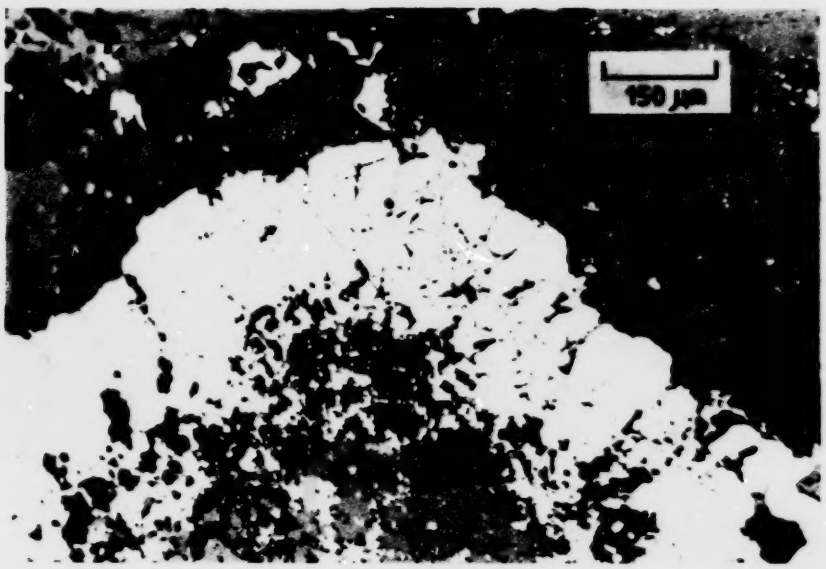

Figure 38. Encrustation of pyrite (white) broken and partly replaced by chalcopyrite (light grey) surrounding and enclosed by sphalerite (dark grey). Note the inclusion-free, enclosing sphalerite compared to the encrusted area. Sulphide matrix ore, lower ore unit, MacLean Extension Orebody. Reflected light (KQB-82-14).

Figure 39. Approximately equant grains of sphalerite (medium grey) enclosed by galena, pyrite (black) and barite (white). Some grains are cut by discontinuous barite veinlets. Lower ore unit, 17 level, MacLean Orebody. Transmitted light (KQB-82-187).

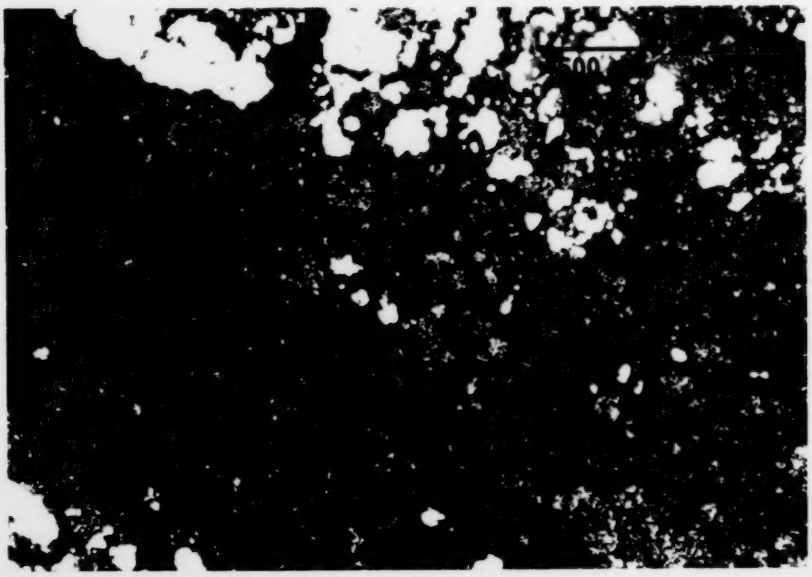

Figure 40. Rounded small grains of sphalerite (medium grey) in an opaque matrix of galena and minor pyrite (black). Small masses of barite (white) border and are intergrown with the granular sphalerite. Sulphide matrix ore, MacLean Extension Orebody. Transmitted light (KQB-82-9).

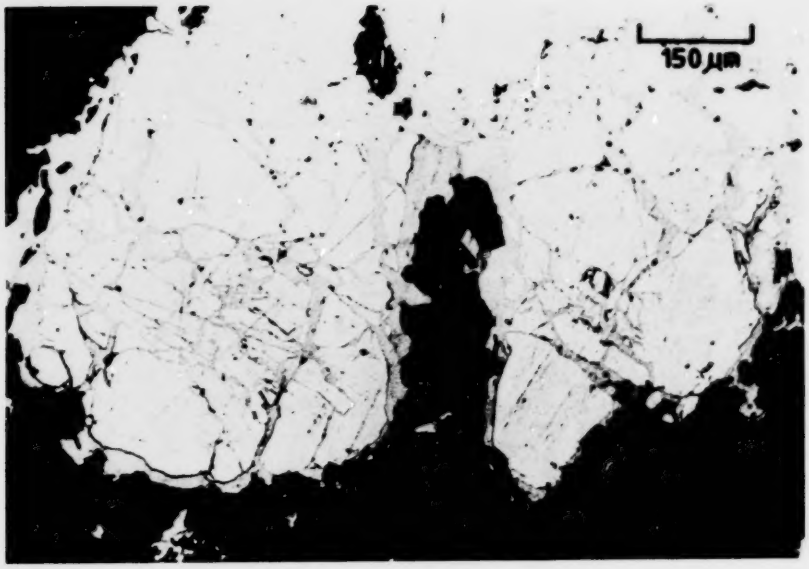

Figure 41. Highly fractured pyrite (white) veined and partially replaced by chalcopyrite (grey) in a clast in polylithic breccia-conglomerate, Lower ore unit, MacLean Extension Orebody. Reflected light (KQB-82-80).

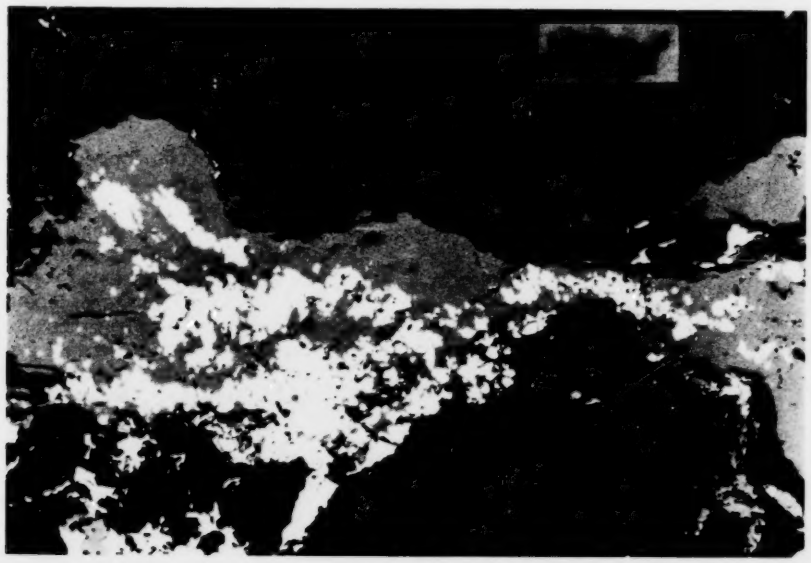

Figure 42. Extremity of a plastically deformed sulphide fragment of sphalerite (medium grey) with chalcopyrite (light grey) and pyrite (white) between lithic detritus (dark grey) which bounds the clast. Lower ore unit, MacLean Extension Orebody. Reflected light (KQB-82-23B).

Cu + Pb + Zn. High grade sulphide matrix ore overlies the polylithic breccia-conglomerate in the MacLean Orebody and extends into the MacLean Extension Orebody where it forms the basal beds of the lower ore unit at some locations. The total metal content of sulphide matrix ore is in excess of 30 per cent Cu + Pb + Zn. The metal content decreases up section with the transition to polylithic breccia-conglomerate and arenaceous conglomerate where sulphides occur principally in clasts. Polylithic breccia-conglomerate typically contains from 5 to 15 per cent Cu + Pb + Zn with the uppermost beds slightly lower grade than the beds immediately overlying sulphide matrix ore. The lowest grade sulphides occur in arenaceous conglomerate with Cu + Pb + Zn typically less than 5 per cent. Barite content of ore-bearing beds is variable, but a general trend to higher barite content within the uppermost ore beds was noted. High barite content occurs in massive barite matrix ore capping the MacLean Orebody, baritic polylithic breccia-conglomerate of the upper bed of the lower ore unit in the MacLean Extension area, and barite matrix ore forming much of the upper ore unit in the MacLean Extension area.

For the stratigraphic units outlined above, the Cu/(Pb + Zn) ratio has been calculated. Massive sulphide orebodies of the Kuroko-type, with which Buchans has been compared (Thurlow and Swanson, 1981), have copper-rich bases and lead- zinc rich tops (Lambert and Sato, 1974). Thus, in an in situ massive sulphide Kuroko deposit, the Cu/(Pb + Zn) ratio would be expected to decrease to the top of the orebody.

In Figure 43 the mean ratios of Cu to Pb + Zn are remarkably constant throughout the lower and upper ore units despite wide variation in ore grade. The mean values are between 0.04 and 0.10 and values for individual drill sections do not fall below 0.025. Sulphide and barite matrix ore are in the range of 0.025 to 0.08 Cu/(Pb + Zn). For stratigraphically higher base metal-bearing beds the mean value of the ratio does not deviate widely but the range of values is greater. This range is probably due to the bouldery nature of the sulphides, with some drillholes cutting more, or larger, copper-rich boulders while others cut lead-zinc-rich detritus.

Variations in base metal and barite contents and ratios indicate that the ore beds were eroded from a heterogeneous source area with Cu, Pb-Zn- and barite-rich areas. In initial debris flows unconsolidated ore detritus was more homogenized than later flows with more ore fragments. An increase in the barite content in later flows indicates that the hydrothermal source areas probably remained active throughout transport and deposition of the transported ore beds.

The only exception to the metal ratio trends is the massive slumped ore in the western part of the MacLean Extension Orebody (Fig. 15, 43). This ore has a combined Cu + Pb + Zn grade in excess of 30 per cent but the ratio of Cu to Pb + Zn is variable and higher than typical MacLean channel transported ores. In absolute amounts the copper content of this bed locally exceeds 10 per cent over 3 m. The high copper content suggests that one particular portion of the source orebody may have been sampled by the slump. No mixing of sulphide fragments occurred in this area and, as the drill core and ore grade indicate, the sulphides were not diluted by barren lithic detritus.

SYNTHESIS AND OVERVIEW

This section reviews the data and suggests transport mechanisms and directions of fragmental ores in the MacLean channel. Some physical parameters of the ore-bearing beds are estimated and some physical features of the depositional basin are inferred.

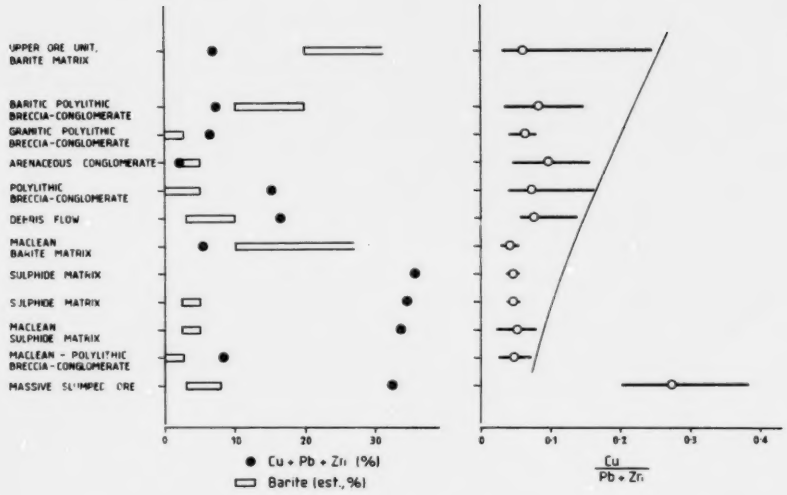

Figure 43. Total copper, lead and zinc content (solid circles), estimated barite content (open bars) and copper to lead plus zinc ratio for selected beds in the lower and upper ore units, MacLean and MacLean Extension areas. Average metal ratios (open circles) and range of metal ratios (solid bars) are shown on the right graph. The curved line represents the maximum metal ratio. All analyses by Asarco Inc. at Buchans.

Transport and deposition

The bouldery nature of the ore in the lower and upper ore units of the MacLean channel, sulphide clasts in a lithic matrix and lithic clasts in a sulphide matrix, and the lack of any underlying stockwork sulphides – alteration zones indicate clearly that the ore beds resulted from transport of sulphide and lithic detritus from distant, external sources. A subtle balance of ore deposition and mass wastage near hydrothermal vents were probably important factors in determining physical characteristics of the ore beds.

Mass wastage phenomena could have included rock falls, landslides and subaqueous sedimentary gravity flows including turbidity currents, fluidized flows, liquified flows, grain flows and debris flows (terminology of Nardin *et al.*, 1979). Previous authors (Thurlow, 1977; Walker and Barbour, 1981; Thurlow and Swanson, 1981 and Calhoun and Hutchinson, 1981), favoured subaqueous sedimentary gravity flows, particularly debris flows, as the mechanism of transport of the detrital ore beds.

Data from the current study indicates the complexity of the basin filling processes for the lower and upper ore units. Concurrent with the conclusions of previous authors, debris flows were probably the dominant transport mechanism but high and normal density turbidity currents and landslide or slump deposits were also involved.

Features of the ore beds in the MacLean channel that indicate debris flow transport are the angularity and extremely poor sorting of the sediment, random internal fabric of most beds and variable nature of both the clast percentages and matrices of the ore beds. Inverse grading occurs at the base of some beds. These features occur in both sulphide matrix ore and polylithic breccia-conglomerate and are indicative of non-turbulent flow in material with high matrix strength. Direct evidence of the matrix strength diagnostic of debris flows is the suspension of large boulders in a matrix of fine grained debris and the blunt, meniscus-shaped terminations of flows. Boulder dams, the coarse deposits which border debris flows, were recognized at several localities in the MacLean channel and are described in detail in this report. These features are preserved by the en masse deposition of the debris flow by 'freezing' in the channel.

As a result of their slow, laminar flow, debris flows do not actively erode their substrate throughout most of their course. In the MacLean channel no direct evidence was observed for extensive scouring at the base of flows. Locally, the flows were deposited on poorly lithified felsic tuff and irregular contacts developed due to loading. Laminar shear throughout the mass of the flow is indicated in the sulphide matrix ore where elongate discontinuous areas of pure sphalerite-galena or pyrite-chalcopyrite coexist with lithic-rich layers. Laminar shear transport of incompletely lithified, hydrothermally precipitated sediments (i.e. sulphides and barite) resulted in obliteration of clast boundaries and development of crude discontinuous layering during flow.

Polylithic breccia-conglomerates contain discrete clasts of sulphides which underwent brittle fracture in the source area and remained coherent clasts during transport and deposition.

An enigmatic feature of the ore beds in the MacLean channel is the presence of granitoid clasts (Stewart, 1983, 1987). They are the only clast type that occurs in the ore unit but is not found in autochtonous rocks in any potential source area. These coarse grained, well-rounded clasts were deposited preferentially at the margins of debris flows, although finer grained granitoid detritus was observed in all ore beds. The presence of coarse grained granitoid detritus in the debris flows suggests that the process that produced the granitoid clasts could have triggered the debris flows, e.g. explosive volcanic eruptions (e.g. Stewart, 1987).

Not all sediment transport into the MacLean channel was by debris flows. On 12 level, at the east end of the exposed MacLean channel, several beds of barite matrix ore exhibit

both density sorting in the matrix and sorting of clasts by size. Individual beds are thick and contain coarse grained lithic and lesser sulphide detritus. Each bed is underlain by coarse grained unsorted detritus with little matrix. Grain interaction, escaping pore fluid and fluid turbulence are the sediment support mechanisms which result in particle size segregation. Lowe (1979) suggested the term 'high-density turbidity current' for flows which originate as Bingham plastic substances but involve fluid turbulence. The section on 12 level could represent deposits from debris flows which became turbulent with the addition of interstitial water, deposited the coarse sediment as an unsorted lag, and subsequently deposited sorted clasts from a high-density turbidity current.

In turbidity currents (low-density turbidity currents of Lowe, 1979) the primary sediment support mechanism is the upward component of fluid turbulence. Features of turbidity current deposits include sole marks, load structures, graded beds, plane lamination and ripple cross lamination. Hampton (1972) developed a mathematical model for the generation of turbidity currents by debris flows. In the upper ore unit grading of barite clasts in sandy sediments overlying the first cycle of ore deposition indicates local turbulence in sand- and fine pebble-sized detritus resulting from the debris flow emplacement of barite matrix ore. Within the lower ore unit local graded beds in arenaceous conglomerate suggest fluid turbulence as a method of transport for some sandy sediments. Despite this evidence for local turbidity current deposition, no evidence was observed for extensive turbidity current deposits in ore units in the MacLean channel.

Arenaceous conglomerate flanking the debris flow boulder dams shows a measure of matrix strength but was not deposited directly by the debris flow process. Grain flows or fluidized flow are more likely processes for the local transport of this sandy sediment away from the flow.

Elastic failure results in slump and slide deposits with shear failure on discrete planes and little internal deformation of the sediment mass. In the MacLean channel at 2400W a deposit is recognized which is termed massive slumped ore (Fig. 15). By November, 1983 (the last field studies for this report) insufficient exposures existed to assess the degree of bedding disturbance in this deposit. Limited exposures and drill-core data indicate that the ore was a massive accumulation of pyrite, chalcopyrite, sphalerite, galena and barite with no admixed lithic detritus. Metal ratios for the ore are atypical with a very high copper content relative to lead and zinc. The tnick lens-shaped body was deposited on unaltered volcanic and sedimentary rocks of the MacLean channel basin fill sequence and was bounded to the south by the main MacLean Fault and the west by the original north wall of the MacLean channel. Sulphide matrix ore and polylithic breccia-conglomerate overlie the ore lens to the north and east.

The siltstone unit of the ore sequence which underlies the lower ore unit was also deposited by sedimentary gravity flows. In the eastern part of the MacLean channel and extending beneath the Rothermere and Lucky Strike orebodies, the siltstone unit comprises siltstone and fine grained sandstone with plane lamination, ripple-drift cross-lamination, graded beds and deformed loaded contacts providing evidence of turbidity current deposition (Fig. 4). Further west, underlying the MacLean Extension Orebody, no autochthonous siltstone was observed and the unit includes pebble- to boulder-sized siltstone, altered siltstone and minor rhyolite detritus in a silty to tuffaceous matrix. The poor sorting and angularity of detritus in the siltstone breccia-conglomerate beds indicates debris flow transport. Thin beds of brecciated siltstone occur at the top of the siltstone unit in the MacLean Orebody.

In the east the siltstone was deposited, and at least in part lithified, in a basin with its western limit to the east of the MacLean Extension area. Synsedimentary tilting resulted in disruption of the autochthonous siltstone and debris flow transport of siltstone breccia-conglomerate to the west into the newly formed basin in the MacLean Extension area. This slope reversal preceeded the major episode of transported ore deposition in the MacLean and MacLean Extension areas.

The direction of transport for the sedimentary gravity flows and slumps that fill the MacLean channel result from the interaction of gravity acting on the sediment and basinal slopes and walls at the time of deposition. Transport directions are not necessarily a reflection of the source area for the ore as a flow, once 'captured', will continue to move downslope along the axis of the channel. For the orebodies under consideration, the primary flow direction was from east to west in the main MacLean channel with minor flow to the north, probably due to plugging of the main channel by debris. In the extreme western end of the exposed MacLean channel, ore transport, at least locally, was probably from the south or southwest.

Some physical parameters of debris flows

Estimates of some physical parameters of the debris flows in the MacLean channel were calculated by Binney (1984). The methods of calculation and additional results are presented and alternative transport mechanisms for some coarse clasts in the upper ore unit are suggested.

The yield strength (k) of debris in critical equilibrium is estimated by measurement of the thickness (c) of coarse boulders supported in the debris flow. Variables include the unit weight (density·acceleration of gravity) of the debris flow (δd) and the block (δb) and the depth of penetration of the block into the flow (1/n).

$$K \approx \frac{c}{4}\left(\gamma b - \frac{\gamma d}{n}\right) \quad (1)$$ (Johnson, 1970, p. 486-490)

With all units expressed in kg, m, sec, the resultant value for the yield strength (k) of the debris flow is in $N.m^{-2}$ where $1N = 1\ kg.m.sec^{-2}$.

The relationship between the yield strength of the debris in critical equilibrium (k), the slope (δ), the thickness of the flow (τ_c) and the unit weight of the debris (γd) is:

$$K = \tau_c\ \gamma d \sin \delta \quad (2)$$ (Johnson, 1970, p. 488)

The estimated yield strength (k) from equation 1 can be used to calculate the paleoslope.

Binney (1984) calculated estimated yield strengths of 1.0 to 1.5 $\times$ 10^3 $N.m^{-2}$ for a baritic polylithic breccia-conglomerate bed and 9 $\times$ 10^3 $N.m^{-2}$ for extremely coarse detritus in another polylithic breccia-conglomerate bed. These estimated yield strengths are related to calculated slopes of 3 degrees for the baritic polylithic breccia-conglomerate and approximately 11 degrees for the other polylithic breccia-conglomerate.

Further estimates of both yield strength and paleoslope have been calculated and are presented in Table I. At the base of the ore sequence in the MacLean Extension area is siltstone breccia-conglomerate with beds comprising large angular siltstone blocks in a sandy to tuffaceous matrix. For this unit which only locally contains sulphide blocks and predates the major ore beds, a flow density of 2.0 $\times$ 10^3 $kg.m^{-3}$ is assumed. The calculated yield strength of the debris flow is 1.9 $\times$ 10^3 $N.m^{-2}$ and the critical slope needed for flow is 3 degrees. The yield strength and slope needed for flow are consistent with data calculated for the stratigraphically younger, lower and upper ore units.

Most debris flow deposits in the upper and lower ore units of the MacLean Extension Orebody give calculated yield strengths of 1.0 to 4.0 $\times$ 10^3 $N.m^{-2}$ with slopes of less than 6 degrees needed for flow. No consistent lateral or vertical trends are observed in the calculated slopes, although the baritic polylithic breccia-conglomerate needed slightly lower slopes for flow than the underlying debris flow deposits. The limited lateral exposures of individual beds and the approximate nature of the calculations limit study of lateral slope variations within beds.

The debris flow exposed in sublevel 20-6-1 gives high calculated slopes of 11 degrees. Detailed mapping of the sublevel indicated flow was to the north at this location and present measured slopes flatten from 12 to 15 degrees to less than 5 degrees within the sublevel. Deposition of the beds occurred at the base of a steep slope. Calculated data support this interpretation and suggest that the present attitudes are a reflection of the paleotopography.

Data for the sulphide matrix ore are inconsistent with calculated paleoslopes for both the underlying and overlying beds. The sulphide matrix ore does not contain large lithic clasts. In the MacLean Orebody the paleoslopes would have had to exceed 10 to 15 degrees to allow for transport through this area of the coarse grained sediments found in the MacLean Extension Orebody. Binney (1984) calculated the yield strength of a sulphide matrix debris flow on a 10 degree slope. The yield strength, 4 $\times$ 10^4 $N.m^{-2}$, is an order of magnitude higher than polylithic breccia-conglomerate debris flow deposits in the MacLean Extension Orebody.

Inconsistency of the calculated slopes, potential for boulder transport and known size distribution of material in the sulphide matrix ore all indicate that these ores are not adequately described by Johnson's model for debris flow. The flow density may be well in excess of 2.4 $\times$ 10^3 $kg.m^{-3}$ and considering admixed water with the sulphide detritus, the density is more likely to be 3.2 $\times$ 10^3 $kg.m^{-3}$. This density would result in buoyant forces acting on the lithic detritus. The damping effect of the high density sulphide matrix would aid in trapping the lithic clasts within the flow. Laminar shearing within the sulphide mass also aids retention of the lithic detritus in the flow. The fabric of the sulphide matrix ore is consistent with pervasive laminar shear of the sediment during flow. The mass, behaving like a plastic, is described by Johnson's second equation ($k = \tau_c \gamma d \sin \delta$).

Table I. Calculated yield strength and paleoslope for some debris flow deposits in the ore sequence, MacLean channel

Unit	location	yield strength k ($N.m^{-2}$)	slope (°)
upper ore unit	2400W	3.5×10^3	4
		3.1×10^3	4
	2600W	1.1×10^3	4
		2.6×10^3	8
lower ore unit			
baritic polylithic	1350W	1.5×10^3	3
breccia-conglomerate	1400W	1.6×10^3	4
	1600W	1.2×10^3	2
granitic polylithic	1350W	2.0×10^3	5
breccia-conglomerate	1400W	0.9×10^3	5
debris flow,	1800W	2.6×10^3	6
south channel	2000W	3.7×10^3	4
debris flow,	1000W	9.0×10^3	11
sublevel 20-6-1		7.5×10^3	11
sulphide matrix ore	200E	0.8×10^2	< 1
	1700W	0.3×10^3	< 1
siltstone unit			
siltstone breccia-conglomerate	3000W	1.9×10^3	3

A revised estimate of the shear stress needed to cause movement can be calculated using a flow density of 3.2×10^3 kg.,$^{-3}$:

$$k = (10m)(3.2 \times 10^3 kg.m^{-3})(9.8m.sec^{-2}) \sin 10° = 5 \times 10^4 N.m^{-2}$$

With the high internal yield strength, the sulphide matrix ore would freeze on much steeper slopes than the lithic-rich flows which predominate in the MacLean Extension Orebody. Deposition can occur by a decrease in slope, by a decrease in thickness of the flow or by entrapment behind a boulder dam.

Upper ore unit calculations, based on measurement of coarse blocks of detritus in both ore depositional cycles, give consistent slopes of 4 degrees for deposition of the barite matrix ore. An exception to the calculated results is a coarse block of sphalerite-galena ore located at the base of the upper ore bed (Fig. 19). This block gives an estimated yield strength for the debris flow of 2.6×10^3 N.m^{-2} and a calculated slope of 8 degrees, double the result from the other clasts and a slope inconsistent with observed geology. These calculated results indicate an additional undefined mechanism of clast movement was operative in the barite matrix ore of the upper ore unit.

Shield's diagram may be used to calculate the shear stress and velocity of the fluid needed to move a given diameter sphere as bed load (Blatt *et al.*, 1972). Considering the sphalerite-galena block in the upper ore unit, the parameters for using Shield's diagram include; fragment diameter (d_s) 0.5 m, fragment density 5.4×10^3 kg.m^{-3} and flow density (assumed) 2.4×10^3 kg.m^{-3}. The kinematic viscosity (dynamic viscosity/density) is assumed to be 0.04 m^2.sec^{-1} as calculated from a dynamic viscosity of approximately 10^2 N.sec.m^{-2} for naturally occurring subaerial flows (Johnson, 1970, p. 513) and a density of 2.4×10^3 kg.m^{-3}. The resultant shear stress from Shield's diagram (Blatt *et al.*, 1972, p. 91) is 1×10^3 N.m^{-2} and the bed velocity of the flow is 0.5 m.sec^{-1}. The boundary Reynolds number is 6, indicating laminar flow in the boundary layer, consistent with debris flow conditions. The value for shear stress is in close agreement with other data for the yield strength (equals shear stress at critical equilibrium) for the upper ore unit at this location (Table I). Velocities at the bed of 0.5 m.sec^{-1} are within the range of measured average velocities of subaerial flows by Johnson (1970, p. 512) (1 m.sec^{-1}) and Sharp and Nobles (1953) (0.3 to 4.4 m.sec^{-1}). These velocities indicate that the debris flows filling the MacLean channel were instantaneous events in the geological history of the basin.

These results suggest that some coarse detritus in the upper ore unit, initially transported by the matrix strength of the debris flow, was rolled along the substrate as the slope and competency of the flow decreased.

In summary, calculation of some physical parameters of MacLean channel debris flows has allowed testing of observed geological features against a model for transport. Results of the calculations indicate the non-ideal behaviour of some dense sulphide matrix ore and the multiple transport mechanisms possible for some coarse detritus in the flows.

Ore deposition in the MacLean channel

Models for the deposition of the massive sulphide and transported sulphide ores at Buchans have been suggested by Walker and Barbour (1981), Thurlow and Swanson (1981), Henley and Thornley (1981) and Hutchinson (1981). The present study was too limited in scope to develop a complete model for the ore-forming process; however specific features that bear on genesis of transported ores in the MacLean channel will be reviewed.

The MacLean and MacLean Extension orebodies occur in a fault-bounded remnant of the MacLean channel. The Rothermere and Lucky Strike transported ore beds were probably also deposited in the MacLean channel but with an incomplete understanding of later thrust faults bounding the overbodies (e.g. Thurlow ans Swanson, 1987) details of correlations or orebodies are not well understood.

Stratigraphy and lithology of the rocks in the ore sequence suggest that deposition of the siltstone unit (Fig. 2) may mark the formation of the MacLean channel. In situ siltstone underlying the MacLean, Rothermere and Lucky Strike orebodies was deposited from turbidity currents in a basin centred east of the study area. A reversal in slope following deposition of the in situ siltstone permitted siltstone breccia-conglomerate debris flows to move from east to west into the newly formed MacLean channel.

The aerial distribution of felsic crystal-lithic tuff overlying the siltstone unit is unknown, however, the tuff pinches out to the east and thins to the west (Fig. 2). The area of thick tuff deposits at the east end of the MacLean Extension Orebody may have been a basinal depression or a slope change where the subaqueous tuffs were deposited preferentially.

The provenance and distribution of the lower and upper ore units is better understood than the surrounding rocks since mine records, mapping and drill core were available in addition to information gathered in this study. Stratigraphic reconstruction, clast orientations and debris flow mapping have indicated at least two sources of sulphide, barite and lithic detritus. Most transported ore in the study area was deposited by westward moving debris flows. A small proportion of transported ore in the extreme western end of the MacLean Extension Orebody was derived from the south and southwest. Multiple sulphide sources may exist for each of these transport directions as gravity driven mass wastage phenomena like debris flows will, once captured by an elongate sloping depression, tend to flow along its length. The sulphide-bearing debris flows stopped when decreasing slopes would not provide sufficient gravitational force to overcome either the flow's internal shear strength or the shear strength of a boulder dam containing the flow.

At the close of the main episode of sulphide transport which deposited the lower ore unit, the MacLean channel was blanketed by felsic crystal and lithic tuff. The thickness and distribution of these tuffs are unknown.

Instability in the hydrothermal source areas continued later in the west or southwest and two barite-rich debris flows

formed the upper ore unit (Fig. 32). The lower, narrow part of the channel had been filled at this time and the upper ore unit extends across a broad area outside the known limits of the lower ore unit (Fig. 11).

Exploration guidelines

Effective geological exploration for transported ore is aided by an understanding of the mass wastage phenomena responsible for the downslope transport of sulphide and barite detritus. In the MacLean channel transport processes include slumps, debris flows and high density turbidity currents. Low density turbidity currents transported silt-, sand- and fine pebble-sized lithic detritus into a basin (channel) but were not responsible for transport of ore-grade sulphide material. The transport of sulphides away from volcanic centres by turbidity currents has been reported for Kuroko deposits (Kajiwara, 1970; Ito *et al.*, 1974). Thus, a complete range of subaqueous sediment gravity flow processes may reconcentrate sulphide and barite detritus into viable "transported ore deposits".

Transport processes result in progressive mechanical deformation, destruction and reworking of original ore material. This produces a range of deposit lithologies which can be crudely related to the proximity of the transported ore to its source deposit. Massive slumped ore involves en masse movement of sulphides or barite down a steep slope with some internal disturbance of bedding but no incorporation of lithic detritus. These deposits should be in close proximity and directly downslope of their source area. Both sulphide matrix ore and polylithic breccia-conglomerate result from debris flow transport of sulphides and can be found in excess of 1 km from their source area. In sulphide matrix ore, laminar shear during flow destroys the identity of individual, poorly lithified sulphide fragments. Lithic detritus is dispersed in the sulphide matrix. In polylithic breccia-conglomerate sulphides occur as discrete clasts.

Coarse bouldery breccia-conglomerate is found on the margins of some debris flows. At Buchans these debris flow margins represent grade boundaries between economic sulphides within the flow and low-grade, subeconomic arenaceous conglomerate adjacent to the flow. Mapping of the marginal deposits helps define high grade ore and indicates the direction of flow, a critical parameter in exploration for other deposits of both transported and in situ ore.

Paleotopography influences the shape and distribution of the transported orebodies. If broad basinal depressions with low slopes exist adjacent to a hydrothermal source, transported ore may form relatively thick accumulations of sediment that taper off gently over an extensive area. Insufficient relief would inhibit transport by debris flows and the transported ore would build into a mound until the slope of the mound was steep enough to allow flow further from the source. In channels with moderate to steep internal slopes, like the MacLean channel, individual flows can originate along the margins of the depression and once 'captured' by it, flow along the length. Therefore, in searching for in situ sources for the transported ore, the sides as well as the ends of channels should be explored.

Individual debris flows, because of their matrix strength, do not fill the entire channel. Several juxtaposed, overlapping flows will fill the channel. Therefore, isopach maps of ore unit thickness can be used to indicate the extent and nature of the channel at the time of ore emplacement.

Debris flows freeze in position when the slope decreases and the shear stress, due to gravity, cannot overcome the internal strength of the debris or the strength of a confining boulder dam. Measurements of the course blocks in a debris flow deposit (breccia-conglomerate) allow calculation of the approximate paleoslope. A decrease in the paleoslope may result in deposition of concentrations of sulphide detritus. An increase in paleoslope will result in non-deposition of debris flows until another basin is encountered. Thus, one orebody can be "drilled off" only to have another related orebody discovered further down the paleoslope.

In summary, geological exploration for transported and related in situ ore will be most effective when detailed sedimentological studies are used to determine the shape of the depositional basin, transport processes, flow directions and paleoslope. All of these factors determine the size, shape and grade of the transported ore deposit and suggest areas of potential for the discovery of in situ deposits.

REFERENCES

Binney, W.P.
1984: Estimation of physical parameters of MacLean channel sulphide-bearing debris flows, Buchans, Newfoundland; in Current Research, Part A, Geological Survey of Canada, Paper 84-1A, p. 495-498.

Binney, W.P., Thurlow, J.G. and Swanson, E.A.
1983: The MacLean Extension orebody, Buchans, Newfoundland; in Current Research, Part A, Geological Survey of Canada, Paper 83-1A, p. 313-319.

Blatt, H., Middleton, G. and Murray, R.
1972: Origin of Sedimentary Rocks; Prentice-Hall Inc., Englewood Cliffs, New Jersey, 634 p.

Calhoun, T.A. and Hutchinson, R.W.
1981: Determination of flow direction and source of fragmental sulphides, Clementine deposit, Buchans, Newfoundland; in The Buchans Orebodies: Fifty Years of Geology and Mining, ed. E.A. Swanson, D.F. Strong and J.G. Thurlow; Geological Association of Canada, Special Paper 22, p. 187-204.

Cook, H.E.
1979: Ancient continental slope sequences and their value in understanding modern slope development; Society of Economic Paleontologists and Mineralogists, Special Publication 27, p. 287-305.

Fisher, R.V.
1971: Features of coarse-grained, high-concentration fluids and their deposits; Journal of Sedimentary Petrology, v. 41, p. 916-927.

Hampton, M.A.
1972: The role of subaqueous debris flow in generating turbidity currents; Journal of Sedimentary Petrology, v. 42, p. 775-793.

Henley, R.W. and Thornley, P.
1981: Low grade metamorphism and the geothermal environment of massive sulphide formation, Buchans, Newfoundland; in The Buchans Orebodies: Fifty Years of Geology and Mining, ed. E.A. Swanson, D.F. Strong and J.G. Thurlow; Geological Association of Canada, Special Paper 22, p. 187-204.

Hutchinson, R.W.
1981: A synthesis and overview of Buchans geology: in The Buchans Orebodies: Fifty Years of Geology and Mining, ed. E.A. Swanson, D.F. Strong and J.G. Thurlow; Geological Association of Canada, Special Paper 22, p. 325-350.

Ito, T., Takahashi, T. and Omori, T.
1974: Submarine volcanic-sedimentary features in the Matsumine Kuroko deposits, Hanaoka mine, Japan; Society Mining Geologists Japan, Special Issue 6, p. 115-131.

Johnson, A.M.
1970: Physical Processes in Geology; Freeman, San Francisco, California, 577 p.

Kajiwara, Y.
1970: Syngenetic features of the Kuroko ore from the Shakanai mine; in Volcanism and Ore Genesis, ed. T. Tatsumi; University of Tokyo Press, p. 197-206.

Lambert, I.B. and Sato, T.
1974: The Kuroko and associated ore deposits of Japan; a review of their features and metallogenesis; Economic Geology, v. 69, p. 1215-1236.

Lindsay, J.F.
1968: The development of clast fabric in mudflows; Journal of Sedimentary Petrology, v. 68, p. 1242-1253.

Lowe, D.R.
1979: Sedimentary gravity flows: their classification and some problems of application to natural flows and deposits; Society of Economic Paleontologists and Mineralogists, Special Publication 27, p. 75-82.

Middleton, G.V. and Hampton. M.A.
1976: Subaqueous sediment transport and deposition by sedimentary gravity flows; in Marine Sediment Transport and Environmental Management, ed. D.J. Stanley and D.J.P. Swift; John Wiley and Sons, p. 197-218.

Nardin, T.R., Hein, F.J., Gorsline, D.S. and Edwards, B.D.
1979: A review of mass movement processes, sediment and acoustic characteristics, and contrasts in slope and base-of-slope systems versus canyon-fan-basin floor systems; Society of Economic Paleontologists and Mineralogists, Special Publication 27, p. 61-73.

Sharp, R.P. and Nobles, L.M.
1953: Mudflow of 1941 at Wrightwood, Southern California; Geological Society of America, Bulletin, v. 64, p. 547-560.

Stewart, P.W.
1983: Granitoid clasts in boulder breccias of MacLean Extension orebody, Buchans, Newfoundland; in Current Research, Part A, Geological Survey of Canada, Paper 83-1A, p. 321-324.
1987: Geology and gensis of granitoid clasts in the MacLean Extension transported orebody; in Buchans Geology, Newfoundland, ed. R.V. Kirkham, Geological Survey of Canada, Paper 86-24, Report 10.

Swanson, E.A. and Brown, R.L.
1962: Geology of the Buchans orebodies; Canadian Institute of Mining and Metallurgy, Bulletin, v. 55, p. 618-626.

Thurlow, J.G.
1977: Occurrence, origin and significance of mechanically transported sulphide ores at Buchans, Newfoundland (abstract); in Volcanic Processes in Ore Genesis; Geological Society of London, Special Publication, no. 7, p. 127.

Thurlow, J.G., Swanson, E.A. and Strong, D.F.
1975: Geology and lithogeochemistry of the Buchans polymetallic sulphide deposits, Newfoundland; Economic Geology, v. 70, p. 130-144.

Thurlow, J.G. and Swanson, E.A.
1981: Geology and ore deposits of the Buchans area, central Newfoundland; in The Buchans Orebodies: Fifty Years of Geology and Mining, ed. E.A. Swanson, D.F. Strong and J.G. Thurlow; Geological Association of Canada, Special Paper 22, p. 113-142.
1987: Stratigraphy and structure of the Buchans Group; in Buchans Geology, Newfoundland, ed. R.V. Kirkham; Geological Survey of Canada, Paper 86-24, Report 2.

Walker, P.N. and Barbour, D.M.
1981: Geology of the Buchans ore-breccias; in The Buchans Orebodies: Fifty Years of Geology and Mining, ed. E.A. Swanson, D.F. Strong and J.G. Thurlow; Geological Association of Canada, Special Paper 22, p. 161-185.

Walker, R.G.
1975: Generalized facies models for resedimented conglomerates of turbidite association; Geological Society of America, Bulletin, v. 86, p. 737-748.
1979: Turbidites and associated coarse clastic deposits; in Facies Models, ed. R.G. Walker; Geological Association of Canada, p. 91-103.

- 9 -

Geology and genesis of granitoid clasts in the MacLean Extension transported orebody

Contract No. 1583327

Peter W. Stewart[1]

Stewart, P.W., Geology and genesis of granitoid clasts in the MacLean Extension transported orebody; in Buchans Geology, Newfoundland, ed. R.V. Kirkham; Geological Survey of Canada, Paper 86-24, p. 149-176, Report 9, 1987.

Abstract

Granitoid clasts occur in sulphidic and non-sulphidic breccia-conglomerate and conglomerate in the MacLean Extension area at Buchans. The granitoid clasts occupy from less than 0.1% to 4.5% (by volume) of these subaqueous debris flow deposits and are typically the most rounded clast lithology. They are largest (maximum average size = 17.1 × 10.6 cm) and most abundant proximal to the most sulphidic sections of the debris flow deposits. Although variable in colour and texture, these differences (including the continuum of grain size and igneous textures from intrusive to subvolcanic) in the granitoid clasts appear to reflect the effects of hydrothermal alteration and the timing and environment of crystallization rather than different source areas. Grain size and textural differences provide a means to classify the clasts into six types that can be reduced into 'granitic' (types 1 and 3), 'aplitic' (types 2, 4 and 5) and 'other' (type 6) groups.

The fine- to medium-grained, porphyritic and moderately to strongly altered 'granitic' clasts dominate the granitoid clast population adjacent to ore-grade sulphidic debris flow deposits. Fine grained, weakly porphyritic and weakly altered 'aplitic' clasts increasingly dominate the granitoid clast population in debris flow deposits that flank and overlie the main transported ore zones.

Granitoid clasts have similar typically 'immobile' element (Zr, Y, TiO_2, V, Ga, Nb, REE) compositions that appear to have originated from a common volcanic-arc magma system. Buchans Group felsic flows and coeval subvolcanic intrusions (Feeder Granodiorite) have similar compositions and also originated from the same magma system.

The granitoid clasts are cognate plutonic to subvolcanic fragments that were rounded, altered and transported to the surface in breccia pipe(s) that emanated from the Buchans Group magma system. This process probably occurred as a result of the exsolution of an aqueous phase from the magma during crystallization. The explosive activity necessary for transportation upward may have initiated debris flow movement when the breccia pipe reached the surface. This event disrupted the hydrothermal system responsible for sulphide mineralization and possibly resulted in the eventual termination of this system. However, the location of this breccia pipe is not known at present.

Résumé

On trouve des clastes granitoïdes dans des brèches-conglomérats et des conglomérats sulfurés et non sulfurés aux alentours de la prolongation de MacLean, à Buchans. Les clastes granitoïdes représentent entre moins de 0,1 % et 4,5 % (par volume) des gisements produits par des coulées de débris subaquatiques ces clastes sont normalement les plus arrondis. Ils sont plus gros (en moyenne, 17,1 cm × 10,6 cm) et plus abondants près des sections les plus sulfurées des gisements. Bien que leur couleur et leur texture

[1]Department of Earth Sciences, Memorial University of Newfoundland St. John's, Newfoundland.
Present Address: Department of Geology, University of Western Ontario, London, Ontario N6A 5B7

varient, ces différences, y compris la continuité de la grosseur des grains et des structures ignées dans les roches intrusives et hypabyssales, semblent traduire les effets de l'altération hydrothermale, ainsi que de la chronologie et du milieu de cristallisation, plutôt que des sources distinctes. La différence dans la grosseur des grains et dans la structure permettent de classer les clastes en six catégories dites "granitiques" (catégories 1 et 3), "aplitiques" (catégories 2, 4 et 5) et "autres" (catégorie 6).

Les clastes "granitiques", porphyriques et modérément ou fortement altérés, à grain fin ou moyen, dominent la population des clastes granitoïdes près des gisements de sulfures laissés par les coulées de débris. Les fragments "aplitiques", faiblement porphyriques et altérés, à grain fin, dominent de plus en plus la population de fragments granitoïdes dans les gisements produits par les coulées de débris, qui sont contigus et sous-jacents aux principales zones de minerai déplacé.

Composition en éléments typiquement "immobiles" (Zr, Y, TiO_2, V, Ga, Nb, éléments des terres rares) est similaire dans tous les clastes granitoïdes; elle aurait évoluée dans un magma commun d'arc insulaire. Les coulées felsiques du groupe de Buchans et les intrusions hypabyssales contemporaines (granodiorite Feeder) ont des compositions similaires et auraient été formées à partir du même magma.

Les clastes granitoïdes sont des fragments plutoniques ou hypabyssaux syngénétiques qui ont été arrondis, altérés et transportés en surface dans une ou plusieurs cheminées volcaniques provenant du magma du groupe de Buchans. Ce processus aurait été provoqué par l'exsolution d'une phase aqueuse durant la cristallisation du magma. L'activité explosive nécessaire pour le transport vers le haut pourraient avoir provoqué des coulées de débris lorsque la cheminée volcanique a atteint la surface. Cet événement a perturbé le réseau hydrothermal qui a produit la minéralisation sulfurée et aurait même fini par le faire disparaître. Cependant, on a pas encore découvert l'emplacement de la cheminée volcanique.

INTRODUCTION

The Pb-Zn-Cu-Ag-Au massive sulphide deposits at Buchans are considered to be Paleozoic analogues to the Tertiary massive sulphide deposits of the Kuroko district in Japan (Thurlow, 1977; Thurlow and Swanson, 1981). The formation of siliceous and pyritic Cu-rich stockwork orebodies and massive Pb-Zn-Cu sulphide orebodies by precipitation of sulphide minerals from hydrothermal fluids is postulated at Buchans (Thurlow and Swanson, 1981; Henley and Thornley, 1981) and in Japan (Ohmoto and Skinner, 1983). Portions of the massive orebodies at each location have been mechanically transported from their original site of deposition (Thurlow and Swanson, 1981; Hashiguchi, 1983). At Buchans, the transported orebodies occur as lenses of sulphidic breccia-conglomerate that have been deposited by subaqueous sediment debris flows (Thurlow and Swanson, 1981; Walker and Barbour, 1981; Binney et al., 1983; Binney, 1987).

Prior to the recognition of the syngenetic deposition of the in situ orebodies with the hosting Buchans Group volcanic rocks and the transported origin of some sulphidic lenses, Swanson and Brown (1962) noted the presence of a distinctive rock unit, the 'granite conglomerate', in close spatial relationship with the orebodies. Thurlow and coworkers (Thurlow and Swanson, 1981; Walker and Barbour, 1981) demonstrated the transported nature of some orebodies at Buchans and noted a spatial relationship between the transported orebodies and the presence of large, typically well-rounded granitoid clasts. These granitoid clasts were considered to be enigmatic because all other clast lithologies present in the debris flow deposits, with the exception of rare carbonate clasts (see Nowlan and Thurlow, 1984, 1987), could be correlated with known rock units within the Buchans Group (Thurlow and Swanson, 1981).

This report contains the results of a detailed investigation of the geology and geochemistry of the granitoid clasts in the MacLean Extension transported orebody. Thurlow (1981a, b) suggested that geochemically and mineralogically similar intrusive bodies near the margins of the Buchans Group, the Feeder Granodiorite, are exposures of the source of the granitoid clasts. The most logical source for the granitoid clasts, their relationship to the Feeder Granodiorite and a model to explain their presence and spatial relationship to the transported orebodies are presented.

REGIONAL GEOLOGY

The sulphide orebodies are hosted by the Buchans Group (Fig. 1), a complex assemblege of dominantly submarine, volcanic, volcaniclastic and sedimentary rocks (Thurlow, 1981a, b) of Middle Ordovician age (Nowlan and Thurlow, 1984, 1987; Stewart, 1985). Recent interpretation of the structures at Buchans has resulted in a simplification of Buchans Group stratigraphy but has presented a much more complex structural interpretation (Thurlow and Swanson, 1987; McClay, 1987). South-eastward directed thrust faults in the Buchans area produced a series of imbricate thrust slices bounded by major fault surfaces (McClay, 1987; Thurlow and Swanson, 1987). Each slice, or thrust block, contains a partial stratigraphic section through the Buchans Group (Fig. 2). Movement was localized on bedding surfaces in many areas and resulted in the repetition of several sequences within the volcanic pile, including the sulphide-bearing layers. It is now interpreted that all economic orebodies are contained in the Buchans River Formation, a sequence of dominantly felsic volcanic rocks (Thurlow and Swanson, 1987). Further details of the structure and stratigraphy of the Buchans Group are given elsewhere in this volume.

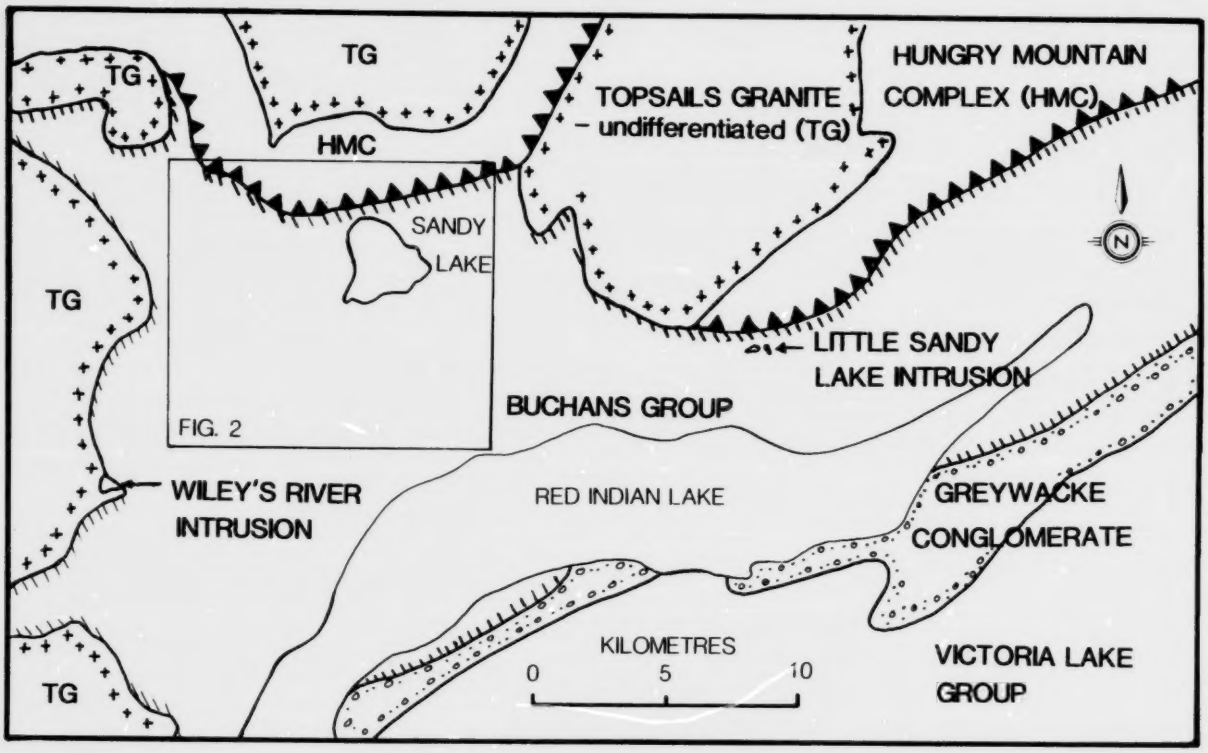

Figure 1. Simplified geological map of the Buchans/Red Indian Lake area, including the locations of the Feeder Granodiorite bodies (Wiley's River and Little Sandy Lake Intrusions).

Historically, the Buchans Group has been correlated with the Roberts Arm Group (Swanson and Brown, 1962). It has been shown to have geochemical differences with other volcanic rocks in central Newfoundland, for example, the Victoria Lake Group (Strong, 1977; Swinden and Thorpe, 1984). The Buchans and the Roberts Arm groups have geochemical similarities to modern 'late' or post-island arc volcanic rocks (Strong, 1977). Together, these groups and the Chanceport and Cottrell's Cove groups are informally referred to as the Buchans-Roberts Arm Belt (Swinden and Kean, 1984).

The absolute age of deposition of the rocks of the Buchans-Roberts Arm Belt and their position within central Newfoundland stratigraphy relative to a period of sedimentation during the Caradocian stage of the Ordovician period (Strong, 1977; Kean *et al.*, 1981; Swinden and Kean, 1984; Stephens *et al.*, 1984) is still conjectural. These aspects of Buchans Group geology are discussed more fully elsewhere in this volume (Thurlow and Swanson, 1987; Whalen and Currie, 1987; Nowlan and Thurlow, 1987).

GEOLOGICAL SETTING OF THE MACLEAN EXTENSION OREBODY

The following description of the MacLean Extension Orebody is based largely on Binney *et al.* (1983) and Thurlow and Swanson (1987). For further descriptions of this and other transported orebodies in the Buchans area, see Thurlow and Swanson (1981), Walker and Barbour (1981), Calhoun and Hutchinson (1981) and Binney (1987).

The MacLean Extension Orebody is hosted within the Buchans River Formation at the same stratigraphic interval as the Rothermere and MacLean transported orebodies and the Lucky Strike in situ orebody (Thurlow and Swanson, 1987). It occurs down paleoslope from the Rothermere and MacLean transported bodies in a linear arrangement extending northwest from the Lucky Strike in situ orebodies (Fig. 2) (Thurlow and Swanson, 1981). In the Lucky Strike and Rothermere area, the in situ and transported orebodies overlie altered and sulphide-bearing sections of the Ski Hill and Buchans River formations. The MacLean and MacLean Extension orebodies typically overlie less altered Buchans River Formation lithologies (Thurlow and Swanson, 1981, 1987). The Buchans River Formation stratigraphy in the MacLean Extension area consists of lenses of sulphide-bearing and barren breccia and breccia-conglomerate, barren arenaceous conglomerate, siltstone and rhyolitic flows within a sequence of felsic pyroclastic rocks. The breccia and breccia-conglomerate are interpreted as being deposited by subaqueous debris flows (Walker and Barbour, 1981; Binney *et al.*, 1983; Binney, 1987). Although a detailed description of the

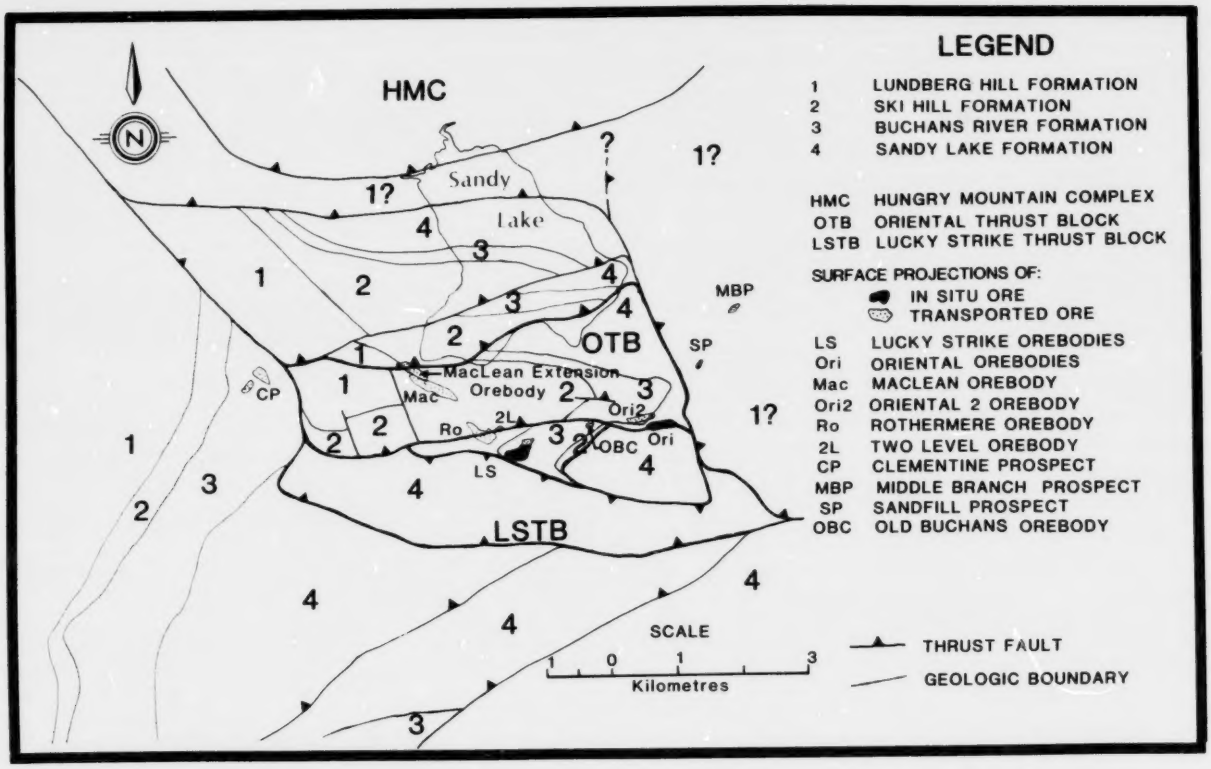

Figure 2. Schematic geological map of the Buchans Group in the immediate vicinity of the massive sulphide orebodies showing some important thrust blocks and projections of the orebodies to the surface (after Thurlow and Swanson, 1987).

Buchans River Formation is presented elsewhere (Binney, 1987), the MacLean Extension Orebody and related strata are described briefly below.

The direction of mass sediment transport and the site of deposition of these flows was apparently controlled by paleotopographic depressions and channels in the underlying felsic pyroclastic rocks (Thurlow and Swanson, 1981; Walker and Barbour, 1981). Several channels containing economic accumulations of sulphides have been recognized in the Buchans area (Walker and Barbour, 1981). The most important channel from an economic viewpoint is the MacLean-Rothermere channel which has yielded over 7 million tonnes of ore (Thurlow and Swanson, 1981). The source of the sulphides in the Rothermere, MacLean and MacLean Extension transported orebodies is considered to be in the vicinity of the in situ Lucky Strike orebody (Thurlow and Swanson, 1981; Hutchinson, 1981; Binney, 1987), although the precise source of the transported ore has not yet been identified.

The transported orebodies in this channel were possibly deposited originally as a semi-continuous series of debris flow deposits (Thurlow and Swanson, 1987; Binney, 1987). The MacLean Extension Orebody consists of upper and lower ore units (Binney *et al.*, 1983). The lower ore unit may be visualized as a continuum of lithological subunits based on changes in the proportion of sulphide and lithic components, the average clast size, and abundance and angularity of the lithic fragments (Fig. 3). Polylithic breccia-conglomerate forms the broad central portion of this continuum of debris flow subunits (Binney, 1987). One end member (sulphide matrix ore) consists of dominantly sulphide clasts and sporadic lithic clasts in a sulphide-rich matrix. The other end member (arenaceous conglomerate) consists of predominantly sub- to well-rounded lithic clasts and minor sulphide grains and rare fragments in a lithic-rich coarse sand-sized matrix (Binney *et al.*, 1983; Binney, 1987).

Polylithic breccia-conglomerate deposits contain angular to rounded clasts that range from boulders several metres in diameter to pebble size in a silt- and sand-sized matrix (Binney *et al.*, 1983). Many diverse lithologies occur as clasts (Walker and Barbour, 1981; Binney, 1987). The sulphide component (clasts and matrix) decreases and lithic material (clasts and matrix) increases across the continuum from sulphide matrix ore to arenaceous conglomerate (Fig. 3). These changes are accompanied by a decrease in average clast size and increase in the degree of rounding of all clast lithologies. With the use of modifiers, such as 'ore-

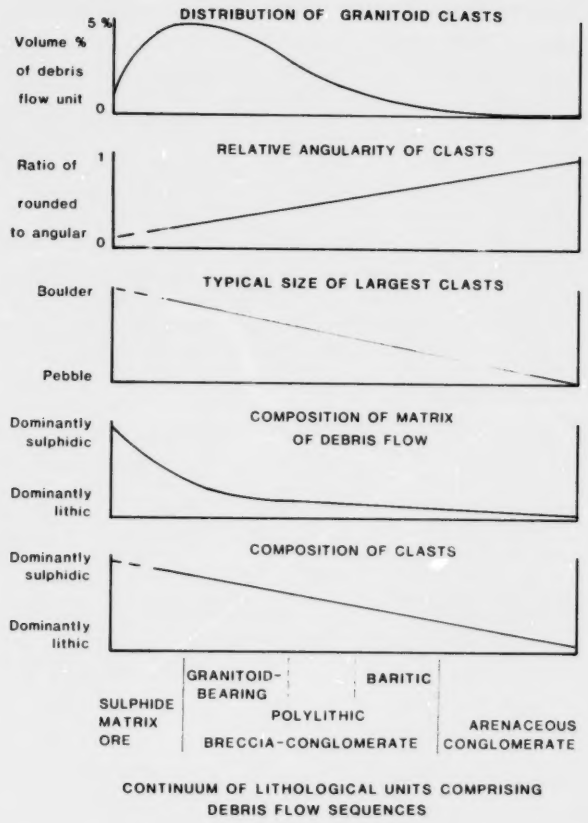

Figure 3. Schematic representation of changes in matrix composition, dominant composition of clasts, size of clasts, relative angularity of clasts and abundance of granitoid clasts that describe the lithologic continuum of sedimentological units comprising transported orebodies and genetically related strata in MacLean Extension area.

grade', 'granitoid-bearing' and 'baritic', discrete sections of polylithic breccia-conglomerate beds may be distinguished (Binney *et al.*, 1983) (Fig. 3).

The schematic and composite cross-section of the MacLean Extension Orebody (Fig. 4) shows the typical stratigraphic arrangement of these subunits. Sulphide matrix ore occupies the base of the flow unit. This generally grades upward and outward laterally into granitoid-bearing polylithic breccia-conglomerate with large sphalerite-galena clasts (Fig. 5a), or less commonly, chalcopyrite-pyrite clasts (Fig. 5b). The increasingly lithic-rich subunits that overlie and flank the main sulphide-bearing sections of debris flow sequence are subeconomic polylithic breccia-conglomerate and arenaceous conglomerate deposits. Most of the lower ore unit was subsequently capped by baritic polylithic breccia-conglomerate flows (Fig. 4).

The upper ore unit conformably overlies 30 to 50 m of felsic pyroclastic rocks (Binney *et al.*, 1983) that form the hangingwall to the lower ore unit (Fig. 4). The upper ore unit consists of baritic polylithic breccia-conglomerate with mainly sub-economic sulphide accumulations (Thurlow and Swanson, personal communication, 1982, 1983). Unlike the lower ore unit, no granitoid clasts occur in the upper ore unit. The upper ore unit is overlain by felsic pyroclastic rocks (Fig. 4).

The units shown in schematic cross-section (Fig. 4) can be related to the plan of the MacLean Extension orebodies (Fig. 6). At study locations 1 and 2 (Fig. 6), sulphide matrix ore, granitoid-rich polylithic breccia-conglomerate and subeconomic polylithic breccia-conglomerate are exposed. Subeconomic granitoid- rich polylithic breccia-conglomerate and baritic polylithic breccia-conglomerate, and barren arenaceous conglomerate occur at study location 3. These differences reflect distance away from sulphide matrix ore cores of the debris flows at locations 1 and 2 into the overlying and flanking subunits (Fig. 4). The debris flows exposed at location 4 (Fig. 6) appear to be a different set than that seen in locations 1, 2 and 3 (Fig. 6) (W.P. Binney, personal communication, 1983). In this area, a lens of polylithic breccia-conglomerate that lacks a sulphide matrix ore core apparently occurs north of the larger debris flow lens that contains a sulphide matrix ore core (Fig. 4). However, economic accumulations of sulphides within baritic and granitoid-rich polylithic breccia-conglomerate subunits are present at this locality.

GRANITOID CLASTS IN THE MACLEAN EXTENSION AREA

Introduction

The diversity in lithologies present as clasts in the MacLean Extension area (Binney *et al.*, 1983; Binney, 1987) is similar to that seen in other transported orebodies at Buchans (Walker and Barbour, 1981; Calhoun and Hutchinson, 1981). The macroscopic distinction between the igneous rocks formed in volcanic, hypabyssal (sub-volcanic) and plutonic environments, without critical field relationships, is not always possible. To ensure that all clasts of possible plutonic origin were included in the study, the following field definition of 'granitoid clast' was employed: "any clast greater than 1 cm in length with observable crystals (phenocrysts or groundmass) that could not be definitely ascribed to a volcanic origin."

Granitoid clasts are characterized by: 1) small average crystal grain size – 1 mm or less; 2) porphyritic texture – from weakly to strongly developed; 3) highly variable colour – light brown, medium brown, brown-green, brick-red, white, pink-red and pink-grey.

Petrography and classification of the granitoid clasts

The granitoid clasts in MacLean Extension area were initially classified into twelve types using macroscopic field characteristics (Stewart, 1983). In decreasing order of emphasis, the

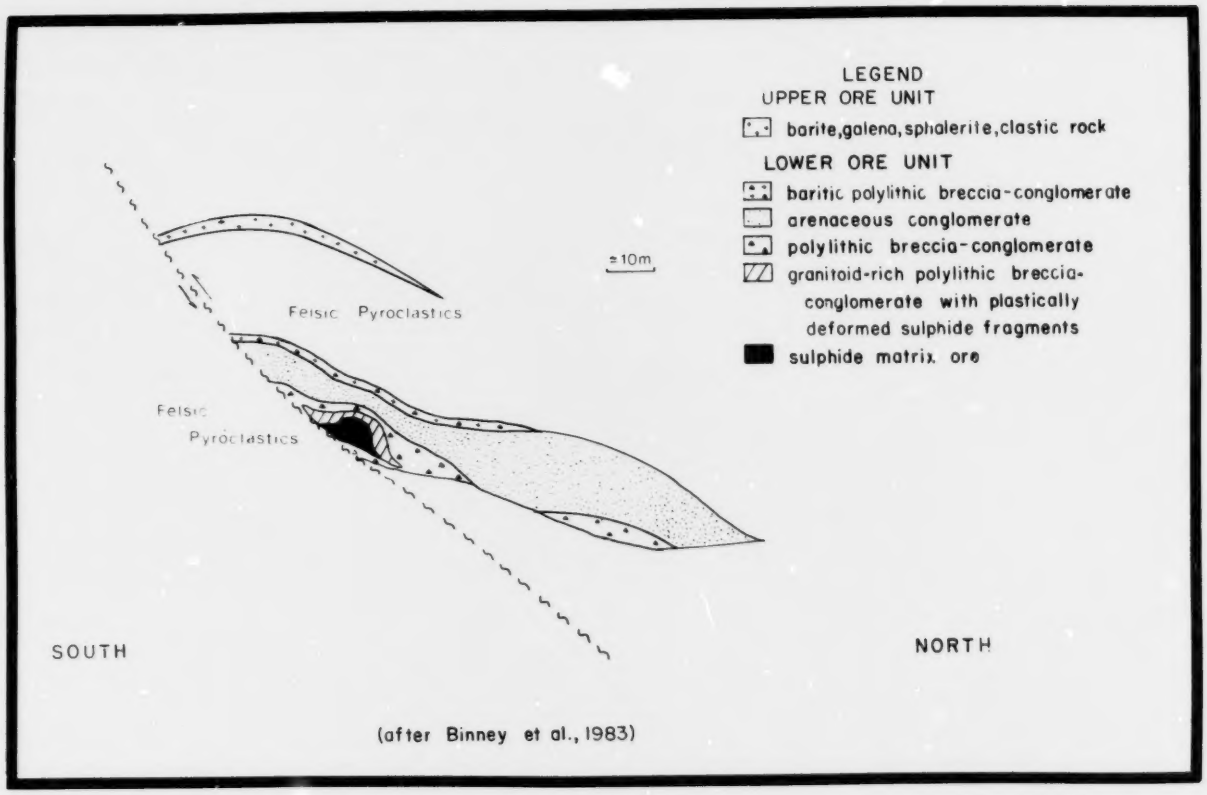

Figure 4. Schematic composite cross-section through the MacLean Extension Orebody showing the idealized distribution of the debris flow lithologic subunits including the main granitoid-rich zone of polylithic breccia-conglomerate (modified from Binney *et al.*, 1983).

macroscopic criteria used were: 1) the dominant colour of the groundmass (i.e. the overall colour of the rock); 2) average grain size of the groundmass; 3) presence or absence of phenocrysts; 4) average size and type of phenocrysts; 5) the amount of mafic minerals present and; 6) whether mafic minerals were fresh or altered. However, microscopic examination suggested that colour differences reflect mainly the variable degree of hydrothermal alteration rather than differences in the primary composition. As well, textural similarities and differences between granitoid clasts that were not recognized previously because of the fine grain size of the clasts provided the means for a microscopic classification. This scheme (Stewart, 1984) reduced the number of defined 'types' of granitoid clasts by half, and is employed in this paper with only minor modifications.

Emphasis in classification is placed on igneous textures and relative grain sizes because differences in the relative proportions of the primary minerals are slight. With the exception of type 6 clasts (see below), quartz and feldspar typically comprise 97% or more of the primary minerals with quartz comprising 30-50% and feldspar 45-65% by volume. Potassium feldspar was not recognized petrographically, and all feldspar grains appear to be plagioclase. The predominant mafic phase is biotite which is now partially to completely altered to chlorite plus or minus opaques. Biotite and its alteration products occupy typically 3% or less of the clasts. Amphibole crystals have been observed in less than 5% of the samples, and clinopyroxene in only five clasts. Amphibole and pyroxene crystals are found typically in the least altered and coarsest grained clasts and are very subordinate in proportion to biotite. Accessory minerals are magnetite, apatite, zircon and rare sphene.

Clasts are assigned to types based on the average groundmass grain size and the degree of equigranularity, and the abundance, type and size of phenocrysts (Fig. 7). The coarsest grained clasts with the best developed phaneritic texture, i.e., most truly plutonic, have been assigned to type 1 (Fig. 8a). Finer grained, weakly to non-porphyritic and highly granophyric clasts have been assigned to type 5 (Fig. 8e). Clasts types 2, 3 and 4 are intermediate in average grain size between the two end members (Fig. 8b, c, d). In general, groundmass grain size decreases, phenocrysts decrease in size and relative abundance and the texture becomes increasingly aplitic and granophyric with the transition from type 1 through to type 5 clasts (Fig. 8).

Figure 5a. Photograph of two large 'granitic' clasts with large sphalerite and galena-rich clasts in granitoid-bearing polylithic breccia-conglomerate within 30 m of sulphide matrix ore (location 2, Fig. 6).

Clast type 6 is texturally and mineralogically distinct from the other granitoid clast types. These clasts contain a greater proportion of plagioclase crystals (50-70% by volume) and mafic minerals (5-10%) and less quartz (20-30%) than the other five types and lack quartz phenocrysts or granophyric patches (Stewart, 1984). Abundant subhedral to euhedral plagioclase grains produce a distinctive 'lath-like' texture in these clasts (Fig. 8f). Type 6 clasts are largely restricted in the MacLean Extension area to the siltstone breccia underlying the MacLean Extension ore horizon (location 6, Fig. 6). This unit appears to have been deposited by debris flows as well, but contains no sulphides. No other types of granitoid clasts occur in this unit. A small number of type 6 clasts occur within the overlying MacLean Extension debris flow subunits.

The following descriptions apply to clast types 1 through to 5.

Igneous textures appear to range from intrusive to subvolcanic. The porphyritic nature of most of the clasts and abundance of granophyric textures suggest rapid crystallization. Porphyritic nature, granophyric textures and fine grain size suggest that the granitoid clasts crystallized at a high crustal level. These textural differences, the similar mineralogy and relatively consistent mineral proportions in each clast type are interpreted to reflect differences in the depth and crystallization history of a magma.

The granitoid clasts are best classified as (micro) trondhjemites and granophyric aplites. This designation is based on the absence of K-feldspar, greater than 20% quartz by volume, the low Fe content of these clasts (as indicated by the low proportion of mafic minerals), and dominance of biotite as the primary magmatic mafic mineral (Barker, 1979; Bowden *et al.*, 1984).

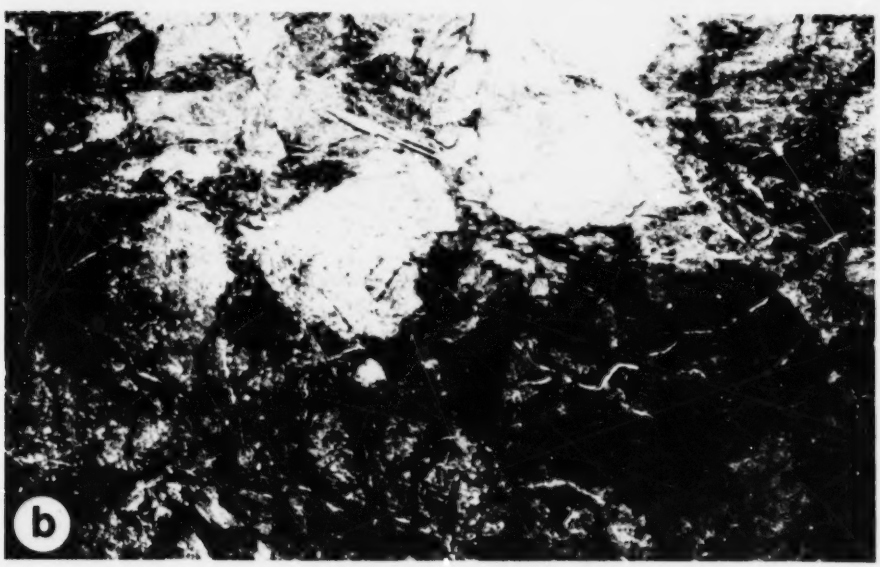

5b. Photograph of variably coloured, quartz-porphyritic 'granitic' clast with chalcopyrite-rich clast in granitoid-bearing polylithic breccia-conglomerate overlying sulphide matrix ore (location 1, Fig. 6).

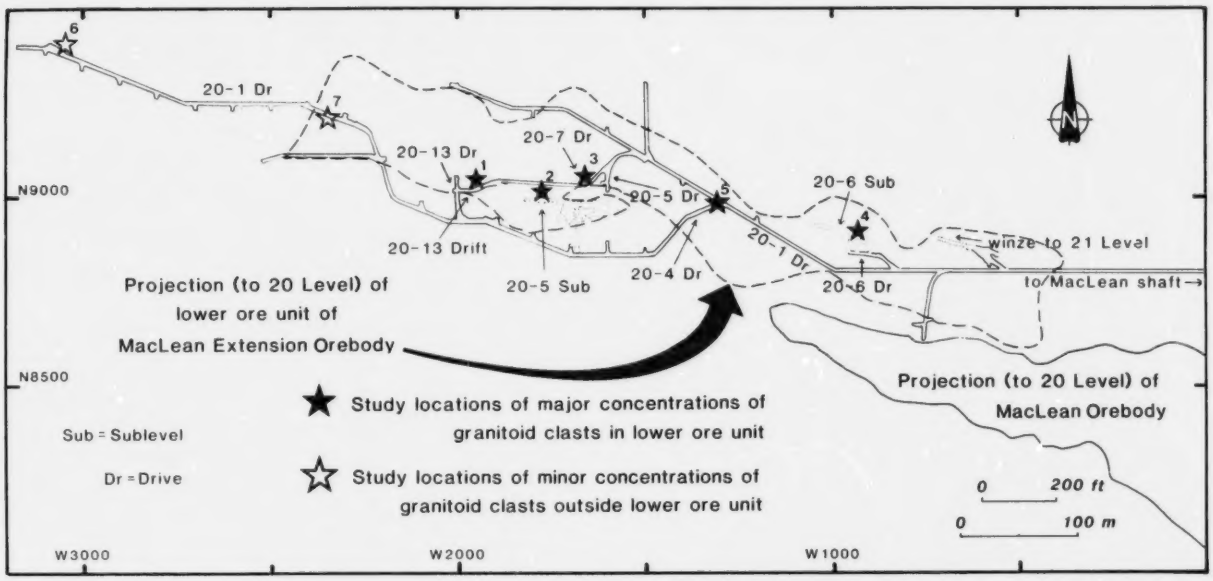

Figure 6. Plan of 20 level, MacLean Mine (MacLean Extension area) showing outlines of the MacLean Extension orebodies and study locations.

Quartz phenocrysts are large (up to 10 mm in type 1 and 3 clasts), rounded, usually glomerocrystic and slightly larger than the plagioclase phenocrysts (up to 6 mm in type 1 and 3 clasts). Type 3 clasts are hiatal porphyritic whereas type 1 clasts are seriate porphyritic with a continuous range in grain size from groundmass to phenocrysts. Type 2 clasts are equigranular relative to these two types and intermediate in average grain size (Fig. 7). Although type 5 clasts are slightly finer grained than type 4 clasts, the greater abundance of granophyric intergrowths in type 5 clasts is characteristic.

Alteration of plagioclase grains is ubiquitous, but variable in relative intensity and consists of two types: 1) very fine grained, red-brown dust (hematite) clouding the grains; and 2) the partial to complete replacement of plagioclase crystals by fine grained calcite and sericite. Locally, barite, chlorite and rarely epidote are also seen to partially replace plagioclase.

Plagioclase phenocrysts in the most altered clasts are replaced partially by fine grained aggregates of sericite and calcite and groundmass plagioclase is almost completely replaced by fine grained sericite, calcite and barite (and possibly cryptocrystalline quartz). Quartz crystals (phenocrysts especially) are relatively unaffected by this alteration, and stand out in a "sea" of alteration products. In contrast, plagioclase phenocrysts in types 4 and 5 clasts characteristically have partially to strongly altered (to sericite and calcite) cores while the groundmass plagioclase is typically strongly dusted by hematite without significant calcite or sericite replacement. Type 2 clasts commonly display an intermediate degree of alteration between strongly hematized type 4 and 5 clasts and pervasively altered type 1 and 3 clasts. In less pervasively altered type 1, 2 and 3 clasts, plagioclase grains display weak to strong hematite dusting.

The mafic phases (biotite and rare amphibole) are partially to completely replaced by chlorite and opaque minerals or less typically by sericite and/or epidote. The degree of chloritization appears to correlate with the degree of alteration of plagioclase grains. In moderately altered clasts, biotite is replaced entirely by chlorite. In pervasively altered samples, biotite and chlorite are absent with only rare opaque minerals present. Type 4 and 5 clasts have a slightly lower abundance of primary mafic minerals (approximately 1% biotite) and biotite is typically better preserved than in types 1, 2 or 3.

The colour of granitoid clasts appear to reflect variable alteration. Colour variations within individual clasts demonstrate the secondary nature of the observed colours. Quartz plus calcite plus barite veins with bleached halos in the adjacent host rock terminate at clast boundaries (Fig. 9). This feature plus highly variable colours in adjacent clasts within one debris flow demonstrate that the colour differences in granitoid clasts probably occurred prior to their incorporation in the debris flows.

Phenocrysts typically show sets of fine fractures that are parallel within one phenocryst but show different orientations in phenocrysts within a single thin section. Larger fractures and embayments in quartz phenocrysts are filled typically with very fine grained groundmass material or alteration products. Both fractured and unfractured quartz phenocrysts characteristically show undulous extinction.

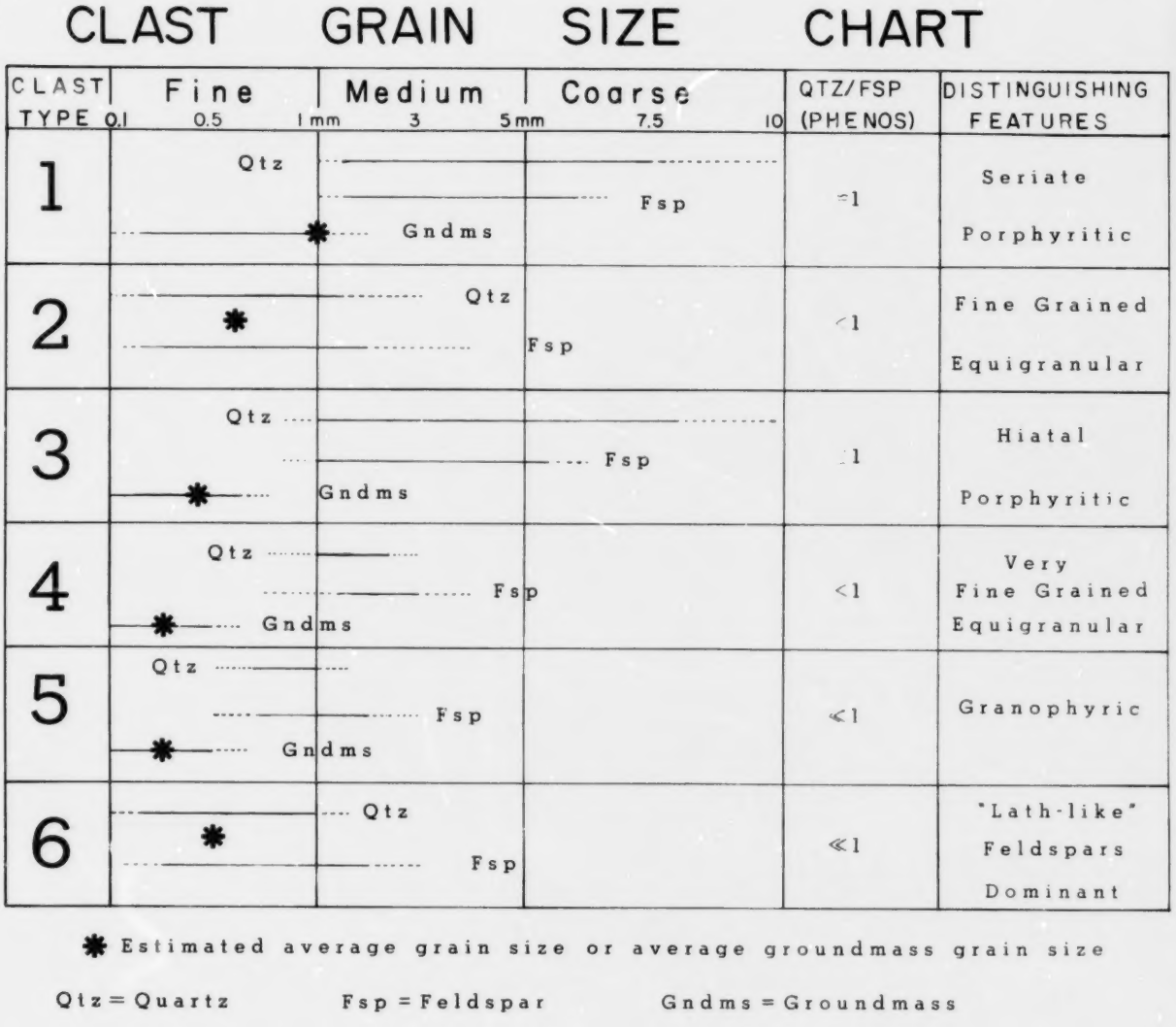

Figure 7. Graphical representation of phenocryst and groundmass grain size and textural criteria used to classify granitoid clast types in the MacLean Extension area.

The porphyritic and coarsest grained clasts typically show the most intense fracturing, veining and alteration. Some quartz phenocrysts are fractured and slightly 'pulled apart' similar to quartz phenocrysts in volcanic rocks of the underlying Lundberg Hill Formation (Fig. 10). The lack of a systematic orientation to these fractures negates their origin by a later deformational event. These features indicate phenocryst deformation prior to their incorporation in the debris flows.

Cryptocrystalline quartz (possibly intergrown with plagioclase) occurs filling open spaces as veins and as a cement for mineral grains in highly altered, fractured and brecciated clasts. These features imply that brecciation, alteration and silicification of the clasts occurred before their incorporation in the debris flow.

Although type 6 clasts are similar mineralogically to the other types, they contain more plagioclase, biotite and magnetite and less quartz. The larger grain size and subhedral nature of the plagioclase indicates that it probably began to crystallize earlier than the other phases. Quartz phenocrysts are absent and quartz occurs interstitial to the larger plagioclase laths and biotite grains, indicating that it was a late crystallizing phase.

Type 6 clasts appear to represent an earlier, slightly less differentiated magma product than the other clast types (see section on geochemistry). The rare occurrence of type 6

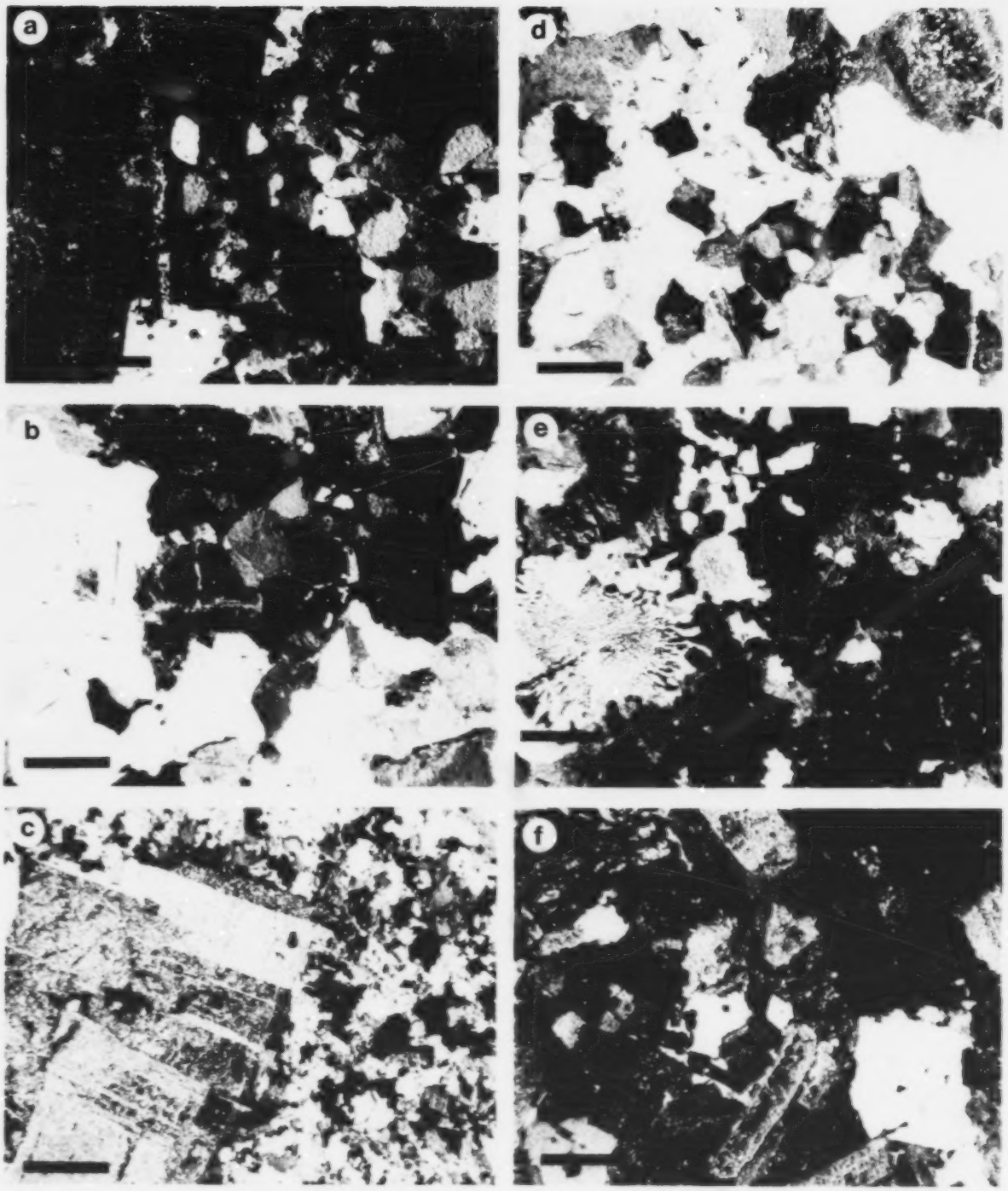

Figure 8. Representative photomicrographs of: (**a**) granitoid clast type 1; (**b**) granitoid clast type 2; (**c**) granitoid clast type 3; (**d**) granitoid clast type 4; (**e**) granitoid clast type 5; (**f**) granitoid clast type 6. Bar scale is 5 mm.

Figure 9. Photograph of granitoid clast showing calcite + quartz + barite veinlets (and associated bleached margins) terminating at clast boundaries.

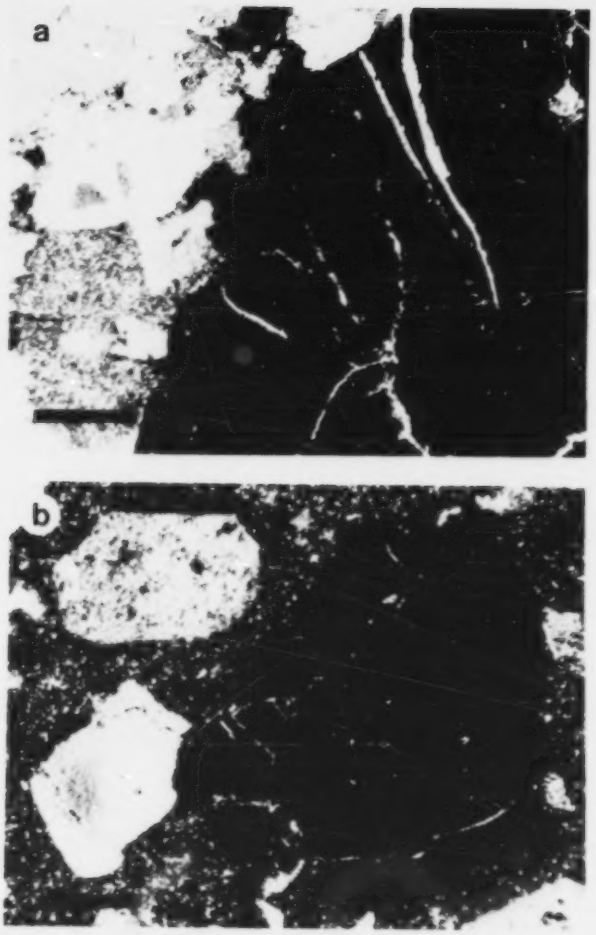

Figure 10. Photomicrographs of (**a**) a typical porphyritic granitoid clast (type 3) and (**b**) a quartz porphyritic volcanic rock of the Lundberg Hill Formation. Bar scale is 5 mm.

material as rounded 'globules' within other granitoid clast types and its restriction to the siltstone breccia underlying the MacLean Extension debris flow sequence support this interpretation.

Granitoid clast characteristics

Clast length is defined as the longest observable dimension; width is the maximum distance perpendicular to the length. Average granitoid clasts dimensions at each study location are given in Table 1.

Granitoid clasts are found to be of unequal dimensions, typically oval or elongate in form (Table 1). The area of each granitoid clast is estimated using the formula for the area of an ellipse to reflect the inequal average dimensions (Table 1). The sum of these areas was compared to the total area of the study location to determine the percentage area occupied by granitoid clasts. The volume of a debris flow occupied by granitoid clasts is extrapolated from the per cent area occupied by granitoid clasts (Table 1). This extrapolation is based on the assumption that the unobserved third dimension is not significantly and consistently longer or shorter than the two observed dimensions. This assumption is considered valid for the following reasons: 1) no evidence exists of preferred orientation in any clast type within these debris flows (Binney, 1987); 2) no evidence of any extensive tectonically produced flattening or stretching of lithic clasts within the Buchans Group is observed; 3) study locations are parallel, perpendicular and oblique to the presumed debris flow direction. Therefore, the measured cross-section through each clast is considered to be nonpreferential and no consistent bias toward either over- or under-estimating the unobserved dimension should exist.

The study locations are exposures of the most obvious concentrations of granitoid clasts in the MacLean Extension area, thus the volume per cent estimates are considered max-

Table 1. Average dimensions, volume per cent, estimated degree of roundness and abundances of groups of granitoid clasts on 20 level, MacLean Extension area (see Fig. 6 for study locations)

LOCATIONS STUDY	UNDERGROUND REFERENCE	ROCK UNIT(S)	AVERAGE DIMENSIONS n	LENGTH (cm)	WIDTH (cm)	VOLUME %	ROUNDNESS CLASSES[1] 1	2	3	4	5	6	CLAST GROUPINGS[2] Granitic	Aplitic	Others
1	20-13 Drift (north face)	granitoid-rich ore polylithic breccia - conglomerate	70	17.1	10.6	4.58			1	34	34	1	54	15	1
	20-13 Drive (both faces)	polylithic breccia - conglomerate	34	nd	nd	nd			1	13	17	3	6	28	
2	20-5 Sub (south face)	granitoid-rich ore polylithic breccia - conglomerate	37	16.1	9.4	3.62			8	18	11		28	7	2
3	20-7 Drive (north face)	polylithic arenaceous breccia-conglomerate, granitoid-bearing polylithic brecia - conglomerate and baritic polylithic breccia - conglomerate (undivided)	171	6.8	3.6	2.90			1	43	97	30	71	92	8
4	20-6 Sublevel (south face)	granitoid-bearing polylithic breccia - conglomerate and minor baritic	158	6.0	4.0	1.16			1	43	74	40	17	141	
	20-6 Sublevel (north face)	polylithic breccia - conglomerate and arenaceous conglomerate (undivided)	262	4.7	3.2	0.55				26	154	82	11	249	2
5	20-4 Drive (south face)	baritic polylithic breccia - conglomerate and granitoid - bearing	150	3.7	2.5	1.16			2	23	79	46	12	137	1
	20-4 Drive (north face)	arenaceous breccia - conglomerate (undivided)	100	4.6	3.3	1.02				16	64	20	20	75	5
	20-1 Drive	baritic polylithic breccia -conglomerate	22	nd	nd	nd				3	12	7		22	
6	20-1 Drive (north face)	siltstone breccia	30	nd	nd	nd				16	14		5	18	7
7	20-1 Drive	hangingwall dacitic pyroclastics	3	nd	nd	nd					2	1		3	
2	20-5 Sublevel (south face)	footwall dacitic pyroclastics	36	6.8	5.6	0.58			1	17	17	1	10	22	4
3	20-7 Drive (north face)	footwall dacitic pyroclastics	9	7.8	3.5	0.10					6	3	5	4	

1: Roundness classes from Jackson (1970); 2: based on microscopic classification of Stewart (1983); nd = not determined, estimated volume less than 0.1%; n = number of samples

imums (Table 1). Average dimensions and volume calculations of granitoid clasts in the siltstone breccia and felsic pyroclastic rocks in MacLean Extension area are shown for comparison. The volume was not calculated for locations with few granitoid clasts (less than 0.1% by volume).

The largest (average size) granitoid clasts and the maximum volume occupied by granitoid clasts occur in granitoid-bearing polylithic breccia-conglomerate near sulphide matrix ore (locations 1 and 2, Fig. 6) (Table 1). The average size and volume per cent occupied by granitoid clasts decreases in granitoid-bearing polylithic breccia-conglomerate as one moves away from sulphide matrix ore (locations 3 and 5, Fig. 6) (Table 1). In ore-grade, granitoid-bearing polylithic breccia-conglomerate that lacks associated sulphide matrix ore (location 4, Fig. 6), granitoid clasts are slightly larger but occupy a similar volume to those at locations 3 and 5 (Table 1). Granitoid clasts are a minor component in debris flow subunits outside the ore zones.

The relative angularity of each granitoid clast was estimated by the 'comparison chart of visual estimation of roundness' (Jackson, 1970, p. 329). On this scale, one indicates a very angular clast or grain and six represents a well-rounded clast or grain. The overwhelming majority of granitoid clasts (99%) were assigned values (4, 5 or 6) that correspond with the sub-rounded, rounded and well-rounded classes (Table 1).

The greater degree of roundness of the granitoid clasts relative to other clast lithologies was noted previously (Thurlow, 1981a; Walker and Barbour, 1981; Binney *et al.*, 1983). These workers observed that the granitoid clasts typically exhibit the highest degree of rounding of all clast lithologies in debris flow deposits.

Grouping of granitoid clast types

Two groupings can be made from the five main granitoid clast types based on grain size and textural similarities. Types 1 and 3 are highly porphyritic with the best developed 'granitic' groundmass texture and form the 'granitic' group. Types 4 and 5 are finer grained and relatively equigranular with only rare quartz and plagioclase phenocrysts, typically contain granophyric patches and have an overall 'aplitic' texture. Type 2 clasts, because of their relative equigranular nature and predominantly aplitic texture are grouped with types 4 and 5 into the 'aplitic' group. Type 6 clasts are distinct and constitute a separate group.

The microscopic classification is difficult to apply underground. However, similar groupings can be made from the macroscopic classification (Stewart, 1983). Clast types 1, 4 and 6 in the original scheme form the 'granitic' group, while types 2, 5 and 7 constitute the 'aplitic' group based on groundmass textural similarities and the absence of phenocrysts. The 'other' group consists of all other clast types in the macroscopic classification not assigned to the 'granitic' or 'aplitic' groups. The close correlation between the relative per cent distribution of the 'granitic', 'aplitic' and 'other' clast groups at the main study locations based on both microscopic and macroscopic classification methods is shown in Figure 11b. This correlation suggests that the distribution of the 'granitic', 'aplitic' and 'other' granitoid clast groups defined macroscopically (Table 1) closely approximates the distribution patterns of these groups based on the improved, but non-applicable in the field, microscopic classification.

Distribution of granitoid clasts

The 'granitic' group clearly predominates where sulphide matrix ore is present (i.e. 20-13 Drift and 20-5 Sublevel, Fig. 11b; Table 1), whereas the 'aplitic' group predominates in the 20-6 Sublevel where sulphide matrix ore is absent (Table 1; Fig. 11b). At 20-7 Drive, each group is present in approximately equal proportions (Table 1; Fig. 11b). The latter location is east of 20-13 Drift (location 1) and slightly east of and beneath 20-5 Sublevel (location 2, Fig. 6) and is probably an exposure of the flank of the flows exposed at locations 1 and 2 (W.P. Binney, personal communication, 1983). As sulphide concentrations decrease (locations 3 and 5), debris flow subunits are increasingly dominated by 'aplitic' group clasts (Table 1). Although most granitoid clasts in arenaceous conglomerate are too small to study in detail, they appear to be predominantly 'aplitic' with 'granitic' group clasts absent to rare in this unit. Granitoid clasts are entirely absent from the baritic, polylithic breccia-conglomerate subunit that constitutes the upper ore unit (Binney *et al.*, 1983).

The changes in the granitoid clast population indicate a strong correlation between the 'granitic' group and the most sulphide-rich sections of the debris flows. There is a correlative decrease in the volume per cent of the debris flow occupied by granitoid clasts. The largest granitoid clasts (average clast size) and the maximum volume of granitoid clasts are also found intimately associated with the greatest concentration of base metal sulphide mineralization (Fig. 11a).

No mechanism other than density would presumably sort clasts during debris flow movement. The greater density of the sulphide clasts relative to all other clast lithologies may explain their concentration at the base of the debris flow sequence (Fig. 4). However, no such density difference exists between the granitoid clasts and other clast lithologies. The observed distribution patterns of the 'granitic' and 'aplitic' granitoid clasts is, therefore, considered to reflect the character of and changes in source areas rather than processes active during debris flow movement.

It is noted that the size, abundance and character of the granitoid clasts varies within one debris flow sequence (e.g. locations 1, 2 and 3, Fig. 6,11). Therefore, changes in the source area of the granitoid clasts must have occurred within the time needed to initiate, transport and deposit one debris flow sequence. Similarly, the changes in the granitoid group population between this debris flow sequence and that exposed in 20-6 Sublevel (Location 4; Fig. 6) also must have occurred within a short period of time as these flows occupy

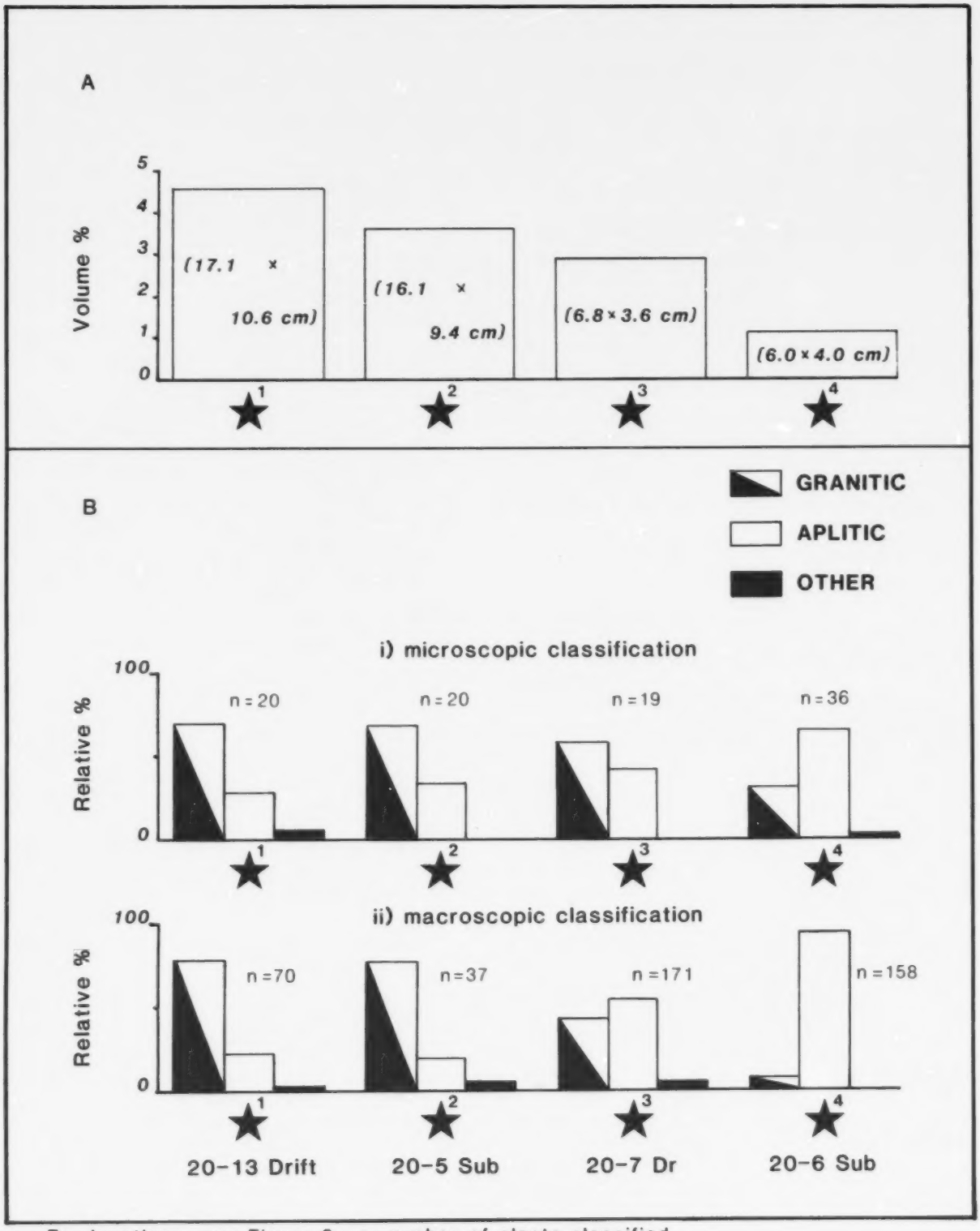

For locations, see Figure 6; n = number of clasts classified

Figure 11. (**a**) Estimated volume per cent of debris flows occupied by granitoid clasts at main study locations (see Fig. 6). Average granitoid clast size (in cm) at each location is shown inside each histogram; **b**) Relative per cent of each group of granitoid clasts at the main study locations; groupings based on macroscopic classification of Stewart (1983) and microscopic classification of Stewart (1984).

the same stratigraphic position in the MacLean Extension area (Thurlow and Swanson, 1987; Binney, 1987).

FEEDER GRANODIORITE

The Feeder Granodiorite underlies two small areas in the Buchans Group east and west of Buchans townsite (Thurlow and Swanson, 1981). These occurrences are informally referred to as the Little Sandy Lake intrusion (0.15 km^2) and the Wiley's River intrusion (1.1 km^2), respectively (Fig. 1) (Stewart, 1985).

The Little Sandy Lake intrusion intrudes the Buchans Group. The Wiley's River intrusion is seen to have been intruded by the Topsails alkali feldspar granite and related mafic intrusive rocks (Stewart, 1983). However, the contact between the Wiley's River intrusion and the Buchans Group volcanic rocks is not exposed (Stewart, 1985).

Each plutonic body is allotriomorphic, inequigranular and characterized by prominent (up to 10-15 mm), rounded quartz phenocrysts and smaller (up to 8 mm) subhedral plagioclase phenocrysts set in fine- to very fine-grained groundmasses. However, in the Little Sandy Lake intrusion, phenocrysts occupy 20% by volume or less and are subordinate volumetrically to the groundmass. Whereas in the Wiley's River intrusion, groundmass material (5-20% by volume) is subordinate to phenocrysts. K-feldspar rims plagioclase crystals and occurs as a groundmass component in the Wiley's River intrusion. However, K-feldspar is absent in the Little Sandy Lake intrusion. Granophyric intergrowths occur locally in the Wiley's River intrusion and near the margins of the Little Sandy Lake intrusion. Biotite is the primary mafic component in each body and appears to have crystallized interstitial to the quartz and plagioclase phenocrysts. Rare subhedral amphibole crystals occur in the Wiley's River intrusion. Partial to complete alteration of biotite and amphibole to chlorite is common in each, but is more pervasive in the Little Sandy Lake intrusion, as is the development of epidote. Amphibole has not been recognized in the Little Sandy Lake intrusion.

Porphyritic textures, fine grain size of the groundmass and the presence of granophyric intergrowths and aplitic textures suggest that each body was intruded at a high crustal level. The anhedral, 'ragged' appearance of the quartz and feldspar crystals, the interdigitating nature of the quartz and feldspar crystal contacts and the presence of inclusions of feldspar in quartz and vice versa suggest relatively rapid crystallization. Strain features, such as the development of undulous extinction preferentially in the phenocryst phases and rare bent twin planes in plagioclase, suggest high-temperature ductile deformation prior to final crystallization.

GEOCHEMISTRY

Introduction

The main purposes of the geochemical investigation were: 1) to determine the chemical composition of the granitoid clasts and the Feeder Granodiorite; 2) to compare these data with the chemical composition of Buchans Group felsic volcanic rocks (from Thurlow, 1981a); 3) to identify plausible sources of the clasts and eliminate others. The petrographic evidence of variable degrees of hydrothermal alteration of the granitoid clasts emphasizes the importance of comparisons of only those elements typically immobile during hydrothermal alteration and other secondary processes. Elements selected to examine the primary composition of the granitoid clasts are Zr, Y, TiO_2, V, Ga, Nb and REE. These are elements of large ionic charge and size, i.e., high field strength (HFS) elements. Their abundances can be useful indicators of the degree of magmatic differentiation and the potential sources of an igneous rock (Pearce and Cann, 1973; Hanson, 1978; Briqueu *et al.*, 1984; Pearce *et al.*, 1984). The HFS elements also appear to be relatively immobile during most secondary processes (Humphris and Thompson, 1978; Ludden *et al.*, 1982), although some mobility in these elements has been reported within zones of intense hydrothermal alteration associated with massive sulphide (MacGeehan and MacLean, 1980; Finlow-Bates and Stumpfl, 1981), Cu porphyry (Taylor and Fryer, 1982) and lode Au deposits (Rosylyakova and Rosylyakova, 1975; Ludden *et al.*, 1984).

An empirical evaluation of the chemical changes resulting from hydrothermal alteration is difficult, if not impossible, to make without a means to demonstrate the primary unaltered magmatic composition of the clasts. Correspondingly, no attempt can be made to model the petrogenesis of the granitoid clasts.

Tables of the complete chemical data, analytical methods and estimates of accuracy and precision are presented elsewhere (Stewart, 1985).

Composition of the granitoid clasts

The mean major and trace element composition of the granitoid clast types are given in Table 2. They all have similar sodic, silica-rich (i.e. high-silica rhyolites) compositions with the exception of the more rhyodacitic type 6 clasts. The more intermediate character of type 6 clasts (lower SiO_2, higher Fe_2O_3, MgO, TiO_2) relative to the felsic composition of the other clast types is evident (Table 2). The small range of SiO_2 values (66% to 77%) of the clasts limits the usefulness of Harker diagrams but decreases in Fe_2O_3, MgO and TiO_2 with increasing SiO_2 contents are seen. Trace element abundances are similar for all granitoid clasts, e.g. low Zr, Y, Ni, Cr, U abundances. This is exemplified by the tight cluster of points in Figure 12. Differences between the clasts are recognizable however, as shown by the separation of type 6 clasts from the other types in Figure 13. A correlation between decreasing Ti and V from type 6 clasts to 'granitic' clasts (types 1 and 3) to 'aplitic' clasts (types 2, 4 and 5) is developed imperfectly. This trend may be explicable by the fractional crystallization of a mafic phase containing these elements, such as ilmenite or titano-magnetite (Briqueu *et al.*, 1984).

The slightly greater concentration of both Zr and Y in the 'aplitic' clasts (Fig. 14) relative to the 'granitic' clasts sug-

Table 2. Averaged chemical analyses of granitoid clasts subdivided by type

	TYPE 1		TYPE 2		TYPE 3		TYPE 4		TYPE 5	TYPE 6	
SiO_2	72.31	(2.00)	74.02	(2.18)	74.13	(1.77)	77.00	(.79)	77.3	68.17	(1.08)
TiO_2	0.18	(.06)	.19	(.08)	.13	(.05)	.15	(.06)	.13	.39	(.05)
Al_2O_3	11.78	(.80)	10.94	(.73)	10.86	(1.08)	10.70	(.49)	11.6	13.77	(.31)
Fe_2O_3*	1.98	(.91)	1.51	(.76)	1.10	(.59)	1.11	(.19)	.85	3.94	(.52)
MnO	.07	(.02)	.05	(.02)	.05	(.01)	.05	(.01)	.03	.07	(.02)
MgO	.76	(.34)	.59	(.34)	.48	(.27)	.35	(.16)	.30	1.32	(.40)
CaO	2.54	(.50)	1.69	(.32)	2.44	(.51)	1.58	(.59)	1.17	3.16	(.74)
Na_2O	3.73	(.58)	4.45	(1.07)	3.72	(.51)	4.84	(1.11)	3.93	4.65	(.59)
K_2O	1.30	(.29)	0.95	(1.10)	1.18	(.32)	.53	(.47)	3.08	.93	(.43)
P_2O_5	.06	(.10)	.03	(.04)	.04	(.02)	.04	(.07)	.03	.21	(.15)
LOI	3.20	(.72)	2.53	(.68)	3.41	(.69)	2.09	(.84)	1.26	2.57	(.91)
TOTAL	97.91		96.95		97.54		98.44		99.68	99.18	
					TRACE ELEMENTS (ppm)						
Pb	172	(245)	110	(126)	74	(54)	66	(34)	43	16	(8)
Th	12	(3)	12	(5)	12	(4)	16	(2)	20	8	(2)
U	2	(2)	1	(2)	1	(2)	3	(2)	5	1	(1)
Rb	22	(5)	16	(17)	20	(5)	9	(8)	39	14	(10)
Sr	304	(112)	310	(126)	403	(238)	244	(16)	170	277	(56)
Y	18	(7)	25	(8)	15	(5)	32	(12)	19	28	9
Zr	100	(18)	116	(22)	80	(13)	127	(27)	86	105	(31)
Nb	4	(1)	5	(1)	5	(2)	5	(3)	7	5	(1)
Zn	157	(93)	142	(138)	143	(102)	64	(35)	29	98	(93)
Cu	37	(19)	57	(63)	36	(12)	25	(8)	14	19	(6)
Ni	0		0		0		0		0	0	
Ba	7943	(7515)	12455	(8566)	13456	(11510)	8055	(2403)	3942	1829	(2314)
V	38	(14)	30	(20)	33	(15)	17	(6)	12	70	(9)
Cr	0		0		0		0		0	0	
Ga	10	(3)	10	(2)	8	(3)	9	(1)	7	12	(1)
n	11		4		12		6		1	3	

* = total Fe reported as Fe_2O_3
0 = measured abundance is below analytical detection limit (approx. 1 ppm); standard deviations (1σ) in brackets;
n = number of samples; data from Stewart (1985)

gests their origin is from a slightly more evolved or differentiated magma source than the 'granitic' clasts. This relationship is common between comagmatic aplites and granites (e.g. Lynch and Pride, 1984).

The REE abundances in all granitoid clasts are similar (Table 3). On chondrite normalized REE plots, all granitoid clast types analyzed show evidence of moderate light REE enrichment with La contents varying between 20 and 60 times chondrite and Er contents between 3 and 10 times chondrite (Fig. 15). Type 1, 2, 3 and 6 clasts appear to lack a consistent Eu anomaly (Fig. 15a, b). However, a slight and relatively consistent negative Eu anomaly occurs in the type 4 clasts (Fig. 15b). Negative Eu anomalies typically indicate the removal of plagioclase during crystallization thereby depleting the melt in Eu (Hanson, 1980).

Calcite, sericite, barite and chlorite are the result of hydrothermal alteration and all contain volatile elements. Therefore, loss-on-ignition (LOI) provides a qualitiative measure of the intensity of alteration. The greater degree of alteration of the 'granitic' group clasts (types 1 and 3) observed petrographically relative to the other types is evident in Table 2 (higher LOI, CaO, Ba). No clear evidence of the light and middle REE depletions that result from intense hydrothermal alteration associated with massive sulphide deposition are apparent (e.g. Campbell *et al.*, 1984; Fig. 15).

In summary, the similar abundances of relatively 'immobile' trace elements (Ti, Zr, Y, Nb and REE) that display evidence of magmatic differentiation suggest that the clasts have a common magmatic source. The similar mineralogy and the gradation in igneous textures of the different granitoid clast types (except type 6 clasts) also suggests that the clasts may have a common origin. 'Aplitic' group clasts appear to be slightly more evolved relative to the 'granitic' group. Type 6 clasts are less evolved than either group. No geochemical data are recognizably contradictory to a common magmatic origin for the granitoid clasts.

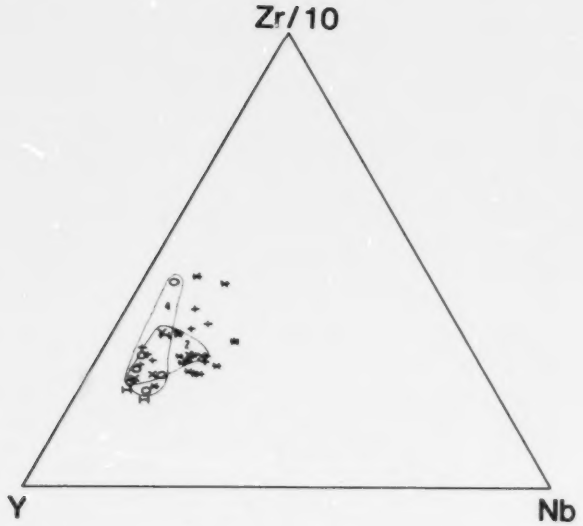

Figure 12. Zr/Y/Nb diagram for granitoid clast types. Crosses (+) represent type 1 clasts, (X) represent type 2 clasts, asterisks (*) represent type 3 clasts, circles (0) represent type 4 clasts, the star represents the type 5 clast and (H) represent type 6 clasts. Fields of 'aplitic' group clasts (types 2 and 4) are shown.

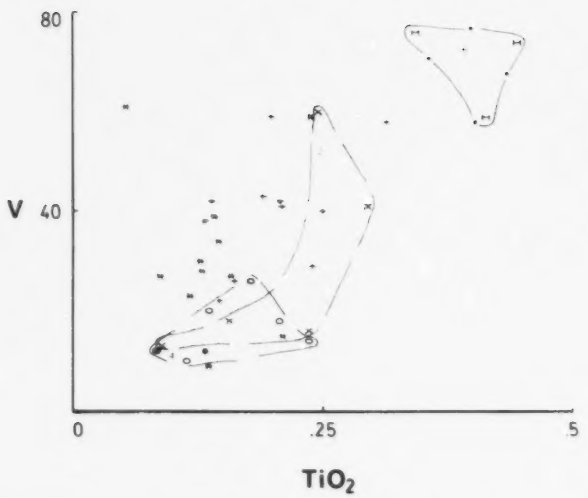

Figure 13. TiO_2 (weight %) versus V (in ppm) variation diagram for granitoid clast types. Fields of 'aplitic' group clasts (types 2 and 4) and 'other' clasts (type 6) are shown. Symbols as defined in Figure 12.

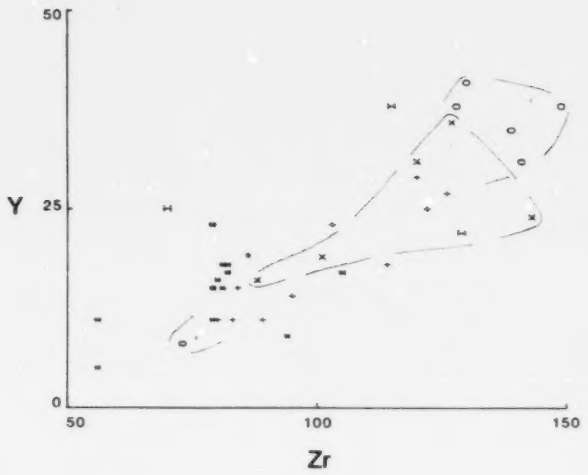

Figure 14. Zr versus Y (both in ppm) variation diagram for granitoid clast types. Symbols as defined in Figure 12.

Comparison of chemistry of granitoid clasts, Feeder Granodiorite and Buchans Group felsic flows

The major, trace and REE geochemistry of the granitoid clasts, the Feeder Granodiorite (Wiley's River and Little Sandy Lake intrusions) and Buchans Groups felsic flows have been compared to evaluate the comagmatism of these suites proposed by Thurlow (1981a, b). Lithogeochemical data for Buchans Group flows with greater than 65% SiO_2 from Thurlow (1981a) augment those from this study for a Buchans River Formation rhyolite in MacLean Extension and five Buchans Group rhyolitic flows from the Little Sandy Lake area. REE data for Buchans Group volcanic rocks from Strong (1984) are also used. The Topsails granite is younger than the Buchans Group (Whalen and Currie, 1987), and has been shown to have major and trace element abundances that are different from those of the granitoid clasts (Stewart, 1984). Topsails granite data have been plotted on some figures for reference and not as a possible source of the granitoid clasts.

The populations of interest (i.e., excluding the Topsails granite) are: 1) silica-over-saturated, 2) subalkaline (after Irvine and Baragar, 1971), and 3) peraluminous (Al_2O_2/$CaO + Na_2O + K_2O$ greater than 1). The granitoid clasts have slightly lower mean abundances of TiO_2, Fe_2O_3 and Al_2O_3 than other rock units (Table 4). The clasts contain greater Pb, Zn and Cu abundances than the other populations but this is attributable to the presence of base metal sulphides within the clasts or more likely as contaminants from the sulphide-rich host strata. However, no significant differences in the trace element compositions are apparent. This is shown by the overlap in the fields for each population (Fig. 16, 17, 18).

The granitoid clasts have similar V, Y and Zr abundances to the Feeder Granodiorite bodies (Table 4), but at slightly

Table 3. Rare earth element contents (in ppm) of granitoid clast types 1, 2, 3 and 4, and the Wiley's River intrusion

	TYPE 1							TYPE 3				TYPE 6
	007	008	031	014	051	082	127	002	004	043	073	067
La	13.88	9.43	6.79	8.20	8.13	13.01	18.53	12.92	7.02	5.52	13.06	20.76
Ce	31.07	26.67	18.10	20.95	20.16	30.25	39.88	29.78	19.87	16.99	32.31	49.21
Nd	12.13	13.74	8.60	9.82	11.10	13.19	15.23	11.92	11.94	7.73	16.23	23.12
Sm	2.07	2.81	1.74	1.91	2.61	2.54	2.25	2.14	2.92	1.80	3.17	4.84
Eu	0.74	0.88	0.66	0.58	0.90	0.76	0.70	0.88	0.62	0.81	1.01	1.60
Gd	1.91	2.59	1.93	1.73	2.82	2.38	2.85	2.21	2.79	1.73	3.08	4.40
Dy	1.50	2.28	1.18	1.39	2.51	1.81	1.31	1.63	2.36	1.51	2.14	2.85
Er	0.61	1.13	0.79	0.86	1.70	0.82	0.64	1.15	1.42	1.18	1.03	1.24

	TYPE 2			TYPE 4			WILEY'S RIVER INTRUSION						
	040	058	099	086	119	118	187	189	190	191	196	198	199
La	11.41	7.87	14.81	14.25	20.41	20.25	9.11	7.74	8.53	9.10	11.62	17.04	6.06
Ce	30.35	26.24	37.76	37.98	50.49	53.28	27.22	21.56	26.32	29.45	32.79	42.76	18.18
Nd	15.67	17.38	20.10	19.31	24.60	26.97	15.48	11.71	15.55	15.95	17.14	21.04	10.88
Sm	3.59	3.89	4.44	4.21	5.04	5.44	3.57	2.68	3.33	3.29	3.60	4.71	2.67
Eu	0.84	1.11	1.19	1.01	0.83	1.14	0.26	0.39	0.65	0.44	0.71	0.59	0.31
Gd	3.37	3.22	3.90	3.83	4.63	5.18	3.84	2.97	4.19	4.08	4.00	5.16	3.29
Dy	2.56	3.32	3.10	2.68	3.42	4.07	3.24	2.63	3.78	4.47	3.39	4.64	3.37
Er	1.17	2.15	1.81	1.92	2.06	2.26	1.05	1.30	1.57	2.10	1.50	2.49	1.75

ALL SAMPLES ARE KQS-82-xyz - GSC sample number; data from Stewart (1985)

higher SiO_2 values and with greater variability (Fig. 16). Buchans Group felsic flows have TiO_2 and Zr abundances that show considerable overlap with the fields for both Feeder Granodiorite bodies as well as approximating (albeit at slightly lower SiO_2 contents) the measured abundances in the granitoid clasts (Fig. 16, 17). Rhyolitic flows of the Lundberg Hill Formation in the Little Sandy Lake area and the Buchans River Formation have similar trace element abundances to both Feeder Granodiorite bodies, the granitoid clasts and other Buchans Group felsic flows (Fig. 16, 17). The separation of the Topsails granite from all other rock units is evident on these diagrams.

The fields for the two Feeder Granodiorite bodies are virtually coincident if other trace elements (Nb, Ga, Sr) are considered with Zr and Y (Fig. 18). These fields fall entirely within the larger field described by the granitoid clasts when Ga and Nb are plotted (Fig. 18a, b). Topsails granite is separated on these three plots with only a slight overlap on the Zr/Y/Ga plot (Fig. 18b).

On the Zr/Y/Sr plot, the field of the granitoid clasts extends from the fields of the Feeder Granodiorite bodies toward the Sr apex (Fig. 18c). Sr has been added to the 'granitic' clasts during the formation of calcite by hydrothermal alteration shifting the field for the granitoid clasts toward the Sr apex (Stewart, 1984, 1985). The less altered 'aplitic' group clasts predominate on the left side of the granitoid clast field (Stewart, 1985) closest to the fields of Feeder Granodiorite bodies suggesting similar compositions in these rock units.

Bell and Blenkinsop (1981) determined similar initial Sr isotopic compositions of 0.7068 and 0.7072 for the Wiley's River intrusion and the Buchans Group, repectively. No attempts were made to determine this ratio in the clasts after recognition of Sr mobility during alteration of the granitoid clasts.

REE patterns for the Wiley's River intrusion and felsic volcanic rocks from the Lundberg Hill Formation (data from

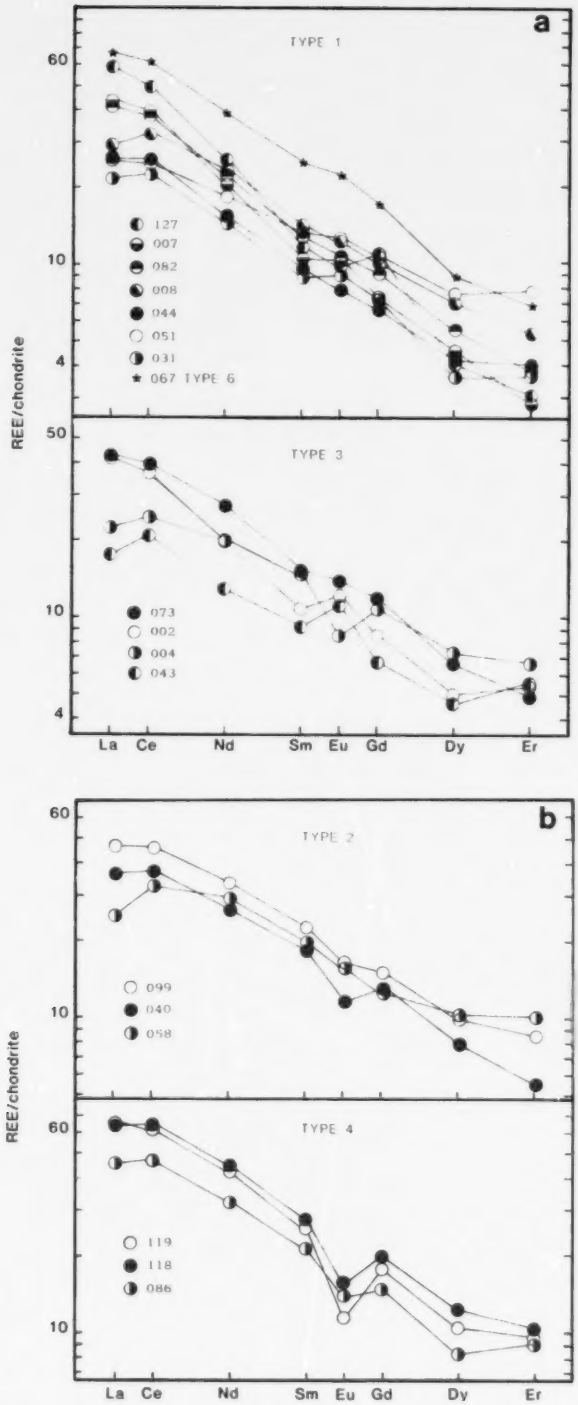

Figure 15. **a**) Chondrite normalized (to chondrite values of Taylor and Gorton, 1977) rare earth element plots for granitoid clast types 1, 3 and 6; **b**) Chondrite normalized rare earth element plots for granitoid clast types 2 and 4. Symbols and accompanying numbers designate the sample analysed (all numbers are KQS-82-xyz).

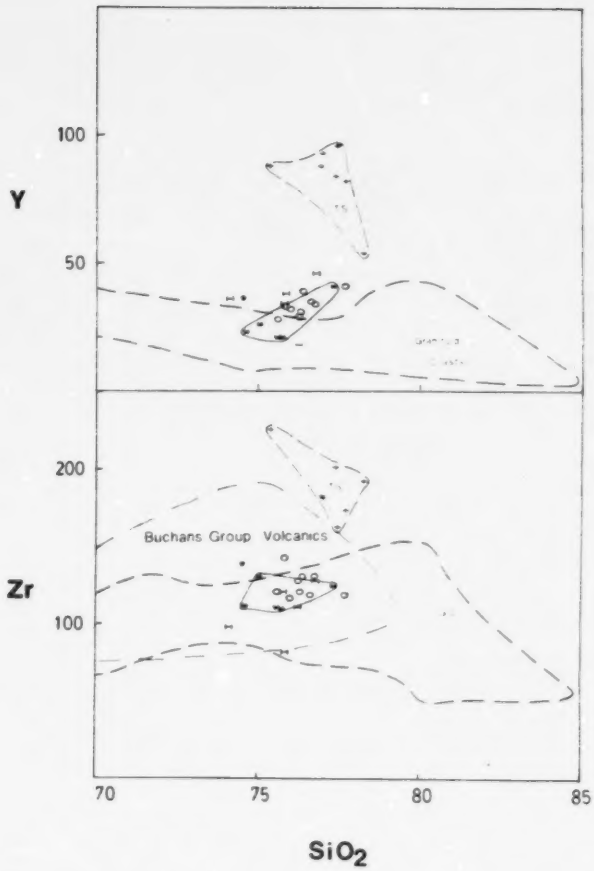

Figure 16. SiO_2 (weight %) versus Y and Zr (in ppm) variation diagrams; Crosses (+) represent Topsails alkali feldspar granite, asterisks (*) represent Little Sandy Lake intrusion, circles (0) represent Wiley's River intrusion, the star represents the Buchans Formation rhyolite used in the geochronology study, and (H) represent Lundberg Hill Formation rhyolites from the Little Sandy Lake area. Fields of Buchans Group felsic flows (BV) (data from Thurlow, 1981a) and granitoid clasts (GC) are shown.

Strong, 1984) are shown in Fig. 19. Similar light REE enriched patterns are shown by each rock unit, despite some variability in the patterns of the Buchans Group flows. The consistent negative Eu anomaly of the Wiley's River intrusion indicates that its magma source was probably affected by plagioclase fractionation during crystallization (Hanson, 1980) and is, therefore, slightly more evolved than the volcanic rocks. Buchans Group flows do not demonstrate a consistent negative or positive Eu anomaly.

Comparison of these patterns with the REE patterns of the granitoid clast types (Fig. 15) reveals little substantial difference in the patterns or in the range in REE abundance levels between the populations. An increasingly negative and more consistent Eu anomaly can be seen when comparing the

Table 4. Averaged chemical analyses of granitoid clasts, Feeder Granodiorite (Wiley's River intrusion and Little Sandy Lake intrusion), Buchans Group felsic flows and Topsails alkali feldspar granite

	Granitoid Clasts		Wiley's River Intrusion		Little Sandy Lake Intrusion		Buchans Group Felsic Flows #		Little Sandy Lake Felsic Flows		Topsails Granite	
SiO_2	73.66	(2.81)	75.10	(.82)	73.48	(1.15)	71.44	(3.56)	73.86	(1.06)	76.24	(1.04)
TiO_2	.18	(.04)	.23	(.03)	.23	(.05)	.34	(.17)	.22	(.06)	.13	(.07)
Al_2O_3	11.36	(1.15)	12.09	(.24)	12.38	(.40)	13.31	(1.17)	12.36	(.25)	11.96	(.44)
Fe_2O_3*	1.63	(1.02)	2.06	(.14)	3.19	(.47)	2.94	(1.57)	2.79	(.87)	1.39	(.30)
MnO	.05	(.02)	.05	(.01)	.08	(.02)	.07	(.05)	.10	(.01)	.03	(.02)
MgO	.62	(.38)	.46	(.11)	1.16	(.14)	.83	(.69)	1.35	(.68)	.11	(.07)
CaO	2.26	(.70)	1.50	(.32)	.93	(.33)	1.69	(1.00)	1.05	(.30)	.33	(.22)
Na_2O	4.07	(.84)	4.31	(.20)	4.80	(.26)	4.08	(.96)	4.42	(1.09)	3.94	(.08)
K_2O	1.11	(.63)	2.15	(.32)	.78	(.27)	2.57	(1.28)	1.26	(.62)	4.64	(.15)
P_2O_5	.06	(.08)	.05	(.02)	.08	(.02)	nd		.09	(.05)	.03	(.02)
LOI	2.90	(.89)	.59	(.19)	1.54	(.22)	1.96	(1.02)	2.03	(.46)	.51	(.09)
TOTAL	97.90		98.90		98.65		99.23		99.53		99.31	
TRACE ELEMENTS (ppm)												
Pb	101	(147)	13	(5)	7	(2)	nd		6	(3)	18	(5)
Th	12	(4)	11	(2)	10	(4)	nd		5	(4)	30	(2)
U	2	(12)	2	(2)	0		nd		0		8	(3)
Rb	19	(10)	54	(11)	17	(7)	45	(24)	24	(13)	152	(21)
Sr	321	(162)	129	(11)	118	(27)	155	(82)	70	(20)	24	(14)
Y	21	(10)	34	(4)	26	(8)	nd		34	(10)	84	(14)
Zr	100	(25)	126	(8)	118	(10)	130	(35)	108	(18)	189	(21)
Nb	5	(2)	5	(1)	4	(5)	8	(4)	3	(1)	35	(5)
Zn	128	(97)	21	(7)	35	(9)	nd		47	(9)	28	(9)
Cu	35	(26)	11	(7)	15	(6)	nd		15	(3)	16	(15)
Ni	0		0		0		nd		0		0	
Ba	9708	(8748)	982	(198)	368	(181)	894	(431)	281	(192)	342	(113)
V	34	(19)	19	(3)	38	(3)	28	(23)	13	(11)	4	(4)
Cr	0		0		0		nd		0		0	
n =	38		9		5		23		5		7	

* = total Fe reported as Fe_2O_3; n = number of samples
standard deviation (1σ) in brackets; nd = not determined;
0 = measured abundance is below analytical detection limit (approx. 1 ppm)
\# = data from Thurlow (1981a); all other data from Stewart (1985)

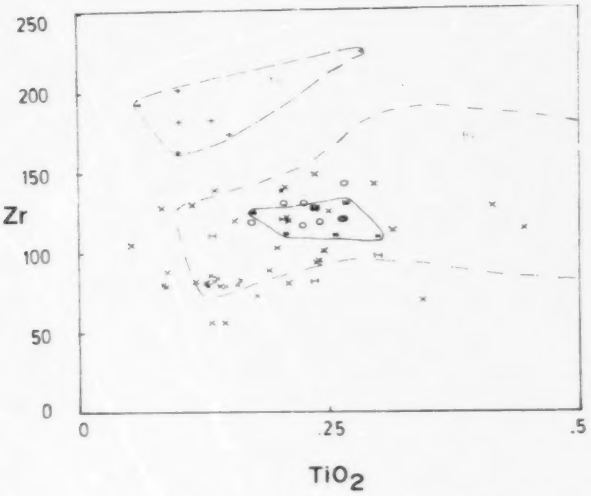

Figure 17. TiO_2 (weight %) versus Zr (in ppm) variation diagram. Field of Buchans Group felsic flows (BV) (data from Thurlow, 1981a) is shown. Symbols as defined in Figure 16, plus (x) represent granitoid clasts.

Buchans Group volcanic rocks to the 'granitic' clasts to the 'aplitic' clasts to the Wiley's River intrusion (Fig. 15, 19). The continual crystallization of plagioclase in the source magma chamber is a feasible explanation of this relationship.

Tectonic setting

The island arc setting of the Buchans Group volcanic rocks (Strong, 1977; Thurlow, 1981a) is supported on trace element discrimination diagrams for the tectonic interpretation of granitic rocks (Pearce *et al.*, 1984). The granitoid clasts, Feeder Granodiorite and Buchans Group felsic flows plot within the volcanic arc granite (VAG) field (Fig. 20). The identification of a different magmatic source for the Topsails granite is clear (Fig. 20b).

The fields for the granitoid clasts and Feeder Granodiorite bodies do not coincide exactly. However, loss of potassium during alkali metasomatism of the granitoid clasts may explain the lower Rb contents in some (Fig. 20a). Limited mobility of the "immobile" HFS elements or the effects of

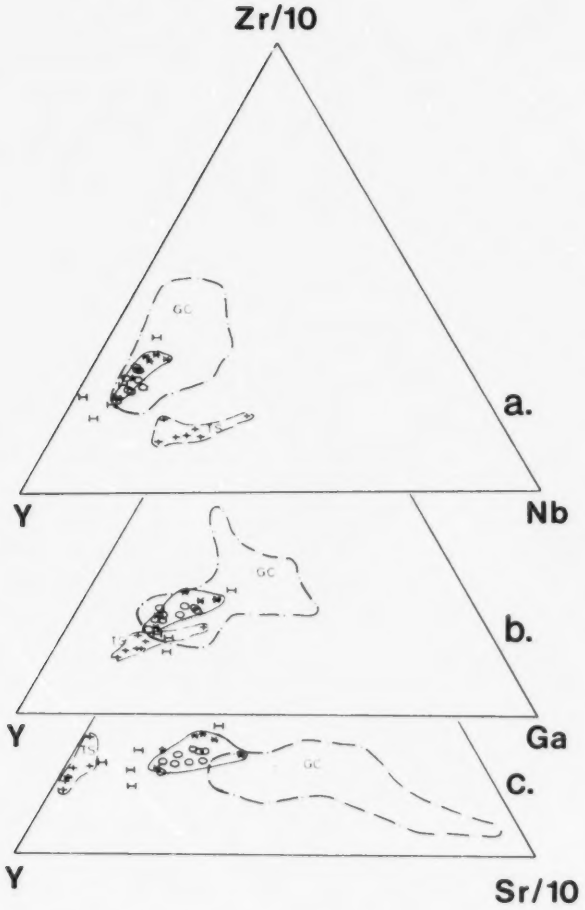

Figure 18. Triangular plots of trace elements (Zr, Y, Nb, Ga and Sr, in ppm). Field of granitoid clasts (GC) is shown. Symbols as defined in Figure 16.

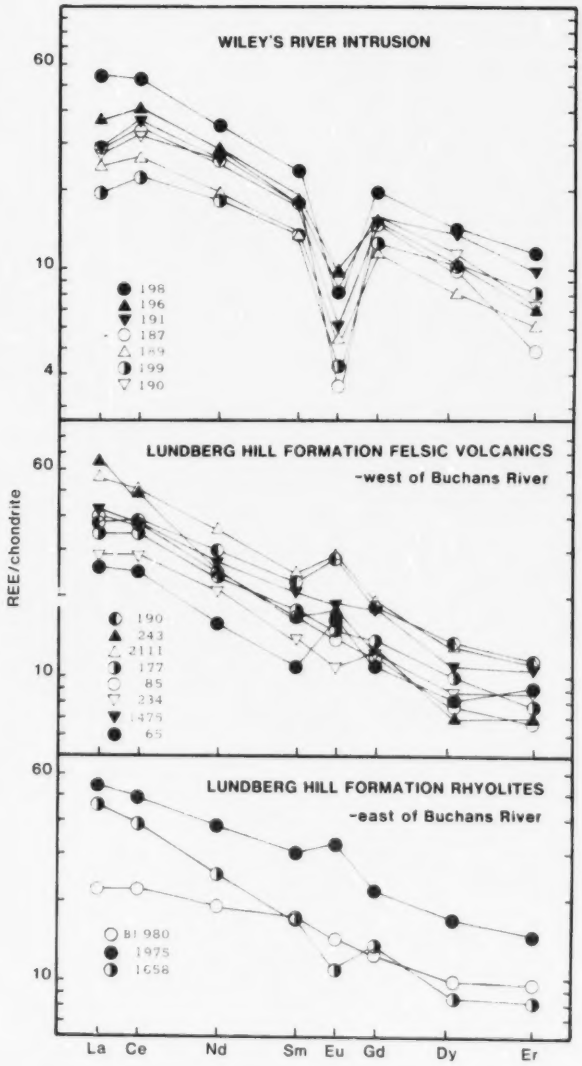

Figure 19. Chondrite normalized (to chondrite values of Taylor and Gorton (1977)) rare earth element plots for Lundberg Hill Formation rhyolites of the Buchans Group (data from Strong, 1984), and Wiley's River intrusion (WRI). Symbols and accompanying numbers designate the sample analysed. Wiley's River area samples are all KQS-82-xyz.

dilution on their measured abundances due to additions of other elements during alteration probably best explains the scatter parallel to the Y + Nb axis of the granitoid clast samples.

The loss of K during alkali metasomatism from the Little Sandy Lake intrusion, similar to that of some granitoid clasts, is expressed by its lower Rb contents (Fig. 20b). The slight shift upward and to the right of the Wiley's River intrusion relative to the other rock units is indicative typically of a slightly greater degree of differentiation (Pearce *et al.*, 1984).

In summary, the "immobile" trace element data for the granitoid clasts, Buchans Group felsic flows and the Feeder Granodiorite are very similar. Evidence of slight differences in the degree of magma evolution for these rock units is seen. The geochemical data are compatible with a common magmatic source for these rock groups.

GEOCHRONOLGY

U-Pb zircon age-dates have been completed for the largest granitoid clast in the MacLean Extension Orebody (Fig. 9) and a quartz and plagioclase-phyric rhyolite of the Buchans River Formation within 30 m stratigraphically underneath the debris flow deposit that contained the granitoid clast. Unfortunately, in addition to the fine grain size and scarcity of zircons in each sample, analytical problems during the study

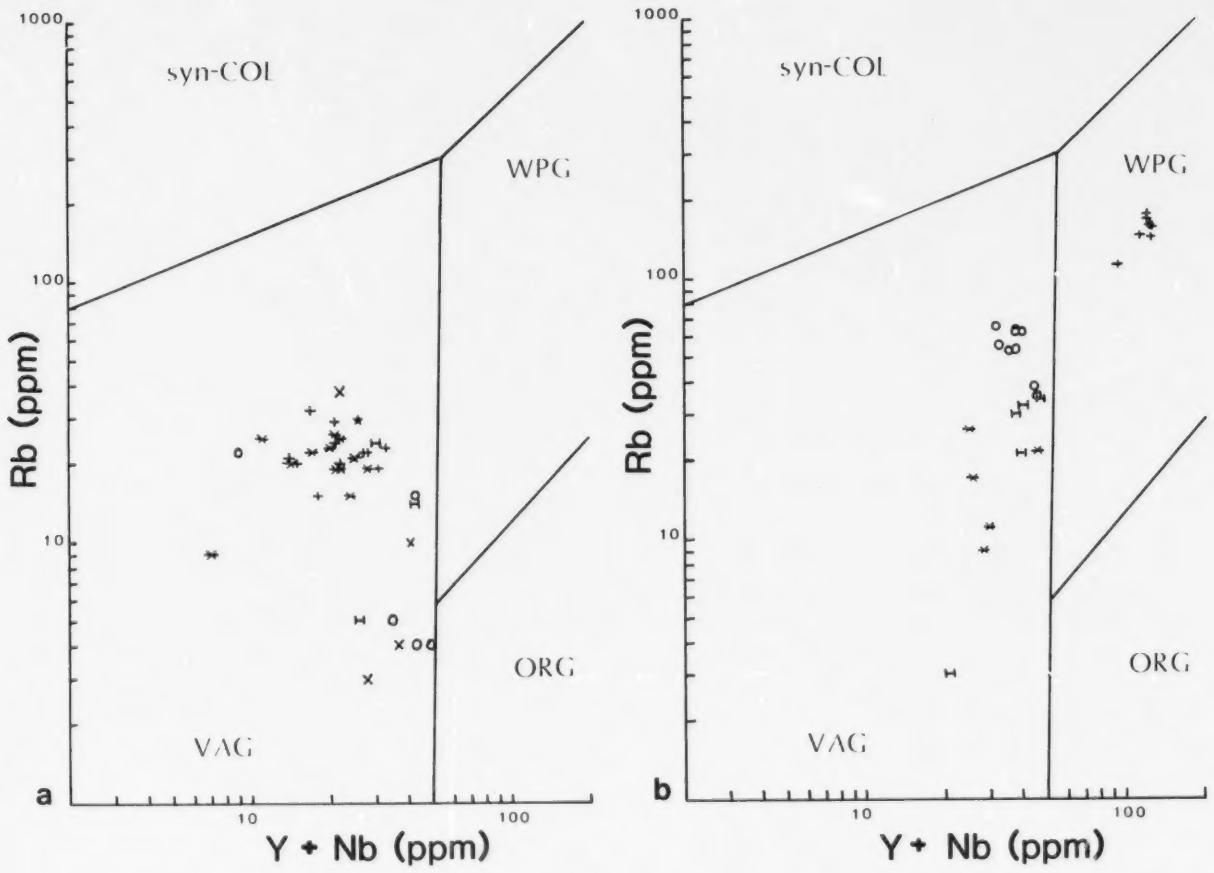

Figure 20. Tectonic discrimination diagram of Pearce et al. (1984) with fields for volcanic arc granites (VAG), ocean ridge granites (ORG), within plate granites (WPG) and syn-collosion granites (syn-COL) shown: **a**) for granitoid clast types, symbols as defined in Figure 12; **b**) other populations considered, symbols as defined in Figure 16.

have resulted in imprecise data and require the data to be considered tentative and preliminary.

Zircons in both samples have stubby euhedral morphologies characteristic of high-level or extrusive felsic rocks. Model ages for two zircon fractions from the rhyolite show significant discordance (up to 55 Ma) that is considered to be due to recent lead loss and/or a small component of older cores (R.W. Sullivan, personal communication, 1986). However, two other zircon fractions from the rhyolite are more concordant and have an average $^{207}Pb/^{206}Pb$ model age with broad uncertainty limits of 465 ± 10 Ma. This age is taken to represent the time of extrusion of the rhyolite (R.W. Sullivan, personal communication, 1986). Although the model ages for the granitoid clast zircon fraction analyzed are relatively concordant, a large uncertainty on the $^{207}Pb/^{206}Pb$ model age (464 ± 40 Ma) is considered appropriate because of the analytical uncertainties.

Despite the broad uncertainy limits, the geochronological data are considered to support the hypothesis that the granitoid clasts were derived from high-level intrusions coeval with Buchans Group volcanism (R.W. Sullivan, personal communication, 1986). Further geochronological work is clearly necessary to resolve the absolute age of the Buchans Group within the Middle Ordovician.

ORIGIN OF THE GRANITOID CLASTS

The proposed model is based primarily on observations of granitoid clasts in MacLean Extension area. Insufficient observations and lack of accessibility preclude definitive statements regarding the differences or similarities to granitoid ciasts in other transported orebodies at Buchans.

Stable isotope studies at Buchans indicate that the mineralizing fluids were composed dominantly of seawater, but with a minor component of magmatic fluids (Kowalik *et al.*, 1981). These data suggest the existence of a magma chamber beneath the Buchans orebodies at the time of ore deposition. Major, trace and rare earth element abundances in the granitoid clasts indicate that all types probably had a common

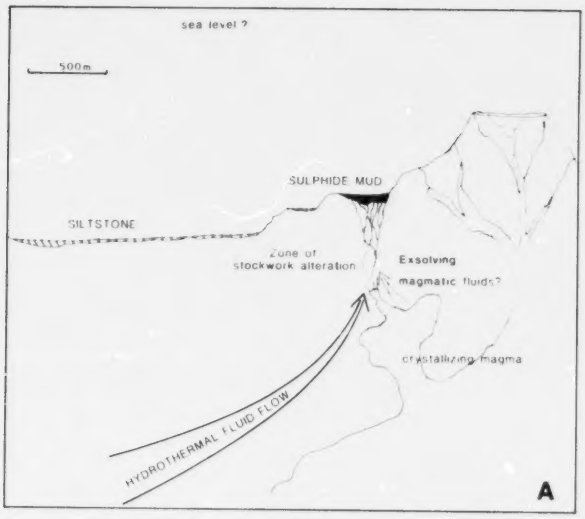

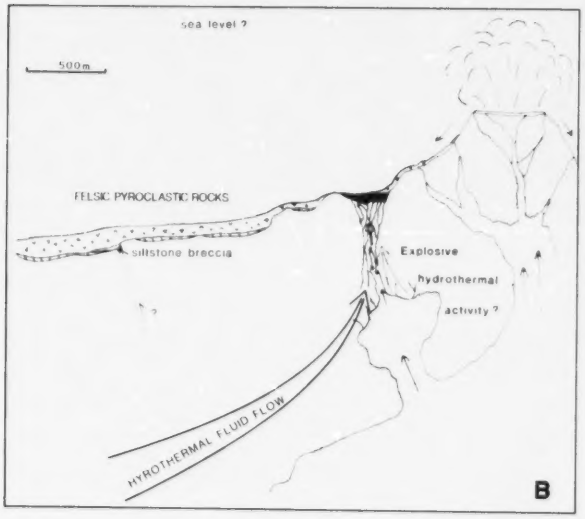

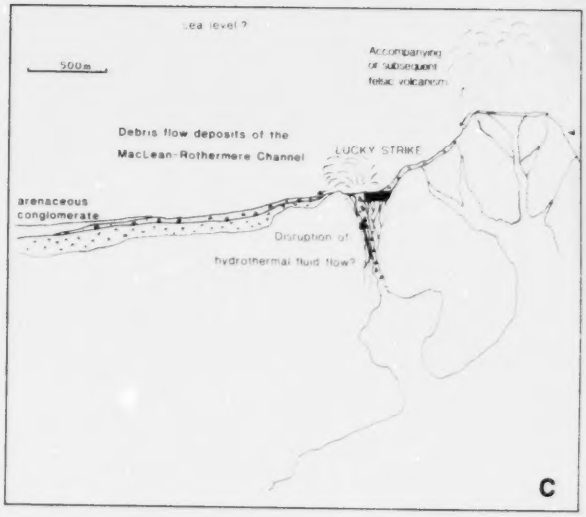

Figure 21. Model for the genesis of the granitoid clasts associated with MacLean Extension and related transported sulphide orebodies. **A**) Hiatus in felsic volcanism with deposition of in situ sulphide bodies and siltstone unit, partial crystallization of underlying magma chamber resulting in the exsolution of a volatile phase that fractures the intruded rock and possibly contributes fluid and metals to the mineralizing hydrothermal fluids. **B**) Period of felsic pyroclastic volcanism, propagation of breccia pipe from magma chamber due to exsolving hydrothermal fluids, these fluids round, alter and transport granitoid clasts upward. **C**) Either accompanying or preceeding another period of felsic pyroclastic activity, the breccia pipe explosively breaches the surface in the vicinity of the in situ sulphide deposits ejecting the granitoid clasts and probably initiating the debris flows. Subsequent debris flows are increasingly less sulphide- and granitoid-rich and are presumed to indicate a waning of sulphide mineralization and the explosiveness of the associated hydrothermal activity.

magmatic source. Similarly, major, trace and REE abundances suggest that the granitoid clasts, Feeder Granodiorite and Buchans Group felsic volcanic rocks also had a common magmatic source.

A volatile phase becomes concentrated in the melt during magma crystallization with the melt eventually becoming saturated with volatiles and exsolving a hydrous fluid phase (i.e., second boiling, Burnham, 1979). The exsolution of this fluid may rupture the enclosing strata and, if it occurs at shallow enough depths, may vent explosively to the surface (Burnham, 1985). This process is considered to be the cause of breccia pipes with or without rounded intrusive fragments associated with some Kuroko and porphyry copper orebodies (Norton and Cathles, 1973; Takanouchi, 1978; Urabe *et al.*, 1983; Sillitoe, 1985). The rounding of granitoid clasts by the expulsion of hydrous fluids from a magma system is particularly well evidenced at Cornwall, England (Allman-Ward *et al.*, 1982).

Periodic, explosive felsic volcanism typifies the Buchans River Formation with the deposition of siltstone and massive sulphide in situ orebodies recording a period of volcanic quiescence (Fig. 21a). It is proposed that during this hiatus a breccia pipe began to emanate from the magma chamber as a result of an increase in fluid pressure generated by second boiling (Burnham, 1985). As the pipe propagated toward the surface, crystalline intrusive material was transported upward from the magma chamber (Fig. 21b). It is clear that previously mineralized and altered stockwork rocks were also apparently brought from depth and subsequently incorporated into Buchans debris flows (Thurlow and Swanson, 1981; Henley and Thornley, 1981; Binney, 1987).

Figure 22. Photograph of polylithic breccia-conglomerate showing irregular outer surface of granitoid clast in contrast to smooth, rounded surface of nearby rhyolite clast.

The 'fluidization' model of Reynolds (1954) is commonly invoked to explain the transportation of rock material from crustal depths (Allman-Ward *et al.*, 1982; McCallum, 1985). However, the relative density differences between the fluid and any transported rock material require very high velocity fluid streaming to suspend or transport rock material (Wolfe, 1980). For this reason Wolfe and the author favour explosions rather than a constant high velocity fluid flow to provide the required velocities for transport of subsurface material upward, i.e., they are moved ballistically.

No evidence exists that the greater degree of rounding of the granitoid clasts relative to other clast lithologies is a result of sedimentary processes. The elongate form and irregular surface of many granitoid clasts (Fig. 22) are atypical of boulders and cobbles of undeformed felsic intrusive rocks rounded by sedimentary processes. Rounding, brecciation and alteration of the granitoid clasts is believed to have occurred during their transportation to the surface by hydrothermal fluids in a breccia pipe.

The high degree of rounding of some granitoid clasts may indicate repeated episodes of these explosions as the breccia pipe(s) was being propogated to the surface. Periodic movement on faults, which also probably control breccia pipe locations (Mitcham, 1974), would both promote rounding by comminution in zones of constriction and by promoting the periodic explosive release of fluid. A periodicity in explosive activity may also be expected if mineral deposition blocks fluid channelways and builds up fluid pressure until it exceeds lithostatic pressure. The correlation between the degree of rounding, intensity of alteration and clast grain size (i.e., 'granitic' group clasts) suggests a longer exposure time to the hydrothermal fluids responsible for alteration and transportation (i.e., greater distance travelled?).

The location of such a breccia pipe within the Buchans Group is unknown. However, the distribution of the granitoid clasts in the MacLean Extension area is interpreted to constrain the location of the source of the granitoid clasts. The occurrence of the most sulphide-rich section at the base of the earliest debris flows may be considered explicable by density sorting during transportion (Binney, 1987). However, the correlation of the most granitoid-rich sections of the debris flows with the sulphide matrix ore can not be explained by density sorting. No concentration of other clast lithologies with the sulphide-rich zones of the debris flows is apparent. This suggests that the source of the granitoid clasts and the site of the sulphide deposition were spatially associated prior to the incorporation of the clasts in the debris flows. The hydrothermal alteration of the granitoid clasts is similar to that typically seen in volcanic rocks associated with Buchans and other massive sulphide deposits, i.e. chloritization of mafic minerals, sericitization of plagioclase, and the introduction of carbonate and silica (Thurlow, 1981a; Franklin *et al.*, 1981; Urabe *et al.*, 1983). This suggests exposure of the granitoid clasts to the hydrothermal fluids responsible for sulphide mineralization prior to their incorporation in the debris flows. These features suggest that the breccia pipe was located within the zone of stockwork alteration and sulphide mineralization underlying the in situ orebodies.

Debris flow movement was initiated apparently by some high energy event, such as explosive hydrothermal or volcanic activity or earthquakes related to either process (Thurlow and Swanson, 1981; Walker and Barbour, 1981; Binney *et al.*, 1983; Binney, 1987). The presence of the largest, most altered, most abundant and coarsest grained granitoid clasts with the sulphide-rich sections of the earliest debris flows suggest that the explosions that transported the granitoid clasts to the surface may have also inititated the debris flow movement (Fig. 21c). The decrease in the ratio of sulphides to barite in subsequent debris flows indicates that a significant change of the hydrothermal system occurred during the deposition of the debris flows.

The change in the character of the granitoid clasts (i.e. from 'granitic' to 'aplitic' group clasts) reflects a change in the source region of the granitoid clasts during the period of debris flow movement. The more evolved composition, finer grain size and abundant granophyric textures of the 'aplitic'

clasts indicate that they probably crystallized more rapidly at shallower levels than the 'granitic' group of clasts. The lower degree of alteration in the 'aplitic' clasts possibly indicates a more rapid transportation history than for the 'granitic' clasts. These differences plus the absence of any granitoid clasts in the upper ore unit suggest a diminishing energy level of the explosive activity. A drop in the explosive energy may be expected after breccia pipes breach the surface releasing confined hydrothermal pressures. The lack of known economic sulphide concentrations at higher stratigraphic levels indicates the possible termination of sulphide mineralization as a result of this explosive activity.

No other potential source for the granitoid clasts can account for the following features: the apparent comagmatism of all granitoid clasts, coeval subvolcanic intrusions and the hosting volcanic rocks; the similar (but imprecise radiometric) ages for a Buchans Group rhyolite and a granitoid clast; the range of igneous textures present in the granitoid clasts; the variable hydrothermal alteration of the granitoid clasts; the correlation between degree of roundness, alteration and brecciation demonstrated by some granitoid clasts; the intimate association of the largest, most altered 'granitic' clasts with maximum sulphide accumulations in debris flows; and the subsequent increase in the proportion of smaller, less volumetrically important and less hydrothermally altered 'aplitic' clasts in later lower grade debris flows.

A weakness of this model is the absence of known breccia pipes in the vicinity of the in situ and stockwork orebodies. However, the recent recognition of the thrust duplex structures formed during a period of thrust movement of the Buchans Group and the resulting improvements in the stratigraphic model of the Buchans Group adds to the plausibility of this model. The localization of thrust movements on bedding planes and zones of previous movement and/or alteration suggested by Thurlow and Swanson (1987) is significant. The zone of intense alteration underlying the original sites of in situ sulphide mineralization would almost certainly be one of the zones affected by the later thrust movement. The presence of the in situ Oriental Orebodies at the base of the Oriental thrust block is an example of this relationship (Thurlow and Swanson, 1987). The removal of the in situ orebodies from their original site of deposition by faulting seems probable. The direction of thrusting toward the southeast (Thurlow and Swanson, 1981, 1987) suggests that the original site may have been overthrust and occurs at depth northwest of Buchans. This could be a feasible explanation why no breccia pipes are observed near Buchans.

SUMMARY AND CONCLUSIONS

Granitoid clasts are products of the magma system responsible for the felsic volcanic rocks of the Buchans Group. The granitoid clasts were altered, rounded and transported to the surface in breccia pipes by explosive release of volatiles, at least in part due to the exsolution of aqueous fluids from the underlying magma. The explosive hydrothermal events that transported the granitoid clasts (and fragments of previously deposited lithologies) to the surface also may have initiated the movement of the debris flows. This explosive activity might have resulted in the eventual cessation of massive sulphide deposition at Buchans.

The Feeder Granodiorite is considered to be a high-level plutonic facies of the Buchans Group, and evidence of a slightly more evolved magma than that which produced the Buchans Group felsic volcanic rocks and granitoid clasts. Textural, mineralogical and geochemical similarities between the granitoid clasts and comagmatic subvolcanic intrusions suggested by Thurlow (1981a, b) are considered to be verified.

ACKNOWLEDGMENTS

Financial support for the field and geochronological work was provided by a Canada Department of Energy, Mines and Resources personal research contract (Contract No. 1583327).

ASARCO Ltd. and Abitibi-Price Co. Ltd. co-operated completely with the author during his stay in Buchans. Permission to go underground, access to drill core and to company files, maps and other material in their offices at Buchans was essential for the success of this study. The occasional use of company vehicles and contracted helicopter services, greatly assisted the conduction of the study and is greatly appreciated.

This work constitutes the results of an M.Sc. thesis at Memorial University of Newfoundland. The period of residency at Memorial University (1982-84) was provided by a Natural Sciences and Engineering Research Council Postgraduate Scholarship, which is gratefully acknowledged. Some financial assistance during this period was also provided from NSERC Operating Grant No. A7975 to D.F. Strong.

The guidance and advice of D.F. Strong (M.U.N.), R.V. Kirkham (G.S.C.), E.A. Swanson (ASARCO), and especially J.G. Thurlow (Abitibi-Price) throughout this study is most appreciated. Thanks are extended to many workers at the Geological Survey of Canada Geochronology Laboratory, Ottawa, in particular R.W. Sullivan, for their assistance, cooperation and good humor during the somewhat ill-fated radiometric age study. This manuscript has benefitted greatly from reviews by R.V. Kirkham.

REFERENCES

Allman-Ward, P., Halls, C., Rankin, A., and Bristow, C.M.
1982: An intrusive hydrothermal breccia body at Wheal Remfry in the western part of the St. Austell granite pluton, Cornwall, England; in Metallization Associated with Acid Magmatism v. 6, ed. A.M. Evans; Wiley, Chichester, p. 1-28.

Barker, F.
1979: Trondhjemite: definition, environment and hypotheses of origin; in Trondhjemites, Dacites and Related Rocks, ed. F. Barker; Elsevier, Amsterdam, p. 1-12.

Bell, K. and Blenkinsop, J.
1981: A geochronologic study of the Buchans area, Newfoundland; in The Buchans Orebodies: Fifty years of Geology and Mining, ed. E.A. Swanson, D.F. Strong and J.G. Thurlow; Geological Association of Canada, Special Paper 22, p. 91-111.

Binney, W.P.
1987: A sedimentological investigation of MacLean channel transported sulphide ores; in Buchans Geology, Newfoundland, ed. R.V. Kirkham; Geological Survey of Canada, Paper 86-24, Report 8.

Binney, W.P., Thurlow, J.G., and Swanson, E.A.
1983: The MacLean Extension orebody, Buchans, Newfoundland; in Current Research, Part A, Geological Survey of Canada, Paper 83-1A, p. 313-319.

Bowden, P., Batchelor, R.A., Chappell, B.W., Didier, J., and Lameyre, J.
1984: Petrological, geochemical and source criteria for the classification of granitic rocks: a discussion; Physics of the Earth and Planetary Interiors, v. 35, p. 1-11.

Briqueu, L., Bougault, H., and Joron, J-L.
1984: Quantification of Nb, Ta, Ti and V anomalies in magmas associated with subduction zones: petrogenetic implications; Earth and Planetary Science Letters, v. 68, p. 297-308.

Burnham, C.W.
1979: Hydrothermal fluids at the magmatic stage; in Geochemistry of Hydrothermal Ore Deposits, ed. H.L. Barnes; John Wiley and Sons, New York, p. 71-136.

Burnham, C.W.
1985: Energy release in subvolcanic environments: implications for breccia formation; Economic Geology, v. 80, p. 1515-1522.

Calhoun, T.A. and Hutchinson, R.W.
1981: Determination of flow direction and source of fragmental sulphides, Clementine deposit, Buchans, Newfoundland; in The Buchans Orebodies: Fifty Years of Geology and Mining, ed. E.A. Swanson, D.F. Strong and J.G. Thurlow; Geological Survey of Canada, Special Paper 22, p. 187-204.

Campbell, I.H., Lesher, C.M., Coad, P., Franklin, J.M., Gorton, M.P., and Thurston, P.C.
1984: Rare-earth element mobility in alteration pipes below massive Cu-Zn- sulphide deposits; Chemical Geology, v. 45, p. 181-202.

Finlow-Bates, T. and Stumpfl, E.P.
1981: The behavior of so-called immobile elements in hydrothermally altered rocks associated with volcanogenic submarine-exhalative ore deposits; Mineralium Deposita, v. 16, p. 319-328.

Franklin, J.M., Lydon, J.W., and Sangster, D.F.
1981: Volcanic-associated massive sulphide deposits; Economic Geology, 75th Anniversary Volume, p. 485-627.

Hanson, G.N.
1978: The application of trace elements to the petrogenesis of igneous rocks of granitic composition; Earth and Planetary Science Letters, v. 38, p. 26-43.

1980: Rare earth elements in petrogenetic studies of igneous systems; Annual Review of Earth and Planetary Sciences, v. 8, p. 371-406.

Hashiguchi, H.
1983: Penecontemporaneous deformation of Kuroko ore at the Kosaka mine, Akita, Japan; Economic Geology Monograph 5, p. 167-183.

Henley, R.W. and Thornley, P.
1981: Low grade metamorphism and geothermal environment of massive sulphide ore formation, Buchans, Newfoundland; in The Buchans Orebodies: Fifty Years of Geology and Mining, ed. E.A. Swanson, D.F. Strong and J.G. Thurlow; Geological Association of Canada, Special Paper 22, p. 205-228.

Humphris, S.E. and Thompson, G.
1978: Trace element mobility during hydrothermal alteration of oceanic basalts; Geochimica et Cosmochimica Acta, v. 42, p. 127-136.

Hutchinson, R.W.
1981: A synthesis and overview of Buchans geology; in The Buchans Orebodies: Fifty Years of Geology and Mining, ed. E.A. Swanson, D.F. Strong and J.G. Thurlow; Geological Association of Canada, Special Paper 22, p. 325-350.

Irvine, T.N. and Baragar, W.R.A.
1971: A guide to the chemical classification of the common volcanic rocks; Canadian Journal of Earth Sciences, v. 8, p. 523-548.

Jackson, K.C.
1970: Textbook of Lithology; McGraw Hill, New York, 552 p.

Kean, B.F., Dean, P.L., and Strong, D.F.
1981: Regional geology of the central volcanic belt of Newfoundland; in The Buchans Orebodies: Fifty Years of Geology and Mining, ed. E.A. Swanson, D.F. Strong and J.G. Thurlow; Geological Association of Canada, Special Paper 22, p. 65-78.

Kowalik, J., Rye, R., and Sawkins, F.J.
1981: Stable isotope study of the Buchans polymetallic sulphide deposits; in The Buchans Orebodies: Fifty Years of Geology and Mining, ed. E.A. Swanson, D.F. Strong and J.G. Thurlow; Geological Association of Canada, Special Paper 22, p. 229-254.

Ludden, J., Gelinas, L., and Trudel, P.
1982: Archean metavolcanics from the Rouyn-Noranda district, Abitibi Greenstone Belt, Quebec: 2. Mobility of trace elements and petrogenetic constraints. Canadian Journal of Earth Sciences, v. 19, p. 2276-2287.

Ludden, J., Daigneault, R., Robert, F., and Taylor, R.P.
1984: Trace element mobility in alteration zones associated with Archean Au lode deposits; Economic Geology, v. 79, p. 1131-1141.

Lynch, G.V. and Pride, C.
1984: Evolution of a high-level, high-silica magma chamber: the Pattison pluton, Nisling Range alaskites, Yukon; Canadian Journal of Earth Sciences, v. 21, p. 407-414.

MacGeehan, P.J. and MacLean, W.H.
1980: An Archean sea-floor geothermal system, 'calc-alkaline' trends and massive sulphide genesis; Nature, v. 286, p. 767-771.

McCallum, M.E.
1985: Experimental evidence for fluidization processes in breccia formation; Economic Geology, v. 80, p. 1523-1543.

McClay, K.R.
1987: Aspects of the structural geology of the Buchans area; in Buchans Geology, Newfoundland, ed. R.V. Kirkham; Geological Survey of Canada, Paper 86-24, Report 3.

Mitcham, T.
1974: Origin of breccia pipes; Economic Geology, v. 69, p. 412-413.

Norton, D.L. and Cathles, L.M.
1973: Breccia pipes- products of exsolved vapor from magmas; Economic Geology, v. 68, p. 540-546.

Nowlan, G.S. and Thurlow, J.G.
1984: Middle Ordovician conodonts from the Buchans Group, central Newfoundland, and their significance for regional stratigraphy of the Central Volcanic Belt; Canadian Journal of Earth Sciences, v. 21, p. 284-297.

Nowlan, G.S. and Thurlow, J.G.
1987: Middle Ordovician conodonts from the Buchans Group; in Buchans Geology, Newfoundland, ed. R.V. Kirkham; Geological Survey of Canada, Paper 86-24, Report 4.

Ohmoto, H. and Skinner, B.J. (ed.)
1983: The Kuroko and related volcanogenic massive sulphide deposits; Economic Geology Monograph 5, 604 p.

Pearce, J.A. and Cann, J.R.
1973: Tectonic setting of basic volcanic rocks using trace element analyses; Earth and Planetary Science Letters, v. 19, p. 290-300.

Pearce, J.A., Harris, N.B.W., and Tindle, A.G.
1984: Trace element discrimination diagrams for the tectonic interpretation of granitic rocks; Journal of Petrology, v. 25, p. 956-983.

Reynolds, D.
1954: Fluidization as a geological process, and its bearing on the problem of intrusive granites; American Journal of Science, v. 252, p. 577-613.

Rosylyakova, N.V. and Rosylyakova, N.A.
1975: Endogenic aureoles of gold deposits – Translation Precis *by* R.W. Boyle; Journal of Geochemical Exploration, v. 6 (1976), p. 383-387.

Sillitoe, R.H.
1985: Ore-related breccias in volcanoplutonic arcs; Economic Geology, v. 80, p. 1467-1514.

Stephens, M.B., Swinden, H.S., and Slack, J.F.
1984: Correlation of massive sulphide deposits in the Appalachian-Caledonian orogen on the basis of paleotectonic setting; Economic Geology, v. 79, p. 1442-1478.

Stewart, P.W.
1983: Granitoid clasts in boulder breccias of MacLean orebody, Buchans, Newfoundland; in Current Rsearch, Part A, Geological Survey of Canada, Paper 83-1A, p. 321-324.
1984: Geochemistry of granitoid clasts from MacLean Extension orebody, Buchans, Newfoundland, and implications on their possible source; in Current Research, Part A, Geological Survey of Canada, Paper 84-1A, p. 462-467.
1985: Geology, geochemistry, geochronology and genesis of granitoid clasts in breccia-conglomerates, MacLean Extension orebody, Buchans, Newfoundland; unpublished M.Sc. thesis, Memorial University of Newfoundland, 327 p.

Strong, D.F.
1977: Volcanic regimes in the Newfoundland Appalachians; in Volcanic Regimes in Canada, ed. W.R.A. Baragar, L.C. Coleman and J.M. Hall; Geological Association of Canada, Special Paper 16, p. 61-90.
1984: Rare earth elements in volcanic rocks of the Buchans area, Newfoundland; Canadian Journal of Earth Sciences, v. 21, p. 775-780.

Swanson, E.A. and Brown, R.L.
1962: Geology of the Buchans orebodies; Canadian Institute of Mining and Metallurgy Bulletin, v. 55, p. 618-626.

Swinden, H.S. and Kean, B.F.
1984: Volcanogenic sulphide mineralization in the Newfoundland Central Mobile Belt; in Mineral Deposits in Newfoundland – a 1984 Perspective, compiled by H.S. Swinden; Newfoundland Department of Mines and Energy, Mineral Development Division, Report 84-3, p. 55-77.

Swinden, H.S. and Thorpe, R.I.
1984: Variations in style of volcanism and massive sulphide deposition in Early to Middle Ordovician island-arc sequences of the Newfoundland Central Mobile Belt; Economic Geology, v. 79, p. 1596-1619.

Takanouchi, S.
1978: High salinity fluid inclusions in breccias of intrusive dikes in Hokuroku Kuroko area, Japan (abstract); International Association on the Genesis of Ore Deposits, 5th Symposium, Program with Abstracts, p. 188.

Taylor, R.P. and Fryer, B.J.
1982: Rare earth element geochemistry as an aid to interpreting hydrothermal ore deposits; in Metallization Associated with Acid Magmatism, ed. A.M. Evans; Wiley and Sons, Chichester, p. 357-365.

Taylor, S.R. and Gorton, M.P.
1977: Geochemical application of spark source mass spectrography III. Element sensitivity, precision and accuracy; Geochimica et Cosmochimica Acta, v. 41, p. 1375-1380.

Thurlow, J.G.
1977: Occurrence, origin and significance of mechanically transported sulphide ores at Buchans, Newfoundland (abstract); Volcanic Processes in Ore Genesis, Geological Society of London, Special Publication No. 7, p. 127.

1981a: Geology, ore deposits and applied rock geochemistry of the Buchans Group, Newfoundland; unpublished Ph.D. thesis, Memorial University of Newfoundland, 305 p.

1981b: The Buchans Group: its stratigraphic and structural setting; in The Buchans Orebodies: Fifty Years of Geology and Mining, ed. E.A. Swanson, D.F. Strong and J.G. Thurlow; Geological Association of Canada, Special Paper 22, p. 79-90.

Thurlow, J.G. and Swanson, E.A.

1981: Geology and ore deposits of the Buchans area, central Newfoundland; in The Buchans Orebodies: Fifty Years of Geology and Mining, ed. E.A. Swanson, D.F. Strong and J.G. Thurlow; Geological Association of Canada, Special Paper 22, p. 113-142.

Thurlow, J.G. and Swanson, E.A.

1987: Stratigraphy and structure of the Buchans Group; in Buchans Geology, Newfoundland, ed. R.V. Kirkham; Geological Survey of Canada, Paper 86-24, Report 2.

Urabe, T., Scott, S.D., and Hattori, K.

1983: A comparison of footwall-rock alteration and geothermal systems beneath some Japanese and Canadian volcanogenic massive sulphide deposits; Economic Geology, Monograph 5, p. 345-364.

Walker, P.N. and Barbour, D.M.

1981: Geology of the Buchans ore horizon breccias; in The Buchans Orebodies: Fifty Years of Geology and Mining, ed. E.A. Swanson, D.F. Strong and J.G. Thurlow; Geological Association of Canada, Special Paper 22, p. 161-186.

Whalen, J.B. and Currie, K.L.

1987: The relationship of the Topsails igneous terrane to the Buchans Group; in Buchans Geology, Newfoundland, ed. R.V. Kirkham; Geological Survey of Canada, Paper 86-24, Report 6.

Wolfe, J.A.

1980: Fluidization versus phreatomagmatic explosions in breccia pipes; Economic Geology, v. 75, p. 1105-1109.

- 10 -

Evaluation of a resurgent caldera and aspects of ore deposition and deformation at Buchans

R.V. Kirkham and J.G. Thurlow[1]

Kirkham, R.V. and Thurlow, J.G., Evaluation of a resurgent caldera and aspects of ore deposition and deformation at Buchans; in Buchans Geology, Newfoundland, ed. R.V. Kirkham; Geological Survey of Canada, Paper 86-24, p. 177-194, Report 10, 1987.

Abstract

Detailed studies in classic districts, such as Kuroko in Japan and the Noranda camp in Quebec, have led to refinements of the models of volcanogenic massive sulphide deposits settings and genesis. These studies indicate that submarine calderas were instrumental in localizing ore-forming, hydrothermal exhalative activity. A caldera model of ore formation is examined for the Buchans area. Caldera resurgence and synchronous gaseous or phreatomagmatic eruptions could have been important in disrupting syngenetic sulphide and baritic mounds and initiating ore-bearing slumps and debris flows at Buchans.

The synvolcanic disruption of the ores and subsequent major faulting and shearing in the area have led to significant textural modifications of the ores. These modifications are not fully understood but even a partial knowledge of them could be helpful during exploration and development of new orebodies. This paper brings together information from various sources, discusses aspects of the settings of the deposits and presents some working hypotheses for ore deposition and deformation at Buchans.

Résumé

L'étude détaillée de districts classiques, tels que le district de Kuroko au Japon et le camp de Noranda au Québec, ont permis de perfectionner les modèles des milieux et de la genèse des gisements de sulfures massifs d'origine volcanique. Ces études révèlent que des calderas sous-marines ont contribué à localiser l'activité hydrothermale qui a produit les exhalaisons minéralisatrices. Le minerai de Buchans pourrait s'être accumulé dans une caldera. Le soulèvement d'une caldera et des éruptions phréatomagmatiques ou gazeuses synchrones pourraient avoir contribué à la perturbation des monticules syngénétiques du sulfures et de barytine et au déclenchement des coulées et des effondrements de débris métallifères à Buchans.

La perturbation synvolcanique des minerais a été suivie par une importante période de cisaillement et de formation de failles; ces activités ont modifié considérablement la structure des minerais. L'importance de ces modifications n'est pas parfaitement connue, mais même une connaissance partielle de ces changements peut aider l'exploration et la mise en valeur des nouveaux gisements. Cette étude rassemble des renseignements provenant d'une gamme de sources, discute des différents aspects des milieux des gisements et présente quelques hypothèses de travail concernant l'accumulation et la déformation des minerais à Buchans.

[1]BP Canada-Selco Division, Box 789, Corner Brook, Newfoundland A2H 6G7

INTRODUCTION

This paper examines some tentative models of ore deposition and deformation in the light of recent studies at Buchans and elsewhere. It is a discussion paper outlining possibilities rather than offering concrete, well-tested models. The structural complexity at Buchans, primarily a result of an intricate pattern of thrust faults (e.g. Thurlow and Swanson, 1987; McClay, 1987; Calon and Green, 1987), and important gaps in information make more rigorous models impossible at this time. Despite these limitations, working hyphotheses could be of value in exploration and directing further studies at Buchans.

What was the nature of the volcanic environment at Buchans? Was it a submerged or partially submerged calc-alkaline volcanic arc as suggested by several workers or was it more akin to the deeply rifted and submerged bimodal volcanic environment dominated by calderas as in the classic Kuroko districts of Japan? This paper suggests a close analogy to the Kuroko districts, rather than a constructive volcanic arc environment, and explores the possibility of submarine calderas at Buchans.

Thurlow and Swanson (1981) outlined the interrelationship of in situ and transported orebodies at Buchans. However, the question arises as to whether or not 'in situ' orebodies at Lucky Strike, Old Buchans and Oriental were the source of known transported ores or did the transported ores come from somewhere else? Were these 'in situ' orebodies deposited on hydrothermal vent systems or have they also been 'transported' to some degree? What were the trigger mechanisms for the ore-bearing debris flows and how did the granitoid clasts get incorporated into them? Also, what was the nature of processes operating in the debris flows that led to such marked segregation of materials (Binney *et al.*, 1983; Binney, 1987)? What textural modifications of sulphides occurred at this syndepositional stage and can these textural modifications be distinguished from ones formed later during tectonic deformation? These and related questions are addressed in this paper.

POSSIBLE CALDERA ENVIRONMENT OF ORE FORMATION

Thurlow *et al.* (1975) and Thurlow and Swanson (1981) suggested that a strong analogy exists between Middle Ordovician sulphide orebodies at Buchans and Miocene Kuroko ores in the Green Tuff region of Japan. Ohmoto (1978), Kouda and Koide (1978) and Ohmoto and Takahaski (1983) recently emphasized the importance of calderas in the genesis of the Kuroko ores. Evidently calderas averaging 4 to 8 km in diameter in the Hokuroku district were critical in localizing the ore deposits. Some calderas contain several large, rich orebodies while others contain only minor occurrences or are barren. Gibson and Watkinson (1986) and Gibson *et al.* (1986) also recently proposed a caldera origin for the Central Mine Sequence which contains the main volcanogenic massive sulphide deposits in the Noranda camp. In this case the postulated caldera was 20 km in diameter and contained 3000 m of fill. Such a caldera is large by modern standards but is comparable in size to the large Tertiary calderas underlain by Precambrian crust in the Basin and Range Province of the western United States (Walker, 1984). Taube (1986) suggested that the gold- and copper-bearing volcanogenic massive deposit at Mount Morgan in Australia is related to a penecontemporaneous fault that could be part of a large cauldron resurgent structure.

In view of the structural complexity and the uncertainities of the stratigraphic evolution of the Buchans area, identification of possible calderas is difficult. Nevertheless, if calderas could have played an important role in determining the geology of the area and localizing orebodies, even an incomplete knowledge of their nature and distribution could be useful in exploration (e.g. Ohmoto and Takahaski, 1983).

Calderas, except for ones related to large mafic shield volcanoes, typically form during and after explosive eruption of large volumes of pyroclastic material. They are more or less circular volcanic depressions inferred to form by the collapse of the roof of a magma chamber by evacuation of magma from below. The size of collapse feature, in most areas, is related to the volume of pyroclastic material expelled (Lipman, 1984; Walker, 1984). More irregular volcanic-tectonic depressions and volcanic subsidence structures regardless of shape, size, depth of erosion or connection with surface volcanism, called cauldrons, could form by similar processes (Smith and Bailey, 1968; Fig. 1). Quaternary calderas vary widely in size, ranging from 1.6 to over 50 km in diameter with median size being 6.5 km (Walker, 1984). They can be from about 100 to greater than 3000 m deep. In most areas they result from the catastrophic eruption of large volumes of magma, but Walker (1984) argued that they may also form incrementally in several stages related to a series of eruptions.

Caldera-forming eruptions can be followed by a resurgence or uplift within the caldera (cauldron) usually forming a structural resurgent dome(s) (Smith and Bailey, 1968). The causes of resurgence are poorly understood, however, Marsh (1984) suggested that the most likely causes are the combined effects of regional detumescence or subsidence and magmatic vesiculation. The resurgence can be accompanied by post-caldera lava domes and volcanoes both within and outside the limits of the caldera (e.g. Walker, 1984). The uplift can be accompanied by the emplacement of magma in the vicinity of the resurgent dome at shallow depth or a few (4 to 6) kilometres below the surface (e.g. Nielsen and Hulen, 1984; Elbring and Rundle, 1986).

At Buchans the volcanic suite is dominated by pillowed and brecciated basalt and fragmental rhyolite (Thurlow and Swanson, 1987) which is comparable to the submarine bimodal volcanism in Kuroko region of Japan. If caldera collapse was triggered by large volume felsic pyroclastic eruptions, then the Lundberg Hill and Buchans River formations (Thurlow and Swanson, 1987) would be logical places in the stratigraphy in which to search for evidence of calderas. The basalt-dominated Ski Hill Formation, separating the Lundberg Hill and Buchans River formations, and the Sandy Lake Formation, comprised mainly of basalt and arkose,

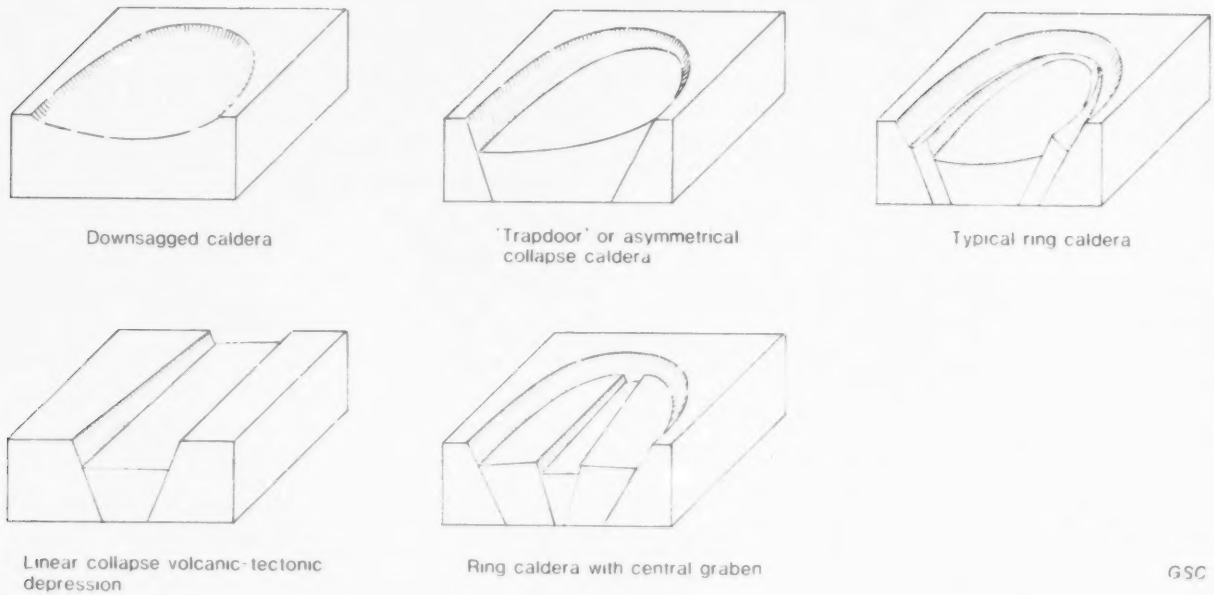

Figure 1. Some typical volcanic collapse structures. Constructed from information in papers on calderas, such as Smith and Bailey, 1968; Lipman, 1984; Walker, 1984.

which overlies the Buchans River Formation, are not likely to have been accompanied by major caldera collapse. Limited information is available to constrain the location of possible calderas formed after pyroclastic eruptions in the Lundberg Hill and Buchans River formations. The thickest and most widespread felsic pyroclastic units occur in the oldest recognized unit, the Lundberg Hill Formation; therefore, the greatest amount of caldera collapse likely would have occurred at this time. The regional extent of felsic pyroclastic rocks in the Lundberg Hill Formation is strong circumstantial evidence for caldera collapse during deposition of the Lundberg Hill Formation. The Ski Hill and Buchans River formations, which overlie the Lundberg Hill Formation, apparently are restricted to the mine area (see Fig. 2 of Thurlow and Swanson (1987) for approximate distributions of Ski Hill and Buchan River formations). Conceivably they could have been deposited in a caldera about 13 km in diameter following pyroclastic eruptions in the Lundberg Hill Formation. No firm evidence exists for such a caldera except for large blocks up to 30 m in diameter that occur in the Lundberg Hill Formation in the Wiley's Lakes area near the known limits of the Ski Hill and Buchans River formations. Such large blocks in a megabreccia could be rock fall or slide deposits located near the rim of a caldera (e.g. Smith and Bailey, 1968; Lambert, 1974; Busby-Spera, 1984; Lipman, 1984).

According to Ohmoto and Takahaski (1983), the Kuroko deposits formed in depressions immediately after caldera collapse and all of the calderas underwent resurgent igneous activity. Since no ore is known in the Lundberg Hill Formation, the Buchans River Formation is the only unit at Buchans in which to examine possible caldera-related ore formation. Figure 2 shows a restored distribution of in situ and transported orebodies at Buchans and some indicated synvolcanic normal faults. The effects of late thrust faults have been removed. The insets show two possible caldera configurations. No simple explanation is possible for the postulated early normal fault geometric relationships but a few possibilities are considered. The indicated movements for synvolcanic block faults (Sandfill-Middle Branch area west side up and the MacLean-Rothermere area south side up) do not support the concept that these are marginal ring faults of a caldera. However, they could be second-order rift structures within a larger caldera (e.g. Inset A, Fig. 2). Alternatively, the MacLean-Rothermere-Lucky Strike-Old Buchans faults may have been curvilinear rim faults and the more linear Sandfill-Middle Branch faults were possibly a related second-order rift within a nested caldera about 5 to 6 km in diameter (Inset B, Fig. 2). However, such curvilinear structures in the Lucky Strike and Old Buchans areas are not sufficiently well documented to be certain of such an interpretation. At present, the first of the two suggested caldera configurations is favoured. The linear array of rhyolite domes and breccias from the Old Buchans to Middle Branch area indicates that this structure probably localized igneous activity but that the MacLean-Rothermere structure had no associated igneous activity (Fig. 2).

Thurlow and Swanson (1987) and Binney (1987) indicate that the stratigraphic units in the vicinity of the transported orebodies in the MacLean channel are thickest in the south abutting reactivated steep faults and tend to pinch-out in a

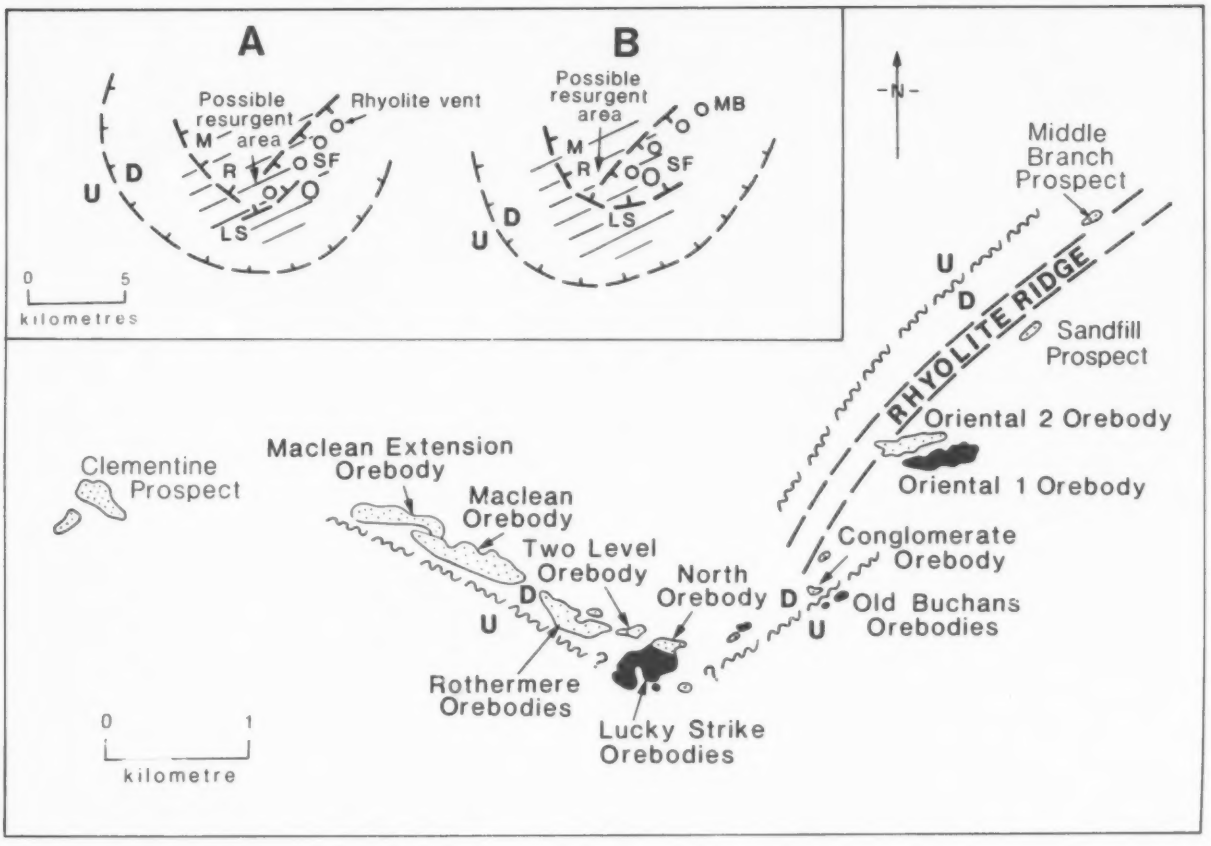

Figure 2. A reconstruction of the location of early normal faults and rhyolite domes and breccias in the vicinity of the Buchans orebodies. Oriental (O), Sandfill (SF) and Middle Branch (MB) deposits have been moved 1 km north to remove displacement on the Ski Hill Fault. The small, late thrust displacement between the Rothermere (R) and MacLean orebodies has also been removed by moving the MacLean (M) and MacLean Extension orebodies to the south. The insets show two possible configurations of calderas: A) One large caldera formed during and/or following eruption of Lundberg Hill felsic pyroclastic rocks with ore-bearing grabens formed on a resurgent dome centred in the general Lucky Strike (LS) area, and B) the same large caldera related to the Lunderg Hill Formation but containing a smaller nested caldera and associated resurgent dome related to the Buchans River Formation. In situ orebodies are solid black and transported orebodies are stippled; D indicates down and U, up movements on postulated synvolcanic faults.

northerly direction. Such stratigraphic thinning away from bounding faults supports the concept of a rotated, down-dropped fault block as would be expected along a steeply north-dipping, syndepositional normal fault. If this was a deep, graben-like structure, as suggested by Thurlow and Swanson (1987), then either the down-dropped block was a half-graben hinged to the north or differential movement occurred on the bounding faults with less movement along the north bounding fault. Many calderas contain deep rift structures (e.g. Smith and Bailey, 1968; Walker, 1984). Some of these rifts are centrally located in the calderas but others are more irregularly distributed. Such second-order rift structures within a caldera are a plausible explanation for the origin for the ore-bearing 'channels'.

As mentioned above, Ohmoto and Takahaski (1983) indicated that all calderas associated with Kuroko ores in the Hokuroku district underwent resurgence and that, in general, the Kuroko deposits formed in paleotopographic lows. Since no unequivocal in situ ores have been identified at Buchans, with the possible exception of some of the Lucky Strike Orebodies (Jambor, 1987), the original sites of ore deposition are unknown. However, bedded siltstone that occurs stratigraphically below the ore at Buchans could yield important information about the paleotopography just prior to ore for-

mation. Binney (1987) indicates that this bedded siltstone unit probably formed in a paleotopographic depression as fine grained, distal turbidites. As the bedded siltstone is not present in the MacLean channel in the MacLean Extension area (except as thin, <1 m, discontinuous lenses), he concludes that the main depression in which the siltstone was deposited occurred to the east of the MacLean Extension area. Nonchannelized turbidites in the bottom of Crater Lake, Oregon (Nelson *et al.*, 1986) and pyritic muds and distal turbidites in the lower Mesozoic subaqueous Vanderver Mountain caldera in the southern Sierra Nevada, California (Busby-Spera, 1984) are similar to the siltstone at Buchans and support the idea that the siltstone at Buchans was deposited in a caldera. At present the bedded siltstone unit is most extensive in the MacLean channel. Because it shows no facies changes near the walls of the channel, the siltstone probably was deposited in a broader basin, possibly the floor of a caldera, immediately prior to the formation of the MacLean channel. However, because this siltstone or correlative sedimentary units have not been identified in many areas outside of the MacLean channel, the configuration of the basin of deposition of this unit remains unknown.

As pointed out by Binney (1987), the incorporation of siltstone clasts in debris flows in the MacLean and MacLean Extension areas indicates that a topographic inversion must have occurred in the area between deposition of the siltstone and siltstone breccia (Fig. 3, stratigraphically lowest indicated debris flow breccia-conglomerate unit). Such a topographic inversion at this stratigraphic position is compatible with caldera resurgence (insets Fig. 2). The centre of the resurgent block or dome was possibly near the town of Buchans, immediately east of the Lucky Strike Orebodies. Although it has not been attempted, considering that the siltstone was probably deposited in a basin on a low-relief surface, reconstructed dips of the siltstone prior to late faulting could outline the position of a resurgent dome. Paleotopographic relief in the vicinity of such a structure could have been considerable, as discussed below. The MacLean channel and Sandfill-Middle Branch structures could have been deep longitudinal and/or radial grabens formed by stresses developed during uplift of a resurgent dome similar to those documented in many calderas (e.g. Smith and Bailey, 1968; Johnson, 1970; Lipman, 1984). As indicated by Walker (1984), some of these rift structures, especially longitudinal grabens, control postcollapse volcanism while others do not.

DEBRIS FLOW PROCESSES

For a clearer understanding of the processes that led to and operated during debris flow transport of sulphides and barite, a knowledge of the paleotopography and its relationship to the volcanic setting, the trigger mechanisms of the debris flows, nature of materials in the debris flows, segregation processes and textural modifications are essential. Binney (1987) and Stewart (1987) consider most of these points but they are also examined in this paper, especially their possible relationship to caldera resurgence.

Paleotopography during ore deposition and resedimentation into the ore-bearing debris flows were important factors controlling the present distribution of orebodies. The debris flows containing abundant siltstone, sulphide and barite clasts and sulphide slump or slide deposits in the MacLean channel are evidence of high paleotopographic relief. The debris flows indicate that, at the time of sedimentation, the sulphide- and barite-rich source areas must have been in unstable, topographically high positions (e.g. Fig. 3). In the MacLean channel the ore-bearing material was transported at least 4 km down the paleoslope primarily to the northwest (Binney, 1987). Binney's work (1984, 1987) indicates that the paleoslope was probably similar to the present slope from the Two Level Orebody near surface to the MacLean Extension Orebody about 1100 m vertically below surface, despite the fact that the area is cut by numerous faults. Although his calculations are approximate, he indicates that paleoslopes were in the order of 6 to 10° for the lower ore unit and 3° for the siltstone breccia-conglomerate and baritic upper ore unit in MacLean Extension area. However, he suggests that paleoslopes in excess of 10 to 15° in the MacLean area might have been necessary for the debris flows to transport the large clasts through this area to the MacLean Extension Orebody. Assuming an average paleoslope of 10° over 4 km, the paleotopographic relief in the MacLean channel during ore deposition would have been about 700 m. Paleoslopes of 5° and 15° would have resulted in about 350 and 1070 m of paleotopographic relief, respectively. Therefore, a paleotopographic relief of 600 to 1000 m over a distance of 4 to 5 km along the MacLean channel is not unreasonable. A northwest dipping paleoslope in the MacLean channel during ore deposition is consistent with a resurgent dome centred somewhere to the east of Lucky Strike. The source area(s) for material in the ore-bearing debris flows, prior to thrust faulting, was probably in the general vicinity of the town of Buchans. Altered, sulphide-bearing footwall rocks are most abundant near Lucky Strike, Old Buchans and Rothermere suggesting close proximity to a number of large hydrothermal vents.

In the MacLean Extension area, a large mass of disrupted copper- and zinc- rich sulphides contained none of the conspicuous clasts characteristic of the debris flow deposits of the area. This mass also had metal ratios that were very different from those of the debris flow deposits in the area (Binney, 1987). No hydrothermal feeder system is known in the vicinity of this deposit. This mass is best viewed as a slump or slide deposit transported down a steep slope from the south (Binney, 1987; depicted in Fig. 3). Jambor (1987) notes also that remants of the Lucky Strike Main Orebody have a fragmented or disrupted texture also consistent with slumping of the ore.

The main clast types in the ore-bearing debris flows are massive sulphides, barite, altered volcanic rocks, stockwork, siltstone, basalt, rhyolite and granitoids (e.g. Walker and Barbour 1981; Calhoun and Hutchinson, 1981; Binney *et al.*, 1983; Binney, 1987; Stewart, 1987). For the most part the clasts were consolidated, but compaction and load features (e.g. Fig. 4, 5a) indicate that at least some sulphide and

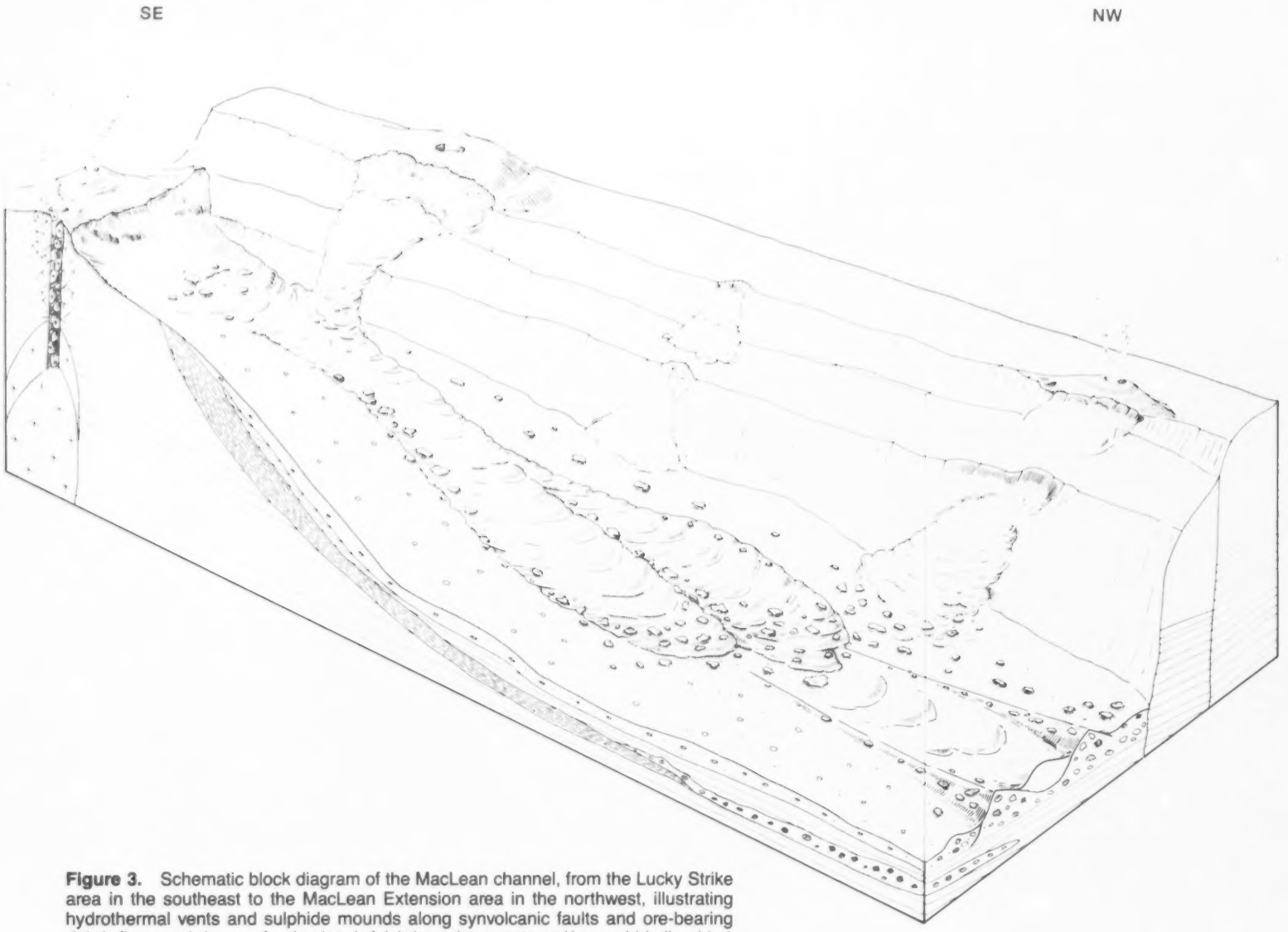

Figure 3. Schematic block diagram of the MacLean channel, from the Lucky Strike area in the southeast to the MacLean Extension area in the northwest, illustrating hydrothermal vents and sulphide mounds along synvolcanic faults and ore-bearing debris flows and slumps. A subvolcanic felsic intrusion penetrated by a pebble (boulder) dyke or breccia pipe, bedded siltstone (dashed pattern), siltstone breccia-conglomerate (stratigraphically lowest breccia-conglomerate unit), overlying sulphide- and barite-rich slumps and debris flows and flanking arenaceous conglomerate are shown.

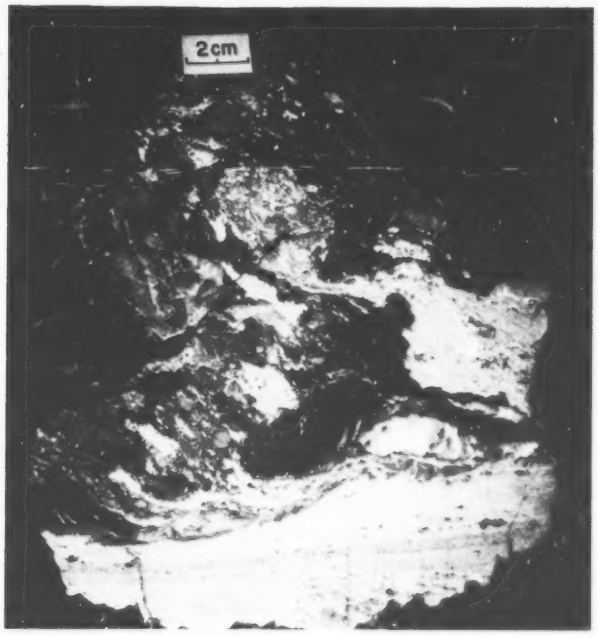

Figure 4. Polylithic breccia-conglomerate with highly contorted and compacted sulphide clasts (mainly sphalerite and galena) between more rigid lithic clasts, 20 level, MacLean Extension Orebody. Layered sphalerite-galena-rich mass at base of specimen is very fine grained ('steely') and shows evidence of extensive grain comminution and strain (KQB-83-14; collected by W.P. Binney; GSC 204266-G).

siltstone clasts were only semi-consolidated and probably underwent plastic or soft-sediment deformation during sediment transport and after deposition in the debris flows. Figure 5b shows ragged sulphide clasts and the conformable lower contact, with prominent load features, of the Two Level Orebody. Because the underling silty sandstone is unsheared and contains a heavy sulphide clast with a ragged contact, that has sunk into the unconsolidate sand, the ragged nature of the sulphide clasts is most likely a sedimentary compaction, rather than a tectonic, feature. As pointed out by Binney (1987), the stress necessary to generate these 'soft' clasts had to be high for the material to fail in an elastic or brittle manner. Although synsedimentary shear and soft-sediment plastic deformation of unmetamorphosed volcanogenic massive sulphide deposits have not been described extensively in the literature, references have been made to "schlieren" structures and synsedimentary plastic deformation of clasts in fragmental Kuroko ores (e.g. Ishikawa and Yanagisawa, 1974; Ito *et al.*, 1974; Watanabe, 1974). These features in the unmetamorphosed Kuroko deposits support the concept of synsedimentary plastic of soft-sediment deformation of sulphides at Buchans.

The separation of debris flows into massive sulphide- or barite-rich centres with steep sulphide and polylithic boulder-rich breccia-conglomerate margins grading out into arenaceous conglomerate, as documented by Binney *et al.* (1983) and Binney (1987), indicates extensive segregation of materials during transport. Poorly consolidated clasts were probably completely disaggregated forming the dense, sulphidic, baritic, viscous, mud-water slurries with Bingham characteristics in the cores of the flows (e.g. Johnson, 1970; Hampton, 1972; Carter 1975; Middleton and Hampton, 1976; Lowe, 1979; Binney, 1987). Studies of the transport of materials in the centres of debris flows indicate that they would be carried by laminar flow along innumerable shear surfaces probably with a rigid plug in the centre of the transport channel (e.g. Johnson, 1970; Hampton, 1972; Middleton and Hampton, 1976; Fisher, 1982; Postma, 1986; Fig. 6). Any turbulence or eddies would tend to be eradicated (Johnson, 1970, p. 442). Coherent, large clasts would be ejected from the dense mud-water mixture in the cores of the flows and accumulate in lateral and terminal (frontal) breccia-conglomerate deposits (e.g. Johnson, 1970; Pierson, 1984; Binney, 1987).

The precise relationship and mechanism of transport and deposition of the external arenaceous conglomerate to the sulphide- and barite-rich debris flows have not been established with any degree of assurance (see Binney, 1987). The relatively massive nature of these deposits and close proximity to the debris flows suggest deposition from high-density turbidity currents or possibly cohesionless grain flows or fluidized flows (e.g. Hampton, 1972; Middleton and Hampton, 1976; Lowe, 1982; Postma, 1986; Binney, 1987). Turbulent mixtures conceivably could have been generated during debris flow transport at the top and near the front of the debris flows in the vicinity of the shear surface with the surrounding water (e.g. Hampton, 1972; Fig. 6). Cossey and Ehrlich (1979) described a transitional sequence of breccia-conglomerate to turbiditic sandstone units in Jurassic slope deposits in northern Tunisia, with some similarities to the transition from polylithic breccia-conglomerate to arenaceous conglomerate at Buchans. They suggested that a variety of gravity flow mechanisms, including submarine slides, debris flows, grain flows and turbulent mixtures, possibly were responsible for the gradation of one deposit type to another. In Paleocene submarine canyon fill at Point Lobos, California, Clifton (1984) documented some gravity-flow, gradational conglomerate-sandstone couplets somewhat analogous with the polylithic breccia-conglomerate and arenaceous conglomerate units at Buchans. He suggested that during deposition perhaps a mechanism transitional between debris flow and grain flow may have been involved. The channelized nature of these deposits is similar to that postulated for the debris flows at Buchans.

Stewart (1987) presents strong circumstantial evidence supporting a subvolcanic intrusion(s) related to Buchans Group rhyolite, as the source of the granitoid clasts in the debris flows. Gaseous or phreatomagmatic eruptions that were derived from or penetrated the subvolcanic intrusion(s) are a logical means by which the granitoid clasts could have been brought to surface and rounded during transport through diatremes or pebble dykes. They also could have disrupted the

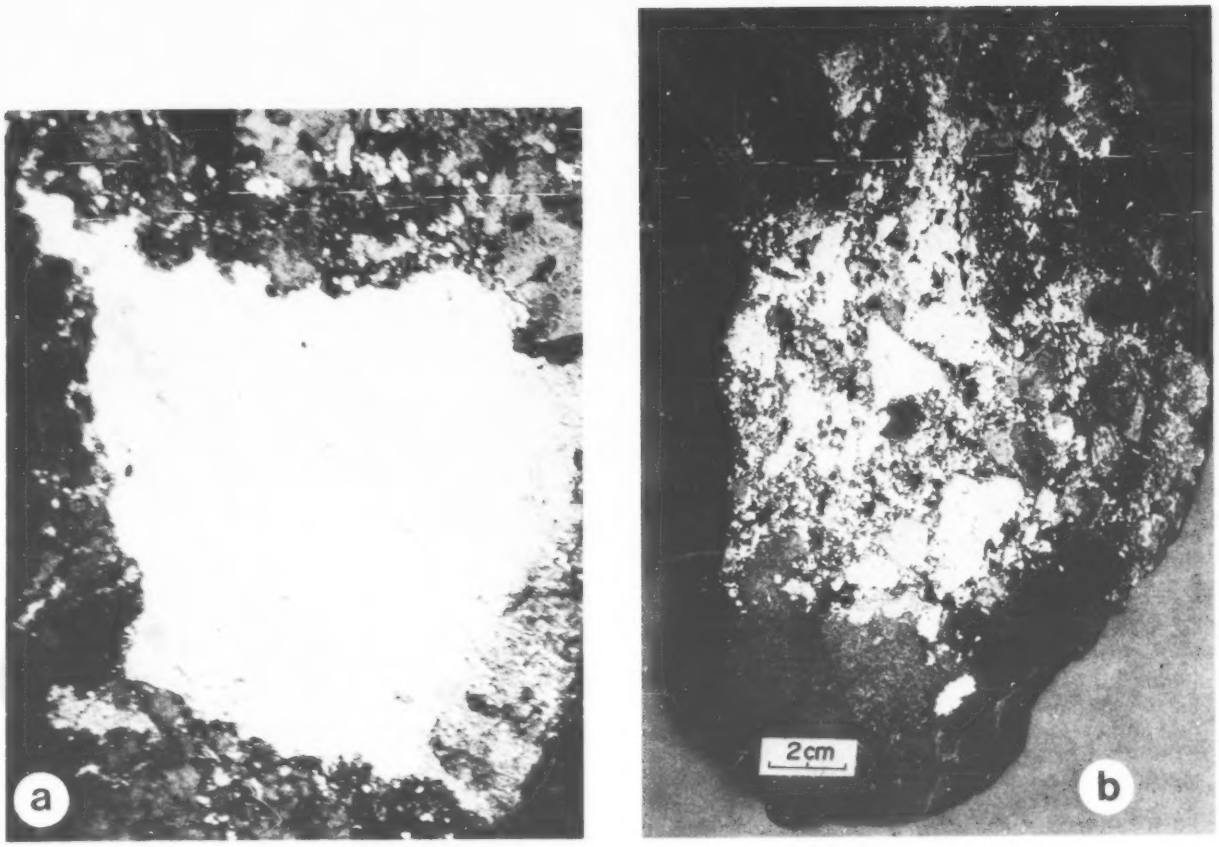

Figure 5

a. Spalerite (medium grey) -galena (pale grey) clast, seven centimetres long, with scalloped margin in polylithic breccia-conglomerate, MacLean Extension Orebody (KQ-84-32A; GSC 204266-P).

b. Fragmental ore of the Two Level Orebody with abundant sphalerite (medium grey) – galenal (pale grey) and lithic (medium and dark grey) clasts in comfortable contact with silty sandstone, northeast corner of Lucky Strike glory hole. The sulphide clasts have very irregular, ragged margins and the lithologic contact shows prominent load structures with a heavy sphalerite-galena and dark siltstone clasts that sunk into the silty sandstone before it was consolidated (Collected by J.L. Jambor; GSC 204266-M).

overlying sulphide and barite mounds triggering numerous, voluminous debris flows. Figure 3 is a schematic illustration of such an environment and such processes. Gaseous eruptions centred on a resurgent dome are consistent with the views of Smith and Bailey (1968) and Marsh (1984) that magma vesiculation could be an important contributing factor to resurgence. Smith and Bailey (1968, p. 614, 632) suggested that resurgent calderas are more closely related to ore formation than other types of calderas and that many resurgent domes contain pervasively hydrothermally altered rocks. They suggested (p. 643) also that larger, longer lived caldera collapse cycles might also have longer lived, more intense associated hydrothermal systems. Marsh (1984) pointed out that, after a large caldera-forming eruption, deep magma undersaturated in H_2O rising to shallower levels could become saturated in H_2O resulting in vesiculation that could be a contributing factor to resurgence. Burnham's (1983) calculations indicated that explosive volcanic eruptions, as a result of vesiculation or exsolution of H_2O from the magma, are quite feasible even under considerable depths of water.

To gain a better understanding how deposits might have formed and materials segregated in the ore-bearing debris flows, an examination of theoretical models and observations of debris flows are instructive. Figure 6 shows an idealized, moving debris flow at an instant in time (after Johnson, 1970). The flow has a steep bouldery snout and lateral deposits indicating matrix strength. The centre of the flow is more mobile and moves in a series of waves or surges in a channel behind the retaining bouldery snout between the bouldery

lateral deposits. The flow freezes when the mobile core no longer has the energy to exceed the matrix strength of the snout and bounding deposits. This configuration could account for the segregation of materials in the debris flows at Buchans into the sulphide and barite matrix ores in the centres of the flows flanked by coarse breccia-conglomerate deposits (Binney *et al.*, 1983; Binney, 1987). The debris flows in the MacLean channel were evidently strongly channelized along a rotated fault block dipping south towards the postulated synvolcanic, normal MacLean Fault (Fig. 3).

The lower part of Figure 6 is a theoretical model showing the stress distribution in a subaqueous debris flow confined to a semi-circular channel. Many workers have concluded that the movement in debris flows is primarily by laminar flow (e.g. Johnson, 1970; Hampton, 1972; Middleton and Hampton, 1976). Their calculations also indicate that a rigid plug in the core of the flow should exist with no internal deformation (Fig. 6). Movement is accomplished by laminar flow between the plug and dead or immobile regions along the sides and at the base of the channel. These movement zones would be areas of intense shear. Presumably at Buchans this would have occurred in the outer and lower parts of the dense sulphide-and/or barite-rich mud-water slurries that 'froze' to produce the matrix ores. In the zones of debris flow generation and of laminar flow, extensive disaggregation and remolding of materials probably occurred.

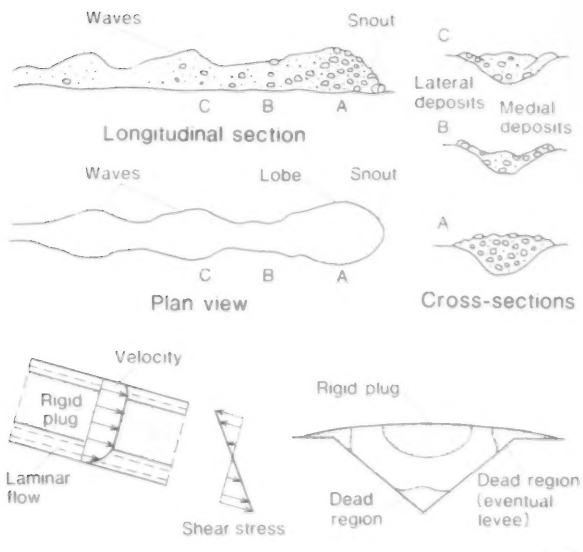

Figure 6. Idealized debris flow at an instant in time and theoretical characteristics of a subaqueous debris flow moving in a semi-circular channel (after Johnson, 1970; Hampton, 1972; Middleton and Hampton, 1976).

DEVELOPMENT OF ORE TEXTURES

Violent disruption of only partially consolidated sulphide and barite mounds and transport down paleoslopes as slumps and debris flows led to significant modification of original ore textures. Attempts to find original bedding and to gain an accurate impression of the nature of in situ ores at Buchans have not been entirely successful. Neither in possible in situ orebodies such as Lucky Strike and Oriental nor in sulphide clasts in debris flows was well-preserved original bedding observed. Undeformed megascopic colloform chemical or delicate particulate layering that could be indicative of original bedding in massive sulphides could not be located. Photomicrographs presented by Strong (1981), Binney (1987) and Jambor (1987) show colloform growth layers on a microscopic scale but similar features on a megascopic scale are rare. The highly deformed layering in the sulphide clast shown in Figure 7 is a possible candidate for original bedding.

Figure 7. Flattened sulphide clasts in baritic polylithic breccia-conglomerate, Two Level Orebody, northeast corner of Lucky Strike glory hole. Folded dark (barite) and light (galena) layers in large, flattened sphalerite-galena clast in centre of specimen are probably deformed bedding (KQ-83-19A; GSC 204266-K).

Figure 8. Brecciated or disrupted sphalerite with minor galena (medium grey), pyrite (light) and minor chalcopyrite (light), Main Orebody, Lucky Strike. Collected by J.L. Jambor from centre of glory hole. Field of view is about 10 cm. (GSC 204327-R).

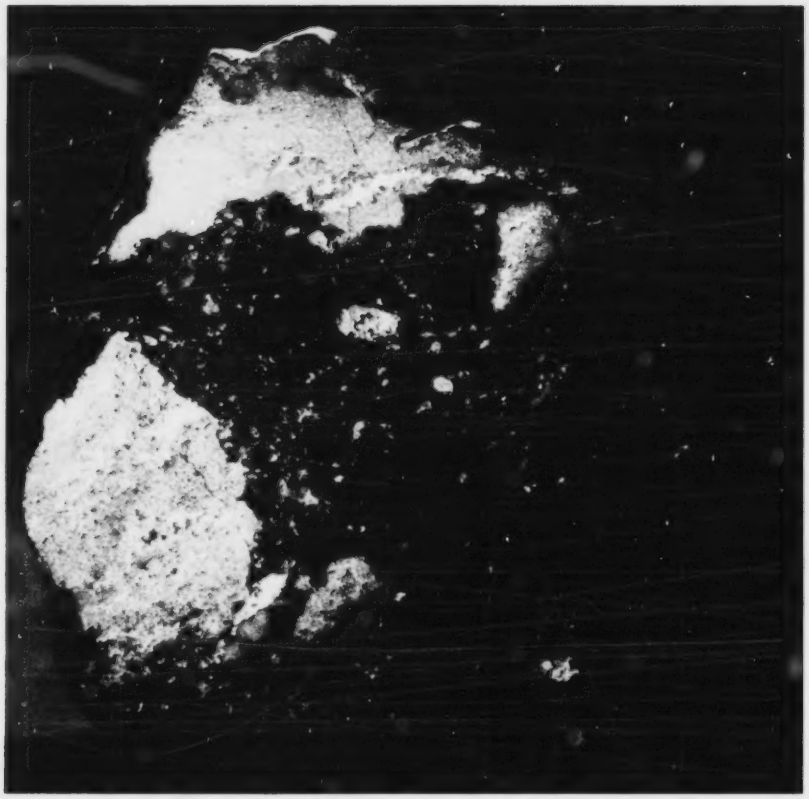

Figure 9. Polylithic breccia-conglomerate with abundant rigid lithic clasts (dark) and relatively uncompacted sulphide clasts (medium and light grey; mainly sphalerite and galena), MacLean Extension Orebody. Specimen is approximatley 11 cm wide; (KQ-83-15A; GSC 204327-P).

Relics of postulated 'in situ' orebodies are not much help either inasmuch as much of the 'in situ' ore remaining at Lucky Strike shows a disrupted, brecciated texture (Jambor, 1987; Fig. 8) and 'in situ' ore at Oriental is highly deformed and occurs as a multitude of small transposed, sheared lenses (McClay, 1987; Calon and Green, 1987). As many of these massive sulphide lenses are interlayered in part with friable, unaltered felsic crystal-vitric tuff, a reasonable probability exists that these are somewhat transported rather than strictly in situ ores. Numerous faults in the Lucky Strike, Old Buchans and Oriental areas and the close proximity of transported debris flow orebodies to the in situ sulphide deposits indicate that caution should be used before accepting any of the identified 'in situ' orebodies as the source(s) of the transported ores.

Structural complexity, as a result of late thrust faults; lack of unequivocal in situ orebodies, poor knowledge of the interrelationship of orebodies; paucity of good ore exposures, and preliminary nature of our observations result in considerable uncertainty in the interpretation of ore textures at Buchans. Nevertheless, ore depositional and deformational histories indicate that several textural transformations of ores should have occurred and that even a rudimentary understanding of these transformations could be helpful in determining the genesis of individual orebodies, their possible relationship to other orebodies and for directing further studies.

Abundant sulphide clasts in the polylithic breccia-conglomerate beds indicate that sulphides could be transported as more-or-less coherent clasts which retained their general original shapes when they came to rest, provided that sufficient rigid lithic clasts were present to support the softer sulphide clasts (Thurlow and Swanson, 1981; Fig. 9). In areas where only soft, incompletely consolidated sulphide clasts were present, the clasts underwent extensive compaction and probably synsedimentary shearing to produce the discontinuous, 'wispy' bedding characteristic of the transported sulphide matrix ores (e.g. Fig. 10, 11). Recognizable flattened sulphide clasts are concentrated in the transition zone between the relatively massive matrix sulphide cores and outer sulphide clast-rich parts of the polylithic breccia-conglomerate margins of the debris flows. Scalloped edges of sulphide clasts, produced by loading, indicate that the clasts were not completely consolidated at the time that they were incorporated into the debris flows (Fig. 5a). Similar scalloped edges are also common on some siltstone clasts (Fig. 12).

Barite, on the other hand, must have been more consolidated than the sulphides since fragments of large barite crystals and coarse grained colloform or cockscomb layered barite are abundant (e.g. Fig. 13, 14). Nevertheless, much fine grained barite occurs intimately intergrown with sulphides suggesting that in places the two were precipitated together and dismembered masses, beds and veins(?) of barite also indicate that it was disaggregated to some degree during sedimentary transport (e.g. Fig. 10).

Matrix sulphide and barite ores tend to be massive, with or without a crude layering. 'Pull-apart' or gash veinlets are

Figure 10. Discontinuous wispy-layered, highly deformed sulphide matrix ore, 20-1 sub-level, MacLean Orebody. Scattered rigid clasts are visible. The light and medium grey lenses could be compacted sphalerite- and galena-rich clasts, respectively. The layering probably resulted from laminar flow in a sulphide-rich, mud-water mixture during sedimentary transport and compaction of semi-consolidated sulphide mud and larger clasts (GSC 204266-X).

characteristic, suggesting that a 'new' mechanical equilibrium was attained during and after deposition (e.g. Fig. 10, 15). This material was probably thoroughly remolded and sheared during transport in the debris flows and obtained a new equilibrium during sedimentary transport and compaction after deposition. Large clasts tended to be cast out of this material during transport, although scattered clasts remained (e.g. Fig. 16). If the wispy layering displayed in this specimen had a tectonic rather than a sedimentary origin, one would expect that the delicate irregularities in the contact of the siltstone clast (probably produced by loading) would have been destroyed during shearing. Sigmoidal layering, dismembered asymmetrical folded barite and/or calcite layers and veins; rotated clasts with tails, and rotated and fractured, resistant clasts in more ductile sulphide-rich matrices could be useful kinematic indicators of the sedimentary transport direction (e.g. Fig. 17, 18, 19). However, these features in the matrix ores were recognized only in polished specimens after mining had ceased and could not be confirmed underground as products of sedimentary rather than tectonic shear. Nevertheless, typical, wispy layered, sheared matrix sulphide ore has been observed in many places overlying unsheared, relatively incompetent crystal-vitric rhyolitic tuff tens of metres away from the nearest fault and grading laterally into unsheared polylithic breccia-conglomerate, supporting the concept that this shearing was sedimentary and not tectonic. However, once consolidated, massive units of soft sulphides could be expected to deform more readily than the surrounding rocks (McClay, 1983) and evidence of tectonic deformation could be present in the sulphide ores and not in other rocks. Presumably sedimentary laminar flow in a dense mixture in a cold environment would be accomplished primarily by intergranular movements, whereas tectonic shear at elevated temperatures would involve ductile deformation of grains, including crystal glide. Microscopic work necessary to discriminate between the two types of deformation has not been done.

In general, the mine area at Buchans is of low regional metamorphic grade, in the prehnite-pumpellyite facies (Henley and Thornley, 1981), and has mainly undergone brittle deformation with only local ductile deformation along fault zones. In or near fault zones sulphides have been highly strained, comminuted and have developed local mylonitic fabrics or layering (Fig. 20). Barite and sulphide tension veins near faults, indicate some late solution transport of ore constituents. Small-scale extensional and compressive faults are abundant in the orebodies.

In the Lucky Strike glory hole blocks or 'knockers'[1] of sulphides and resistant white rhyolite occur in siliceous, sericitic, chloritic, pyritic schistose host rocks which are probably shear zones (Fig. 21). In local areas the sulphide blocks are of diverse nature such as massive sphalerite and galena, massive chalcopyrite and pyrite, siliceous pyritic rocks and zinc-rich baritic transported ores. Examination of a number of large knockers, with K.R. McClay in 1984, indicated that they have sheared contacts. The diverse nature of knockers in local areas and their sheared contacts suggest that they have been transported tectonically significant distances in the shear zones and may not be close to their original sources. Similar sulphide-bearing blocks have also been recognized in fault zones in MacLean Extension and Old Buchan areas and in the Old Buchans Fault about 175 m, and an unnamed fault about 484 m, below the Lucky Strike Orebodies.

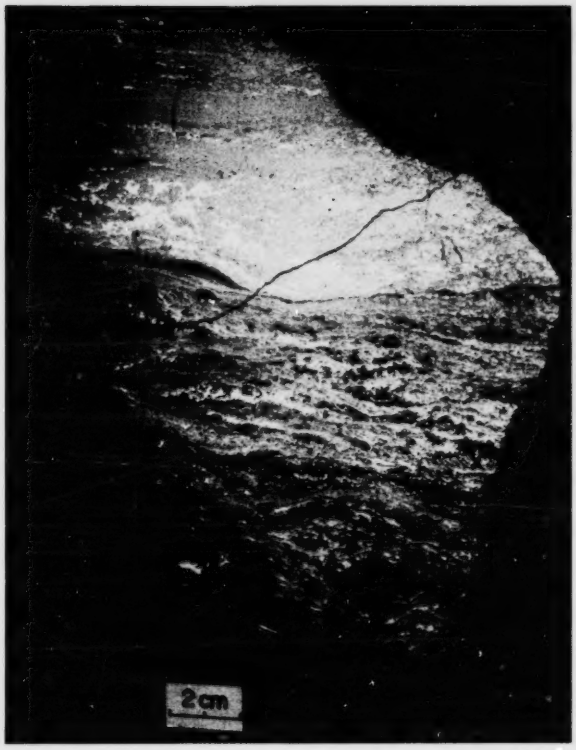

Figure 11. Typical wispy-layered, sphalerite (medium grey), galena (pale), sulphide matrix ore, 20-1 sublevel, MacLean Orebody (same locality as Figure 10). Prominent dark lithic clasts are siltstone and smaller less conspicuous dark 'clasts' are dismembered barite with sulphides in tension gashes. Galena and sphalerite in the matrix vary greatly in grain size (some 'steely') and show evidence of high but variable strain. Sigmoidal, anastomosing layering is evident in areas of lower strain (KQ-74-35; GSC 204266-N). This unit was in contact with unsheared rhyolitic crystal-vitric tuff.

SUMMARY AND CONCLUSIONS

Many aspects of the geology of the mine area are permissive for a large submarine caldera that underwent resurgence at

[1]Knocker in this context refers to a resistant block in a shear or fault zone. This is slightly different than the usage by Berkland et al. (1972) to refer to blocks at surface in the Franciscan terrane that are resistant to weathering.

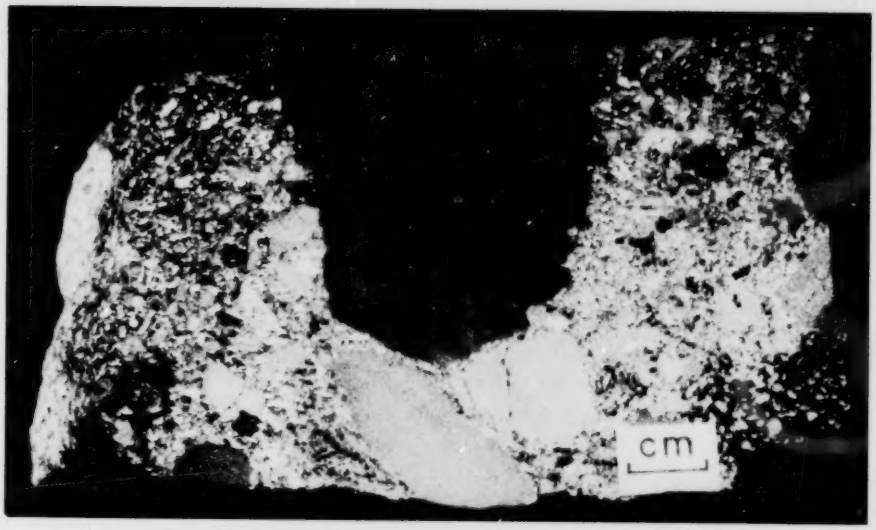

Figure 12. Arenaceous polylithic breccia-conglomerate with large, well-bedded siltstone clast with scalloped margin, MacLean Extension area (KQB-83-18; collected by W.P. Binney; GSC 204266-0).

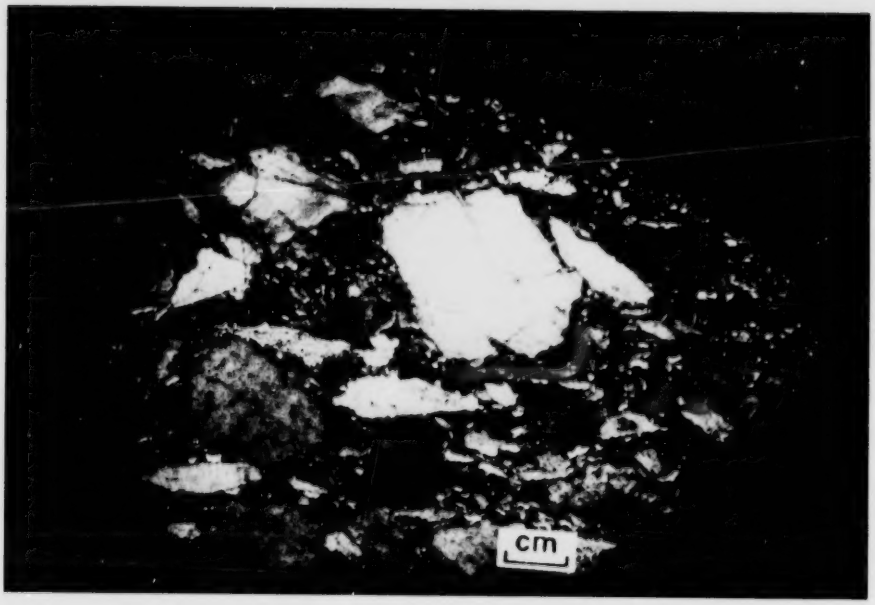

Figure 13. Polylithic breccia-conglomerate with large white barite crystal fragments, elongate sulphide clasts and grey lithic (volcanic, granitoid and siltstone) clasts, 20 level, MacLean Extension Orebody (KQB-82-104; collected by W.P. Binney; GSC 204266-Q).

the time of ore formation. Nevertheless, lack of pertinent data and the complex, post-volcanic fault history mean that any caldera hypothesis at present must be viewed as speculative.

Paleotopographic relief in the order of 800-1100 m in the Buchans mine area at the time of ore formation, or shortly following, is reasonable and the incorporation of pre-ore turbiditic siltstone in debris flows supports a major topographic inversion (Binney, 1987) compatible with syn-ore caldera resurgence. The ores conceivably accumulated at hydrothermal seafloor vents on or near a resurgent dome. Phreatomagmatic or gaseous eruptions, possibly related to magma vesiculation, could have brought granitoid clasts to surface, rounded them in transit and have triggered the debris flows and ore slumps. This disruption of sulphide and baritic material and internal deformation in the debris flows as well as later tectonic deformation in and near faults and shear zones have led to extensive modification of the ores. The resurgent caldera model provides a unifying hypothesis for the coexistence of a submarine caldera, resurgent dome, synvolcanic faults, magma vesiculation, hydrothermal activity, triggering of large-scale sulphide- and barite-rich debris flows and incorporation of granitoid clasts in the debris flows. Conceivably a topographically high resurgent dome could also have been the site of limestone deposition after hydrothermal and volcanic activity waned. It is a reasonably

Figure 14. Large barite clast with cockscomb layers in polylithic breccia- conglomerate, 20 level, MacLean Extension Orebody (GSC 204266-Y).

Figure 15. Massive, sphalerite-rich (medium grey) sulphide matrix ore with galena and chalcopyrite (pale grey) in small, discontinuous 'pull-apart', tension gashes, 20 level, MacLean Extension Orebody (KQ-83-13; GSC 204266-V).

Figure 16. Sulphide matrix ore with discontinuous layering and relic sulphide clasts and dark siltstone clasts with irregular scalloped margins, MacLean Extension Orebody (KQ-84-32C; GSC 204266-H).

Figure 17. Rotated, elongate, somewhat deformed porphyritic (quartz) rhyolitic pumice fragment (4 cm in longest diagonal dimension), consistent with dextral shear, in mylonitic sphalerite-rich sulphide matrix ore, McLean Extension Orebody. Pale flattened metallic clast to left in "lee" of pumice fragment is mainly chalcopyrite with minor included pyrite. Some dark lithic clasts are visible and bright metallic grains and areas are mainly pyrite and galena (KQ-83-15C; GSC 204327-J).

Figure 18. Rotated, pyritic, altered, bedded siltstone(?) clast with tails, (1 cm diameter), is consistent with sinistral shear, set in a fragmental barite, lithic sulphide matrix. Specimen contains many flattened sulphide and pumiceous clasts similar to the dark sphalenite-rich clast immediately below and left of the central clast with tails and the pale pumiceous clast below both those clasts. Many of the white clasts are fragments of barite crystals and some dark, round quartz grains are also visible. Upper ore unit, 20 level, MacLean Extension Orebody (KQ-84-24; GSC 204327-K).

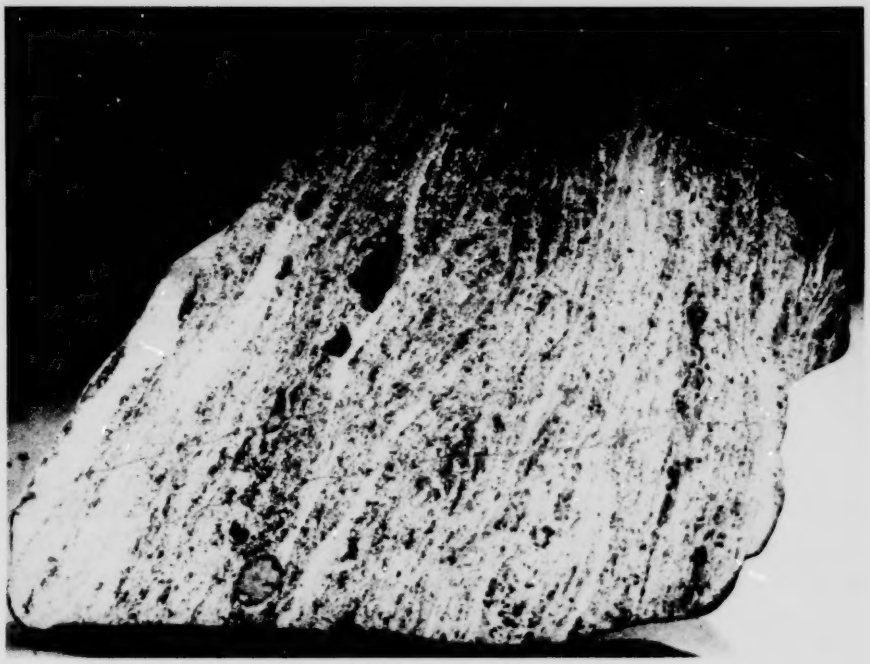

Figure 19. Sulphide matrix ore with dark barite and lithic clasts and anastomosing, sigmoidal layering consistent with sinistral shear, MacLean Extension Orebody (KQ-84-32C; 204327-N). Specimen is 12.5 cm wide.

Figure 20. 'Streaky', mylonitic layered sphalerite (dark grey)-chalcopyrite-pyrite (light grey) ore, 20 level, MacLean Extension Orebody (KQB-82-11; collected by W.P. Binney; GSC 204266-J).

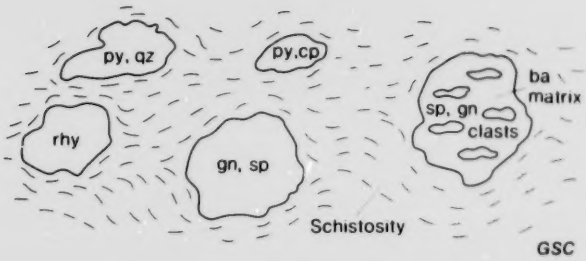

Figure 21. Schematic diagram illustrating sulphide knockers or blocks in a shear zone. Ba = barite, cp = chalcopyrite, gn = galena, qz = quartz, rhy = rhyolite and sp = sphalerite.

source area for the conodont-bearing limestone clasts found in the lower part of the Sandy Lake Formation (Nowlan and Thurlow, 1987).

Although tectonic deformation of ores at Buchans along fault zones is reasonably well established, synsedimentary deformation, based on a knowledge debris flows, should also have been intense. Kinematic evidence of shear is present in the transported sulphide matrix ores but further work is necessary to resolve what shear deformation was sedimentary and what was tectonic.

On a regional scale the thrust faults at Buchans deflected around an area about 6 km wide in an east-west direction in the vicinity of the town of Buchans (see maps in Thurlow and Swanson, 1987; McClay, 1987; Calon and Green, 1987). Conceivably the structure that deflected the thrust faults was the resurgent dome.

ACKNOWLEDGMENTS

This paper relies heavily on information generated in other studies at Buchans, especially Binney's studies of debris flows in the MacLean channel (Binney *et al.*, 1983; Binney, 1984, 1987). Discussions with K.H. Poulsen and C.S. van Staal of textures displayed in polished hand specimens of ore were most helpful in clarifying aspects of their deformational histories. Ron Hill's artistic talents in drawing the block diagrams have put 'life' in geological ideas. W.P. Binney, M.B. Lambert and W.D. Sinclair reviewed the manuscript and made several useful comments.

REFERENCES

Berkland, J.O., Raymond, L.A., Kramer, J.C., Moores, E.M., and O'Day, M.
1972: What is Franciscan?; American Association of Petroleum Geologists, Bulletin, v. 56, p. 2295-2302.

Binney, W.P.
1984: Estimation of physical parameters of MacLean channel sulphide-bearing debris flows, Buchans, Newfoundland; in Current Research, Part A, Geological Survey of Canada, Paper 84-1A, p. 495-498.
1987: A sedimentological investigation of MacLean channel transported sulphide ores; in Buchans Geology, Newfoundland, ed. R.V. Kirkham; Geological Survey of Canada, Paper 86-24, Report 8.

Binney, W.P., Thurlow, J.G. and Swanson, E.A.
1983: The MacLean Extension orebody, Buchans, Newfoundland; in Current Research, Part A, Geological Survey of Canada, Paper 83-1A, p. 313-319.

Burnham, C.W.
1983: Deep submarine pyroclastic eruptions; in The Kuroko and Related Volcanogenic Massive Sulfide Deposits, ed. H. Ohmoto and B.J. Skinner, Economic Geology, Monograph 5, p. 142-148.

Busby-Spera, C.J.
1984: Large-volume rhyolite ash flow eruptions and submarine caldera collapse in the lower Mesozoic Sierra Nevada, California; Journal of Geophysical Research, v. 89, no. B10, p. 8417-8427.

Calhoun, T.A. and Hutchinson, R.W.
1981: Determination of flow direction and source of fragmental sulphides, Clementine deposit, Buchans, Newfoundland; in The Buchans Orebodies: Fifty Years of Geology and Mining, ed. E.A. Swanson, D.F. Strong and J.G. Thurlow; Geological Association of Canada, Special Paper 22, p. 187-204.

Calon, T.J. and Green, F.J.
1987: Preliminary results of detailed structural analysis at Buchans; in Buchans Geology, Newfoundland, ed. R.V. Kirkham; Geological Survey of Canada, Paper 86-24, Report 17.

Carter, R.M.
1975: A discussion and classification of subaqueous mass-transport with particular application to grain-flow, slurry-flow, and fluxoturbidites; Earth-Science Reviews, v. 11, p. 145-177.

Clifton, H.E.
1984: Sedimentation units in stratified resedimented conglomerate, Paleocene submarine canyon fill, Point Lobos, California; in Sedimentology of Gravels and Conglomerates, ed. E.H. Koster and R.J. Steel; Canadian Society of Petroleum Geologists, Memoir 10, p. 429-441.

Cossey, S.P. and Ehrlich, R.
1979: A conglomeratic, carbonate flow deposit, northern Tunisia; a link in the genesis of pebbly mudstones; Journal of Sedimentary Petrology, v. 49, p. 11-22.

Elbring, G.L. and Rundle, J.B.
1986: Analysis of borehole seismograms from Long Valley, California; implications for caldera structure; Journal of Geophysical Research, v. 91, no. B12, p. 12651-12660.

Fisher, R.V.
1982: Debris flows and lahars; in Pyroclastic Volcanism and Deposits of Cenozoic Intermediate to Felsic Volcanic Islands with Implications for Precambrian Greenstone-belt Volcanoes, ed. L.D. Ayres; Geological Association of Canada, Short Course Notes, v. 2, p. 136-190.

Gibson, H.L. and Watkinson, D.H.
1986: The Central Mine Sequence, Noranda, Quebec: A caldera-fill sequence (abstract); Joint Annual Meeting Geological Association of Canada – Mineralogical Association of Canada – Canadian Geophysial Union, Program with Abstracts, v. 11, p. 72.

Gibson, H.L., Watkins, D.H., and Bonneau, J.
1986: Location of volcanogenic massive sulphide deposits within the Central Mine Sequence, Noranda, Quebec (abstract); Joint Annual Meeting Geological Association of Canada – Canadian Geophysical Union, Program with Abstracts, v. 11, p. 72-73.

Hampton, M.A.
1972: The role of subaqueous debris flow in generating turbidity currents; Journal of Sedimentary Petrology, v. 42, p. 775-793.

Henley, R.W. and Thornley, P.
1981: Low grade metamorphism and the geothermal environment of massive sulphide ore formation, Buchans, Newfoundland; in The Buchans Orebodies: Fifty Years of Mining and Geology, ed. E.A. Swanson, D.F. Strong and J.G. Thurlow; Geological Association of Canada, Special Paper 22, p. 205-228.

Ishikawa, Y. and Yanagisawa, Y.
1974: Geology of the Ainai mine, with special reference to syngenetic origin of the Daikoku deposits; in Geology of Kuroko Deposits, ed. S. Ishihara; Mining Geology, Special Issue, No. 6, p. 79-88.

Ito, T., Takahashi, T. and Omori, Y.
1974: Submarine volcanic – sedimentary features in the Matsumine Kuroko deposits, Hanaoka mine, Japan; in Geology of Kuroko Deposits ed. S. Ishihara; Mining Geology, Special Issue, No. 6, p. 115-130.

Jambor, J.L.
1987: Geology and origin of orebodies in the Lucky Strike area; in Buchans Geology, Newfoundland, ed. R.V. Kirkham; Geological Survey of Canada, Paper 86-24, Report 7.

Johnson, A.M.
1970: Physical Processes in Geology; Freeman, Cooper and Company, San Francisco, 577 p.

Kouda, R. and Koide, H.
1978: Ring structures, resurgent cauldron and ore deposits in

the Hokuroku volcanic field, northern Akita, Japan; Mining Geology, v. 28, p. 219-232.

Lambert, M.B.
1974: The Bennett Lake cauldron subsidence complex, British Columbia and Yukon Territory; Geological Survey of Canada, Bulletin 227, 213 p.

Lipman P.W.
1984: The roots of ash flow calderas in western North America: windows into the tops of granitic batholiths; Journal of Geophysical Research, v. 89, no. B10, p. 8801-8841.

Lowe, D.R.
1979: Sediment gravity flows: their classification and some problems of application to natural flows and deposits; in Geology of Continental Slopes, ed. L.J. Doyle and O.H. Pilkey; Society of Economic Paleontologists and Mineralogists, Special Publication, no. 27, p. 75-82.
1982: Sediment gravity flows: II. Depositional models with special reference to the deposits of high-density turbidity currents; Journal of Sedimentary Petrology, v. 52, p. 279-297.

Marsh, B.C.
1984: On the mechanisms of caldera resurgence; Journal of Geophysical Research, v. 89, no. B10, p. 8245-8251.

McClay, K.R.
1983: Structural evolution of the Sullivan Fe-Pb-Zn-Ag orebody, Kimberley, British Columbia, Canada; Economic Geology, v. 78, p. 1398-1424.
1987: Aspects of the structural geology of the Buchans area; in Buchans Geology, Newfoundland, ed. R.V. Kirkham; Geological Survey of Canada Paper 86-24, Report 3.

Middleton, G.V. and Hampton, M.A.
1976: Subaqueous sediment transport and deposition by sediment gravity flows; in Marine Sediment Transport and Environmental Management, ed. D.J. Stanley and D.J.P. Swift; John Wiley and Sons, New York, p. 197-218.

Nelson, C.H., Meyer, A.W., Thor, D. and Larsen, M.
1986: Crater Lake, Oregon: A restricted basin with base-of-slope aprons of nonchannelized turbidites; Geology, v. 14, p. 238-241.

Nielsen, D.L. and Hulen, J.B.
1984: Internal geology and evolution of the Redondo Dome, Valles Caldera, New Mexico; Journal of Geophysical Research, v. 89, p. 8695-8713.

Nowlan, C.S. and Thurlow, J.G.
1987: Middle Ordovician, conodonts from the Buchans Group; in Buchans Geology, Newfoundland, ed. R.V. Kirkham; Geological Survey of Canada, Paper 86-24, Report 4.

Ohmoto, H.
1978: Submarine calderas: A key to the formation of volcanogenic massive sulfide deposits?; Mining Geology, v. 28, p. 219-232.

Ohmoto, H. and Skinner, B.J. (ed.)
1983: The Kuroko and Related Volcanogenic Massive Sulfide Deposits; Economic Geology Publishing Company, Monograph 5, 604 p.

Ohmoto, H. and Takahashi, T.
1983: Geologic Setting of the Kuroko deposits, Japan: Part III. Submarine calderas and Kuroko genesis; in The Kuroko and Related Volcanogenic Massive Sulfide Deposits, ed. H. Ohmoto and B.J. Skinner; Economic Geology, Monograph 5, p. 39-54.

Pierson, T.C.
1984: Why debris flows stop (abstract); Geological Society of America, Abstracts with Programs, v. 16, no. 6, p. 623.

Postma, G.
1986: Classification of sediment gravity-flow deposits based on flow conditions during sedimentation; Geology, v. 14, p. 291-294.

Smith, R.L. and Bailey, R.A.
1968: Resurgent cauldrons; in Studies in Volcanology, ed. R.R. Coats, R.L. Hay and C.A. Anderson; Geological Society of America, Memoir 116, p. 613-662.

Stewart, P.W.
1987: Geology and genesis of granitoid clasts in the MacLean Extension transported orebody; in Buchans Geology, Newfoundland, ed. R.V. Kirkham; Geological Survey of Canada, Paper 86-24, Report 11.

Strong, D.F.
1981: Notes on ore mineralogy of the Buchans district; in The Buchans Orebodies: Fifty Years of Geology and Mining, ed. E.A. Swanson, D.F. Strong and J.G. Thurlow; Geological Association of Canada, Special Paper 22, p. 143-160.

Taube, A.
1986: The Mount Morgan gold-copper mine and environment, Queensland: A volcanogenic massive sulfide deposit associated with penecontemporaneous faulting; Economic Geology, v. 81, p. 1322-1340.

Thurlow, J.G.
1981: The Buchans Group: Its stratigraphic and structural setting; in The Buchans Orebodies: Fifty Years of Geology and mining, ed. E.A. Swanson, D.F. Strong and J.G. Thurlow; Geological Association of Canada, Special Paper 22, p. 79-90.

Thurlow, J.G. and Swanson, E.A.
1981: Geology and ore deposits of the Buchans area, central Newfoundland, in The Buchans Orebodies: Fifty years of Geology and Mining, ed. E.A. Swanson, D.F. Strong and J.G. Thurlow; Geological Association of Canada, Special Paper 22, p. 113-142.
1987: Stratigraphy and structure of the Buchans Group; in Buchans Geology, Newfoundland, ed. R.V. Kirkham; Geological Survey of Canada, Paper 86-24, Report 2.

Thurlow, J.G., Swanson, E.A. and Strong, D.F.
1975: Geology and lithogeochemistry of the Buchans polymetallic sulphide deposits, Newfoundland; Economic Geology, v. 70, p. 130-144.

Walker, G.P.L.
1984: Downsag calderas, ring faults, caldera sizes and incremental caldera growth; Journal of Geophysical Research, v. 89, p. 8407-8416.

Walker, P.N. and Barbour, D.M.
1981: Geology of the Buchans ore-breccias; in The Buchans Orebodies: Fifty years of Geology and Mining, ed. E.A. Swanson, D.F. Strong and J.G. Thurlow; Geological Association of Canada, Special Paper 22, p. 161-185.

Watanabe, M.
1974: On the textures of ores from the Daikoku ore deposit, Ainai mine, Akita Prefecture, Northeast Japan, and their implications in the ore genesis; in Geology of Kuroko Deposits, ed. S. Ishihara; Mining Geology, Special Issue, No. 6, p. 337-348.

- 11 -

Geology and geochemistry of the Skidder Basalt

J. Wayne Pickett[1]

Pickett, J.W., Geology and geochemistry of the Skidder Basalt; in Buchans Geology, Newfoundland, ed. R.V. Kirkham; Geological Survey of Canada, Paper 86-24, p. 195-218, Report 11, 1987.

Abstract

The Skidder Basalt comprises a spilitized assemblage of basaltic pillow lava, pillow breccia and massive flows plus lesser mafic pyroclastic rocks and chert. Trondhjemitic pods and dykes intrude the unit locally. Spilitization of the rocks has resulted in redistribution of SiO_2 and Fe, removal of K_2O and MgO, and extensive addition of Na_2O. The rocks are classified dominantly as sub-alkaline basalts; define tholeiitic trends, and plot close to the boundary between ocean-floor basalt and island-arc tholeiite fields on trace element variation diagrams. The suggested paragenesis of the Skidder Basalt is olivine + Cr-spinel ± plagioclase, olivine + plagioclase and, late in the crystallization history, clinopyroxene + plagioclase + magnetite + apatite. The plagiogranites are low Al_2O_3 oceanic type trondhjemites and are chemically more similar to trondhjemites considered to represent late magmatic differentiates of basaltic magma than to those suggested to have formed by partial fusion of amphibolites. The Skidder Basalt is geologically and geochemically more similar to the pillow lava sections of ophiolitic complexes than to the Buchans Group basalts.

Résumé

Le basalte de Skidder se compose d'une association spilitisée de laves basaltiques en coussins, de brèches en coussins et de coulées massives, ainsi que de plus petites quantités de roches pyroclastiques mafiques et de chert. Par endroits, des lentilles allongées et des filons de trondhjémite percent le basalte. La spilitisation des roches a provoqué la redistribution de SiO_2 et de Fe, l'enlèvement de K_2O et de MgO et l'addition de vastes quantités de Na_2O. Les roches sont surtout des basaltes subalcalins; elles présentent des tendances tholéiitiques et, dans les diagrammes de variation des éléments-trace, elles se situent près de la limite entre le basalte des fonds océaniques et les nappes de tholéiites d'arc insulaire. Le basalte de Skidder aurait une paragenèse à olivine + spinelle à chrome ± plagioclase, à olivine + plagioclase et, vers la fin de la cristallisation, à clinopyroxène + plagioclase + magnétite + apatite. Les plagiogranites sont des trondhjémites de type océanique pauvres en Al_2O_3; chimiquement, ils ressemblent à des trondhjémites caractéristiques du produit de la différenciation tardive d'un magma basaltique, plutôt qu'à des trondhjémites formées par fusion partielle d'amphibolites. La géologie et la géochimie du basalte de Skidder ressemblent à celles des laves en coussins des complexes ophiolitiques, plutôt qu'à celles du basalte du groupe de Buchans.

INTRODUCTION

The Skidder Basalt underlies an area of approximately 20 square kilometres about 10 kilometres south of the town of Buchans in central Newfoundland (Fig. 1). It is composed dominantly of basaltic pillow lava, pillow breccia, plus lesser mafic pyroclastic rocks and chert. Trondhjemitic pods and dykes intrude the unit locally.

The Skidder Basalt had previously been included in the "Footwall Basalt" of the Buchans Group (Thurlow, 1981). However, in contrast to the Footwall Basalt, now part of the Sandy Lake Formation (Thurlow and Swanson, 1986), the Skidder Basalt is spilitized; pillows are variolitic in some areas and generally contain fewer in number and smaller amygdules; and the rocks have a high magnetic susceptibility (see GSC Aeromagnetic Map 7049G, Red Indian Lake). On the basis of these differences the rocks were assigned to a new unit called the Skidder Basalt (Pickett and Barbour, 1984).

Mafic volcanic rocks of the Skidder Basalt host the Skidder Prospect (Fig. 2, 3), a volcanogenic massive sulphide deposit. The prospect was discovered in 1971 by ASARCO Inc. and later delineated by diamond drilling by

[1]Department of Earth Sciences, Memorial University of Newfoundland, St. John's, Newfoundland A1B 3X5

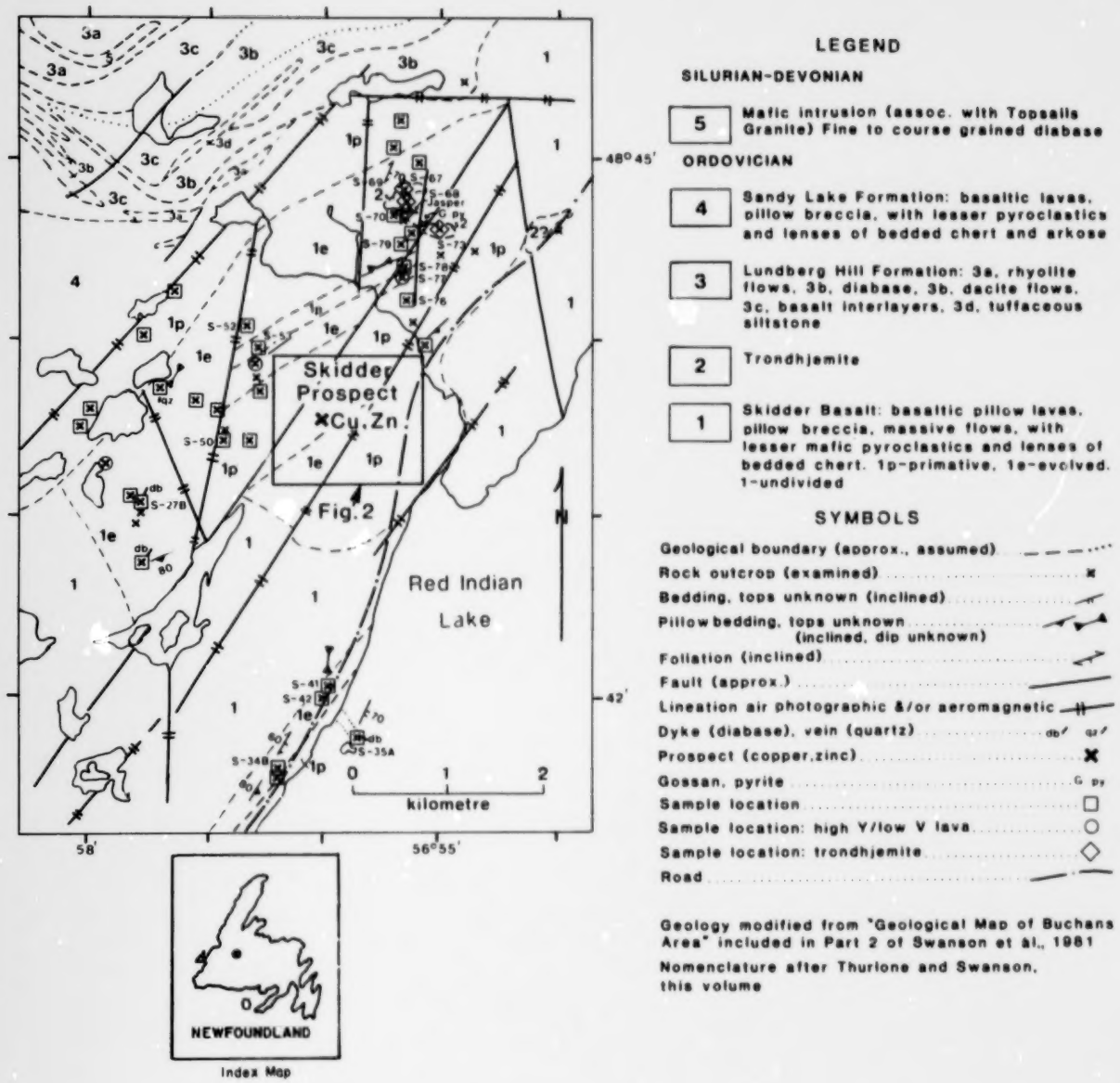
LEGEND
SILURIAN-DEVONIAN
5 Mafic intrusion (assoc. with Topsails Granite) Fine to course grained diabase
ORDOVICIAN
4 Sandy Lake Formation: basaltic lavas, pillow breccia, with lesser pyroclastics and lenses of bedded chert and arkose
3 Lundberg Hill Formation: 3a, rhyolite flows, 3b, diabase, 3b, dacite flows, 3c, basalt interlayers, 3d, tuffaceous siltstone
2 Trondhjemite
1 Skidder Basalt: basaltic pillow lavas, pillow breccia, massive flows, with lesser mafic pyroclastics and lenses of bedded chert. 1p-primative, 1e-evolved, 1-undivided
SYMBOLS
Geological boundary (approx., assumed)
Rock outcrop (examined)
Bedding, tops unknown (inclined)
Pillow bedding, tops unknown (inclined, dip unknown)
Foliation (inclined)
Fault (approx.)
Lineation air photographic &/or aeromagnetic
Dyke (diabase), vein (quartz)
Prospect (copper,zinc)
Gossan, pyrite
Sample location
Sample location: high Y/low V lava
Sample location: trondhjemite
Road
Geology modified from "Geological Map of Buchans Area" included in Part 2 of Swanson et al., 1981
Nomenclature after Thurlow and Swanson, this volume
Skidder Prospect Cu, Zn
Fig. 2
Red Indian Lake
48°45'
42'
58'
56°55'
0 1 2
kilometre
N
NEWFOUNDLAND
Index Map

Figure 1. Regional geology of the Skidder area.

ASARCO in joint venture with Abitibi Price Mineral Resources. It contains probable and possible reserves totalling approximately 900 000 tonnes averaging approximatly 2% Cu, 2% Zn and containing minor amounts of Pb and Ag (D.M. Barbour, 1977, unpublished report). The deposit consists of three types of sulphide-bearing units 1) a quartz-pyrite stockwork zone that contains minor amounts of chalcopyrite and sphalerite 2) a semi-massive to massive, non-bedded pyrite zone with minor amounts of chalcopyrite and sphalerite and 3) a laminated massive sulphide zone consisting of fine to medium grained pyrite with lesser amounts of chalcopyrite and sphalerite (Pickett and Barbour, 1984). Brecciated, quartz-veined, massive jasper and lesser bedded jasper-rich siltstone are associated with the massive sulphides. Distinct alteration zones characterized by secondary mineral assemblages are present up to 100 m laterally away from the quartz-pyrite stockwork zone (Fig. 3) (Pickett and Barbour, 1984).

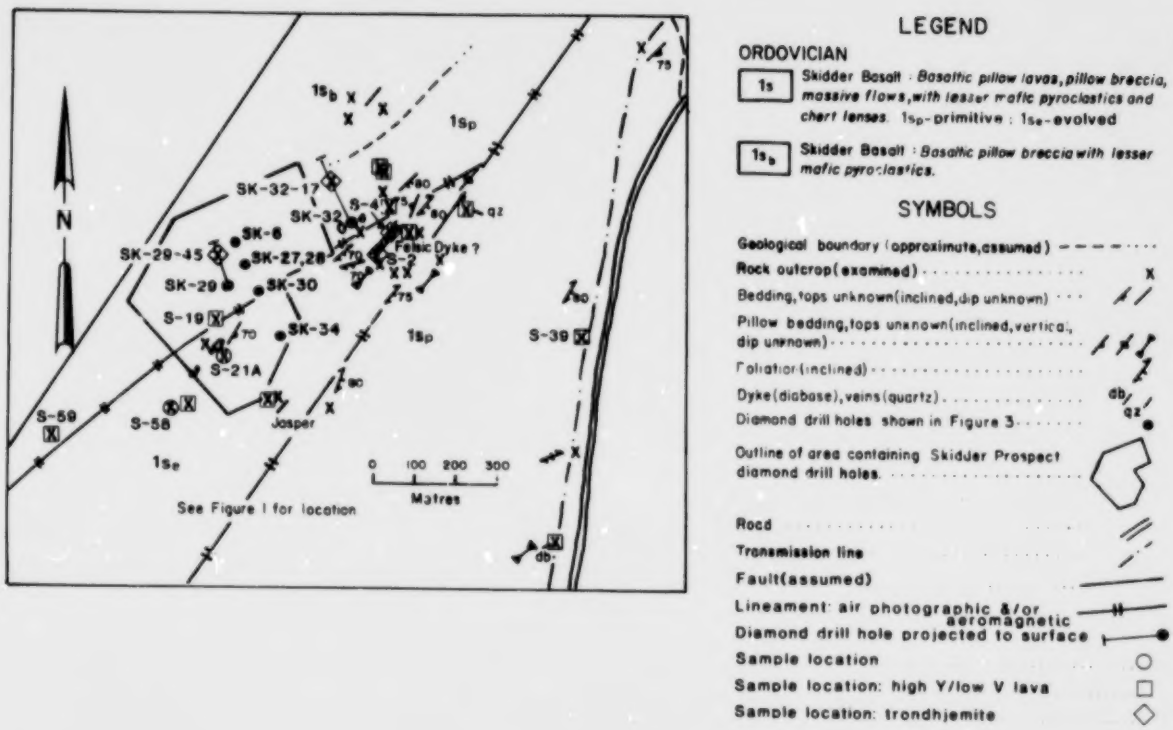

Figure 2. Local geology of the Skidder Prospect.

Mottl (1983a) suggested characteristics secondary mineral assemblages representative of increasing seawater/rock ratios. These assemblages match reasonably well those flanking the quartz-pyrite zone of the Skidder Prospect and indicate that increasing volumes of hydrothermal fluids passed through rocks that are successively more proximal to the stockwork zone (Pickett and Barbour, 1984).

The prospect has more features in common with deposits in ophiolite sequences (Pickett and Barbour, 1984) than to the polymetallic, Kuroko-type massive sulphide deposits of the Buchans area (Thurlow, 1973).

Lithological differences between the Skidder Basalt and mafic rocks of the Buchans Group as well as the contrasting features of the Skidder Prospect when compared to other Buchans area deposits prompted a geochemical study of the Skidder Basalt in an effort to determine possible geochemical differences between it and Buchans Group basalts. This paper concentrates on the results of that study and compares analyses of the Skidder Basalt to analyses of other rocks from various tectonic settings as well as to mafic rocks of the Buchans Group. In addition, the geochemistry of the trondhjemites that intrude the Skidder Basalt is reported, and a qualitative petrogenetic model for the Skidder Basalt is presented.

REGIONAL GEOLOGY

The Skidder Basalt forms part of the Dunnage Zone of south-central Newfoundland (Williams, 1979). The Dunnage Zone comprises Cambro-Ordovician ophiolitic rocks and Ordovician island arc sequences deposited during the early opening and closing of the Iapetus Ocean (Dean, 1978; Williams, 1979). The ophiolitic rocks and island-arc sequences are overlain by Devonian to Carboniferous terrestrial sedimentary rocks and intruded by Ordovician to Carboniferous intrusive rocks.

The Skidder Basalt is bounded to the north and west by the early Middle Ordovician (Nowlan and Thurlow, 1984, 1987) Buchans Group, suggested by previous workers (e.g. Thurlow, 1981) to be a calc-alkaline, volcanic and volcaniclastic suite of rocks of island arc affinity. Early Ordovician volcanic and volcaniclastic rocks of the Victoria Lake Group (Kean and Jayasinghe, 1980) outcrop on the south shore of Red Indian Lake in presumed fault contact with the Skidder Basalt. To the southwest, the Skidder Basalt is intruded by lower Silurian granitoid rocks that are part of the Topsails igneous terrane (Whalen and Currie, 1983; 1987) and to the south it is overlain by Carboniferous sedimentary rocks (Kean and Jayasinghe, 1980). The Skidder Basalt has not been dated either paleontologically or radiometrically.

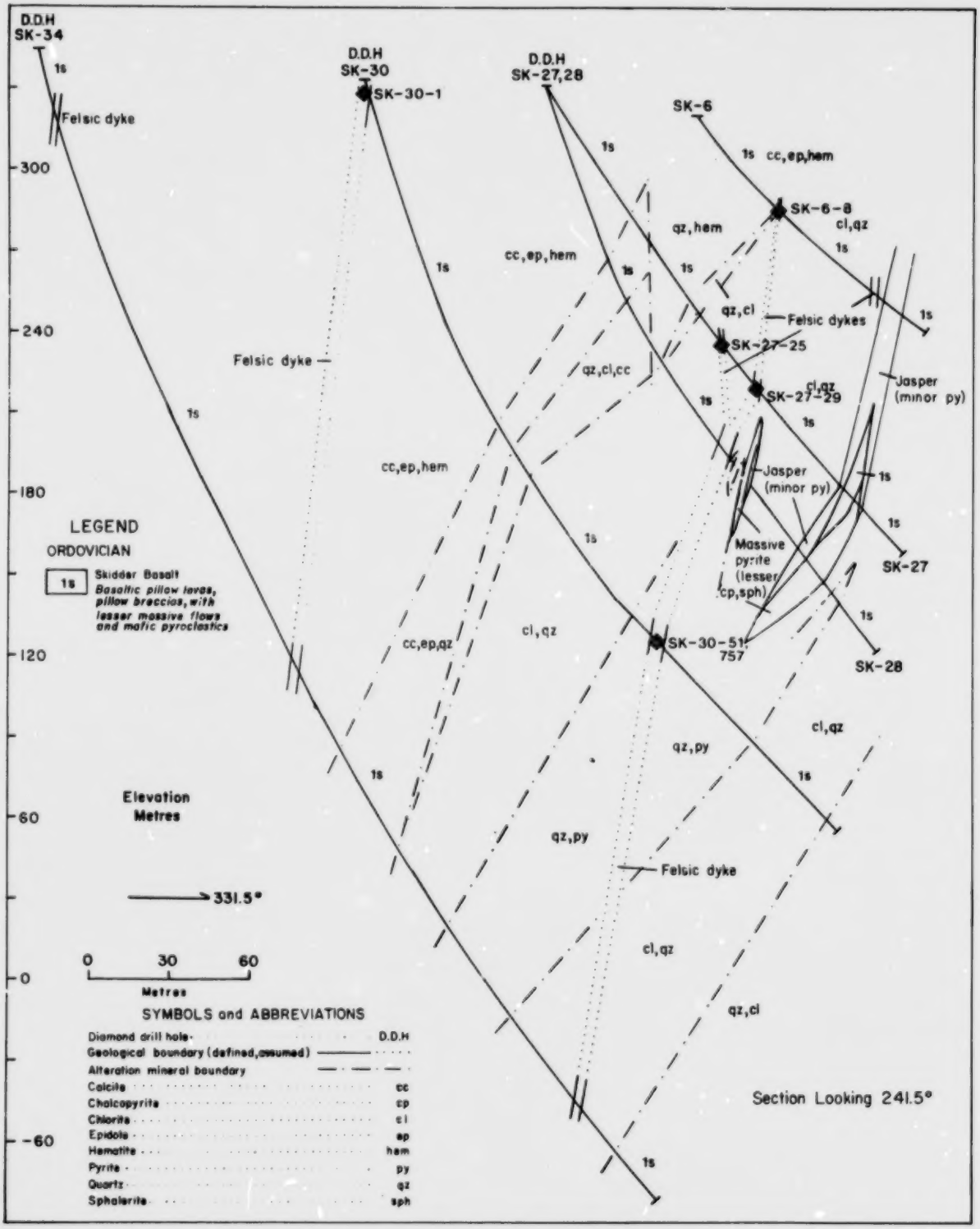

Figure 3. Cross-section through the Skidder Prospect showing the alteration zones that flank the quartz-pyrite stockwork zone. See Figure 2 for location of the diamond-drill holes.

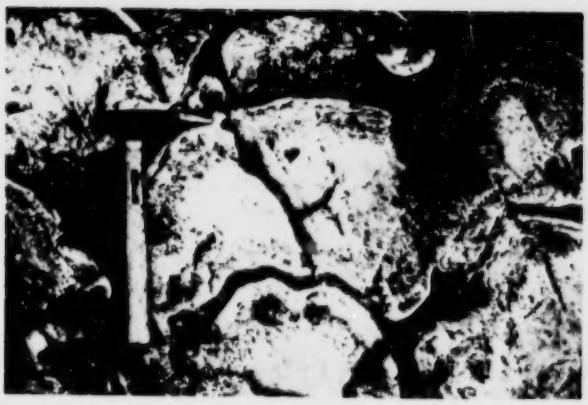

Figure 4. Variolitic pillow lava of the Skidder Basalt near sample location S-35A (Fig. 1; GSC204419-W).

Contact relations of the Skidder Basalt with bounding units were not observed in this study. However, the contact of the Skidder Basalt and the Victoria Lake Group is marked by a topographic lineament through Red Indian Lake suggesting a fault. The contact with the Buchans Group is also marked by lineaments (Fig. 1) that are evident both topographically and also from regional magnetic susceptibility contrasts.

LOCAL GEOLOGY

Skidder Basalt

The Skidder Basalt (unit 1, Fig. 1, 2) comprises a sequence of basaltic pillow lava, pillow breccia, massive flows and lesser mafic pyroclastic rocks. The rocks are medium green to medium grey and are fine to medium grained.

Pillows are dominantly small (15-30 cm in diameter) but locally are up to 1 m in diameter. They are round but irregular in cross-section. Interpillow material is generally more chloritic than that making up the pillows themselves and in some areas small irregular jasper bodies fill pillow interstices. Some pillows contain light grey varioles, 3-6 mm in diameter, within a green chloritic matrix (Fig. 4a, 4b). These variolitic pillows have been noted structurally beneath the Skidder massive sulphide prospect as well as in outcrop to the south, presumably stratigraphically below the deposit.

Pillow breccias consist of angular basaltic fragments within a chloritic and, in many areas, epidote-rich matrix. Other pillow breccias are more characteristic of isolated pillow breccia (Carlisle, 1963). These rocks consist of rounded "mini-pillows", 5-20 cm in diameter, within a darker green, more chloritic matrix. The matrix characteristically comprises 30 to 60 per cent of the rock. In some areas these "mini-pillows" are variolitic and are similar to the variolitic pillows in the flows.

Massive flows are medium grey to medium green and fine to medium grained. Locally the flows have been autoclastically brecciated. An estimated 30 per cent of the massive and pillowed flows are amygdaloidal. These amygdules, commonly filled by calcite and less commonly by epidote and chlorite, are generally 2-4 mm in diameter and, where present, make up less than 10 per cent of the rock.

Mafic pyroclastic rocks consist dominantly of medium green-grey ash-crystal tuffs. These tuffs have an overall massive appearance and are poorly bedded with bedding planes visible only on the weathered surface making them difficult to distinguish from massive flows in drill core. One outcrop of matrix supported lapilli tuff is exposed 400 m northeast of the Skidder Prospect. The lapilli are angular, 2-8 cm in length, and constitute approximately 10 per cent of the rock. The matrix to the lapilli is chloritic to siliceous.

Jasper and red cherty siltstone occur as interpillow material and as discontinuous massive and in rare localities bedded units (Fig. 1, 3).

Mafic intrusive rocks exposed in the area include fine to medium grained diabase dykes and coarser grained gabbroic bodies (dykes?). The latter occur in two outcrops to the west of the Skidder Prospect. The rocks contain visible ophitic intergrowths of plagioclase and pyroxene.

Trondhjemite

A small body of trondhjemite outcrops about 2.5 km northeast of the Skidder Prospect (Fig. 1). Discordant contacts suggesting intrusion of the trondhjemite into adjacent mafic rocks are exposed in some areas. However, a 1 m-thick unit of jasper separates the trondhjemite from basalt in at least one locality. The trondhjemite is generally grey to green, fine grained and massive. A second similar "pod" outcrops approximately 1 km to the east (Fig. 1).

Light grey-green, fine grained trondhjemite dykes intrude the Skidder Basalt immediately adjacent to the Skidder Prospect, as seen in outcrop (Fig. 2) and in drill core (Fig. 3). The dykes, which are generally less than 5 m thick, strike approximately northeast and dip steeply to the southeast. In some areas they contain 5 per cent of 1 to 3 mm feldspar phenocrysts in a dense matrix. In many dykes layering is present within 30 cm of their contact with adjacent units. The layering is defined by alternating light and dark grey-green to buff-coloured 0.5 to 1 cm wide zones that parallel the dyke contact.

These dykes as well as those that are presumed to have "fed" the trondhjemite pods are thought to have been emplaced along faults. The trondhjemitic dykes near the Skidder Prospect probably were intruded along the same fault zone that provided access to the surface for the metal-bearing hydrothermal fluids that formed the deposit. The trondhjemitic pod exposed to the northeast of the prospect occurs along the northeast extension of this assumed fault (Fig. 1, 2).

Structure

Individual flow units as well as pyroclastic and sedimentary rocks examined within the Skidder Basalt strike generally northeasterly and dip steeply to the southeast (Fig. 1). Pillows

are typically not suitable for determining stratigraphic tops but locally can be determined to be northwest facing. Foliations trend predominantly northeasterly (Fig. 1) and in a few localities, a second foliation striking approximately 075° is present (Fig. 1, 2); dips in both cases are steep. Several topographic lineaments are evident on aerial photographs and many of these correspond to linear magnetic features. The linears strike in three dominant directions: northeast, northerly, and approximately northwest (Fig. 1, 2).

PETROGRAPHY

Skidder Basalt

In thin section, extrusive rocks of the Skidder Basalt are dominated by secondary mineral assemblages. Rare, variably altered plagioclase phenocrysts occur in a matrix of albite, actinolite, chlorite, calcite and in places epidote. Albite occurs typically as randomly oriented laths less than 0.5 mm in length. The actinolite occurs as elongated crystals or fibrous masses and in places is altered to talc or chlorite. Secondary epidote occurs typically as rounded masses 1.5 to 2 mm in diameter as well as in veins. In a few thin sections radially aligned needles of epidote are present. Epidote also fills veins and amygdules. Calcite occurs typically as irregular masses and as veins. Chlorite is present as fine grained masses usually interstitial to albite laths. Secondary quartz, where present, fills veins and amygdules and also occurs with albite as irregular patches.

Thin sections of Skidder Basalt rocks containing greater amounts of secondary ferro-magnesian minerals are composed typically of actinolite, chlorite, albite and calcite. Chlorite, in some sections, displays anomalous blue interference colours. Albite occurs as elongated laths throughout. Lesser amounts of opaque minerals (chromite?) also occur as tiny subhedral grains. Relict plagioclase (phenocrysts?) extensively altered to calcite are seen in some sections. No relict ferromagnesion phases have been seen in these more mafic rocks, however in some instances masses of chlorite display shapes that may be pseudomorphic after olivine crystals.

Varioles are present in the more mafic flows in some areas. The varioles are generally defined by a greater abundance of albitized plagioclase which, in some thin sections, occurs as radial growths around a common centre. In places these rosettes form the core of the varioles, the core being surrounded by an intermediate "ring" of chlorite and an outer layer of calcite. Actinolite, chlorite and lesser albite dominate material outside the varioles.

Other Skidder Basalt flows are characterized by plagioclase (mostly albite) as the dominant mineral. These rocks are composed of intersertal intergrowths of albite laths, chlorite, actinolite and, in places, relict clinopyroxene. Finely disseminated opaque minerals (magnetite ?, ilmenite ?, titanomagnetite ?) are also present.

The ubiquitous presence of albite, chlorite and, in many places, actinolite and calcite indicate that rocks of the Skidder Basalt have a mineralogy similar to that of spilites (cf. Amstutz, 1974).

Trondhjemite

In thin section, the trondhjemites, commonly exhibit 2 to 3 mm-long plagioclase and lesser quartz phenocrysts in a matrix of intergrown quartz and plagioclase. Secondary quartz and quartz-chlorite veins and vugs are present in a few places. 'Myrmekitic' quartz-chlorite intergrowths are present in thin sections of rocks from the trondhjemitic pod. In one thin section of these rocks rounded shapes defined by sericite were observed. Minor amounts of opaque minerals are present locally.

SKIDDER BASALT GEOCHEMISTRY

Sample preparation and geochemical methods

Whole rock geochemical analyses were done on 33 samples of pillowed flows and 15 samples of massive flows collected by the author during mapping of the Skidder Basalt. The samples were collected outside the Skidder Prospect alteration zone. Weathered material and any veins and amygdules present in the samples were removed prior to crushing.

With the exception of phosphorus and loss on ignition, major element analyses were performed by atomic absorption spectrophotometry. Samples were prepared in a manner similar to that described by Langmhyr and Paus (1968) and the elements were analysed on a Perkin-Elmer Model 370 atomic absorption spectrometer with digital readout. Phosphorus was determined colorimetrically using a Bausch and Lomb Spectronic 20 Colorimeter, based on a modification of the method described by Shapiro and Brannock (1962). Loss on ignition was determined from weight loss after heating a portion of the powdered sample to approximately 1000°C for about 90 minutes. Duplicate analyses of several samples and four analyses of Skidder Basalt sample S-60 were run to determine the precision of the major element analyses. Table 1 shows the mean, standard deviation, minimum and maximum values obtained from the duplicate analyses of sample S-60.

Table 1. Duplicate major element analyses by atomic absorption spectrophotometry

Skidder Basalt samples S-60 (4 analyses)				
	Mean	Standard deviation	Minimum	Maximum
SiO_2	51.48	0.43	50.90	51.90
TiO_2	1.31	0.06	1.27	1.40
Al_2O_3	14.93	0.21	14.70	15.20
Fe_2O_3[1]	13.64	0.06	13.57	13.71
MnO	0.13	0.01	0.13	0.14
MgO	6.60	0.08	6.52	6.66
CaO	4.02	0.01	4.00	4.03
Na_2O	5.57	0.07	5.50	5.63
K_2O	0.09	0.00	0.09	0.09
P_2O_5[2]	0.14	0.03	0.10	0.17
LOI[3]	2.35	0.11	2.25	2.48

[1]Total iron as Fe_2O_3
[2]Analyzed by colorimetry
[3]Determined by weight difference after heating to 1000°C for 90 minutes

Trace elements were determined by X-ray fluorescence techniques on 10-gm, pressed, whole rock powder pellets using a Phillips 1450 X-ray fluorescence spectrometer with a rhodium tube. U.S.G.S. standard W-1 was included with each batch of pellets analysed by X-ray fluorescence. Table 2 shows the mean, standard deviation, and the minimum and maximum trace element values obtained from 26 repeat analyses of W-1. Also, the accepted trace element values for W-1 according to Abbey (1980) and the detection limits of the elements (D. Press, personal communication) are listed. The elements Sr, Y, Zn, Cu, Ni, V and Cr have low standard deviations relative to the mean, have a limited range, are close to accepted values, and concentrations of these elements in the Skidder Basalt (Table 3) are generally well above the detection limits by the XRF method. Zr values are also consistent but approximately 10 ppm lower than the accepted value for W-1. Ga, Rb and Nb have acceptable range and standard deviation relative to the mean and are similar to the accepted values for W-1. However, concentrations of Rb and Nb within the Skidder Basalt (Table 3) are close to the detection limits for these elements by the XRF method. Pb values obtained are extremely variable and Pb concentrations in the Skidder Basalt are close to or below the detection limit. Ba analyses are highly variable but the mean is close to the accepted value for Ba in W-1.

Introduction

Eighteen representative whole rock analyses of the Skidder Basalt samples are presented in Table 3. The Skidder Basalt has been geochemically subdivided into two types (Fig. 1, 2). Those basalts which contain higher contents of elements such as Cr (>150 ppm) and Ni, which are compatible with early liquidus phases, and relatively low contents of "incompatible" elements such as (<25 ppm), Zr and P have been termed "primitive" compositions. Samples with lower concentrations of the compatible minor elements and higher contents of the incompatible elements have been termed 'evolved'. The distribution of primitive and evolved rocks, shown on Figure 1, suggests that the Skidder Basalt as now exposed occurs in a series of thrust slices.

The geochemical results are used in the following discussion to: 1) suggest the chemical effects of spilitization on the Skidder Basalt, 2) to geochemically classify the rocks and suggest the possible tectonic setting in which they formed and 3) develop a qualitative petrogenetic model.

Spilitization

Mottl (1983a and 1983b) attempted to apply experimental data on seawater-basalt interaction to the observed secondary mineralogy of altered basalts. He concluded that an estimate can be made of the seawater/basalt mass ratio on the basis of the secondary minerals observed in the altered basalts. Secondary minerals present in the Skidder Basalt (outside the Skidder Prospect alteration zone) are calcite, epidote, actinolite, albite, chlorite and minor quartz and hematite. Mottl (1983a) suggests this mineral assemblage to be characteristic of relatively low water to rock ratios less than 30. According to experimental results summarized by Rosenbauer and Bischoff (1983), the effects of seawater interaction with rocks under the low water/rock ratios (presumed to have prevailed during alteration of the Skidder Basalt) should be an overall increase in Mg and probably Na, an overall decrease in Ca and K and redistribution of SiO_2, Fe, Mn and Zn.

In order to examine the possible effects of alteration on the contents of these elements in the Skidder Basalt, binary plots of elements versus zirconium and element versus yttrium were done. These latter elements were chosen since they are incompatible with early formed mafic phases and can thus be used as differentiation indices and moreover they are considered to be resistant to hydrothermal alteration (Winchester and Floyd, 1976; Pearce and Norry, 1979; Perfit *et al.*, 1980; "Basaltic Volcanism Study Project" (BVSP), 1981a). Figures 5a,b,c and d are plots of SiO_2[1], total iron as Fe_2O_3, MgO and Na_2O versus yttrium. SiO_2 and total iron as Fe_2O_3 show moderate scatter on these diagrams and the range of values at a given yttrium content suggests addition of silica and iron to some samples but removal from others. Redistribution rather than overall addition or removal of these elements is supported by the similarity of their average contents in the Skidder Basalt when compared to relatively unaltered ocean-floor and island-arc basalts (Table 4). As shown in Table 4, the average content of MgO is lower in the Skidder Basalt than in average ocean-floor basalt and island-arc basalt (with the exception of those from the northwestern Pacific) but the average Na_2O content of the Skidder Basalt is considerably higher than the others. This suggests that hydrothermal alteration has resulted in an overall addition of Na_2O to and removal of MgO from the Skidder Basalt. The extreme scatter shown by MgO and Na_2O on Figures 5c and 5d suggests that the amount of removal/addition of these elements was somewhat independent of the original, unaltered composition of the rocks. Thus, the negative correlation of MgO with Na_2O shown in Figure 6 is probably not totally a result of magmatic processes but also because hydrothermal addition of Na_2O to the rock was probably accompanied by removal of MgO. The average contents of K_2O and Sr in the Skidder Basalt are also less than average unaltered ocean-floor and island-arc basalts (Table 4) indicating a probable depletion of these elements in the Skidder Basalt as a result of alteration. Average CaO contents of the Skidder Basalt are also less than the others. This may also be due to alteration but removal of calcite veins from the analysed samples has introduced a sampling bias since Ca removed from feldspars as a result of albitization may have been redeposited as calcite in veins.

The chemical effects of spilitization on alkalies are further illustrated on a diagram of Hughes (1973) (Fig. 7).

[1]On all plots presented that include major element oxides, loss on ignition has been excluded and each major element analysis recalculated to 100% before plotting.

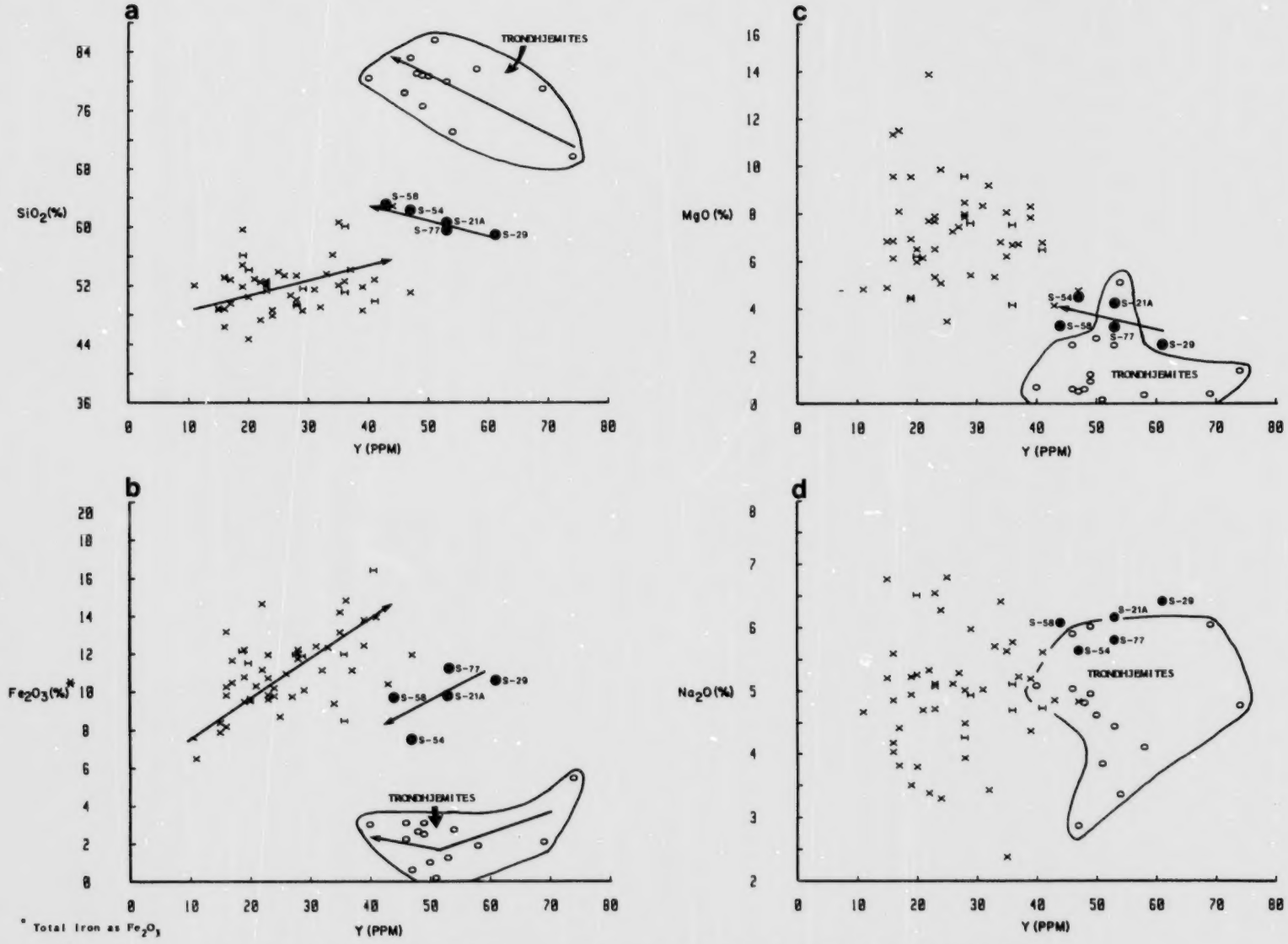

Figure 5. Selected major oxide versus yttrium plots of the Skidder samples. Arrows show suggested differentiation trends. X – Skidder Basalt lavas; H – mafic dykes from Skidder area; solid dots – high Y/low V lavas; open circles – Skidder trondhjemites.

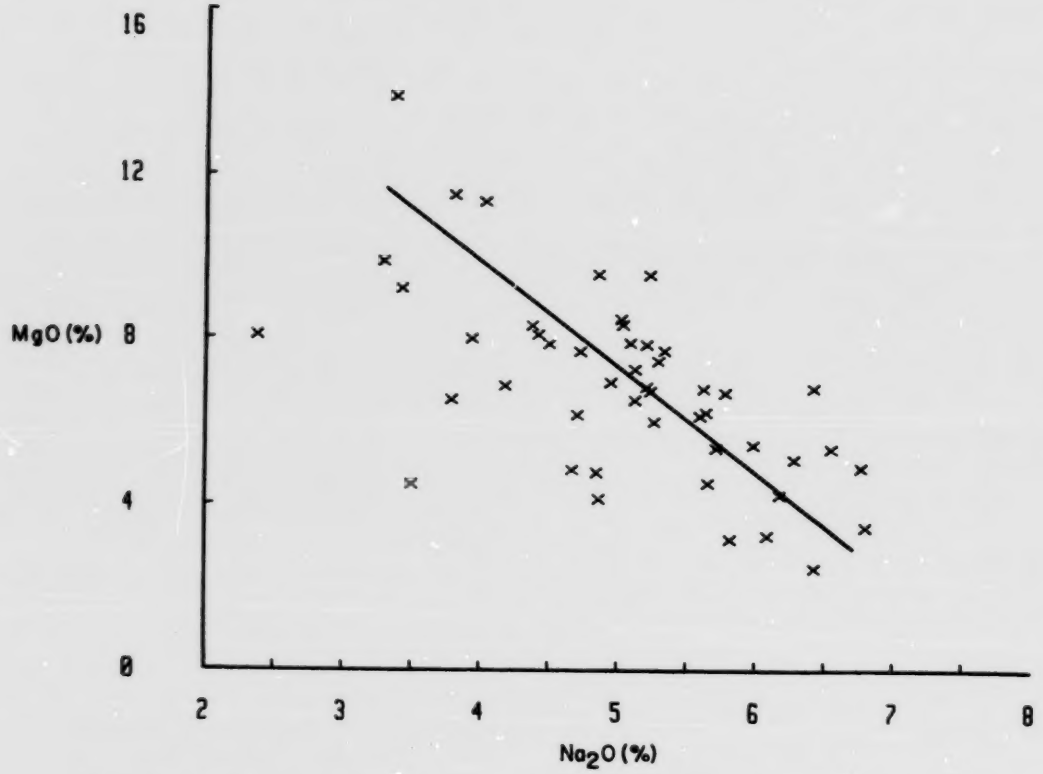

Figure 6. MgO versus Na_2O plot of Skidder basalts showing marked negative correlation.

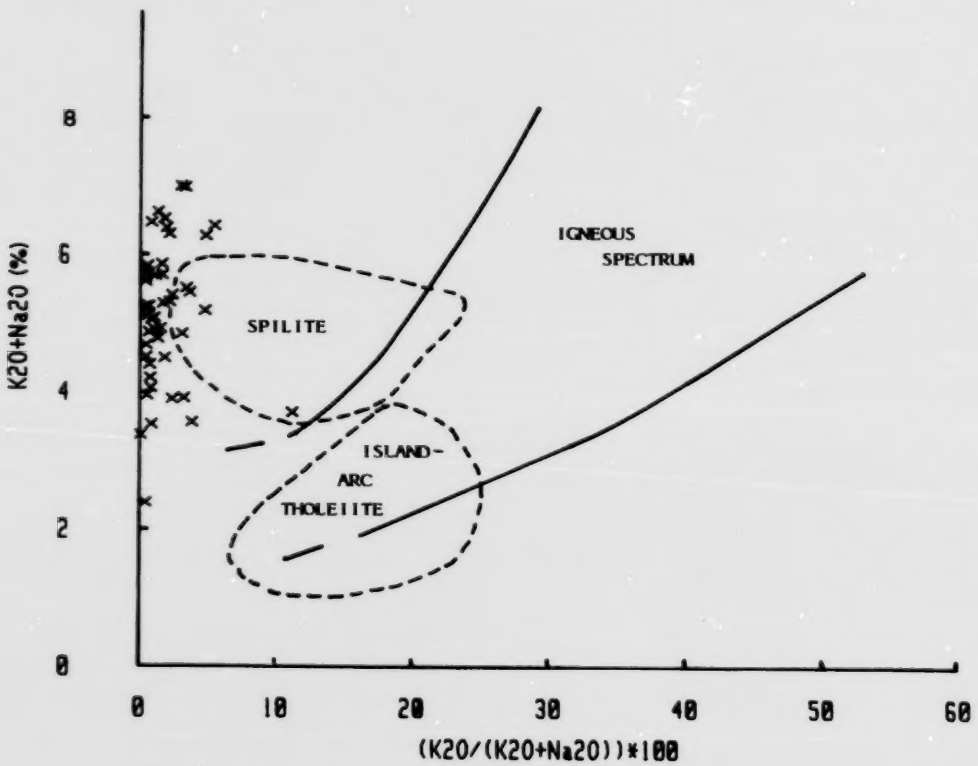

Figure 7. Skidder basalts plotted on the 'igneous spectrum' diagram of Hughes (1973). Island-arc tholeiite field after Stauffer et al. (1975).

Table 2. Duplicate minor element analyses by X-ray fluorescence

	U.S.G.S. standard W-1 (26 analyses)								
	Mean($\bar{x}$)	Standard deviation(s)	Minimum	Maximum	($s/\bar{x}$) × 100	Accepted value (v) (Abbey, 1980)	$\bar{x}$ – v	($\bar{x}$ – v)/v × 100	Detection limit
Pb	9	3.4	3	18	38%	7.8	1.2	15%	6.4
Th	5	2.6	0	10	52%	2.4	2.6	108%	4.4
U	1	1.4	0	6	140%	0.58	0.42	72%	1.7
Rb	22	2.6	17	27	12%	21	1	5%	3.4
Sr	183	2.8	176	188	2%	190	−7	−4%	3.1
Y	24	1.6	21	28	6%	25	0	0%	3.8
Zr	95	2.5	90	100	3%	105	−10	−10%	4.6
Nb	11	1.6	7	13	15%	9.5	1.5	16%	3.5
Zn	84	4.9	65	89	6%	86	−2	−2%	2.3
Cu	116	5.1	100	124	4%	110	7	6%	2.5
Ni	77	4.2	62	82	5%	76	1	1%	2.8
La	13	5.7	0	23	44%	9.8	3.2	33%	6.3
Ba	161	38	46	208	24%	160	1	1%	5.4
V	253	4.2	242	261	2%	260	−7	−3%	2.0
Ce	71	20	30	132	28%	23	48	209%	6.5
Cr	121	2.9	113	126	2%	115	6	5%	1.8
Ga	19	2.8	14	29	15%	16	3	19%	2.1

Table 3. Representative analyses of the Skidder Basalt. See Figure 2 for sample locations

	Major elements																	
	S 76	S 35A	S 59	S 78	S 39	S 34B	S 53	S 19	S 50	S 42	S 52	S 79	S 70	S 27B	S 41	S 77	S 21A	S 58
SiO_2	42.30	48.50	47.90	50.60	50.60	49.60	50.90	48.10	52.70	49.60	52.20	49.40	50.90	52.80	49.80	57.70	58.70	61.30
TiO_2	0.69	0.62	0.49	0.87	0.79	0.84	1.09	1.13	1.16	1.20	1.03	1.15	1.53	1.65	1.23	1.34	1.60	1.22
Al_2O_3	14.40	14.50	15.10	14.60	16.60	14.50	14.00	14.50	13.60	15.80	14.80	15.30	15.20	12.90	14.00	14.10	14.30	14.10
Fe_2O_3[1]	12.04	8.86	10.12	9.35	10.75	9.65	9.51	9.23	11.87	11.95	12.00	13.49	14.35	10.82	11.95	10.95	9.45	9.45
MnO	0.21	0.16	0.16	0.18	0.15	0.15	0.16	0.16	0.16	0.16	0.19	0.19	0.21	0.19	0.13	0.19	0.15	0.14
MgO	10.37	8.94	11.13	9.12	7.43	5.77	7.64	7.08	7.77	8.04	5.21	5.90	6.48	6.56	7.55	3.07	4.09	3.17
CaO	7.60	7.07	8.03	5.91	4.66	8.60	8.46	9.43	6.93	4.57	6.29	4.04	2.28	7.34	6.16	3.38	2.09	1.65
Na_2O	3.68	4.89	3.68	4.63	5.14	4.41	4.92	5.02	4.44	4.85	5.56	5.35	5.59	5.10	5.00	5.64	5.98	5.93
K_2O	0.03	0.03	0.09	0.07	0.18	0.14	0.03	0.12	0.02	0.05	0.03	0.06	0.09	0.02	0.11	0.03	0.13	0.34
P_2O_5	0.04	0.03	0.01	0.07	0.12	0.13	0.10	0.16	0.13	0.20	0.07	0.04	0.16	0.11	0.19	0.59	0.38	0.17
LOI	8.12	5.56	3.75	4.14	3.25	5.70	3.35	5.59	1.83	3.51	2.12	2.83	3.17	1.48	4.73	2.89	2.39	1.84
Total	99.48	99.16	100.46	99.54	99.67	99.49	100.16	100.52	100.61	99.93	99.50	97.75	99.96	98.97	100.85	99.88	99.26	99.31
	Minor elements																	
	S 76	S 35A	S 59	S 78	S 39	S 34B	S 53	S 19	S 50	S 42	S 52	S 79	S 70	S 27B	S 41	S 77	S 21A	S 58
Pb	3	nd	nd	3	nd	5	3	1	1	7	2	4	8	nd	7	5	6	nd
Rb	nd[2]	nd	nd	2	nd	2	nd	3	nd	nd	nd	nd	nd	nd	5	3	4	nd
Sr	44	52	67	35	150	98	67	110	89	46	57	56	73	32	64	38	31	32
Y	16	19	17	16	22	21	23	27	28	31	33	35	36	37	39	53	53	44
Zr	30	38	16	46	50	52	66	62	73	58	80	78	69	74	68	88	95	100
Nb	2	1	4	4	5	4	7	3	8	3	6	6	3	2	4	3	5	4
Zn	92	87	68	71	77	60	55	66	36	84	94	110	120	43	75	80	120	110
Cu	15	130	84	56	81	56	39	51	36	110	32	20	45	99	14	11	nd	14
Ni	330	150	150	69	88	37	53	67	72	32	13	5	6	22	20	nd	nd	nd
Ba	2	nd	nd	13	9	2	8	17	11	19	13	nd	41	nd	28	62	52	1
V	290	300	190	280	380	330	280	250	270	440	370	420	540	310	340	90	130	120
Cr	550	550	370	150	230	93	180	140	280	87	42	37	45	24	63	nd	nd	3
Ga	15	14	13	15	15	14	12	10	12	13	17	17	16	12	15	20	16	19

[1]Total iron as Fe_2O_3
[2]nd = not detected

Table 4. Comparison of average Skidder Basalt to averages of ocean-floor and island-arc basalts as well as the Annieopsquotch ophiolite and Sandy Lake Formation basalts of the Buchans Group

Major elements

	Ocean-floor basalts			Annieopsquotch ophiolite		Skidder Basalt (average)	Island-arc basalts			Buchans Group basalts		
	1a	1b	2	3a	3b		4	5a	5b	6	7a	7b
weight %												
SiO_2	50.53	50.93	49.56	49.28	50.69	50.02	51.90	50.73	50.63	52.00	48.80	46.60
TiO_2	1.56	1.19	1.42	1.24	1.35	1.02	0.80	0.83	0.86	0.83	0.83	0.87
Al_2O_3	15.27	15.15	16.09	14.92	14.94	14.59	16.00	17.38	18.16	17.30	15.47	16.81
Fe_2O_3	-	-	-	2.70	2.56	10.30[1]	-	3.01	3.29	-	8.63[1]	11.54[1]
FeO	10.46[2]	10.32[2]	10.17[2]	8.20	8.09	-	9.56[2]	6.96	7.79	7.53	-	-
MnO	-	-	-	0.20	0.26	0.15	0.17	0.19	0.19	0.19	0.14	0.13
MgO	7.47	7.69	7.69	7.56	7.14	6.48	6.77	6.97	5.61	7.39	5.80	6.72
CaO	11.49	11.84	11.34	11.05	7.14	7.11	11.80	11.51	11.15	11.70	9.90	6.27
Na_2O	2.62	2.32	2.80	2.36	3.99	4.77	2.42	2.06	1.96	2.26	3.00	1.82
K_2O	0.16	0.14	0.24	0.09	0.06	0.09	0.44	0.26	0.27	0.42	0.97	1.40
P_2O_5	0.13	0.10	-	0.10	0.12	0.15	0.11	0.09	0.10	0.13	-	-
Mg'	0.59	0.60	0.60	0.59	0.59	0.58	0.58	-	-	-	-	-
				n=42	n=7	n=48		n=43	n=89	n=12	n=5	n=8

Minor elements

	Ocean-floor basalts		Annieopsquotch ophiolite		Skidder Basalt (average)	Island-arc basalts				Buchans Group basalts	
					Large low valency cations						
ppm	8.	9a.	3a.	3b.		9b.	5a.	5b.	6.	7a.	7b.
K	1064	1660	750	500	750	3570	2160	2240	3490	8050	11600
Rb	1.0	2	1	1	2	4.7	4.1(22)*	2.4(2)	5.7	22	34
Ba	12.2	20	62	50	18	60	90.2(21)	195(8)	63.3	410	720
Pb	-	-	2	3	3	-	4.0(18)	5.28(1)	2.4	25	30
Sr	127	121	95	83	84	231	224(22)	247(3)	337.6	260	250
					Large high valency cations						
Zr	-	90	57	70	63	40	31(21)	313(3)	41	72	80
Ti	-	8390	7430	8090	6120	5040	4980	5160	4980	4980	5220
Nb	-	4.6	1	2	5	1.7	1.7(5)	-	1.6	-	-
Y	-	33	36	42	29	17	16(21)	17(1)	17	-	-
					Ferro-magnesian elements						
Cr	270	251	170	120	150	111	82(20)*	31(1)	176	240	130
V	250	-	330	350	310	-	286(20)	240(1)	254	180	330
Ni	135	90	74	44	54	18	36(20)	38(1)	69	48	40
Cu	86	-	30	30	45	-	98(20)	40(1)	94	52	66
Zn	85	-	86	140	72	-	78(21)	-	71	64	90
Ga	17	-	14	14	15	-	-	-	15.2	-	-

[1] Total Iron as Fe_2O_3
[2] Total Iron as FeO
n = number of samples
* Values in parentheses indicate number of analyses

1. Melson et al. (1976): Average basaltic glass a) Atlantic, Pacific, and Indian Ocean spreading centre b) Indian Ocean spreading centre.
2. Pearce (1976): Average ocean-floor basalt.
3. Dunning (1984); Annieopsquotch ophiolite a) Average-sheeted dykes b) Average-lavas.
4. Jakes and White (1972); Average island-arc tholeite.
5. Ewart (1982): Average basalts of low K orogenic volcanic rocks: a) South-Western Pacific; b) North-Western Pacific.
6. Basaltic Volcanism Study Project (1981b): Average New Britain Island Arc Basalts.
7. Thurlow (1981): Buchans Group, Sandy Lake Formation: a) mafic flows b) mafic pyroclastic rocks.
8. Basaltic Volcanism Study Project (1981a): Type 1 oceanic tholeiites.
9. Pearce (1982): a) Mid-ocean-ridge tholeiite; b) tholeiitic volcanic arc basalts.

Hughes showed that unaltered igneous rocks plot in the igneous spectrum field on this diagram. The Skidder basalt rocks plot outside the igneous spectrum, close to the spilite field, indicative of enrichment of Na_2O relative to K_2O in the rocks.

The redistribution of SiO_2 and total Fe as well as the decrease in K as a result of alteration of the Skidder Basalt is supportive of the conclusions of Rosenbauer and Bischoff (1983). However, the decrease in Mg and substantial increase in Na that has occurred in the Skidder Basalt is not predicted by the experimental results. Mottl (1983b) uses metamorphic differentiation to explain the discrepancy in the amount of Na increase predicted by experiments on basalt/seawater interaction and the greater increase noted in altered basalts. He suggests that Na diffuses away from the 'reaction front' under natural conditions, a process not duplicated in the experiments.

Classification

Major elements such as Si, Fe, Mg and alkalies, commonly used for classifying volcanic rocks, in the Skidder Basalt, have been affected by hydrothermal alteration and are therefore not used. Instead the rocks are classified using minor and trace elements less affected by alteration.

Winchester and Floyd (1977) defined fields for the common volcanic rocks on a binary plot of Zr/TiO_2 (used as a differentiation index) versus Nb/Y (used as an index of alkalinity) (cf. Pearce and Cann, 1973). The Skidder basalts are classified as sub-alkaline on this diagram (Fig. 8) and fall dominantly in the sub-alkaline basalt and basalt/andesite fields. Two of the rocks are classified as andesite. The fields of tholeiitic and calc-alkaline basalts on the Ti-Zr diagram defined by Pearce and Cann (1973) were modified slightly by Garcia (1978). Tholeiitic magma types show an increase in Ti with differentiation whereas calc-alkaline magmas do not. The Skidder basalts define a tholeiitic trend on this diagram (Fig. 9). Samples of less differentiated rocks (containing lower amounts of Ti and Zr) plot dominantly in the overlapping island-arc tholeiite/ocean-floor basalt field and more differentiated rocks (those with greater amounts of Ti and Zr) plot mostly in the ocean-floor basalt field.

Tectonic setting

Many authors eg. (Perfit et al., 1980; Basaltic Volcanism Study Project (BVSP), 1981a, b; Pearce, 1982) have noted that mid-ocean ridge basalt suites have higher contents of the high field strength (HFS) cations Ti, Zr and Y, as well as the compatible element Cr, and have much lower contents of the large ion lithophile (LIL) elements such as K, Rb, Ba and Sr than do island-arc tholeiites.

Table 4 lists the average contents of elements in the Skidder Basalt along with average contents for ocean-floor basalts, island-arc basalts, the Sandy Lake Formation basalts of the Buchans Group (Thurlow, 1981) and the Annieopsquotch Complex (Dunning, 1984) exposed to the south of the Skidder area. The average contents of large ion lithophile elements are lower in the Skidder basalts relative to island-arc tholeiites and Buchans Group basalts and are comparable to those of average ocean-floor basalts and the Annieopsquotch ophiolite. However, hydrothermal alteration has affected the contents of these elements in the Skidder Basalt limiting their use as a discriminant. Nevertheless, Hart (1976) indicates that, of these elements, Sr is affected least as a result of hydrothermal alteration by seawater. Also, Basaltic Volcanism Study Project authors (1981a) suggest that Sr abundances of less than 200 ppm separate ocean-floor tholeiitic rocks from those of other tectonic regimes. The average content of Sr (83.5 ppm) for the Skidder Basalt is approximately equal to that of the dykes and lavas of the Annieopsquotch ophiolote and both have significantly lower average contents than island-arc tholeiites and Buchans Group basalts and are somewhat less than average values for ocean-floor basalts. Other elements used to discriminate between ocean-floor and island-arc tholeiites eg. Ti, Zr, Cr and Ni have contents, in the Skidder Basalt, intermediate between the two types. The average content of Y in the Skidder Basalt is only slightly less than the average for ocean-floor basalts and the Annieopsquotch ophiolite but is somewhat higher than average contents for island-arc tholeiites.

Trace element variation diagrams commonly used to distinguish basalts from different tectonic settings are shown in Figure 10. The Skidder basalts plot dominantly within the ocean-floor basalt field and a few in the low-potassium tholeiite area on Figure 10a (Pearce and Cann, 1973). They plot in the MORB-arc lava and MORB-within plate lava fields with some scatter into the field of island-arc lavas on Figure 9b (Pearce, 1980). On another diagram from Pearce (1980), the Skidder basalts overlap the MORB-within-plate lava and island-arc tholeiite fields at higher Cr contents and plot in the within-plate basalt and island-arc tholeiite fields at lower Cr contents (Fig. 10c). They plot close to the boundary of island-arc and ocean-floor tholeiites at higher Ni contents and predominantly within the island-arc tholeiite field at lower Ni contents on Figure 10d (Beccaluva *et al.*, 1979).

Petrogenetic model

According to several authors (e.g. Bender et al., 1978, BVSP, 1981a) MORB chemistry is dominated by low pressure fractional crystallization of olivine + Cr-spinel followed by olivine + plagioclase and only late in the crystallization history does clinopyroxene become a liquidus phase. This contrasts with the liquid line of descent proposed for island-arc tholeiites (cf. Perfit et al., 1980) in which clinopyroxene instead of plagioclase is the early mineral phase. Clinopyroxene replaces olivine as the liquidus phase at pressures greater than 12 kb (about 40 km depth) (BVSP, 1981c). Also, Holloway and Burnham (1972) showed that plagioclase is not a stable phase under hydrous magmatic conditions and that the important crystallizing phases under these conditions are clinopyroxene, olivine and magnetite. This prompted Perfit et al. (1980) to suggest that the substitution of clinopyroxene for plagioclase as an early mineral phase in island-arc tholeiites may be due to crystallization at greater depths or at higher P_{H_2O} conditions. Hence, the presence or absence of plagioclase or clinopyroxene as the early liquidus phase can provide further information as to the possible tectonic setting and also the P_{H_2O} and the fO_2 conditions under which the Skidder basalts formed.

Carbonatized plagioclase crystals are the only relict phenocrysts noted in thin sections of the Skidder Basalt. Fractionation of plagioclase is also consistent with the trend defined by the Skidder flows on Figure 11 (Pearce and Flower, 1977). According to Le Roex et al. (1982), Sr has a distribution coefficient of 2 between plagioclase and liquid. Thus, fractionation of plagioclase is also supported by the relatively low average content of Sr in the Skidder Basalt.

Pearce and Norry (1979) modeled the effects of fractionation of several minerals with regard to Zr and Y. These effects are shown as vectors on Figure 12. The trend outlined by

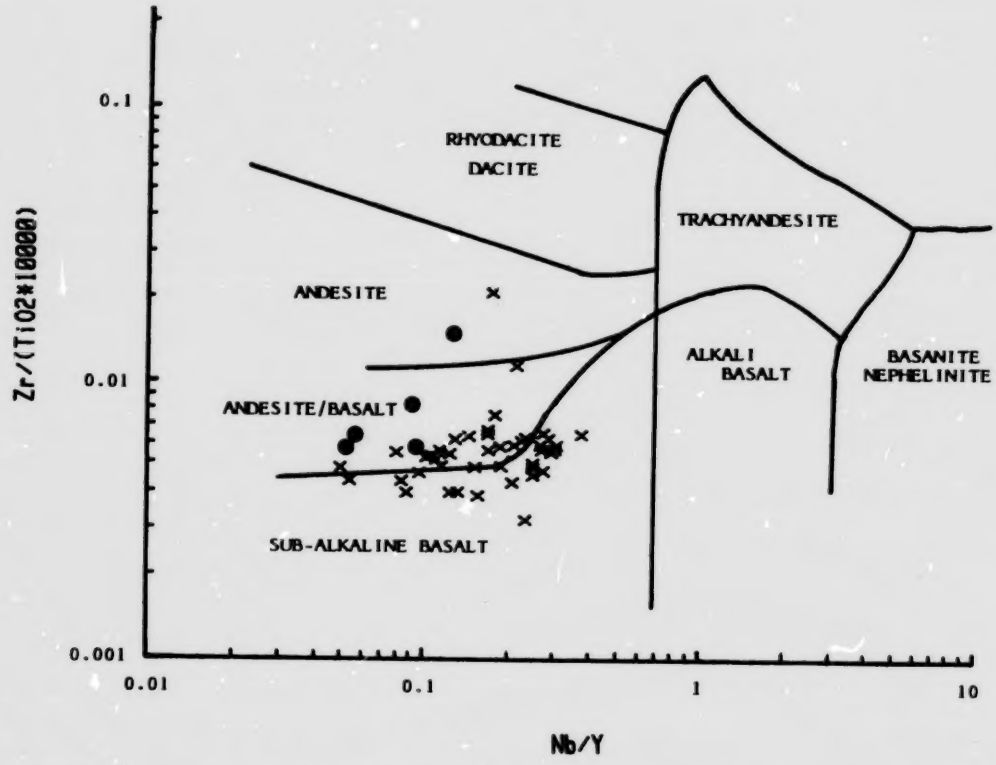

Figure 8. Skidder flows plotted on classification diagram after Winchester and Floyd (1977). Solid dots – high Y/low V lavas.

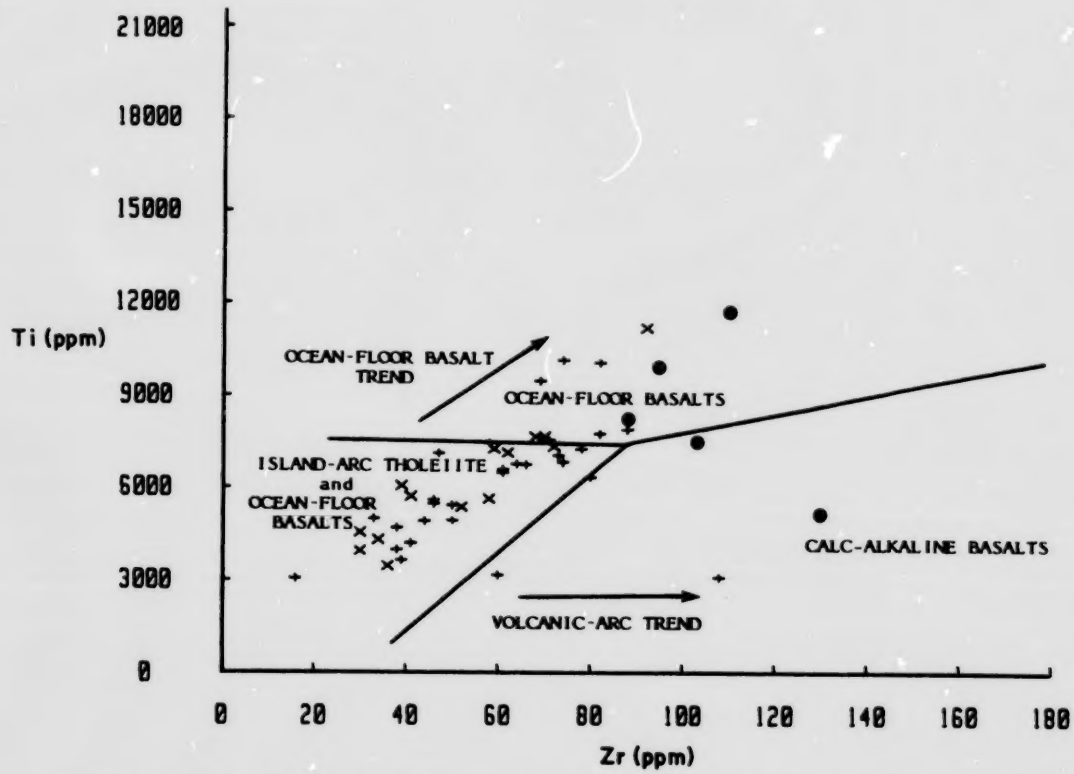

Figure 9. Skidder flows plotted on environmental discriminant diagram after Garcia (1978). + – pillowed flows; X – massive flows; solid dots – high Y/low V lavas.

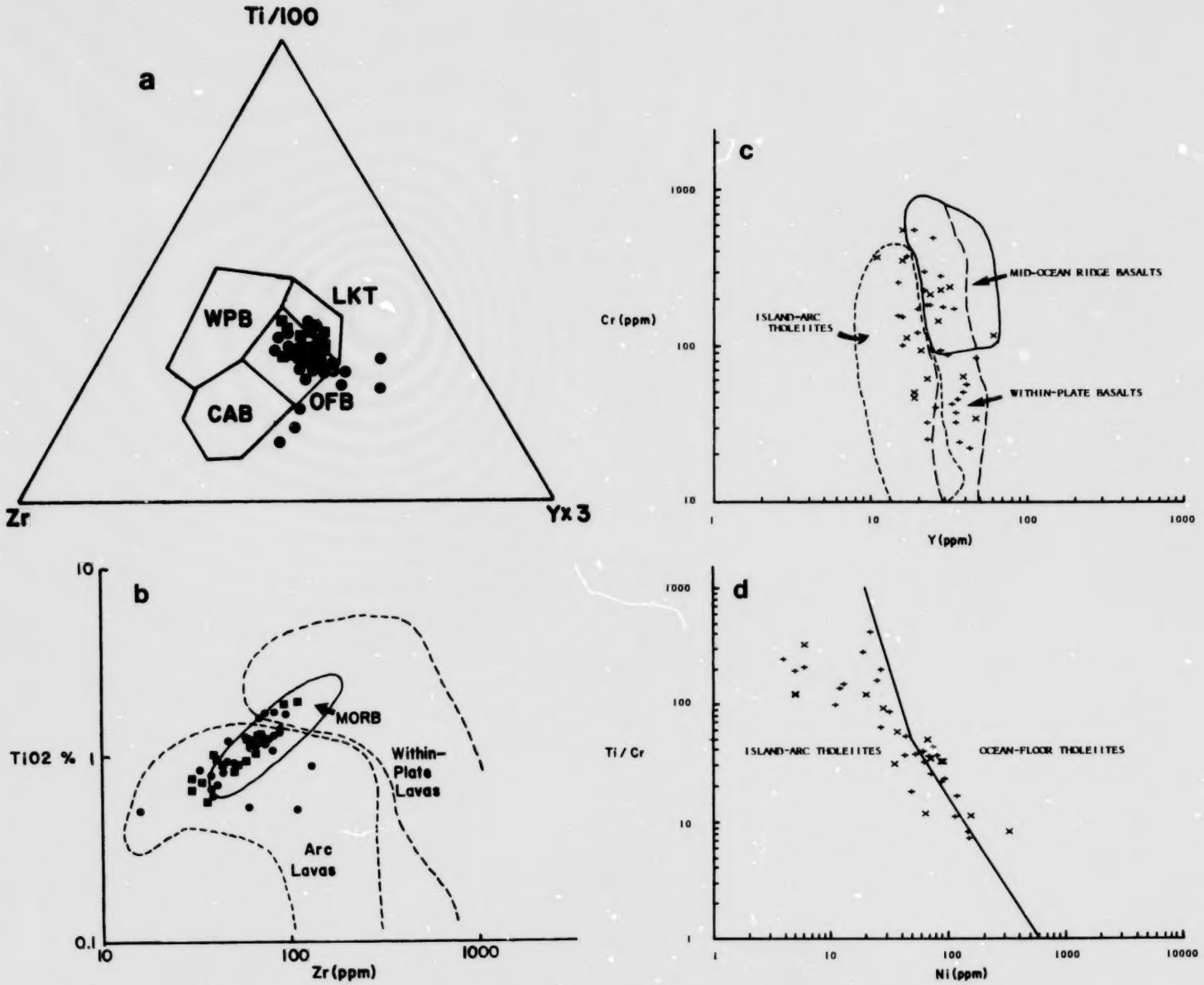

Figure 10. Skidder flows plotted on typical trace element variation diagrams used to distinguish basalts of different tectonic settings. WPB – within-plate basalts; LKT – low-potassium tholeiites; CAB – calc-alkaline basalts; OFB – ocean-floor basalts; MORB – mid-ocean-ridge basalts; solid dots and plus sign – pillowed flows; solid squares and "X" – massive flows.

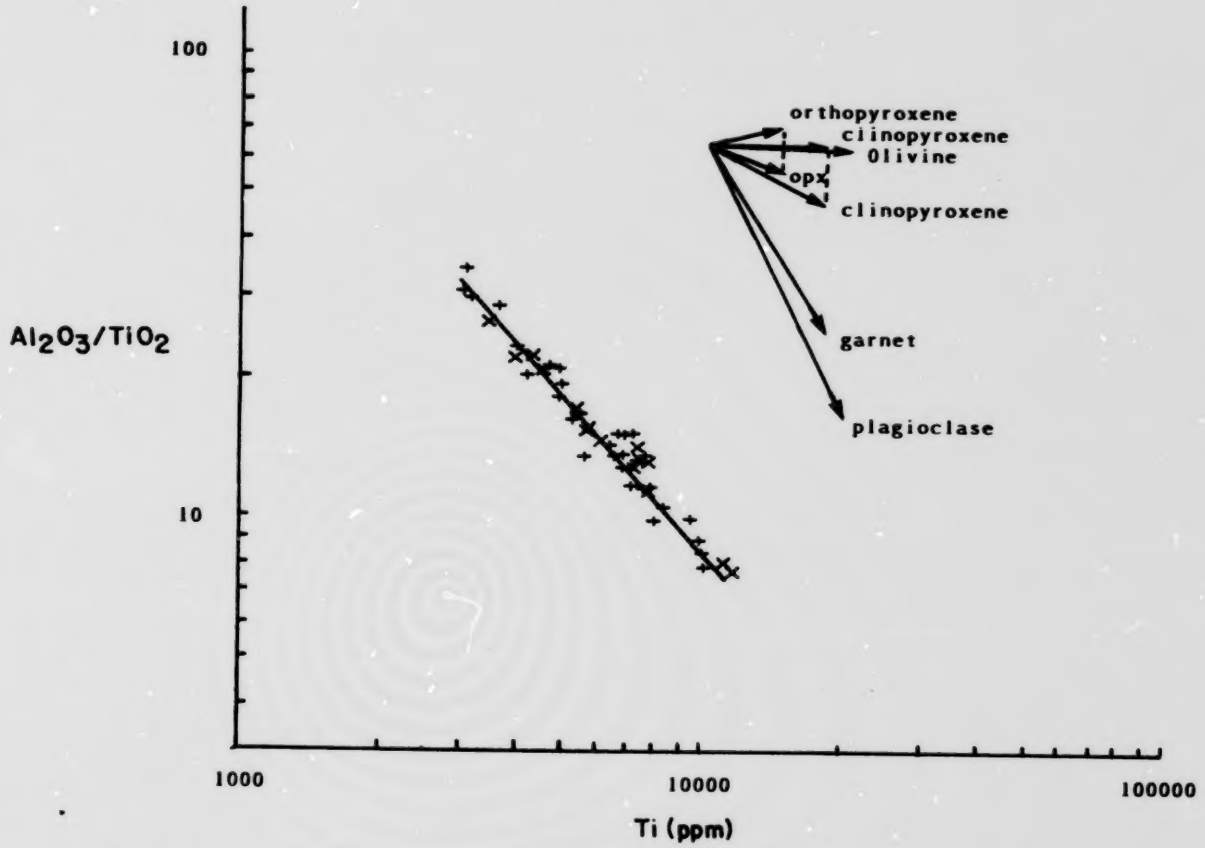

Figure 11. Skidder basalts plotted on a chemical fractionation diagram of Pearce and Flower (1977). Arrows show the effects of fractionation of various minerals. + – pillowed flows, X – massive flows.

Skidder flows is consistent with fractionation of olivine and plagioclase. Extensive fractionation of clinopyroxene which would tend to lower the Y/Zr ratio is not indicated.

Figure 13 is a plot of log Ni versus log Cr, on which a 'best fit' line composed of five segments has been drawn (by eye) through the trend outlined by the Skidder Basalt and Annieopsquotch ophiolite. The behaviour of Ni and Cr in basaltic magmas is dominated by the three phases: olivine, Cr-spinel and clinopyroxene. Nickel partitions into olivine and Cr into Cr-spinel, which crystallize early from basaltic magmas, and both Ni and Cr partition into clinopyroxene having distribution coefficents of 2 and 10, respectively (Sun et al., 1979). Segment A is thought to be representative of co-fractionation of olivine and Cr-spinel. The steepening of the slope shown by segment B is indicative of an increase in the amount of Cr precipitation relative to Ni presumably due to an increase, relative to olivine, of the amount of Cr-spinel fractionation. This increased Cr-spinel frationation may have occurred at the onset of anorthite precipitation. The flattening of the trend to being subparallel to the Ni axis (Trend C) is probably indicative of the co-precipitation of olivine and anorthite and presumably marks the reduction and eventual cessation of Cr-spinel fractionation. The Annieopsquotch ophiolite dykes and some Skidder Basalt samples display a progressively steepened trend (Segment D) subparallel to the Cr axis. This steepened trend is suggested to mark the onset of clinopyroxene and the cessation of olivine fractionation. However, many of the Skidder Basalt rocks continue trend C and then follow trend C' which is parallel to the Ni axis suggestive of continued co-frationation of olivine and anorthite without clinopyroxene.

Since plagioclase is an early crystal phase in Skidder Basalt frationation, crystallization probably occurred under low fO_2 conditions (Holloway and Burnham, 1972). Vandium is compatible with Cr-spinel (Sun et al., 1979) and under low oxygen fugacity (less than or equal to log fO_2 of -10) is also compatible with clinopyroxene (Shervais, 1982). Hence, vanadium contents in the Skidder Basalt should show the effects of fractionation of Cr-spinel and clinopyroxene.

Figures 14a and b illustrate the behaviour of V with respect to the compatible elements Cr and Ni. The range of Ni

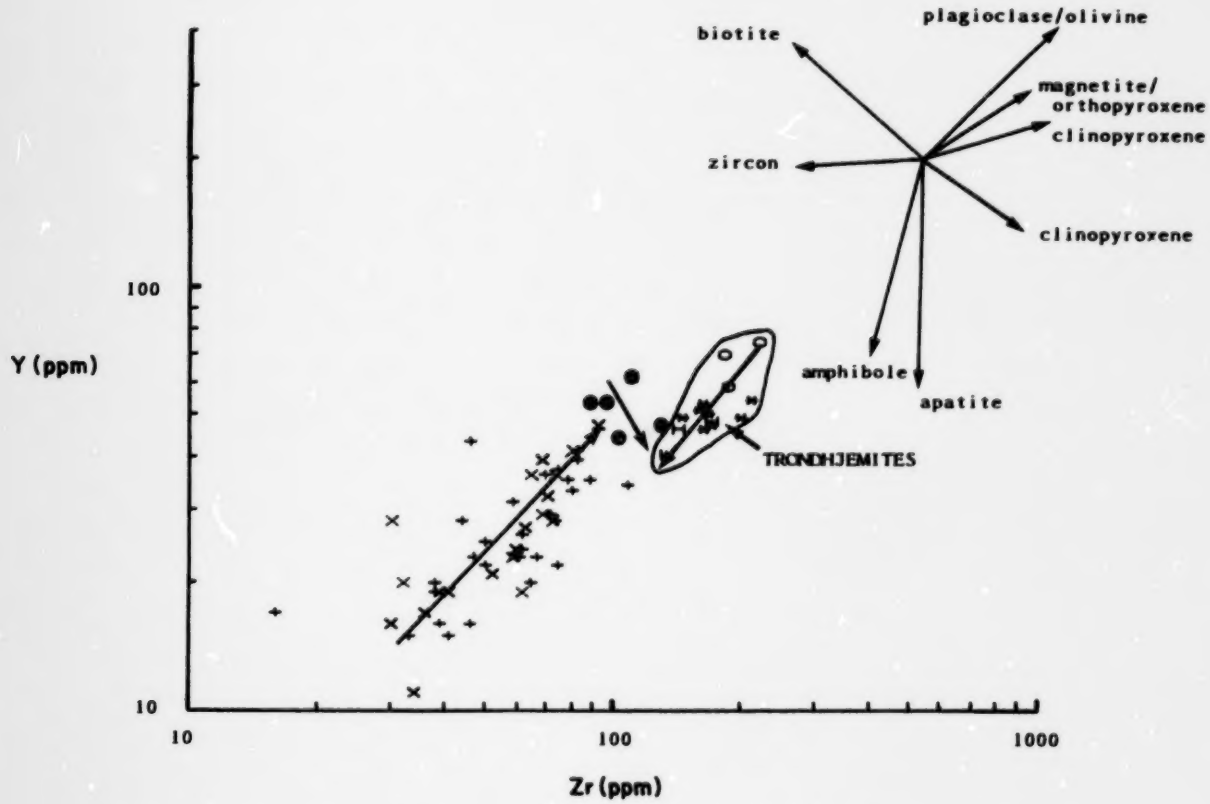

Figure 12. Log Y – log Zr plot of Skidder flows and trondhjemites. Arrows showing the effects of fractionation of various minerals are after Pearce and Norry (1979). Suggested differentiation trends for the Skidder flows and trondhjemites are shown as arrows. + – pillowed flows; X – massive flows; solid dots – high Y/low V lavas; O, *, H, – trondhjemites.

or Cr values included in each line segment labelled A, B, C and C′ on these diagrams is equivalent to the range of values included in each of the similarly labelled line segments on Figure 13. Vanadium increases slightly during the suggested fractionation of olivine and Cr-spinel (Trend A) then decreases moderately along with Cr and to a lesser extent Ni during the proposed increased precipitation of Cr-spinel (Trend B). The considerable increase in V represented by Trends C and C′ further supports the continued co-fractionation of olivine and plagioclase without clinopyroxene, as suggested previously. Trend D′, although not clearly defined, indicates possibly the late crystallization of clinopyroxene.

Skidder Basalt samples fall into two groups on Figure 15a. The greater number of samples define an overall trend of increasing V with increasing Y. However five samples, shown as large dots on the diagram, are separated from the main group. These samples have high Y yet low V concentrations and their high Zr, Y and SiO_2 contents (Fig. 5a, 15b) indicate that they are some of the most evolved lavas of the Skidder Basalt. These high Y/low V lavas define a trend on Figure 5a that is the reverse of that shown by the main body of samples. Samples of the high Y/low V rocks which contain higher SiO_2 contents contain lower concentrations of Y. They also show a similar but less well-defined tend to higher Zr values at lower Y contents (Fig. 15b). This trend suggests that a mineral such as apatite with which Y is compatible (Deer et al., 1966; Goff, 1984) was a fractionating phase in the magma which produced these rocks (Fig. 12). This conclusion is further supported by the considerable reduction of P_2O_5 with decreasing Y shown in Figure 15c. Note, however, that the high P_2O_5 content of some of these samples may be the result of apatite accumulation. The reduction of total iron as Fe_2O_3 and TiO_2 with decreasing Y shown by the high Y/low V lavas (Fig. 5b, 15d) can be explained by fractionation of magnetite.

The gap between the more evolved of the main group of Skidder basalt rocks and the high Y/low V samples seen on Figure 5a and 15a suggest that either the two groups are different petrogenetic suites or that between eruption of the main group of Skidder Basalt lavas and the high Y/low V lavas

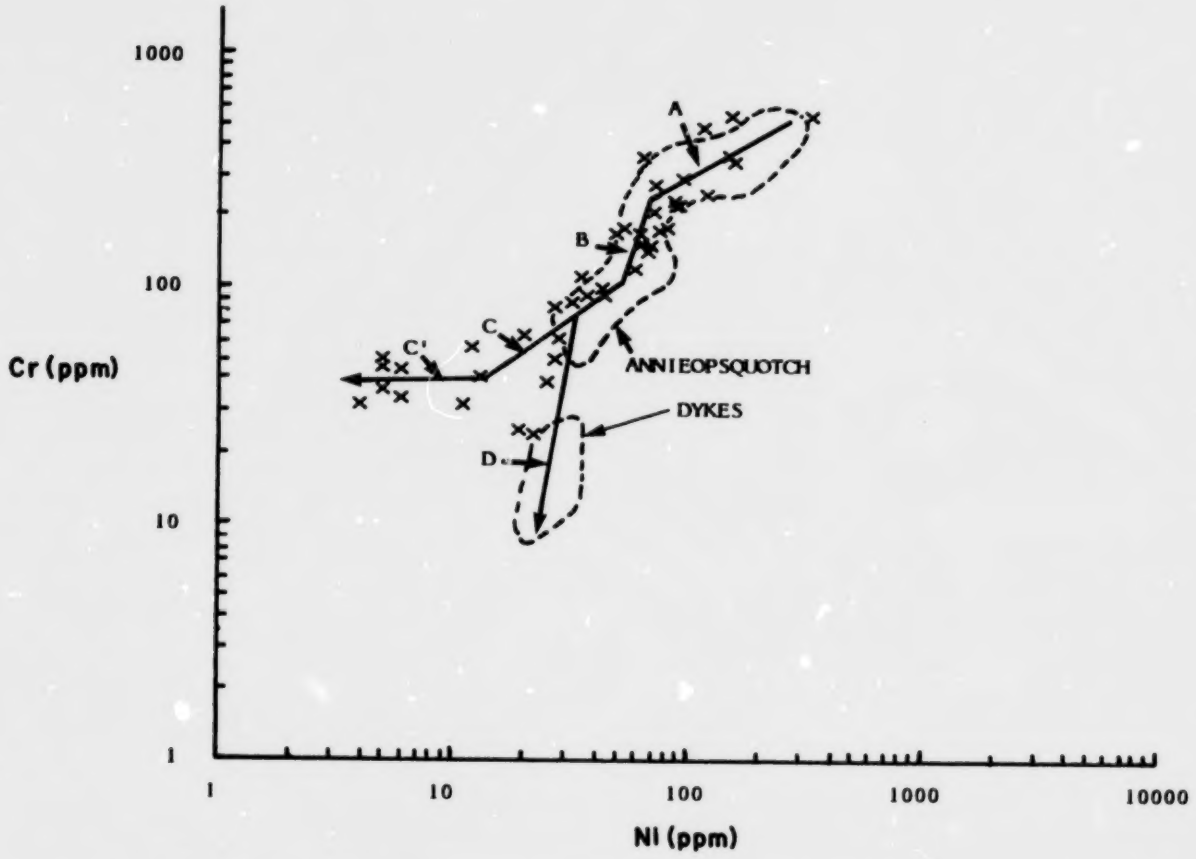

Figure 13. Log-log plot of Cr and Ni contents of Skidder basalts. The fields in which Annieopsquotch dykes plot (data from Dunning, 1984) are also indicated. Arrows show the suggested differentiation trends.

the magma for a period of time acted as a closed system. During this period clinopyroxene would probably have been an important fractionating phase depleting the magma in V. However, minor oxides such as magnetite were probably not liquidus phases since the high Y/low V lavas that contain the lowest contents of SiO_2 and Zr, presumably the least evolved, have high TiO_2 contents.

TRONDHJEMITE GEOCHEMISTRY

Included in Table 5 are eleven whole rock analyses of trondhjemitic dykes that intrude rocks near the Skidder Prospect (Fig. 2, 3) and three analyses of rocks from the trondhjemite pod exposed approximately two km northeast of the Skidder Prospect (Fig. 1). Sample preparation and analytical methods used are the same as those described previously for the Skidder Basalt analyses. Trondhjemite samples are included on Figures 5, 12 and 15. Arrows shown on some diagrams indicate a suggested differentiation trend.

The rocks fit reasonably well the definition of low Al_2O_3 (oceanic) type trondhjemites described by Barker (1979). Table 6 compares Skidder trondhjemites with other oceanic type trondhjemites. The Visnes plagiogranites and trondhjemites in the Bay of Islands Complex are thought to have formed by magmatic differentiation of basaltic magma (Pederson and Malpas, 1984; Malpas, 1979). The Karmoy trondhjemites are considered to have formed by partial melting of amphibolite (Pederson and Malpas, 1984) and the Little Port and Twillingate trondhjemites by partial melting of mafic tholeiites (amphibolites) that are basement to or occur at the base of island-arc sequences (Malpas, 1979; Payne and Strong, 1979). The higher average Si and lower average Al contents of the Skidder trondhjemites suggest that they are generally more differentiated than the other suites. Also, the high Mg and unusually low Ca contents of the Skidder trondhjemites indicate that they have probably been hydrothermally altered. Pederson and Malpas (1984) noted that the Visnes and Karmoy trondhjemites can be distinguished by the higher contents of Y and Zr of the former. As shown in Table 6, the trondhjemites thought to have formed by magmatic differentiation have higher average contents of Y and higher average Zr contents than the trondhjemites considered

to have formed by partial fusion. Skidder trondhjemites have significantly higher average Y content than the Little Port and Karmoy trondhjemites and have higher average Zr content than the Little Port and Twillingate trondhjemites. These features suggest that Skidder trondhjemites are more akin to those presumed to have formed by magmatic differentiation than those considered to have formed by partial fusion.

Watson (1979) concluded that melts with molar rations of $(Na_2O + K_2O)/Al_2O_3$ below 1.0 could become saturated with respect to zircon with less than 100 ppm Zr in the melt. Thus, zircon is probably a liquidus phase in a trondhjemitic melt and, if differentiation of the melt occurs, trondhjemites formed from early differentiates will probably contain more Zr and Y (which is compatible with zircon) than rocks

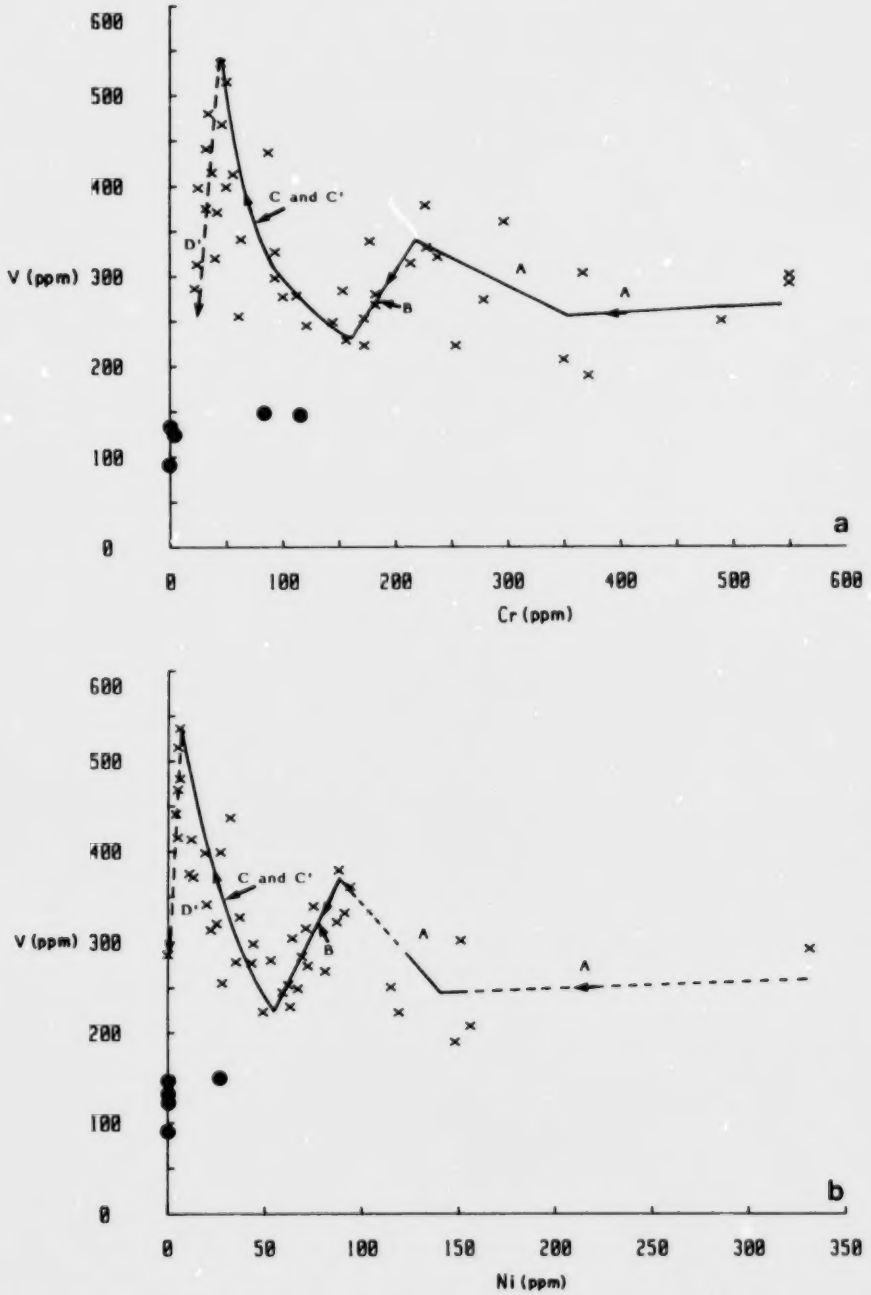

Figure 14. Vanadium plotted against Cr (14a) and Ni (14b) for Skidder flows. Suggested differentiation trends shown as arrows. Solid dots - high Y/low V lavas.

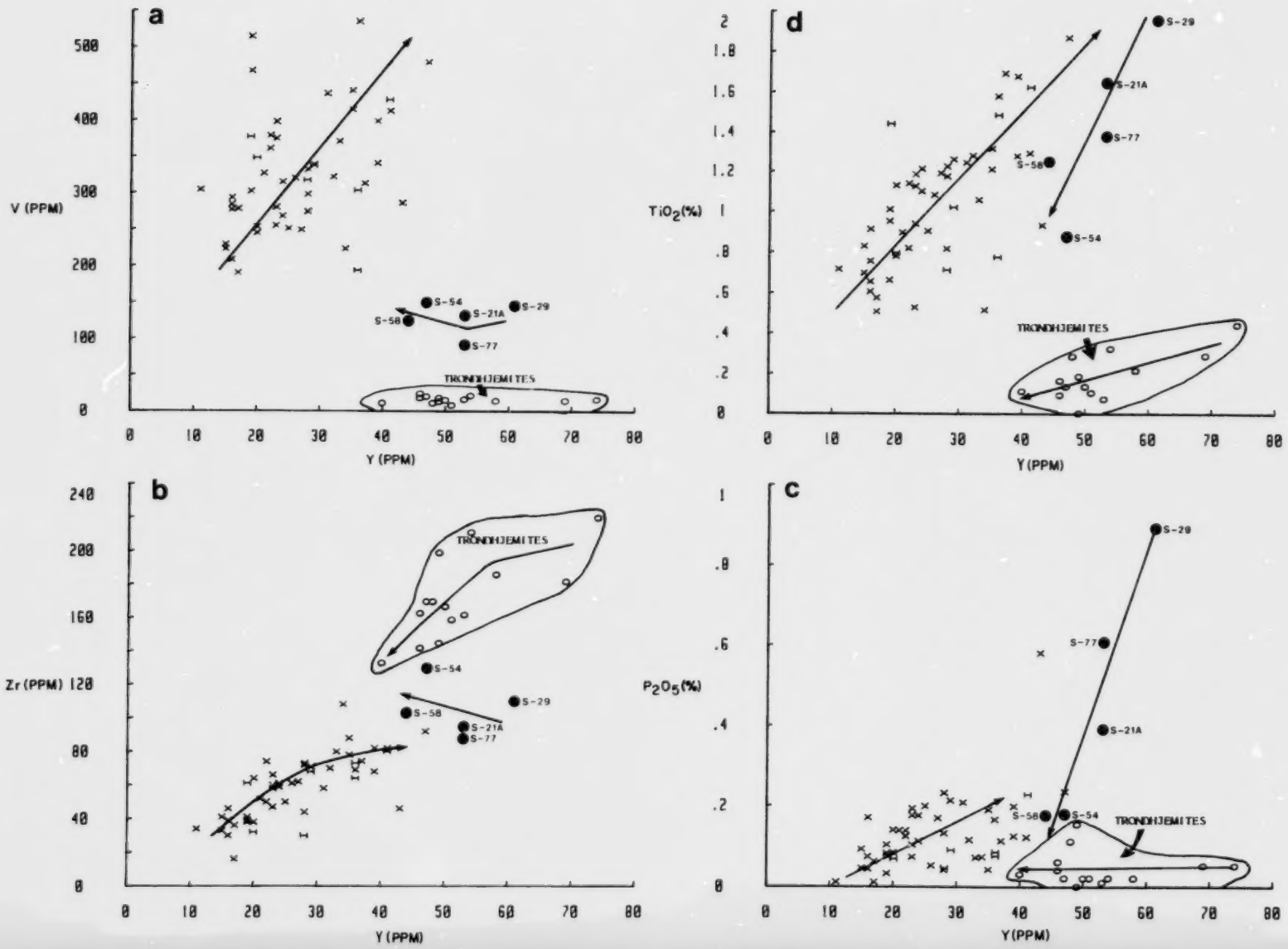

Figure 15. Selected minor and trace elements versus yttrium plots for Skidder rocks. X – Skidder lavas; solid dots – high Y/low V lavas; H – mafic dykes from Skidder area; open circles – trondhjemites.

formed from later differentiates of the melt. Fractionation of zircon is supported by the negative correlation of yttrium with SiO_2 (Fig. 5a) and the positive correlation of Y with Zr (Fig. 15b) in the Skidder trondhjemites. Fractionation of other Y bearing minerals in addition to zircon is suggested by the trend shown on Figure 12. Greater differentiation of the trondhjemitic melt provides one explanation for the slightly lower average Zr and Y contents of the Skidder trondhjemites compared to those of the Bay of Islands ophiolite and the significantly lower contents of these elements in the Skidder and Bay of Islands trondhjemites as compared to the Visnes plagiogranites.

Using the results of experiments on basaltic liquids, Dixon and Rutherford (1979) suggested that plagiogranites may be produced as a result of liquid immisciblity. Philpotts (1979) and others have described occurrences of immiscible glasses in tholeiitic basalts. Watson (1976) experimentally determined partition coefficents for several elements between immiscible mafic and felsic liquids in the system K_2O-$A12O_3$-FeO-SiO_2 at 1180°C and 1 atmosphere. He found that phosphorus is most strongly partitioned into the mafic melt and that Ca, Zr, Ti, Sr, Ba, Cr, Mn, Mg and rare earth elements also partition strongly into the mafic melt. Philpotts (1982) showed that if immiscibility of an Fe enriched basalt occurs at SiO_2 contents below 52 per cent, the felsic melt will be enriched in Na and that K will enter the mafic melt. This situation is reversed if immiscibility occurs at higher SiO_2 contents. An alternate explanation for the origin of the Skidder trondhjemites, therefore, could be that they formed as a result of immiscibility of a late-stage, relatively low SiO_2, Fe-enriched melt. This is supported by the very low contents of P, Ca, Sr, Ba and the relatively low contents of Zr and Y in the Skidder trondhjemites.

COMPARISON WITH OTHER OPHIOLITIC COMPLEXES

Spilitization, the presence of variolitic pillow lavas, the sparseness and smaller size of amygdules, the high magnetic susceptibility and tholeiitic chemistry distinguish the Skidder Basalt from the Buchans Group basalts and illustrate its similarity to the upper portion of the Annieopsquatch Complex (Dunning, 1984) and the Lushes Bight Group of northeastern Newfoundland (Kean, 1984), considered to be ophiolitic (Smitheringale, 1972; Strong, 1973). The ore metal content of the Skidder Prospect that is, Cu and Zn and only a very minor amount of Pb and the occurrence of the prospect in basalts rather than felsic volcanic rocks further support an ophiolitic environment of formation. The presence of trondhjemite dykes and pods in the Skidder Basalt is also consistent with an ophiolitic environment.

Beccaluva et al. (1980) state the ophiolites such as the Troodos and Vourinos complexes, which plot in the island-arc tholeiite field on trace element variation diagrams have common characteristics. Many of these complexes contain lavas that have very low Ti and incompatible element contents

Table 5. Analyses of Skidder trondhjemites. See Figures 1, 2 and 3 for sample locations

	Trondhjemite dykes (drill core)								Trondhjemite dykes (outcrop)			Trondhjemite pod		
	SK 6-8	SK 27-25	SK 27-29	SK 29-45	SK 30-1	SK 30-51	SK 30-757	SK 32-17	S 2	S 4	S 73	S 67	S 68	S 69
Major elements														
SiO_2	78.00	76.90	78.80	70.30	75.00	83.50	81.10	78.40	77.40	80.20	80.00	80.00	67.90	76.90
TiO_2	0.07	0.16	0.13	0.31	0.18	0.10	0.13	0.00	0.09	0.11	0.28	0.21	0.43	0.28
Al_2O_3	10.70	11.20	10.30	12.80	12.10	8.84	10.30	9.30	11.40	10.10	10.00	10.20	14.60	11.50
Fe_2O_3 [1]	1.23	2.20	0.99	2.63	2.45	0.18	0.60	3.00	3.06	3.01	2.61	1.86	5.32	2.04
MnO	0.03	0.04	0.03	0.05	0.03	0.01	0.01	0.02	0.03	0.06	0.02	0.02	0.06	0.02
MgO	2.39	2.42	2.67	4.90	0.91	0.16	0.50	1.19	0.60	0.69	0.59	0.36	1.35	0.39
CaO	0.18	0.07	0.08	0.14	0.18	0.18	0.20	0.24	0.04	0.25	0.10	0.13	0.89	0.14
Na_2O	4.34	4.95	4.52	3.23	5.90	3.75	2.80	4.82	5.83	5.08	4.76	4.03	4.66	5.89
K_2O	0.54	0.10	0.09	1.73	0.97	0.75	1.81	0.06	0.11	0.16	0.20	1.08	2.00	0.03
P_2O_5	0.01	0.04	0.02	0.02	0.15	0.02	0.02	0.00	0.06	0.03	0.11	0.02	0.05	0.05
LOI	1.50	1.17	1.34	2.74	0.52	1.00	1.58	1.76	0.85	1.01	0.87	0.89	2.38	0.62
Total	98.99	99.25	98.97	98.85	98.39	98.49	99.05	98.79	99.47	100.70	99.54	98.80	99.64	97.86
Minor elements														
Pb	9	nd [2]	5	6	7	3	6	4	1	6	3	nd	7	7
Rb	6	2	nd	26	7	10	23	3	2	4	1	20	35	2
Sr	39	43	34	29	35	37	32	30	22	26	21	19	48	23
Y	53	46	50	54	49	51	47	49	46	40	48	58	74	69
Zr	160	160	170	210	200	160	170	150	140	130	170	190	220	180
Nb	5	7	4	8	6	6	7	6	2	5	6	6	6	6
Zn	36	67	34	72	31	40	34	38	51	73	53	21	90	61
Cu	14	18	17	12	19	20	24	13	11	6	17	14	29	17
Ni	nd	nd	nd	nd	nd	nd	nd	nd	nd	nd	nd	nd	nd	nd
Ba	100	19	25	140	86	45	160	5	15	16	4	21	88	nd
V	15	23	14	20	17	7	19	12	17	10	10	13	15	13
Cr	5	10	4	nd	8	10	12	4	nd	nd	5	6	1	3
Ga	13	12	9	17	14	11	12	12	12	12	13	12	20	13
DDH	SK-6	SK-27	SK-27	SK-29	SK-30	SK-30	SK-30	SK-32						
Depth(m)	43.6	115.7	135.3	210.6	3.4	229.4	230.7	159.4						

[1] Total iron as Fe_2O_3
[2] nd = not detected

Table 6. Comparison of average Skidder area trondhjemites to average trondhjemites suggested to have been formed by magmatic differentiation and others thought to have been formed by partial fusion

	Trondhjemites suggested to have been formed by magmatic differentiation			Trondhjemites suggested to have been formed by partial fusion of amphibolites		
	Bay of Islands 1	Visnes Plagiogranites 2	Skidder Trondhjemites	Little Port Complex 1	Karmoy 2	Twillingate 3
	65% SiO_2	63% SiO_2				
SiO_2	75.06	73.50	77.46	71.42	76.40	74.45
TiO_2	0.20	0.32	0.18	0.23	0.17	0.22
Al_2O_3	13.10	12.64	10.95	13.56	13.19	13.02
FeO	1.33	0.48	—	2.09	0.47	—
Fe_2O_3[1]	1.30	3.76	2.23[1]	0.81	0.49	2.62[1]
MnO	0.06	0.06	0.03	0.11	0.03	0.07
MgO	0.19	0.24	1.37	0.94	0.36	0.28
CaO	1.02	4.28	0.20	2.25	2.97	1.85
Na_2O	6.07	4.73	4.61	4.96	5.69	5.03
K_2O	0.72	0.13	0.69	0.70	0.27	0.47
P_2O_5	0.00	0.07	0.04	0.05	0.20	0.01
			Minor elements			
Sr	80	230	31	130	77	97
Y	76	120	52	21	13	—
Zr	230	590	170	69	210	88
Nb	8	11	6	6	4	5
V	7	18	15	43	10	—
Cr	7	18	5	8	15	—
Ni	3	4	0	1	9	—
Cu	9	130	17	11	95	17
Zn	61	7	52	46	22	39
Rb	8	—	10	12	—	10
Ba	190	—	52	68	—	74
Ga	21	—	13	13	—	14
Pb	1	—	5	3	—	3
	n = 3	n = 12	n = 14	n = 10	n = 9	

[1] Malpas (1979)
[2] Pederson and Malpas (1984)
[3] Payne and Strong (1979)
n = number of samples
[1] Total iron as Fe_2O_3

as well as very high Cr and Ni contents. Coish and Church (1979) describe flows with similar characteristics in the Betts Cove Ophiolite. Other effusive rocks present in these ophiolites are more depleted in incompatible elements and compatible elements such as Cr and Ni than typical ocean-floor tholeiites. Beccaluva et al. (1980) further state that the variation in the modal mineralogy of the Troodos and Vourinos ophiolitic rocks define a fractional crystallization order of Cr-spinel plus olivine, clinopyroxene and orthopyroxene followed by plagioclase, similar to that described for island-arc tholeiites (Perfit et al., 1980). Miyashiro (1973) suggested that the Troodos Ophiolite formed in a island-arc environment and Beccaluva et al. (1980) conclude that the Troodos and Vourinos ophiolites probably originated by "spreading processes above a subduction zone close to an intraoceanic converging plate margin". According to Beccaluva et al. (1980) cumulus minerals in the gabbroic complexes and phenocryst phases in the lavas of the Northern Apenine ophiolites, which have MORB-type chemistry, indicate a crystallization order of Cr-spinel plus olivine, plagioclase, clinopyroxene, Ca-poor pyroxene, Fe-Ti oxides and finally apatite. Pearce et al. (in preparation) conclude that ophiolites with MORB chemistry, which include the McQuarie Island ophiolite (Griffin and Varne, 1980) and the Bay of Islands ophiolite (Suen et al., 1979) may have formed in "incipient oceans, major oceans, leaky transforms" or, in "back-arc basins".

The Skidder basalts have low contents of the large ion lithophile elements similar to ocean ridge basalts but typically plot close to the boundary of MORB and island-arc tholeiite fields on many trace element variation diagrams. The lack of lavas with low incompatible trace element and high Cr and Ni contents in the Skidder Basalt and its proposed paragenesis, that is, Cr-spinel plus olivine ± plagioclase, olivine plus plagioclase, and, late in the fractionating history, clinopyroxene plus magnetite and apatite, suggest a greater similarity of the Skidder Basalt to MORB type ophiolites.

The Skidder Basalt contains more fractionated rocks and has lower average contents of incompatible elements than typical ocean-floor basalts. Stern and de Wit (1980) state that

these characteristics are typical of ophiolites formed at slow spreading ridges. They explain this by indicating that slow spreading ridges would probably have magma chambers that act as closed systems for longer periods of time than those at fast spreading centres where magma chambers would be replenished constantly with batches of primitive magma.

CONCLUSIONS

The Skidder Basalt comprises a spilitized, tholeiitic, subalkaline, assemblage of basaltic pillow lava, pillow breccia and massive flows. Lesser amounts of mafic pyroclastic rocks and chert are present and trondhjemitic pods and dykes intrude the unit in places. Spilitization of the rocks has resulted in redistribution of SiO_2 and total iron, removal of K_2O and MgO, and extensive addition of Na_2O. Skidder Basalt samples define tholeiitic trends and typically plot close to the boundary between ocean-floor basalt and island-arc tholeiite fields on trace element variation diagrams.

The suggested parageneiss of the Skidder Basalt is olivine + Cr-spinel ± plagioclase, olivine + plagioclase and, late in the crystallization history, clinopyroxene + plagioclase + magnetite + apatite.

The plagiogranites are low Al_2O_3 oceanic type trondhjemites. They are chemically similar to trondhjemites considered to represent late magmatic differentiates either produced by normal fractionation or possibly due to liquid immiscibility of late stage Fe-enriched basaltic magma.

The Skidder Basalt shows greater geological and geochemical similarities to the pillow lavas of ophiolitic complexes than to the Buchans Group basalts.

ACKNOWLEDGMENTS

The author thanks J.G. Thurlow, E.A. Swanson, and especially D.M. Barbour, as well as other staff of Abitibi-Price Mineral Resources and ASARCO Inc. for their generous assistance during the summer of 1983. L. Boone provided able assistance in the field. G. Andrews is thanked for operating the atomic absorption spectrophotometric unit used for major element analysis of his rocks. G.R. Dunning is especially thanked for allowing the use of some of the rock geochemical data from the Annieopsquotch Complex to the southwest of the Skidder area.

Financial support for field aspects of this study was provided by the Geological Survey of Canada through contract 19SR.23233-3-0434. Additional financial support was provided by a fellowship from Memorial University of Newfoundland, the Buchans Scholarship Fund of ASARCO Incorporated and by D.F. Strong, who alloted funds from his N.S.E.R.C. grant.

J.M. Duke, G.R. Dunning, R.V. Kirkham, D.F. Strong and H.S. Swinden reviewed the paper and made many useful comments.

REFERENCES

Abbey, S.
1980: Studies in "standard samples" for use in the general analysis of silicate rocks and minerals. Part 6: 1979 edition of "usable" values"; Geological Survey of Canada, Paper 80-14, 30 p.

Amstutz, G.C. (ed.)
1974: Spilites and Spilitic Rocks; International Union of Geological Sciences, Series A, Number 41 Springer-Verlag, Berlin, 471 p.

Barker, F.
1979: Trondhjemite: definition, environment and hypotheses of origin. in Trondhjemites, Dacites and Related Rocks, ed. F. Barker; Developments in Petrology 6, Elsevier Scientific, Amsterdam, p. 1-12.

Basaltic Volcanism Study Project
1981a: Ocean-floor basaltic volcanism; in Basaltic Volcanism Study Project, Basaltic Volcanism on the Terrestrial Planets; Pergamon Press, New York, p. 132-160.
1981b: Island arc basalts; in Basaltic Volcanism Study Project, Basaltic Volcanism on the Terrestrial Planets; Pergamon Press, New York, p. 193-213.
1981c: Experimental petrology of basalts and their source rocks; Introduction; in Basaltic Volcanism Study Project, Basaltic Volcanism on the Terrestrial Planets; Pergamon Press, New York, p. 494-513.

Beccaluva, L., Ohnenstetter, D., and Ohnenstetter, M.
1979: Geochemical discrimination between ocean-floor and island-arc tholeiites – application to some ophiolites; Canadian Journal of Earth Sciences, v. 16, p. 1874-1882.

Beccaluva, L., Piccardo, G.B., and Serri, G.
1980: Petrology of Northern Apennine ophiolites and comparison with other Tethyan ophiolites; in Ophiolites, ed. A. Panayioutou; Proceedings of the International Ophiolite Symposium, Cyprus 1979, p. 314-331.

Bender, J.F., Hodges, F.N., and Bence, A.E.
1978: Petrogenesis of basalts from the project FAMOUS area: experimental study from 0 to 15 kilobars; Earth and Planetary Science Letters, v. 41, p. 227-302.

Carlisle, D.
1963: Pillow breccias and their aquagene tuffs, Quadra Island, British Columbia; Journal of Geology, v. 71, p. 48-71.

Coish, R.A. and Church, W.R.
1979: Igneous geochemistry of mafic rocks in the Betts Cove ophiolite, Newfoundland; Contributions to Mineralogy and Petrology, v. 70, p. 29-39.

Dean, P.L.
1978: The volcanic stratigraphy and metallogeny of Notre Dame Bay, Newfoundland; Memorial University of Newfoundland, Geology Report 7, 205 p.

Deer, W.A., Howie, R.A., and Zussman, J.
1966: An Introduction to the Rock-forming Minerals; Longman Group, London, 528 p.

Dixon, S. and Rutherford, M.J.
1979: Plagiogranites as late stage immiscible liquids in ophiolite and mid-ocean ridge suites: an experimental study; Earth and Planetary Science Letters, v. 45, p. 45-60.

Dunning, G.R.
1984: The geology, geochemistry, geochronology and regional setting of the Annieopsquotch Complex and related rocks of southwest Newfoundland; unpublished Ph.D. thesis, Memorial University of Newfoundland, 402 p.

Ewart, A.
1982: The mineralogy and petrology of Tertiary-Recent orogenic volcanic rocks: with special reference to the andesitic-basaltic compositional range. in Andesites: Orogenic Andesites and Related Rocks, ed. R.S. Thorpe; John Wiley and Sons, Chichester, p. 25-95.

Garcia, M.O.
1978: Criteria for the identification of ancient island arcs; Earth Science Reviews, v. 14, p. 147-165.

Goff, S.P.
1984: The magmatic and metamorphic history of the East Arm, Great Slave Lake, N.W.T.; unpublished Ph.D. thesis, University of Alberta, 295 p.

Griffin, B.J. and Varne, R.
1980: The MacQuarie Island ophiolite complex: Mid-Tertiary oceanic lithosphere from a major ocean basin; Chemical Geology, v. 30, p. 285-308.

Hart, S.R.
1976: LIL-element geochemistry, LEG 34 Basalts; in Initial Reports of the Deep Sea Drilling Project, v. 34, p. 283-288.

Holloway, J.R. and Burnham, C.W.
1972: Melting relations of basalt with equilibrium water pressure less than total pressure; Journal of Petrology, v. 13, p. 1-13.

Hughes, C.J.
1973: Spilites, keratophyres and the igneous spectrum; Geological Magazine, v. 109, no. 6, p. 513-527.

Jakes, P. and White, A.J.R.
1972: Major and trace element abundances in volcanic rocks of orogenic areas; Geological Society of America, Bulletin, v. 83, p. 29-40.

Kean, B.F.
1984: Geology and mineral deposits of the Lushs Bight Group, Notre Dame Bay, Newfoundland in Current Research, Newfoundland Department of Mines and Energy, Mineral Development Division, Report 84-1, p. 141-156.

Kean, B.F. and Jayasinghe, N.R.
1980: Geology of the Lake Ambrose (12A/10) – Noel Paul's Brook (12A/9) map areas, central Newfoundland; Newfoundland Department of Mines and Energy, Mineral Development Division, Report 80-2, 29 p.

Langmhyr, F.J. and Paus, P.E.
1968: The analysis of inorganic siliceous materials by atomic absorption spectrophotometry and the hydrofluoric acid decomposition technique, Part I: The analysis of silicate rocks, Analytica Chimica/Acta, v. 43, p. 397-408.

Le Roex, A.P., Dick, H.J.B., Reid, A.M., and Erlank, J.A.
1982: Ferrobasalts from the Speiss ridge segment of the southwest Indian ridge; Earth and Planetary Science Letters, v. 60, p. 437-451.

Malpas, J.
1979: Two contrasting trondhjemite associations from transported ophiolites in western Newfoundland: initial report; in Trondhjemites, Dacites and Related Rocks, ed. F. Barker; Development in Petrology 6; Elsevier Scientific, Amsterdam, p. 465-487.

Melson, W.G., Vallier, T.L., Wright, T.L., Byerly, G., and Nelan, J.
1976: Chemical diversity of abyssal volcanic glass erupted along Pacific, Altantic and Indian Ocean sea-floor spreading centers; in The Geophysics of the Pacific Ocean Basin and its Margin; American Geophysical Union, Washington D.C., p. 351-367.

Miyashiro, A.
1973: The Troodos ophiolite was probably formed in an island arc; Earth and Planetary Science Letters, v. 19, p. 218-224.

Mottl, M.J.
1983a: Metabasalts, axial hot springs, and the structure of hydrothermal systems at mid-ocean ridges; Geological Society of America, Bulletin, v. 94, p. 161-180.
1983b: Hydrothermal processes at seafloor spreading centers: application of basalt-seawater experimental results; in Hydrothermal Processes at Seafloor Spreading Centers, ed. P.A. Rona, K. Bostrom, L. Laubier, and K.J. Smith; NATO Conference Series IV: Marine Sciences, v. 12, Plenum Press, New York, p. 199-224.

Nowlan, G.S. and Thurlow, J.G.
1984: Middle Ordovician conodonts from the Buchans Group, central Newfoundland, and their significance for regional stratigraphy of the Central Volcanic Belt; Canadian Journal of Earth Sciences, v. 21, p. 284-296.
1987: Middle Ordovician conodonts from the Buchans Group; in Buchans Geology, Newfoundland, ed. R.V. Kirkham; Geological Survey of Canada, Paper 86-24, Report 4.

Payne, J.G. and Strong, D.F.
1979: Origin of the Twillingate trondhjemite, north-central Newfoundland: Partial melting in the roots of an island arc; in Trondhjemites, Dacites, and Related Rocks, ed. F. Barker; Developments in Petrology 6; Elsevier Scientific, Amsterdam, p. 489-516.

Pearce, J.A.
1976: Statistical analysis of major patterns in basalt; Journal of Petrology, v. 17, p. 15-43.
1980: Geochemical evidence for the genesis and eruptive setting of lavas from Tethyan ophiolites. in Ophiolites, ed. A. Panayioutou; Proceedings of the International Ophiolite Symposium, Cyprus, 1979, p. 261-272.
1982: Trace element characteristics of lavas from destructive plate boundaries; in Andesites: Orogenic Andesites and Related Rocks, ed. R.S. Thorpe; John Wiley and Sons, p. 525-548.

Pearce, J.A. and Cann, J.R.
1973: Tectonic setting of basic volcanic rocks determined using trace element analyses, Earth and Planetary Science Letters, v. 19, p. 290-300.

Pearce, J.A. and Flower, M.F.J.
1977: The relative importance of petrogenetic variables in magma genesis at accreting plate margins: a preliminary investigation, Journal of the Geological Society of London, v. 134, p. 1-25.

Pearce, J.A. and Norry, M.J.
1979: Petrogenetic implications of Ti, Zr, Y, and Nb variations in volcanic rocks; Contributions to Mineralogy and Petrology, v. 69, p. 33-47.

Pearce, J.A., Lippard, S.J., and Roberts, S.
– Characteristics and tectonic significance of supra-subduction zone ophiolites.

Pederson, R.V. and Malpas, J.
1984: The origin of oceanic plagiogranites from the Karmoy ophiolite, western Norway; Contributions to Mineralogy and Petrology, v. 88, p. 36-52.

Perfit, M.R., Gust, D.A., Bence, A.E., Arculus, R.J., and Taylor, S.R.
1980: Chemical characteristics of island arc basalts: implications for mantle sources; Chemical Geology, v. 30, p. 227-256.

Philpotts, A.R.
1979: Liquid immiscibility in tholeiitic basalts; Journal of Petrology, v. 20, p. 99-118.
1982: Compositions of immiscible liquids in volcanic rocks; Contributions to Mineralogy and Petrology, v. 80, p. 201-218.

Pickett, J.W. and Barbour, D.M.
1984: Geology of the Skidder prospect, Buchans, Newfoundland; in Current Research, Part A, Geological Survey of Canada, Paper 84-1A, p. 581-586.

Rosenbauer, R.J. and Bischoff, J.L.
1983: Uptake and transport of heavy metals by heated seawater: A summary of experimental results; in Hydrothermal Processes at Seafloor Spreading Centers, ed. P.A. Rona, K. Bostrom, L. Laubier and K.J. Smith; NATO Conference Series IV: Marine Sciences, v. 12, Plenum Press, New York, p. 177-197.

Shapiro, L. and Brannock, W.M.
1962: Rapid analysis of silicate, carbonate and phosphate rocks; United States Geological Survey, Bulletin 1144A, p. A31.

Shervais, J.W.
1982: Ti-V plots and the petrogenesis of modern and ophiolitic lavas; Earth and Planetary Science Letters, v. 59, p. 101-118.

Smitheringale, W.G.
1972: Low potash Lushs Bight tholeiites: ancient oceanic crust in Newfoundland ?; Canadian Journal of Earth Sciences, v. 9, p. 574-588.

Stauffer, M.R., Mukherjee, A.C., and Koo, J.
1975: The Amisk Group: an Aphebian (?) island arc deposit; Canadian Journal of Earth Sciences, v. 12, p. 2021-2035.

Stern, C. and de Wit, M.J.
1980: The role of spreading centre magma chambers in the formation of Phanerozoic oceanic crust: evidence from Chilean ophiolites; in Ophiolites, ed. A. Panayioutou; Proceedings of the International Ophiolite Symposium, Cyprus, 1979, p. 497-506.

Strong, D.F.
1973: Lushs Bight and Roberts Arm Groups of central Newfoundland: possible juxtaposed oceanic and island-arc volcanic suites; Geological Society of America, Bulletin, v. 84, p. 3917-3928.

Suen, C.J., Frey, F.A., and Malpas, J.
1979: Bay of Islands ophiolite suite, Newfoundland: petrologic and geochemical characteristics with emphasis on rare earth geochemistry; Earth and Planetary Science Letters, v. 45, p. 337-348.

Sun, S.S., Nesbitt, R.W., and Sharaskin, A.
1979: Geochemical characteristics of mid-ocean ridge basalts; Earth and Planetary Science Letters, v. 44, p. 119-138.

Swanson, E.A., Strong, D.F. and Thurlow, J.G. (ed.)
1981: The Buchans Orebodies: Fifty Years of Geology and Mining; Geological Association of Canada, Special Paper 22, 350 p.

Thurlow, J.G.
1973: Lithogeochemical studies in the vicinity of the Buchans massive sulphide deposits, central Newfoundland; unpublished M.Sc. thesis, Memorial University of Newfoundland, 172 p.
1981: Geology, ore deposits and applied rock geochemistry of the Buchans Group, Newfoundland; unpublished Ph.D. thesis, Memorial University of Newfoundland, 305 p.

Thurlow, J.G. and Swanson, E.A.
1981: Geological map of the Buchans area, central Newfoundland; in The Buchans Orebodies: Fifty Years of Geology and Mining, ed. E.A. Swanson, D.F. Strong and J.G. Thurlow; Geological Association of Canada, Special Paper 22.
1987: Stratigraphy and structure of the Buchans Group; in Buchans Geology, Newfoundland, ed. R.V. Kirkham, Geological Survey of Canada, Paper 86-24, Report 2.

Watson, E.B.
1976: Two-liquid partition coefficients: experimental data and geochemical implications; Contributions to Mineralogy and Petrology, v. 56, p. 119-134.
1979: Zircon saturation in felsic liquids: Experimental results and application to trace element geochemistry; Contributions to Mineralogy and Petrology, v. 70, p. 407-419.

Whalen, J.B. and Currie, K.L.
1983: The Topsails igneous terrane of western Newfoundland; in Current Research, Part A, Geological Survey of Canada, Paper 83-1A, p. 15-23.
1987: Relationship of the Topsails igneous terrane to the Buchans Group; in Buchans Geology, Newfoundland, ed. R.V. Kirkham; Geological Survey of Canada, Paper 86-24, Report 6.

Williams, H.
1979: Appalachian orogen in Canada; Canadian Journal of Earth Sciences, v. 16, no. 3, p. 792-807.

Winchester, J.A. and Floyd, P.A.
1976: Geochemical magma type discrimination: application to altered and metamorphosed basic igneous rocks; Earth and Planetary Science Letters, v. 28, p. 459-469.
1977: Geochemical discrimination of different magma series and their differentiation products using immobile elements; Chemical Geology, v. 20, p. 325-343.

Geology and mineralogy of the Tulks pyritic massive sulphide deposit

J.L. Jambor[1] and D.M. Barbour[2]

Jambor, J.L. and Barbour, D.M., Geology and mineralogy of the Tulks pyritic massive sulphide deposit; in Buchans Geology, Newfoundland, ed. R.V. Kirkham; Geological Survey of Canada, Paper 86-24, p. 219-226 Report 12, 1987.

Abstract

The Tulks deposit consists of four distinct pyritic massive sulphide lenses which total about 720,000 tonnes grading 5.6% Zn, 2.0% Pb, 1.3% Cu, 41 g Ag/t and 0.4 g Au/t. Host rocks are predominantly greenchist-facies felsic crystal tuffs in the Tulks Hill Volcanics, a group of felsic pyroclastic rocks which form an important part of the Ordovician Victoria Lake Group and occur over a strike length of 65 km and a width of up to 3.5 km. The Tulks massive sulphide lenses are elongate parallel to a prominent northeasterly trending, sub-vertical regional schistosity. All four lenses are of similar size with dimensions in the order of 220 m by 100 m and average thickness of 6 m. Pyrite is the principal sulphide in all of the lenses, and sphalerite, galena, chalcopyrite, tetrahedrite and tennantite account for all but trace amounts of the primary base metals. The silver values are attributable to argentian tetrahedrite and tennantite; argentian gold is the main source of the gold values. Pyrrhotite, much of it altered to marcasite, is present only in modest amounts and only in one lens. The massive sulphides occur in distinct layers or zones which reflect variations both in the total sulphide content and in the base metal values. These variations are not consistent within a lens and have not provided a reliable indication of stratigraphic tops. Weak, but economically undesirable alteration by covellite, digenite and anglesite has affected all of the lenses; the alteration is mainly near surface, but also occurs erratically at depth in one of the lenses.

Résumé

Le gisement Tulks se compose de quatre lentilles distinctes de sulfures massifs pyriteux qui donneraient au total près de 720 000 tonnes d'une teneur de 5,6 % en Zn, 2,0 % en Pb, 1,3 % en Cu, 41 g d'argent par tonne et 0,4 g d'or par tonne. Les roches encaissantes sont surtout des tufs cristallins felsiques du faciès des schistes verts dans les roches volcaniques de Tulks Hill. Ces dernières sont des roches pyroclastiques felsiques qui forment une partie importante du groupe ordovicien de Victoria Lake; on les trouve sur une distance de 65 km parallèlement à la direction, et leur largeur peut atteindre 3,5 km. Les lentilles de sulfures massifs du gisement Tulks sont allongées parallèlement à une schistosité régionale subverticale proéminente, à orientation nord-est. Les quatre lentilles sont de dimensions similaires, soit de l'ordre de 220 mètres sur 100 mètres, et ont une épaisseur moyenne de 6 mètres. Elles ont toutes comme sulfure principale de la pyrite, et la sphalérite, la galène, la chalcopyrite, la tétraédrite et la tennantite sont à l'origine de la plus grande partie des métaux communs primaires. Les premières sources des indices d'argent sont la tétraédrite et la tennantite argentifères; l'or argentifère est la principale source des indices d'or. La pyrrhotite se trouve en faibles quantités dans une seule lentille; une grande partie de cette pyrrhotite a été transformée en marcasite. Les sulfures massifs se présentent en couches distinctes ou en zones qui traduisent les variations dans la teneur totale en sulfures et dans la teneur en métaux communs. Ces variations ne sont pas constantes à l'intérieur d'une seule lentille et ne sont pas une indication fiables des sommets stratigraphiques. Il y a eu formation de covelline, de digénite et d'anglésite, minéraux secondaires économiquement indésirables, dans toutes les lentilles; la transformation a eu lieu surtout près de la surface, mais elle s'est produite également irrégulièrement en profondeur dans une des lentilles.

[1]CANMET, 555 Booth Street, Ottawa, Ontario K1A 0G1
[2]BP Canada-Selco Division, P.O. Box 789 Corner Brook, Newfoundland A2H 6G7 (formerly with Abitibi-Price Inc.)

INTRODUCTION

The Tulks Prospect, held in cotenancy by Abitibi-Price Incorporated and ASARCO Incorporated, is a pyritic massive sulphide deposit about 40 km southwest of Buchans (Fig. 1). Diamond drilling of the deposit, which is surficially marked by gossans, was begun in 1963 and has since delineated four distinct massive sulphide lenses which total about 720,000 tonnes grading 5.6% Zn, 2.0% Pb, 1.3% Cu, 41 g Ag/t and 0.4 g Au/t. The deposit is of particular interest because Tulks was given serious consideration as a potential source of feed to prolong the operation of the now-closed Buchans mill; however, tests of the Tulks ore, including a bulk sample obtained from underground workings, gave unsatisfactorily low metal recoveries. The metallurgical problem was the focus of a detailed mineralogical investigation of the sulphide ore (Jambor, 1984); the present paper provides a more comprehensive view of the deposit in relation to its geological setting.

REGIONAL GEOLOGY

The Tulks deposit occurs in volcanic rocks of the Ordovician Victoria Lake Group (Kean, 1977). These volcanic rocks form part of the Dunnage Zone, a lower Paleozoic volcanosedimentary sequence generated during opening and subsequent closure of Iapetus Ocean (Fig. 1, 2). Conodonts, from limestone lenses at the mouth of Victoria River and from a location 15 km to the northeast, date the Victoria Lake Group as late Llanvirn – early Llandeilo (Stouge, 1978). To the southwest, the Victoria Lake Group is reported to be in fault contact with the Annieopsquotch ophiolite complex (Dunning, 1981). Evidence obtained by one of the writers (D.M.B.) in the Pats Pond area about 15 km southwest of Tulks, supports a conformable relationship upon the ophiolite with areas modified by faulting. This suggests regional correlation of the relationship, well established in Notre Dame Bay, in which pre-Caradocian volcanics of presumed island arc origin lie conformably upon ophiolite (Kean *et al.*, 1981).

In the Red Indian Lake area the Victoria Lake Group is conformably overlain by siltstone of the Harbour Round Formation which occupies a stratigraphic position similar to the Caradocian black shale of Notre Dame Bay (Kean and Jayasinghe, 1980). The Buchans Group structurally overlies all of the above rocks, but contains conodonts of Whiterockian age (latest Arenig – early Llanvirn; Nowlan and Thurlow, 1984). Part of the Buchans Group is thus slightly older than the underlying Victoria Lake Group; the inversion suggests that the contact between the two groups is a thrust fault (Nowlan and Thurlow, 1987).

The Victoria Lake Group consists of interfingered mafic to felsic submarine pyroclastic rocks with associated volcaniclastic sedimentary rocks. Moderate to strong foliation sub-parallel to bedding is a characteristic feature of the Group. Metamorphic grade varies from sub-greenschist to middle greenschist facies, with metamorphic grade and intensity of foliation increasing southwesterly. The Tulks Hill Volcanics are felsic pyroclastic rocks which form an important part of the Victoria Lake Group and occur over a strike length of 65 km and a width of up to 3.5 km; the true thickness is obscured by numerous faults sub-parallel to strike, and by small-scale tight isoclinal foids. Accompanying the felsic pyroclastic rocks, and probably comagmatic with them, are abundant intrusions of quartz-porphyritic quartz monzonite and granodiorite; also present are lesser gabbro and diabase intrusions which are interpreted to be younger. Within the Victoria Lake Group all of the known sulphide deposits, except Tally Pond, are hosted by the Tulks Hill felsic volcanics, i.e., Victoria, Jacks Pond, Tulks East and Tulks (Fig. 2).

LOCAL GEOLOGY AND STRUCTURE

The dominant lithologies in the area of the Tulks deposit are medium grained muscovite-chlorite felsic crystal tuff, coarse crystal tuff and lapilli tuff, and agglomerate with lesser rhyolite and/or subvolcanic intrusions. A large part of the pyroclastic rocks is characterized by clear to bluish quartz eyes, 1 to 3 mm in diameter. In thin sections the rocks can be seen to consist of variable amounts of muscovite, quartz, chlorite and lesser albite in a fine grained recrystallized quartzo-felspathic matrix.

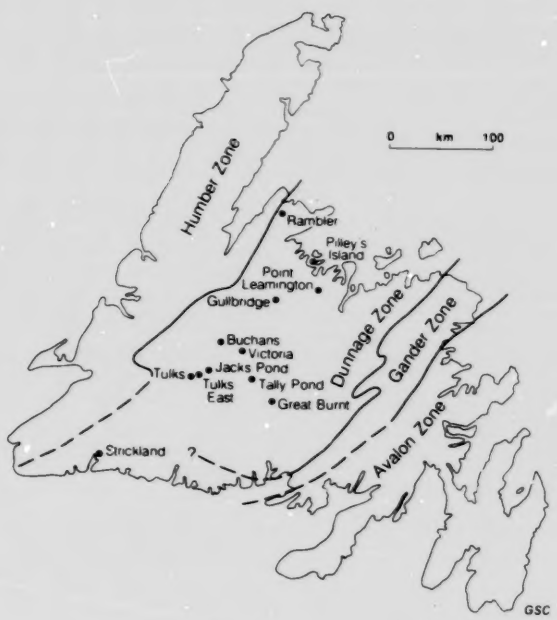

Figure 1. Location of the Tulks deposit with respect to tectonostratigraphic zones of Newfoundland and significant massive sulphide deposits in Ordovician volcanic rocks of the Dunnage Zone. (Does not include ophiolite-related deposits.)

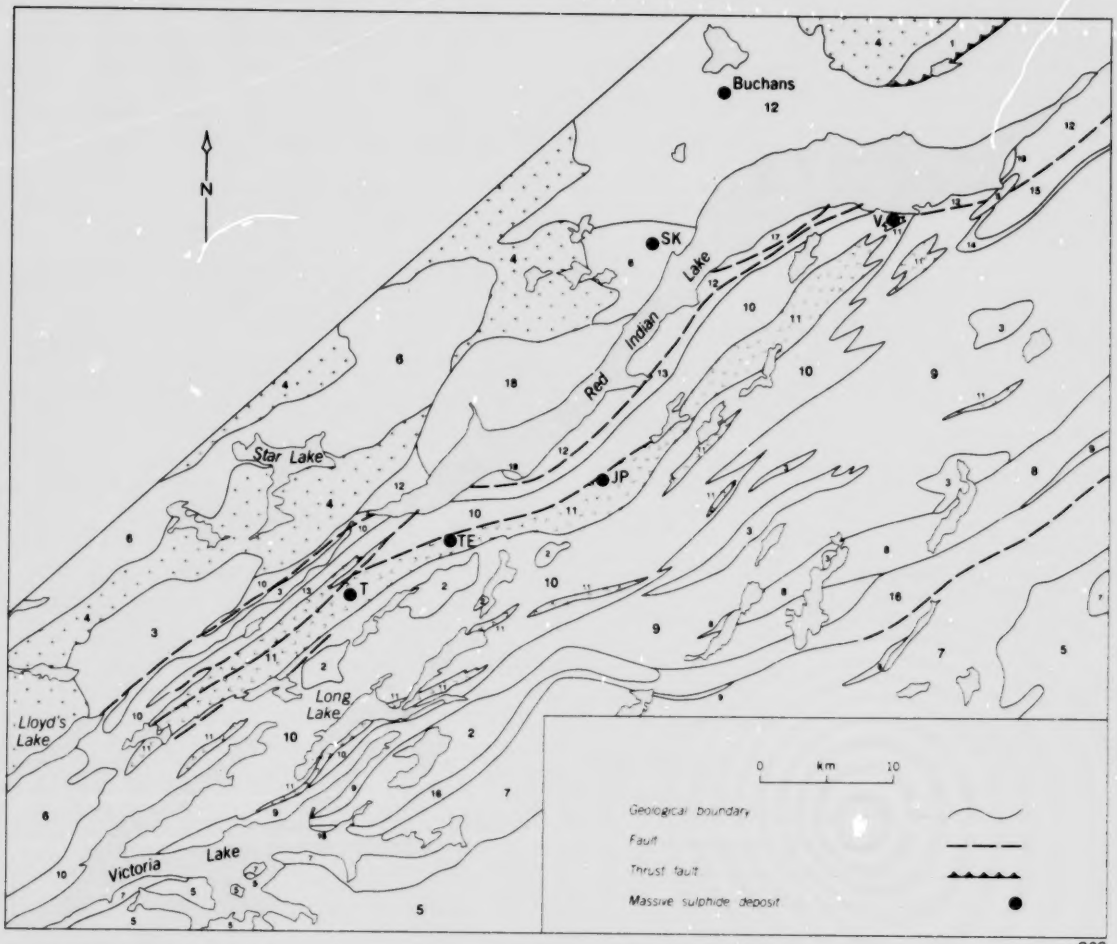

CARBONIFEROUS

18 *Poorly indurated red and grey conglomerate, sandstone, shale, minor limestone*

SILURIAN

17 *Red sandstone, minor conglomerate*

16 *Rogerson Lake Conglomerate: red to grey pebble conglomerate, sandstone, siltstone, mudstone*

ORDOVICIAN

15 *Goldson and Sansom formations: greywacke, conglomerate*

14 *Caradocian black shale, argillite*

13 *Harbour Round Siltstone: finely bedded siltstone, argillite, red chert, tuff, minor breccia*

BUCHANS GROUP

12 *Mafic to felsic lava, volcanic breccia, tuff, arkose*

VICTORIA LAKE GROUP

11 *Tulks Hill volcanics: dominantly felsic pyroclastics, minor flows*

10 *Mafic to intermediate tuff, flow, pillow lava. Includes unseparated felsic volcanics*

9 *Siltstone, argillite, sandstone, greywacke, grey to black slate, chert, bedded tuff*

8 *Tally Pond volcanics: mafic to felsic pyroclastics and flows*

EARLY ORDOVICIAN

7 *Greenschist to amphibolite facies phyllite, siltstone, sandstone, shale. Includes some undifferentiated intrusions*

EARLY ORDOVICIAN-LATE CAMBRIAN

6 *Ophiolite: layered gabbro, sheeted dykes, pillow lava, massive flows, minor ultramafic rock*

INTRUSIVE ROCKS

SILURIAN AND YOUNGER

5 *Brick-red, pink and grey granodiorite, quartz monzonite and granite; minor foliated granite*

4 *Medium- to fine-grained, red to grey granite, quartz monzonite and granodiorite. Includes topsails granite*

3 *Medium- to fine-grained diabase, gabbro, diorite, amphibolite*

ORDOVICIAN

2 *Quartz-porphyritic quartz monzonite, granodiorite and quartz diorite*

ORDOVICIAN AND OLDER

1 *Hungry Mountain Complex: foliated to massive granite, granodiorite, tonalite, diorite, gabbro, minor ultramafic rocks*

Figure 2. Regional geology and location of massive sulphide deposits. Geology based on the compilation map by Kean *et al.* (1981) modified by D.M. Barbour. B. Buchans; SK Skidder; V Victoria; JP Jacks Pond; TE Tulks East; T Tulks.

The lithologic units are lensoid and generally small, typically occurring only on outcrop scale (Fig. 3). This hampers subdivision of the felsic rocks into distinct units and the establishment of a stratigraphic column.

Interfingered with the felsic volcanics are less abundant units of mafic tuff, agglomerate and massive flows whose combined thickness ranges from less than a metre to greater than a hundred metres. Fine grained schistose tuff, composed mostly of chlorite and albite, predominates. Amygdaloidal mafic volcanics are almost absent in the immediate Tulks area. Volcaniclastic and sedimentary rocks are represented mainly by dark grey to black carbonaceous shale which is usually pyritiferous. This rocktype is widespread but occurs as units less than 10 metres thick. Tuffaceous wacke, siltstone and minor chert also are present.

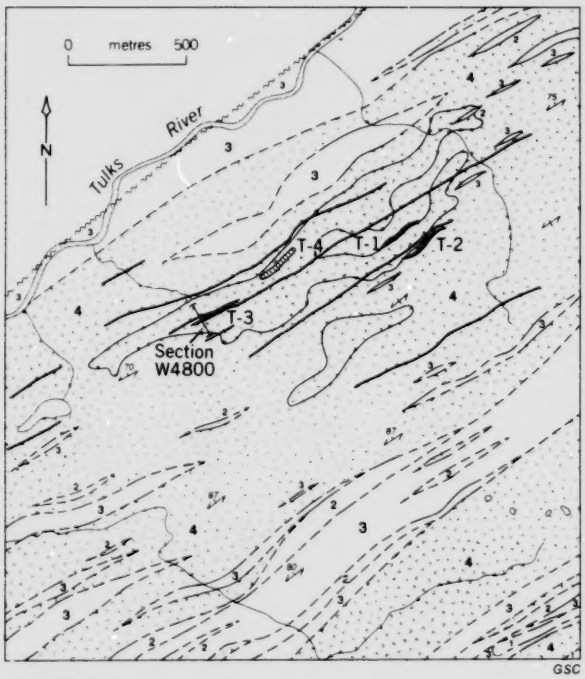

ORDOVICIAN

4 Tulks belt felsic tuff, agglomerate, minor flows and sills

3 Mafic tuff, minor flows and breccia

2 Tuffaceous greywacke, siltstone, minor carbonaceous shale

1 Quartz-porphyritic quartz-monzonite, granodiorite

Pyrite-rich gossan in felsic volcanics

Diabase dyke

Massive sulphide deposit

Surface projection of T-4 massive sulphide deposit

Geological boundary (defined, approximate)

Fault (defined, approximate)

Foliation (inclined, vertical)

Figure 3. Local geology of the Tulks deposit, appellation of the massive sulphide lenses, and location of the W 4800 cross-section (Fig. 5). Geology by D.M. Barbour.

A large intrusion of quartz-porphyritic quartz monzonite and granodiorite occurs approximately 2 km south of the Tulks deposit. The intrusion is weakly foliated parallel to the regional schistosity; near its contact with the Tulks Hill volcanic rocks, the intrusion is coarsely quartz-porphyritic and lithologically similar to the felsic crystal tuffs.

The youngest rocks in the area are fine- to medium-grained diabase dykes which have been observed mainly in diamond-drill cores from the area near the sulphide deposit. The dykes are unfoliated and form long, very straight and continuous units sub-parallel to the regional schistosity. They are interpreted to postdate the main deformation and to be intruded along pre-existing fault planes.

The dominant structural feature in the Tulks area is a prominent northeasterly trending, sub-vertical schistosity defined by alignment of muscovite and chlorite. On Tulks Hill this schistosity is crenulated by a later S_2 cleavage trending northwesterly. Faults parallel to the S_1 schistosity are also a prominent feature which can be recognized as elongate depressions between outcrop areas, as cliff scarps along Tulks Hill, in the underground adit, and as loci for the later diabase dykes. In the Tulks Valley, diamond-drill holes intersected a major fault with a 100-m thickness of gouge and breccia. Sense of movement on the faults is not known but most slickensides are sub-horizontal, thereby suggesting that some displacement was strike-slip. Metamorphism is middle greenschist facies with chlorite-muscovite-albite-quartz being a stable assemblage in appropriate lithological compositions. Moreton (1984) suggests tight to isoclinal folding parallel to S_1. Metamorphism and deformation are considered to be Acadian in age.

HOST ROCKS AND GENERAL MINERALOGY

The Tulks deposit consists of four distinct pyritic massive sulphide lenses which are elongate parallel to the regional schistosity, dip 70° to the northwest, and plunge horizontally. All four lenses, designated T-1 to T-4, are of similar size with dimensions in the order of 220 m by 100 m and average thickness of 6 m. Three of the lenses crop out at bedrock surface; the T-4 lens is subsurface and extends from depths of approximately 100 m to 250 m.

Host rock for the massive sulphide lenses is medium grained, muscovitic-chloritic felsic crystal tuff, locally with prominent quartz eyes. The tuff enclosing the sulphide lenses is characterized by an anomalous pyrite content which forms a zone 1800 m along strike and up to 400 m across strike. The zone produces a strong gossan and contains anomalous base metal values.

Pyrite is the principal sulphide in all of the Tulks lenses, and sphalerite, galena, chalcopyrite and tetrahedrite-tennantite account for all but trace amounts of the primary base metal values. Nearly all of the silver is attributable to argentian tetrahedrite and tennantite; native gold is sufficiently common to account for nearly all of the gold detected by assay. A list of the minerals occurring in the deposit is given in Table 1.

Hand and drill-core specimens of Tulks sulphides are megascopically similar to pyritic massive sulphides from other deposits. Layering of the sulphides is commonly evident, particularly where both pyrite and sphalerite are the main constituents of a rock. The two minerals usually show some degree of segregation, and the assemblage is generally the only one to display thin laminations of sulphides. Layering of sulphides is also commonly evident where the amount of silicates accompanying the sulphides is large. Thus layering arises mainly through variations in the proportions of pyrite and base metal sulphides, but also arises through changes in pyrite grain sizes. Tulks sulphides are generally fairly coarse, with pyrite grain sizes commonly exceeding 0.5 mm. This coarseness is readily apparent in hand specimens. The pyrite is euhedral to anhedral and coarse- to fine-grained, but even the finest grained samples lack colloform or framboidal textures and growth zoning.

Most Tulks sphalerite is associated with abundant pyrite, but in a few places sphalerite layers poor in pyrite are interbedded with tuff and are sufficiently abundant to form semi-massive sulphides. Under the microscope, the most notable feature of the bulk of the sphalerite is its homogeneity: coarse grains in smooth contact with other minerals, and finer grains among the interstices of pyrite account for by far the greatest part of the zinc values, both in high-grade and low-grade samples.

Tulks sphalerite is megascopically brown rather than black, in keeping with the low iron content: electron microprobe analysis of 6 representative samples from the T-1 and T-3 lenses gave Fe values ranging from 1.8 to 4.2 wt %; another sample, the only one in which sphalerite is in contact with pyrrhotite, gave 8.6 wt % Fe. In all the samples Cu content ranges from 0.2 to 0.5 wt %, and Mn ranges from 0.0 to 0.1 wt %.

Galena at Tulks is usually associated with sphalerite and is invariably subordinate to it in both quantity and grain size. Grain boundaries between the two minerals are generally simple and regular. Most of the galena occurs as large to small homogeneous patches in sphalerite, as patches concentrated at the rims of sphalerite, or as grains interposed between pyrite and sphalerite. Penetrative replacement of sphalerite by galena is present in a few samples, but well-defined, cross-cutting linear veinlets of galena are extremely rare.

Nearly all of the primary copper values in the T-1, T-2 and T-3 lenses are attributable to chalcopyrite. In contrast, tennantite is the principal copper mineral in the eastern part of the T-4 horizon. Tennantite also is locally abundant in parts of the T-3 lens, but overall merely supplements the copper values derived from chalcopyrite. Most of the chalcopyrite occurs along pyrite grain boundaries and in the interstices among pyrite crystals, as larger patches which have coalesced to form the matrix hosting pyrite crystals, and as large homogeneous patches in sphalerite and in silicate gangue. The interstitial-type occurrence is especially characteristic of tightly compact massive sulphides low in silicates and galena-sphalerite.

The principal sulphides listed in Table 1 make up the bulk of the Tulks sulphide assemblage and also are the most important in terms of pervasive distribution and economics. The four minor sulphides listed in Table 1, although abundant locally, nevertheless constitute only a small percentage of the Tulks massive sulphides and have a restricted rather than a pervasive spatial distribution.

Arsenopyrite is widespread in that it occurs in all of the Tulks lenses. Maximum volume of arsenopyrite in an individual polished section is about 10%, but in many sections the mineral is absent. The commonest forms of arsenopyrite are

Table 1. Minerals in the Tulks deposit

Principal sulphides	Minor sulphides	Minor oxides	Others	
pyrite	arsenopyrite	magnetite	stannite	tetradymite
sphalerite	tennantite	ilmenite	kesterite	hessite
galena	pyrrhotite	hematite	gold	hedleyite (?)
chalcopyrite	tetrahedrite	cassiterite	silver	unidentified A (Bi_3Te_2)
			bismuth	unidentified B (Bi_2Te)

Principal silicates	Sulphates, carbonates, phosphates	Oxidation and supergene assemblages	
quartz	dolomite	digenite	anglesite
muscovite	calcite	covellite	kaolinite
chlorite	barite	marcasite	cerussite
albite	siderite		goethite
celsian	ankerite		
	apatite		

dispersed crystal clusters, and dispersed individual crystals up to 0.5 mm in length.

Tennantite occurs widely and is locally sufficiently abundant that masses are megascopically identifiable in drill cores, especially those from parts of the T-4 lens. Tetrahedrite also is present at Tulks but is much less abundant as indicated by correlations between microscopic observations and microprobe analyses. Compositions vary from almost end-member tetrahedrite to almost end-member tennantite. Solid-solution silver is consistently present but is generally low in tennantite (minimum 0.2 wt % Ag) and high in tetrahedrite (up to 12.3 wt % Ag).

Blebs of pyrrhotite occur sparingly as inclusions in pyrite in all of the Tulks lenses. Most of the inclusions are round and 15 to 20 micrometres in diameter; many of the individual inclusions consist of both pyrrhotite and chalcopyrite. Coarse grains of pyrrhotite, similar in size to those of the base metal sulphides, occur only in the T-1 lens. Much of this coarse grained pyrrhotite has been altered to extremely fine grained marcasite and secondary pyrite which are accompanied by substantial pitting; the pits reflect the volume reduction which attends the transformation of pyrrhotite to marcasite.

Among the minor oxides (Table 1) only magnetite occurs in appreciable amounts. The magnetite has been found only in the T-1 and T-2 lenses, where it locally constitues up to 5 volume % of the massive sulphide rock. In the category of "other minerals" (Table 1), stannite and kesterite occur sparingly as minute irregular grains in sphalerite. Argentian gold, with compositions extending to aurian silver, is typically associated with chalcopyrite and occurs as blebs averaging 5-15 × 20 micrometres in diameter. Microprobe analyses of six samples gave formula ratios ranging from $Au_{38.9}Ag_{61.1}$ to $Au_{71.2}Ag_{28.8}$. Tetradymite is the main mineral in the telluride assemblage present in trace amounts in the T-3 lens.

The principal silicates listed in Table 1 are components which occur in samples of massive sulphides, and thus are quantitatively minor relative to the associated sulphides. Quartz, muscovite and chlorite are common in variable amounts in all of the sulphide lenses; albite also is widely distributed but forms only a low fraction of a per cent of the silicate gangue. Celsian, $BaAl_2Si_2O_8$, apparently is confined to the T-1 lens but is extensive within it. The mineral occurs among the sulphides as elongate grains up to 1.0 × 0.6 mm, and also as slightly smaller, roughly equant grains.

Dolomite and lesser calcite have been found in all of the Tulks lenses as fine grained aggregates and coarse single grains dispersed among the sulphides. The occurrences are similar to those of quartz, and in most samples the carbonates coexist with silicates, especially where the spaces between the sulphides are sufficient to form an interconnecting network. No massive barite occurs at Tulks; rather, the mineral is locally abundant in association with quartz and carbonates as disseminated grains among the sulphides. Siderite, ankerite and apatite are rare in the deposit.

METAL ZONING

An adit was driven into the T-3 lens to obtain a bulk sample for metallurgical tests. Detailed examination of the lens in the underground workings showed that the sulphides occur in distinct layers or zones (Fig. 4). These zones include (i) massive pyrite with less than 4% base metal sulphides,

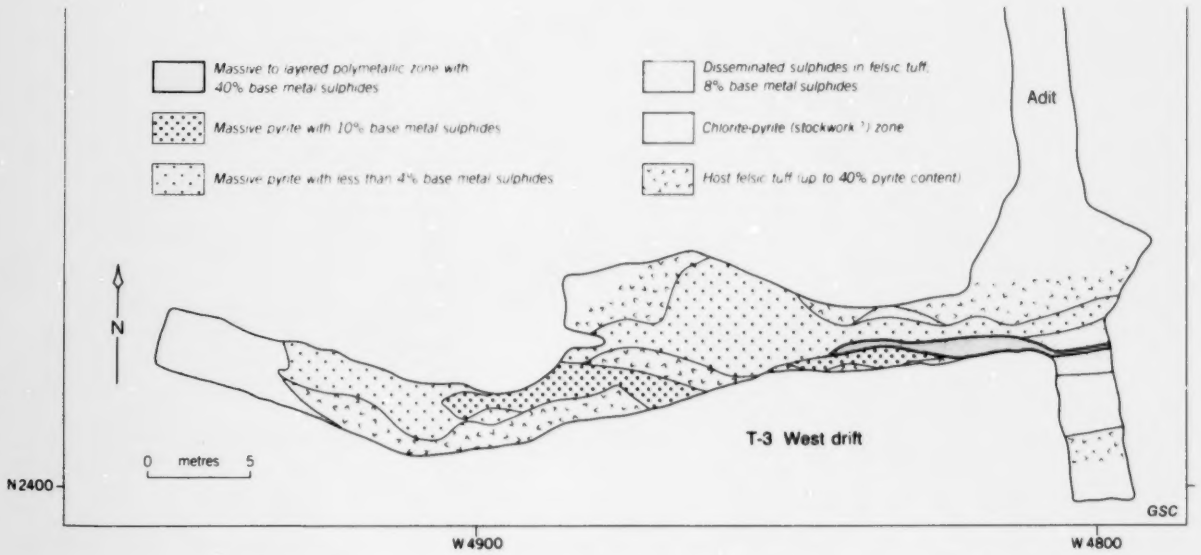
Massive to layered polymetallic zone with 40% base metal sulphides
Massive pyrite with 10% base metal sulphides
Massive pyrite with less than 4% base metal sulphides
Disseminated sulphides in felsic tuff, 8% base metal sulphides
Chlorite-pyrite (stockwork ?) zone
Host felsic tuff (up to 40% pyrite content)
Adit
N
0 metres 5
T-3 West drift
N 2400
W 4900
W 4800
GSC

Figure 4. Plan of the T-3 lens on the adit level (see Fig. 5), showing the sulphide variations within the lens.

(ii) massive pyrite with 10% base metal sulphides, (iii) a massive to banded polymetallic zone with 40% base metal sulphides, and (iv) a disseminated sulphide zone with 8% base metal sulphides. Also present in the adit is a chlorite-pyrite schist zone with minor base metal sulphides. Moreton (1984) suggests that this zone forms part of the stockwork feeder system associated with the massive sulphides.

Sulphides zones similar to those observed underground also are evident in drill sections. In a few cases a stratigraphically upright sequence is evident, that is, chalcopyrite-rich massive sulphides near one contact progress to galena-rich massive sulphides at the other. Typically, however, drill intersections of a lens in a single cross-section give ambiguous zoning, or down-dip reversals in zoning. Conclusions about the stratigraphic directions as derived from metal zoning are therefore tenuous; nevertheless, from the spatial distribution of the various sulphide zones in the T-1 lens, Jambor (1984) suggested that the lens is not overturned and that its stratigraphic top faces north. No conclusions were made about the other lenses, but a weak trend towards concentration of tetrahedrite-tennantite on the north side of the T-3 lens hints at an upright stratigraphy. In contrast, detailed geochemical study led Moreton (1984) to suggest that the T-3 area is overturned and faces southeast. He further noted that the subvolcanic rhyolite intrusion north of T-3 lens (Fig. 5) contains sulphide veinlets, thus possibly indicating that the intrusion played a part in the mineralizing process, i.e., it is comparable to the lava domes and subvolcanic intrusions associated with other volcanogenic massive sulphide deposits.

Several features consistent with a volcanic exhalative origin are present in the Tulks deposit. These include: (i) massive to layered nature of the sulphides (deformation has obscured recognition of bedding), (ii) conformable contacts with the enclosing volcanic rocks, (iii) the deposit occurs within submarine felsic pyroclastic rocks, (iv) alteration of

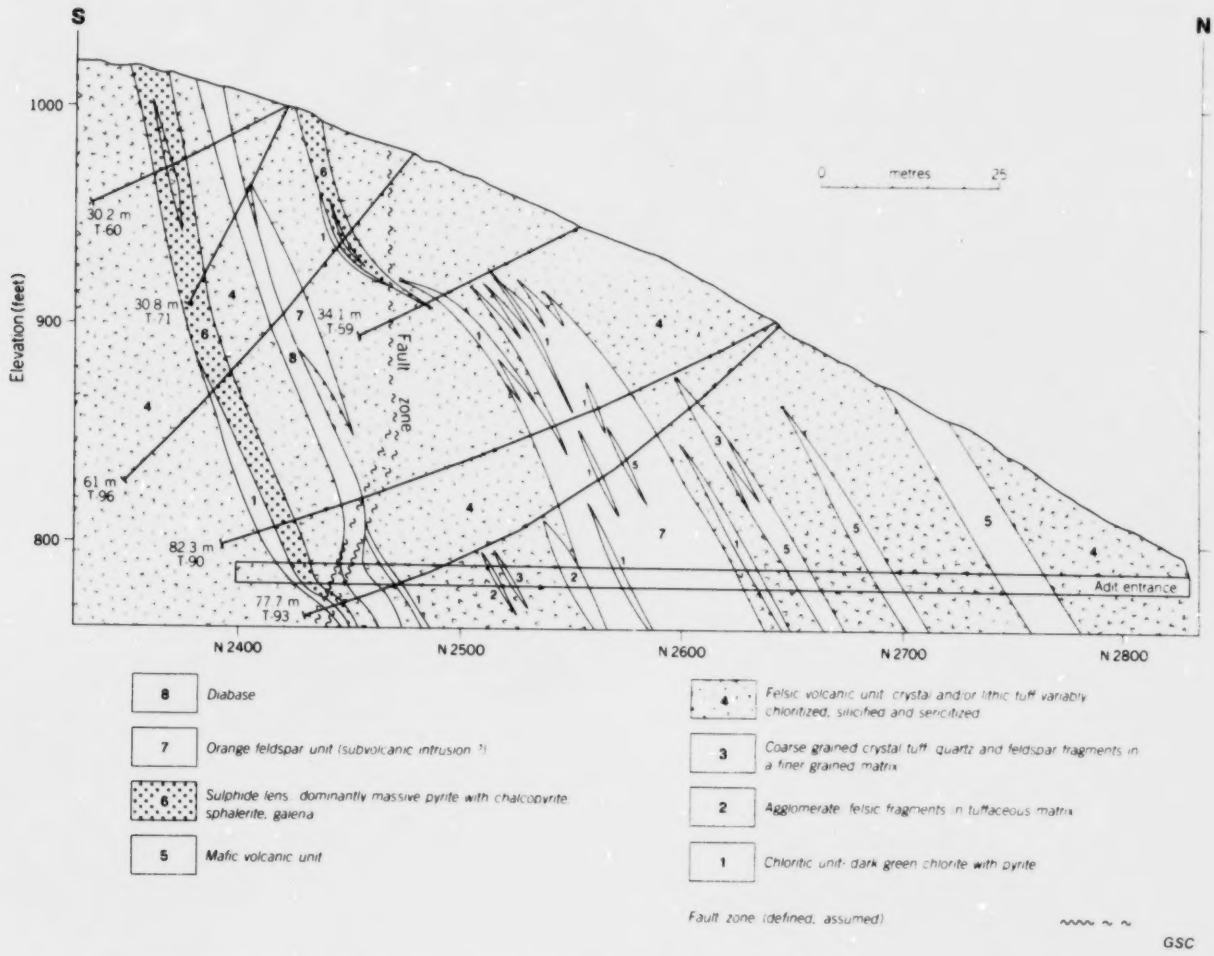

Figure 5. North-south cross-section of the T-3 lens (after Moreton, 1984). Grid co-ordinates and elevations are in feet.

the enclosing volcanic rocks, (v) the presence of possible stockwork alteration, including crosscutting sulphide veinlets, and (vi) the occurrence of a subvolcanic intrusion similar to others associated with many deposits worldwide. Similarities to some New Brunswick massive sulphide deposits are present in many of the lithological and mineralogical characteristics of the Tulks area.

SUPERGENE ALTERATION

The supergene assemblage in the Tulks deposit is listed in Table 1. Digenite and covellite occur in all of the Tulks lenses as hairline veinlets and rims, and as minute specks intermingled with other oxidation products, especially anglesite. Marcasite has been found only in the T-1 and T-2 lenses; in the latter the marcasite is associated with digenite and covellite and is inferred to be supergene. The other alteration minerals given in Table 1 occur only sparingly. Of the various primary sulphides, galena has been by far the most susceptible to replacement by covellite, digenite and anglesite; sphalerite and chalcopyrite have been affected much less in terms of the intensity of alteration of individual grains, the complexity of the alteration products, and the spatial extent of alteration in the lenses.

Although all of the Tulks sulphide lenses have been partly oxidized and supergene-altered, the effects of these alterations generally decrease with depth in the T-1 and T-2 lenses, and possibly also in T-4. Supergene alteration in the T-3 lens seems to be much more erratic in that some cross-sections have only sparse covellite and digenite in near-surface drillholes whereas these minerals are more common at greater depths. Possibly the alteration at depth is related to unspecified fracture zones or minor faults; there seems to be no correlation between the distribution of the alteration minerals and major features such as the lens contacts, or sulphide zones within the lens.

REFERENCES

Dean, P.L.
1977: Geology and metallogeny of the Notre Dame Bay area; Newfoundland Department of Mines, Report 77-10, 17 p.

Dunning, G.R.
1981: The Annieopsquotch ophiolite belt, southwest Newfoundland; in Current Research, Part B, Geological Survey of Canada, Paper 81-1B, p. 11-15.

Jambor, J.L.
1984: Mineralogy of the Tulks Zn-Pb-Cu massive sulphide deposit, Buchans area, Newfoundland; CANMET, Department of Energy, Mines and Resources, Division Report 84-22(TR), 49 p.

Kean, B.F.
1977: Geology of the Victoria Lake map area (12A/6), Newfoundland; Newfoundland Department of Mines, Report 77-4, 11 p.

Kean, B.F. and Jayasinghe, N.R.
1980: Geology of the Lake Ambrose (12A/10) – Noel Paul's Brook (12A/9) map areas, central Newfoundland; Newfoundland Department of Mines, Report 80-2, 29 p.

Kean, B.F., Dean, P.L., and Strong, D.F.
1981: Regional geology of the Central Volcanic Belt of Newfoundland; in The Buchans Orebodies: Fifty Years of Geology and Mining, ed. E.A. Swanson, D.F. Strong and J.G. Thurlow; Geological Association of Canada, Special Paper 22, p. 65-78.

Moreton, C.
1984: The Tulks Hill Massive Sulphide Deposits, Newfoundland; unpublished M.Sc. thesis, Memorial University, Newfoundland.

Nowlan, G.S. and Thurlow, J.G.
1984: Middle Ordovician conodonts from the Buchans Groups, central Newfoundland, and their significance for regional stratigraphy of the Central Volcanic Belt; Canadian Journal of Earth Sciences, v. 21, p. 284-296.
1987: The significance of Middle Ordovician conodonts from the Buchans Group; in Buchans Geology, Newfoundland, ed. R.V. Kirkham; Geological Survey of Canada, Paper 86-24, Report 4.

Stouge, S.
1978: Conodonts from limestone in the Victoria Lake Group; Newfoundland Department of Mines and Energy, Mineral Development Divison, unpublished report.

Williams, H.
1979: Appalachian Orogin in Canada; Canadian Journal of Earth Sciences, v. 16, p. 792-807.

Detailed lead isotope study of Buchans and related ores

G.L. Cumming[1] and D. Krstic[1]

Cumming, G.L., and Krstic, D., Detailed lead isotope study of Buchans and related ores; in Buchans Geology, Newfoundland, ed. R.V. Kirkham; Geological Survey of Canada, Paper 86-24, p. 227-233 Report 13, 1987.

Abstract

Twelve galenas from deposits of the Buchans area are identical within the limits of our measuring error and four more are depleted only slightly in ^{206}Pb relative to the main group. The data points lie significantly below the Stacey and Kramers growth curve and have model ages much younger than the host rocks.

Sphalerites and other sulphide concentrates from several nearby deposits were also analysed, many as leach-residue pairs, in an attempt to obtain additional information which might aid in interpretation of isotope ratios of the Buchans ores. These data along with some additional analyses on galenas, appear to define two steep, diverging linear arrays which may be either mixing lines or multi-stage isochrons.

Large variations in the U/Pb ratio in the sources of deposits on a regional scale are not evident in the compositions of the main Buchans deposits. They were either derived from a very uniform source or the Pb was thoroughly mixed during the process of ore deposition. We have been unable to distinguish clearly between several alternative models that might explain the isotopic coompositions.

Résumé

Douze échantillons de galène tirés des gisements de la région de Buchans sont identiques selon les limites de l'erreur de mesure, tandis que quatre autres sont légèrement appauvris en Pb^{206} par rapport aux groupes principaux. Les données se trouvent bien en dessous de la courbe de croissance de Stacey et Kramers et donnent des âges beaucoup plus récents que les roches encaissantes.

On a également analysé des échantillons de sphalérite et d'autres concentrés sulfurés provenant de plusieurs gisements avoisinants, souvent sous forme de résidus d'attaque, afin d'obtenir d'autres informations qui pourraient aider à interpréter les rapports isotopiques des minerais de Buchans. Ces données, ainsi que les résultats d'autres analyses de la galène, semblent définir deux réseaux linéaires divergents et raides qui pourraient être soit des lignes de mixtion ou des isochrones représentant des étapes multiples.

Les principaux gisements de Buchans ne font pas voir la variation marquée des rapports U/Pb que l'on trouve à l'échelle régionale dans les sources des gisements. Les principaux gisements de Buchans seraient donc dérivés d'une source très homogène, ou encore le plomb a peut-être été complètement mélangé au cours de l'accumulation du minerai. Les auteurs n'ont pas réussi à faire la distinction entre plusieurs modèles différents qui pourraient expliquer les compositions isotopiques.

[1]Department of Physics, University of Alberta, Edmonton, Alberta, Canada T6G 2J1

INTRODUCTION

The isotopic compositions of Pb in large massive sulphide deposits have long been used to construct Pb isotope growth curves for the whole crust-mantle system (e.g. Stacey and Kramers, 1975; Cumming and Richards, 1975; Schlax and Oldenburg, 1984), or for specific subdivisions of this system (Doe and Zartman, 1979). Implicit in these calculations are 1) that individual deposits are uniform in composition and 2) that these compositions are representative of the average Pb isotopic composition of extensive sections of the earth's crust or mantle at the time of ore formation.

In most studies only a few samples have been analysed for a given deposit, whereas regional studies are more common. The case regarding the Buchans area (Fig. 1) is typical of this tendency. Recent studies of the Buchans deposits have resulted in the Pb isotope data as given by Doe and Zartman (1979) – one analysis, Bell and Blenkinsop (1981) – five analyses, and Farquhar and Fletcher (1980) – five analyses, while Swinden and Thorpe (1984) placed the Buchans area in the context of the Newfoundland Central Mobile Belt and demonstrated large variations in the U/Pb ratio for the source regions of deposits. Based on the existing data, the degree to which large regional differences are reflected in the individual mines is uncertain. This work presents data for 16 samples representing most of the major deposits of the immediate Buchans area as well as for 26 additional samples from smaller nearby deposits and showings.

ANALYTICAL TECHNIQUES

Pb was separated from galena samples, or in some cases from sphalerite-rich sulphide mixtures and other sulphide concentrates, by fractional crystallization of $PbCl_2$. Samples of half

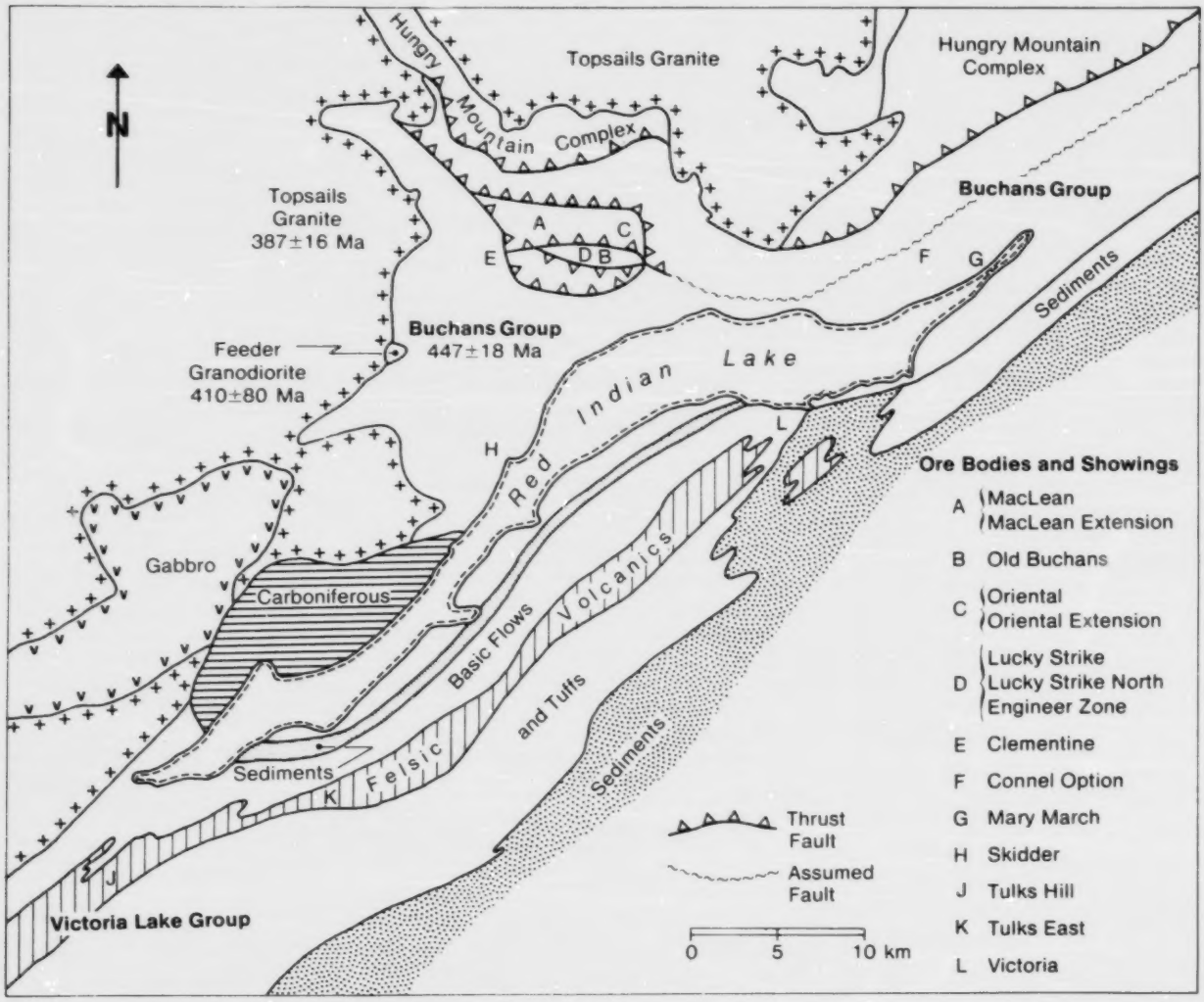

Figure 1. Geologic sketch map of the Buchans area, showing the locations of the deposits for which new isotope data are given in Table 1. Ages after Bell and Blenkinsop (1981).

to one microgram were loaded on a Re filament using the standard silica gel-phosphoric acid technique and analysed on a Micromass MM30 mass spectrometer. The operating temperature was 1250°C as measured on a disappearing filament pyrometer, and reproducibilities at the time these analyses were carried out were 0.21‰, 0.26‰ and 0.29‰ (1 σ) for the $^{206}Pb/^{204}Pb$, $^{207}Pb/^{204}Pb$ and $^{208}Pb/^{204}Pb$ ratios, respectively, as determined by 19 replicate analyses of NBS SRM981 common Pb. One duplicate was run during this study as a check on the consistency of the analyses.

RESULTS AND DISCUSSION

The Buchans deposits

The data of Table 1 from the immediate Buchans mine area are plotted in Figure 2 along with an ellipse representing our nominal measuring error as described above. Thirteen data points (excluding No. 5, 7, 10 and 14) are within the error limits expected from standard measurements. The average value of the 13 points is well below the Stacey and Kramers (1975) growth curve and in fact the second stage U/Pb ratio for the growth curve which passes through the data average is about $\mu = 9.34$, in comparison with a value of 9.74 for their reference curve. The model age for the average Buchans composition is 380 Ma.

The host rocks have been dated by Bell and Blenkisop (1981), who obtained a Rb/Sr age of 447 ± 18 Ma and by Stewart (1987), who reports a U/Pb zircon age of 465 ± 10 Ma. Moreover, Nowlan and Thurlow (1984) discussed the identification of recently discovered conodonts which strongly support a latest Arenig to early Llanvirn age for the rocks. Harland *et al.* (1982) deduced an age of 478 ± 8 Ma for this boundary, indicating that the Rb/Sr date is slightly too young, while the zircon age is within error limits of the suggested value based on fossil evidence. The Pb model age of about 380 Ma is, therefore, much younger than the volcanic host rocks. On the basis of the widely accepted syngenetic model for deposits of this type, the ore formation age should correspond to the age of the volcanic host rocks, and geologic evidence supports the concept that ore formation occurred at the time of volcanism. Thus the simple model age is substantially too young and a more complex model is required to explain the Pb isotope ratios.

The data (Fig. 2) suggest to us that all 17 analyses have significantly more variation in $^{206}Pb/^{204}Pb$ than in $^{207}Pb/^{204}Pb$. This distribution is not what would be expected if material were derived simultaneously from sources with slightly different U/Pb ratios. Such Pb would have ratios along a line of steep slope as discussed by Swinden and Thorpe (1984) in their regional study. The present data may represent a short period Pb/Pb isochron which, for a true age of about 470 Ma, would have a slope of 0.068. This isochron, indicated on Figure 2, is consistent with the data. A linear regression calculated by the method of Cumming *et al.* (1972) yields an approximate slope of 0.053 but fails to converge and gives indeterminate errors, due to the unfavorable distribution of data points. Hence, this calculation is of little help in determining the significance of the data distribution.

The Pb to which a radiogenic component could have been added cannot have been much less radiogenic than the present composition of these samples due to the vast bulk of Pb in the Buchans deposits. A nonradiogenic initial composition would require improbably large amounts of radiogenic material to be added. Thus it is clear that simple models are insufficient to account for the compositions of the main group of Buchans deposits.

Leaching of sulphides

In an attempt to obtain further useful compositional information from the Pb isotope ratio distributions, we carried out leaching experiments on sulphides from several of the deposits (Connel, Skidder, Mary March and Tulks East). These sulphides were presumed to have low lead contents compared to galena samples. Differential leaching of sulphides can yield information about the time interval since the last resetting of the U/Pb system and is particularly useful for minerals where the U/Pb ratio is relatively large, since differences in Pb isotope ratios may be large and reliable age estimates may be obtained (Cummming *et al.*, 1982). Our attempts were not particularly successful for any of the analyses reported here, since all samples were in fact very high in trace Pb. As is apparent in Table 1 and Figure 3, more difference exists between galena speciments from the same deposit than was observed between fractions in the leaching analyses. Between-sample variation for the Skidder deposit (No. 25 to 32) suggests that the data lie along a line of relatively shallow slope, whereas for Tulks East (No. 35 to 40) the variation is along a much steeper isochron discussed below. The reason for the difference in behavior of the Pb from these two deposits is difficult to assess and contributes to the problems of interpretation of the data.

The pattern of isotopic compositions for the Skidder deposit may result from the accumulation of a radiogenic Pb in sulphides from the time of ore formation to the present day, as implicit in calculations such as those in Cumming *et al.* (1982). An alternative explanation is that an episodic addition of Pb occurred during a relatively short interval following initial galena formation (a short period isochron). Whalen and Currie (1987) report that the Topsails intrusive rocks were all emplaced at about 420-430 Ma. Thus a time interval of 30 to 50 Ma is available in which to generate the radiogenic additions contained in the Skidder sulphides and this, in turn, implied a U/Pb ratio of about 10 to 12 in the source rocks. Perhaps Skidder sulphides had their Pb isotope compositions fixed by recrystallization associated with the Topsails igneous episode. A short period addition of radiogenic Pb is thus feasible for the Skidder sulphides since only a relatively small amount of radiogenic Pb is required, whereas this model is quite improbable for the main Buchans deposits, since so much radiogenic Pb would be needed in order to produce the compositional changes required by such a model.

Regional variations

Table 1 and Figure 3 show additional data from other deposits and showings in the area near the Buchans deposits. All the data points except one (No. 30) fall on one of two di-

Table 1. Pb isotopic ratios for samples from the Buchan's area

No.	$^{206}Pb/^{204}Pb$	$^{207}Pb/^{204}Pb$	$^{208}/^{204}Pb$	Sample I.D.	
	Buchans Area				
1	17.829	15.492	37.620	SP-689	(McLean)
2	17.823	15.490	37.612	TQ72-67	(McLean)
3	17.823	15.488	37.612	TQ72-69	(McLean)
4	17.821	15.488	37.606	KQ81-55	(McLean Extension)
5	17.820	15.490	37.621	KQB82-4	(McLean Extension)
6	17.832	15.496	37.628	KQB82-127	(McLean Extension No. 4)
7	17.818	15.496	37.654	KQ74-18	(Old Buchans Pit)
8	17.827	15.490	37.626		(Oriental)
	17.831	15.498	37.640		repeat
9	17.823	15.491	37.610	KQ81-58	(Oriental No. 1 East Pit)
10	17.825	15.497	37.632	KQ83-33	(Oriental No. 1 West Pit)
11	17.832	15.496	37.634	KQ83-21	(Lucky Strike Main)
12	17.829	15.493	37.619	KQ83-22	(Lucky Strike Main)
13	17.826	15.492	37.617	KQ83-17	(Lucky Strike North)
14	17.815	15.489	37.606	KQ83-19A	(Lucky Strike North)
15	17.833	15.495	37.624	KQ74-28	(Engineer Zone)
16	17.828	15.491	37.613	1884-1097	(Clementine)
	Other Deposits				
17	17.735	15.488	37.560	outcrop	(Connel Option) sphal.
18	17.731	15.486	37.543	specimen	(Connel Option) (R)
19	17.732	15.486	37.543		(Connel Option) (L)
20	17.723	15.480	37.543	KQ84-35	(Connel Option) R12-97.5'
21	17.965	15.527	37.662	KQ84-36	(Mary March) mixed (R)
22	17.965	15.529	37.677		(Mary March) sulf. (L)
23	17.943	15.519	37.634	KQ84-37	(Mary March) mixed (R)
24	17.941	15.523	37.635		(Mary March) sulf. (L)
25	17.639	15.457	37.458	KQ83-72	(Skidder)
26	17.586	15.445	37.498	KQ82-73	(Skidder)
27	17.629	15.442	37.463	KQ83-78	(Skidder sulfide) (R)
28	17.634	15.445	37.461	KQ83-78	(Skidder sulfide) (L)
29	17.644	15.445	37.464	KQ83-77	(Skidder sulfide) (R)
30	17.638	15.452	37.491		(Skidder sulfide) (L)
31	17.684	15.455	37.492	KQ83-08	(Skidder sulfide) (R)
32	17.685	15.455	37.481		(Skidder sulfide) (L)
33	18.144	15.571	37.957	TQ82-1	(Tulks Hill)
34	18.142	15.575	37.955	TQ81-50	(Tulks Hill)
35	18.203	15.591	37.997	KQ84-42	(Tulks East) mixed (R)
36	18.204	15.590	37.998		(Tulks East) sulf. (L)
37	18.180	15.584	37.963	KQ84-41	(Tulks East) mixed (R)
38	18.173	15.578	37.958		(Tulks East) sulf. (L)
39	18.177	15.581	37.967	KQ84-40	(Tulks East) mixed (R)
40	18.186	15.586	37.995		(Tulks East) sulf. (L)
41	18.139	15.604	38.060	KQ83-29	(Victoria)
42	18.134	15.597	38.045	KQ83-30	(Victoria)

L - leach in dilute HCl
R - residue decomposed in HNO_3
Code numbers are GSC identification.
All samples are galena except where noted.

verging lines as indicated on the figure. For line A, with a slope of 0.285 (Cumming *et al.*, 1972), we obtain intersections with the Stacey and Kramers (1975) growth curve at 3271 ± 55 Ma and 380 ± 11 Ma with mean squared weighted deviates (MSWD) of 0.56. For line B, with a slope of 0.256, the intersections are at 3131 ± 36 MMa and 279 ± 9 Ma with MSWD = 0.53. In view of the age of the host rocks and the syngenetic origin of these deposits as discussed above, we may discount the younger intersections as being of no direct age significance.

These arrays may be compared with other data sets from eastern North America. LeHuray (1982) postulated that Buchans Pb isotopic ratios lay close to a line of slope 0.399 defined by data from massive sulfide deposits of the southern Appalachians and Swinden and Thorpe (1984) calculated a slope of 0.44 for all available data from deposits of the Central Mobile Belt of Newfoundland. This latter calculation is based on the inclusion of data which we now propose belong to different linear arrays (e.g. Victoria and Buchans) while the correlation proposed by LeHuray is for deposits separated by some 2500 km and, hence, may not be valid. On the other hand, all of these discussions agree that Appalachian Pb isotope ratios tend to lie on very steep "isochrons" which have lower intersections with the Stacey and Kramers (1975) growth curve at times in excess of 3000 Ma and have upper intersections indicating apparent mineralization ages which are too young by about 100 Ma.

The significance of the two linear arrays (A and B) proposed in Figure 3 is difficult to assess. Line B seems well established since subsets of the data from related deposits appear to be distributed along the line. Line A may be fortuituous since only three well-separated clusters of points define the line.

Taken at face value, the two lines intersect at a point ($^{206}Pb/^{204}Pb$ = 17.14, $^{207}Pb/^{204}Pb$ = 15.32) close to a growth curve with m = 8.75 and at a time of 550 Ma. We have tried calculations involving mixing of such depleted mantle Pb with crustal Pb represented by high values of U/Pb and find it difficult to generate compositions similar to those of Buchans ores, using any reasonable values of the parameters.

We have also investigated the possibilities of three-stage models as elucidated by Gale and Mussett (1973). On the premise that our two lines A and B might be representative of arrays diverging from the standard growth curve at about

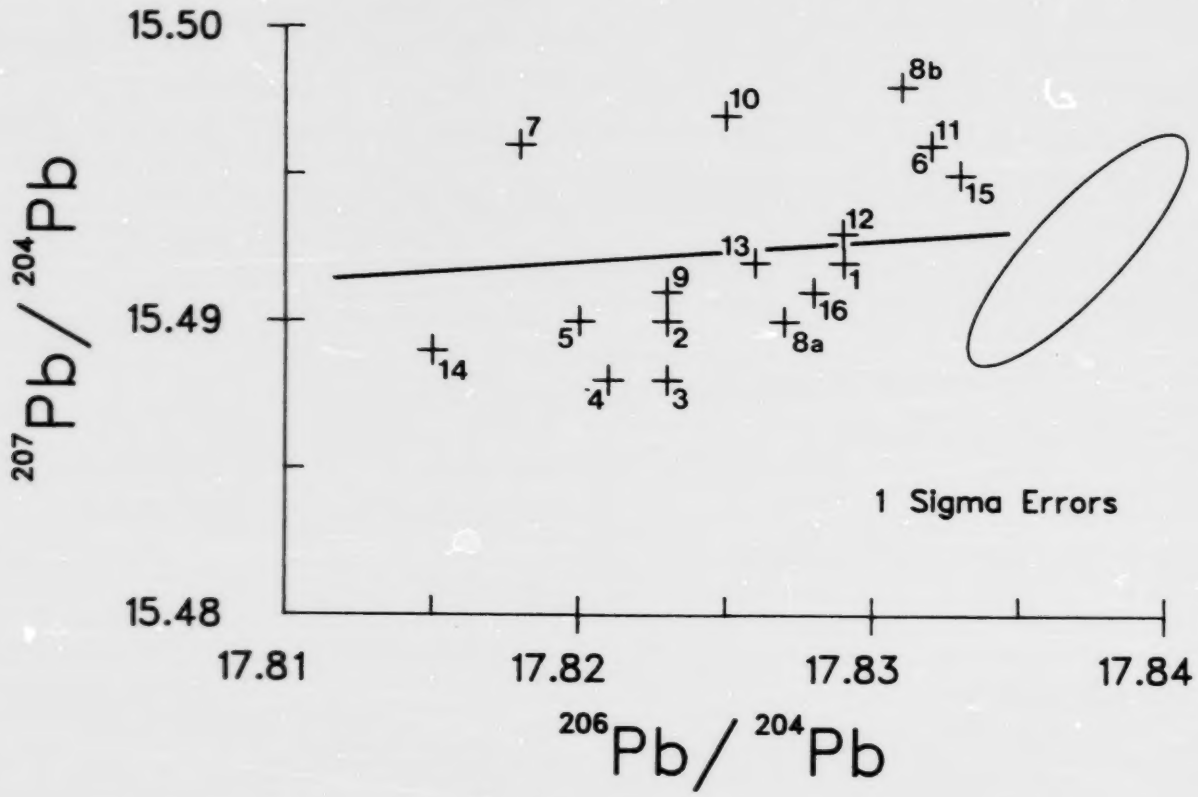

Figure 2. $^{207}Pb/^{204}Pb$ versus $^{206}Pb/^{204}Pb$ for 17 analyses from the Buchans area. The error ellipse shown is estimated from 19 replicate analyses on NBS SRM981. The line represents the expected slope of a short-period Pb/Pb isochron at 470 Ma.

3200 Ma, one is led to consider a three-stage model with constant second- stage fractionation factor (equation A59, page 84 of Gale and Mussett (1973)). The age information which is available from analysis of the data in these terms is limited and provides no useful limits on the time of ore formation. Furthermore, for the Buchans deposits we are constrained to a very short third-stage time interval since the ores are penecontemporaneous with the host rocks. This in turn requires very large values of m for the last stage and extremely large volumes of rock in order to generate enough Pb to satisfy the mass balance restrictions of the large bulk of Buchans ores. This is, of course, the problem of short-period isochrons as discussed previously.

Other possible models have been investigated by Swinden and Thorpe (1984) and need not be reiterated here except to note that a model involving continuously changing U/Pb ratios is at least partially successful in yielding satisfactory model ages, but a single model which is satisfactory for all deposits is diffcult to identify.

CONCLUSIONS

Variations exist in the isotopic composition of the main group of Buchans deposits over a distance of approximately 8 km, from Clementine to the Oriental deposits. However, within this area the variations are small, just larger than the detection limits of our present measuring capabilities. The data distribution is consistent with a short period of Pb evolution in the volcanic environment soon after formation, and is difficult to explain in any other way.

Outside the immediate Buchans area, variations in Pb isotope composition are much larger which implies significant differences in the U/Pb ratios of the Pb source regions. The results may imply a major differentiation of the U/Pb

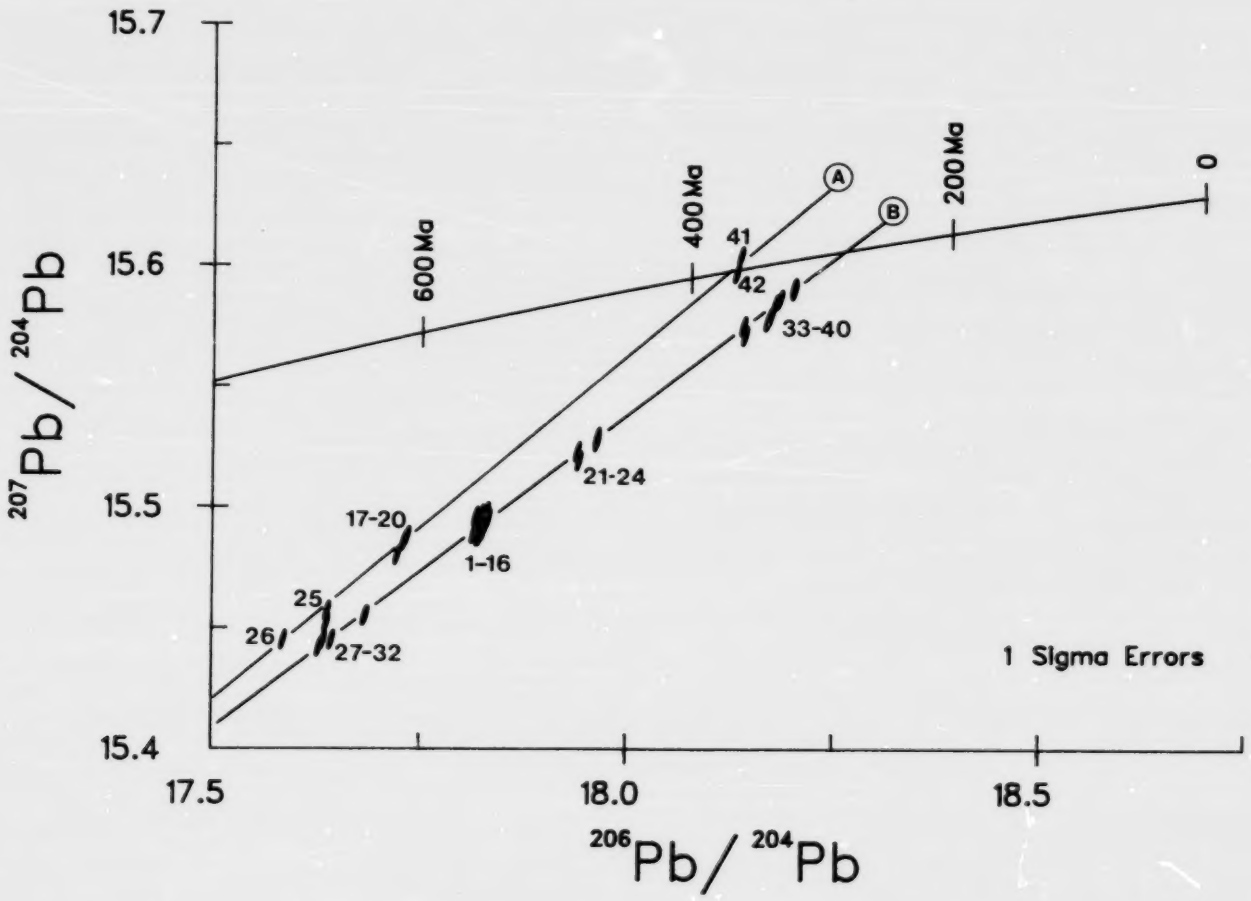

Figure 3. $^{207}Pb/^{204}Pb$ versus $^{206}Pb/^{204}Pb$ for the data of Table 1. Stacey and Kramers (1975) growth curve is shown for reference. Note the discrepancy between the geologic age for the Buchans deposits (~ 470 Ma) and the apparent isotopic age (< 400 Ma). The two lines shown (A and B) diverge from the growth curve near 3200 Ma and may be multistage isochrons or mixing lines.

ratio of the source rocks at about 3200 Ma. Since almost all the data lie well below the Stacey and Kramers (1975) growth curve, relatively low values of m were maintained in the source rocks throughout much of their subsequent history. However, simple models are not easy to devise, since model ages tend to be much too young for most models evaluated. The data lie on one of two steep isochrons, neither of which agrees with that proposed by Swinden and Thorpe (1984) who obtained a much steeper slope and hence an older age for the time of first differentiation.

Short-period Pb evolution for the data from the Buchans deposits is indicated and if our interpretation of the data is correct, then the implication is that at least some of the massive sulphide deposits contain Pb which has undergone more than one stage of development. Therefore great care must be exercised in choosing data which are relevant to the calculation of Pb growth curves for the earth.

ACKNOWLEDGMENTS

We thank the many members of the Geological Survey of Canada and others who supplied the samples and wish to particularly thank R.I. Thorpe and R.V. Kirkham who reviewed the manuscript and made helpful comments. This work was supported in part by an operating grant to G.L. Cumming from the Natural Sciences and Engineering Research Council of Canada.

REFERENCES

Bell, K. and Blenkinsop, J.
1981: A geochronological study of the Buchans area, Newfoundland, in The Buchans Orebodies: Fifty Years of Geology and Mining, ed. E.A. Swanson, D.F. Strong and J.G. Thurlow; Geological Association of Canada, Special Paper 22, p. 91-112.

Cumming, G.L., Eckstrand, O.R. and Peredery, W.V.
1982: Geochronologic interpretations of Pb isotope ratios in nickel sulfides of the Thompson Belt, Manitoba; Canadian Journal of Earth Sciences, v. 19, p. 2306-2324.

Cumming, G.L. and Richards, J.R.
1975: Ore lead isotope ratios in a continuously changing Earth; Earth and Planetary Science Letters, v. 28, p. 155-171.

Cumming, G.L., Rollett, J.S., Rossotti, F.J.C. and Whewell, R.J.
1972: Statistical methods for the computation of stability constants. Part I. Straight-line fitting of points with correlated errors; Journal of the Chemical Society of London, Dalton Transactions: Inorganic Chemistry, p. 2652-2658.

Doe, B.R. and Zartman, R.E.
1979: Plumbotectoics. I. The Phanerozoic; in Geochemistry of Hydrothermal Ore Deposits, 2nd edition, ed. H.L. Barnes; Wiley-Interscience, New York, p. 22-70.

Farquhar, R.M. and Fletcher, I.R.
1980: Ore-lead isotopes and Grenville plate tectonics; in The Continental Crust and Its Mineral Deposits, ed. D.W. Strangway; Geological Association of Canada, Special Paper 20, p. 771-788.

Gale, N.H. and Mussett, A.E.
1975: Eposodic uranium-lead models and the interpretation of variations in the isotopic composition of lead in rocks; Reviews of Geophysics and Space Physics, v. 11, p. 37-86.

Harland, W.B., Cox, A.U., Llewellyn, P.G., Pickton, C.A.G., Smith, A.G. and Walter, R.
1982: A Geologic Time Scale; Cambridge University Press, 131 p.

LeHuray, A.P.
1982: Lead isotopic patterns of galena in the Piedmont and Blue Ridge ore deposits, southern Appalachians; Economic Geology, v. 77, p. 335-351.

Nowlan, G.S. and Thurlow, J.G.
1984: Middle Ordovician conodonts from the Buchans Group, central Newfoundland and their significance for regional stratigraphy of the Central Volcanics Belt; Canadian Journal of Earth Science, v. 21, p. 284-296.

Schlax, M. and Oldenburg, D.W.
1984: Age bounds from lead isotope data; Earth and Planetary Science Letters, v. 68, p. 413-421.

Stacey, J.S. and Kramers, J.D.
1975: Approximation of terrestrial lead isotope evolution by a two-stage model; Earth and Planetary Science Letters, v. 26, p. 207-221.

Stewart, P.W.
1987: Geology and genesis of granitoid clasts in the MacLean Extension transported ore body; in Buchans Geology, Newfoundland, ed. R.V. Kirkham; Geological Survey of Canada, Paper 86-24, Report 9.

Swinden, H.S. and Thorpe, R.I.
1984: Variations in style of volcanism and massive sulfide deposition in Early to Middle Ordovician island arc sequences of the central Newfoundland mobile belt; Economic Geology, v. 79, p. 1596-1619.

Whalen, J.B. and Currie, K.L.
1987: The relationship of the Topsails igneous terrane to the Buchans Group; in Buchans Geology, Newfoundland, ed. R.V. Kirkham; Geological Survey of Canada, Paper 86-24, Report 6.

- 14 -

Deep multifrequency and transient electromagnetic surveys near Buchans

A.K. Sinha[1] and L.E. Stephens[1]

Sinha, A.K. and Stephens, L.E., Deep multifrequency and transient electromagnetic surveys near Buchans; in Buchans Geology, Newfoundland, ed. R.V. Kirkham; Geological Survey of Canada, Paper 86-24, p. 235-250, Report 14, 1987.

Abstract

Deep electromagnetic (EM) surveys using multifrequency and transient sources were conducted over two sites near Buchans, Newfoundland. The purpose was to examine the capabilities of the two systems to detect and delineate poorly conductive transported sulphide bodies buried at large depths. The first site was the Clementine Prospect, a sphalerite-barite-rich transported sulphide body occurring at an average depth of more than 300 m. The other site was at Mary March, 34 km east of Buchans where silicified and seriticized felsic volcanics are present. This survey was directed toward detection and delineation of any conductive body present at depths up to 300-400 m from the surface.

The transient EM system was not successful in detecting any strongly conductive body at either site. The multifrequency system, however, recorded weak anomalies on three lines over the Clementine Prospect. The system also detected two weak conductive bodies with good line-to-line correlation at the Mary March site. The weak multifrequency response at the two sites, however, meant that quantitative interpretation of the data could not be done with confidence. The nature of the Mary March conductors should be explained once the conductors are drilled.

Résumé

Des levés électromagnétiques en profondeur ont été effectués au-dessus de deux emplacements près de Buchans, à Terre-Neuve, en utilisant des sources multifréquences et des sources transitoires. Ces levés avaient pour objet d'examiner la capacité des deux systèmes de déceler et de délimiter des masses de sulfures transportées qui sont des mauvais conducteurs enfouis à très grande profondeur. Le premier emplacement examiné a été l'indice Clementine, une masse de sulfures transportés riche en sphalérite et en barytine dont la profondeur moyenne est supérieure à 300 mètres. L'autre emplacement, celui de Mary March, se situe à 34 km à l'est de Buchans; on y trouve des roches volcaniques felsiques séricitisées et silicifiées. Le levé avait pour objet de déceler et de délimiter tout corps conducteur enfoui à un maximum de 300 à 400 m.

Le système électromagnétique transitoire n'a pas décelé de corps fortement conducteur à l'un ou l'autre des emplacements. Cependant, le système multifréquence a enregistré de faibles anomalies sur trois lignes de vol au-dessus de l'indice Clementine. Il a également décelé deux corps faiblement conducteurs caractérisés par une bonne corrélation entre les lignes à l'emplacement de Mary March. Cependant, étant donnée la faiblesse de la réponse multifréquence aux deux emplacements, il est impossible d'interpréter quantitativement certaines des données. Il devrait être possible de déterminer la nature des conducteurs de l'emplacement de Mary March une fois qu'on y aura entrepris des travaux de forage.

[1]Geological Survey of Canada, 601 Booth Street, Ottawa, K1A 0E8

INTRODUCTION

As part of the Canada-Newfoundland co-operative mineral program, a deep transient and multifrequency electromagnetic (EM) survey was conducted over two sites near Buchans, Newfoundland, in 1982. The work was carried out by personnel from GSC with active co-operation and help from geologists and owners of the properties, Abitibi-Price Inc. and ASARCO Inc. The first survey site was the Clementine Prospect, a deep sulphide deposit about 4.4 km northwest of the town of Buchans. The other site was at Mary March, about 34 km east of Buchans off Highway 370. The two sites were investigated using the Maxi-Probe multi frequency and Geonics EM-37 transient EM systems. Both systems are capable of detecting good conductors several hundred metres below the surface.

The Clementine Prospect was discovered in 1960 by blind drilling of favourable volcanics as part of the general exploration program. Later, 21 diamond-drill holes intersected the zone at depths ranging from 207 m to 485 m below the surface. It is estimated to contain about 369 000 metric tonnes of zinc-lead-copper sulphides containing 15-25% of sphalerite and barite (J.G. Thurlow, personal communica-

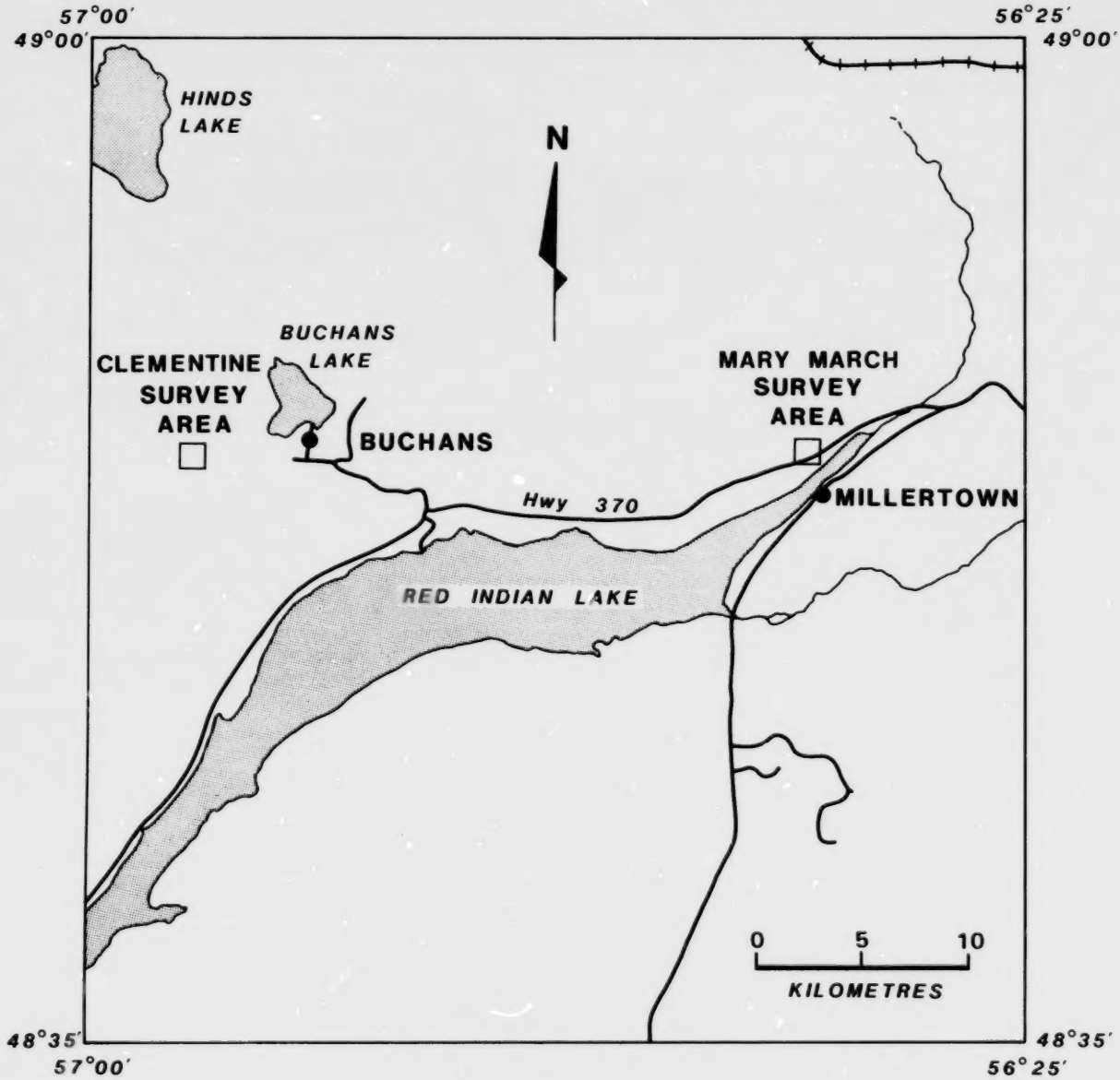

Figure 1. Location map of the two survey areas near Buchans, Newfoundland.

tion, 1985), two electrically resistive minerals. Clementine is a classic case of a deposit of transported sulphides, the source of which is unknown. Previous ground electrical, EM and Induced Polarization (I.P.) surveys as well as airborne EM surveys have failed to detect the sulphide body. The reason for the lack of response is twofold: (a) the deposit is rather deep with an average depth exceeding 300 m, and (b) the overall electrical conductivity of the deposit is not high because it contains a high percentage of barite and sphalerite and because of the fragmental, disconnected nature of the conductive sulphides. Hence, the electrical and EM response of this body is too low for standard electrical and EM systems in use which have depth penetration of the order of 200 m. A high voltage power line is present in the area as well, producing electrical noise for all electrical and EM surveys. The purpose of our tests at this site was to evaluate the effectiveness of two deep sounding EM systems to detect and, if possible, delineate this deep, poorly conductive body from the surface.

The Mary March site has previously been mapped in detail by company geologists who detected its ore potential by the presence of altered rocks such as silicified and sericized felsic volcanics at several locations. Ground VLF and horizontal loop EM surveys at the site also detected several weak, shallow conductors of unknown origin (J.G. Thurlow, personal communication, 1982). A deep EM survey was, therefore, considered appropriate for this site in an attempt to locate better conductors at depth.

Survey grid lines were cut at both sites by personnel from Abitibi-Price Inc. The two survey locations are shown in Figure 1. At the Clementine site, the transient EM survey was conducted on eight NW-SE oriented lines, 120 m apart, using two rectangular transmitter loops. The lengths of the survey lines varied from 500 to 800 m, and were limited by the electrical noise from a nearby high tension power line. The multifrequency survey was conducted on three parallel lines each about 500 m long oriented NW-SE. At the Mary March site, the transient EM survey was carried out on five NNW-SSE oriented lines, 100 m apart, the lengths of the lines varying from 600 to 800 m. The multifrequency survey at this site consisted of measurements taken along seven parallel lines, each about 400 m long oriented NNW-SSE. The station intervals for both EM surveys at the two sites were 25 m.

GEOLOGY OF THE SURVEY AREAS

The geology of the ore deposits at Buchans has been described by Thurlow and Swanson (1981). In addition, flow directions and source of fragmental sulphides at the Clementine Prospect has been evaluated by Calhoun and Hutchinson (1981). The Buchans ores are high-grade Kuroko-like polymetallic massive sulphide deposits associated with Ordovician submarine felsic volcanic rocks. The orebodies consist of three types of deposits based on their structure and origin: (a) stockwork zones consisting of subeconomic to low-grade networks of disseminated and vein sulphides within strongly altered host rock; (b) in situ primary sulphides consisting of high-grade sphalerite-galena-chalcopyrite-pyrite-barite ores lying stratigraphically above the

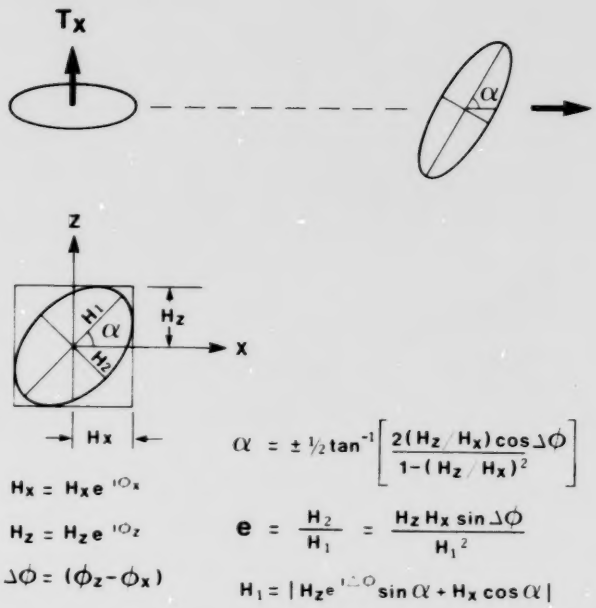

Figure 2. Mode of operation and parameters measured in multifrequency EM measurements.

stockwork zones; (c) transported sulphide ores consisting of low- to high-grade accumulations of sulphide fragments derived from in situ ore but transported by submarine turbidity flows from their source.

The Clementine Prospect is a breccia-textured, volcanic sulphide-barite-rich transported ore occurrence which appears to be on the same stratigraphic horizon as the MacLean and Rothermere orebodies, two transported deposits which have been mined successfully in the past (Thurlow and Swanson, 1981, 1987). Criteria developed for relating MacLean and Rothermere orebodies to the Lucky Strike in situ orebody suggest that an undiscovered source of the Clementine Prospect might lie to the northwest of it (Calhoun and Hutchinson, 1981). The Clementine Prospect has a lower grade ore than MacLean and Rothermere and consists of three units: 1) felsic clast-rich breccia, 2) andesitic clast-rich breccia and, 3) baritic clast-rich breccias, each occurring in separate stratigraphic levels (Calhoun and Hutchinson, 1981). The three units are designated as upper, middle and lower units, respectively. The sulphide clasts of the lower unit consists of pyrite and chalcopyrite while the sulphide fragments of the middle unit are mainly sphalerite and galena. The upper unit contains more baritic clasts and less sulphide clasts than the two other units. Drillholes intersect the sulphide zone at the Clementine Prospect at depths of 207 to 485 m below the ground. It has a strike of N45°E and a dip of 35°SE. The topography of the area is generally flat and boggy with numerous swamps and ponds.

The geology of the Mary March area is less well known since no mineral occurrence of significant size has been reported in the area and drillhole information is not available.

The Mary March survey area, shown in Figure 1 is south of an abandoned railway track and north of Red Indian Lake. Lithologically, the area is similar to the Buchans mine area. The rocks consist of silicic to intermediate to mafic volcanic rocks which are folded and faulted on a fairly broad scale (Neale and Nash, 1963). The topography of the area is flat and boggy north of Hwy 370 and fairly undulating south of the highway with the terrain generally sloping towards the lake. Geological mapping in this area has led to the discovery of characteristic altered rocks indicating the potential presence of massive sulphide bodies within the area. The survey was conducted at this site to examine this hypothesis.

PREVIOUS GEOPHYSICAL SURVEYS

The history of geophysical exploration at Buchans has been summarized by Moss and Perkins (1981). The earliest geophysical method tried at Buchans was the 'equipotential line' method by Hans Lundberg in 1926 which led to the discovery of two massive sulphide orebodies, the Lucky Strike and Oriental No. 1. Since those discoveries, various surface, drill hole and airborne geophysical methods have been tried over the massive and transported orebodies with limited success. The second most important geophysical contribution to discovery of ore at Buchans was made in 1954, when an electrical potential survey using surface and drillhole techniques assisted in the discovery of the Oriental No. 2 orebody. In retrospect, electrical methods have been successful only in cases where the orebody is shallow and contains a high percentage of conductive sulphides. In the case of transported ores containing significant amounts of barite and sphalerite, the success rate is poor to nil, especially if the orebody is at a substantial depth from the surface.

The presence of abundant metallic sulphides in Buchans orebodies would normally suggest that these may be suitable targets for EM surveys. However, the fragmental nature of the orebodies and high proportions of two resistive minerals, barite and sphalerite in the ores, result in poor observed EM responses in ground EM systems. Induced Polarization and ground and airborne EM surveys over the Clementine Prospect had failed to detect the presence of the sulphide deposit in previous surveys. A Very Low Frequency (VLF) survey over the Clementine and Mary March sites only detected several shallow conductors, presumably fracture zones (J.G. Thurlow, personal communication, 1982).

Considering the lack of EM response in previous surveys, the success of the multifrequency and transient EM surveys over these prospects seemed uncertain. Clementine was an especially difficult site since the low-grade sulphide body occurs at a substantial depth. At the Mary March site, little information was available about the possible presence or extent of any orebody except that characteristic altered rocks had been detected at the site. A VLF survey conducted earlier by Abitibi-Price Inc. had detected several conductors of unknown origin but no information was available about the locations of the VLF conductors when the GSC survey began.

DESCRIPTIONS OF THE EM SYSTEMS

A Maxi-Probe deep EM system was used for multifrequency surveys. The system has been described by Sinha (1979, 1983). However, for the Buchans survey, the system was used in a different mode. Instead of sounding over layered media, it was used in a traverse mode for the detection of conductive bodies by measuring the tilt angle and ellipticity of the polarization ellipse. The technique will be described later in this section.

Figure 2 shows the mode of operation of the Maxi-Probe system. The transmitter Tx is a horizontal loop (for this survey three loops connected in parallel to form a cloverleaf) placed on the ground which may be energized to transmit up to 128 discrete sinusoidal frequencies from 1 Hz to 60 kHz. The receiver consists of a pair of orthogonal horizontal and vertical coils to measure the in-phase and quadrature components of the vertical (H_z) and horizontal (H_x) magnetic field components respectively at various distances from the transmitter. The transmitter and the receiver are synchronized at the beginning of the survey using two crystal clocks. This eliminates the necessity for a long connecting cable between the transmitter and the receiver for the phase reference. The receiver usually is placed at various locations from about 150 m to 600 m from the transmitter. Beyond 600 m, the EM fields are usually too weak to be measured accurately. From the measured horizontal and vertical magnetic field components, the ratios of the field amplitudes and their phase differences are determined.

As the primary field is not 'bucked out' at the receiver, the total field measured at the receiver consists of both the primary field from the transmitter and the secondary field generated by subsurface conductors, which will normally have some phase difference between them. The resultant field at the receiver is, therefore, elliptically polarized. The parameters of the ellipse (tilt angle α and ellipticity e) shown in Figure 2 may be determined from the amplitude ratio H_z/H_x and phase difference $\emptyset_z$-$\emptyset_x$ at each frequency. From plots of tilt angle and ellipticity along a survey line, one may be able to detect the presence of conductive bodies beneath the ground. It has been shown (Ward *et al.*, 1974) that when the receiver passes across a conductor, the tilt angle and ellipticity values decrease, thus indicating the presence of a conductor. Such tilt angle and ellipticity measurements have been used successfully for the detection of good conductors in mining environments (Sinha and Stephens, 1984). For such surveys, station separations are set at 25 m or less for defining conductors with sufficient precision.

A transient or time-domain EM system differs from a frequency-domain system in that instead of transmitting sinusoidal currents at different frequencies, a pulse of known base frequency is passed through a transmitter, most commonly, a single strand rectangular loop lying on the ground. The configuration of the transmitter loop in relation to a subsurface conductor is shown in Figure 3. The loop is normally laid on the ground with its longer side parallel to the expected strike of the conductor. A steady current, most commonly,

20 to 25 amperes is passed through the loop long enough (slightly over 8 milliseconds for the 30 Hz base frequency) for the turn-on transients in the ground to dissipate. The steady current is then abruptly terminated as shown in lower part of Figure 3. According to Faraday's laws of induction, the rapid reduction of current in the transmitter in a very short period causes the magnetic flux to collapse, thereby inducing a secondary electromotive force (e.m.f.) in nearby conductors. This e.m.f. causes eddy currents to flow in nearby conductors which will decay in a characteristic fashion depending on the shape, size and conductivity of the conductors. The decay currents generate a secondary magnetic field, whose time rate of change is measured by a mobile receiver loop placed on the ground along the survey line. The decay of the secondary field is measured at several time windows or channels in the absence of the primary field as shown in the

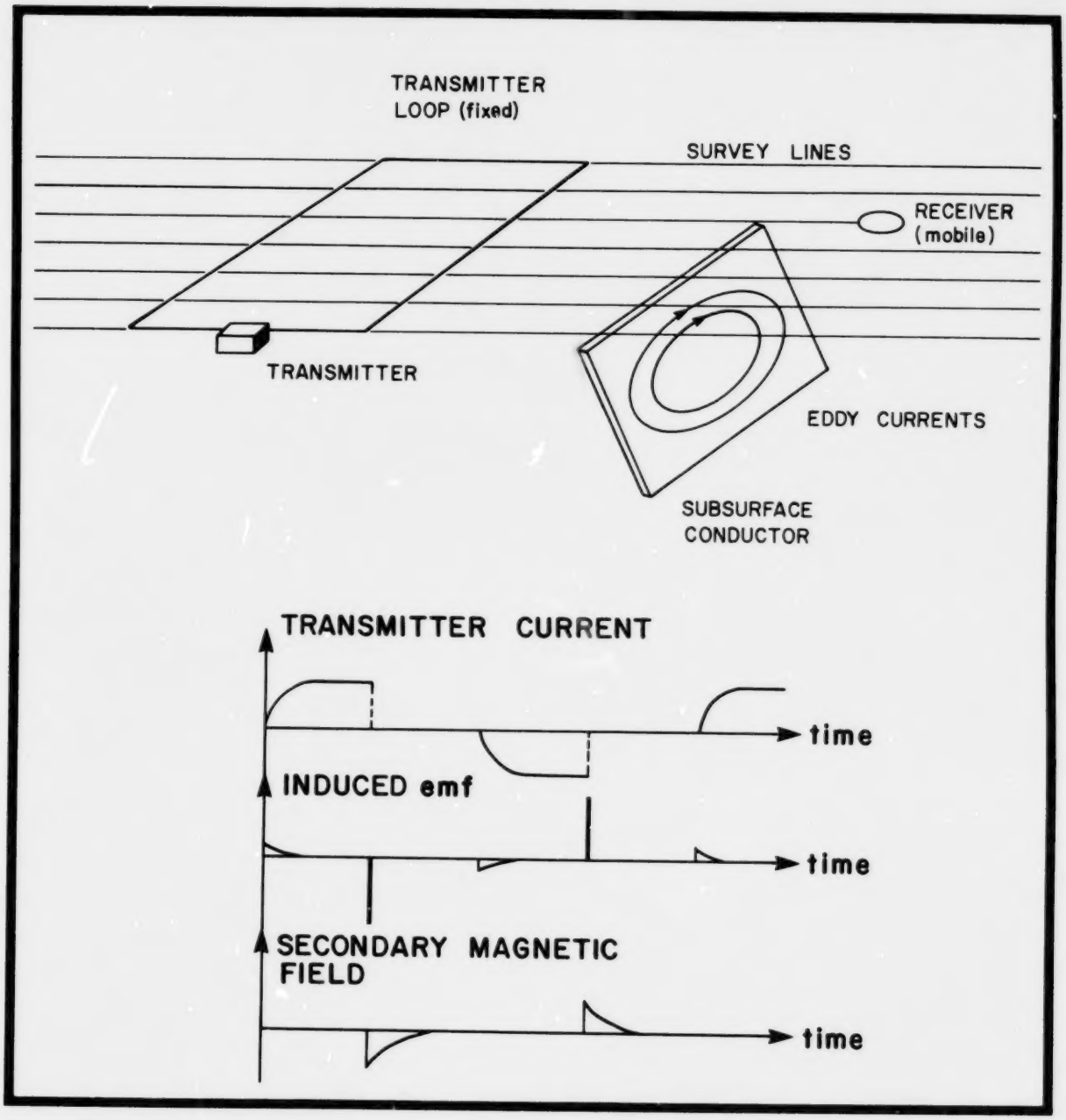

Figure 3. Schematic diagram of a transient EM system showing transmitter pulse and induced secondary effects.

diagram. After the 'off' period, (equal to the 'on' period) the current is turned 'on' again rapidly but in the negative sense and then, abruptly brought back to zero as shown in Figure 3. The decay voltages are measured over many cycles to enhance the signal/noise ratios after applying suitable amplification to the measured signal.

A Geonics EM-37 transient system was used for the present survey. The system has been described earlier by Sinha (1983) and Sinha and Stephens (1983). For this survey, an oven-warmed crystal was used for synchronizing the transmitter to the receiver (for stable and precise synchronization) which eliminated the need for a cable between the transmitter

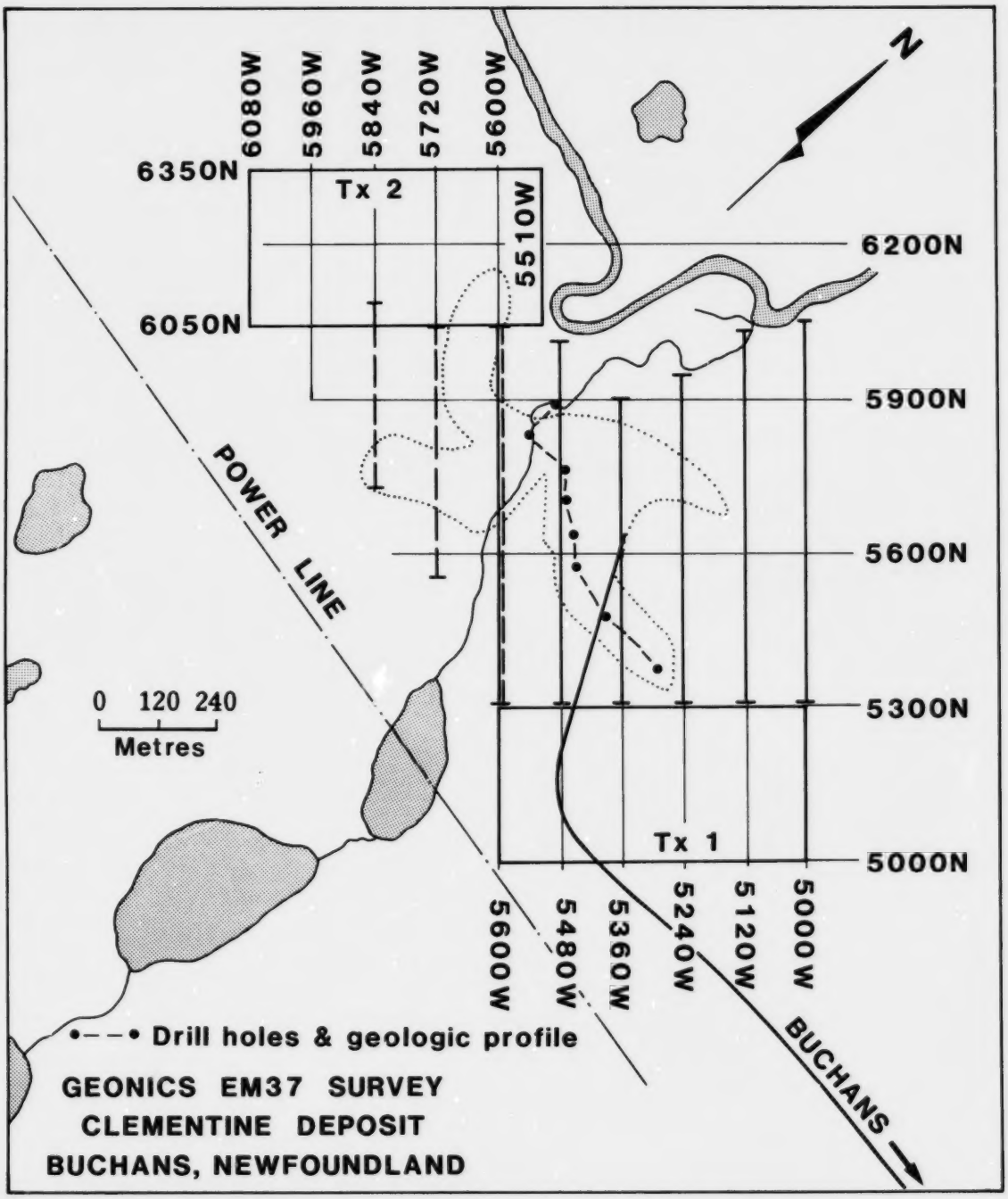

Figure 4. Survey area for the transient EM survey over the Clementine Prospect.

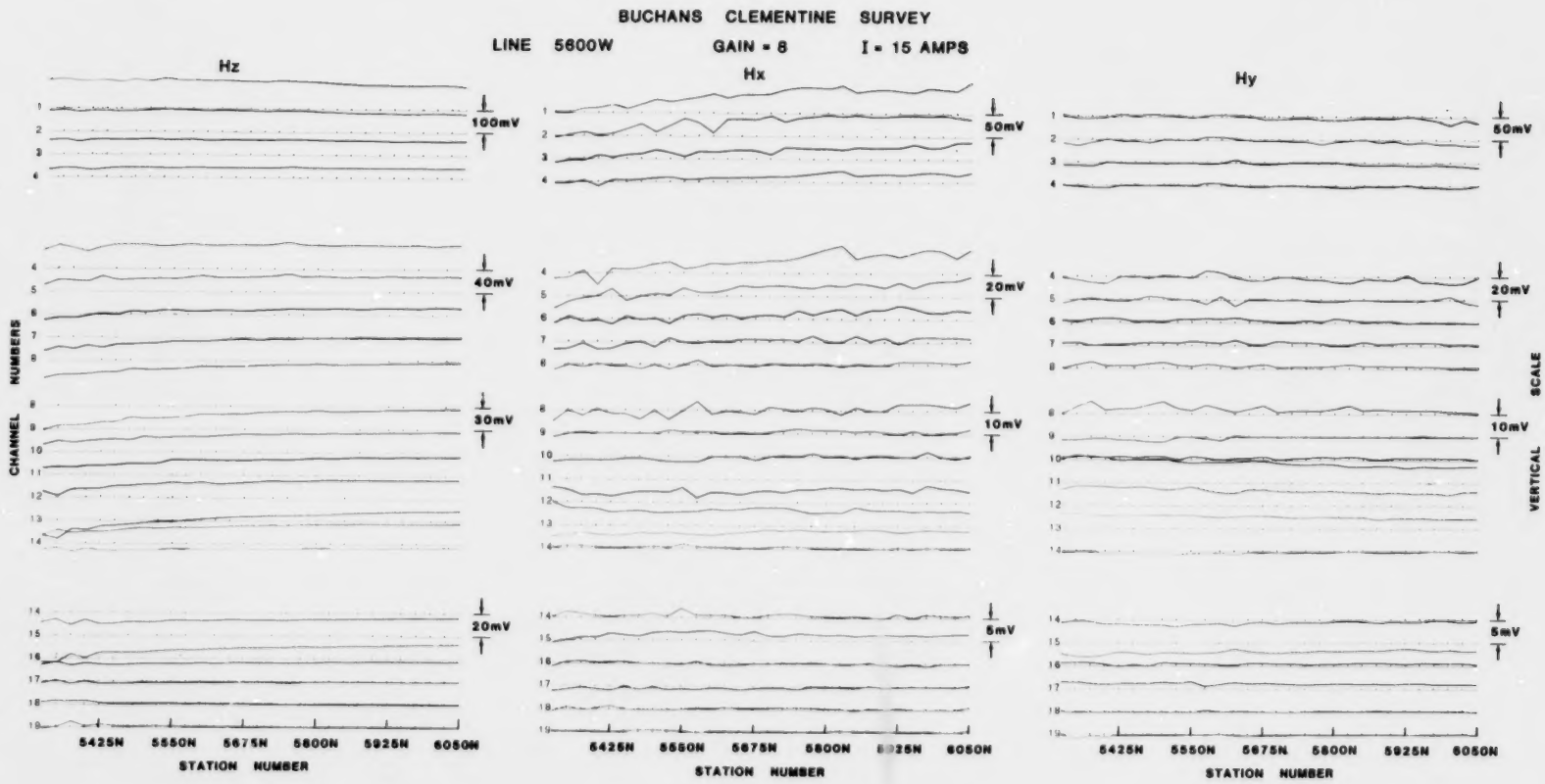

Figure 5. Plot of the decay of the orthogonal magnetic field components on line 5600 W at Clementine.

and the receiver for phase reference. This type of synchronization is not affected by rough topography, or the distance between the transmitter and the receiver. With this system, it is possible to measure the decay of the magnetic fields in three orthogonal directions in 20 discrete time channels from 86 microseconds to over 7 milliseconds after the turn-off using the base frequency of 30 Hz. A lower base frequency of 3 Hz was not used in this survey because of poor results at the more sensitive higher frequency of 30 Hz.

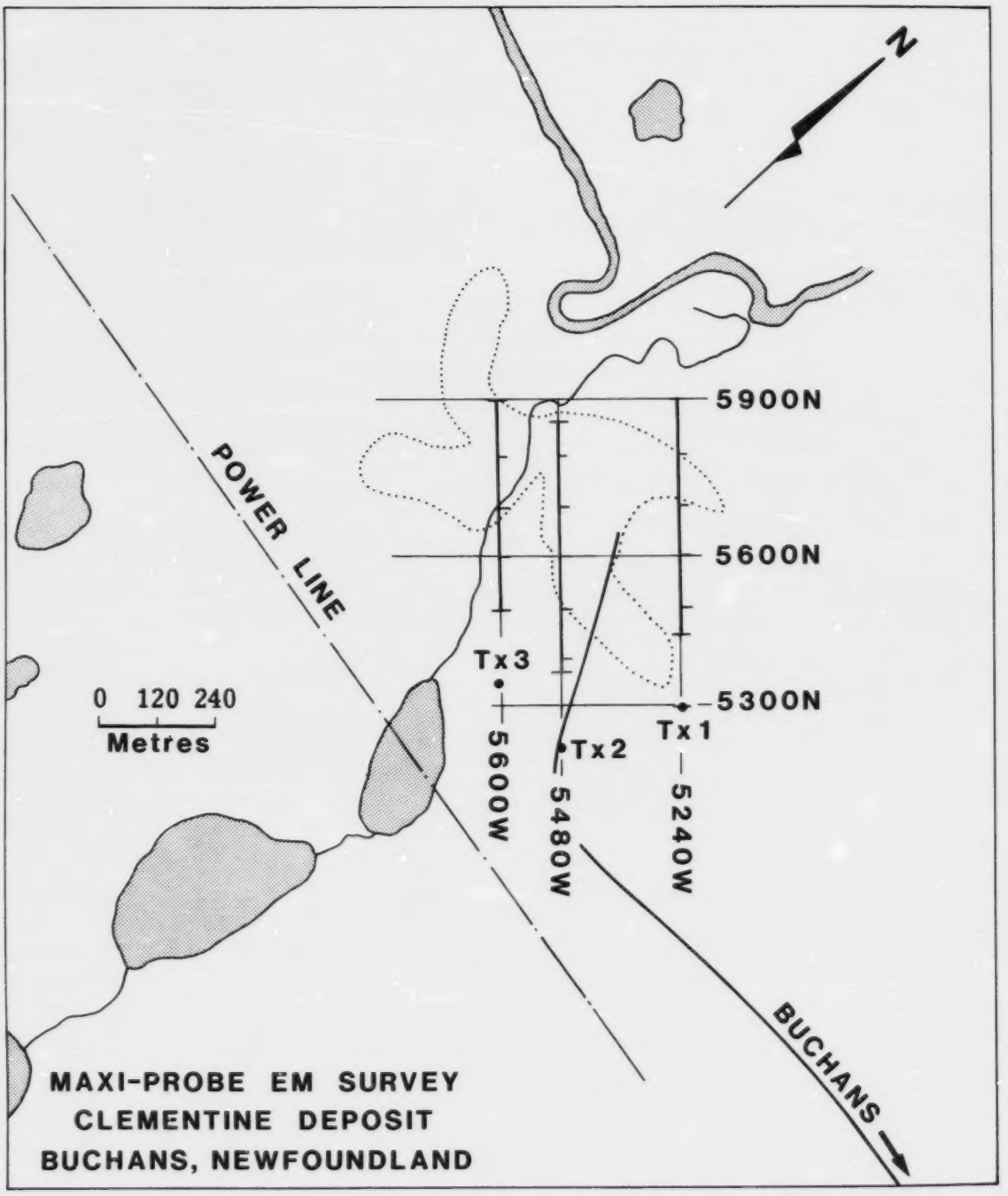

Figure 6. Survey area for the multifrequency EM survey over the Clementine Prospect.

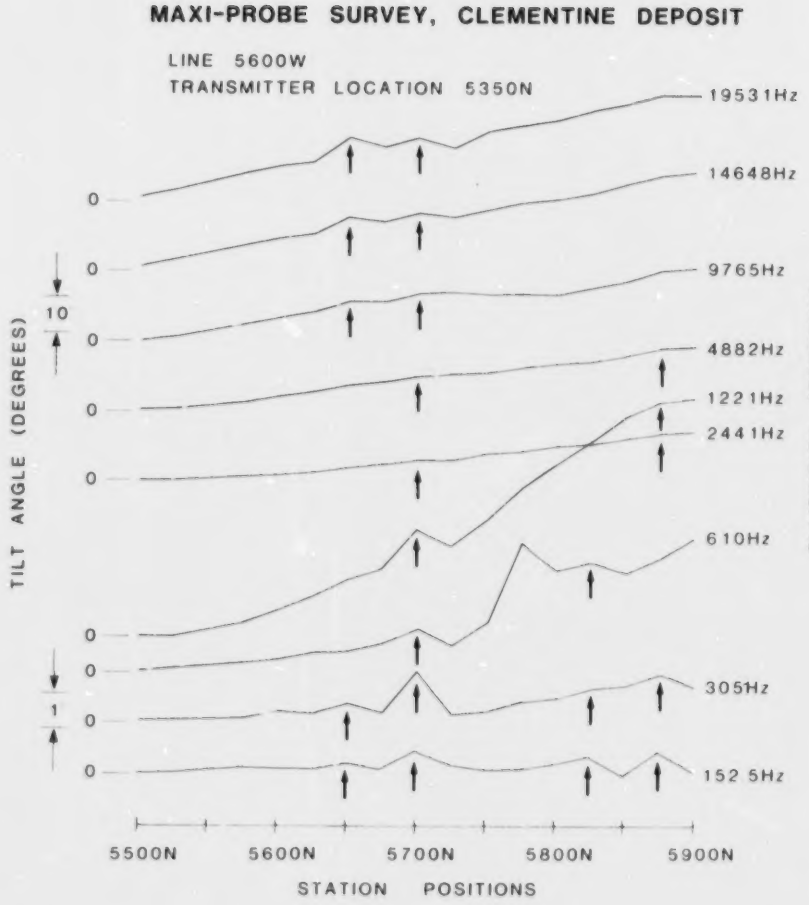

Figure 7. Plot of the variation of the tilt angle in degrees versus station positions on line 5600 W at Clementine.

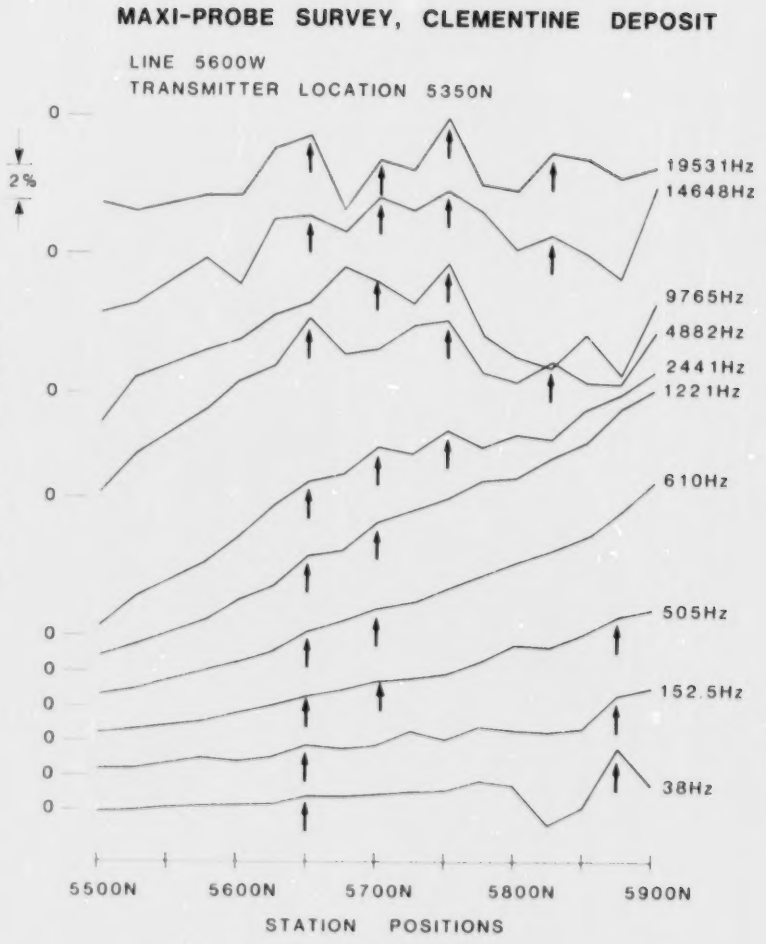

Figure 8. Plot of the variation of the ellipticity in per cent versus station positions on line 5600 W at Clementine.

RESULTS OVER CLEMENTINE PROSPECT

Figure 4 shows the area surveyed by the transient EM system over the Clementine Prospect. An outline of the sulphide body derived from drilling information is shown by dotted lines. Two transmitter loops were used during the survey. These are indicated by T_{x1} and T_{x2} on the figure and the dimensions were 300 m by 600 m in both cases. Six lines, 120 m apart were surveyed using T_{x1} while three lines were surveyed using T_{x2} with line 5600 W being common to both. The presence of a high tension power line in the area made the lengths of lines surveyed with T_{x2} rather short, since the receiver had to be at least 400 m away from the power line to prevent overloading of the circuitry.

The field data set consists of the measurements of the decay of the secondary field voltages in three orthogonal directions for 20 channels at each station position, 25 m apart. The direction of the survey line is chosen by convention to be the X-direction while the orthogonal horizontal direction is taken to be the Y-direction. Z-direction is taken to be vertically upward. The presence of a discrete conductor is indicated by a crossover type response in z-component and a maximum in the x-component. The y-component response gives an indication about the direction of the strike and the strike length (Sinha, 1983).

Early channel data are equivalent to high frequency response on frequency- domain systems. Hence, these are mostly affected by near-surface materials. Late channel data, on the other hand, are mostly affected by deeper inhomogeneities. Figure 5 shows the response of the field components H_z, H_x and H_y on line 5600 W for the transmitter loop T_{x1}. The channel numbers (1 to 19) are indicated on the left, the 20th channel was not recorded because it was noisy. Since earlier channels have higher amplitudes, they have been plotted with a smaller scale, e.g. 100 or 50 mV/division. The decreasing amplitude in later channels necessitated plotting those data at progressively larger scales to display the decays of the fields in a clear fashion. The vertical scales are shown to the right of the plots. To facilitate the comparison of data plotted with different scales, data from a channel is plotted with two scales whenever a change of scale takes place. The station locations are indicated in the abscissa. None of the three components H_z, H_x or H_y show any definite anomalous pattern with good channel to channel correlation. The occasional small spikes are most likely caused by noise originating from slight receiver coil misorientations, atmospheric noise or local inhomogeneities. The same lack of response from subsurface conductors is observed on all survey lines. It was therefore concluded that the transient system was unable to detect the sulphides at the Clementine Prospect.

The multifrequency survey using the Maxi-Probe system was conducted at this site on three parallel lines, namely 5240 W, 5480 W and 5600 W. The locations of the survey lines in relation to the Clementine Prospect and the three transmitter locations T_{x1}, T_{x2} and T_{x3} are shown in Figure 6. The purpose of the survey was to determine if tilt angle and ellipticity measurements can detect the conductive sulphides on these lines. Time limitations prevented a more thorough survey at this site. The sitings of the transmitter loops were irregular for two reasons. First, the transmitter loops require level or semi-level ground for reliable survey data (Sinha, 1981). Thus level ground was chosen for the loops whenever available. Secondly, the tilt angle and ellipticity values cannot be measured with this system for distances closer than 150 m and at distances greater than 600 m from the transmitter. The usable length of a survey line is therefore only about 450 m. The transmitter sites were therefore chosen in such a way that the distances to the edges of the Clementine Prospect would be less than 600 m and that the edges would be roughly perpendicular to the survey lines for good coupling to the conductor.

Figure 7 shows a plot of the corrected tilt angles in degrees versus station positions on line 5600 W. The measured tilt angle data are first corrected for the effects of topography by subtracting from the measured values the tilt angle at the lowest frequency at each station. The effect of the half-space is then subtracted from the reduced response to yield the corrected tilt angle due to any subsurface conductive inhomogeneity. To apply the second correction, several EM

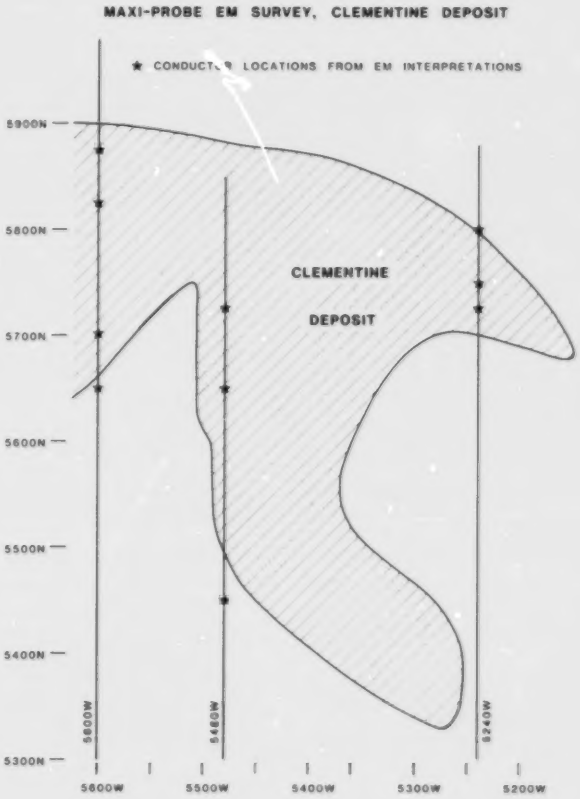

Figure 9. Plan map of the Clementine Prospect and conductor locations on three lines based on multifrequency surveys.

depth soundings were conducted to determine the nature of the half-space. The tilt angle response from such a half-space model was computed at several frequencies and at different distances from the transmitter which was then used in applying the second correction.

The variation of the tilt angle values on the line is rather small, which is not surprising considering the low conductivity of the sulphide zone. At high frequencies (9765 H_z and over), the tilt angles indicate the presence of conductors at 5650 N and 5700 N. At intermediate frequencies (1221 to 4882 H_z), conductors are located at 5700 N and 5875 N. At frequencies lower than 610 H_z (low frequencies), conductors are indicated at 5825 N and 5875 N in addition to the two conductors at 5650 N and 5700 N. A decrease in tilt angle is also indicated at 5775 N at 610 H_z. However, other frequencies do not show corresponding responses; hence this response is considered to be due to noise. According to drill hole data, the line should intersect the deposit at 5680 N and 5900 N and the tilt angle data seem to detect the southern and the northern edges of the conductor reasonably well.

Figure 8 illustrates a plot of the corrected ellipticity values in per cent versus station positions on the line. Ellipticity values appear to be somewhat erratic especially at higher frequencies, presumably because of effects from shallower sources with conductors indicated at 5650 N, 5700 N, 5750 N and 5825 N. At low frequencies, the variations are more subdued with conductors being indicated at 5650 N and 5875 N. Intermediate frequencies indicate conductors at 5650 N and 5700 N. Minor conductors are detected at several locations around 5775 N with poor correlation between different frequencies. Hence, the ellipticity results also appear to be useful in detecting the southern and northern edges of the deposit. Both tilt and ellipticity plots indicate the northern boundary of the conductor at 5875 N in contrast to 5900 N in plan maps from drillhole data. The discrepancy may be due to some misinterpretation of interpolated drillhole data or due to the scattered nature of the conductor boundary. The conductors around 5800 N may be discrete conductors or may represent a change in ore grade in the same deposit.

The survey line 5240 W also detected the southern and northern edges of the conductor. But line 5480 W did not

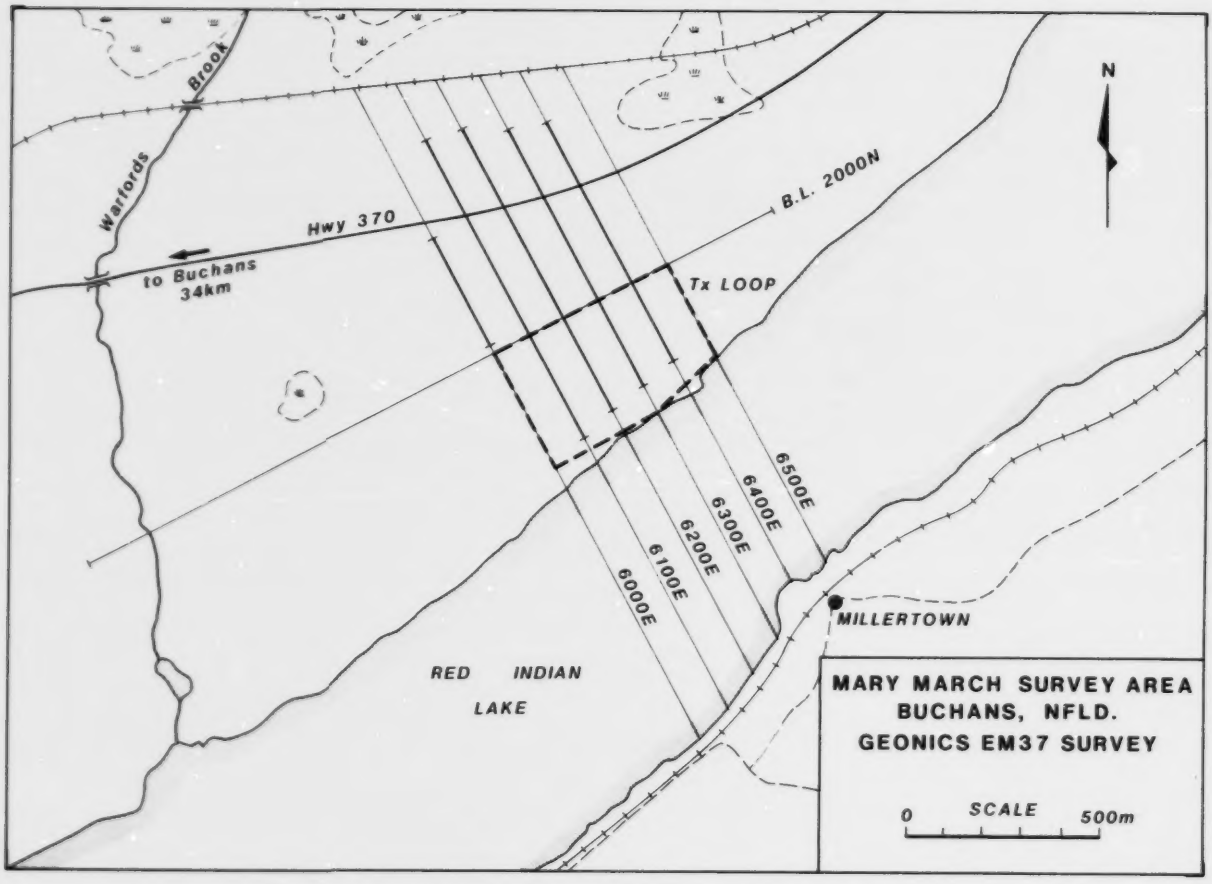

Figure 10. Survey area for the transient EM system at the Mary March site.

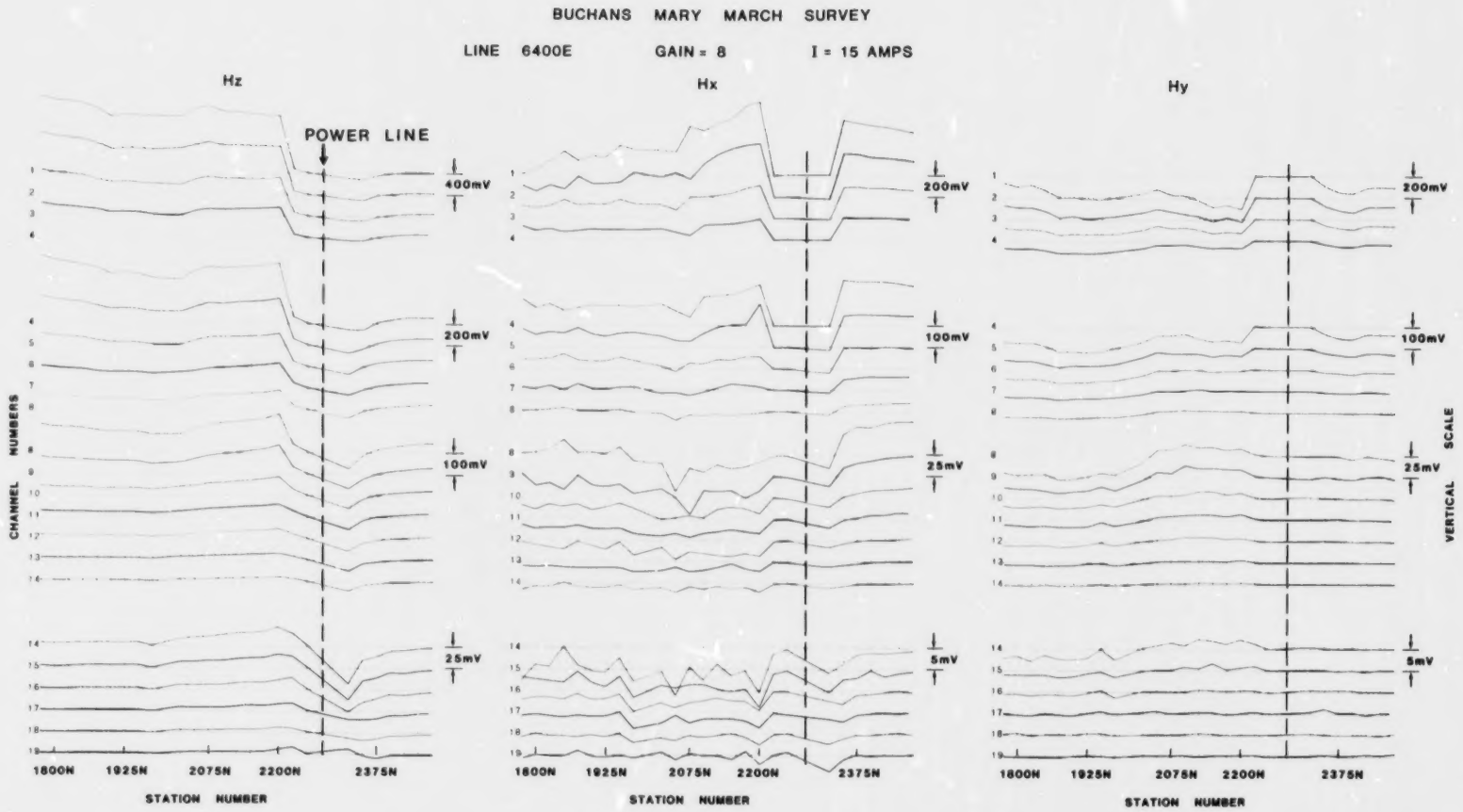

Figure 11. Plot of the decay of orthogonal magnetic field components on line 6400 E at the Mary March site.

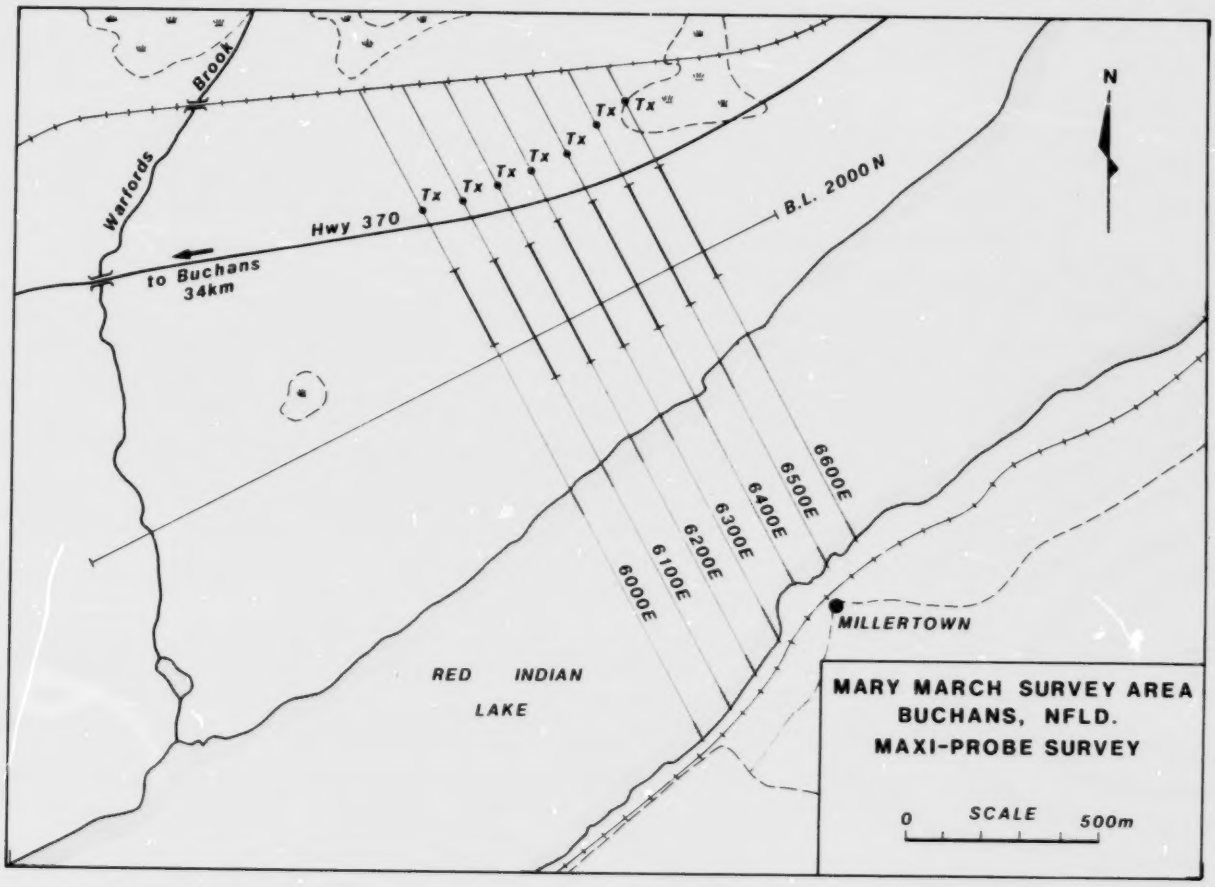

Figure 12. Survey area for the multifrequency EM survey at the Mary March site.

extend far enough to the north to detect the northern edge of the conductor. Figure 9 shows a plan map of the Clementine Prospect and the conductor locations indicated by the EM surveys. The correlation is good on all lines except at the southern edge of line 5480 W, where the discrepancy is about 50 m. A possible reason for this may be the poor coupling of the exciting field with the southern edge of the conductor, which is almost parallel to the survey line. The small tilt angle and ellipticity anomalies may also be partly responsible for the discrepancy.

RESULTS OVER MARY MARCH AREA

The locations of the survey lines and the transmitter loop for the transient EM survey at the Mary March survey area are shown in Figure 10. The NNW trending survey lines extended from an abandoned railway track to the north of the Survey grid to the northern shore of Red Indian Lake. An approximately rectangular loop, 300 m by 500 m, was laid south of the baseline (2000 N) as shown in Figure 10. The lengths of survey lines are indicated by 'tick' marks and they generally averaged about 800 m. A high voltage power line along highway 370 produced electrical noise in its vicinity, which prevented the recording of the small secondary fields within 50 m of the line.

Figure 11 shows the transient decay plots of the secondary magnetic fields in three orthogonal directions on line 6400 E. The z-component does not show any variation except near the power line which crossed the survey line at 2280 N. The two horizontal components in x and y directions were more noisy without any definite trend. The same pattern was repeated on all other lines. In order to determine whether weaker anomalies could be detected in the absence of current passing through the power line, a request was made to the local power company to shut off power to the line for a brief period. The line was resurveyed when the power was shut-off. The response did not change significantly even after the power shut-off. The reason for that became clear when it was noticed that the power line had been grounded at several places. The spurious signals are, therefore, caused by the grounding of the power line which behaved like large electric dipoles. Aside from the power line response, the transient EM system, therefore, did not detect any conductor at Mary March area.

The multifrequency survey was conducted on seven survey lines as shown in Figure 12. On all lines, the transmitters

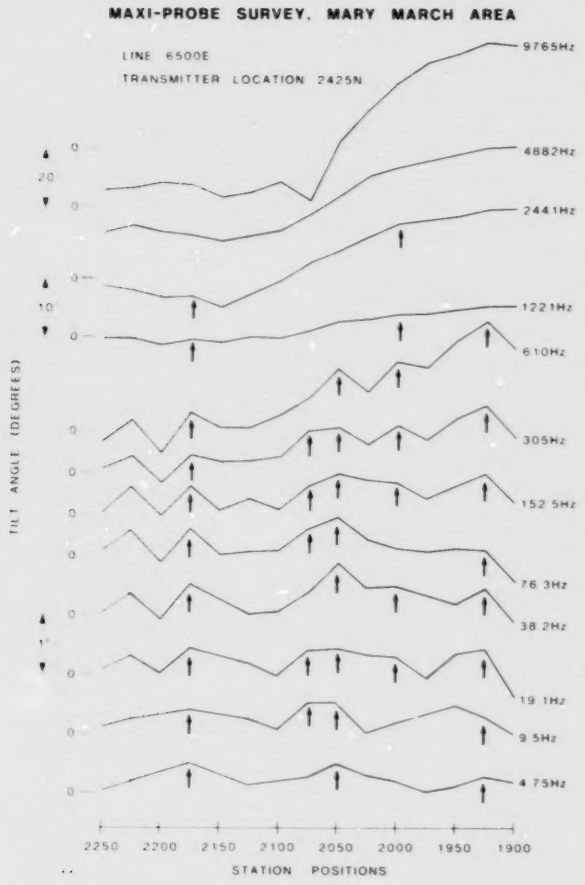

Figure 13. Plot of the variation of the tilt angle in degrees versus station positions on line 6500 E at Mary March.

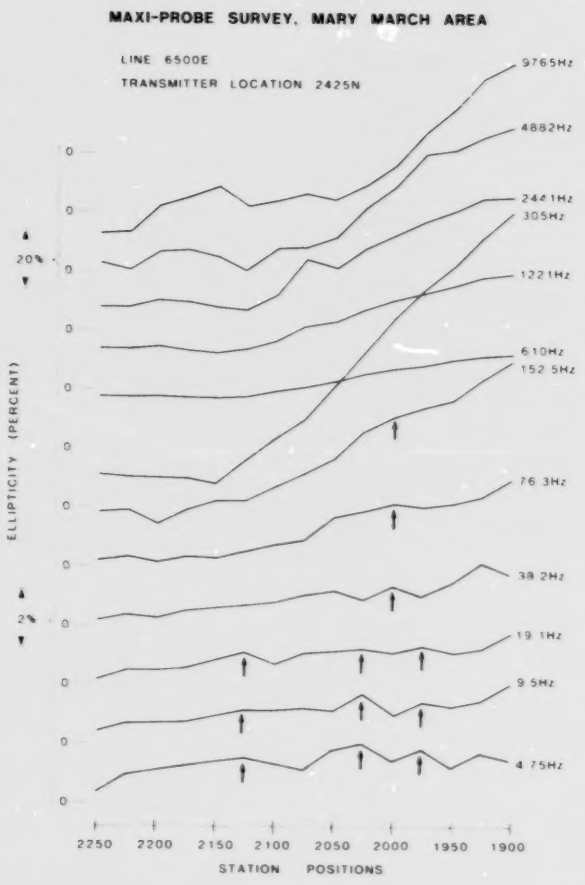

Figure 14. Plot of the variation of the ellipticity in per cent versus station positions on line 6500 E at Mary March.

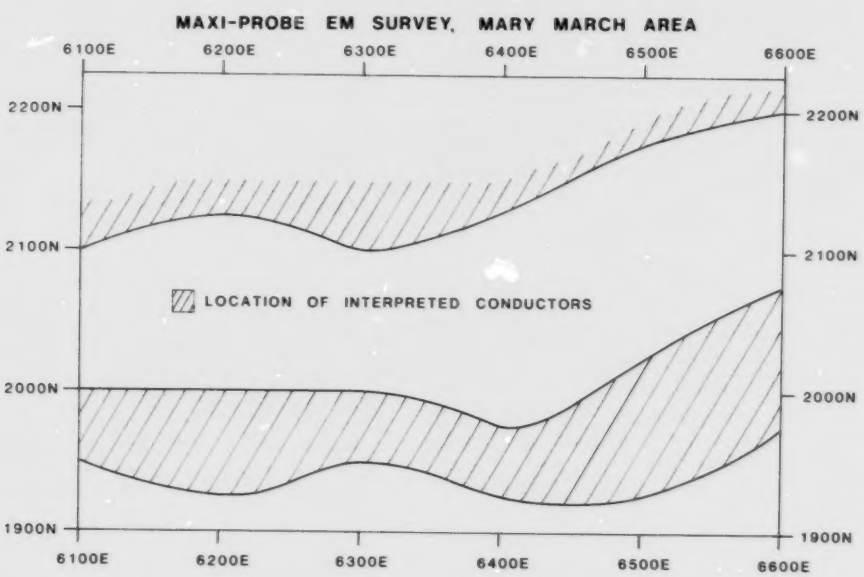

Figure 15. Map showing the location of interpreted conductors at the Mary March site from multifrequency surveys.

indicated by T_x, were located between the highway and the railway track since the ground was level and this permitted tilt and ellipticity measurements to begin from just south of the road and without any need to cross the power line. The Maxi-Probe system was also found to be less susceptible to power line noise possibly because of better line filters. This allowed the first receiver stations to be as close as 25 m from the power line. The lengths of the survey lines are shown by 'tick' marks. The topography of the area south of the highway was very uneven which limited the range of data collection to 500-550 m from the transmitter on most lines.

Figures 13 and 14 show the variation of corrected tilt angle and ellipticity parameters versus station positions on line 6500 E. In Figure 13, the tilt values have been plotted with three scales because of the wide variation of this parameter on this line. The raw tilt angle values have been corrected for the effects of topography and half-space as discussed in the previous section. The response is large and noisy in high and intermediate frequencies, possibly due to the presence of shallow, discrete conductors. For lower frequencies (610 H_z and lower), several distinct conductors are detected at 1925 N, 2000 N, 2050 N and 2175 N and a weak one at 2075 N. The conductive signature at 2225 N has been ignored since it is too close to the transmitter and the power line. The ellipticity data (Fig. 14) show less variation than the tilt angle data especially at lower frequencies. Conductors are detected at 1975 N, 2025 N and 2125 N in the low frequency band. But, none of the anomalies are large or consistent from frequency to frequency. The ellipticity responses at high frequencies are as large and noisy as the tilt angle responses.

Similar results were plotted for other lines from 6000 E to 6600 E. Line 6000 E was somewhat short because of an instrumental problem and, hence, the data on that line were not taken into consideration for interpretation. From the conductor locations obtained on the six lines, an areal conductor map was prepared for the survey area. Figure 15 shows the conductor location map at the Mary March area. The multifrequency survey detected a narrow conductor, 50-75 m wide in the southern end of the survey grid. Another conductor was detected in the northern end of the grid, its southern end being located between 2100 N and 2200 N. Its northern edge was not mapped since the lines did not extend far enough to the north because of the power line. Some indication exists that its northern boundary could be at 2225 N on line 6500 E (Figure 13), but the evidence is unclear on other lines.

CONCLUSIONS

Surveys with transient and multifrequency EM systems were conducted at two sites near Buchans to detect poorly conductive sphalerite-barite-rich polymetallic sulphide deposits buried at large depths. Both systems are capable of detecting bodies with good conductivity at depths of several hundred metres. The Clementine Prospect, a poorly conductive transported sulphide deposit was especially difficult to detect since its average depth exceeds 300 m. No surface electrical or EM system had detected the deposit in previous surveys. The work at Mary March was more like a reconnaissance survey since no sulphide deposits had been detected in the area except for the presence of altered rocks such as silicified and seriticized felsic volcanics at several places.

The transient EM survey did not detect any conductors at either site. The responses were generally low and erratic, with poor correlation between different channels, possibly reflecting the poor signal/noise ratios in the survey data. The multifrequency survey using tilt angle and ellipticity measurements was more successful in detecting the Clementine sulphides on three lines although the signal/noise ratio was poor. The discrepancy on the location of this deposit from borehole information and our data generally does not exceed 25 m on the lines surveyed. At the Mary March site, the multifrequency system detected two conductive bodies. Although the tilt and ellipticity responses were weak on all lines, the correlation between the response from one frequency to another and from line to line was good. The reason for the apparent success of the Maxi-Probe system at the two sites where other EM systems have failed in earlier tests may lie in the use of much stronger primary fields (10 to 100 times larger) than used in other commercially available EM systems. This, along with better noise filters and careful processing of data indicated the presence of weak conductive anomalies. Perhaps the Mary March anomalies will be drilled to determine the nature of the conductors. This survey demonstrated that ground EM methods will be difficult to use in areas like Buchans where the electrical conductivities of the sulphides are not high and where the deposits occur at substantial depths below the surface.

ACKNOWLEDGMENTS

We are thankful to Abitibi-Price Inc. and ASARCO Inc. for providing facilities for carrying out the work. We are particularly indebted to Dr. J.G. Thurlow, resident geologist, Abitibi-Price for providing geological information and maps prior to and during the field work. We also thank Mr. Derek Gresham our colleague at GSC who spent considerable time editing and plotting the field data on the computer.

REFERENCES

Calhoun, T.A. and Hutchinson, R.W.
1981: Determination of flow direction and source of fragmental sulphides, Clementine Deposit, Buchans, Newfoundland; in The Buchans Orebodies – Fifty Years of Mining and Geology, ed. E.A. Swanson, D.F. Strong and J.G. Thurlow; Geological Association of Canada, Special Paper 22, p. 187-204.

Moss, C. and Perkins, E.W.
1981: History of geophysical exploration at Buchans, Newfoundland; in The Buchans Orebodies – Fifty Years of Mining and Geology, ed. E.A. Swanson, D.F. Strong and J.G. Thurlow; Geological Association of Canada, Special Paper 22, p. 285-310.

Neale, E.R.W. and Nash, W.A.
1963: Sandy Lake (east half) map-area, Newfoundland; Geological Survey of Canada, Paper 62-28.

Sinha, A.K.
1979: Maxi-Probe EMR-16: A new wide-band multifrequency ground EM system; Geological Survey of Canada, Paper 79-1B, p. 23-26.

Sinha, A.K.
1980: A study of topographic and misorientation effects in multifrequency electromagnetic soundings; Geoexploration, v. 18, no. 2, p. 111-133.

Sinha, A.K.
1983: Deep multifrequency EM sounding at a site near Bowmanville, Ontario; in Current Research, Part A, Geological Survey of Canada, Paper 83-1A, p. 133-137.

Sinha, A.K.
1983: Deep transient electromagnetic soundings over the McClean uranium deposits; in Uranium Exploration in Athabasca Basin, Saskatchewan, Canada, ed. E.M. Cameron, Geological Survey of Canada, Paper 82-11, p. 273-280.

Sinha, A.K. and Stephens, L.E.
1983: Deep electromagnetic sounding over the permafrost terrain in the Mackenzie Delta, N.W.T., Canada; in Permafrost: Fourth International Conference, Proceedings, National Academy of Sciences, Washington, D.C., p. 1166-1171.
1984: Detection and mapping of a complex conductor near Timmins, Ontario by the transient and multifrequency electromagnetic systems; presented at the 46th Meeting of the European Association of Exploration Geophysicists, London, England.

Thurlow, J.G. and Swanson, E.A.
1981: Geology and ore deposits of the Buchans district, Central Newfoundland; in the Buchans Orebodies – Fifty Years of Mining and Geology, ed. E.A. Swanson, D.F. Strong and J.G. Thurlow; Geological Association of Canada, Special Paper 22, p. 113-142.
1987: Stratigraphy and structure of the Buchans Group; in Buchans Geology, Newfoundland, ed. R.V. Kirkham; Geological Survey of Canada, Paper 86-24, Report 2.

Ward, S.H., Pridmore, D.F., Rijo, L., and Glenn, W.E.
1974: Multispectral electromagnetic exploration for sulphides; Geophysics, v. 39, no. 5, p. 666-682.

- 15 -

Mise-à-la-masse experiments in the Maclean Extension Orebody

C.J. Mwenifumbo[1]

Mwenifumbo, C.J., Mise-à-la-masse experiments in the MacLean Extension Orebody; in Buchans Geology, Newfoundland, ed. R.V. Kirkham; Geological Survey of Canada, Paper 86-24, p. 251-261, Report 15, 1987.

Abstract

Drill hole mise-à-la-masse (MALM) potential and induced polarization (IP) measurements were conducted underground in the MacLean Extension Orebody. Parts of the MacLean Extension polymetallic sulphide deposit were found to be highly conductive and correlation of ore intersections between holes was accomplished easily with the mise-à-la-masse method. The ore lying between sections W2300 and W2400 was shown to be electrically continuous and forms a single ore lens.

Résumé

On a mesuré dans les trous de forage souterrains par les méthodes de mise à la masse et de polarisation induite, le potentiel électrique du gisement de la prolongation de MacLean. Certaines parties de ces gisements de sulfures polymétalliques sont très conductives et, grâce à la méthode de la mise à la masse, il a été possible de mettre en corrélation le point d'intersection du minerai d'un sondage à l'autre. Le minerai situé entre les sections W2300 et W2400 présente une continuité électrique et forme une seule lentille de minerai.

INTRODUCTION

The mise-à-la-masse (MALM) electrical method of prospecting is used generally after a conductive mineralized zone has been located. It involves placing a current electrode directly in contact with the mineralized zone, and then mapping the resulting electric potential field distribution either at the surface or in the subsurface via drillholes or underground openings. The potential field reflects the shape, size and orientation of the energized conductive zone. This technique is used mainly for mapping the size and orientation of a deposit and for determining the continuity of the mineralization from hole-to-hole. It is also possible to detect conductive orebodies in the vicinity of the energized body that are not directly connected. The MALM method has been applied extensively and successfully during detailed mapping of massive sulphide orebodies with high electrical conductivity (McMurry and Hoagland, 1956; Parasnis, 1967; Ketola, 1972; Mansinha and Mwenifumbo, 1983).

MALM experiments were carried out underground in the MacLean Extension Orebody. The MacLean Extension Orebody is structurally and stratigraphically complicated. A number of ore intersections cannot be easily correlated from section-to-section or from hole-to-hole along a given section. There is also a high degree of variability in the proportions of lead, zinc and copper sulphides (galena, sphalerite and chalcopyrite). Some of the sulphide ores contain a high percentage of sphalerite, barite and rock fragments which are poor electrical conductors. The overall conductivity of the ore, however, is fairly high relative to that of the host rock. The MALM field tests were conducted to investigate the possibility of using the technique to trace sulphides from hole-to-hole and to determine any possible extension of the orebody that may have been missed by drilling.

GEOLOGY

The geology and ore deposits of the Buchans area have been described in detail by Thurlow and Swanson (1981) and the geology of the MacLean Extension deposit has been described by Binney, *et al.* (1983) and Binney (1987). The Buchans ores are barite-rich, polymetallic massive sulphide deposits associated with submarine felsic volcanic rocks. They are mainly zinc-lead-copper sulphides. Three major ore types occur at Buchans; 1) stockwork, 2) in situ ore and

[1]Geological Survey of Canada, 601 Booth Street, Ottawa, K1A 0E8

3) mechanically transported fragmental ore. The MacLean Orebody is mechanically transported ore and consists of low- to high-grade accumulations of sulphide fragments derived from an unknown massive sulphide source. The ore has apparently been transported by debris flows for considerable distances from its source and deposited in paleotopographic depressions. In the MacLean Extension Orebody, some sections consist of massive, high grade, copper-rich ores and others comprise mainly low to high grade lead-zinc ores. In general, the ore comprises varying proportions of sphalerite, galena and chalcopyrite in different ore lenses.

Figure 1 is a map of level 20 of the MacLean Extension Orebody where the MALM experiments were carried out. Three sections where these measurements were taken (W2300, W2350 and W2400) are indicated on the map. Figure 2a shows the geology of section W2300, where the ore consists of moderate to high grade ore breccia (mainly Pb-Zn ore) within the dacitic tuff unit. The ore zone approximates a curved tabular body, dipping to the south at about 40 degrees. The geology of section W2350 is shown in Figure 2b. The ore outline is approximately elliptical and the ore consists of moderate to high grade Cu-Pb-Zn sulphides. Figure 2c shows the geology of section W2400. The ore along this section is massive Cu-rich, high grade Cu-Pb-Zn ore. The ore outline is circular, only 100 feet away from the curved, tabular ore zone of section W2300. These three geologic sections indicate the complex morphology of the MacLean Extension Orebody. Only the geology below the drift level is displayed in these figures. In all these sections there are ore lenses above the drift level. There has been extensive drilling in all these sections and the holes used in the experiments are indicated on the sections.

EQUIPMENT AND FIELD PROCEDURE

The equipment used in the MALM measurements consisted of a battery operated Huntec M4 LOPO transmitter and a Huntec M4 receiver. Both the receiver and the transmitter can be used for time and frequency domain IP and complex resistivity measurements. However, the MALM IP and potential measurements conducted in the MacLean Extension Orebody were carried out in the time domain only. Primary voltages, self potentials (SP) and chargeability information from ten windows of equal width (175 milliseconds) were recorded on cassette tapes. The complete waveforms were also recorded on the tapes. The period of the transmitter current waveform was 8 seconds (two repeat cycles of 2 seconds current on and 2 seconds off, with polarity reversed after each cycle). The current electrode used to energize the sulphide zone was a copper clad steel rod about 1 metre in length. The electrodes used for potential measurements were made of platinum wire mesh about 5 cm in length and 1.25 cm in diameter. The remote potential electrode was a non-polarizable copper-copper sulphate electrode whereas the other distant current electrode was a copper clad steel electrode. Accurate depth measurements along the hole lengths were accomplished with a mechanical depth encoder having a resolution of 1 cm. MALM IP and potential measurements were made at 1 metre intervals down hole using a two conductor shielded cable. All the holes logged were water-filled. Geological logs and contact resistance measurements were used to locate the grounding points in the ore intersections. The locations of the remote potential electrode (P ∞) and the distant current electrode (C ∞) are shown in Figure 1. All measurements were made with reference to these remote electrodes. Electrode layouts for measurements

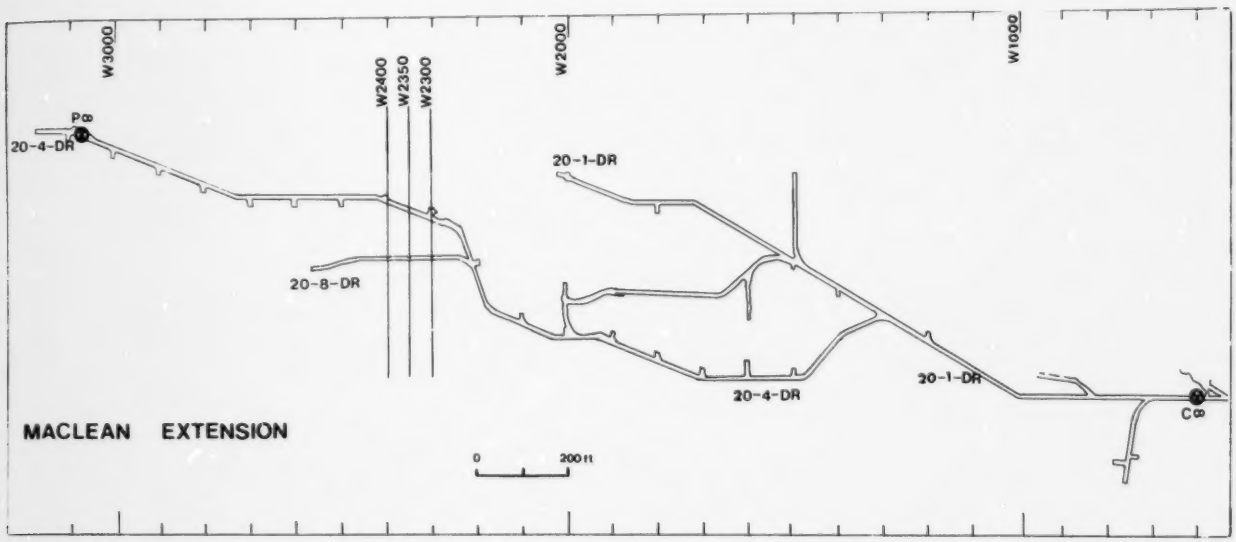

Figure 1. Plan map of level 20 of the MacLean Extension Orebody showing the location of remote electrodes and the geologic sections where the mise-à-la-masse measurements were carried out.

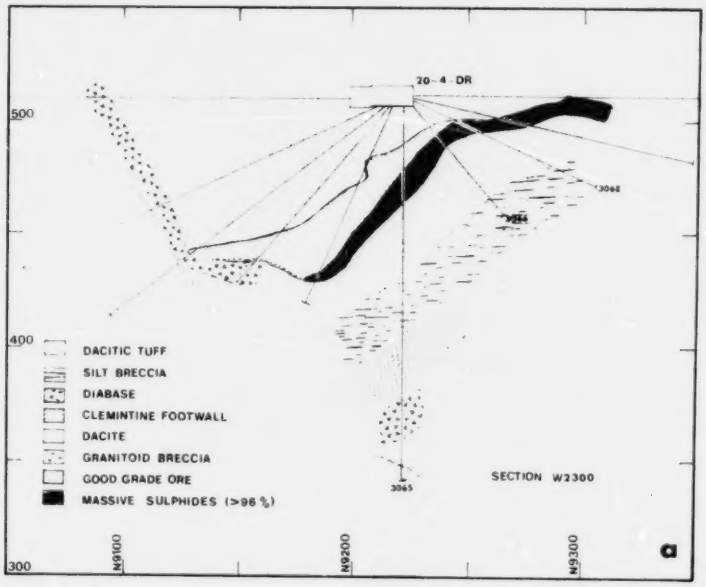

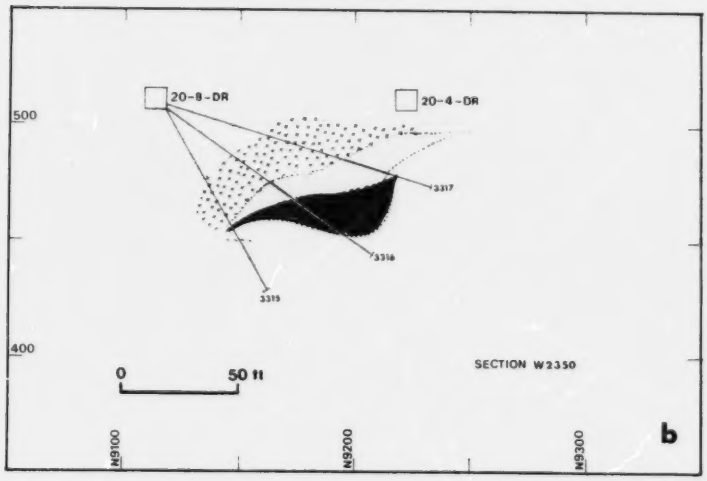

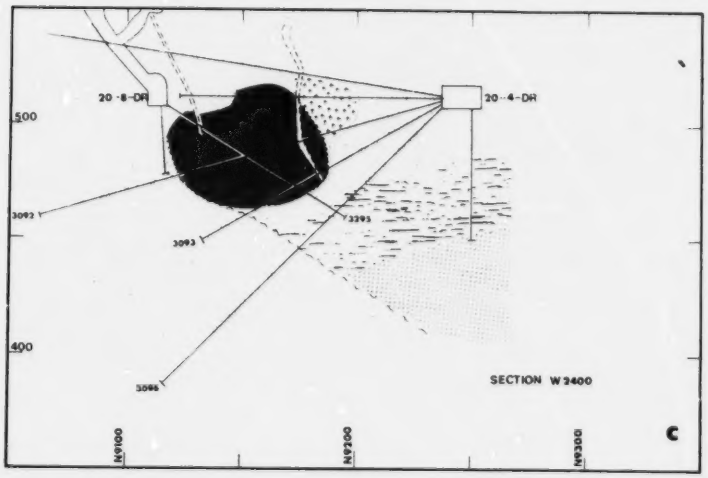

Figure 2. Geologic sections along W2300, W2350 and W2400 on level 20, MacLean Extension (geology from company sections). The holes used in the present study are numbered.

in underground workings were dictated by accessibility into various drifts. Metal objects such as steel pipes, railway tracks and operating machinery also presented problems in electrode layouts and measurements underground.

MISE-À-LA-MASSE POTENTIAL AND IP MEASUREMENTS

Figure 3 shows MALM potential and IP measurements along hole 3065 in section W2300 with the energizing current electrode in the ore zone in hole 3068, at a depth of 7.5 metres along the hole. Displayed in Figure 3a are the MALM potentials, standard IP (chargeability), SP and chargeabilities from the 10 windows. The chargeabilities are the normalized time integral of the decay voltage and the standard IP chargeability is integrated from 0.45 to 1.1 seconds after current switch off. The 10 windows are of equal width (175 milliseconds) with the first window integrated from 100 to 275 milliseconds. In all the figures to follow, the IP window with the highest chargeability is the first window (W1) and the one with the lowest chargeability is the last window (W10). All the chargeability values are expressed in milliseconds. The MALM potentials in each drillhole are measured at a constant current. However, to be able to compare potentials measured in different holes on the property, the potentials are normalized to one current value. The MALM results indicate a flat, potential high outlining the position of the ore intersection. This indicates that the ore intersections in hole 3068 and 3065 are in electrical continuity. An Almost constant

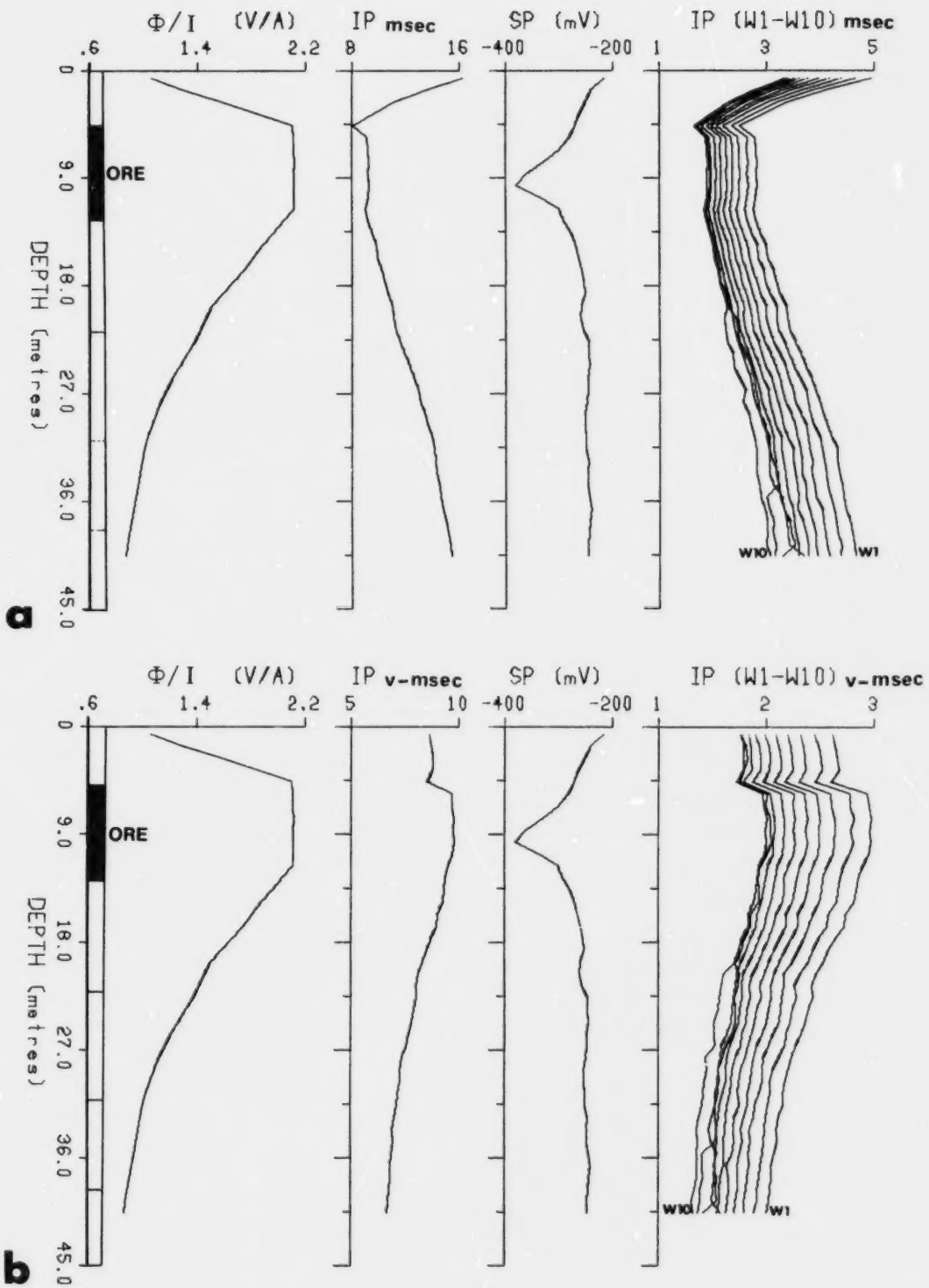

Figure 3. Mise-à-la-masse potential and IP measurements along hole 3065-W2300 (Fig. 2) with the energizing current electrode in the ore at 7.5 m in hole 3068- W2300. IP values are normalized and expressed in milliseconds in Figure 3a and are not normalized and expressed in volt-milliseconds in Figure 3b. The MALM potential values are normalized with respect to the primary current.

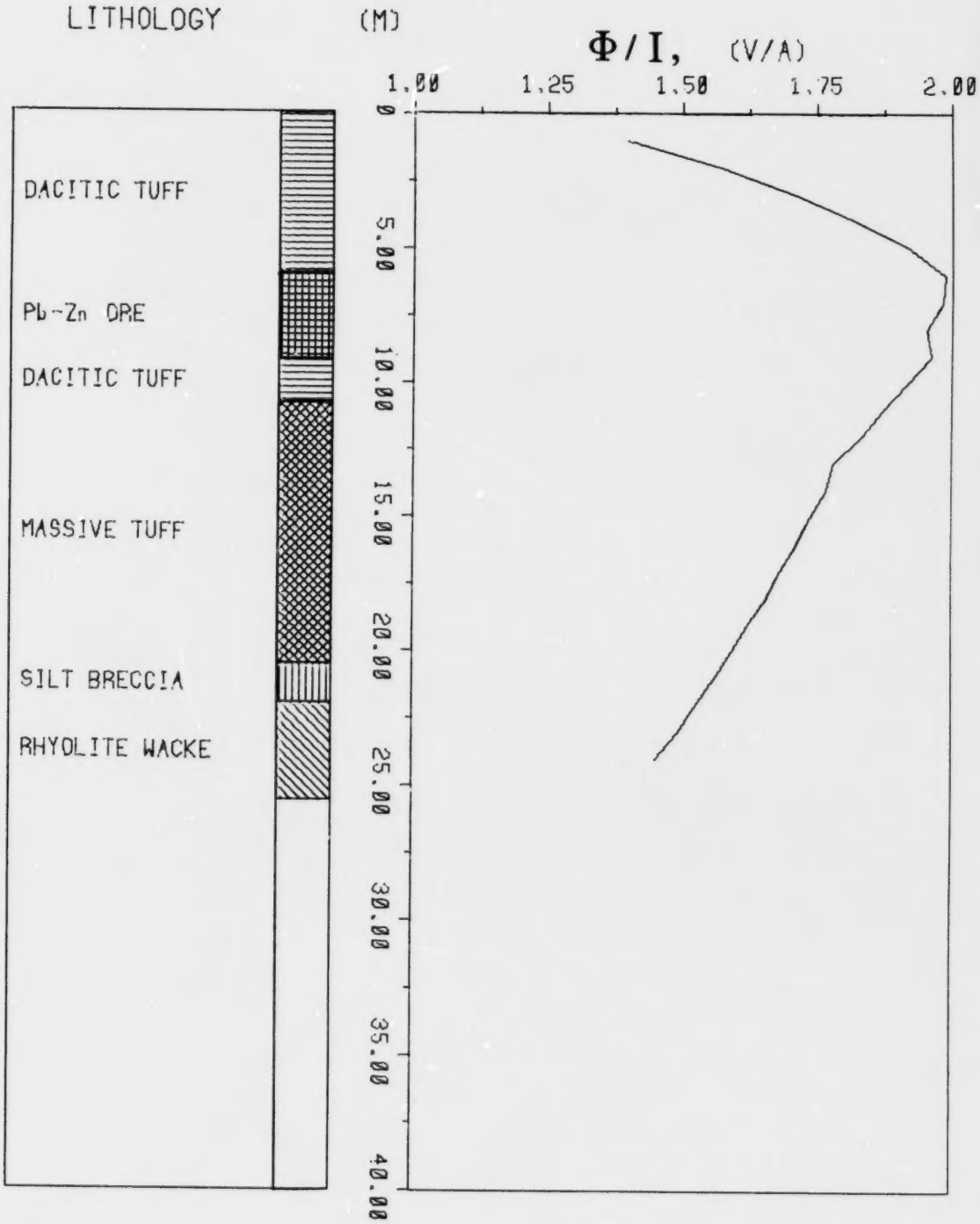

Figure 4. Mise-à-la-masse potential measurements along hole 3068-W2300 with the current electrode in the ore at 9 m in hole 3065-W2300 (Fig. 2).

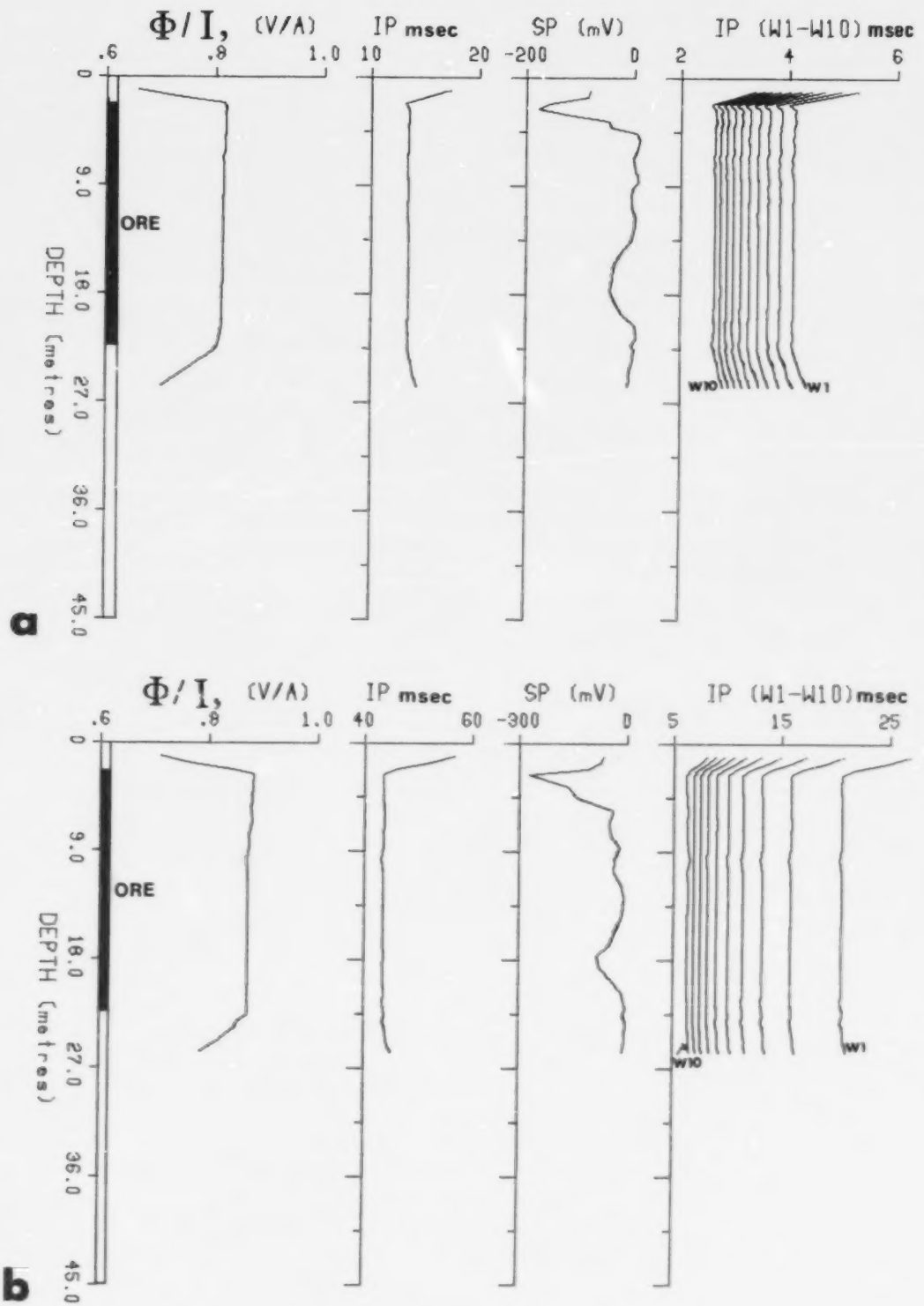

Figure 5. Mise-à-la-masse potential and IP measurements carried out along hole 3295-W2400 (Fig. 2). Figure 5a with the current electrode in ore at a depth of 24 m in hole 3316-W2350 (Fig. 2). Figure 5b with the current electrode in hole 3065-W2300 at a depth of 9 m. (Fig. 2) IP values are in milliseconds.

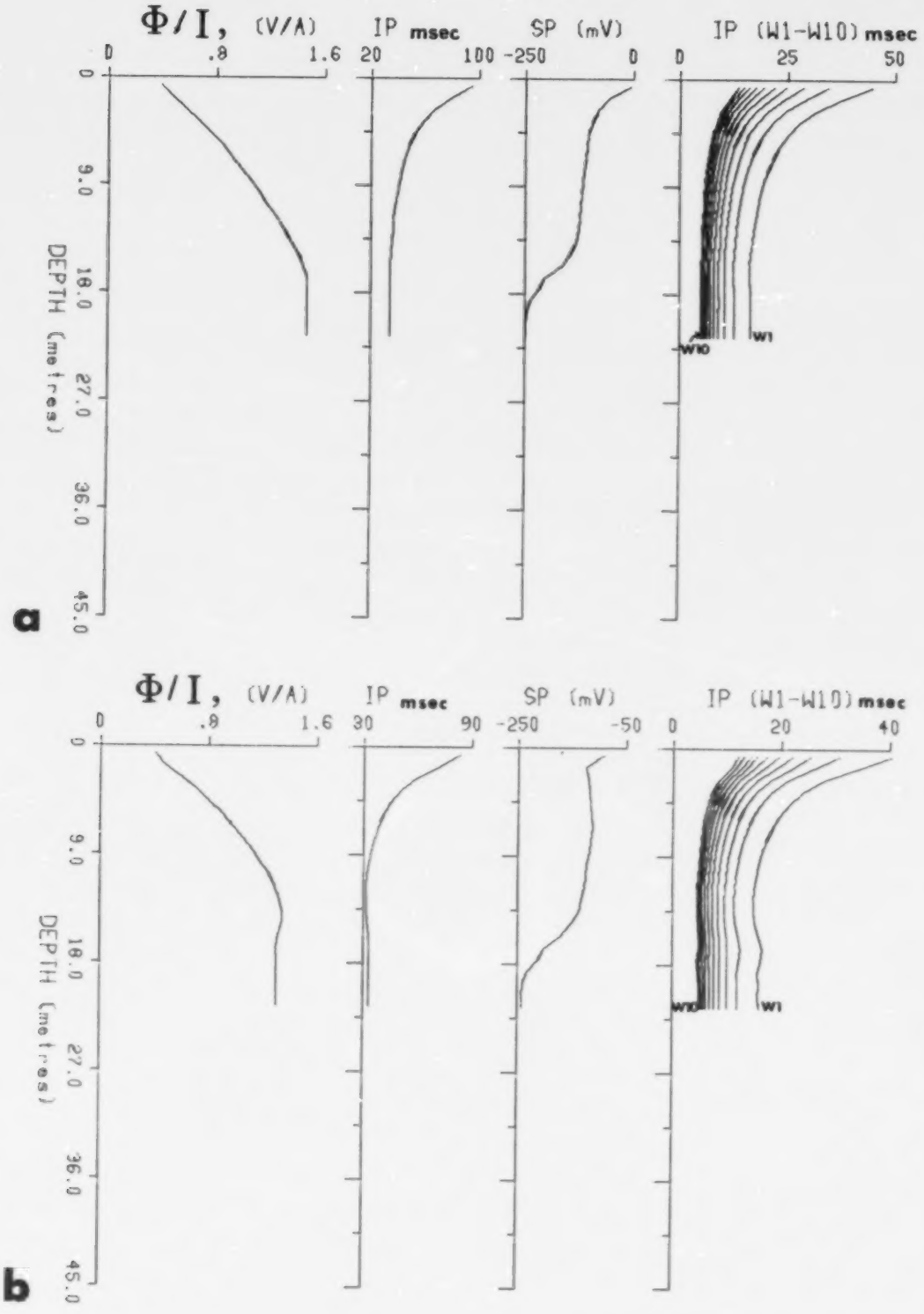

Figure 6. Mise-à-la-masse potential and IP measurements along hole 3093-W2400 (Fig. 2). Figure 6a with the current electrode in the ore section at a depth of 24 m in hole 3316-W2350 and Figure 6b with the current electrode at a depth of 23 m in hole 3295-W2400 (Fig. 2).

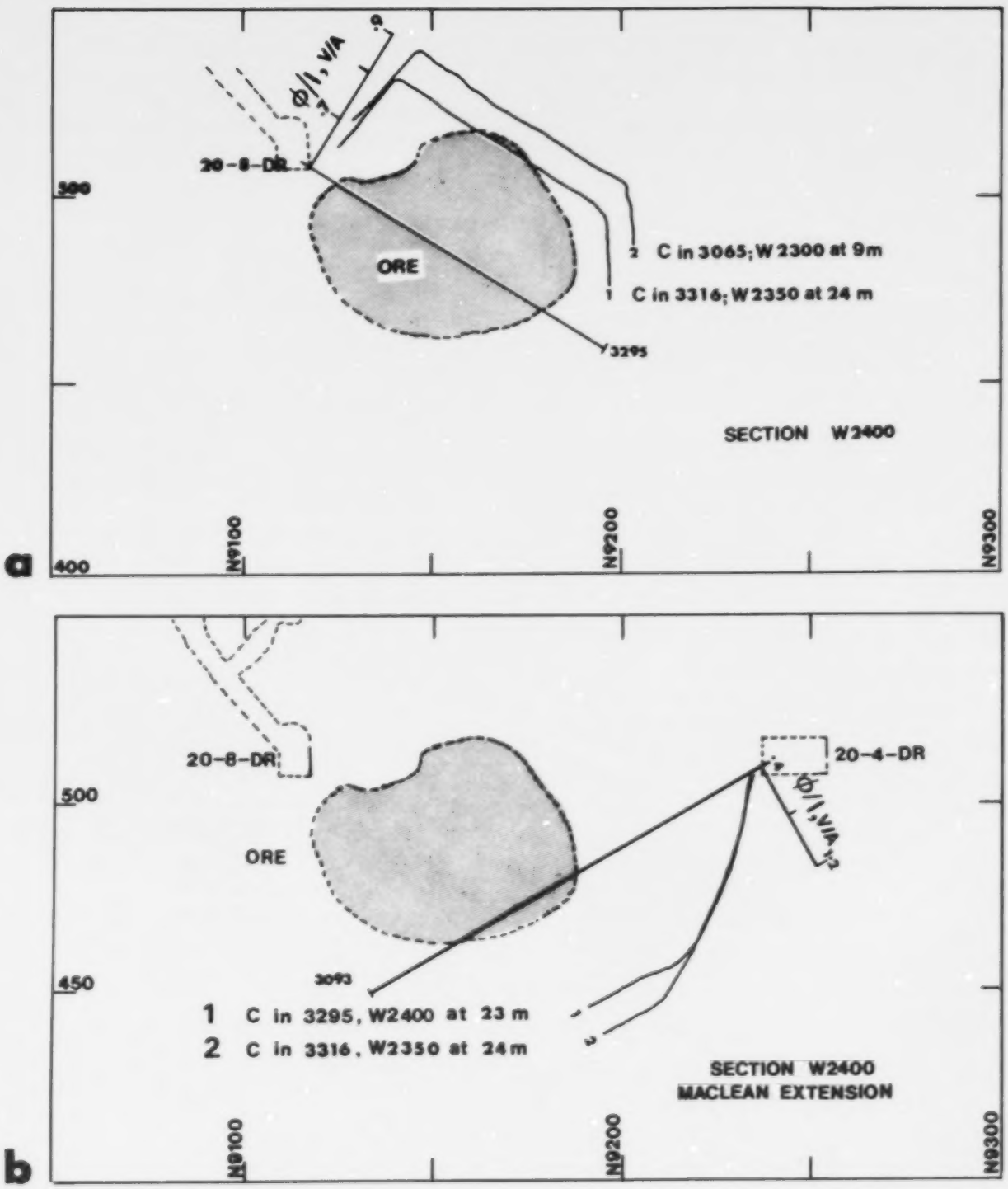

Figure 7. Mise-à-la-masse potential measurements along hole 3295-W2400 (Fig. 7a) and along hole 3093-W2400 (Fig. 7b) for various current electrode locations.

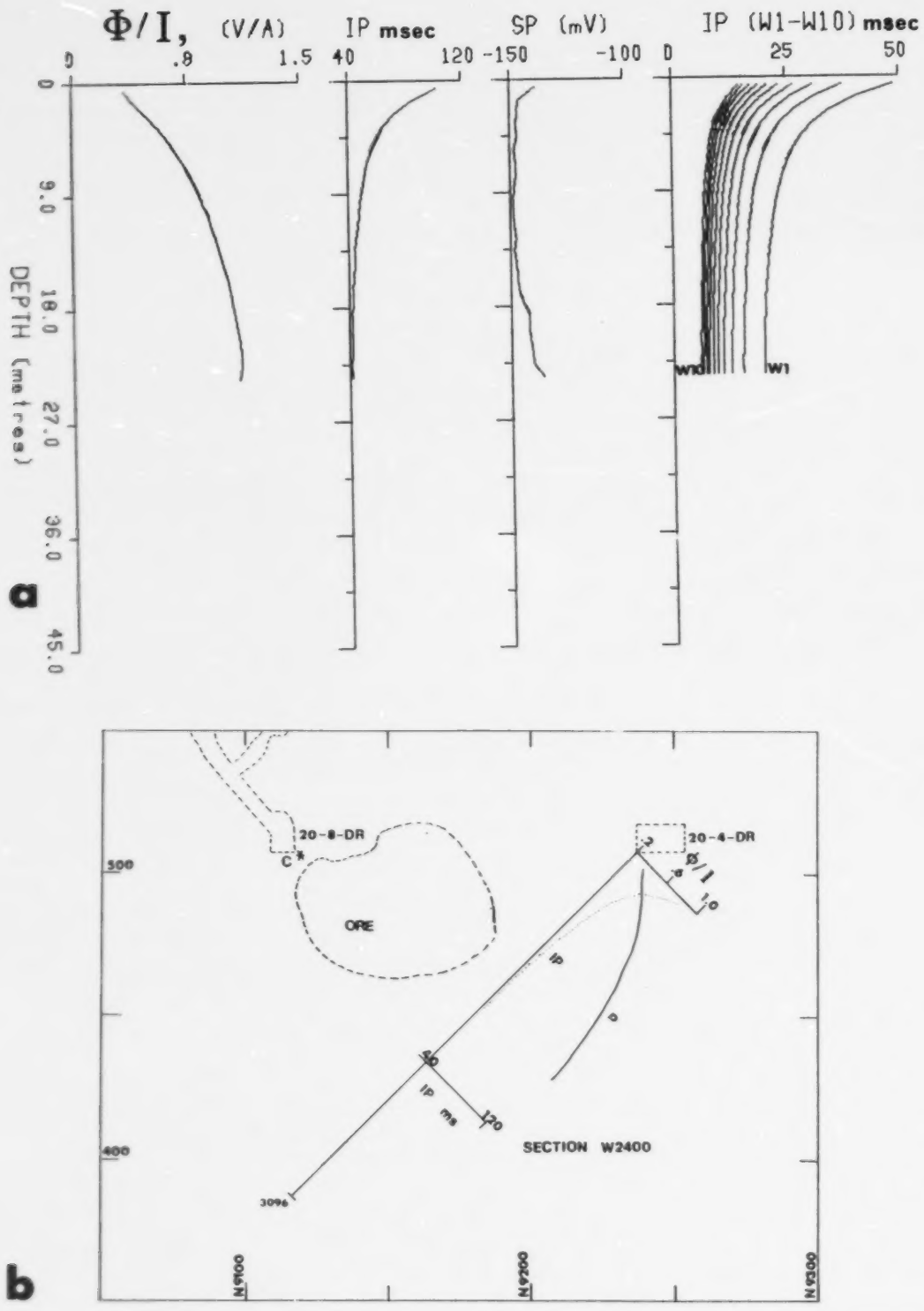

Figure 8. Mise-à-la-masse potential and IP measurements along a barren hole 3096-W2400 with the energizing current electrode placed in an unmineralized section at 1 m depth in hole 3295-W2400 (Fig. 2).

potential high across the intersection indicates that the ore is highly conductive. It should be noted that the potentials decrease at a slower rate down hole from the ore indicating that the sulphides extend down the hole below the ore. This is in agreement with the geologic section of Figure 2a. The standard IP shows an inverse relationship to the potentials, because the IP data presented here are the normalized time integral of the decay voltage. The area under the decay curve is normalized by the primary potential. If the primary potential normalization is removed (the area under the decay curve with units in volt-milliseconds) we obtain the results displayed in Figure 3b. We notice a high IP response over the ore intersection with a gradual decrease on the down hole side.

With the MALM, the continuity of the sulphide zone is established when the location of potential maximum coincides with that of the indicated location of the ore. However, this does not always happen. In many cases the ore deposit consists of a number of ore lenses with differing resistivities and dimensions, and also within the limits of the ore deposit other conducting structures such as faults may be present. In such complex geologic situations the potential field distribution is complicated and to determine accurately the geoelectrical structure between the holes, measurements of the potential field are carried out in a number of holes for different locations of the energizing current electrodes. In order to verify the continuity of the energized ore section from hole 3068 to hole 3065, a current electrode was placed in 3065 and potential measurements were made in hole 3068. The results are presented in Figure 4. The location of the potential maximum coincides with the ore intersection.

To study the continuity of the ore intersections between the three sections, a number of measurements were carried out along holes in all the sections with the current electrodes placed in different mineral intersections. Figure 5 shows MALM IP and potential measurements in hole 3295, section W2400 with the current electrodes located in ore intersections in hole 3316, section W2350 at 24 metres (Fig. 5a) and in hole 3065, section W2300 at 9 metres (Fig. 5b). An almost constant potential maximum is observed across the ore intersection for both the current electrode positions indicating that the orebody is electrically continuous between these holes (sections W2300 and W2350 to section W2400). The IP measurements similarly show an inverse relationship to the potential measurements. MALM IP and potential measurements along hole 3093, section W2400 are presented in Figure 6. Figure 6a shows measurements with the current source in hole 3316, section W2350 at 24 metres and Figure 6b for the current electrode in hole 3295, section W2400 at 23 metres. There is a gradual increase in potential values with increasing depth. The potentials reach a maximum at about 14 metres and then flatten out. This depth coincides with the upper boundary of the ore intersection. The potential field distribution could not be determined below the lower contact because the hole was plugged at about 23 metres. The gradual increase in the potentials indicate that the conductive ore comes close to the hole above the upper contact, in contrast to an almost step-like change in the observed potentials along hole 3295 (see Fig. 5).

Figure 7 shows the potential measurements recorded in the two holes on section W2400 (Fig. 6) plotted along the section with the ore outline indicated as the shaded area. The two potential curves in Figure 7a are practically identical. The distinct potential maximum, with constant potentials within the ore intersection indicates that the ore is highly conductive and forms a single continuous ore zone between the holes. The same conclusion applies to the observations along hole 3093 (Fig. 7b). The potential field distribution was also studied along hole 3065, section W2300 with current sources located in holes in sections W2350 and W2400. The potential maxima were observed to coincide with the ore intersections indicating, conclusively, the continuity of conductive sulphides between these sections.

When two or more holes do not intersect ore, it is often necessary to determine if there is any ore between the holes. Current electrodes are grounded in various positions in one hole while potential measurements are recorded in the other hole. By comparing the observed measurements with theoretical results from simple models it is possible to establish the presence or absence of conductive sulphides between the holes. Figure 8 shows IP and potential measurements along a barren hole 3096 in section W2400 with the current source grounded in an unmineralized part of hole 3295 at a depth of 1 metre. The measurements were not carried out past the projection of the sulphide zone because the hole was plugged. A broad potential high is observed directly opposite the projection of the ore zone onto the drill hole. This observation alone does not conclusively indicate the presence of conductive mineralization between the holes. Other geophysical and/or geological data are needed to establish the possible occurrence of sulphides between the holes. The high negative SP values observed along hole 3096 are an indication of sulphides in the vicinity.

The MacLean Extension Orebody is a complex assemblage of polymetallic sulphides. A number of faults within the ore area seem to offset some ore lenses. A number of holes were drilled above and below the drift intersected base metal sulphides while others were barren. The MacLean Extension appeared to present an ideal situation for the study of the MALM potential field distribution. Unfortunately all drillholes except those studied were plugged.

CONCLUSIONS

The MALM IP and potential measurements carried out in the MacLean Extension Orebody, although limited only to three sections and a few holes, indicate that the sulphide zones within this part of the orebody are highly conductive and the ore sections can be correlated easily between holes. The normalized MALM IP data show an inverse relationship to the potentials, low IP coinciding with high potentials across the mineral intersections. No additional information can be obtained on the geometry and nature of the ore zones from the IP data. A more comprehensive analysis of the decay waveforms (time constants) may reveal additional information on the polarizability of the sulphides.

The MALM measurements can answer a number of questions encountered in mineral exploration and development. In cases where an orebody consists of a number of ore lenses, the MALM measurements can be used to determine which of the lenses are connected between drillholes. This information is useful in planning mining operations. The MALM measurements can also be used to determine the direction of dip of a discovered conductor and to evaluate its extension within a given area. This information is again useful in siting subsequent drillholes aimed at intersecting the same sulphide lens. The MALM measurements can also be used to determine the structure between the holes which in turn may aid in the discovery of missed ore zones.

ACKNOWLEDGMENTS

This work was carried out under the Canada-Newfoundland Cooperative Mineral Program. Thanks are due to the staff of ASARCO and Abitibi-Price Mineral Resources for providing the geologic information and logistical help required for carrying out this study.

REFERENCES

Binney, W.P.
1987: A sedimentological investigation of MacLean Channel transported sulphide ores; in Buchans Geology, Newfoundland, ed. R.V. Kirkham; Geological Survey of Canada, Paper 86-24, Report 8.

Binney, W.P., Thurlow, J.G. and Swanson, E.A.
1983: The MacLean Extension orebody, Buchans, Newfoundland; in Current Research, Geological Survey of Canada, Paper 83-1A, Part A, p. 313-319.

Ketola, M.
1972: Some points of view concerning mise-à-la-masse measurements; Geoexploration, v.10, p. 1-23.

Mansinha, L. and Mwenifumbo, C.J.
1983: A Mise-à-la-masse survey at the Cavendish geophysical test site; Geophysics, v. 48, p. 1252-1257.

McMurry, H.V. and Hoagland, A.D.
1956: Three dimensional applied potential studies at Austin-

Parasnis, D.S.
1967: Three dimensional mise-à-la-masse surveys of an irregular lead-zinc-copper deposit in Central Sweden; Geophysical Prospecting, v. 15, no. 3, p. 407-437.

Thurlow, J.G. and Swanson, E.A.
1981: Geology and ore deposists of the Buchans area, central Newfoundland; in The Buchans Orebodies: Fifty Years of Mining and Geology, ed. E.A. Swanson, D.F. Strong and J.G. Thurlow; Geological Association of Canada, Special Paper 22, p. 113-142.
ville, Virginia; Geological Society of America, Bulletin, v. 67, p. 683-696.

Natural gamma ray logging in volcanic rocks: the Mudhole and Clementine base metal prospects

C.J. Mwenifumbo[1] and P.G. Killeen[1]

Mwenifumbo, C.J. and Killeen, P.G., Natural gamma ray logging in volcanic rocks: the Mudhole and Clementine base metal prospects; in Buchans Geology, Newfoundland, ed. R.V. Kirkham; Geological Survey of Canada, Paper 86-24, p. 263-272, Report 16, 1987.

Abstract

Natural gamma ray logging was carried out in two holes at the Mudhole Prospect and one hole at the Clementine Prospect near Buchans, Newfoundland. The holes intersect volcanic, volcaniclastic and sedimentary rocks which include andesite, rhyolite, dacite, diabase intrusions, tuff, agglomerate, arkose, siltstone and greywacke. These rock units can be characterized easily by their natural gamma ray activity. The total count gamma ray logs show rhyolite as producing the highest gamma ray count rate while the diabase intrusions are characterized by their extremely low gamma ray activity.

Résumé

On a effectué la diagraphie par rayons gamma naturels de deux trous de forage à l'indice Mudhole et d'un trou de forage à l'indice Clementine, près de Buchans, à Terre-Neuve. Les trous de forage traversent des roches volcaniques, des roches volcaniques clastiques et des roches sédimentaires, y compris de l'andésite, de la rhyolite, de la dacite, des intrusions de diabase, du tuf, de l'agglomérat, de l'arkose, de l'aleurolite et du grauwacke. Il est facile de caractériser ces unités lithologiques grâce aux rayons gamma qu'elles émettent. Les diagrammes de rayons gamma montrent que la rhyolite émet la plus grande quantité de rayons gamma, tandis que les intrusions de diabase en produisent de très faibles quantités.

INTRODUCTION

Although natural gamma ray logging is standard practice in uranium exploration, oil exploration and coal evaluation, there has been a limited application of the technique to base metal exploration and geologic mapping in igneous and metamorphic terranes. A few papers dealing with the use of gamma ray well logs for interpreting the geology in igneous and metamorphic terranes include those by West and Laughlin (1976), Keys (1979), Daniel *et al.* (1981), Stefansson *et al.* (1982) and Chapman and Thompson (1984).

In oil exploration and coal evaluation, natural gamma radiation detected by a gamma ray probe originates mainly from the radioelement potassium-40. The main minerals contributing to an increase in potassium-40 are the K-feldspars and micas. Differences in the percentages of these minerals in various sedimentary rock units makes it possible to identify and characterize different sedimentary units by their levels of radioactivity. In uranium exploration the main contribution to gamma radiation generally originates from the uranium decay series no matter what the rock type, because locating anomalous concentrations of uranium is the objective. Under ordinary conditions in metamorphic and igneous environments, however, gamma radiation may be contributed approximately equally from the uranium decay series, potassium-40 and the thorium decay series. Here again, the K-feldspars and micas contribute most of the gamma radiation originating from potassium-40. Usually the uranium and thorium in igneous rocks are contained in minerals such as allanite, apatite, monazite, sphene and zircon. Serra et al. (1980), list a number of thorium, thorium-bearing, uranium and uranium-bearing minerals which may be present in igneous rocks in varying proportions. These radioelement concentrations may be detected and measured in boreholes with a natural gamma-ray logging probe.

With the foregoing discussion in mind, natural gamma ray logging was carried out at two base metal prospects near Buchans, Newfoundland to evaluate the technique as a mapping tool in a volcanic environment.

Total count gamma ray logs were obtained in two boreholes at the Mudhole Prospect and one borehole at the Clementine Prospect. The locations of these two prospects are shown in Figure 1. The drillholes were logged with the Geological Survey of Canada research and development logging system. The logging speed was 3 m/minute and data

[1]Geological Survey of Canada, 601 Booth Street, Ottawa, K1A 0E8

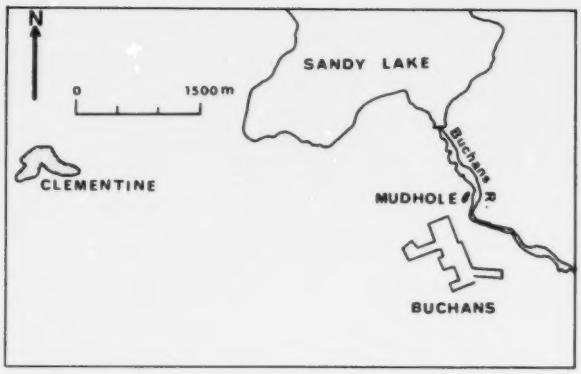

Figure 1. Location of the two base metal prospects at Buchans.

were recorded every 4 seconds onto nine-track tape in 256 channels covering a gamma ray energy range from approximately 0.1 MeV to 3.0 MeV. The scintillation detectors used in the present study included a 25 × 76 mm Bismuth Germanate ($Bi_4Ge_3O_{12}$, commonly called BGO), a 25 × 76 mm and a 19 × 76 mm thallium activated sodium iodide (NaI(Tl)) detector. Only the total count window logs (covering an energy range between 0.4 to 3.0 MeV) are presented in this report. In this volcanic environment the radioelement concentrations are very low compared to those observed in uranium exploration and hence gamma ray count rates are also very low. Consequently the energy windows used for spectral gamma ray analysis (K, U, Th windows) had very poor counting statistics and no attempt was made to produce quantitive logs of potassium, uranium and thorium from the present data.

LITHOLOGY INTERSECTED BY THE DRILLHOLES

The two drillholes in the Mudhole Prospect (hole MH890 and MH2572) intersected mainly volcanic rocks. Numerous diabase intrusions transect the area. The volcanic rocks intersected by the drillholes include andesite, rhyolite and dacite flows. The bottom of the holes intersect the Sandy Lake Formation which consists mainly of arkose, pyritic siltstone and greywacke. Between the Sandy Lake Formation and the volcanic flows lie the pyroclastic rocks which host the lead-zinc sulphides of the Mudhole Prospect. These holes, however did not intersect any base metal sulphides. The drillhole at the Clementine Prospect (hole CL1911) passed through rhyolites, dacites, andesites and volcaniclastic rocks. This hole intersected low-to-medium grade lead-zinc transported ore, the sulphides being hosted by the volcaniclastic units (volcanic wacke, conglomerate and lithic tuffs).

RESULTS AND DISCUSSIONS

As mentioned above, all the holes were logged at 3 m/minute. Gamma ray counts were accumulated and recorded every 4 seconds, giving a measurement every 20 cm along the hole. The count rate values are reduced to counts per second in all the following presentations.

Figure 2 shows the lithologic log derived from the diamond drill core log and the total count gamma ray log for drillhole MH2572, obtained with the 25 × 76 mm BGO detector. The geologic log indicates that the hole intersects two major volcanic units and diabase intrusions. These different rock units can be readily distinguished on the gamma ray log. The rhyolite flows have a higher gamma ray response than the andesite flows. The upper rhyolite flow (10-50 m) has a lower gamma ray activity than the lower feldspar-phyric rhyolite (127-164 m). These two flows may have been derived from different sources or may have undergone different degrees of alteration (possible enrichment in potassic minerals within the lower rhyolite flow unit). The diabase intrusions are characterized by extremely low gamma ray activity. All of these units have a fairly uniform distribution of the radioelements which indicates probable chemical homogeniety within the individual units. An interesting note is that within the andesite flow (175-275 m) two sections with higher than average gamma ray count rate were identified; one from 195 to 200 m and another one from 200 to 206 m. The lithologic log does not indicate a separate flow unit within this region, nor does it indicate any changes in alteration. A re-evaluation of the core in this section of the hole may reveal the reason for these high gamma ray values (e.g. changes in lithology or alteration). Since this was not done, we can only speculate on the reasons. The gamma ray count rate in the section from 195 to 200 m seem to suggest that it could be an amygdaloidal andesite flow unit whereas the section from 200 to 206 m has count rates similar to those observed in the rhyolite flow (9 - 58 m). The amygdaloidal andesite flows (between the intervals 58 - 80 m and 91 - 110 m) seem to have slightly higher levels of radioactivity than more massive andesite.

Figure 3 shows the total count gamma ray log and lithologic log for hole MH890. The gamma ray log was obtained with 19 × 76 mm NaI(Tl) detector. As in hole MH2572, the diabase intrusions are defined clearly and characterized by a very low gamma ray response. The core log description identifies the section between 9 and 198 metres as silicic, acid to intermediate flows with a number of diabase dykes. The flows are porphyritic with feldspar phenocrysts. The gamma ray log shows two levels of radioactivity between these depths indicating two probable volcanic flow units. The lower count rate region from 9 to 90 metres is probably a rhyolite flow and the higher count rate region between 90 to 198 is probably equivalent to the feldspar-phyric rhyolite flow unit in hole MH2572. This rock sequence may be correlated with that of hole MH2572 drilled approximately 100 metres away. From 198 to 225 m the core log indicates agglomerates, amygdaloidal andesites and diabase dykes. These can be easily identified from the gamma ray log. From 300 to 340 metres the hole intersects alternating layers of pyroclastics (agglomerate and tuffs) and diabase dykes. These have been lumped together on the lithologic log, however, the gamma ray log clearly separates the diabase and the agglomerates. The arkosic and dacitic tuffs between 317 and 334 m are characterized by high gamma ray activity. The siltstone and

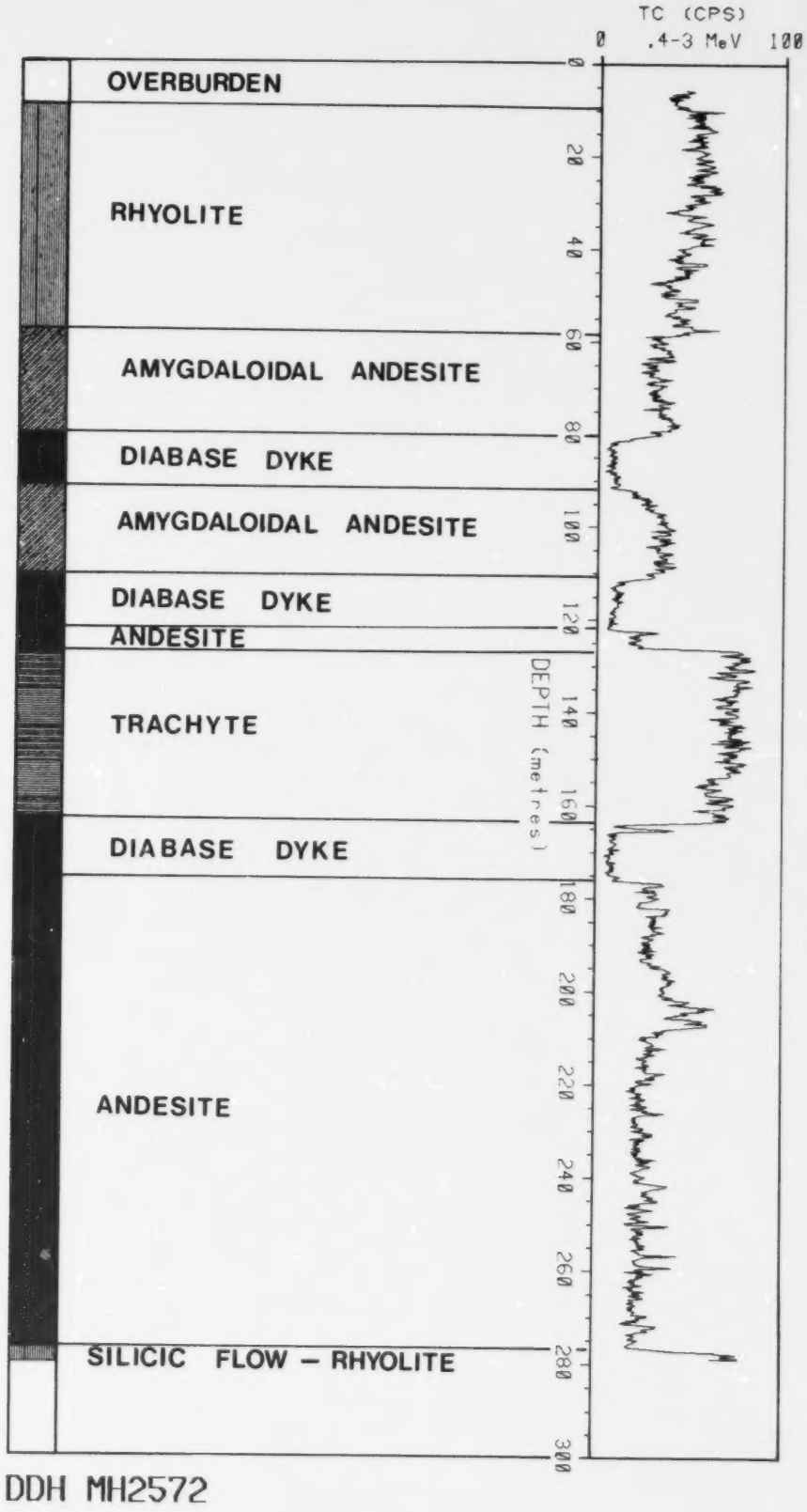

Figure 2. Total count gamma ray log recorded in hole MH2572 at the Mudhole Prospect using a 25 × 76 mm BGO detector, logging velocity of 3 m/minute and sample time of 4 seconds (Z = 20 cm). The lithology (based on core description) intersected by the drillhole is indicated on the left.

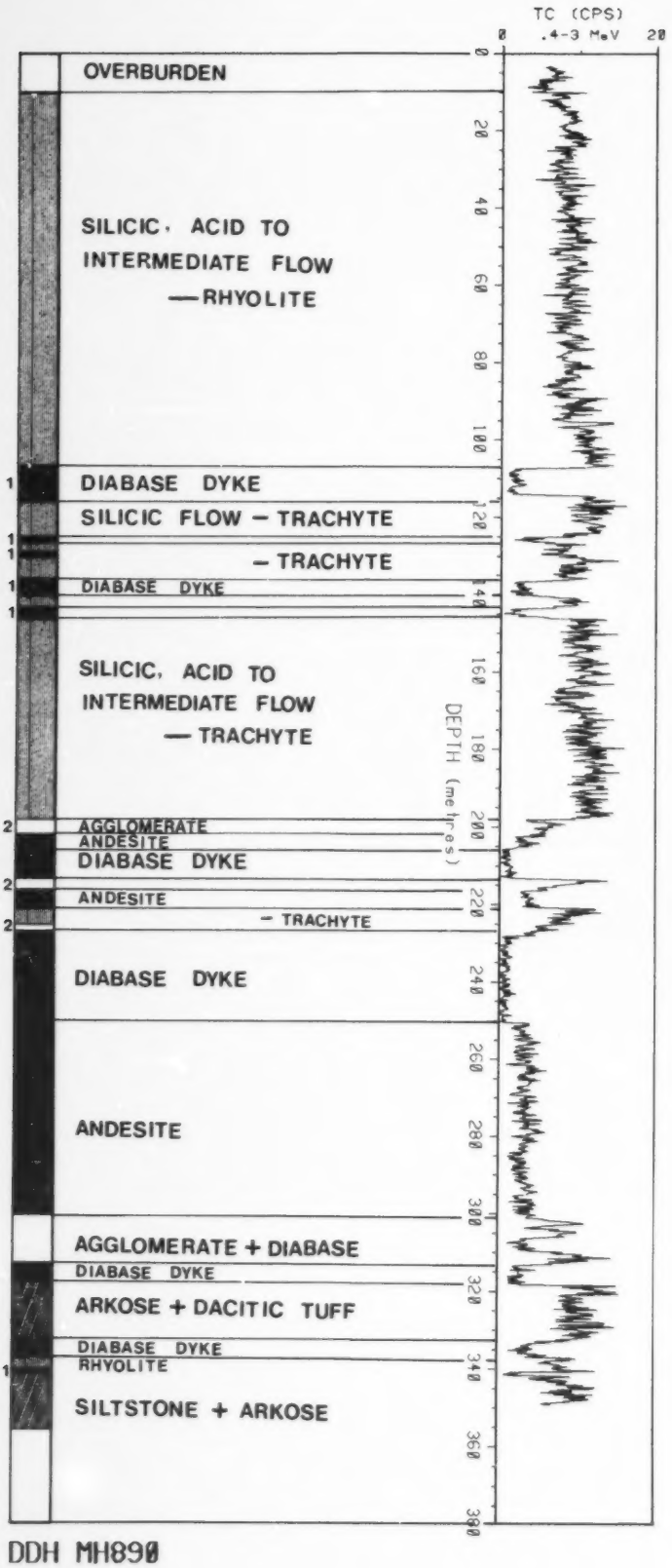

Figure 3. Total count gamma ray log recorded in hole MH890 at the Mudhole Prospect using a 19 × 76 mm NaI(Tl) detector, logging velocity of 3m/minute and sample time of 4 seconds ($Z = 20$ cm). The lithology (based on core description) intersected by the drillhole is shown on the left.

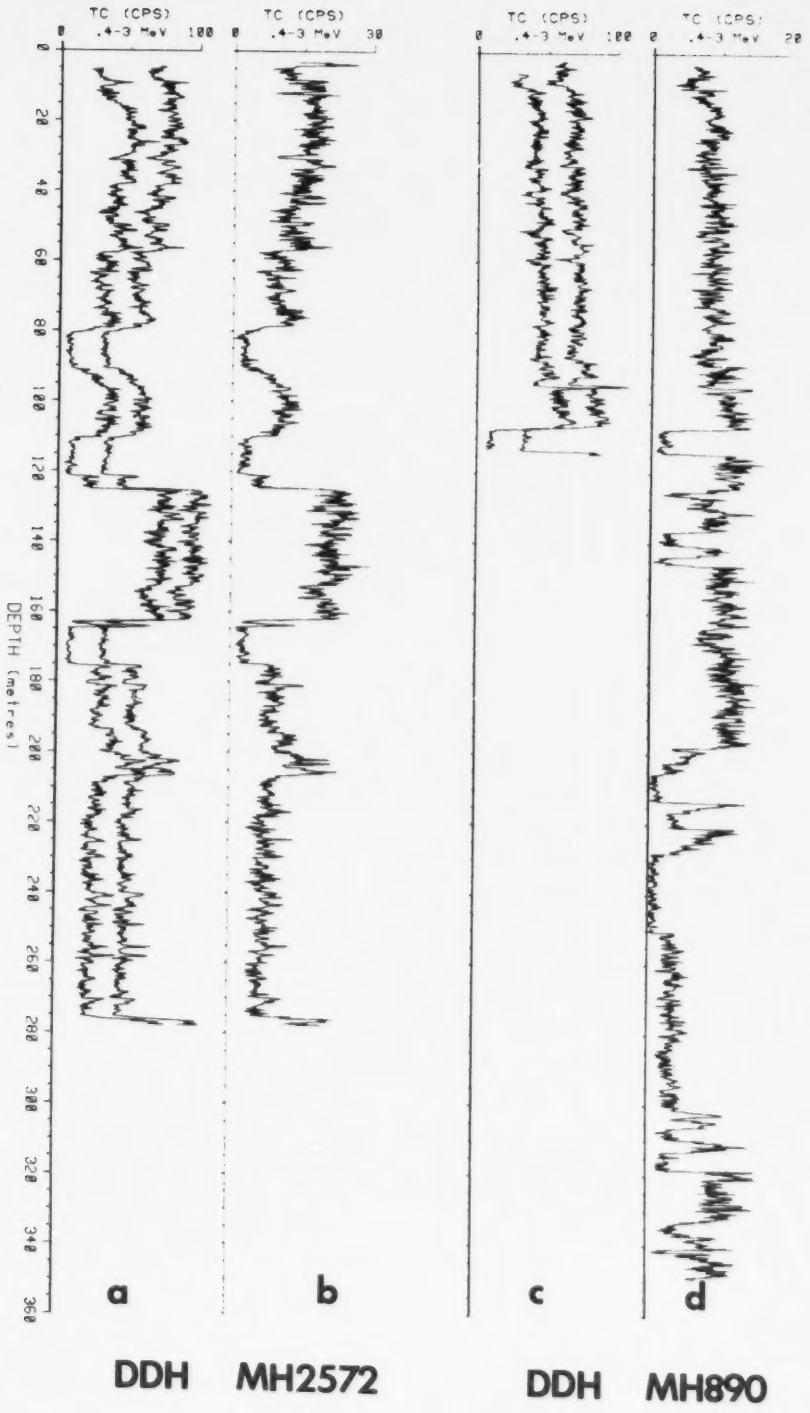

Figure 4. Total count gamma ray logs recorded at the Mudhole Prospect showing the repeatability of the measurements. Figure 4a, uphole and downhole runs recorded in hole MH2572 using a 25 × 76 mm BGO detector. Figure 4b, log recorded with a 25 × 76 NaI(Tl) detector in hole MH2572. Figure 4c, repeat logs in hole MH890 with 25 × 76 mm BGO detector. Figure 4d, log recorded in MH890 with a 19 x 76 mm NaI(Tl) detector.

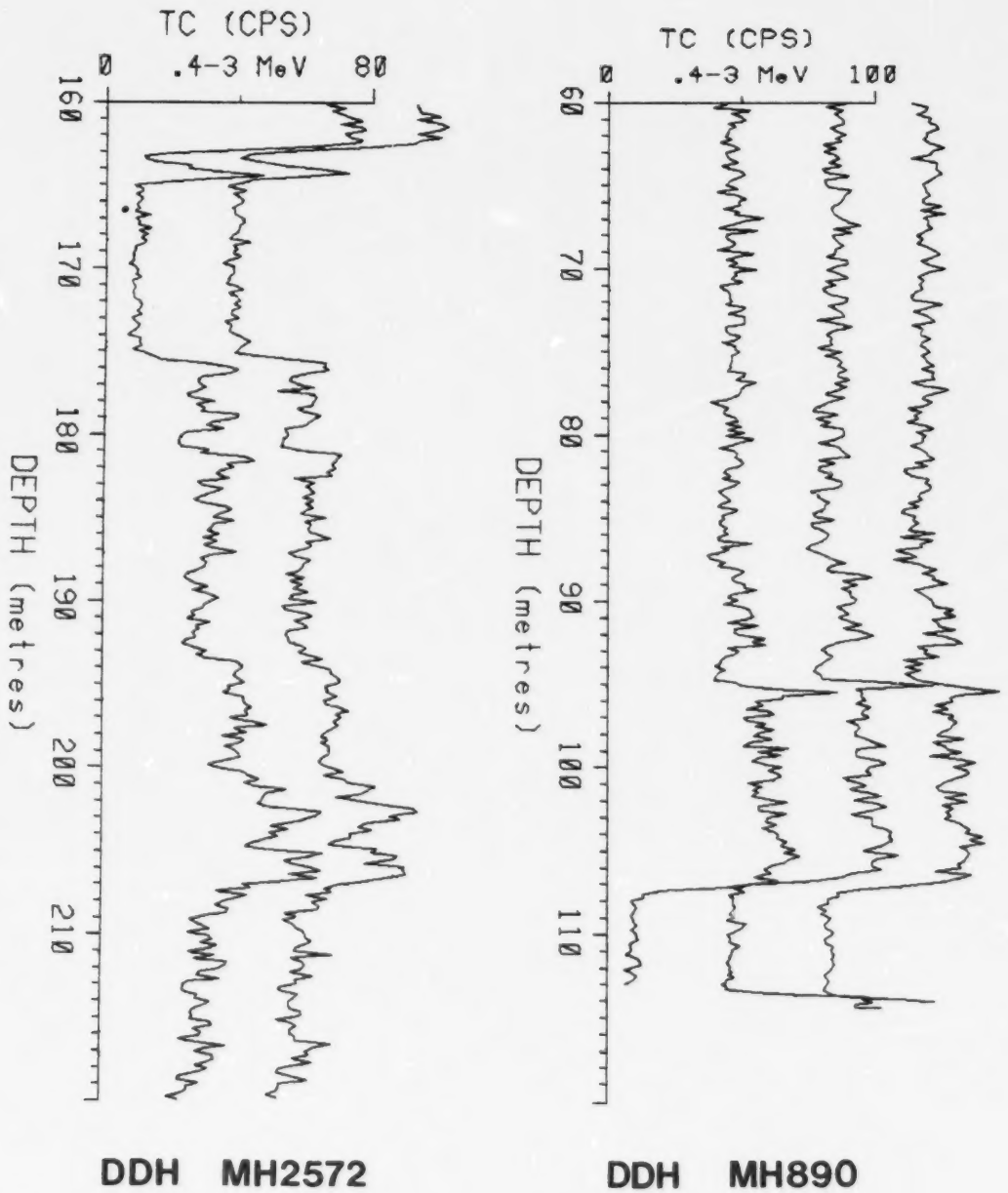

Figure 5. Expanded sections from Figure 4 showing that the fine details of the gamma ray signature are repeatable.

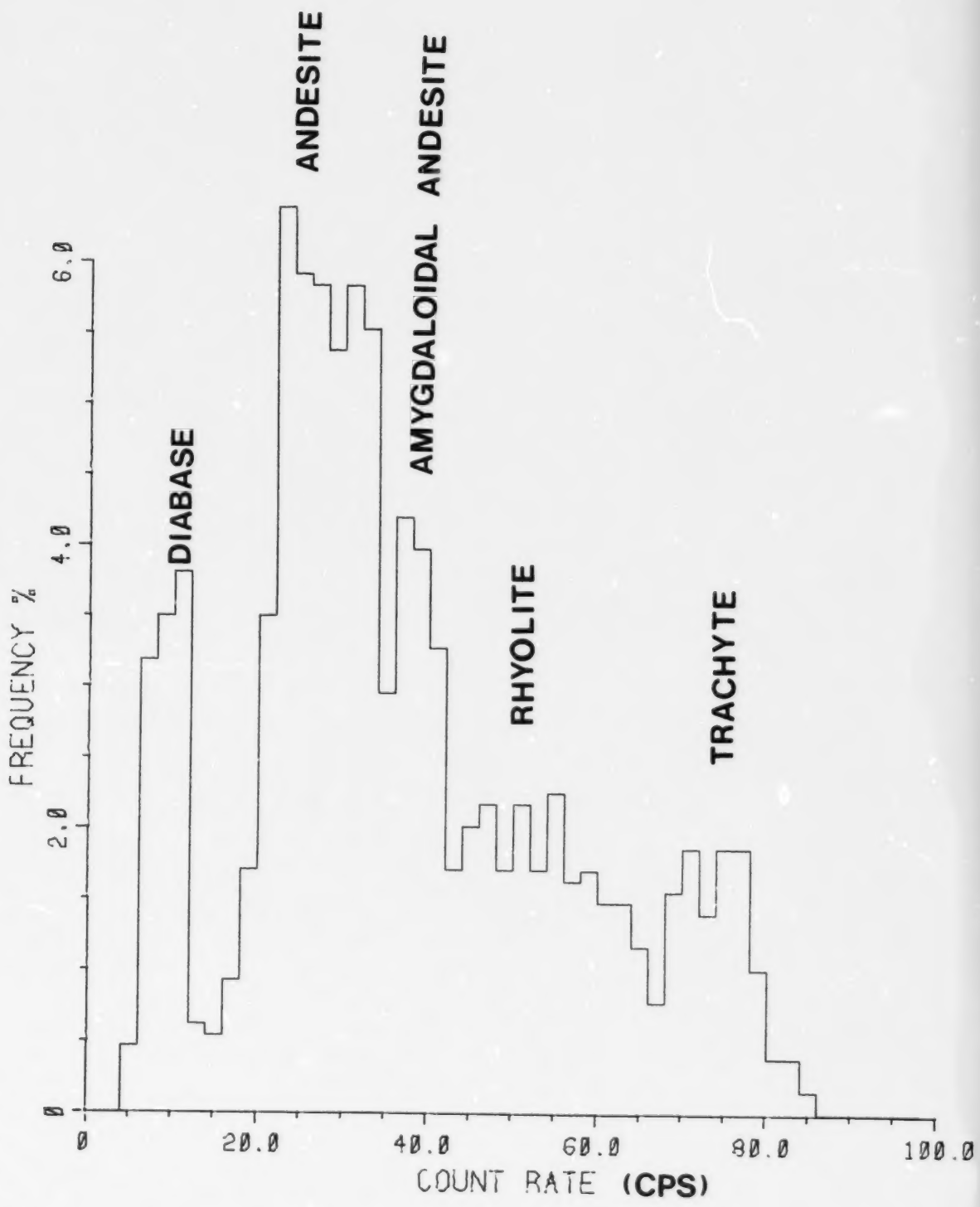

Figure 6. Frequency distribution plot of gamma ray total count log for hole MH2572.

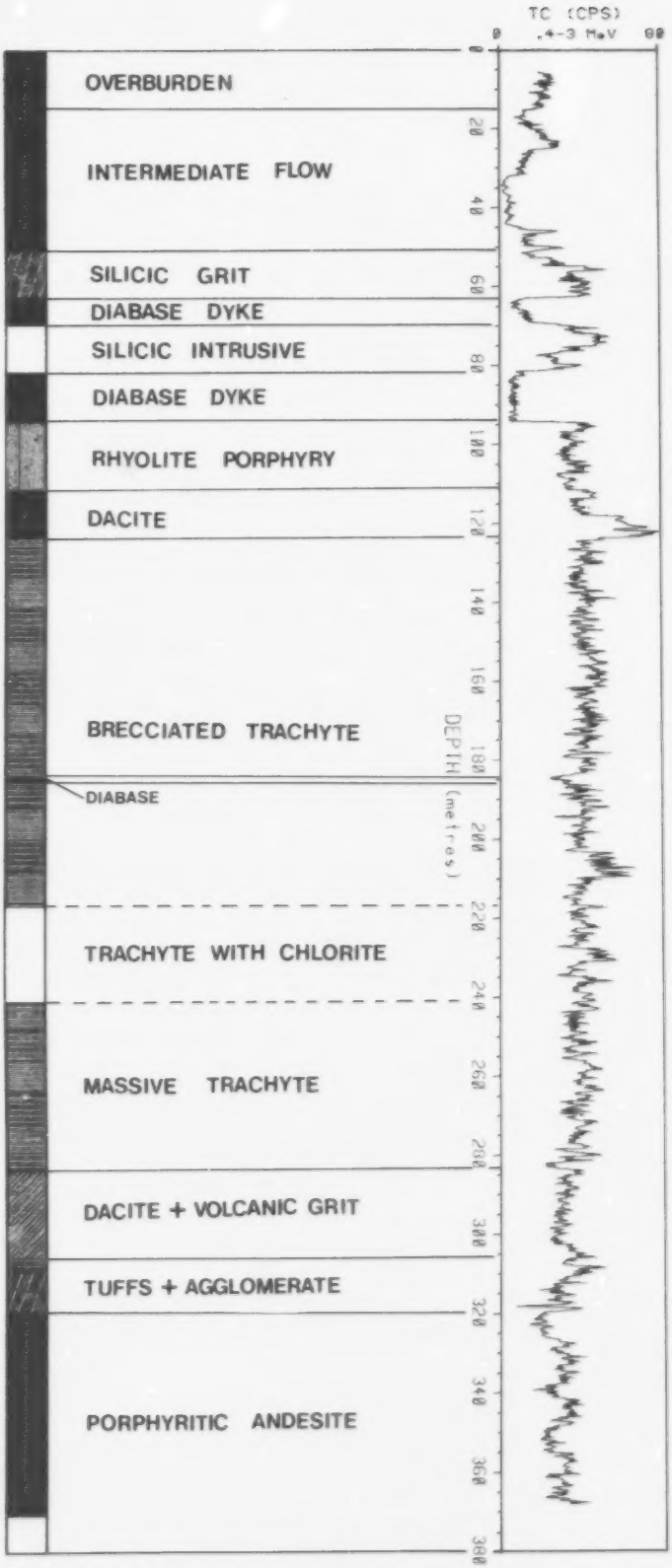

Figure 7. Total count gamma ray log recorded in hole CL1911 at the Clementine Prospect using a 25 × 76 mm BGO detector, logging velocity of 3 m/minute and sample time of 4 seconds ($Z = 20$ cm). The lithology (based on core description) intersected by the drillhole is shown on the left.

arkose below 340 m have nearly the same level of radioactivity as the pyroclastic rocks. It is difficult to separate the rhyolite, pyroclastic rocks and sedimentary units using the total count gamma log (especially when they are adjacent to each other) because the levels of radioactivity are essentially the same. However, the spectral gamma ray log, which determines the relative contribution of the radioelements, K, U and Th to the overall radioactivity, may distinguish the sedimentary rock units from the volcanic flows. To do this, a slower logging speed or larger detector would have to be used.

The count rates for all the logs obtained with either the BGO detector or the NaI(Tl) detector are fairly low (less than 100 counts per second). Considerable statistical scatter exist in the data. This could lead to the conclusion that some of the finer variations in the gamma ray count rate might be attributed to this statistical scatter. However the following discussion demonstrates that useful geologic information is contained in the smallest variations in the gamma ray logs recorded. Figure 4 is an illustration of the repeatability of the measurements acquired in these holes. Figure 4a shows two repeat logs obtained in hole MH2572 with the 25 × 76 mm BGO detector. The logs are offset for clarity. Figure 4b shows a log obtained along the same hole (hole MH2572) with the 25 × 76 mm NaI(Tl) detector. These logs illustrate that the changes in the gamma ray response are a true reflection of the lithologic changes along the drillhole. Two repeat logs run in hole MH890 with a 25 × 76 mm BGO detector are shown in Figure 4c. The logs are again offset for clarity. These logs were run only to a depth of 114 m because of an obstruction at that depth. A smaller probe with a 19 × 76 mm NaI(Tl) detector was run to the bottom of hole and the logs are displayed in Figure 4d. Again the gamma ray signature repeats very well. Expanded sections of repeat logs along holes MH890 and MH2572 displayed in Figure 5 show excellent duplication of the fine variations in the count rate indicating the validity of the information contained in even the smaller fluctuations in the log.

Figure 6 is a frequency distribution plot of gamma ray count rate data in Figure 2 for hole MH2572. It indicates a multimodal distribution representing the respective volcanic flow units intersected by the drillhole. A similar frequency distribution was obtained for the gamma ray log of hole MH890. The possibilities for use of the gamma ray log as an aid to geologic interpretation are readily apparent. For example, Stefansson et al. (1982), in their study of gamma ray responses of Icelandic rocks, have shown that a linear relationship exists between the gamma ray activity and the silica content of volcanic rocks. The more felsic the rocks, the higher the gamma activity, that is, silicic rocks such as rhyolites (69-75 % silica) have a higher gamma activity than intermediate rocks such as andesites and dacites (63-69 % silica). This observation was also reported by Keys (1979).

The lithologic and total count gamma ray logs for the Clementine hole (hole CL1911) are presented in Figure 7. This log was obtained with the 25 × 76 mm BGO detector. All major changes in lithology along the drillhole are shown and most of them are defined clearly on the gamma ray log. A few particularly interesting points are present on the gamma ray log. From 14 to 50 m the lithologic log indicates an intermediate flow with scattered amygdules. However, the gamma ray log shows considerable variation within this section of the hole. The very low gamma ray activity in the region between 32 and 43 metres suggests that this may be a zone of diabase intrusions. The interval between 111 and 123 m is identified as dacite from the core description. The upper section (111-118 m) is coarse grained dacite and the lower section (118-123 m) is medium grained dacite. These two sections are distinguished clearly on the gamma ray log. The medium grained dacite has a fairly high level of radioactivity. The coarse grained dacite has almost the same level of radioactivity as the rhyolite porphyry above. This observation suggests that the two dacites may be of different chemical composition as well as being texturally different. The coarse grained dacite may also have been incorrectly identified, and may be a rhyolite porphyry. The rhyolite flow in the interval 123 to 283 metres is fairly uniform with a gradual decrease in radioactivity with increasing depth. The brecciated rhyolite (123-217 m) has slightly higher gamma ray activity than the massive rhyolite (240-283 m). In addition minor fluctuations in the levels of radioactivity are present within the rhyolite; for example, a high count rate at 205 m. This increase may be due to alteration (increases in potassium) or to changes in the concentrations of the radioelements within an unaltered rhyolite. The diabase dyke at about 185 m is too thin to be resolved clearly on the gamma ray log. However, an indication of its presence is apparent on the log. The gamma ray activity within the rhyolite flow (125-280 m) is similar to that observed within the rhyolites at the Mudhole Prospect (hole MH2572 log with a 25 × 76 mm BGO detector). This feature suggests that the rhyolites at the two prospects have similar compositions.

CONCLUSIONS

This study has indicated that the total count gamma ray logs may be applied in the Buchans area with a high degree of confidence for the identification of the different volcanic rock types. Because contacts between major volcanic units are well defined on the gamma ray logs, determination of the thicknesses of individual units may also be achieved easily. Gamma ray logs, in conjunction with the geological logs can be used to provide a more complete and reassuring geological interpretation of the lithology intersected in diamond-drill holes. The use of gamma ray spectral logs in the area might provide additional information on the relative concentrations of the naturally occurring radioelements, U, Th, and K, permitting further subdivision of the geologic units and subdividing alteration types not possible on the basis of the total count logs alone.

ACKNOWLEDGMENTS

This work was carried out under the Canada-Newfoundland co-operative mineral program 1982-1984. Geologic core log descriptions of the holes logged were provided by the staff of ASARCO Inc. and Abitibi-Price Inc.

REFERENCES

Chapman, B.H. and Thompson, D.T.
1984: Application of geophysical logging within skarn-type deposits: The Log Analyst, v. XXV, p. 13-24.

Daniels, J.J., Scott, J.H., and Olhoeft, G.
1981: Interpreting Precambrian metamorphic geology from geophysical well logs; Society of Professional Well Log Analysts Twenty-Second Annual Logging Symposium Transactions, p. T1-T17.

Keys, W.S.
1979: Borehole geophysics in igneous and metamorphic rocks; Society of Professional Well Log Analysts Twentieth Annual Logging Symposium Transactions, p. OO1-OO26.

Serra, O., Baldwin, J. and Quirein, J.
1980: Theory, interpretation and practical application of natural gamma ray spectroscopy; Society of Professional Well Log Analysts Twenty-First Annual Logging Symposium, Transactions, p. Q1-Q30.

Stefansson, V., Gudmundsson, A. and Emmerman, R.
1982: Gamma ray logging in icelandic rocks; The Log Analyst, v. XXIII, p. 11-16.

West, F.G. and Laughlin, A.W.
1976: Spectral gamma logging in crystalline basement rocks; Geology, v. 4, p. 617.

Preliminary results of a detailed structural analysis of the Buchans Mine area[1,2]

Contract 06ST. 23233-5-0382

T.J. Calon[3] and F.K. Green[3]

Calon, T.J., and Green, F.K., Preliminary results of a detailed structural analysis of the Buchans Mine area; in Buchans Geology, Newfoundland, ed. R.V. Kirkham; Geological Survey of Canada, Paper 86-24, p. 273-288, Report 17, 1987.

Abstract

Structural surface mapping and analysis of mine level plans and diamond-drill core and logs in the Buchans Mine area confirm that the volcanic and sedimentary rocks of the Buchans Group comprise an extensive thrust system. It is exposed in the form of eyelid windows through a broad, east-west trending culmination with complex internal structure. An interpretation is presented for the geometry and stacking order of the duplexes that build the culmination, using the recently revised stratigraphy for the Buchans Group. Detailed analysis of the Oriental #1 Orebody and preliminary work on the Lucky Strike Orebodies show that these deposits occur in intensely imbricated antiformal stacks. A kinematic model for the evolution of the thrust system is proposed involving south-southeast directed imbrication by progressive footwall collapse of the Buchans Group beneath the advancing Hungry Mountain thrust complex.

Résumé

La cartographie de la structure en surface et l'analyse des galeries, des diagraphies et des échantillons de carottage au diamant dans la région de la mine Buchans confirment que les roches volcaniques et sédimentaires du groupe du Buchans forment une vaste séquence de nappes de charriage. Le groupe affleure sous forme de fenêtres dans une vaste culmination à orientation est-ouest et à structure interne complexe. Les auteurs se fondent sur la stratigraphie révisée du groupe de Buchans afin de présenter une interprétation de la géométrie et de l'ordre d'empilage des duplex qui forment la culmination. L'analyse détaillée du gisement Oriental n° 1 et l'étude provisoire des gisements de Lucky Strike révèlent que ces gîtes se présentent dans des antiformes fortement imbriquées. On propose un modèle cinématique de l'évolution de la séquence de nappes de charriage qui comprend l'imbrication vers le sud-sud-est à la suite de l'effondrement progressif du mur du groupe de Buchans sous le complexe de charriage de Hungry Mountain.

---

[1]Contribution to the Canada-Newfoundland Mineral Development Agreement 1984-89

[2]Editor's note. This work was started after Thurlow and Swanson (1987) and McClay (1987) papers were written and the authors had copies of these papers and recommendations of K.R. McClay for further structural geology studies at Buchans

[3]Department of Earth Sciences and Centre for Earth Resources Research, Memorial University of Newfoundland, St. John's, Newfoundland A1B 3X5

INTRODUCTION

Volcanic rocks of the Ordovician Buchans Group host the well-known polymetallic massive sulphide-barite Buchans orebodies in the central Newfoundland Appalachians. The stratigraphy and structure of the Buchans Group are presently the subject of major studies in an attempt to identify new exploration targets. The structural analysis of the Buchans Mine area, initiated in 1985, was designed to resolve the complex geometry and kinematics of thrusting and folding that affected the Buchans Group. In particular, it was directed to reassess the present distribution of the Buchans orebodies in terms of thrust tectonic controls. The work involved detailed structural analysis of geological surface exposures along four transects trending approximately north-south across the various Buchans orebodies (Fig. 1). It also included relogging of a large number of diamond-drill cores from holes along the four transects and re-interpretation of available mine level and stope plans.

Recent structural interpretations of the Buchans area indicate the presence of a complex array of thrust faults that control the distribution of lithostratigraphic units of the Buchans Group (Thurlow, 1984; Thurlow and Swanson, 1987; McClay, 1987). They lend support to an idea suggested earlier by Thurlow and Swanson (1981, p. 125) that "the Oriental and Lucky Strike ore horizon sequences represent structurally stacked thrust blocks which originally lay at the same stratigraphic horizon".

The first part of this report presents an interpretation of the structural geometry and stacking order of the Buchans thrust stack and attempts to formalize the nomenclature of the various thrust systems. The second part describes the structure of the Oriental #1 Orebody exposed in the Oriental West and East pits and presents a preliminary interpretation of the structure of the Lucky Strike Orebodies exposed in the Lucky Strike glory hole. The macroscopic and mesoscopic structural data are used to formulate a kinematic model for the evolution of the thrust stack.

BUCHANS GROUP STRATIGRAPHY

Recognition that the volcanic, volcaniclastic and sedimentary rocks of the Buchans Group comprise an extensive thrust belt has led to a new stratigraphic framework, that is considerably simplified over the pre-existing stratigraphic scheme (Thurlow, 1984; Thurlow and Swanson, 1987). In the new stratigraphic column, shown in Table 1, the Buchans Group is subdivided into four lithostratigraphic units: from lowest to highest, the Lundberg Hill Formation, Ski Hill Formation, Buchans River Formation and Sandy Lake Formation. The Buchans River Formation hosts all of the known volcanogenic sulphide orebodies in the area.

The units of the Buchans Group are structurally repeated in a number of thrust systems (Fig. 1a,b). The new stratigraphic column is defined in the Oriental block, immediately north of the Ski Hill – Buchans River Fault (Thurlow and Swanson, 1987), but can be extrapolated to the other thrust systems with only minor changes (J.G. Thurlow, personal communication, 1985). The application of the new stratigraphic column to the geometrical interpretation of the Buchans thrust stack allows the construction of restorable cross-sections comprising most of the thrust systems. This lends additional support to the validity of the new stratigraphic scheme.

MACROSCOPIC STRUCTURE OF THE BUCHANS THRUST STACK

The Buchans area can be envisaged as a fold and thrust belt in which lithostratigraphic units of the Buchans Group are repeated in a large number of thrust systems (Fig. 1). The interpretation of the geometry of the thrust stack is illustrated in an idealized section shown in Figure 2. The proposed nomenclature and stacking order for the thrust systems are presented in Table 2. The interpretation is based on an, as yet, incomplete compilation of available surface and subsurface data concerning locations and attitudes of the bounding faults of the thrust systems and formational contacts and imbricate faults within the thrust systems. Subsurface data to a depth of 1000 metres below the present erosional level of the thrust stack are most concentrated in an area surrounding the main orebodies (Fig. 1). Consequently, the geometrical interpretation is constrained best for the thrust systems occupying the hangingwall and footwall of the Ski Hill – Buchans River Fault near the Buchans town site.

At present, detailed structure contour maps have been constructed for the Ski Hill – Buchans River Fault (courtesy J.G. Thurlow, 1986) and the eastern segment of the Airport Fault (this study). These maps incorporate information on the positions of leading and lateral branch lines (Hossack, 1983) of these two major thrusts, leading branch lines of the main imbricates in the Sandy Lake duplex, and formational cut-off lines (Boyer and Elliott, 1982) on large parts of the hangingwall and footwall of the Ski Hill-Buchans River Fault. It is believed that this data set reasonably constrains the geometry

Table 1. Stratigraphy of the Buchans Group (after Thurlow and Swanson, 1987)

Sandy Lake Formation Basaltic pillow lava, pillow breccia, felsic volcaniclastic sedimentary rocks. Locally abundant pyroclastic and tuffaceous sedimentary rocks.
Buchans River Formation Felsic pyroclastics and breccia, rhyolite, pyritic siltstone, polylithic breccia-conglomerate, granite-boulder conglomerate, massive sulphide and barite orebodies.
Ski Hill Formation Basaltic to andesitic pyroclastics, pillow lava and pillow breccia, massive mafic flows and minor felsic tuff.
Lundberg Hill Formation Felsic pyroclastics and breccia, rhyolite, tuffaceous sedimentary rocks and minor chert.

Table 2. Proposed nomenclature and stacking order of thrust systems at Buchans

1. Hungry Mountain Complex

Hungry Mountain Thrust

2. Middle Branch Duplex
   - Upper metamorphic imbricates (2a)
   - Lower non-metamorphic imbricates (2b)

Airport Fault

3. Sandy Lake Duplex
   - Upper imbricate (3a)
   - Intermediate imbricate (3b)
   - Oriental imbricate (3c)
   - Antiformal stacks of Oriental Orebodies (3d)

Ski Hill–Buchans River Fault

4. Lake 3 Duplex
   (part of Lucky Strike duplex ?)

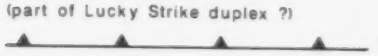

Wiley's River Fault

5. Lucky Strike Duplex
   (Old Buchans, Lucky Strike, Rothermere and MacLean orebodies)

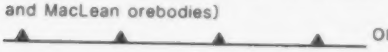

Old Buchans Fault

6. Arkose Duplex
   (Imbricates ?)

Unnamed Thrust

7. Buchans Duplex
   (Culmination of Imbricates, base not exposed)

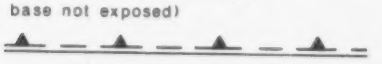

Unnamed Thrust

8. Lower Buchans Group Thrust System
   - Wiley's River Imbricate (8a)
   - Tilley's Pond Imbricate (8b)
   - Lower Imbricates

Sole Thrust ?

of the upper part of the thrust stack, involving units 2b, 3, 4 and 5 to a depth of one kilometre in the area north of the surface trace of the Ski Hill – Buchans River Fault (Fig. 2). On the other hand, data compilation for the units in the lower part of the thrust stack (base of unit 5 and units 6, 7 and 8 in Figure 2) is in a preliminary stage, while the geometrical interpretation is made difficult by a general lack of deep drillhole data in the area south of the surface trace of the Skill Hill – Buchans River Fault. The geometry of this part of the thrust stack is therefore conjectural. The sole thrust of the Buchans thrust stack is nowhere exposed and has not been intersected in deep drillholes. It may lie at considerably greater depth than shown in Figure 2.

Figures 1 and 2 show that the Buchans thrust stack defines a broad, east – west trending structural culmination that rests with a gentle inclination to the east on top of the lowermost thrust systems of the Buchans Group (unit 8) exposed in the area. The culmination is built up by the stacking, or "bunching" (Boyer and Elliott, 1982), of a number of larger and smaller thrust systems (units 3-7) of the Buchans Group. The structure may thus be regarded as a huge antiformal stack (Boyer and Elliott, 1982). The Airport Fault at the floor of the Middle Branch duplex (unit 2b in Figure 2) and the Hungry Mountain Thrust are folded over the roof of the antiformal stack. The thrust systems within the core of the culmination are each bound by a floor and roof thrust and contain internally a number of imbricates. They represent duplex structures (Dahlstrom, 1970), and on the basis of the geometry of the imbricates three types can be distinguished (Boyer and Elliott, 1982). Units 3a-c, 5 and 7 define hinterland-dipping duplexes, unit 4 represents a foreland-dipping duplex (Thurlow and Swanson, 1987), and unit 3d contains two small antiformal stacks comprising the Oriental #1 Orebody (see below). Due to erosional removal of the upper thrust systems of the stack, the duplexes that occupy the core of the culmination are now exposed in a pattern resembling eyelid windows (Boyer and Elliott, 1982; also see McClay, 1987). However, no duplex is completely framed by an overlying thrust sheet (Fig. 1).

Structure contour maps for the Ski Hill – Buchans River Fault and Airport Fault west and east of the Buchans town site show that these thrust surfaces are listric in shape. They dip steeply north near the erosional surface, and the amount of dip decreases gradually towards the north. The thrusts are interpreted to merge asymptotically with the sole thrust (Fig. 2). Other floor thrusts of the duplexes are assumed to show the same geometry, except in the area directly south of the town site where the floor thrust of the Lake 3 duplex (unit 4), and possibly the Lucky Strike duplex (unit 5), are folded over the core of the culmination and locally show south-dipping attitudes (Fig. 2; also see Thurlow and Swanson, 1987).

The surface traces of the bounding thrusts of the various duplexes show a complex geometrical pattern (Fig. 1). This arises to a large extent from folding of the duplexes that are structurally higher in the stack over the duplexes that occupy the core of the culmination. To some extent, however, the surface trace pattern of the thrusts also indicates the presence of an intricate system of frontal, oblique and lateral ramps (Butler, 1982) for the duplexes. The presence of a large, gently east-plunging hangingwall anticline in the Oriental imbricate (unit 3c) north of the Ski Hill – Buchans River Fault indicates that the north-dipping segment of this thrust is a frontal hangingwall ramp situated at the leading edge of the Sandy Lake duplex (Fig. 1, 2). Similar geometries are observed on a smaller scale in units 3a, 3d (see below), and units

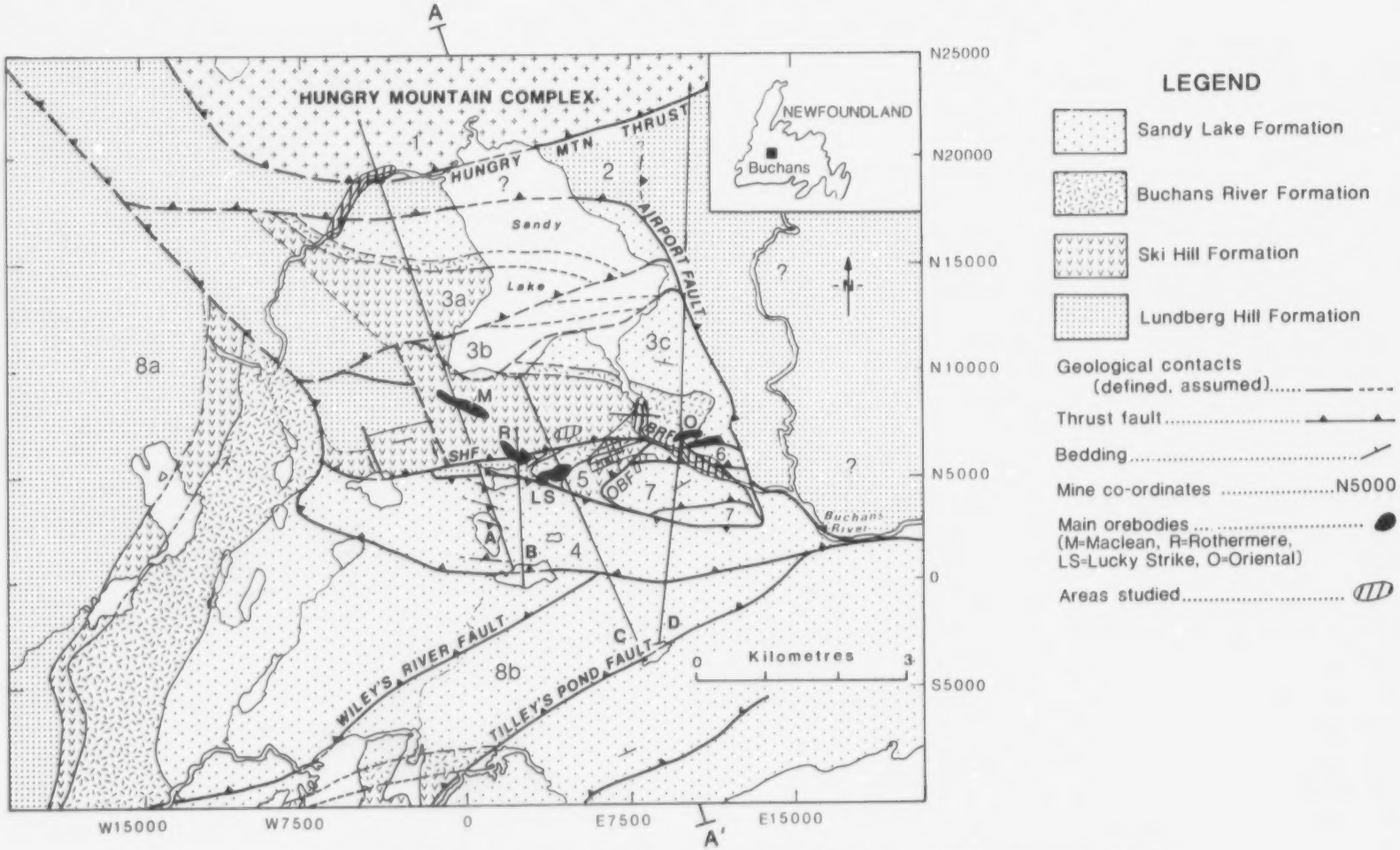

Figure 1a. Geological map of the Buchans area showing the distribution of lithostratigraphic units and structure of the Buchans Group. (after Thurlow and Swanson, 1986) The locations of the structural transects A, B, C, and D and the cross-section shown in Figure 2 are indicated. BRF – Buchans River Fault, OBF-Old Buchans Fault, SHF – Ski Hill Fault.

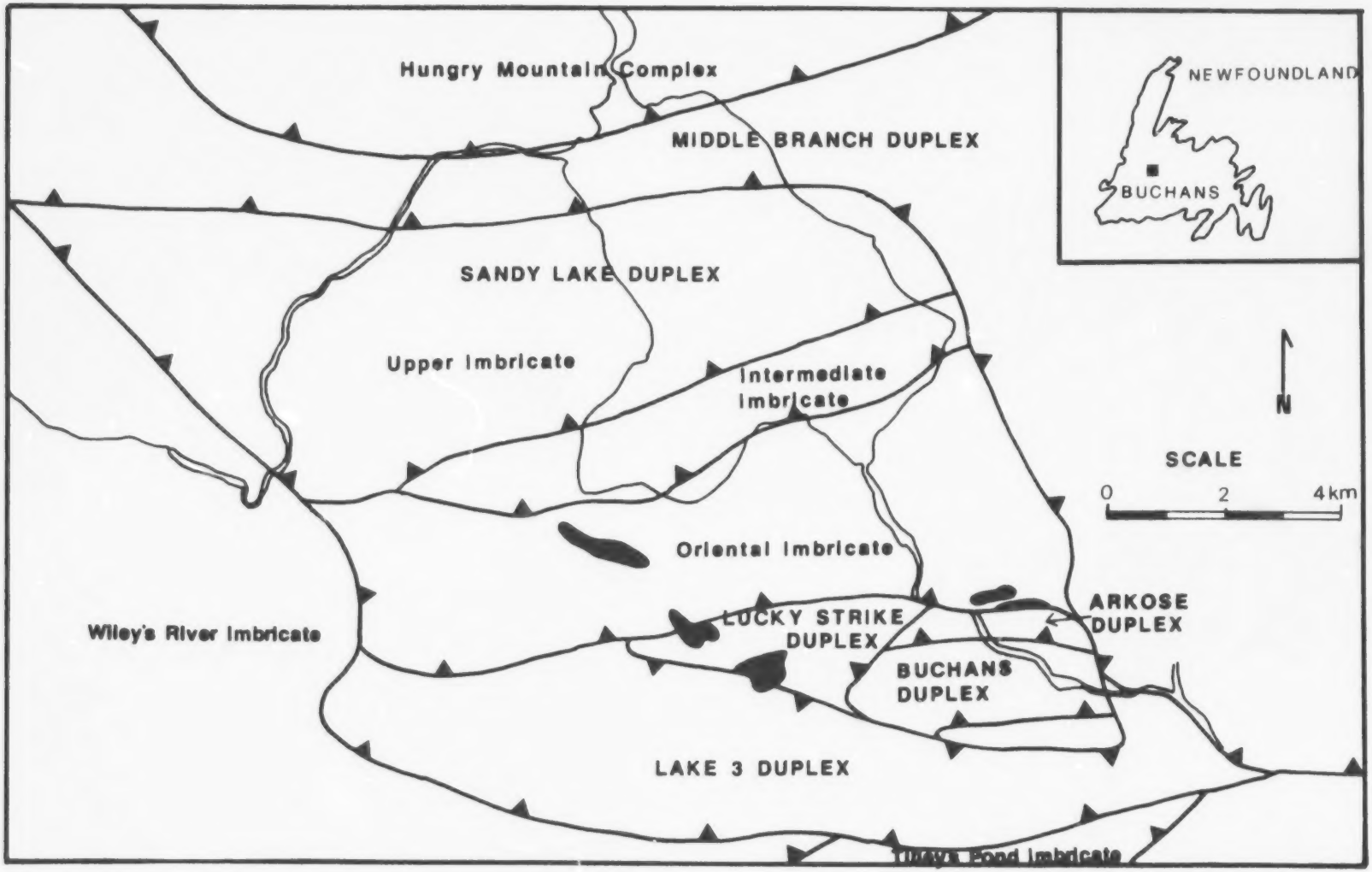

Figure 1b. Simplified map showing proposed nomenclature of thrust systems at Buchans.

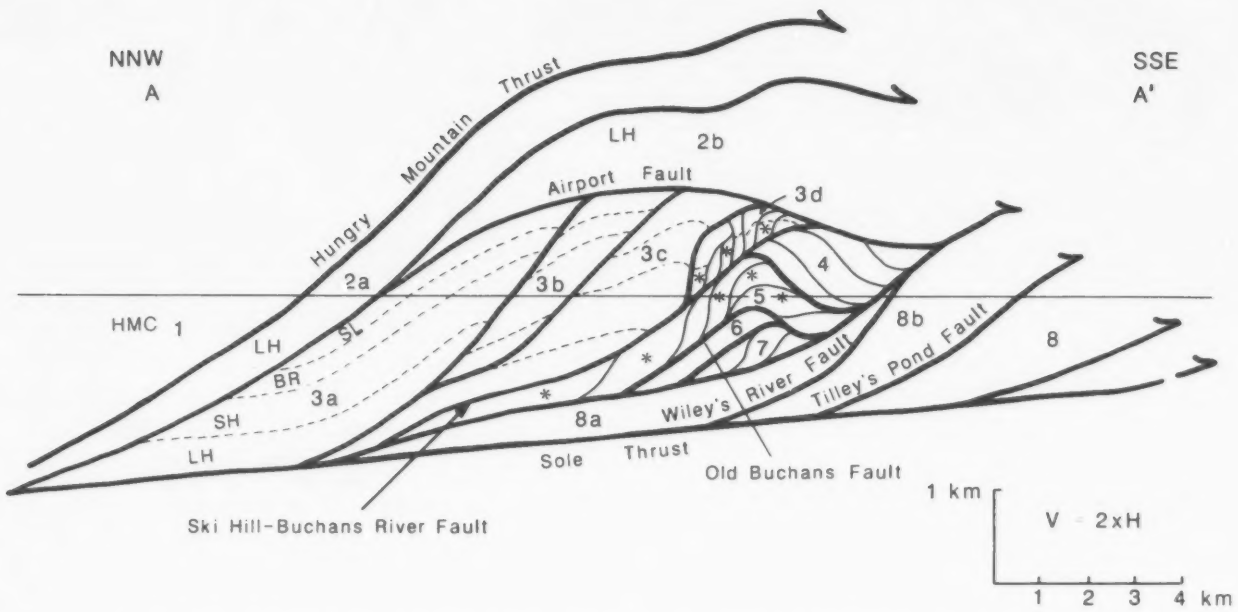

Figure 2. Schematic cross-section showing the structural geometry of the Buchans thrust stack. Numbers on the cross-section refer to structural units listed in Table 2. Location of section is shown in Figure 1. Asterisks indicate positions of the main Buchans orebodies. BR – Buchans River Formation, HMC – Hungry Mountain Complex, LH – Lundberg Hill Formation, SH – Ski Hill Formation, SL – Sandy Lake Formation.

4 and 5 (Thurlow and Swanson, 1987). The N-S to NW-SE striking segments of the Ski Hill – Buchans River and Airport faults (Fig. 1a) are interpreted to represent gently east-dipping lateral ramps. A north-plunging lateral branch line defined by the intersection of these two faults can be delineated in the subsurface near Middle Branch River, approximately 1.5 kilometres east of the N-S striking segment of the Airport Fault (Fig. 1). As a consequence of the movement of the Middle Branch and Sandy Lake duplexes over an irregular system of frontal and lateral ramps, the duplexes are now partly overlapping in a shingle-like fashion. Similar stacking geometries are displayed by units 5, 6 and 7 in the area south of the Ski Hill – Buchans River Fault (Fig. 1a).

As originally suggested by Thurlow and Swanson (1981), the main Buchans orebodies occur at two distinct structural levels in the thrust stack separated from one another by the Ski Hill – Buchans River Fault (Fig. 1, 2). The Oriental #1 and 2 orebodies are contained in an intensely imbricated system at the base of the Sandy Lake duplex (unit 3d). The Old Buchans, Lucky Strike, Rothermere and MacLean orebodies are contained in the structurally lower Lucky Strike duplex. The two thrust systems appear to overlap to some extent near the branch point of the Old Buchans Fault with the Buchans River Fault (Fig. 1). The lithostratigraphic sequences contained in the two thrust systems may have been separated from one another during thrusting by an easterly dipping oblique or lateral ramp segment which now lies in the Ski Hill – Buchans River Fault. The two ore "blocks" may thus not be truly thrust-repeated in the sense that they are stacked on top of one another along frontal ramps as suggested by the geometry shown in Figure 2.

The salient features of the stratigraphy and structure of the various thrust systems that comprise the Buchans culmination are presented in the following section.

DESCRIPTION OF THRUST SYSTEMS

The Hungry Mountain Complex forms the structurally highest thrust sheet exposed in the Buchans area. It consists of polydeformed tonalitic gneisses that are lithostratigraphically unrelated to the Buchans Group. The contact between the gneiss complex and the Buchans Group is nowhere exposed. East of Sandy Lake (Fig. 1a), amphibolite grade S-C mylonites (Lister and Snoke, 1984) derived from granitoid rocks at the base of the complex appear to overlie submetamorphic volcanic rocks, assigned to the Lundberg Hill Formation of the Buchans Group. (Thurlow and Swanson, 1987). The mylonite zone is characterized by a shallowly north- to northwest-dipping foliation and a strong, down-dip mineral elongation lineation. This fabric is deformed locally in north- to northwest-plunging, asymmetric (east-verging) reclined folds. Thurlow (1981) interpreted the mylonite zone to have formed during north- to south-directed emplacement of the complex onto the Buchans Group. In view of its

pronounced contrast in metamorphic grade with the underlying Buchans Group, the complex must be regarded as a far-travelled, originally deep-seated unit. Kinematic indicators in the mylonites, including biotite fish and tailed feldspar porphyroclasts, confirm a south-directed, early movement phase. The movement pattern of the younger folds is presently uncertain. Considering its large regional distribution, the gneiss complex may be considered as a dominant thrust sheet (Boyer and Elliott, 1982), whose movement may have caused the stacking of the Buchans Group in its footwall. The Hungry Mountain Thrust appears to be folded over the roof of the Buchans culmination in the area east of Middle Branch River (see geological map of Buchans area by Thurlow and Swanson, 1981), but unfortunately a large section of the folded roof is intruded by the Topsails Granite.

The Middle Branch duplex forms the uppermost thrust system of the Buchans Group. Its roof thrust is the Hungry Mountain Thrust, and it overlies a number of Buchans Group duplexes along the Airport Fault. At present the duplex is subdivided in two units (Figs. 1, 2). Unit 2a is exposed to the west of Sandy Lake and contains penetratively deformed, mafic volcanic rocks of greenschist to epidote amphibolite grade. The rocks have a north-dipping foliation with down-dip mineral elongation lineation parallel to the mylonitic fabric of the overlying gneisses of the Hungry Mountain Complex. The shape and attitude of the floor thrust of this unit are poorly constrained, but the fault appears to be north-dipping. Thurlow (1981) interpreted the metamorphism of the unit as a result of the "hot" emplacement of the Hungry Mountain Complex onto the Buchans Group. Unit 2b is exposed in a large area east of Sandy Lake and contains a variety of submetamorphic volcanic and volcaniclastic rocks that are mildly deformed, mostly in a cataclastic manner. Drill-core data show that east of Sandy Lake the Airport Fault dips gently eastwards, and defines a small, east-plunging antiform near the branch point with the floor thrust of unit 3a (see below). The floor thrust of unit 2b, east of the Buchans town site, dips steeply north at the surface and flattens gradually at depth. Virtually no information is available on the internal structural geometry of the unit. The rocks of both units have been assigned tentatively to the Lundberg Hill Formation by Thurlow and Swanson (1987). The contrasts between the units in metamorphic grade and structural style, on the one hand, and the similarities in these aspects between unit 2a and the Hungry Mountain Complex, on the other hand, seem to indicate that units 2a and 2b followed fundamentally different displacement paths. Unit 2a appears to have been subjected to thrusting together with the Hungry Mountain Complex at much greater depth than recorded by any of the other thrust systems of the Buchans Group. This may imply that unit 2a is a far-travelled, isolated horse (Boyer and Elliott, 1982) of exotic material that was accreted to the sole of the Hungry Mountain Complex prior to the juxtaposition of the latter with the Buchans Group.

The Sandy Lake duplex occupies the footwall of the Airport Fault. The geometry of its floor thrust, defined by the Ski Hill – Buchans River Fault, is described in an earlier section. The structure of the western boundary of the duplex is poorly constrained due to a lack of surface and subsurface data. Three large imbricates (units 3a-c) are postulated to comprise the bulk of the duplex. They preserve the most complete lithostratigraphic sections of the Buchans Group, but in each section the bottom and the top of the succession are defined by faults (Thurlow and Swanson, 1987). The positions of the floor thrusts of units 3a and 3b are poorly constrained due to a lack of drill core data around Sandy Lake. The small, east-plunging culmination on the Airport Fault east of Sandy Lake (see above) is interpreted to trace the position of a hangingwall anticline developed in the underlying imbricate 3a. The southern limb of the culmination contains the branch line of the Airport Fault with the floor thrust of the imbricate (Fig. 1). Unit 3d forms the lowermost imbricate system of the duplex, exposed in the southeastern part of its outcrop area. It is described and illustrated in detail in the following section.

The Lake 3 duplex lies in the immediate footwall of the Ski Hill Fault in the western part of the area (Fig. 1). Further east, its floor thrust splays of the Ski Hill Fault and is interpreted to fold over the Lucky Strike and lower duplexes (units 6 and 7). This geometry suggests that the Lake 3 duplex immediately underlies the Sandy Lake duplex in the regional stacking order (Table 2), and further that it is folded over an antiformal stack of units 5-7 in its footwall. Its internal structure defines a foreland-dipping duplex (Fig. 2; also see Thurlow and Swanson, 1987), in which the imbricate thrust surfaces curve asymptotically from the roof thrust down to the floor thrust. Available drill-core data indicate that this duplex contains only rocks of the Sandy Lake Formation at the top of the Buchans Group.

The Lucky Strike duplex represents the economically most important duplex of the thrust stack, hosting the majority of the known Buchans orebodies including Old Buchans, Conglomerate, Lucky Strike, Two Level, Rothermere, MacLean and MacLean Extension orebodies. The internal structural geometry of the duplex is very complicated and has only been studied in detail in the area of the MacLean and MacLean Extension orebodies (Thurlow and Swanson, 1987). Rocks of the Ski hill and Buchans River formations, comprise the bulk of the duplex. They are arranged in a number of hinterland-dipping imbricates that contain the main orebodies (Fig. 2). The geometrical relationships between these orebodies and the ones contained in the Sandy Lake duplex were discussed in a previous section. Preliminary notes on the structure of the Lucky Strike orebodies are presented in a later part of this report.

The Arkose duplex represents a small thrust system that is clearly overlain by the Lucky Strike duplex along the Old Buchans Fault (Fig. 1). It also occupies the footwall of the Buchans River Fault, lying immediately beneath the imbricate system that contains the Oriental Orebodies. These geometrical relationships between units 3d, 5 and 6 point to the presence of a complex frontal – lateral ramp configuration, requiring an east-dipping oblique or lateral ramp between units 3d and 5, as suggested earlier. These relationships cannot be shown properly in a single section as Figure 2. The

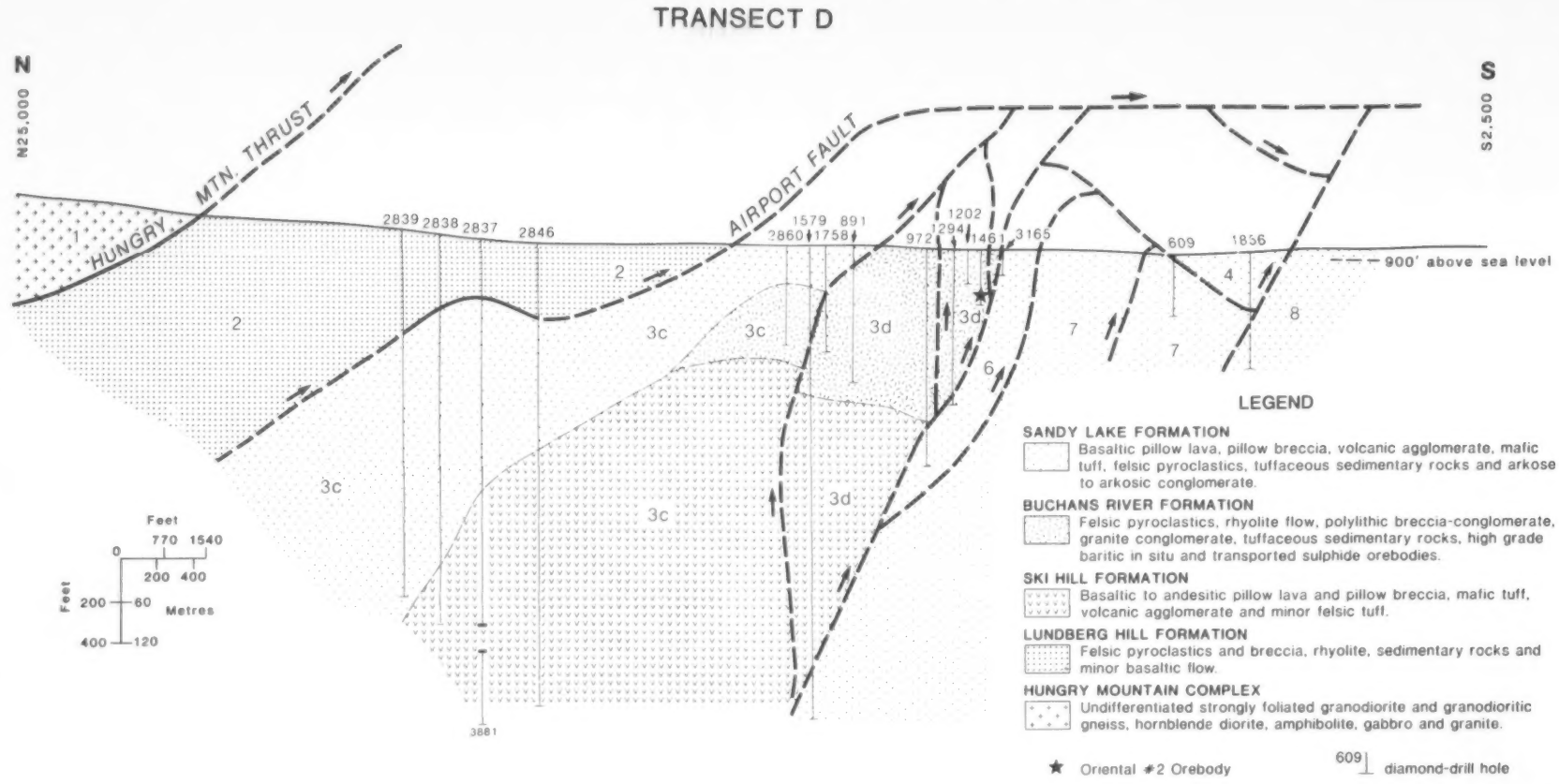

Figure 3. Detailed north-south cross-section through the Oriental area (Transect D). Vertical scale is exaggerated to four times horizontal scale. Numbers on the cross-section refer to structural units listed in Table 2.

internal geometry of the Arkose duplex is virtually impossible to decipher due to the massive nature of the arkoses of the Sandy Lake Formation that comprise the unit. A few north-dipping bedding attitudes suggest that it represents a hinterland–dipping duplex structure.

The Buchans duplex lies in the exposed core of the culmination involving all of the duplexes described previously (Fig. 1, 2). It exposes only rocks of the Sandy Lake Formation, but may contain lower lithostratigraphic units at its base. The floor thrust of the duplex has not been penetrated by diamond-drill holes, and it is, therefore, not known whether or not the unit forms the structural base of the Buchans culmination.

The lowermost thrust system of the stack is exposed in the western and southern part of the Buchans area (Fig. 1), underlying units 2b, 3 and 4. Its internal structure is poorly constrained because of very limited surface exposures and virtually no diamond-drill hole data. The unit is tentatively divided into a number of imbricates separated by northeast-striking thrust faults. Wiley's River imbricate, the highest unit of the thrust system, comprises a large lithostratigraphic section of the Buchans Group exposed in an east-dipping and east-facing monocline. Lower imbricates expose only rocks of the Sandy Lake Formation with northwesterly dipping bedding attitudes. The geometry of this duplex suggests that it did not play a role in the formation of the Buchans culmination which rests on its roof (Fig. 2). The floor thrust of this duplex may represent the sole thrust to the Buchans thrust stack. It may coincide with the major northeast-striking structural lineament that passes through Red Indian Lake to the south-east of the Buchans area (Thurlow, 1981, 1984). Alternatively, the sole thrust may be blind, in which case conceivably it is truncated by the Red Indian Lake Fault.

STRUCTURE OF THE ORIENTAL # 1 OREBODY

The Oriental # 1 and # 2 orebodies are contained in a small, intensely imbricated thrust system (unit 3d in Figures 1 and 2) situated at the base of the Sandy Lake duplex. The thrust system contains exclusively rocks of the Sandy Lake and Buchans River formations. It is exposed in the form of an eyelid window, framed to the east along part of its roof by unit 2b of the Middle Branch duplex and to the north along the remainder of its roof by rocks of the Buchans River and Sandy Lake formations contained in unit 3c of the Sandy Lake duplex (Fig. 3). This part of the roof thrust is at present still poorly delineated, because it separates virtually identical lithostratigraphic sequences in its hangingwall and footwall. The floor thrust of the system is formed by the Buchans River Fault, exposed in Buchans River near the town site and in the southern wall of the Oriental West pit. The footwall of the thrust system consists of massive arkose of the Sandy Lake Formation contained in the Arkose duplex. To the west, the thrust system may overlie a small part of the Lucky Strike duplex as indicated by the presence of a thin unit of highly sheared tuffaceous rocks of the Buchans River Formation exposed in the hangingwall of the Buchans River Fault west of its branch point with the Old Buchans Fault. The positions of the branch lines of the roof thrust with the Buchans River and Airport faults are undetermined and will be very difficult to locate given the presently available subsurface information.

The thrust system is characterized by an overall northerly dipping internal structure defined by numerous imbricate thrust surfaces and the long limbs of south-verging folds contained within the imbricates. It may be subdivided into three main units. The uppermost unit, not further discussed in this section, contains the Oriental # 2 Orebody in what appears to be a single, be it intensely sheared (Alcock, 1961), imbricate thrust sheet that lies completely blind in the footwall of unit 3c. The massive sulphide – barite lenses of the in situ Oriental # 1 Orebody (Thurlow and Swanson, 1981) are contained in two intensely imbricated antiformal stacks situated between the Oriental # 2 imbricate and the Buchans River Fault. All three units rest, with a marked thrust contact of rocks of the Buchans River Formation, on top of arkoses of the Sandy Lake Formation situated in the footwall of the thrust system. The two antiformal stacks of the Oriental # 1 Orebody are well exposed in the Oriental West and East pits. Detailed plane table mapping of the geology of these pits has helped outline the probable structural geometry of the orebody.

Oriental West pit

The geological map of the Oriental West pit (Fig. 4) illustrates the plan view geometry of part of the western antiformal stack. The Buchans River Fault is well exposed in the southern wall of the pit. It shows small dextral offsets along a set of en echelon faults with steep northerly dips, containing moderately east-plunging slickensides. The overall attitude of the floor thrust is steeply north-dipping. The Sandy Lake Formation in the footwall consists of highly fractured conglomeratic arkose.

The immediate hangingwall of the floor thrust consists of penetratively deformed, felsic tuffs that are generally considered to lie stratigraphically above the ore horizon (J.G. Thurlow, personal communication, 1985). These tuffs contain a well-developed, moderate to steep north-dipping foliation which is locally crenulated along discrete, gently north-dipping shear bands. Assuming that the two planar fabrics represent a C-S plane relationship (Simpson and Schmid, 1983), a south-directed thrust sense may be inferred for the base of the imbricates of the Buchans River Formation. The tuffs show two linear fabrics on the foliation plane. The first consists of curvilinear bedding/cleavage intersection lineations which plunge to the north. These lineations are locally parallel to the hinges of rootless, isoclinal folds of competent layers in the tuff. The second fabric is a fine grained mineral lineation plunging moderately northeast (also see McClay, 1987). The tuffs are interpreted to represent a zone of high strain developed during south-directed movement of the thrust stack over its footwall of arkose. Folds which initially developed with axes at high angle to the movement direction of the shear zone became progressively rotated towards the shear direction during thrusting. The significance of the min-

eral lineation is presently enigmatic. It may represent a stage of northeast – southwest directed movement, as suggested by McClay (1987), but the timing of this event is uncertain.

The basal imbricate of sheared tuffs is overlain in the eastern part of the pit by a number of poorly exposed imbricates that once contained the larger ore lenses. The imbricates situated on the northeastern slope of the pit overlie directly these ore lenses. They contain repetitions of conformable sequences which contain from bottom to top: siliceous pyritic stockwork, layered massive sulphide ore lenses and red and green layered tuffs. The thrust surfaces and bedding within the imbricates are generally steeply north-dipping. Gently west- and east-plunging, tight folds with well-developed, north-dipping axial planar cleavage are common (McClay, 1987). A number of these folds show vergence to the south.

The eastern belt of imbricates can be traced westwards across the pit above the basal imbricate of sheared tuff. They are partly overlain by a number of very gently north-dipping imbricates consisting of tuffs normally underlying the ore lenses (J.G. Thurlow, personal communication, 1986), small lenses of highly sheared ore set in a schistose tuffaceous matrix and large lenses of pyritic stockwork. These uppermost imbricates fold in the northeastern part of the pit over the lower imbricates as indicated by their change in attitude. The lower imbricates thicken clearly eastwards due to the stacking of thick ore lenses. In this way an east-west trending, gently west-plunging antiformal stack is formed directly above the floor thrust, resulting in bending of the overlying imbricates.

It is noteworthy, that rocks of the Sandy Lake Formation do not occur in the imbricates of the antiformal stack, at least

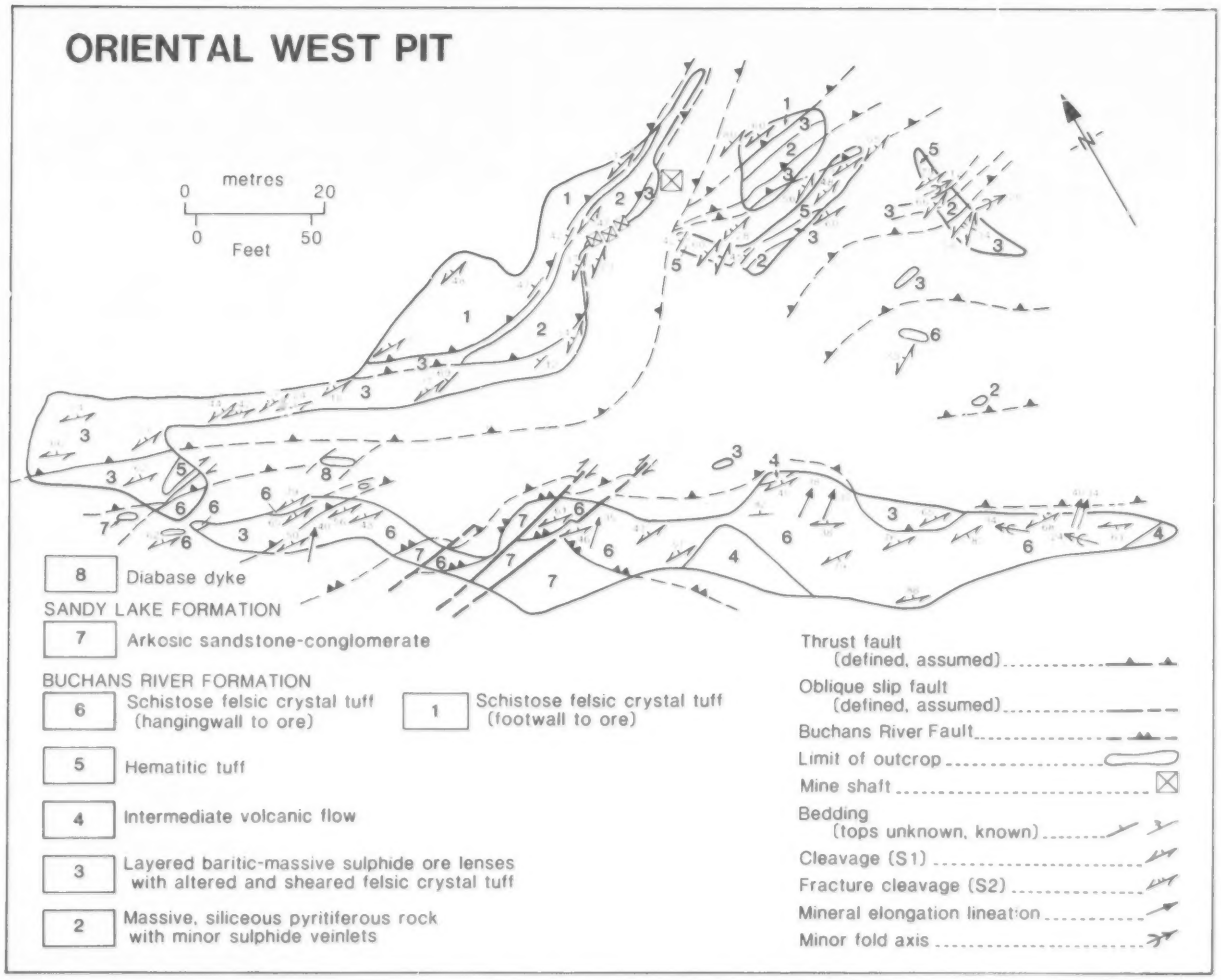

Figure 4. Geological map of the Oriental West pit.

at the present level of exposure. It implies that the formation of the western antiformal stack occurred largely by imbrication within the Buchans River Formation. The contact of the Sandy Lake and Buchans River formations in this part of the thrust system must, therefore, be structural rather than stratigraphic in nature. Unfortunately, this contact is not exposed, but it is intersected in numerous drillholes situated to the northeast of the pit along the trend of the antiformal stack. Arkoses overlie with sharp contact rocks of the Buchans River Formation in these holes. These arkoses, designated "Upper Arkose" in the earlier stratigraphic scheme (Thurlow and Swanson, 1981), were considered to overlie conformably rocks of the Buchans River Formation. The relationships observed in the West pit suggest that this contact is an important intracutaneous thrust. Structure contours for this thrust show that it defines an open, gently northeast plunging synform situated in the area between the Oriental West and East pits.

Oriental East pit

The geological map of the Oriental East pit (Fig. 5) illustrates the geometry of part of the eastern antiformal stack. The floor thrust (Buchans River Fault) of the stack is not exposed in the pit, but lies buried under gravel just to the south of the southern slope of the pit. Subsurface data show that it is a steeply north-dipping plane.

The overlying thrust stack consists of a large number of imbricates that are moderately to steeply north- and northwest-dipping. The surface traces of the imbricate faults are curved in the southern part of the pit, suggesting that the individual thrust sheets were folded over large, massive ore lenses that were extracted from the centre of the pit. Unfortunately, the positions of many of the thrust surfaces exposed along the western slope of the pit cannot be traced with confidence across the pit, even after inspection of available mine level and stope planes. The subsurface data indicate,

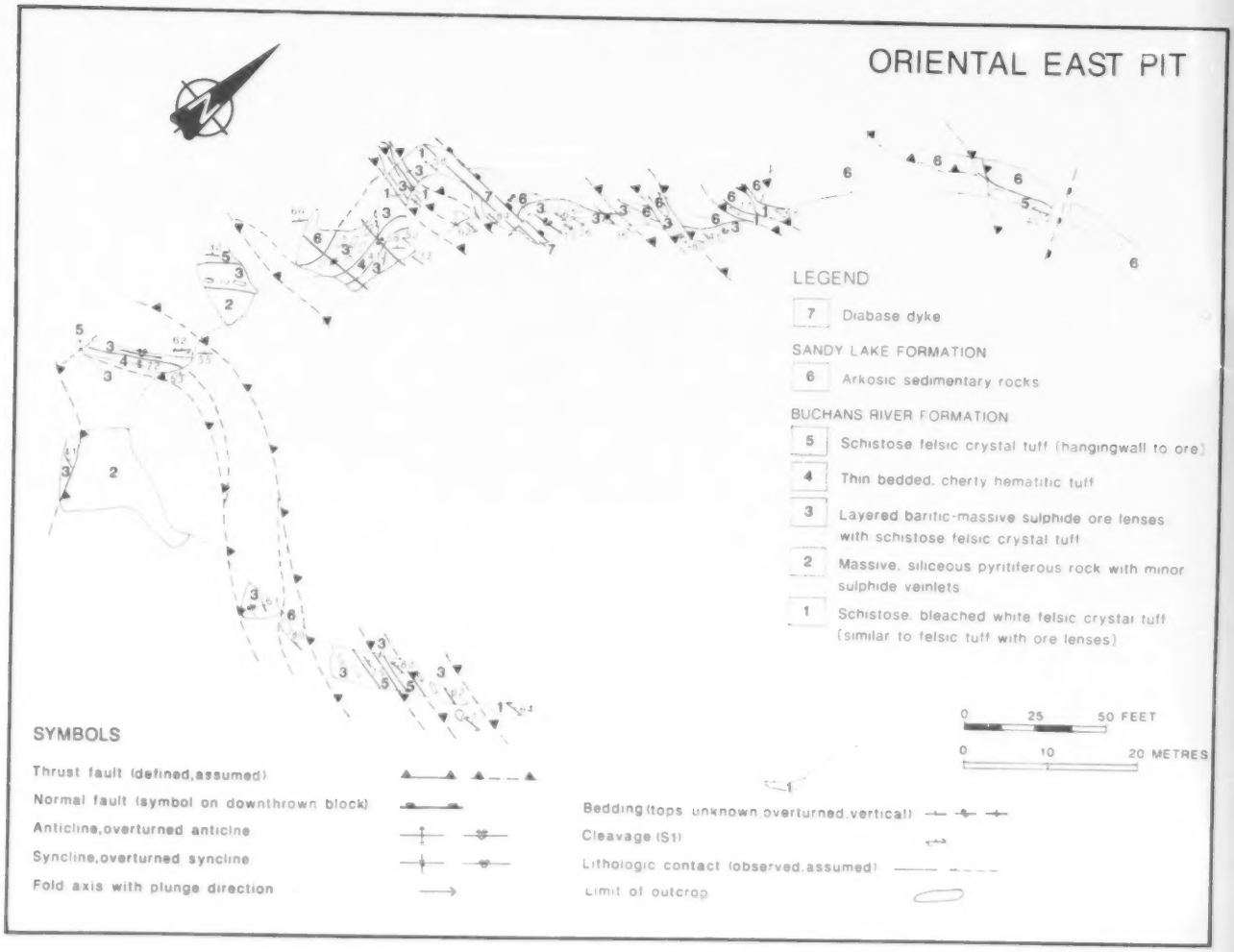
ORIENTAL EAST PIT
LEGEND
7 Diabase dyke
SANDY LAKE FORMATION
6 Arkosic sedimentary rocks
BUCHANS RIVER FORMATION
5 Schistose felsic crystal tuff (hangingwall to ore)
4 Thin bedded, cherty hematitic tuff
3 Layered baritic-massive sulphide ore lenses with schistose felsic crystal tuff
2 Massive, siliceous pyritiferous rock with minor sulphide veinlets
1 Schistose, bleached white felsic crystal tuff (similar to felsic tuff with ore lenses)
0 25 50 FEET
0 10 20 METRES
SYMBOLS
Thrust fault (defined,assumed)
Normal fault (symbol on downthrown block)
Anticline,overturned anticline
Syncline,overturned syncline
Fold axis with plunge direction
Bedding (tops unknown,overturned,vertical)
Cleavage (S1)
Lithologic contact (observed,assumed)
Limit of outcrop

Figure 5. Geological map of the Oriental East pit.

however, that a general change occurs from east-trending structures in the western part of the pit to northeast-trending structures in the easternmost part of the pit. This change in trend conforms with the axial trend of the synform of the so-called "Upper Arkose" (i.e. Sandy Lake Formation) located to the northwest of the pit.

In contrast to the Oriental West pit, most of the imbricates in the East pit contain sequences, up to 10 metres thick, of massive conglomeratic arkose representing the Sandy Lake Formation. In some cases, the arkose overlies conformably normal lithostratigraphic sequences of the Buchans River Formation. At other localities, the contact of the arkose with underlying rocks of the Buchans River Formation is tectonically disturbed. In a few imbricates the contact and bedding planes in the underlying rocks are folded in large, asymmetric folds that verge to the south. Fold axes plunge gently east or west, and the folds carry a steeply north-dipping axial plane cleavage which is well developed in tuffaceous rocks of the Buchans River Formation. In one imbricate at the base of the stack, the presence of an overturned succession of the Buchans River Formation is indicated by the fact that cleavage dips more gently than bedding.

Stratigraphic and structural relationships in the East pit indicate that imbrication occurred by the development of numerous closely spaced thrust surfaces. Many hangingwall- and footwall-ramps are observed in the imbricates exposed on the west slope of the pit, indicating that the thrusts ramped steeply through the rocks of the Buchans River Formation and penetrated at least the basal part of the overlying Sandy Lake Formation. Evidence of folding of the higher thrust sheets over lower ones, particularly those containing the massive ore lenses, is much less convincing than in the West pit.

A structure contour map drawn for the base of the arkose overlying the Buchans River Formation using drillhole data for the area to the northeast of the pit shows that this contact defines an open, gently northeast-plunging antiform. This structure is complementary to the synform situated to the northwest (see above). The antiform delineates the crest of the antiformal stack formed by the imbricates exposed in the East pit. It follows that the level of erosion of the imbricates in the pit lies too low in the stack to show the effects of folding of the thrust sheets.

Synthesis

The Oriental # 1 Orebody occurs in a composite thrust system that lies in the hangingwall of the Ski Hill – Buchans River Fault. It consists of numerous large and small lenses of sheared massive sulphide and barite hosted by thin sequences of highly cleaved and folded felsic tuffs of the Buchans River Formation. The ore units are contained in a large number of thin imbricate thrust sheets that appear to be rather continuous along strike. These imbricates show generally a moderate to steep northwesterly to northerly dip, except in areas where imbricates that are structurally higher in the thrust stack are folded over ones lower in the stack. Such folding is particularly common around imbricates containing large ore lenses. Most of the imbricates contain mesoscopic, asymmetric fold structures that verge to the south or southeast. Folding was associated with the formation of a northerly dipping axial plane cleavage which is well developed in incompetent lithologies. It is not certain that the observed northeast-plunging mineral lineations are related to the folds. Numerous shear fractures, joints and tension gashes are developed in the competent lithologies such as pyritic stockwork and arkose. The bounding thrust surfaces of the imbricates are either discrete fault planes or narrow shear zones, depending on the lithology in which they are developed, and they occur as both flats and ramps. Stratigraphic cut-off lines on hangingwall and footwall ramps are subhorizontal, trending east or northeast. The basal imbricate of the thrust system exposed in the West pit is a zone of high strain developed in felsic tuff that is locally at least 20 metres thick.

The various aspects of the style and orientation patterns of the mesoscopic structures developed in the thrust system all suggest that imbrication of the orebody and its host rocks, as well as the Sandy Lake Formation arkose, occurred in a direction with azimuth in the southeastern quadrant. This is contrary to a conclusion reached by McClay (1987) based on the orientation of stretching lineations in the West pit, that thrust movement on the Ski Hill – Buchans River Fault was in part towards 227°.

The macroscopic structure of the thrust system containing the Oriental # 1 ore lenses involves two antiformal stacks that show a gradual change in trend of their culmination axes from virtually east-west in the western part of the thrust system to northeast - southwest in its eastern part. The two stacks are clearly distinguished by their lithostratigraphic make-up. The western stack, partly exposed in the West pit, appears to consist exclusively of rocks of the Buchans River Formation. The eastern stack, partly exposed in the eastern pit, consists mainly of imbricates that preserve above the rocks of the Buchans River Formation at least the basal succession of the Sandy Lake Formation arkose. This implies that the Sandy Lake Formation was detached from the Buchans River Formation during imbrication of the western stack and must form a separate duplex somewhere above its roof. Further, the floor thrust of the western stack must have ramped through at least part of the Sandy Lake Formation to allow the incorporation of arkose in the imbricates of the eastern stack. The synform of arkose situated between the two pits delineates the boundary between the two stacks and represents a leading synform (Boyer and Elliott, 1982) of the roof thrust of the western stack. The eastern antiform of the base of the arkose delineates the crest of the eastern stack. The folding of imbricates situated higher in the stacks over "bunched" imbricates, which contain the main ore lenses lower in the stacks, provides good evidence that imbrication occurred by the progressive collapse of the footwall of the evolving stacks (i.e. in piggy back fashion; Elliott and Johnson, 1980; Boyer and Elliott, 1982). As argued before, this imbrication occurred in a southerly to southeasterly direction. The Buchans River Fault dips consistently to the north, and the two antiformal stacks are thus obliquely inclined to their floor thrust. This

implies that the fault represents an oblique ramp with respect to its hangingwall and supports the suggestion made earlier that the Oriental and Lucky Strike orebodies were separated from one another during thrusting by an oblique – lateral ramp system. The Buchans River and Ski Hill Fault segments show presently a consistent strike to the east, implying that the ramps were straightened during subsequent movement of the Sandy Lake duplex.

An attempt was made to reinterprete the actual geometry of the orebody using the new surface data of the pits, as well as available mine data which included detailed mine level and stope planes covering the interval between 450' - 700' mine levels. Figure 6 illustrates two north – south cross-sections constructed for the West pit and East pit along mine grid lines East 10,950 and East 11,800, respectively. It should be noted that the sections are oblique to the trend of the antiformal stacks. Each section cuts the area of main concentration of ore lenses in the stacks. The two sections show that the ore lenses are tightly stacked in thin imbricates at the base of the antiformal stacks. Folding of the ore lenses and their host rocks within the imbricates appears to be common. However, some of the interpreted folds may in fact be closely packed ore lenses separated by additional thrust faults with a thin veneer of host rock. The complete absence of Sandy Lake Formation arkose in the western stack is apparent. The synform of arkose situated in the roof at the leading edge of the western antiformal stack is shown in the northern part of the East pit section. Only one imbricate with a folded contact of the Buchan River and Sandy Lake formations is shown in the upper part of the eastern stack. The surface data for the East pit show that such imbricates are common at a slightly higher level in this stack.

PRELIMINARY NOTES ON THE STRUCTURE OF THE LUCKY STRIKE OREBODIES

The Lucky Strike glory hole exposes small, unmined portions of the Main, Two Level and North orebodies. Three days of

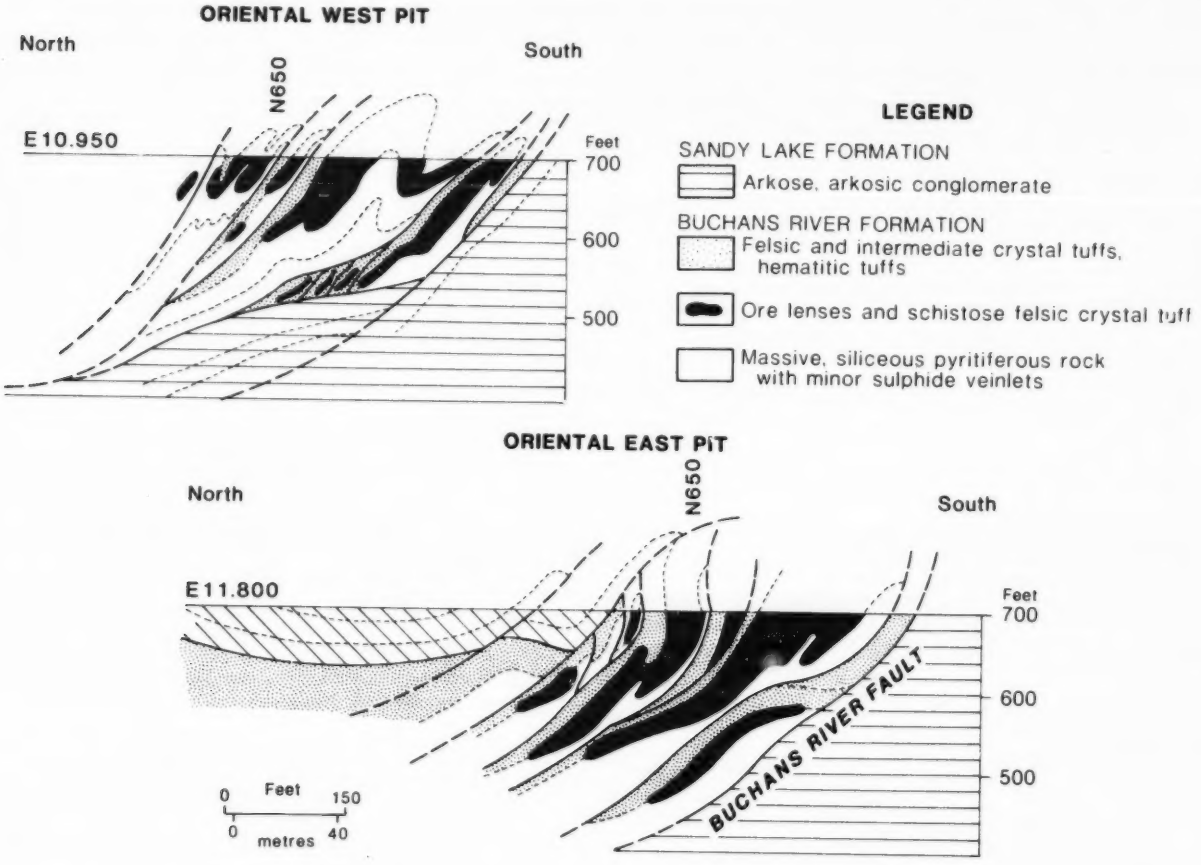

Figure 6. Schematic north-south cross-sections through the Oriental #1 ore lenses in the Oriental West and East pits. Cross-sections were constructed using old mine level and stope plans and elevations are given with respect to 0 foot sea level.

structural analysis were carried out in the glory hole, just prior to flooding, in an attempt to record as much important structural information as possible. At a later stage this material will be analyzed in conjunction with available mine data to reconstruct the geometry of the orebodies.

Remnants of the Main Orebody are exposed along the base of the central part of the pit. They are underlain by an intensely deformed unit of altered, pale green felsic crystal tuff. This unit shows abundant, mesoscopic folds that are north-verging. The rocks have a well-developed cleavage that is axial planar to the folds. This planar fabric is north-dipping and contains a down-dip mineral lineation. The unit is thought to represent a major movement zone along which the orebody was thrusted to the south. The waste band of schistose felsic tuff that transects the orebody with a steep attitude (Jambor, 1987) represents possibly the location of an imbricate thrust fault that splays upwards from the main movement zone.

In the northeastern part of the pit, the North and Two Level orebodies and two pyritic stockwork units are contained in imbricate thrust sheets which appear to fold over the roof of the Main Orebody. The few exposed contacts of the imbricates are shear zones up to one metre wide consisting of chlorite schist. Shear bands and slickensides developed in pyritic chlorite schist at the base of the north-dipping North Orebody indicate south-directed thrusting of the orebody and the overlying imbricates.

The above mentioned preliminary observations, in conjunction with the recognized structural geometry of the Oriental # 1 Orebody, indicate that the Lucky Strike Orebodies occur in an imbricate thrust system with the overall geometry of an antiformal stack.

KINEMATIC MODEL FOR THRUSTING IN THE BUCHANS AREA

The results of the detailed geometrical analysis of the Buchans thrust stack presented in the foregoing sections can be used to formulate a general kinematic model for thrusting in the Buchans area. The main results can be summarized in the following points:

1. The Buchans Group comprises an extensive fold and thrust belt which contains a major east - west trending culmination formed by the stacking of a large number of duplex structures. The stacking order of the duplexes is outlined in Table 2.
2. The top of the thrust stack contains two metamorphic thrust sheets which are interpreted to have been emplaced onto the Buchans Group from a deeper crustal level. They are considered to be far-travelled units that are stratigraphically unrelated to the Buchans Group.
3. The folding of the Hungry Mountain Complex over the roof of the culmination formed by the Buchans Group duplexes implies that the complex was emplaced on the Buchans Group prior to imbrication of the latter. Thrust-

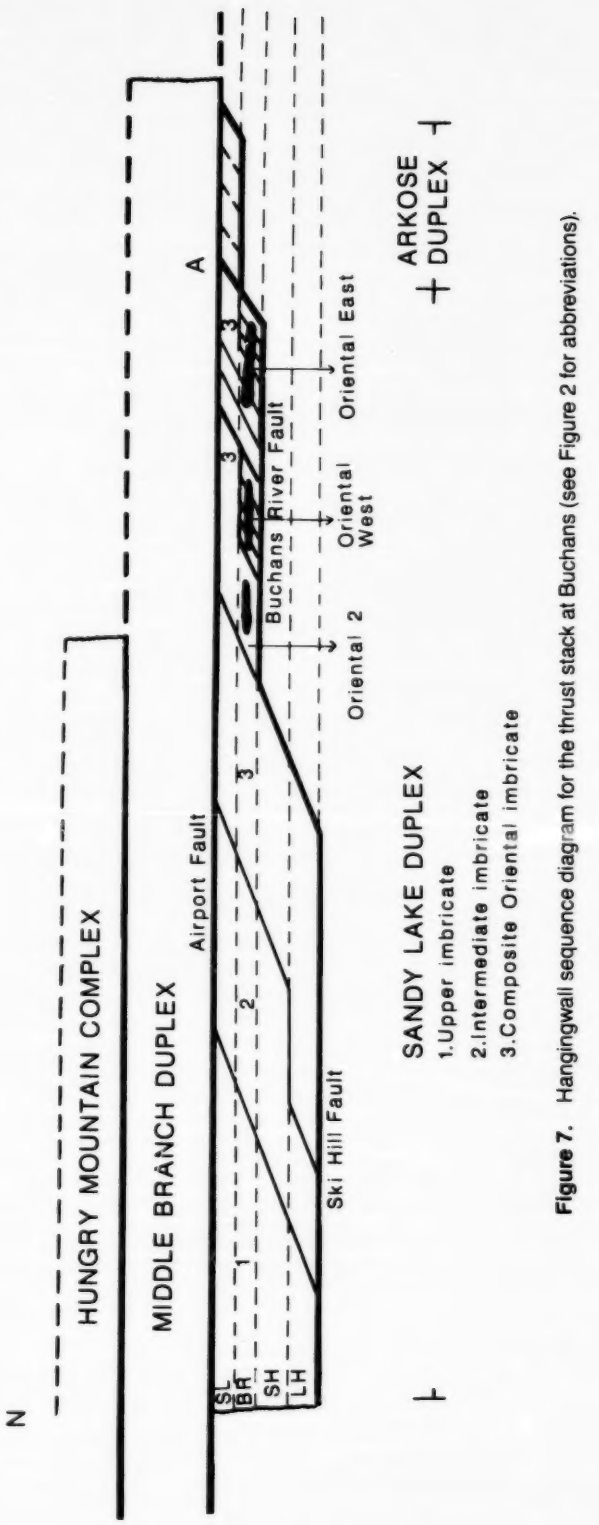

Figure 7. Hangingwall sequence diagram for the thrust stack at Buchans (see Figure 2 for abbreviations).

ing within the Buchans Group may have been initiated by the movement of this dominant thrust sheet.

4. The Buchans culmination is a huge antiformal stack that contains at least seven major duplexes of Buchans Group lithologies. Folding of structurally higher duplexes over the ones lower in the stack shows that the structure formed according to a thrust sequence involving progressive footwall collapse (i.e. in piggy-back fashion). This mode of thrusting is observed also for the stacking of individual imbricates within the duplexes. No deviations from this pattern have been observed.

5. Geometrical relationships shown by the various duplexes and aspects of the internal geometry of the duplexes have been used to deduce the ramp configuration of the thrust systems. The duplexes are bound to a large extent by north-dipping listric thrust surfaces. The presence of large, east - west trending hangingwall anticlines and hangingwall- and footwall-ramps with east - west trending stratigraphic cut-off lines indicate that these north-dipping fault segments represent frontal ramps. Lateral and oblique ramps have been recognized in a few instances and appear to be generally dipping east to northeast. One of these separates the Oriental and Lucky Strike orebodies.

6. The regional direction of thrusting for the Buchans area is inferred to be towards the south or southeast. This is based on the interpretation of the ramp geometry and various aspects of the structural style of the rocks contained in the imbricates such as orientation and vergence of mesoscopic folds, foliation and lineation attitudes and rare kinematic indicators. No evidence was found to substantiate a sequence of regional thrusting events with different movement directions as proposed by McClay (1987).

7. The distribution of lithostratigraphic units of the Buchans Group in the duplexes that form the culmination appears to follow a regular pattern. The higher duplexes in the stack contain more complete lithostratigraphic sequences, while the lower duplexes contain sequences that are restricted to the upper two units of the Buchans Group. This distribution pattern through the thrust stack implies that the floor thrust of the culmination ramped southwards through successively younger units of the Buchans Group.

8. The antiformal stack that forms the Buchans culmination rests on a lower thrust system that also contains rocks of the Buchans Group. The sole thrust of the belt as a whole is blind and may be truncated by the Red Indian Lake lineament.

The kinematic model for thrusting in the Buchans area involves regionally south-directed imbrication of the Buchans Group by footwall collapse during or following the emplacement of the Hungry Mountain Complex. The imbrication occurred along a complex system of frontal, lateral and oblique ramps. Large duplex structures were formed building up a huge antiformal stack. Due to the complex ramp geometry, the internal structure of this stack is of bewildering complexity. A time frame for the evolution of the stack is illustrated in Figure 7 in the form of a hangingwall sequence diagram. It considers the development of the Sandy Lake duplex at a point in time following the emplacement of the Hungry Mountain Complex and the Middle Branch duplex over an as yet undisturbed footwall of the rocks of the Buchans Group. A schematically restored section of the Sandy Lake duplex is shown below the floor thrust of the Middle Branch duplex. This restored section illustrates the position of the floor thrust of the Sandy Lake duplex, defined by the Ski Hill – Buchans River Fault, as well as the positions of the various imbricate thrust surfaces. The stacking of the duplex occurs sequentially from unit 1 to unit 6, each unit first climbing over its footwall before imbrication of the footwall continues. The geometry of the end-product is shown schematically in Figure 2. Work presently in progress involves the construction of a number of these hangingwall sequence diagrams in an attempt to palinspastically restore the Buchans thrust belt.

ACKNOWLEDGMENTS

The project was funded during 1985-86 by the Geological Survey of Canada under DSS contract 06ST.23233-5-0382 to T.J. Calon. Work was continued during the 1986 field season when F.K. Green was employed by the Geological Survey of Canada. Special thanks are due to J.G. Thurlow for introducing the authors to the geology of the Buchans area and for many helpful discussions while fieldwork was in progress. Asarco mine manager G. Neary is thanked for allowing easy access to all available mine data. Permission from J.L. Jambor for use of his geological map of the Lucky Strike glory hole is gratefully acknowledged. R.V. Kirkham, J.G. Thurlow and H.S. Swinden are thanked for reviewing drafts of the manuscript.

REFERENCES

Alcock, J.B.
1961: Oriental No. 2 orebody; Unpublished B.Sc. Thesis, Royal School of Mines London, 65. p.

Boyer, S.E. and Elliott, D.
1982: Thrust systems; American Association of Petroleum Geologists, Bulletin, v. 66, p. 1196-1230.

Butler, R.W.H.
1982: The terminology of structures in thrust belts; Journal of Structural Geology, v. 4, p. 239-245.

Dahlstrom, C.D.A.
1970: Structural geology of the eastern margin of the Canadian Rocky Mountains; Society of Canadian Petroleum Geologists, v. 18, p. 332-406.

Elliott, D. and Johnson, M.R.W.
1980: Structural evolution in the northern part of the Moine thrust zone; Transactions Royal Society Edinburgh, v. 71, p. 69-96

Hossack, J.R.
1983: A cross-section through the Scandinavian Caledonides constructed with the aid of branch line maps; Journal of Structural Geology, v. 5, p. 103-111.

Jambor, J.L.
1987: Geology and origin of the orebodies in the Lucky Strike area; in Buchans Geology, Newfoundland, ed. R.V. Kirkham; Geological Survey of Canada, Paper 86-24, Report 7.

Lister, G.S. and Snoke, A.W.
1984: S-C mylonites; Journal of Structural Geology, v. 6, p. 617-638.

McClay, K.R.
1987: Aspects of the structural geology of the Buchans area; in Buchans Geology, Newfoundland, ed. R.V. Kirkham; Geological Survey of Canada, Paper 86-24, Report 3.

Simpson, C. and Schmid, S.M.
1983: An evaluation of criteria to deduce the sense of movement in sheared rocks; Geological Society of America, Bulletin, v. 94, p. 1281-1288.

Thurlow, J.G.
1981: The Buchans Group: Its stratigraphic and structural setting; in The Buchans Orebodies: Fifty Years of Geology and Mining, ed. E.A. Swanson, D.F. Strong and I.G. Thurlow; Geological Association of Canada, Special Paper 22, p. 79-90.
1984: A geological field guide to the Buchans area; in Mineral Deposits of Newfoundland – A 1984 Perspective, compiled by H.S. Swinden; Newfoundland Department of Mines and Energy, Report 84-3, p. 141-146.

Thurlow, J.G. and Swanson, E.A.
1981: Geology and ore deposits of the Buchans area, central Newfoundland; in The Buchans Orebodies: Fifty Years of Geology and Mining, ed. E.A. Swanson, D.F. Strong and J.G. Thurlow; Geological Association of Canada, Special Paper 22, p. 113-142.

Thurlow, J.G. and Swanson, E.A.
1987: Stratigraphy and structure of the Buchans Group; in Buchans Geology, Newfoundland; ed. R.V. Kirkham; Geological Survey of Canada, Paper 86-24, Report 2.

MAPS
NOT
FILMED

CARTES
OMISES